

# Four new species of *Anyphaena* Sundevall, 1833 from Xizang, China (Araneae, Anyphaenidae)

Shikai Li<sup>1</sup>, Shilin Wang<sup>1</sup>, Xiaoqi Mi<sup>1</sup>, Cheng Wang<sup>1</sup>

<sup>1</sup> Guizhou Provincial Key Laboratory for Biodiversity Conservation and Utilization in the Fanjing Mountain Region, Tongren University, Tongren, 554300 Guizhou, China  
Corresponding author: Cheng Wang ([wchengspider@163.com](mailto:wchengspider@163.com))

## Abstract

Four new species of the genus *Anyphaena* Sundevall, 1833 collected from Xizang, China, are described: *A. cibagou* Wang & Mi, **sp. nov.** (♂♀), *A. linzhi* Wang & Mi, **sp. nov.** (♂♀), *A. shufui* Wang & Mi, **sp. nov.** (♀) and *A. yejiei* Wang & Mi, **sp. nov.** (♀). Diagnostic photos of the habitus and copulatory organs and a distributional map are provided.

**Key words:** DNA barcodes, ghost spider, morphology, southwest China, taxonomy

## Introduction

*Anyphaena* Sundevall, 1833, the most species-rich genus of the family Anyphaenidae Bertkau, 1878, is represented by 106 wander-hunting species widely distributed in Asia, Europe and the Americas (WSC 2024; Rivera-Quiroz and Álvarez-Padilla 2023). In contrast to the taxonomic study of the genus in the Americas, it remains poorly known in Asia, which only has 17 species records, most of them sporadically described and only known from the original description (Durán-Barrón et al. 2016; WSC 2024). To date, eight endemic species known from both sexes are recorded from China, which is much higher than in nearby countries, such as Japan (3), Russia (3) and India (1) (WSC 2024). Among the Chinese species, half of them were described by Lin et al. (2021), including the only species recorded in Xizang, China.

Recently, spider surveys in two National Nature Reserves in Linzhi City, Xizang, China, were carried out, and more than twenty specimens of Anyphaenidae have been collected. After examination, four species belonging to *Anyphaena* are recognized as new to science and described herein.

## Material and methods

Specimens were collected by beating shrubs or hand collecting. They were preserved in 90% ethanol. Specimens are deposited in the museum of Tongren University (TRU) in Tongren, China. They were examined with an Olympus SZX 16 stereomicroscope. After dissection, the vulvae were cleared in trypsin enzyme solution before examination and imaging. Left male palps were used for the descriptions and illustrations. Photographs of the copulatory organs and habitus were taken



Academic editor: Alireza Zamani  
Received: 25 January 2024  
Accepted: 23 February 2024  
Published: 21 March 2024

ZooBank: <https://zoobank.org/DB6879AF-4EED-4ACE-950F-5A8D8CF760BB>

Citation: Li S, Wang S, Mi X, Wang C (2024) Four new species of *Anyphaena* Sundevall, 1833 from Xizang, China (Araneae, Anyphaenidae). ZooKeys 1196: 1–14. <https://doi.org/10.3897/zookeys.1196.119509>

Copyright: © Shikai Li et al.  
This is an open access article distributed under terms of the Creative Commons Attribution License ([Attribution 4.0 International – CC BY 4.0](https://creativecommons.org/licenses/by/4.0/)).

with a Kuy Nice CCD camera mounted on an Olympus BX43 compound microscope. Compound focus images were generated using Helicon Focus v. 6.7.1. Drawings of the schematic course of the copulatory duct were generated by Adobe Illustrator CC 2018. ArcGIS v. 10.4 software was used to create a distribution map.

A partial fragment of the mitochondrial cytochrome oxidase subunit I (COI) gene of the four species was amplified and sequenced using the primers LCO11490 and HCOI2198 (Folmer et al. 1994). The accession numbers are provided in Table 1. The pairwise genetic distances (Kimura two-parameter [K2P]) (see Table 2) were calculated using MEGA 6.0 to assess the genetic differences (Li and Zhang 2023).

All measurements are given in millimetres. Leg measurements are given as total length (femur, patella, tibia, metatarsus, tarsus). References to figures in the cited papers are listed in lowercase type (fig. or figs), and figures in this paper are noted with an initial capital (Fig. or Figs). Abbreviations used in the text and figures are as follows:

**AG** accessory gland; **ALE** anterior lateral eye; **AME** anterior median eye; **At** atrium; **C** conductor; **CD** copulatory duct; **E** embolus; **FD** fertilization duct; **MA** median apophysis; **MS** median septum; **PLE** posterior lateral eye; **PME** posterior median eye; **PPA** prolateral patellar apophysis; **PTA** prolateral tibia apophysis; **RTA** retro-lateral tibia apophysis; **VTA** ventral tibial apophysis; **S** spermatheca.

**Table 1.** Voucher specimen information.

Species	Voucher code	Sex	GenBank accession number
<i>Anyphaena cibagou</i> Wang & Mi, sp. nov.	TRU-XZ-ANY-0001	♂	PP356956
	TRU-XZ-ANY-0002	♀	PP356957
<i>A. linzhi</i> Wang & Mi, sp. nov.	TRU-XZ-ANY-0005	♂	PP356958
	TRU-XZ-ANY-0006	♀	PP356962
<i>A. shufui</i> Wang & Mi, sp. nov.	TRU-XZ-ANY-0014	♀	PP356960
	TRU-XZ-ANY-0015	♀	PP356961
<i>A. yejiei</i> Wang & Mi, sp. nov.	TRU-XZ-ANY-0017	♀	PP356959
	TRU-XZ-ANY-0018	♀	PP356963
	TRU-XZ-ANY-0019	♀	PP356964

**Table 2.** Intraspecific and interspecific nucleotide divergences for four *Anyphaena* species using Kimura two-parameter model.

Species	ANY-0001	ANY-0002	ANY-0005	ANY-0006	ANY-0017	ANY-0018	ANY-0019	ANY-0014	ANY-0015
<i>A. cibagou</i> ANY-0001									
<i>A. cibagou</i> ANY-0002	0.000								
<i>A. linzhi</i> ANY-0005	0.019	0.019							
<i>A. linzhi</i> ANY-0006	0.016	0.016	0.003						
<i>A. yejiei</i> ANY-0017	0.019	0.019	0.022	0.019					
<i>A. yejiei</i> ANY-0018	0.019	0.019	0.022	0.019	0.000				
<i>A. yejiei</i> ANY-0019	0.019	0.019	0.022	0.019	0.000	0.000			
<i>A. shufui</i> ANY-0014	0.033	0.033	0.034	0.033	0.036	0.036	0.036		
<i>A. shufui</i> ANY-0015	0.033	0.033	0.034	0.033	0.036	0.036	0.036	0.000	

## Taxonomy

Family Anyphaenidae Bertkau, 1878

Genus *Anyphaena* Sundevall, 1833

*Anyphaena cibagou* Wang & Mi, sp. nov.

<https://zoobank.org/1179C7E2-BBB7-42DB-94D2-9A7857BA90A7>

Figs 1A–C, 2, 4A, 6A

**Type material.** *Holotype* ♂ (TRU-XZ-ANY-0001), CHINA: Xizang Autonomous Region, Linzhi City, Chayu County, Cibagou National Nature Reserve (28°36.03'N, 97°4.01'E, ca 2200 m), 14 Aug. 2023, C. Wang and H. Yao leg. *Paratypes* 1 ♀ (TRU-XZ-ANY-0002), same data as for holotype; 1 ♀ (TRU-XZ-ANY-0003), Cibagou National Nature Reserve (28°41.43'N, 97°2.86'E, ca 2570 m), 25 Jun. 2023, C. Wang leg.

**Etymology.** The specific name is a noun in apposition and refers to the type of locality, Cibagou National Nature Reserve.

**Diagnosis.** The species is closely similar to that of *A. linzhi* sp. nov., in habitus and copulatory organs, but it can be easily distinguished by the following: 1) the main portion of the median apophysis is almost oval, and slightly longer than wide in ventral view (Fig. 2B), vs elongate-oval, more than two times longer than wide in *A. linzhi* sp. nov. (Fig. 3B); 2) the conductor is acutely narrowed distally (Fig. 4A), vs almost tapered at distal half in *A. linzhi* sp. nov. (Fig. 4B); 3) the atrium is wider than long, and the median septum has a pair of laterally extended lamellar processes (Fig. 2D), vs atrium is longer than wide, and the median septum lacks similar processes in *A. linzhi* sp. nov. (Fig. 3D); 4) the accessory glands are located terminally on copulatory ducts (Fig. 2E), vs located medially in *A. linzhi* sp. nov. (Fig. 3E); and 5) the spermathecae are elongate-oval (Fig. 2E), vs almost spherical in *A. linzhi* sp. nov. (Fig. 3E). The male also somewhat resembles that of *A. tibet* Lin & Li, 2021 in having similar palp, especially the invert L-shaped conductor in retrolateral view, but it can be easily distinguished by the retrolateral tibial apophysis, which has a dorsal ramus about one-fifth the ventral ramus length and with a blunt end in retrolateral view (Fig. 2C), vs the dorsal ramus more than half the ventral ramus length and with a somewhat pointed tip in *A. tibet* (Lin et al. 2021: fig. 7C), and by the smooth conductor (Figs 2C, 4A), vs serrated on the inner margin in *A. tibet* (Lin et al. 2021: fig. 13B).

**Description. Male** (holotype; Figs 1A, B, 2A–C, 4A). Total length 6.72. Carapace 3.20 long, 2.78 wide. Abdomen 3.53 long, 2.35 wide. Clypeus 0.15 high. Eye sizes: AME 0.12, ALE 0.15, PME 0.17, PLE 0.18. Legs: I 9.84 (2.24, 0.79, 3.06, 2.49, 1.26), II 8.48 (2.39, 0.75, 2.66, 1.90, 0.78), III 5.99 (1.95, 0.65, 1.62, 1.26, 0.51), IV 8.67 (2.46, 0.64, 2.34, 2.41, 0.82). Carapace pale yellow to brown, with sub-oval thorax, slightly elevated cephalon, and big, irregular, brown markings; fovea longitudinal, dark red. Chelicerae red-brown, with four promarginal and seven retromarginal teeth. Endites yellow, longer than wide, bearing dense dark setae on inner portion of anterior margins. Labium darker than endites, bearing dark setae at distal margin. Sternum yellow to red-brown, covered with dense short setae, and with three pairs of anteromedian yellow spots laterally. Legs yellow to red-brown, with triangular ventral apophyses on base of coxae. Abdomen elongate-oval, dorsum red-brown to dark brown, spotted, with longitudinal, anterior pale band, irregular, median, dark patch, and two pairs of medium muscle depressions; venter pale to red-brown.

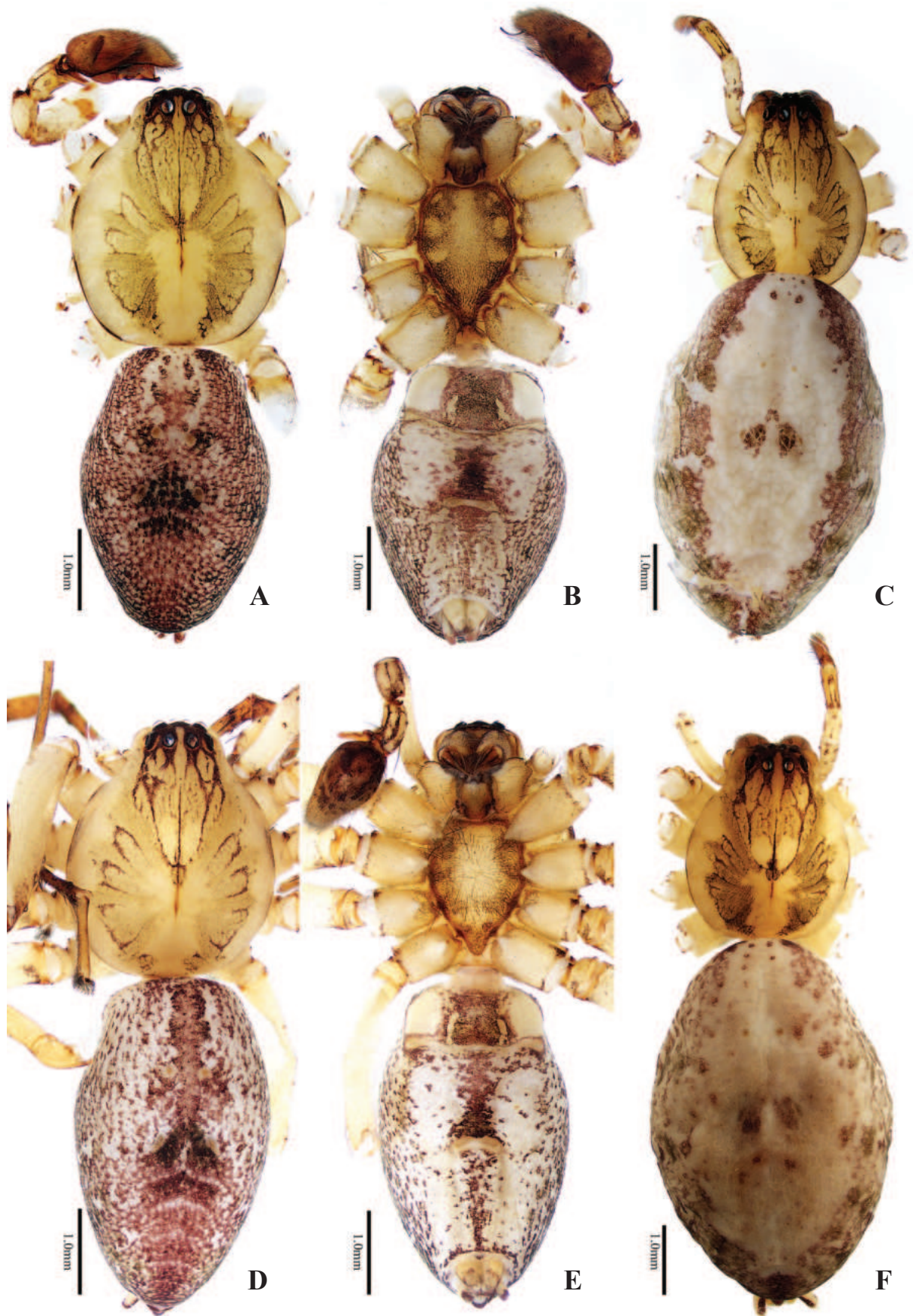


**Figure 1.** Habitus of *Anyphaena* spp. **A–C** *A. cibagou* Wang & Mi, sp. nov. **D–F** *A. linzhi* Wang & Mi, sp. nov. **A, B, D, E** male holotypes and **C, F** female paratypes **A, C, D, F** dorsal view **B, E** ventral view. Scale bars: 1.0 mm.

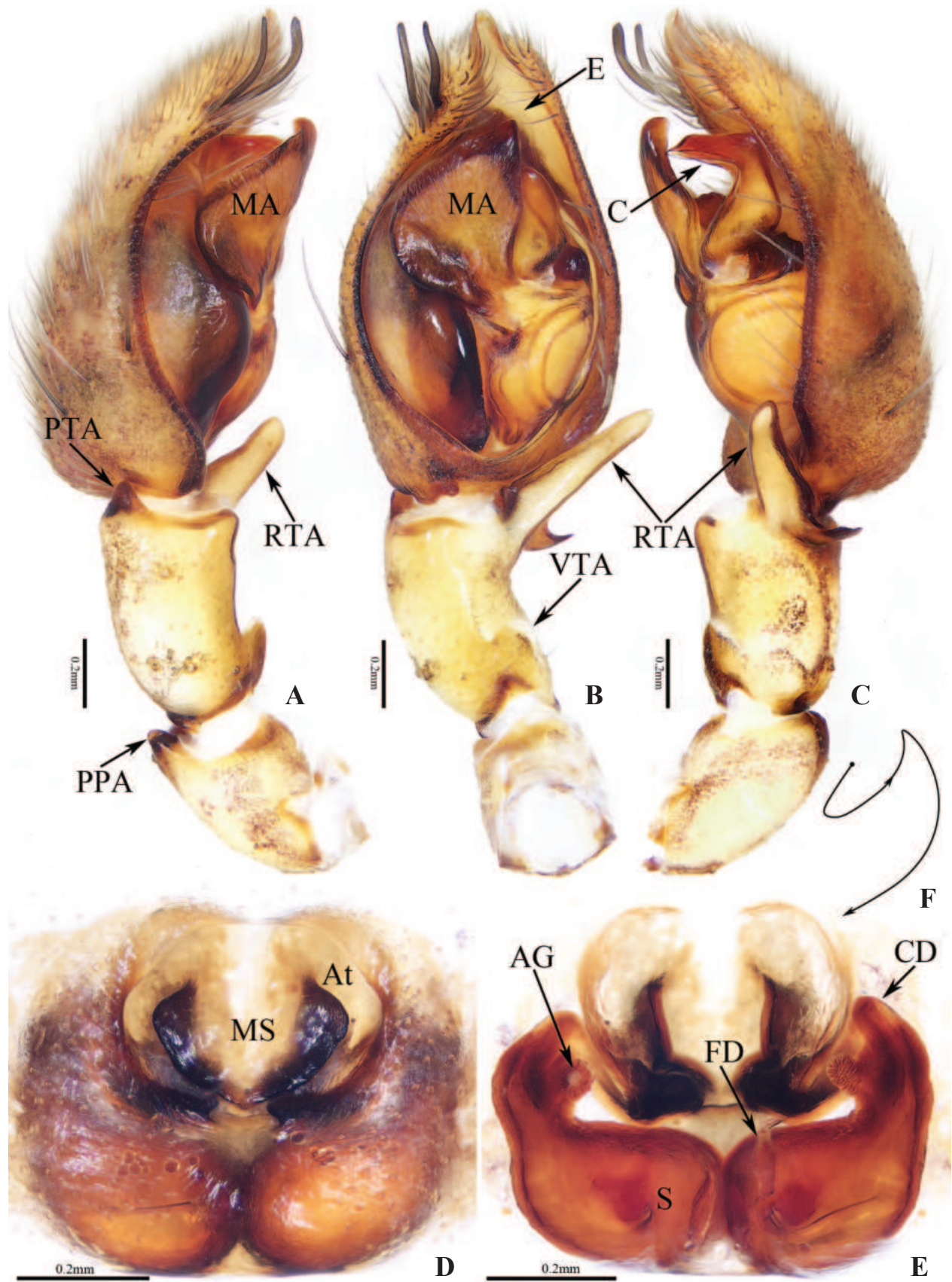


Figure 2. Copulatory organs of *Anyphaena cibagou* Wang & Mi, sp. nov., male holotype and female paratype A male palp, prolateral view B ditto, ventral view C ditto, retrolateral view D epigyne, ventral view E vulva, dorsal view F schematic course of copulatory duct, dorsal view. Scale bars: 0.2 mm.

Palp (Figs 2A–C, 4A): patella slightly longer than wide, with short, sclerotized distro-prolateral apophysis less than one-tenth its length; tibia about 1.5 times longer than wide, with half-round, base-ventral apophysis and bifurcated retro-lateral apophysis, which has long, bar-shaped ventral ramus directed towards ca 11:30 o'clock position apically in retrolateral view, and short, lamellar dorsal ramus; cymbium setose, bearing two distro-prolateral macro-setose; bulb almost oval; tegulum swollen; subtegulum elongated, prolaterally located; median apophysis originates from the medium of retrolateral side of bulb, the main portion almost oval, and with rather pointed tip slightly curved dorsally; embolus thin, weakly sclerotized, partly hidden by conductor in ventral view; conductor anterior to the base of median apophysis, curved into invert L-shape in retrolateral view.

**Female** (TRU-XZ-ANY-0002; Figs 1C, 2D–F). Total length 8.32. Carapace 3.05 long, 2.36 wide. Abdomen 5.59 long, 3.54 wide. Clypeus 0.17 high. Eye sizes: AME 0.11, ALE 0.15, PME 0.16, PLE 0.17. Measurements of legs: I 11.15 (3.03, 1.09, 3.20, 2.48, 1.35), II 9.78 (2.75, 0.93, 2.76, 2.17, 1.17), III 7.56 (2.28, 0.88, 1.74, 1.79, 0.87), IV 10.49 (3.04, 0.92, 2.51, 2.92, 1.10). Habitus (Fig. 1C) similar to that of male except having broad, longitudinal, pale band extending across the whole surface, only with sex retromarginal cheliceral teeth and lacking ventral apophysis on the base of coxae.

Epigyne-vulva (Fig. 2D–F): wider than long, with anteriorly located, oval atrium more than half the epigynal width; median septum medially located on atrium, with strongly sclerotized, laterally extended lamellar processes; copulatory openings invisible; copulatory ducts strongly curved at base and then gradually thickened to connected to the anterolateral portions of elongate-oval, touched spermathecae, with short, terminal accessory glands; fertilization ducts lamellar, originate from the inner-base of spermathecae.

**Distribution.** Known only from the type locality in Xizang, China (Fig. 6A).

***Anyphaena linzhi* Wang & Mi, sp. nov.**

<https://zoobank.org/2D1BE0AA-F5DF-48BB-8B5F-79042CA311BC>

Figs 1D–F, 3, 4B, 6A

**Type material.** **Holotype** ♂ (TRU-XZ-ANY-0004), CHINA: Xizang Autonomous Region, Linzhi City, Bomi County, Gangyunshanlin Scenic Area (29°52.99'N, 95°33.59'E, ca 2680 m), 29 Jun. 2023, C. Wang leg. **Paratypes** 1♂7♀ (TRU-XZ-ANY-0005–0012), same data as for holotype.

**Etymology.** The species name is a noun in apposition and comes from the type locality, Linzhi City.

**Diagnosis.** *Anyphaena linzhi* sp. nov. closely resembles that of *A. cibagou* sp. nov., but it can be distinguished by the following: 1) the main portion of median apophysis is elongate-oval, more than two times longer than wide in ventral view (Fig. 3B), vs almost oval, and slightly longer than wide in *A. cibagou* sp. nov. (Fig. 2B); 2) the conductor is tapered at distal half in retrolateral view (Fig. 4B), vs acutely narrowed distally in *A. cibagou* sp. nov. (Fig. 4A); 3) the atrium is longer than wide, and the median septum lacks process (Fig. 3D), vs atrium is wider than long, and the median septum has laterally extended lamellar processes in *A. cibagou* sp. nov. (Fig. 2D); 4) the accessory glands are located medially on copulatory ducts (Fig. 3E), vs located terminally in *A. cibagou* sp. nov. (Fig. 2E);

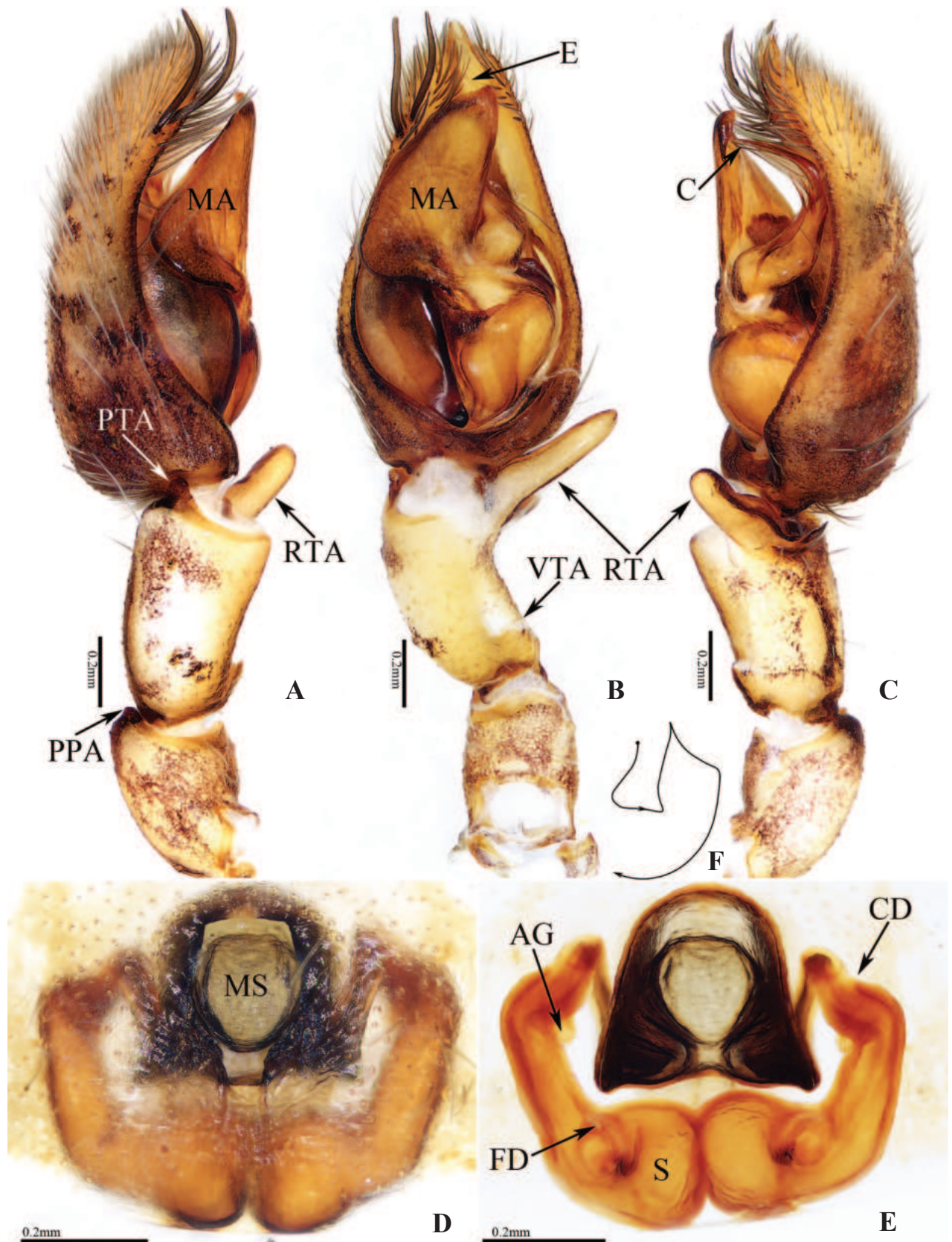


**Figure 3.** Copulatory organs of *Anyphaena linzhi* Wang & Mi, sp. nov., male holotype and female paratype **A** male palp, prolateral view **B** ditto, ventral view **C** ditto, retrolateral view **D** epigyne, ventral view **E** vulva, dorsal view **F** schematic course of copulatory duct, dorsal view. Scale bars: 0.2 mm.

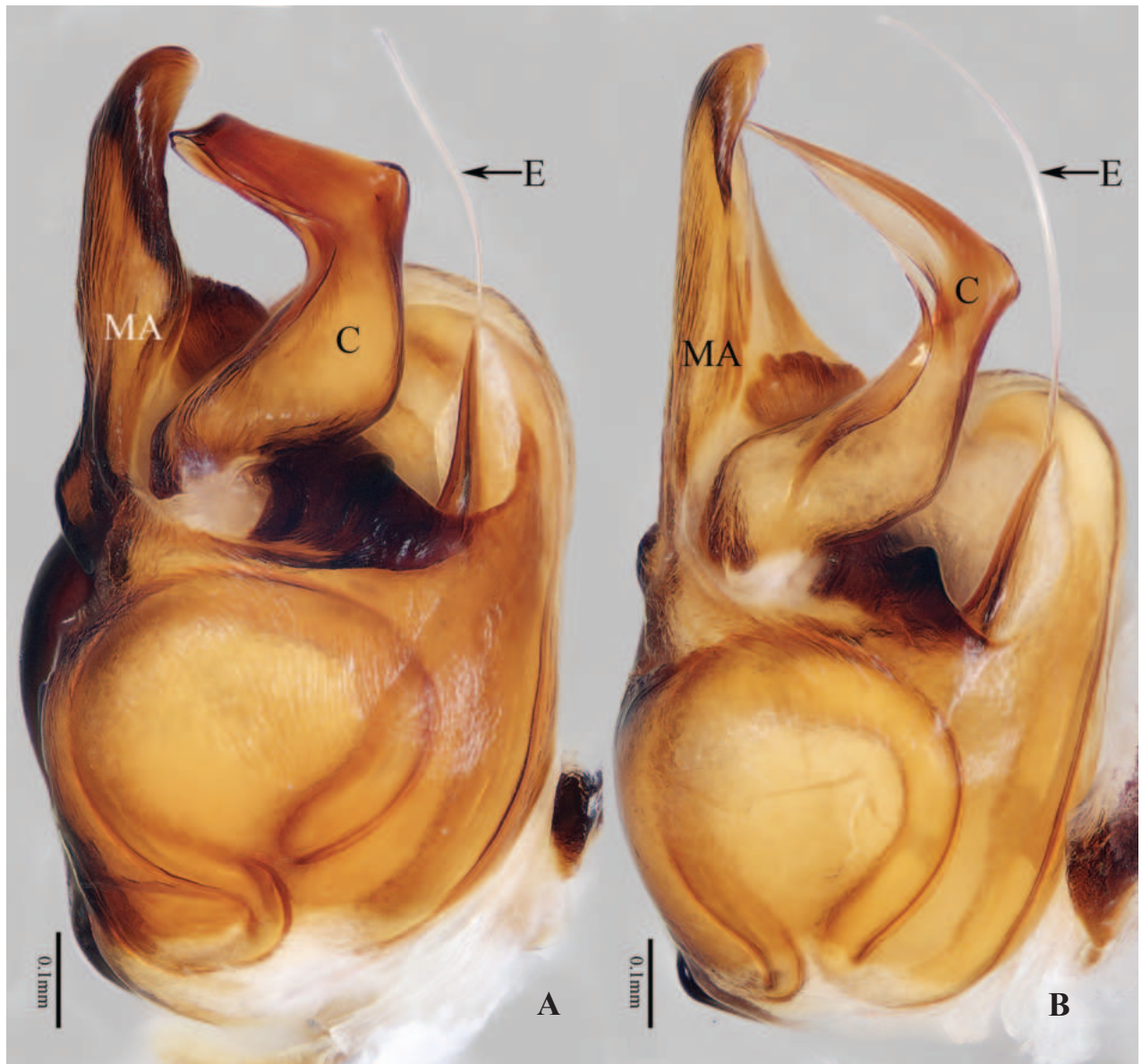


**Figure 4.** Bulb of *Anyphaena* spp., retrolateral view **A** *A. cibagou* Wang & Mi, sp. nov., holotype **B** *A. linzhi* Wang & Mi, sp. nov., paratype. Scale bars: 0.1 mm.

and 5) the spermathecae are about spherical (Fig. 3E), vs elongate-oval in *A. cibagou* sp. nov. (Fig. 2E). The male also somewhat resembles that of *A. tibet* Lin & Li, 2021 in having very similar palpal structure, but it differs in: 1) the ventral ramus of retrolateral tibial apophysis is anteroventrally extending, and about three times longer than the dorsal ramus in retrolateral view (Fig. 3C), vs upward extending, and less than two times longer than the dorsal ramus in *A. tibet* (Lin et al. 2021: fig. 7C); 2) the conductor is smooth (Figs 3C, 4B), vs serrated on the inner margin in *A. tibet* (Lin et al. 2021: fig. 13B).

**Description. Male** (holotype; Figs 1D, E, 3A–C, 4B). Total length 6.52. Carapace 2.82 long, 2.36 wide. Abdomen 3.76 long, 2.25 wide. Clypeus 0.11 high. Eye sizes: AME 0.12, ALE 0.16, PME 0.15, PLE 0.16. Measurements of legs: I 13.27 (3.42, 1.10, 4.12, 3.09, 1.54), II 11.87 (3.14, 1.06, 3.68, 2.69, 1.30), III 8.54 (2.66, 0.79, 2.24, 2.06, 0.79), IV 12.02 (3.31, 0.94, 3.17, 3.46, 1.14). Carapace almost oval, with elevated cephalon, and big, irregular, brown markings; fovea longitudinal,

red-brown. Chelicerae yellow to gray-brown, with four promarginal and eight retromarginal teeth. Endites longer than wide, bearing clusters of dark-brown setae on inner portion of anterior margins. Labium darker than endites. Sternum almost heart-shaped, setose. Legs yellow-brown, with sub-triangular apophyses on the base of coxae. Abdomen elongated, dorsum pale to red-brown, with longitudinal, anteromedian pale band followed by two pairs of muscle depressions and two irregular dark patches medially; venter paler to dark brown.

Palp (Figs 3A–C, 4B): patella slightly longer than wide, with sclerotized, disto-prolateral apophysis; tibia slightly curved medially, with almost half-round ventro-retrolateral apophysis at base and bifurcated disto-retrolateral apophysis, which has straight, bar-shaped ventral ramus directed towards ca 10 o'clock position apically in retrolateral view, and strongly sclerotized, lamellar dorsal ramus; cymbium longer than wide, with two slender, medially curved macrosetae on the distal portion of prolateral margin; bulb almost oval; tegulum swollen; subtegulum elongated, prolaterally located; median apophysis originates from the middle of retrolateral side of bulb, main portion elongated, with somewhat pointed tip; embolus thin, partly visible; conductor retrolateral to the main portion of median apophysis, strongly curved medially, and with tapered distal half extending anteroventrally.

**Female** (TRU-XZ-ANY-0006; Figs 1F, 3D–F). Total length 8.41. Carapace 3.05 long, 2.50 wide. Abdomen 5.50 long, 3.64 wide. Clypeus 0.12 high. Eye sizes AME 0.10, ALE 0.15, PME 0.14, PLE 0.15. Measurements of legs: I 12.89 (3.26, 1.39, 3.60, 3.06, 1.58), II 11.40 (3.00, 1.22, 3.18, 2.74, 1.26), III 8.85 (2.52, 1.16, 2.05, 2.18, 0.94), IV 11.73 (3.12, 1.20, 2.87, 3.38, 1.16). Habitus (Fig. 1F) similar to that of male except having the dorsal abdominal pale band extending the whole surface, seven retromarginal cheliceral teeth, and lacking ventral apophysis on the base of coxae.

Epigyne and vulva (Fig. 3D–F): wider than long; atrium almost hexagonal, anteriorly located; median septum almost linguiform; copulatory ducts curved, gradually thicken, with short, medially located accessory glands less than one-third the largest diameter of copulatory ducts in length; spermathecae sub-spherical, touched; fertilization ducts lamellar.

**Distribution.** Known only from the type locality in Xizang, China (Fig. 6A).

### ***Anyphaena shufui* Wang & Mi, sp. nov.**

<https://zoobank.org/F0B57275-CDBF-4315-A047-4AFB9D08EDF1>

Figs 5A, B, E, F, I, 6B

**Type material.** **Holotype** ♀ (TRU-XZ-ANY-00013), CHINA: Xizang Autonomous Region, Linzhi City, Chayu County, Cibagou National Nature Reserve (28°36.03'N, 97°4.01'E, ca 2200 m), 14 Aug. 2023, C. Wang et al. leg. **Paratypes** 1♀ (TRU-XZ-ANY-00014), same data as for holotype; 1♀ (TRU-XZ-ANY-00015), Cibagou National Nature Reserve (28°41.43'N, 97°2.86'E, ca 2570 m), 25 Jun. 2023, C. Wang leg.

**Etymology.** The species is named after Mr Fu Shu, who helped us with specimens collecting in Linzhi, Xizang; noun (name) in genitive case.

**Diagnosis.** *Anyphaena shufui* sp. nov. closely resembles that of *A. rhyndophysa* Feng, Ma & Yang, 2012 in epigyne-vulva structure, but it can be easily distinguished by the atrium, which is slit-shaped (Fig. 5E), vs oval in *A. rhyndophysa* (Feng et al. 2012: fig. 8).

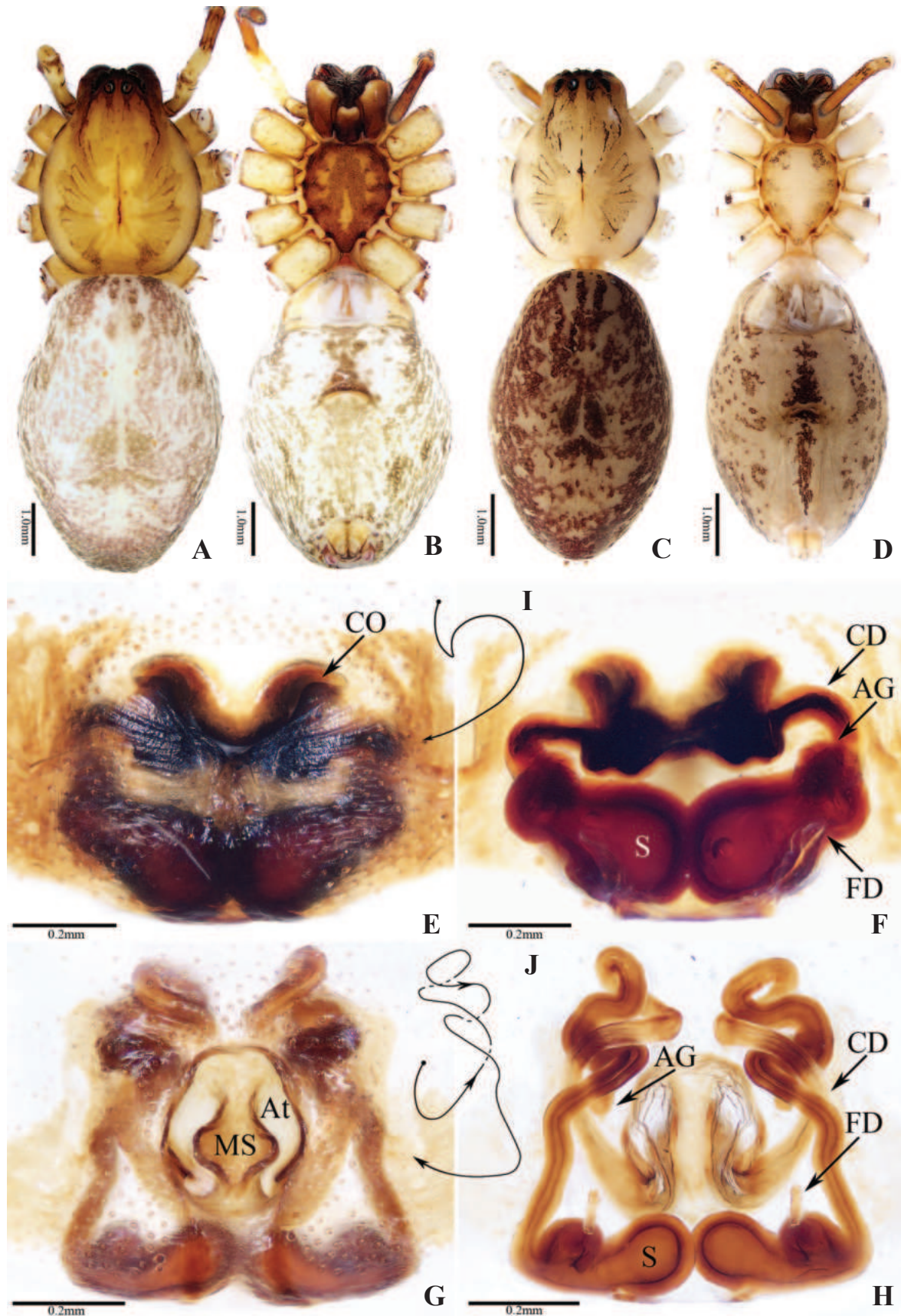


Figure 5. Female holotypes of *Anyphaena* spp. **A, B, E, F, I** *A. shufui* Wang & Mi, sp. nov. **C, D, G, H, J** *A. yejie* Wang & Mi, sp. nov. **A, C** habitus, dorsal view **B, D** ditto, ventral view **E, G** epigyne, ventral view **F, H** vulva, dorsal view **I, J** schematic course of copulatory duct, dorsal view. Scale bars: 1.0 mm (**A–D**); 0.2 mm (**E–H**).

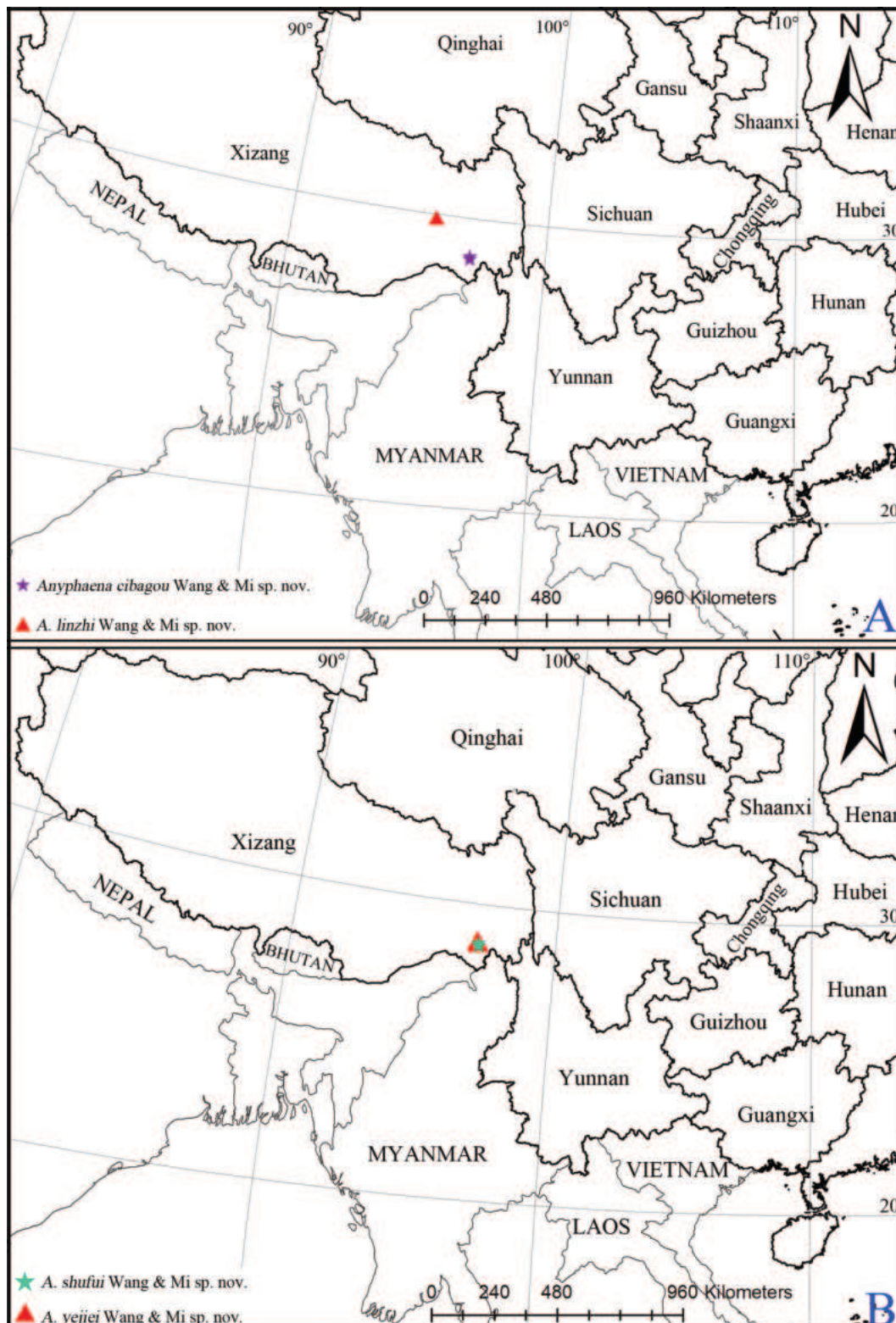


Figure 6. Distributional records of the *Anyphaena* spp. A *A. cibagou* Wang & Mi, sp. nov. and *A. linzhi* Wang & Mi, sp. nov. B *A. shufui* Wang & Mi, sp. nov. and *A. yejie* Wang & Mi, sp. nov.

**Description. Female** (holotype; Fig. 5 A, B, E, F, I). Total length 8.95. Carapace 3.95 long, 3.19 wide. Abdomen 5.76 long, 3.90 wide. Clypeus 0.30 high. Eye sizes: AME 0.11, ALE 0.20, PME 0.19, PLE 0.20. Legs: I 14.99 (4.14, 1.22, 4.45, 3.40, 1.78); II 13.69 (3.91, 1.21, 3.83, 3.25, 1.49); III 10.61 (3.23, 1.08, 2.65, 2.53,

1.12); IV 14.71 (4.40, 1.24, 3.64, 4.12, 1.31). Carapace yellow to brown, with oval thorax and elevated cephalon, bearing big, irregular brown markings; fovea longitudinal, dark red. Chelicerae red-brown, with three promarginal and eight retromarginal teeth. Endites red-brown, ca two times longer than wide. Labium colored as endites. Sternum red-brown, setose, with irregular dark yellow stripes. Legs yellow to brown. Abdomen elongated, dorsum pale to brown, with anterior, longitudinal irregular pale band followed by brown markings, and two pairs of muscle depressions; venter paler than dorsum.

Epigyne-vulva (Fig. 5E, F, I): wider than long; atrium anteriorly located, slit-shaped; copulatory openings located on the lateral sides of atrium; copulatory ducts widened at base, and then folded and acutely narrowed to tube-shaped portions, which curved medially and with oval, terminal accessory glands; spermathecae elongate-oval, touched; fertilization ducts lamellar.

**Male.** Unknown.

**Distribution.** Known only from the type locality in Xizang, China (Fig. 6B).

***Anyphaena yejie* Wang & Mi, sp. nov.**

<https://zoobank.org/71FE6C75-DCE8-4CDB-A4C6-8136566069C7>

Figs 5C, D, G, H, J, 6B

**Type material.** **Holotype** ♀ (TRU-XZ-ANY-00016), CHINA: Xizang Autonomous Region, Linzhi City, Chayu County, Cibagou National Nature Reserve (28°46.62'N, 97°0.86'E, ca 2880 m), 24 Jun. 2023, C. Wang et al. leg. **Paratypes** 4♀ (TRU-XZ-ANY-0017–0020), same data as for holotype; 2♀ (TRU-XZ-ANY-0021–0022), Cibagou National Nature Reserve (28°41.43'N, 97°2.86'E, ca 2570 m), 25 Jun. 2023, C. Wang leg.

**Etymology.** The species is named after Mr Yejie Lin, who contributed to the taxonomic study of Chinese *Anyphaena* species and helped with species identification; noun (name) in genitive case.

**Diagnosis.** *Anyphaena yejie* sp. nov. is similar to that of *A. shenzhen* Lin & Li, 2021 in having a very long, distorted copulatory duct, but it can be easily distinguished by the medially located atrium and medially originated copulatory duct (Fig. 5G, H), vs anteriorly located atrium and anteriorly originated copulatory duct in *A. shenzhen* (Lin et al. 2021: fig. 6A, B). It also resembles that of *A. cibagou* sp. nov. in having a similar median septum, but it can be easily distinguished by the medially located atrium and much thinner and coiled copulatory ducts (Fig. 5G, H), vs anteriorly located atrium and much thicken, and not coiled copulatory ducts in *A. cibagou* sp. nov. (Fig. 2D, E).

**Description. Female** (Fig. 5C, D, G, H, J). Total length 7.84. Carapace 3.00 long, 2.44 wide. Abdomen 4.72 long, 3.00 wide. Clypeus height 0.17. Eye sizes: AME 0.11, ALE 0.16, PME 0.15, PLE 0.17. Measurements of legs: I 7.92 (2.12, 0.75, 2.10, 1.94, 1.01); II 7.18 (1.95, 0.78, 1.77, 1.72, 0.96); III 5.15 (1.36, 0.60, 1.14, 1.46, 0.59); IV 7.39 (2.05, 0.70, 1.77, 2.23, 0.64). Carapace pale yellow to brown, with sub-oval thorax and elevated cephalon bearing big, brown markings; fovea longitudinal, dark red. Chelicerae red-brown, with four promarginal and seven retromarginal teeth. Endites dark yellow, almost paralleled. Labium dark brown, with pale distal portion bearing dense dark setae. Sternum yellow, almost heart-shaped, with small dark-brown spots. Legs pale to brown.

Abdomen elongated, dorsum fuchsia, with irregular yellow and fuchsia markings; venter pale, covered with brown spots laterally.

Epigyne-vulva (Fig. 5G, H, J): longer than wide, with oval, medially located atrium separated by the sub-oval septum; copulatory openings beneath the lateral margin of atrium; copulatory ducts long, forming complicated coils and with medially located, bar-shaped accessory glands extending downward; spermathecae elongated, touched, with two sub-spherical portions; fertilization ducts lamellar, originate at the anterior portions of the outside spherical portions of spermathecae.

**Male.** Unknown.

**Distribution.** Known only from the type locality in Xizang, China (Fig. 6B).

## Acknowledgements

The manuscript benefited greatly from comments by Alireza Zamani (Finland, Turku) and Yejie Lin (Beijing, China). We are grateful to Hong Yao, Nonghao Yao for helping with the fieldwork and Lin Zheng, Shasha Luo for assisting with the molecular work.

## Additional information

### Conflict of interest

The authors have declared that no competing interests exist.

### Ethical statement

No ethical statement was reported.

### Funding

This research was supported by the Scientific Monitoring of Cibagou National Nature Reserve Project, the Scientific Monitoring of Yarlung Zangbo Grand Canyon National Nature Reserve Project, the National Natural Science Foundation of China (NSFC-32200369), the Science and Technology Project Foundation of Guizhou Province ([2020]1Z014), the Key Laboratory Project of Guizhou Province ([2020]2003), the Training Project of High-level Innovative Talents of Guizhou Province (2024-(2022)-050), and the Doctoral Research Foundation of Tongren University (trxyDH2102).

### Author contributions

CW and XM performed morphological species identification. SL, CW, and SW finished the species photos and descriptions. CW, XM, and SL drafted and revised the manuscript. All authors read and approved the final version of the manuscript.

### Author ORCIDs

Shikai Li  <https://orcid.org/0009-0002-3947-2550>

Shilin Wang  <https://orcid.org/0009-0003-0759-5350>

Xiaoqi Mi  <https://orcid.org/0000-0003-1744-3855>

Cheng Wang  <https://orcid.org/0000-0003-1831-0579>

### Data availability

All of the data that support the findings of this study are available in the main text.

## References

- Durán-Barrón CG, Pérez TM, Brescovit AD (2016) Two new synanthropic species of *Anyphaena* Sundevall (Araneae: Anyphaenidae) associated to houses in Mexico City. *Zootaxa* 4103(2): 189–194. <https://doi.org/10.11646/zootaxa.4103.2.11>
- Feng P, Ma YY, Yang ZZ (2012) A new species of genus *Anyphaena* from China (Araneae: Anyphaenidae). *Acta Arachnologica Sinica* 21(2): 72–75.
- Folmer O, Black M, Hoeh W, Lutz R, Vrijenhoek R (1994) DNA primers for amplification of mitochondrial cytochrome c oxidase subunit I from diverse metazoan invertebrates. *Molecular Marine Biology and Biotechnology* 3(5): 294–299.
- Li ZY, Zhang F (2023) Five new species of the long-legged sac spider genus *Cheiracanthium* C.L. Koch, 1839 (Araneae: Cheiracanthiidae) from China. *European Journal of Taxonomy* 900: 81–105. <https://doi.org/10.5852/ejt.2023.900.2303>
- Lin YJ, Marusik YM, Gao CX, Xu H, Zhang XQ, Wang ZY, Zhu WH, Li SQ (2021) Twenty-three new spider species (Arachnida: Araneae) from Asia. *Zoological Systematics* 46(2): 91–152. <https://doi.org/10.11865/zs.2021201>
- Rivera-Quiroz FA, Álvarez-Padilla F (2023) Integration or minimalism: twenty-one new species of ghost spiders (Anyphaenidae: Anyphaena) from Mexico. *European Journal of Taxonomy* 865: 1–94. <https://doi.org/10.5852/ejt.2023.865.2097>
- World Spider Catalog (2024) World Spider Catalog. Version 24.5. Natural History Museum Bern. <https://doi.org/10.24436/2> [Accessed on: 20 January 2024]

# The arboreal snail genus *Amphidromus* Albers, 1850 (Eupulmonata, Camaenidae) of Southeast Asia:

## 1. Molecular systematics of some Vietnamese species and related species from Cambodia, Indonesia, and Laos

Parin Jirapatrasilp<sup>1,2</sup>, Chih-Wei Huang<sup>3</sup>, Chirasak Sutcharit<sup>1</sup>, Chi-Tse Lee<sup>4</sup>

1 Animal Systematics Research Unit, Department of Biology, Faculty of Science, Chulalongkorn University, Bangkok, Thailand

2 Leibniz Institute for the Analysis of Biodiversity Change, Martin-Luther-King-Platz 3, Hamburg, Germany

3 School of Life Science, National Taiwan Normal University, Taipei, Taiwan

4 Department of Life Sciences, National Chung Hsing University, Taichung, Taiwan

Corresponding authors: Chirasak Sutcharit ([jirasak4@yahoo.com](mailto:jirasak4@yahoo.com), [chirasak.s@chula.ac.th](mailto:chirasak.s@chula.ac.th)); Chi-Tse Lee ([leechtse@yahoo.com.tw](mailto:leechtse@yahoo.com.tw))



Academic editor: Thierry Backeljau

Received: 4 September 2023

Accepted: 6 February 2024

Published: 22 March 2024

ZooBank: <https://zoobank.org/7954DFBF-803A-48F5-B791-42DD09FE5D01>

**Citation:** Jirapatrasilp P, Huang C-W, Sutcharit C, Lee C-T (2024) The arboreal snail genus *Amphidromus* Albers, 1850 (Eupulmonata, Camaenidae) of Southeast Asia: 1. Molecular systematics of some Vietnamese species and related species from Cambodia, Indonesia, and Laos. ZooKeys 1196: 15–78. <https://doi.org/10.3897/zookeys.1196.112146>

**Copyright:** © Parin Jirapatrasilp et al. This is an open access article distributed under terms of the Creative Commons Attribution License ([Attribution 4.0 International – CC BY 4.0](https://creativecommons.org/licenses/by/4.0/)).

### Abstract

This paper reassesses the taxonomy and systematics of 11 arboreal snail species in the genus *Amphidromus* from Vietnam, Cambodia, Indonesia and Laos (*A. bozhii* Wang, 2019, *A. buelowi* Fruhstorfer, 1905, *A. costifer* Smith, 1893, *A. haematostoma* Möllendorff, 1898, *A. ingens* Möllendorff, 1900, *A. madelineae* Thach, 2020, *A. metabletus* Möllendorff, 1900, *A. pankowskianus* Thach, 2020, *A. placostylus* Möllendorff, 1900, *A. roseolabiatus* Fulton, 1896, and *A. thachi* Huber, 2015). The taxonomic validity of each species is supported by a phylogenetic analysis of mitochondrial COI and 16S rRNA gene fragments from 17 ingroup taxa. *Amphidromus buelowi* was found to comprise two populations from two distant localities, one from Mount Singgalang, West Sumatra, Indonesia and the other from southern Vietnam. The samples from southern Vietnam were previously described as *A. asper* Haas, 1934 and *A. franzhuberi* Thach, 2016, but they are now treated as junior synonyms of *A. buelowi* in this study. In addition, two species from Vietnam are described as new to science, viz. *A. asperoides* Jirapatrasilp & Lee, **sp. nov.** and *A. ingensoides* Jirapatrasilp & Lee, **sp. nov.**, each of which is conchologically comparable to *A. buelowi* and *A. ingens*, respectively.

**Key words:** Biodiversity, Helicoidei, shell polymorphism, Stylommatophora, taxonomy

## Table of contents

Introduction .....	16
Materials and methods.....	17
Specimen preparation and preliminary species identification .....	17
Molecular phylogenetic analyses .....	17
Species validation.....	19
Abbreviations .....	19
Institutional abbreviations.....	19
Results .....	23
Systematics .....	24
Family Camaenidae Pilsbry, 1895.....	24
Genus <i>Amphidromus</i> Albers, 1850.....	24
<i>Amphidromus ingens</i> Möllendorff, 1900 .....	24
<i>Amphidromus asperoides</i> Jirapatrasilp & Lee, sp. nov. ....	28
<i>Amphidromus bozhii</i> Wang, 2019.....	31
<i>Amphidromus placostylus</i> Möllendorff, 1900.....	36
<i>Amphidromus ingensoides</i> Jirapatrasilp & Lee, sp. nov. ....	40
<i>Amphidromus buelowi</i> Fruhstorfer, 1905.....	43
<i>Amphidromus thachi</i> Huber, 2015.....	47
<i>Amphidromus metabletus</i> Möllendorff, 1900.....	51
<i>Amphidromus haematostoma</i> Möllendorff, 1898 .....	56
<i>Amphidromus madelineae</i> Thach, 2020.....	59
<i>Amphidromus costifer</i> Smith, 1893.....	62
<i>Amphidromus roseolabiatatus</i> Fulton, 1896 .....	66
<i>Amphidromus pankowskianus</i> Thach, 2020.....	69
Discussion .....	70
Acknowledgements .....	72
References.....	73

## Introduction

Since the comprehensive synoptic catalogue of the Southeast Asian arboreal snail genus *Amphidromus* Albers, 1850 by Laidlaw and Solem (1961), most papers on this genus involve the descriptions of new species. As a result, more than 150 species were newly introduced (MolluscaBase 2023). Some studies also revisited the taxonomic status of some species (e.g., Sutcharit et al. 2021; Verbinnen and Segers 2021), while others revised the taxonomy of *Amphidromus* in particular regions (Solem 1965; Sutcharit and Panha 2006; Inkhavilay et al. 2017; Poppe 2020), whereas still fewer papers focussed on molecular phylogenetic relationships (Sutcharit et al. 2007; Lee et al. 2022).

This paper is the first of a series that aims to revise the taxonomy and systematics of *Amphidromus* species from Southeast Asia, following the taxonomic reassessment of *A. cruentatus* (Morelet, 1875) in Lee et al. (2022). We revise some Vietnamese species and related species from Cambodia, Indonesia, and Laos that are phylogenetically related or that are conchologically similar to *A. cruentatus*. These include 11 nominal species: *A. bozhii* Wang, 2019, *A. buelowi* Fruhstorfer, 1905, *A. costifer* Smith, 1893, *A. haematostoma* Möllendorff,

1898, *A. ingens* Möllendorff, 1900, *A. madelineae* Thach, 2020, *A. metabletus* Möllendorff, 1900, *A. pankowskianus* Thach, 2020, *A. placostylus* Möllendorff, 1900, *A. roseolabiatus* Fulton, 1896, and *A. thachi* Huber, 2015. However, the original descriptions and subsequent treatments to delimit these species were primarily based on shell characteristics, which are extremely variable in the genus *Amphidromus* (Haniel 1921; Lee et al. 2022). Therefore, other lines of evidence, especially DNA sequence data, are crucial to define species boundaries more accurately and reassess the taxonomic status of *Amphidromus* species.

Against this background, new specimens of these 11 nominal species were collected in order to study their shell and anatomical characters, compare them with the available type material of species known from the study area, and to infer their phylogenetic relationships using DNA sequence data.

## Materials and methods

### Specimen preparation and preliminary species identification

Empty shells and living specimens were collected from several localities in Cambodia, Indonesia, Laos, and Vietnam (Fig. 1, Table 1). A total of 278 specimens was collected, and all specimens are deposited in the National Museum of Natural Science of Taiwan, Taichung, unless otherwise stated. Live specimens were photographed and fixed in 70% (v/v) ethanol for anatomical examination and 95% (v/v) for DNA analysis. The genitalia of 3–5 specimens per species were examined under a stereomicroscope, and one or two genitalia from each species were selected for photography. The radula of one specimen per species was examined with a scanning electron microscope (SEM; JEOL, JSM-5410 LV). At each collecting site, the specimens were collected within an area of approximately 100 m<sup>2</sup>. Shell measurements are based on adult specimens only.

Preliminary morphospecies identifications were based on (1) the shell characters used in the original descriptions and other relevant literature, such as Zilch (1953), Sutcharit et al. (2015), and Thach (2016, 2017, 2018, 2020a, 2021), (2) the accordance between the collecting localities and the type locality, and (3) comparisons with type specimens and/or reference collections from several natural history museums. The type localities are mentioned in the wording and language of the original descriptions. If possible, the current names and/or regional names of the type localities are provided in square brackets.

### Molecular phylogenetic analyses

The acquisition of new DNA data of both mitochondrial COI and 16S rRNA, and molecular phylogenetic analyses including the calculation of intra- and interspecific *p*-distances and constructions of phylogenetic trees and haplotype networks, follow Jirapatrasilp et al. (2022) and Lee et al. (2022). New sequences were obtained from a total of 127 specimens from 14 *Amphidromus* species. In addition, sequences of *A. perversus* (Linnaeus, 1758) (type species of *Amphidromus*), *A. contrarius* (Müller, 1774) (type species of the subgenus *Syndromus*), and *A. cruentatus* retrieved from GenBank (Köhler and Criscione 2015; Jirapatrasilp et al. 2022; Lee et al. 2022) were included, resulting in a total

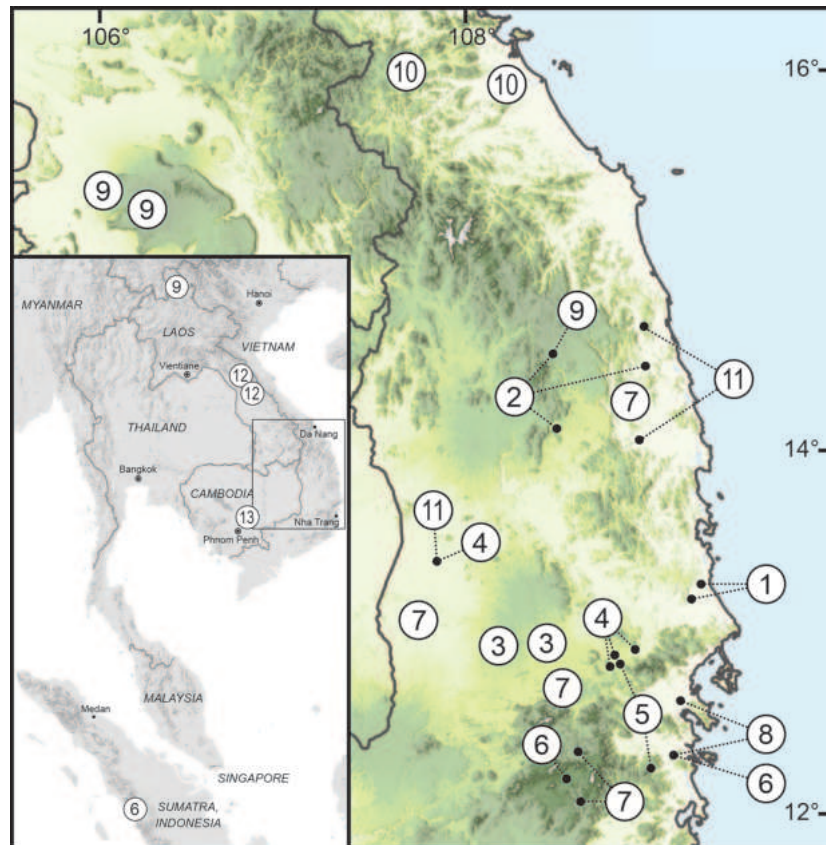


**Figure 1.** Distribution map of *Amphidromus* samples recognised in this study. 1. *Amphidromus bozhii*; 2. *Amphidromus placostylus*; 3. *Amphidromus asperoides* sp. nov.; 4. *Amphidromus ingens*; 5. *Amphidromus ingensoides* sp. nov.; 6. *Amphidromus buelowi*; 7. *Amphidromus thachi*; 8. *Amphidromus metabletus*; 9. *Amphidromus haematostoma*; 10. *Amphidromus madelineae*; 11. *Amphidromus costifer*; 12. *Amphidromus pankowskianus*; 13. *Amphidromus roseolabiatu*s. Species numbers correspond to those in Fig. 2 and Tables 1, 2. The map was produced using QGIS (3.16.0) with SRTM Downloader plugin (<https://github.com/hdus/SRTM-Downloader>), retrieving SRTM data from NASA Earth Data server (<https://urs.earthdata.nasa.gov/>).

of 17 *Amphidromus* species in the dataset. Sequences of *Camaena cicatricosa* (Müller, 1774) and *C. poyuensis* Zhou, Wang & Ding, 2016 from GenBank (Ding et al. 2016) were used as outgroup (Table 1).

The sequence alignments of each gene fragment were performed separately using MAFFT (v. 7, see <https://mafft.cbrc.jp/alignment/server/index.html>), with default options (Kato et al. 2017). The concatenated dataset was prepared in Kakusan4 (v. 4.0.2016.11.04, see <https://www.fifthdimension.jp/products/kakusan/>; Tanabe 2011) with the best-fitting model adjustment for Bayesian inference (BI) analyses. The BI analysis was performed with the best-fitting models of each gene fragment and each codon position of COI (generalised time reversible (GTR) + gamma (G) for the third codon position of COI and Hasegawa–Kishino–Yano (HKY) + G for 16S rRNA and the remaining codon positions of COI) using MrBayes on XSEDE (v.3.2.6, see <http://nbisweden.github.io/MrBayes/>; Ronquist et al. 2012) in the CIPRES Science Gateway (see <https://www.phylo.org/>; Miller et al. 2010). Two independent analyses were run simultaneously and consisted of four chains of five million generations, sampling every 500 generations and discarding the first 50% of samples as burn-in.

In addition, a maximum likelihood (ML) tree was constructed using the IQ-TREE webserver (see <http://iqtree.cibiv.univie.ac.at>), with integrated ModelFinder function (Nguyen et al. 2015; Trifinopoulos et al. 2016; Kalyaanamoorthy et al. 2017). Branch support was estimated using 1000 ultra-fast bootstrap replicates (Hoang et al. 2018), the Shimodaira and Hasegawa-approximate likelihood-ratio (SH-aLRT) test and the approximate Bayes (aBayes) test (Anisimova et al. 2011). A clade was considered to be well supported if the ultra-fast bootstrap support (BS) values were  $\geq 95\%$ , aBayes support values  $\geq 0.95$ , SH-aLRT support values  $\geq 80\%$  and Bayesian posterior probability values (PP) were  $\geq 0.95$  (San Mauro and Agorreta 2010; Anisimova et al. 2011; Hoang et al. 2018).

Uncorrected pairwise genetic distances ( $p$ -distances) among different *Amphidromus* species were calculated in MEGA (v. 7.0, see <https://www.megasoftware.net/>) using pairwise deletion (Kumar et al. 2016). Haplotype networks were constructed using the minimum spanning network method (Bandelt et al. 1999) as implemented in the program PopART (v. 1.7.2, see <http://popart.otago.ac.nz/index.shtml>; Leigh and Bryant 2015).

### Species validation

Preliminary morphospecies identifications were validated by the reciprocal monophyly of each morphospecies in the phylogeny constructed from the concatenated COI + 16S dataset. We adopted the interspecific COI genetic distance of 4%, which has been associated with the optimum intra/inter-specific threshold value for stylommatophoran land snails (Davison et al. 2009), as the threshold to validate the reciprocal monophyly of the preliminary morphospecies.

### Abbreviations

The abbreviations **D** (dextral) and **S** (sinistral) are used in conjunction with numbers of specimens in the material examined sections of each species. Abbreviations for the genital organs in the figure captions follow those defined by Solem (1983) and Sutcharit and Panha (2006).

### Institutional abbreviations

<b>ANSP</b>	Academy of Natural Sciences of Philadelphia, Drexel University, Philadelphia
<b>CUMZ</b>	Chulalongkorn University Museum of Zoology, Bangkok
<b>MNHN</b>	Muséum national d'Histoire naturelle, Paris
<b>NHMUK</b>	when citing specimen lots deposited in the Natural History Museum, London
<b>NMNS</b>	National Museum of Natural Science of Taiwan, Taichung
<b>RBINS</b>	Royal Belgian Institute of Natural Sciences, Brussels
<b>RMNH</b>	Naturalis Biodiversity Center, Rijksmuseum van Natuurlijke Historie, Leiden
<b>SMF</b>	Senckenberg Forschungsinstitut und Naturmuseum, Frankfurt am Main

**Table 1.** List of specimens used in this study with species name, locality details, voucher and GenBank accession numbers. Species numbers correspond to those in Figs 1, 2, and Table 2.

Number	Species	Preliminary species identification in this study	Specimen codes	Voucher numbers	Locality	No. of specimen and chirality	Figure	GenBank accession numbers		References
								COI	16S rRNA	
1	<i>Amphidromus bozhii</i> Wang, 2019	<i>A. bozhii</i>	X10 to X19	NMNS-8764-004 to NMNS-8764-013	Phu Hoa District, Phu Yen Province, Vietnam	10D	8D-E	X10-X18: OR977987-OR977995	X10-X12: OR964283- OR964285 X15: OR964286	This study
			XJ1 to XJ8	NMNS-8764-014 to NMNS-8764-021	Tuy Hoa District, Phu Yen Province, Vietnam	8S	8F	XJ1-XJ8: OR977996-OR978003	-	
2	<i>Amphidromus placostylus</i> Mölldendorff, 1900	<i>A. placostylus</i>	VAM0 to VAM4	NMNS-8764-213 to NMNS-8764-217	Dak Po District, Gia Lai Province, Vietnam	4D + 1S	11C-D	VAM1-VAM4: OR978004- OR978007	VAM1-VAM4: OR964287- OR964290	This study
			VKAA1 to VKAA4	NMNS-8764-218 to NMNS-8764-221	Khang, Gia Lai Province, Vietnam	3D + 1S	11E-F	VKAA2-VKAA4: OR978008- OR978010	VKAA2-VKAA4: OR964291 - OR964293	
			VKBB0 to VKBB9	NMNS-8764-222 to NMNS-8764-231	Hoai An, An Lao, Binh Dinh Province, Vietnam	4D + 6S	11G-I	VKBB0: OR978011 VKBB5: OR978012 VKBB9: OR978013	VKBB0: OR964294 VKBB5: OR964295 VKBB9: OR964296	
			VKBN	NMNS-8764-232	Binh Dinh Province, Vietnam	1D	-	-	-	
3	<i>Amphidromus asperoides</i> Jirapatrasilp & Lee sp. nov.	<i>A. placostylus</i>	VME01 to VME021	NMNS-8764-233 to NMNS-8764-253	Hoai An district, Binh Dinh Province, Vietnam	7D + 14S	-	-	-	This study
			D2-1 to D2-4	NMNS-8764-001 to NMNS-8764-003, NHMUK 20230613	Ea Tu village, Buon Ma Thuat city, Dak Lak Province, Vietnam	4D	8A-C	OR978014- OR978017	OR964297 - OR964300	
			VTAU1 to VTAU20	NMNS-8764-192 to NMNS-8764-211	Krong Pak, Dak Lak Province, Vietnam	20D	-	-	-	
			G3-1 to G3-5	NMNS-8764-082 to NMNS-8764-086	M'drak District, Dak Lak Province, Vietnam	4D + 1S	3D-E	G3-1: OR978018	-	
4	<i>Amphidromus ingens</i> Mölldendorff, 1900	<i>A. ingens</i>	R50	NMNS-8764-087	Ea M'doal Ward, M'drak District, Dak Lak Province, Vietnam	1D	3F	OR978019	OR964301	This study
			U20 to U24	NMNS-8764-088 to NMNS-8764-092	Krong A Ward, M'drak District, Dak Lak Province, Vietnam	4D + 1S	3G	U20-U23: OR978020- OR978023	OR964302 - OR964306	
			YD1 to YD8, YE1 to YE4	NMNS-8764-093 to NMNS-8764-104	Ea Sup District, Dak Lak Province, Vietnam	7D + 5S	3H-I	YD1-YD8: OR978024- OR978031 YE1-YE4: OR978032- OR978035	YD1-YD2: OR964307- OR964308 YD5-8: OR964309 - OR964312 YE1-YE4: OR964313- OR964316	
			G4, P6	NHMUK 20230614, NMNS-8764-105	CuMita Ward, M'drak District, Dak Lak Province, Vietnam	1D + 1S	8G-H	OR978036- OR978037	OR964317 - OR964318	
5	<i>Amphidromus ingensoides</i> Jirapatrasilp & Lee sp. nov.	<i>Amphidromus sp. 2</i>	U10, U11	NMNS-8764-106, NMNS-8764-107	Hon Ba, Khanh Son District, Khanh Hoa Province, Vietnam	1D + 1S	8I-J	OR978038- OR978039	OR964319 - OR964320	This study

Number	Species	Preliminary species identification in this study	Specimen codes	Voucher numbers	Locality	No. of specimen and chirality	Figure	GenBank accession numbers		References
								COI	16S rRNA	
6	<i>Amphidromus buelowi</i> Fruhstorfer, 1905	<i>A. buelowi</i>	SUK1 to SUK4	NMNS-8764-022 to NMNS-8764-025	Mount Singalang, Sepuluh Koto, Tanah Datar Regency, West Sumatra, Indonesia	4D	15E	SUK2-SUK3: OR978040-OR978041	SUK2-SUK3: OR964321-OR964322	This study
		<i>A. asper</i>	VCF, VCI7	NMNS-8764-026, NMNS-8764-027	Lang-Biang plateau, Lac Duong District, Lam Dong Province, Vietnam	2D	15G	VCF: OR978042	VCF: OR964323	
		<i>A. franzhuberi</i>	VCG, VCI1 to VCI6	NMNS-8764-028 to NMNS-8764-034	Nha Trang, Khanh Hoa Province, Vietnam	6D + 1S	15H-I	VCG: OR978043 VCI1-VCI3: OR978044-OR978046	VCG: OR964324 VCI1-VCI3: OR964325-OR964327	
		<i>A. thachi</i>	VBQ1, VBQ2	NMNS-8764-264, NMNS-8764-265	Lac Duong District, Lam Dong Province, Vietnam	2D	17G-H	OR978048-OR978049	OR964329-OR964330	
		<i>A. thachi</i>	VB11 to VB14	NMNS-8764-266 to NMNS-8764-269	Vinh Thanh, Binh Dinh Province, Vietnam	3D + 1S	17D	VB11: OR978047	VB11: OR964328	
		<i>A. thachi</i>	VCD1, VCD2	NMNS-8764-270, NMNS-8764-271	Buon Don District, Dak Lak Province, Vietnam	1D + 1S	17E	OR978050-OR978051	OR964331-OR964332	
7	<i>Amphidromus thachi</i> Huber, 2015	<i>A. thachi</i>	VMAM	NMNS-8764-272	Da Lat, Lam Dong Province, Vietnam	1S	17F	OR978052	OR964333	This study
		<i>A. thachi</i>	XM1, XM2	NMNS-8764-273, NMNS-8764-274	Krong Bong, Dak Lak Province, Vietnam	2D	-	OR978053-OR978054	OR964334-OR964335	
		<i>A. metabletus</i>	P3 to P5, XE1 to XE5	NMNS-8764-123 to NMNS-8764-130	Nha Trang, Khanh Hoa Province, Vietnam	4D + 4S	21C-F	P3-P5: OR978055-OR978057 XE1-XE5: OR978064-OR978068	P3-P5: OR964336-OR964338 XE1-XE5: OR964344-OR964348	
		<i>A. metabletus</i>	VMELa1 to VMELa6, VMELb1 to VMELb6, VMELc1, VMELd1 to VMELd3, VMELe1 to VMELe3	NMNS-8764-131 to NMNS-8764-149	Ninh Hoa, Khanh Hoa Province, Vietnam	15D + 4S	21G-L	VMELa6: OR978058 VMELb6: OR978059 VMELc1: OR978060 VMELd1: OR978061 VMELd3: OR978062 VMELe1: OR978063	VMELa6: OR964339 VMELb6: OR964340 VMELc1: OR964341 VMELd1: OR964342 VMELe1: OR964343	
9	<i>Amphidromus haematostoma</i> Mollendorff, 1898	<i>A. haematostoma</i>	X91 to X94	NMNS-8764-053 to NMNS-8764-056	Samphanh District, Phongsali Province, Laos	4S	24D	-	X92-X94: OR964349-OR964351	This study
		<i>A. haematostoma</i>	ZK0 to ZK9, ZK9a to ZJ9j	NMNS-8764-057 to NMNS-8764-076	Ba Chien, Pakse District, Champasak Province, Laos	20S	24E-F	ZK6-ZK7: OR964352-OR964353	ZK6-ZK7: OR964352-OR964353	
		<i>A. haematostoma</i>	AM36	ex. Maassen collection	Boloven Plateau, Paksong District, Champasak Province, Laos	1S	-	OR978069	-	
10	<i>Amphidromus madeleineae</i> Thach, 2020	<i>A. haematostoma</i>	VMDO1 to VMDO5	NMNS-8764-077 to NMNS-8764-081	Kbang District, Gia Lai Province, Vietnam	5S	24G	VMDO1: OR978070 VMDO4: OR978071 VMDO5: OR978072	-	This study
		<i>A. madeleineae</i>	VB01 to VB05	NMNS-8764-108 to NMNS-8764-112	Duy Xuyen District, Quang Nam Province, Vietnam	5S	24I-J	VB02: OR978076 VB05: OR978077	VB02: OR964354 VB05: OR964355	
		<i>A. madeleineae</i>	VKBG0 to VKBG9	NMNS-8764-113 to NMNS-8764-122	Za Hung, Dong Giang District, Quang Nam Province, Vietnam	10S	24K-M	VKBG1: OR978078 VKBG5: OR978079 VKBG9: OR978080	VKBG1: OR964356 VKBG5: OR964357 VKBG9: OR964358	

Number	Species	Preliminary species identification in this study	Specimen codes	Voucher numbers	Locality	No. of specimen and chirality	Figure	GenBank accession numbers		References
								COI	16S rRNA	
11	<i>Amphidromus costifer</i> Smith, 1893	<i>A. costifer</i>	YW0 to YW9	NMNS-8764-035 to NMNS-8764-044	Tay Son District, Binh Dinh Province, Vietnam	10D	27D-E	-	YW0-YW8: OR964366-OR964374	This study
			YF1 to YF6	NMNS-8764-045 to NMNS-8764-050	Ea Sup District, Dak Lak Province, Vietnam	6D	27F-G	YF4: OR978083	YF2-YF6: OR964361-OR964365	
			VKBE1, VKBE2	NMNS-8764-051, NMNS-8764-052	An Lao District, Binh Dinh Province, Vietnam	2D	27H-I	OR978081- OR978082	OR964359- OR964360	
12	<i>Amphidromus pankowskianus</i> Thach, 2020	<i>A. pankowskianus</i>	CAF1 to CAF3	NMNS-8764-150 to NMNS-8764-152	Khammouan Province, Laos, near Minh Hoa District, Quang Binh Province, Vietnam	2D + 1S	30K-L	CAF1-CAF2: OR978084-OR978085	CAF1: OR964375	This study
			VTAR1 to VTAR40	NMNS-8764-153 to NMNS-8764-191, NMNS-8764-212	Lak Sao, Khamkeut District, Bolikhamsai Province, Laos	23D + 17S	30H-J	VTAR02: OR978086 VTAR06: OR978087 VTAR08-VTAR09: OR978088-OR978089 VTAR11: OR978090 VTAR15: OR978091	-	
13	<i>Amphidromus roseolabiatius</i> Fulton, 1896	<i>A. roseolabiatius</i>	CAB0 to CAB9	NMNS-8764-254 to NMNS-8764-263	Kambong Siem District, Kampong Cham Province, Cambodia	4D + 6S	30D-F	CAB0: OR978092 CAB2-CAB3: OR978093-OR978094 CAB7: OR978095	CAB0: OR964376 CAB2-CAB3: OR964377-OR964378 CAB7: OR964379	This study
14	<i>Amphidromus cruentatus</i> (Morelet, 1875)	<i>A. cruentatus</i>	X71 to X79, X81 to X88	NMNS-8476-001 to NMNS-8476-009, NMNS-8476-034 to NMNS-8476-041	Samphanh District, Phongsali Province, Laos	17S	-	OL352241-OL352248, OL352249-OL352255	X71: OL352062 X73-X79: OL352063-OL352069 X81-X88: OL352070-OL352077	Lee et al. (2022)
			ZY3, ZY4, ZY7	NMNS-8476-054, NMNS-8476-055, NMNS-8476-058	Chu Prong District, Gia Lai Province, Vietnam	3S	-	OL352256-OL352258	ZY3-ZY4: OL352078-OL352079 ZY7: OL352080	
15	<i>Amphidromus contrarius</i> (Müller, 1774)	<i>A. contrarius</i>	AM C.468733	-	6.5 km N of Los Palos, Lautem District, Timor-Leste	1S	-	KP085341	KP085031	Köhler and Criscione (2015)
16	<i>Amphidromus perversus</i> (Linnaeus, 1758)	<i>A. perversus</i>	AM19	CUMZ 4291	Bali Island, Indonesia	1S	-	MW649970	MW652850	Jirapatrasilp et al. (2022)
17	<i>Amphidromus sinistralis</i> (Reeve, 1849)	<i>A. sinistralis</i>	AM38	ex. Maassen collection	Sulawesi, Indonesia	1S	-	OR978096	-	This study
Outgroup										
18	<i>Camaena cicutricosa</i> (Müller, 1774)	<i>C. cicutricosa</i>	FJQBC18503	-	Guiping, Guangxi, China	-	-	KU061276	KU586474	Ding et al. (2016)
19	<i>Camaena poyuensis</i> Zhou, Wang & Ding, 2016	<i>C. poyuensis</i>	FJQBC18484	-	Poyue town, Bama, Hechi, Guangxi, China	-	-	KU061273	KU586468	

## Results

The COI dataset of *Amphidromus* in this study comprised 130 sequences with lengths between 556 and 658 bp, including 284 variable and 265 parsimony-informative sites, from an alignment length of 658 bp. The variation in the COI sequence lengths is due to incomplete sequences at both ends in some sequences. The 16S rRNA dataset comprised 118 sequences with lengths between 343 and 394 bp. The 16S rRNA alignment including gaps was 414 bp, including 136 variable and 125 parsimony-informative sites.

The ML and BI phylogenetic analyses based on the concatenated datasets yielded consistent topologies (Fig. 2, showing BI topology). The preliminary morphospecies identification in this study yielded a total of 16 *Amphidromus* morphospecies (Table 1), of which 11 showed a well-supported reciprocal monophyly (SH-aLRT  $\geq$  80%, aBayes  $\geq$  0.95, BS  $\geq$  95%, PP  $\geq$  0.95) (Fig. 2), supporting their recognition as valid species. In addition, *Amphidromus* sp. 1 and sp. 2 also showed well-supported reciprocal monophyly and were characterised by a distinct shell morphology. Therefore, these latter two taxa were described as new species to science (*A. asperoides* sp. nov. and *A. ingensoides* sp. nov., respectively). Specimens previously identified as *A. asper* Haas, 1934 and *A. franzhuberi* Thach, 2016 belonged to the same clade as *A. buelowi*, and *A. nguyenkhoai* Thach, 2020 belonged to the same clade as *A. costifer*.

The DNA sequence data show that the phylogenetic relationships among the species did not mirror their geographical ties. *Amphidromus contrarius*, *A. perversus*, and *A. sinistralis* each did not belong to the same clades of the other taxa, and the relationships of these three species with other species remain unresolved. *Amphidromus roseolabiatum* and *A. pankowskianus* were retrieved together as sister clades forming a distinct well-supported clade (SH-aLRT  $\geq$  80%, aBayes  $\geq$  0.95, BS  $\geq$  95%, PP  $\geq$  0.95) separate from the clade with the remaining taxa. These latter were grouped in a well-supported clade, with *A. costifer* as a sister taxon to all other species in this clade. *Amphidromus cruentatus*, *A. haematostoma*, and *A. madelineae* were closely related in that *A. cruentatus* was sister to the clade *A. haematostoma* + *A. madelineae*. The remaining taxa belonged to a well-supported clade, where *A. bozhii*, *A. ingens*, *A. placostylus*, as well as the two new species belonged to the same well-supported subclade. *Amphidromus bozhii* was sister to *A. placostylus*, and *A. asperoides* sp. nov. was sister to *A. ingens*.

The COI *p*-distances ranged from 0 to 10.03% (average  $2.78 \pm 3.04\%$ ) within species and from 9.61 to 24.16% (average  $18.30 \pm 3.35\%$ ) between species (Table 2). All interspecific pairwise distances exceed 9%, and 92.6% of them (126 out of 136) exceed 12%. Pairwise distances lower than 12% were observed among *A. bozhii*, *A. ingens*, *A. placostylus*, *A. asperoides* sp. nov., and *A. ingensoides* sp. nov. Intraspecific distances typically fall below or hover around 5%. Notable exceptions are *A. haematostoma* at 10.03% and *A. costifer* at 7.84%.

Comparable patterns were observed for 16S, the *p*-distances of which ranged from 0 to 3.39% (average  $1.07 \pm 1.14\%$ ) within species and from 2.76–16.74% (average  $11.68 \pm 3.79\%$ ) between species (Table 2). All interspecific pairwise distances exceed 3%, except between *A. bozhii* and *A. ingens* (2.76%), and 90% of the interspecific *p*-distances (108 out of 120) exceed 5%. Intraspecific distances typically fall below or hover around 3%.

**Table 2.** Percentage of uncorrected pairwise interspecific distances for the partial COI (above the diagonal) and 16S rRNA (below the diagonal) gene fragments among the *Amphidromus* species in this study. Intraspecific distances for COI/16S rRNA are shown on the diagonal (bold). Species numbers correspond to those in Figs 1, 2, and Table 1. The numbers of sequences used to calculate the distances of each respective gene fragment are given as  $n = \text{COI}, 16\text{S}$  in the first column.

Species	1	2	3	4	5	6	7	8	9	10	11	12	13	14	15	16	17
1. <i>A. bozhii</i> ( $n = 17, 4$ )	<b>0.60/ 0.13</b>	9.61	10.33	10.82	9.99	13.29	13.04	17.30	19.19	18.25	18.88	18.87	17.94	21.40	22.36	18.97	18.85
2. <i>A. placostylus</i> ( $n = 10, 10$ )	4.32	<b>5.47/ 3.14</b>	9.83	10.51	10.53	12.79	13.04	16.57	19.02	18.44	17.89	19.60	18.11	21.09	22.16	19.74	19.75
3. <i>A. asperoides</i> sp. nov. ( $n = 4, 4$ )	3.31	4.68	<b>0/0</b>	10.32	10.69	13.13	12.69	16.72	18.47	18.02	17.12	20.33	18.78	20.76	22.41	18.45	18.29
4. <i>A. ingens</i> ( $n = 18, 16$ )	2.76	4.23	3.02	<b>1.37/ 0.52</b>	10.20	12.23	12.74	15.91	19.12	18.38	17.06	20.01	18.26	20.65	20.71	17.71	20.01
5. <i>A. ingensoides</i> sp. nov. ( $n = 4, 4$ )	4.25	5.14	4.61	4.19	<b>3.32/ 1.45</b>	13.51	12.80	16.27	19.16	19.48	17.63	19.98	19.20	21.76	21.62	18.18	19.23
6. <i>A. buelowi</i> ( $n = 7, 7$ )	5.00	5.60	4.61	4.61	4.89	<b>1.25/ 0.19</b>	13.40	17.05	18.72	18.79	18.47	20.63	18.32	21.01	21.78	18.75	19.04
7. <i>A. thachi</i> ( $n = 8, 8$ )	7.41	8.21	6.22	7.19	6.90	6.36	<b>2.21/ 1.07</b>	16.32	19.81	19.43	16.81	19.67	18.31	20.81	21.03	18.05	19.28
8. <i>A. metabletus</i> ( $n = 14, 13$ )	11.08	12.11	11.67	12.04	10.84	11.40	10.68	<b>1.28/ 0.58</b>	20.40	19.43	16.63	20.47	18.53	20.56	21.53	18.30	19.25
9. <i>A. haematostoma</i> ( $n = 7, 5$ )	10.53	10.80	10.10	9.59	9.66	9.38	10.52	12.59	<b>10.03/ 1.99</b>	13.93	20.61	22.44	21.43	20.76	23.28	21.39	21.74
10. <i>A. madelineae</i> ( $n = 5, 5$ )	9.71	9.89	9.17	8.10	8.78	9.26	9.66	11.63	6.04	<b>2.19/ 0.33</b>	17.81	21.12	19.61	20.26	22.90	21.62	20.60
11. <i>A. costifer</i> ( $n = 3, 16$ )	15.45	15.56	14.85	15.33	14.91	13.44	13.69	14.41	16.00	16.02	<b>7.84/ 3.39</b>	19.53	19.31	20.38	21.73	20.23	18.90
12. <i>A. pankowskianus</i> ( $n = 8, 1$ )	13.72	14.18	14.20	13.44	13.61	12.50	14.31	13.78	14.01	13.15	14.37	<b>0.19/ NA</b>	13.02	20.49	21.57	19.59	20.38
13. <i>A. roseolabiatus</i> ( $n = 4, 4$ )	14.28	14.21	13.91	14.09	15.10	13.23	13.03	15.51	14.56	13.08	15.31	6.14	<b>0/0</b>	20.16	21.93	18.97	19.08
14. <i>A. cruentatus</i> ( $n = 18, 19$ )	10.17	9.93	10.82	9.71	9.90	10.26	11.11	12.04	11.37	12.17	15.39	14.21	15.63	<b>3.15/ 1.17</b>	24.16	20.13	21.37
15. <i>A. contrarius</i> ( $n = 1, 1$ )	15.62	16.12	15.90	16.04	15.56	15.41	15.57	16.74	16.41	15.16	14.91	14.29	14.91	16.11	<b>NA/ NA</b>	21.65	21.95
16. <i>A. perversus</i> ( $n = 1, 1$ )	13.75	14.08	14.00	13.44	14.51	14.70	14.93	16.18	15.89	13.09	13.86	13.61	13.09	15.46	13.45	<b>NA/ NA</b>	18.29
17. <i>A. sinistralis</i> ( $n = 1, 0$ )	NA	NA	NA	NA	NA	NA	NA	NA	NA	NA	NA	NA	NA	NA	NA	NA	<b>NA/ NA</b>

## Systematics

### Family Camaenidae Pilsbry, 1895

#### Genus *Amphidromus* Albers, 1850

*Amphidromus* Albers, 1850: 138. Martens in Albers 1860: 184. Fulton 1896: 66, 94.

**Type species.** *Helix perversus* Linnaeus, 1758 by subsequent designation of E. von Martens in Albers (1860).

#### *Amphidromus ingens* Möllendorff, 1900

Figs 3, 4A, 5A–C, 6A–C, 7

*Amphidromus ingens* Möllendorff, 1900b: 23–24. Type locality: Berg “Mutter und Kind”, Annam [Vietnam]. Pilsbry 1900: 175–176. Fischer and Dautzenberg 1904: 406. Laidlaw and Solem 1961: 529, 629. Richardson 1985: 21. Thach 2005: 235, pl. 73, fig. 22. Schileyko 2011: 50. Sutcharit et al. 2021: fig. 1g.

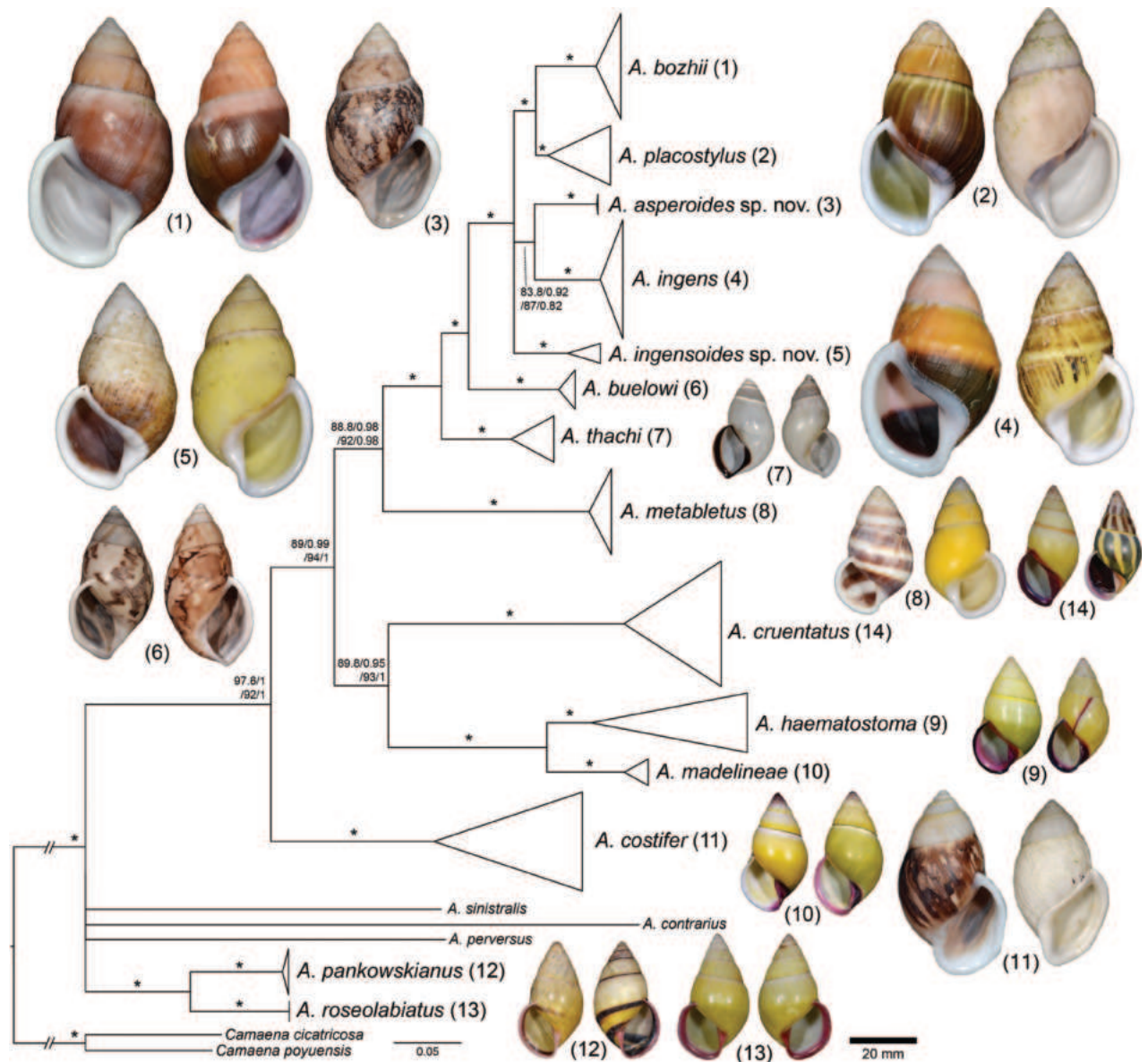


**Figure 2.** Bayesian phylogeny of *Amphidromus* spp. based on mitochondrial COI and 16S genes. Nodal support values are given as SH-aLRT/aBayes/ultra-fast bootstrap (IQ-TREE, ML)/posterior probability (MrBayes, BI). An asterisk on each branch indicates a clade with all well-supported values (SH-aLRT  $\geq$  80%, aBayes  $\geq$  0.95, BS  $\geq$  95%, PP  $\geq$  0.95). Species numbers correspond to those in Fig. 1 and Tables 1, 2.

*Amphidromus* (*Amphidromus*) *ingens*. Zilch 1953: 135, pl. 23, fig. 25.

*Amphidromus naggsi* Thach & Huber, 2014: 35–37, figs 1–13, 15. Type locality: Don Duong district, Lam Dong Province, South Vietnam. Páll-Gergely et al. 2020: 53. Thach et al. 2020: 185, 187, pl. 1, fig. 6a. Thach 2020a: 70, fig. 881 left. Thach 2021: 70. syn. nov.

**Material examined.** VIETNAM: Dextral, **lectotype** of “*Amphidromus ingens*”, SMF 7565/1 (Fig. 3A); 2D + 2S, paralectotypes of “*Amphidromus ingens*”, SMF 7566/4 (Fig. 3B). VIETNAM: Dextral, **holotype** of “*Amphidromus naggsi*”, RMNH.5003908 (Fig. 3C).

**Other material examined.** VIETNAM: 4D + 1S specimens, M’drak District, Dak Lak Province, NMNS-8764-082–NMNS-8764-086 (Fig. 3D, E); 1D specimen, Ea

M'doal ward, M'drak District, Dak Lak Province, NMNS-8764-087 (Fig. 3F); 4D + 1S specimens, Krong A ward, M'drak District, Dak Lak Province, NMNS-8764-088–NMNS-8764-092 (Fig. 3G); 7D + 5S specimens, Ea Sup District, Dak Lak Province, NMNS-8764-093–NMNS-8764-104 (Fig. 3H, I).

**Diagnosis.** Shell large conical and chirally dimorphic (sinistral and dextral coiling). Shell surface with coarse growth lines; last whorl with subsutural depression area and more or less prominent keel on periphery. Genitalia with appendix.

**Differential diagnosis.** *Amphidromus ingens* is unique among all reported Vietnamese species (Schileyko 2011) in having a last whorl with subsutural depression area and more or less prominent keel on periphery. *Amphidromus bozhii* is similar in most of the shell form and sculpture, but the shell sculpture of *A. bozhii* has a very weak spiral depression area and sometimes with or without keel, and the shell colour is generally rose-pink to dark colour, with last whorl stained with dark brown colour below periphery and ~ 1/2 of upper periphery. On the other hand, *A. ingens* has a monochrome (whitish, yellowish, tinted pink) shell, often stained with dark brown to blackish below periphery. *Amphidromus ingens* is also recognised by a distinct clade in the molecular phylogeny (Fig. 2), with the closest *p*-distance to *A. ingensoides* sp. nov. in COI (10.2%) and *A. bozhii* in 16S (2.76%) (Table 2).

**Description.** **Shell** large (height 62.3–74.6 mm, width 38.5–42.5 mm), chirally dimorphic, solid, and ovate conical shape. Spire long conical to elongate conical, apex acute without black spot on tip. Whorls 5–7 convex; suture wide and depressed; last whorl rounded to slightly angulated. Periostracum brownish to thin corneous; varix usually absent. Shell surface generally with irregular and coarse growth lines; below sutural with broad subsutural depression area, and with blunt or low to prominent keel on periphery. Shell colour highly variable: monochrome (whitish, yellowish, tinted pink) to stained with dark brown to blackish below periphery. Parietal callus thickened and white, dilated at umbilical area. Aperture broadly ovate; inner side of outer wall with white, yellow or dark brown to blackish colour. Peristome thickened, expanded, and reflexed but not attached to last whorl; lip whitish. Columella white, straight, or little twisted. Umbilicus imperforate.

**Radula.** Teeth arranged in anteriorly pointed V-shaped rows. Central tooth monocuspid and spatulate with truncated cusp. Lateral teeth bicuspid; endocone small, slightly curved, with wide notch and dull cusp; ectocone large with truncated to slightly curved cusp. Lateral teeth gradually transformed to asymmetric tricuspid marginal teeth (Fig. 4A).

**Genital organs.** Atrium relatively short. Penis slender, conical, and short ~ 1/3 of vaginal length. Penial retractor muscle thickened and inserting on epiphallus close to penis. Epiphallus long, slender tube, slightly narrower than penis. Flagellum short ~ 1/2 of epiphallus and terminating in slightly enlarged folded coil. Appendix short, slender tube, approximately as long as epiphallus, and ~ 2× longer than flagellum. Vas deferens slender tube passing from free oviduct and terminating at epiphallus-flagellum junction (Fig. 5A). Internal wall of penis corrugated, exhibiting series of thickened and swollen longitudinal penial pilasters forming fringe around penial wall, and with nearly smooth to weak folds around base of penial verge. Penial verge short conical with nearly smooth surface, and with opening on the tip (Fig. 5B).

Vagina slender, long cylindrical, and ~ 3× longer than penis. Gametolytic duct enlarged cylindrical tube then abruptly tapering to slender tube terminally and

connected to gametolytic sac (missing during dissecting). Free oviduct short; oviduct compact and enlarged to form lobule alveoli (Fig. 5A). Internal wall of vagina possessing corrugated ridges near genital orifice; ridges becoming thinner and smooth surfaced longitudinal vaginal pilasters, swollen with irregularly shaped and deep crenulations close to free oviduct opening. Spermatophore (in part) dark brown stuck inside gametolytic duct (Fig. 5C).

**Living specimens** generally with pale brown to yellowish body covered with reticulated skin. Foot broad and long with uniform pale brownish to yellowish colour to posterior tail. Dorsal side of anterior body usually with stripe of darkly reticulated skin; head area at base and just behind upper tentacle with orange patch. Upper tentacles drumstick shaped, orange to paler and with dark eyespots on tentacular tips; lower tentacles short and pale orange in colour (Fig. 6A–C).

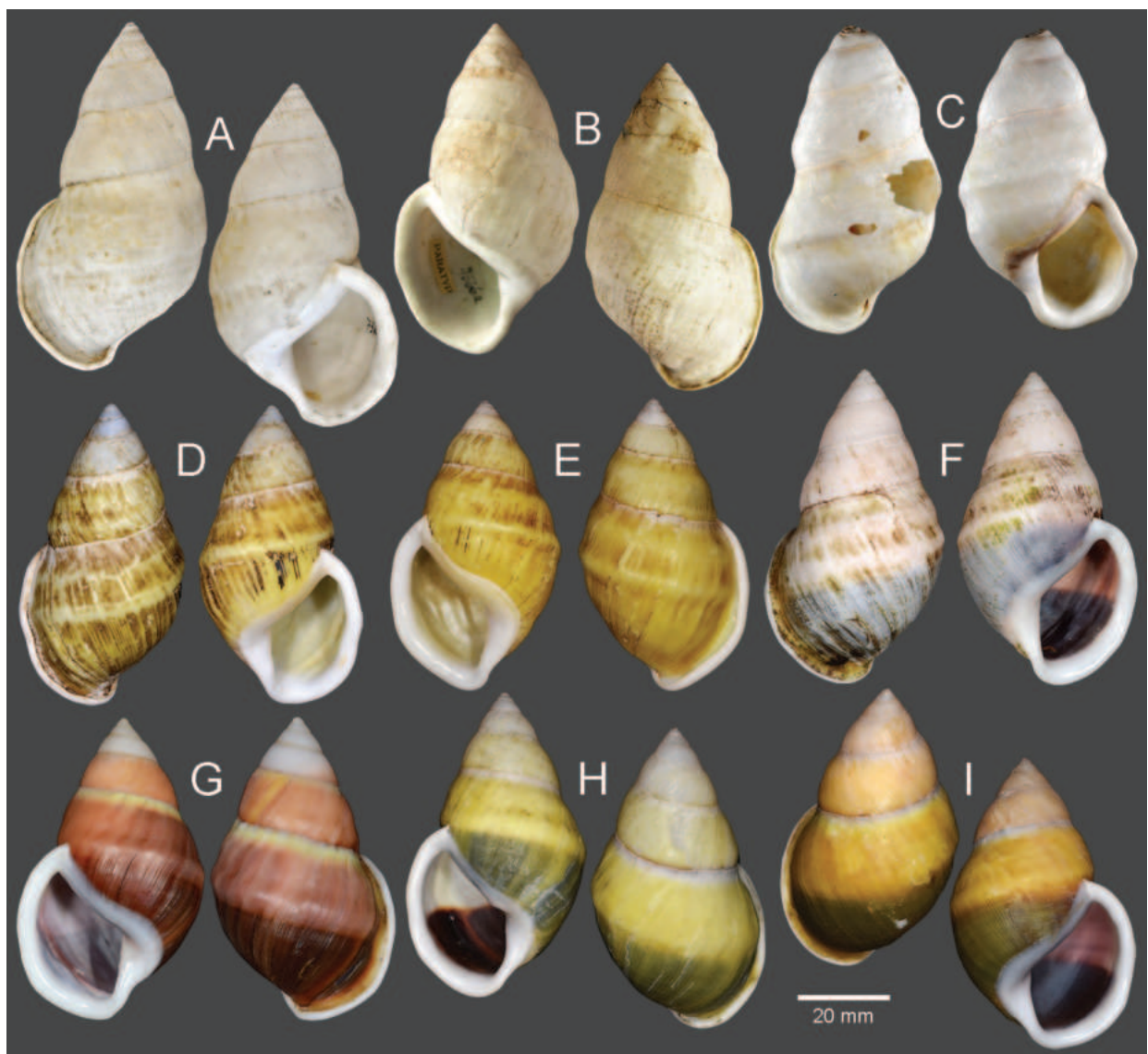


**Figure 3.** Shells of *Amphidromus ingens* Möllendorff, 1900 **A** lectotype of "*Amphidromus ingens*" (SMF 7565) **B** paralectotype of "*Amphidromus ingens*" (SMF 7566) **C** holotype of "*Amphidromus naggsi*" (RMNH.5003908) **D, E** specimens from M'drak, Dak Lak, Vietnam (NMNS-8764-082, NMNS-8764-084) **F** specimen from Ea M'doal, M'drak, Dak Lak, Vietnam (NMNS-8764-087) **G** specimen from Krong A, M'drak, Dak Lak, Vietnam (NMNS-8764-088) **H, I** specimens from Ea Sup, Dak Lak, Vietnam (NMNS-8764-093, NMNS-8764-101). Credit: J. Goud, RMNH (C).

**Haplotype network.** There was a total of 12 COI haplotypes (Fig. 7A) and nine 16S haplotypes (Fig. 7B) of *A. ingens* in this study, and the highest numbers of mutational steps in the COI and 16S minimum spanning networks are 13 and three, respectively.

**Distribution.** The distribution range of the species covers Dak Lak and Lam Dong provinces, Vietnam.

**Remarks.** Thach and Huber (2014) introduced *A. naggsi*, which is described to differ from *A. ingens* in its wrinkled outer surface, the presence of 2–3 broad spiral channels on the body whorl, the more prominent sculpture on the penultimate whorl, and a more elongate aperture. However, upon examining the type specimens of both *A. ingens* and *A. naggsi*, these diagnostic characters were also present in the lectotype and paralectotypes of *A. ingens*, and the holotype of *A. naggsi* agrees well with all the type specimens of *A. ingens* in terms of shell shape, shell surface sculpture, peristome, and apertural shape. Thus, *A. naggsi* is regarded herein as a junior subjective synonym of *A. ingens*.

The shell colour generally varies from whitish (typical) to yellowish to rose-pink colour (Fig. 3). In our examined specimens, many are stained with dark brown colour below periphery and some are stained nearly entirely on the last and penultimate whorl. The shell sculpture generally has two depression areas, one upper periphery and one below suture, and the conspicuous keel to weak keel is generally present on periphery.

***Amphidromus asperoides* Jirapatrasilp & Lee, sp. nov.**

<https://zoobank.org/BB0A2CF5-B568-4CA7-AE3F-59C38CC082E5>

Figs 4B, 5D–F, 6G, 8A–C

*Amphidromus asper* [non Haas]. Thach 2017: 37, pl. 34, figs 432, 433.

**Diagnosis.** Shell large conical and dextral. Shell colour with dark triangular blotches connected with dark zigzag radial streaks. Aperture ovate and rounded anteriorly, columella straight. Genitalia with appendix.

**Differential diagnosis.** The new species differs from the similar species *A. buelowi* in being exclusively dextral, having a straight columella, and lacking an apertural notch and umbilical hump. In contrast, *A. buelowi* is chirally dimorphic, and possesses a distinct twisted columella plait, a prominent umbilical hump encircled columellar area, and an apertural notch projecting anteriorly. In addition, on the soft body of living snail, *A. asperoides* sp. nov. has a uniform brownish yellow to pale brown of the entire body, while *A. buelowi* exhibits a reddish orange body. This new species is also recognised as a distinct clade in the molecular phylogeny (Fig. 2), with the closest *p*-distance to *A. placostylus* in COI (9.83%) and *A. ingens* in 16S (3.02%) (Table 2).

**Etymology.** The specific epithet *asperoides* is from *asper*, and the suffix ‘-oides’, meaning ‘like or resembling’. This name refers to the resemblance in shell morphology of the new species to the nominal species *A. asper*, which is now treated as a junior synonym of *A. buelowi*.

**Type material. Holotype.** VIETNAM: dextral, shell height 61.7 mm, shell width 34.9 mm, with 7 whorls, 15 July 2016, coll. A. N. Pham (NMNS-8764-001, Fig. 8A). **Paratypes.** VIETNAM: 2D specimens, same collecting data as holotype

(NMNS-8764-001–NMNS-8764-003, Fig. 8B); 1D specimen, same collecting data as holotype (NHMUK 20230613, Fig. 8C).

**Type locality.** VIETNAM: Ea Tu village, Buon Ma Thuat city, Dak Lak Province, 12°42'24.4"N, 108°07'25.3"E.

**Other material.** VIETNAM: 20D specimens, Krong Pak, Dak Lak Province, NMNS-8764-192–NMNS-8764-211, 6 Oct. 2022, coll. V. V. Hoang.

**Description.** *Shell* large (height 54.6–61.7 mm, width 31.3–34.9 mm), dextral, solid, and ovate conical shape. Spire long conical with white or pale colour; apex acute without black spot on tip. Whorls 6–7 convex; suture wide and depressed; last whorl ovate. Periostracum thin corneous; varices generally present. Shell surface generally with coarse growth lines. Shell ground colour pale pink, decorated with dark triangular blotches connected with dark zigzag radial streaks. Parietal callus thickened, slightly opaque, white and much thinner in central area. Aperture ovate; without (or very weak) anterior notch and umbilical hump; inner side of outer wall whitish colour; peristome thickened, expanded, and reflexed but not attached to last whorl; lip whitish. Columella white, straight, or weakly twisted. Umbilicus imperforate.

**Radula.** Teeth arranged in anteriorly pointed V-shaped rows. Central tooth monocuspid and spatulate with truncated cusp. Lateral teeth bicuspid; endocone small, with shallow notch and blunt cusp; ectocone large with curved

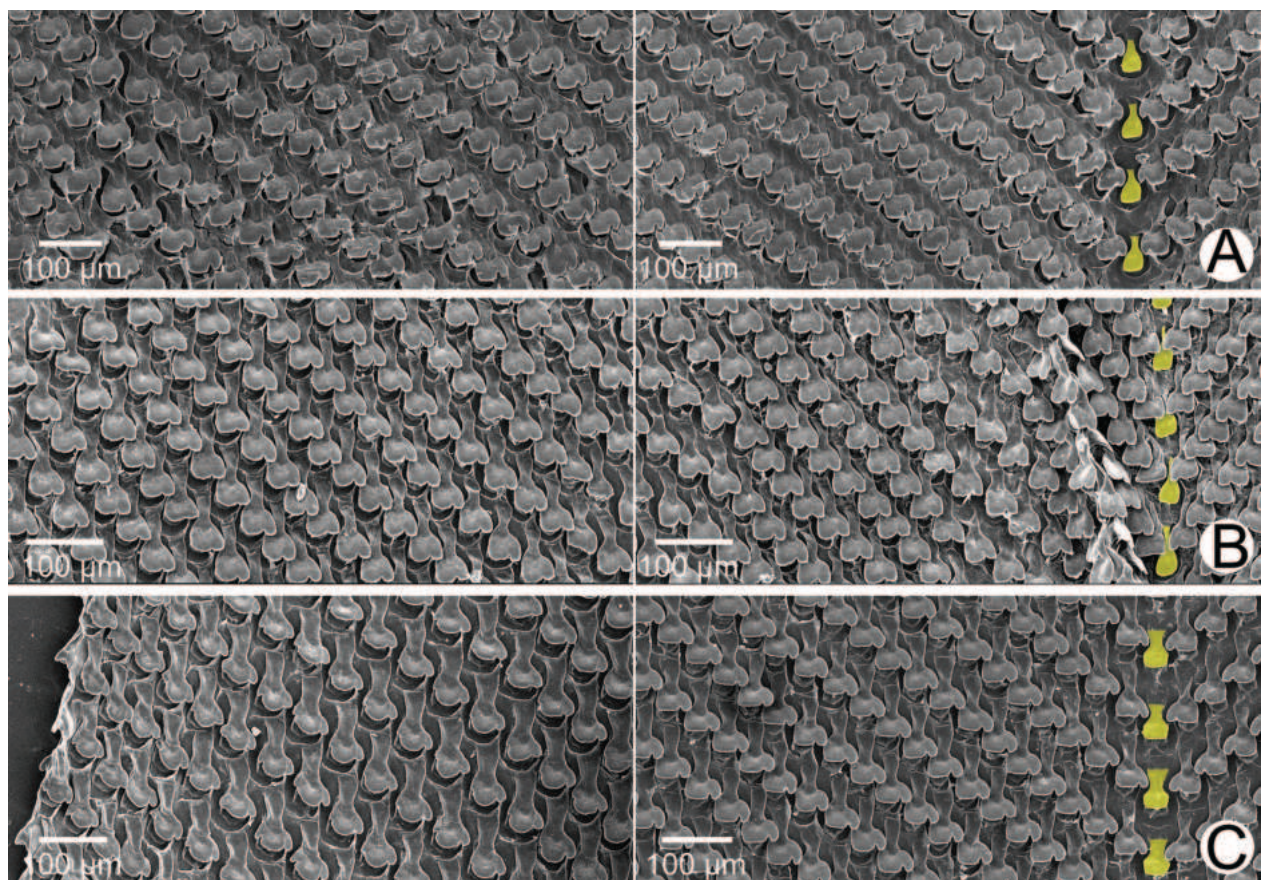


**Figure 4.** SEM images of the radula of *Amphidromus* spp. **A** *Amphidromus ingens* Möllendorff, 1900 from Ea Sup, Dak Lak, Vietnam (NMNS-8764-100) **B** *Amphidromus asperoides* sp. nov. from Ea Tu, Buon Ma Thuat city, Dak Lak, Vietnam (NMNS-8764-001) **C** *Amphidromus bozhii* Wang, 2019 from Tuy Hoa, Phu Yen, Vietnam (NMNS-8764-016). Central teeth are marked in yellow. The left and right images show the outer and inner sections of each radula, respectively.

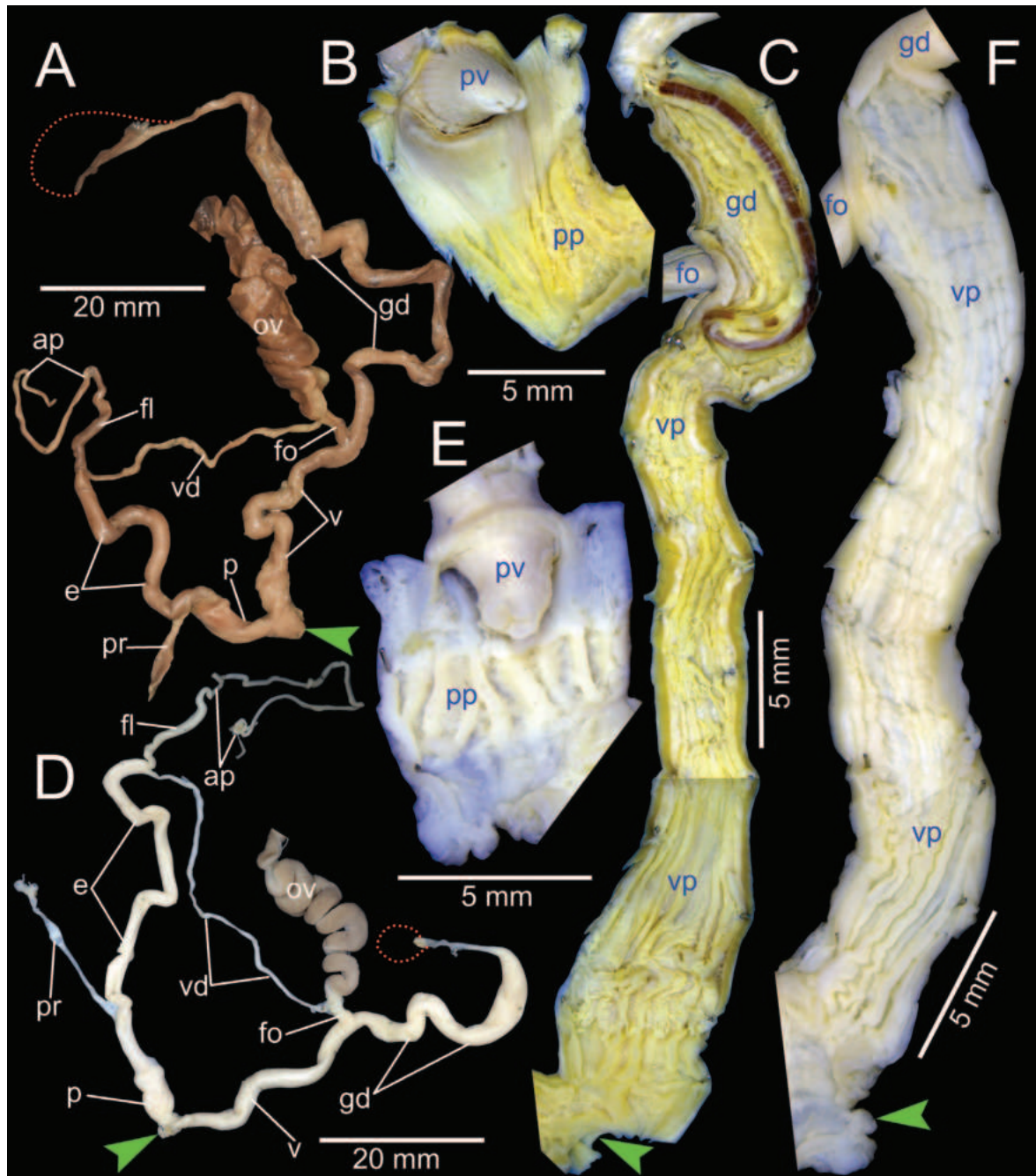


**Figure 5.** Genitalia of *Amphidromus* spp **A–C** *Amphidromus ingens* Möllendorff, 1900 from Ea Sup, Dak Lak, Vietnam (NMNS-8764-100), showing **A** general view of genitalia **B** interior structures of penis **C** interior structures of vagina chamber and gametolytic duct **D–F** *Amphidromus asperoides* sp. nov. from Ea Tu, Buon Ma Thuat city, Dak Lak, Vietnam (NMNS-8764-001), showing **D** general view of genitalia **E** interior structures of penis **F** interior structures of vagina chamber. Red dots indicate the shape of the missing gametolytic sac. Green arrows indicate the genital openings. Abbreviations: ap, appendix; e, epiphallus; fl, flagellum; fo, free oviduct; gd, gametolytic duct; ov, oviduct; p, penis; pp, penial pilaster; pr, penial retractor muscle; pv, penial verge; v, vagina; vd, vas deferens; vp, vaginal pilaster

cusps. Lateral teeth gradually transformed to asymmetric tricuspid marginal teeth (Fig. 4B).

**Genital organs.** Atrium relatively short. Penis slender, conical, and short ~ 1/4 of vaginal length. Penial retractor muscle thickened, long and inserting on epiphallus near penis. Epiphallus very long ~ 2× longer than vagina, and slen-

der tube. Flagellum short, extending from epiphallus and terminating in slightly enlarged tube. Appendix short and slender tube, 4× longer than flagellum and approximately as long as epiphallus. Vas deferens slender tube passing from free oviduct and terminating at epiphallus-flagellum junction (Fig. 5D). Internal wall of penis corrugated, exhibiting series of thickened and swollen longitudinal penial pilasters forming fringe around penial wall, and with nearly smooth to weak folds around base of penial verge. Penial verge short conical with nearly smooth surface, and with opening on the tip (Fig. 5E).

Vagina long, slender, cylindrical, and ~ 2× longer than penis. Gametolytic duct enlarged cylindrical tube then abruptly tapering to slender tube terminally and connected to gametolytic sac (missing during dissection). Free oviduct short; oviduct compact, enlarged to form lobule alveoli (Fig. 5D). Internal wall of vagina possessing corrugated ridges near genital orifice; ridges becoming thinner and smooth surfaced longitudinal vaginal pilasters, swollen with irregularly shaped shallow crenulations close to free oviduct opening (Fig. 5F).

**Living specimens** with soft body morphology generally similar to *A. ingens*. Animals with uniform brownish yellow to pale brown of the entire body including foot, upper and lower tentacles (Fig. 6G).

**Distribution.** This species is known from Dak Lak Province, Vietnam.

**Remarks.** This new species had been previously identified as *A. asper* in Thach (2017). However, based on the difference in shell size and apertural characteristics to the holotype of *A. asper*, those specimens featured in Thach (2017) should be regarded as *A. asperoides* sp. nov. See also under the remarks of *A. buelowi*.

### ***Amphidromus bozhii* Wang, 2019**

Figs 4C, 8D–F, 9A–C, 10

*Amphidromus bozhii* Wang, 2019: 300–301, pl. 3, figs a, b. Type locality: Phu Yen Province, Vietnam.

**Material examined.** VIETNAM: 10D specimens, Phu Hoa District, Phu Yen Province, NMNS-8764-004–NMNS-8764-013 (Fig. 8D, E); 8S specimens, Tuy Hoa District, Phu Yen Province, NMNS-8764-014–NMNS-8764-021 (Fig. 8F).

**Diagnosis.** Shell large conical and chirally dimorphic. Shell surface with coarse growth lines; last whorl nearly absent of spiral depression area and keel. Genitalia with appendix.

**Differential diagnosis.** This species is similar to *A. ingens* in most of the shell form and sculpture. The distinguishing characters are the shell colour which is generally rose-pink to dark colour. The last whorl is stained with dark brown colour below periphery and ~ 1/2 of upper periphery. The shell sculpture has a very weak spiral depression area and sometimes with or without keel. This species looks like an intermediate form between *A. ingens* and *A. placostylus*. *Amphidromus bozhii* is also recognised by a distinct clade in the molecular phylogeny (Fig. 2), with the closest *p*-distance to *A. placostylus* in COI (9.61%) and *A. ingens* in 16S (2.76%) (Table 2).

**Description.** **Shell** large (height 69.1–82.9 mm, width 38.3–42.0 mm), chirally dimorphic, solid, and ovate conical shape. Spire elongate conical with pale colour; apex acute without black spot on tip. Whorls 5–7 convex; suture wide

and depressed; last whorl ovate. Periostracum brownish to thin corneous. Shell surface generally with irregular and coarse growth lines; very weak to nearly absent of spiral depression area and keel. Shell colour generally rose-pink to



**Figure 6.** Living *Amphidromus* spp **A–C** *Amphidromus ingens* Möllendorff, 1900 from Dak Lak, Vietnam **D** *Amphidromus placostylus* Möllendorff, 1900 from Hoai An, An Lao, Binh Dinh, Vietnam **E, F** *Amphidromus ingensoides* sp. nov. from Hon Ba, Khanh Son, Khanh Hoa, Vietnam **G** *Amphidromus asperoides* sp. nov. from Ea Tu, Buon Ma Thuat city, Dak Lak, Vietnam **H, I** *Amphidromus buelowi* Fruhstorfer, 1905 from Lang-Biang plateau, Lac Duong, Lam Dong, Vietnam **J** *Amphidromus thachi* Huber, 2015 from Krong Bong, Dak Lak, Vietnam.

stained with dark brown colour below and ~ 1/2 of upper periphery. Parietal callus thickened, white, and dilated at umbilical area. Aperture broadly ovate; inner side of outer wall with yellow or pale brown colour; peristome thickened, expanded, and reflexed but not attached to last whorl; lip whitish. Columella white, straight, or little twisted. Umbilicus imperforate.

**Radula.** Teeth arranged in anteriorly pointed V-shaped rows. Central tooth monocuspid and short-spatulate with truncated cusp. Lateral teeth bicuspid; endocone small, with wide notch and slightly curved and dull cusp; ectocone large with truncated to blunt cusp. Lateral teeth gradually transformed to asymmetric tricuspid marginal teeth. Outermost teeth with small and curved cusp on endocone and ectocone; mesocone large, with curved cusps (Fig. 4C).

**Genital organs.** Atrium very short. Penis slender, conical, and short ~ 1/2 of vaginal length. Penial retractor muscle thickened and inserting on epiphallus close to penis. Epiphallus long and slender tube. Flagellum short, extending from epiphallus and terminating in slightly enlarged tube. Appendix short,

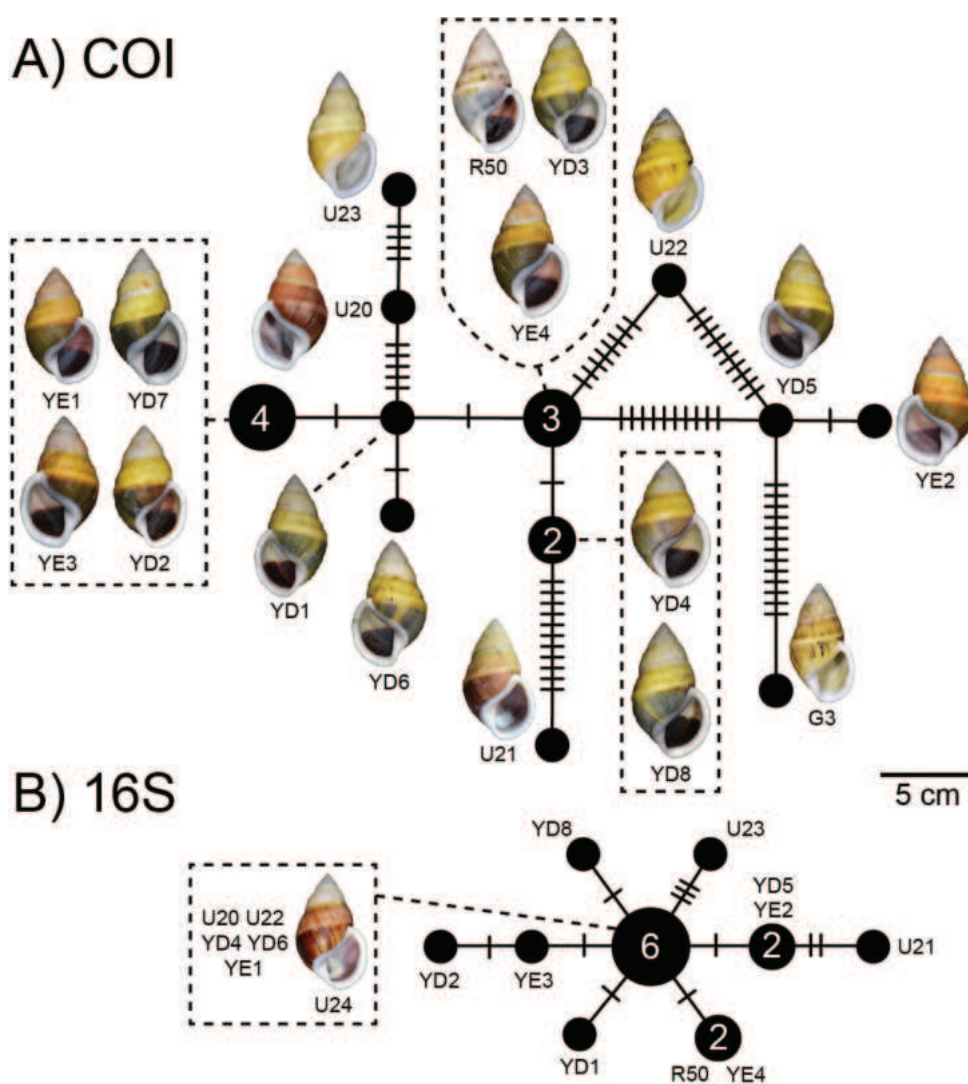


**Figure 7.** Mitochondrial haplotype minimum spanning networks of *Amphidromus ingens* Möllendorff, 1900 **A** COI and **B** 16S rRNA. The size of each circle corresponds to the frequency of that haplotype, also shown as the number in that circle. The bars on the branches indicate the number of mutational steps between haplotypes. Specimen codes correspond to those in Table 1.

slender tube, approximately as long as flagellum, and  $\sim 1/3$  of epiphallus length. Vas deferens slender tube passing from free oviduct and terminating at epiphallus-flagellum junction (Fig. 9A). Internal wall of penis corrugated, exhibiting series of swollen longitudinal penial pilasters forming fringe around penial wall, and with nearly smooth to weak folds around base of penial verge. Penial verge conical with nearly smooth surface (Fig. 9B).

Vagina slender, long cylindrical,  $\sim 2\times$  longer than penis. Gametolytic duct enlarged cylindrical tube then abruptly tapering to slender tube terminally and connected to gametolytic sac (missing during dissection). Free oviduct short;

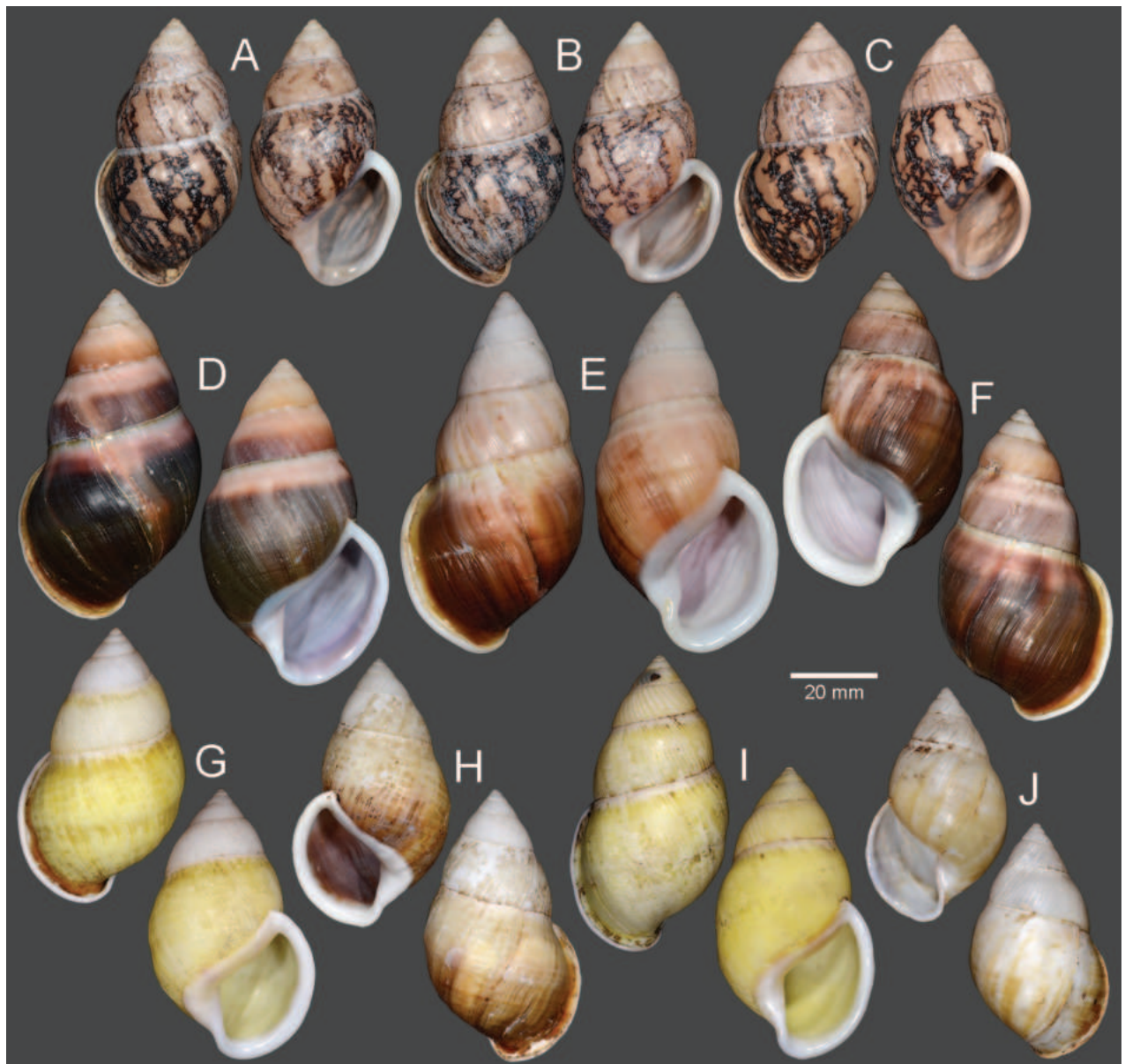


**Figure 8.** Shells of *Amphidromus* spp **A–C** *Amphidromus asperoides* sp. nov. from Ea Tu, Buon Ma Thuat city, Dak Lak, Vietnam **A** holotype (NMNS-8764-001) **B, C** paratypes (NMNS-8764-002 and NHMUK 20230613) **D–F** *Amphidromus bozhii* Wang, 2019 **D, E** specimens from Phu Hoa, Phu Yen, Vietnam (NMNS-8764-009, NMNS-8764-013) **F** specimen from Tuy Hoa, Phu Yen Vietnam (NMNS-8764-014) **G–J** *Amphidromus ingensoides* sp. nov. **G** holotype from Cu'Mta, Mdrak, Dak Lak, Vietnam (NMNS-8764-106) **H** paratype from Cu'Mta, Mdrak, Dak Lak, Vietnam (NHMUK 20230614) **I, J** paratypes from Hon Ba, Khanh Son, Khanh Hoa, Vietnam (NMNS-8764-107, NMNS-8764-106).

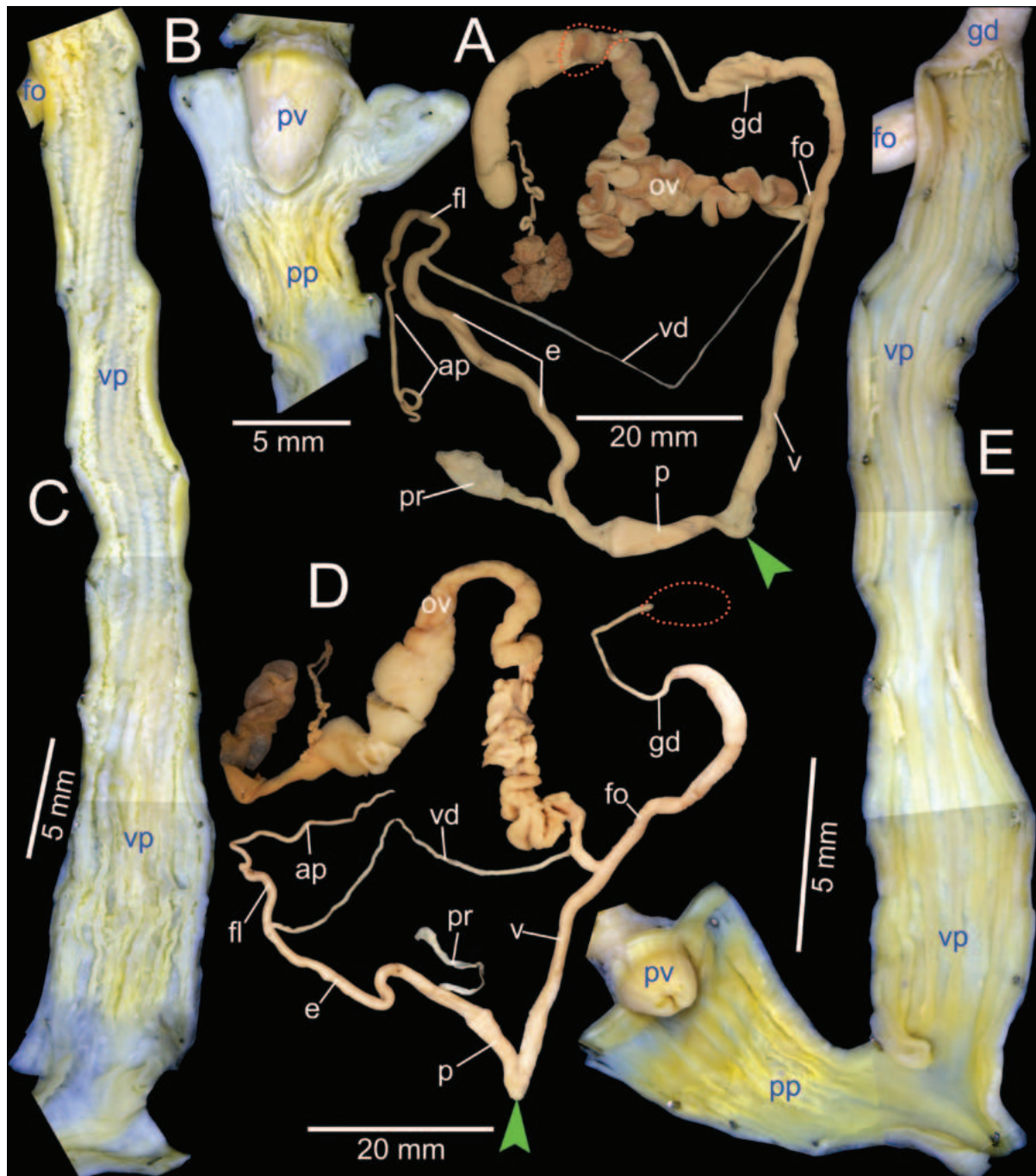


**Figure 9.** Genitalia of *Amphidromus* spp **A–C** *Amphidromus bozhii* Wang, 2019 from Tuy Hoa, Phu Yen, Vietnam (NMNS-8764-016), showing **A** general view of genitalia **B** interior structures of penis **C** Interior structures of vagina chamber **D, E** *Amphidromus placostylus* Möllendorff, 1900 from Dak Po, Gia Lai, Vietnam (NMNS-8764-217), showing **D** general view of genitalia **E** interior structures of penis and vagina chamber. Red dots indicate the shape of the missing gametolytic sac. Green arrows indicate the genital openings. Abbreviations: ap, appendix; e, epiphallus; fl, flagellum; fo, free oviduct; gd, gametolytic duct; ov, oviduct; p, penis; pp, penial pilaster; pr, penial retractor muscle; pv, penial verge; v, vagina; vd, vas deferens; vp, vaginal pilaster

oviduct compact, enlarged to form lobule alveoli (Fig. 9A). Internal wall of vagina possesses strong corrugated ridges near genital orifice, ridges become weaker corrugated vaginal pilasters, and swollen with irregularly shaped deep crenulations close to free oviduct opening (Fig. 9C).

**Haplotype network.** There were seven COI haplotypes of *A. bozhii* in this study, and the highest number of mutational steps in the COI minimum spanning network is ten (Fig. 10).

**Distribution.** This species is found in Phu Yen Province, Vietnam.

### ***Amphidromus placostylus* Möllendorff, 1900**

Figs 6D, 9D, E, 11, 12A, 13

*Amphidromus placostylus* Möllendorff, 1900a: 132. Type locality: Phuc-son [Phuc Son Commune, Tan Yen District, Bac Giang Province, Vietnam]. Pilsbry 1900: 178. Fischer and Dautzenberg 1904: 406. Laidlaw and Solem 1961: 529, 649–650. Richardson 1985: 38. Schileyko 2011: 51. Sutcharit et al. 2021: fig. 1f.

*Amphidromus (Amphidromus) placostylus*. Zilch 1953: 138, pl. 25, fig. 41.

*Amphidromus johnstanisici* Thach & Huber in Thach, 2017: 41, pl. 53, figs 657–663. Type locality: Kbang District, Gia Lai Province, Central Vietnam. Thach 2021: 65. syn. nov.

**Material examined.** VIETNAM: Dextral, **lectotype** of “*Amphidromus placostylus*”, SMF 7593 (Fig. 11A); dextral, **holotype** of “*Amphidromus johnstanisici*”, MNHN-IM-2000-33218 (Fig. 11B).

**Other material examined.** VIETNAM: 4D + 1S specimens, Dak Po District, Gia Lai Province, NMNS-8764-213–NMNS-8764-217 (Fig. 11C, D); 3D + 1S specimens, Kbang, Gia Lai Province, NMNS-8764-218–NMNS-8764-221 (Fig. 11E, F); 4D + 6S specimens, Hoai An, An Lao, Binh Dinh Province, NMNS-8764-222–NMNS-8764-231 (Fig. 11G–I); 1D specimen, Binh Dinh Province, NMNS-8764-232; 7D + 14S specimens, Hoai An district, Binh Dinh Province, NMNS-8764-233–NMNS-8764-253.

**Diagnosis.** Shell large and chirally dimorphic. Periostracum thick corneous with greenish brown radial streaks. Shell surface generally smooth. Genitalia with appendix.

**Differential diagnosis.** *Amphidromus placostylus* is similar to *A. schomburgki* (Pfeiffer, 1860) in having greenish to greenish brown radial streaks on periostracum, but *A. placostylus* has a larger shell (height up to nearly 80 mm) with a whitish apertural lip, and *A. schomburgki* exhibits a relatively smaller shell (height up to 58 mm) with a purplish apertural lip. *Amphidromus placostylus* is also similar to *A. cambojiensis* (Reeve, 1860) in having a relatively large shell and ovate to elongate conical shape, but *A. placostylus* possesses a thick greenish periostracum, uniform whitish shell ground colour, and whitish to dark brown inner side of outer wall. In comparison, *A. cambojiensis* possesses a thin corneous periostracum, with irregular brown to dark brown radial streaks on the shell ground colour, and a bright purplish pink or violet colour on the inner side of outer wall. *Amphidromus placostylus* is also recognised by a distinct clade in the molecular phylogeny (Fig. 2), with the closest *p*-distance to *A. bozhii* in COI (9.61%) and *A. ingens* in 16S (4.23%) (Table 2).

**Description.** **Shell** large (height 64.6–79.5 mm, width 37.4–42.4 mm), chirally dimorphic, solid, and ovate to elongate conical shape. Spire long conical with white colour; apex acute without black spot on tip. Whorls 6–7 convex; suture wide and depressed; last whorl ovate. Periostracum thick corneous or

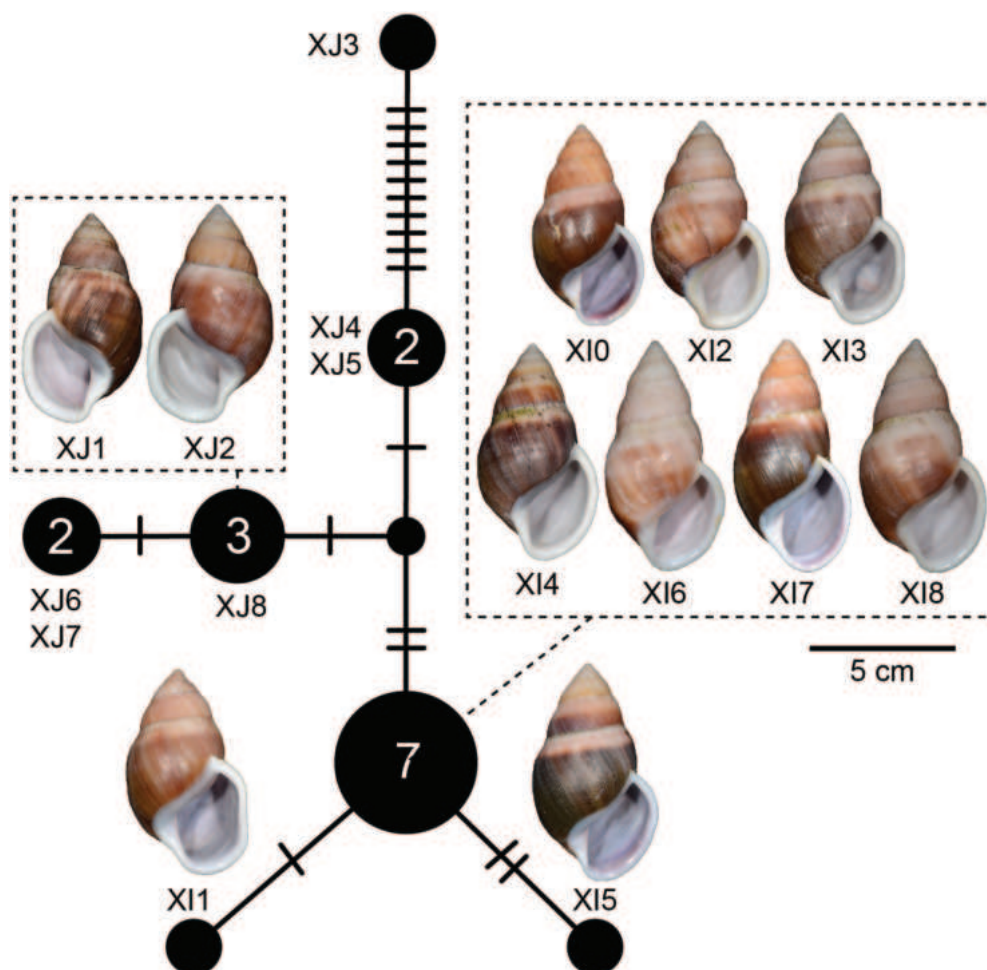


**Figure 10.** Mitochondrial COI haplotype minimum spanning networks of *Amphidromus bozhii* Wang, 2019. The size of each circle corresponds to the frequency of that haplotype, also shown as the number in that circle. The bars on the branches indicate the number of mutational steps between haplotypes. Specimen codes correspond to those in Table 1.

with oblique greenish to greenish brown radial streaks; varix usually absent. Shell surface generally smooth. Shell ground colour monochrome whitish or with dark brownish streaks (without periostracum). Parietal callus thickened and white. Aperture broadly ovate and inner side of outer wall with whitish to dark brown colour; peristome thickened, expanded, and reflexed but not attached to last whorl; lip whitish. Columella white, straight, or little twisted. Umbilicus imperforate.

**Radula.** Teeth arranged in anteriorly pointed V-shaped rows. Central tooth monocuspid and trapezoid-spatulate with truncated cusp. Lateral teeth bicuspid; endocone small, with wide notch and truncated to slightly curved cusp; ectocone large with curved to dull cusp. Lateral teeth gradually transformed to asymmetric tricuspid marginal teeth (Fig. 12A).

**Genital organs.** Atrium relatively short. Penis slender, conical, and short ~ 1/2 of vaginal length. Penial retractor muscle thin, long, inserting on epiphallus close to penis. Epiphallus long, slender tube. Flagellum long, extending from epiphallus and weakly coiled at its end. Appendix short, slender tube, 2× longer than flagellum, and approximately as long as epiphallus. Vas deferens slender tube passing from free oviduct and terminating at epiphallus-flagellum junction (Fig. 9D). Internal wall of penis corrugated, exhibiting series of weak

longitudinal penial pilasters nearly entire inner penis wall. Penial verge short conical, nearly smooth surface and with opening on the tip (Fig. 9E).

Vagina slender, long cylindrical, and ~ 2× longer than penis. Gametolytic duct enlarged cylindrical tube then abruptly tapering to slender tube terminally and connected to gametolytic sac (missing during dissection). Free oviduct short; oviduct compact, enlarged to form lobule alveoli (Fig. 9D). Internal wall of vagina possessing corrugated smooth surface ridges on nearly its entire inner wall; ridges becoming thinner vaginal pilasters in middle, and with little irregular shaped and crenulations close to free oviduct opening (Fig. 9E).

**Living specimens** with soft body morphology generally similar to *A. ingens*. Animals with dark reddish body covered with reticulated skin. Foot broad and long with uniform pale brown colour at foot margin. Head with reddish colour same as body. Upper and lower tentacles with reddish to orange in colour (Fig. 6D).

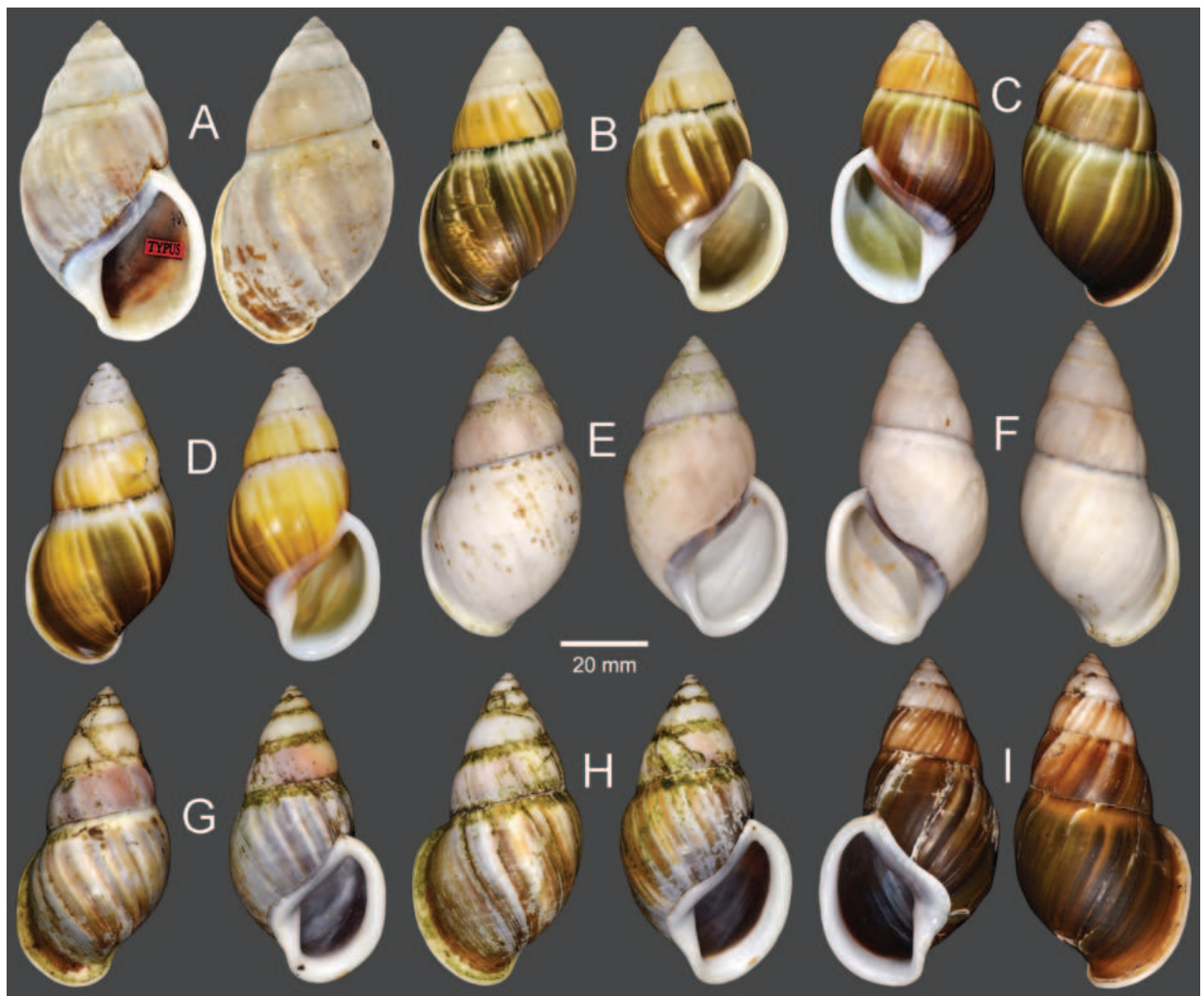


**Figure 11.** Shells of *Amphidromus placostylus* Möllendorff, 1900 **A** lectotype of "*Amphidromus placostylus*" (SMF 7593) **B** holotype of "*Amphidromus johnstanisici*" (MNHN-IM-2000-33218) **C, D** specimens from Dak Po, Gia Lai, Vietnam (NMNS-8764-213, NMNS-8764-215) **E, F** specimens from Kbang, Gia Lai, Vietnam (NMNS-8764-219, NMNS-8764-221) **G–I** specimens from Hoai An, An Lao, Binh Dinh, Vietnam (NMNS-8764-222, NMNS-8764-227, NMNS-8764-231). Credit: M Caballer, MNHN (**B**).

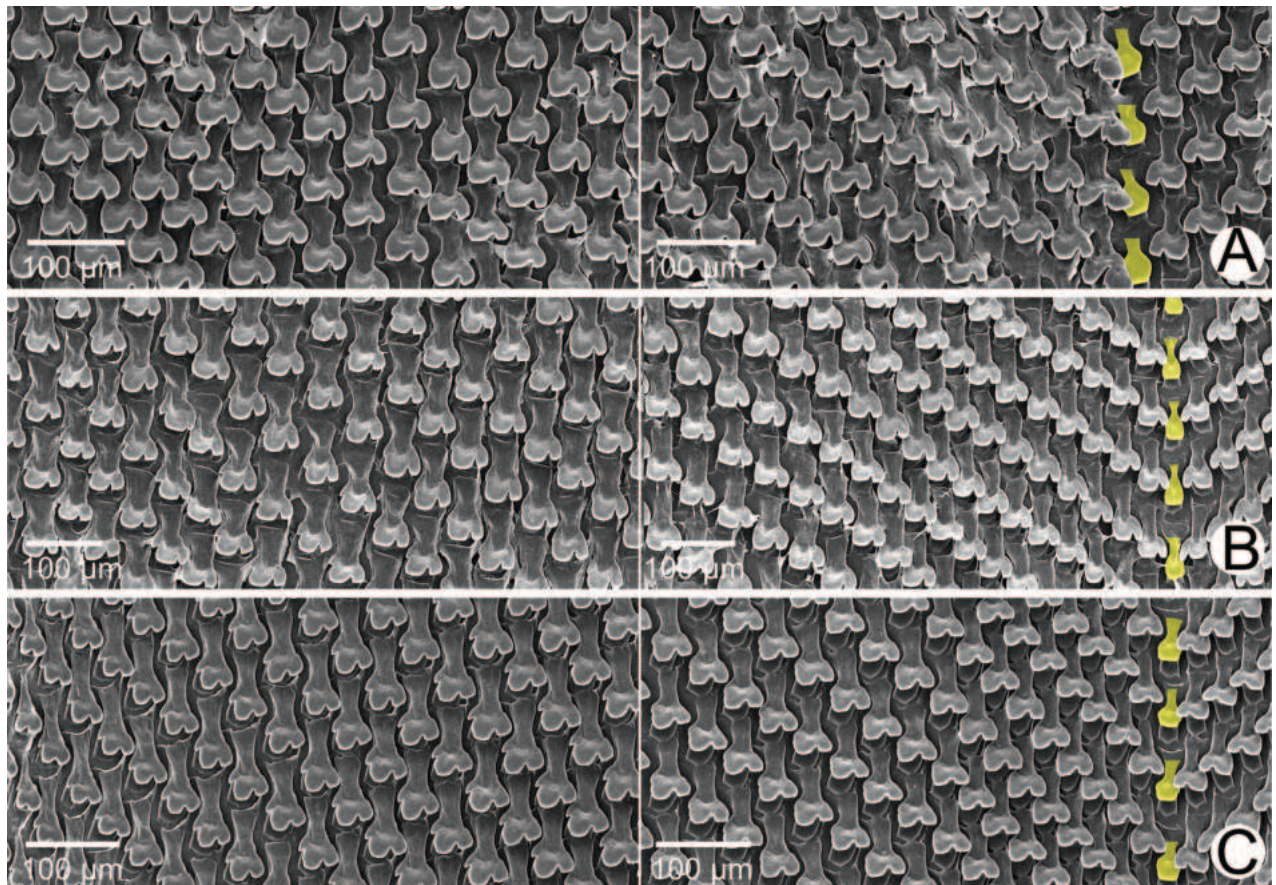


**Figure 12.** SEM images of the radula **A** *Amphidromus placostylus* Möllendorff, 1900 from Dak Po, Gia Lai, Vietnam (NMNS-8764-217) **B** *Amphidromus buelowi* Fruhstorfer, 1905 from Mount Singgalang, Sepuluh Koto, Tanah Datar Regency, West Sumatra, Indonesia (NMNS-8764-024) **C** *Amphidromus thachi* Huber, 2015 from Buon Don, Dak Lak, Vietnam (NMNS-8764-271). Central teeth are marked in yellow. The left and right images show the outer and inner sections of each radula, respectively.

**Distribution.** The distribution range of the species covers Bac Giang, Binh Dinh and Gia Lai provinces, Vietnam.

**Remarks.** As the original description did not explicitly designate a type or state that the description of this species was based on a single specimen (nor could this be inferred), the designation of a holotype by Zilch (1953) in fact constitutes a lectotype designation (ICZN 1999: Art. 74.6).

This species is known only from a single worn-out lectotype, and the remaining periostracum is only traceable behind the apertural lip. Later, Thach and Huber in Thach (2017) introduced *A. johnstanisici*, which is described to differ from *A. placostylus* by the presence of prominent subsutural bands, larger aperture, more voluminous body whorl with dark brown colour, and parietal wall not bordered by a black band. However, both type materials of *A. johnstanisici* and *A. placostylus*, and all the specimens examined herein, especially ones from the type locality of *A. johnstanisici*, possess both subsutural bands and a black band that borders the parietal wall to some extent. These specimens and the holotype of *A. johnstanisici* also match well with the lectotype of *A. placostylus* in shell and apertural shape, and the periostracum colour. Thus, *A. johnstanisici* is regarded herein as a junior subjective synonym of *A. placostylus*. The periostracum colour can vary from greenish to greenish brown in the younger adult

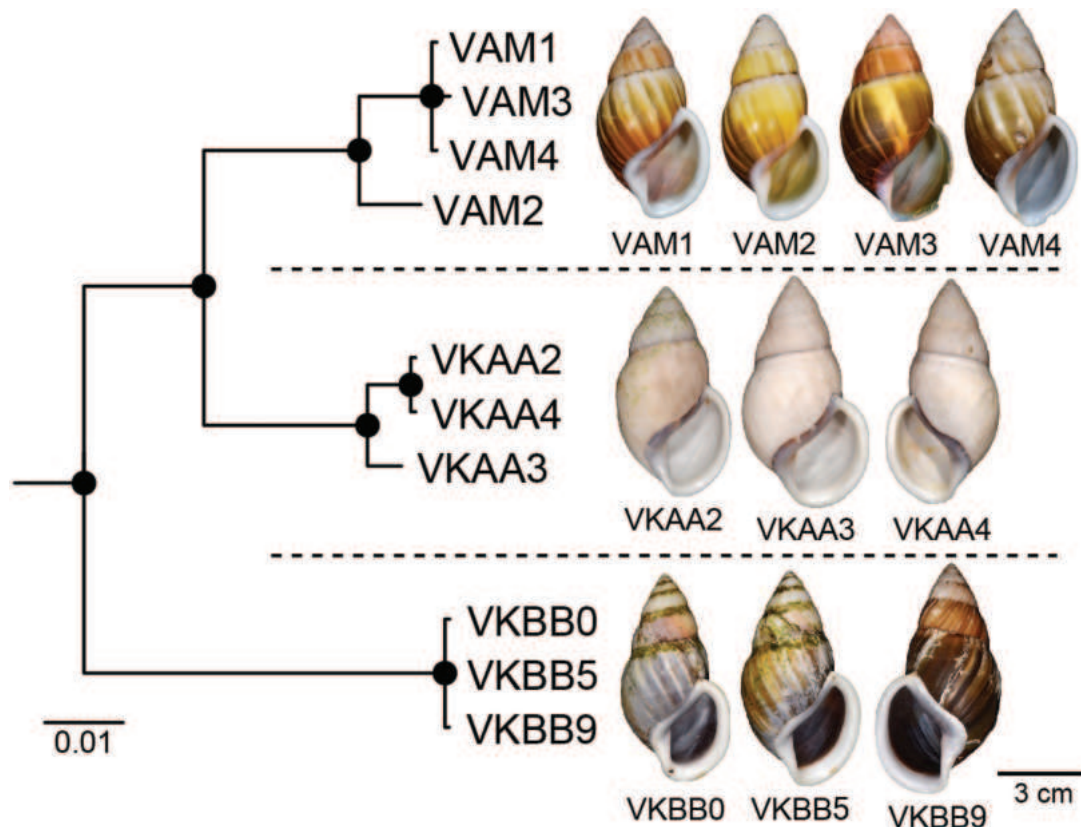


**Figure 13.** Bayesian phylogeny of *Amphidromus placostylus* Möllendorff, 1900 based on mitochondrial COI and 16S genes. Nodal support values are given as SH-aLRT/aBayes/ultra-fast bootstrap (IQ-TREE, ML)/posterior probability (Mr-Bayes, BI). An asterisk on each branch indicates a clade with all well-supported values (SH-aLRT  $\geq$  80%, aBayes  $\geq$  0.95, BS  $\geq$  95%, PP  $\geq$  0.95).

specimens (with thinner apertural lip), while the aged adult specimens (with thicker apertural lip) tend to have yellowish brown to eroded periostracum.

This species also exhibits a prominent population genetic structure, where specimens from the same collecting locality form its own clade (Fig. 13). The COI intraspecific distance among all *A. placostylus* specimens is 5.47%, which is the third highest distance of all *Amphidromus* species in this study. This value is higher than the optimum intra/interspecific threshold value of 4% for stylomatophoran land snails (Davison et al. 2009). In addition, the 16S intraspecific distance among all *A. placostylus* specimens is 3.14%, which is the second highest distance of all *Amphidromus* species in this study. Although each clade constitutes the specimens with the same inner shell colour (Fig. 13), all specimens still have other congruent shell morphology as stated above. We thus refrain from treating each pool of samples from the same collecting locality as a distinct taxon, before more specimens from each locality are critically examined.

***Amphidromus ingensoides* Jirapatrasilp & Lee, sp. nov.**

<https://zoobank.org/BB594FC7-4E23-432C-AAA9-FE4C27BBB633>

Figs 6E, F, 8G–J, 14A–C

**Diagnosis.** Shell large and chirally dimorphic. Shell surface with coarse growth lines crossed by weak spiral ridges. Genitalia with appendix.

**Differential diagnosis.** The new species differs from the closely related *A. ingens* and *A. bozhii* in having a generally rounded last whorl, and coarse growth lines crossed with weak spiral ridges. In comparison, the two latter species having a depression area below suture and prominent blunt or keeled on periphery of the last whorl, and having only irregular growth lines on the shell surface. In addition, this new species is recognised by a distinct clade in the molecular phylogeny (Fig. 2), with the closest *p*-distance to *A. bozhii* in COI (9.99%) and *A. ingens* in 16S (4.19%) (Table 2).

**Etymology.** The specific epithet *ingensoides* is from *ingens*, and the suffix *-oideus*, meaning 'like or resembling'. This name refers to the resemblance in shell morphology of the new species to the nominal species *A. ingens*.

**Type material. Holotype.** VIETNAM: dextral, shell height 62.1 mm, shell width 36.9 mm, with 6½ whorls, 13 Dec. 2016, coll. A. N. Pham (NMNS-8764-105, Fig. 8G). **Paratypes.** VIETNAM: 1S specimen (NHMUK 20230614, Fig. 8H) from the type locality, 19 Sep. 2016, coll. A. N. Pham; 1D + 1S specimens, Hon Ba, Khanh Son District, Khanh Hoa Province, NMNS-8764-106, NMNS-8764-107, 31 Mar. 2017, coll. A. N. Pham (Fig. 8I, J).

**Type locality.** VIETNAM: Cu'Mta ward, Mdrak District, Dak Lak Province, 12°42'22.9"N, 108°45'13.9"E.

**Description. Shell** large (height 54.3–67.0 mm, width 32.8–36.8 mm), chirally dimorphic, solid, and ovate conical shape. Spire long conical to elongate conical, apex acute without black spot on tip. Whorls 5–7 convex; suture wide and depressed; last whorl well rounded to slightly angulated. Periostracum brownish to thin corneous; varix usually absent. Shell surface generally with coarse and irregular growth lines crossed by weak spiral ridges. Shell colour variable: monochrome (whitish, yellowish, tinted pink) to stained with dark brown to blackish below periphery. Parietal callus thickened and white, dilated at umbilical area. Aperture broadly ovate; inner side of outer wall with yellow or dark brown to blackish colour. Peristome thickened, expanded and reflexed but not attached to last whorl, lip whitish. Columella white, straight, or little twisted. Umbilicus imperforate.

**Genital organs.** Atrium relatively short. Penis slender, conical, and short ~ 1/3 of vaginal length. Penial retractor muscle thickened, short and inserting on epiphallus close to penis. Epiphallus long, slender tube, coiled and twisted upon itself. Flagellum long, extending from epiphallus and terminating in slightly enlarged folded coil. Appendix short, slender tube, ~ 2× longer than flagellum, and approximately as long as epiphallus. Vas deferens slender tube passing from free oviduct and terminating at epiphallus-flagellum junction (Fig. 14A). Internal wall of penis corrugated, exhibiting series of prominent and swollen longitudinal penial pilasters forming fringe around penial wall, and with strong roughly surface around base of penial verge. Penial verge short conical with weak roughly surface, and with opening at the tip (Fig. 14B).

Vagina slender, long cylindrical, and ~ 3× longer than penis. Gametolytic duct enlarged cylindrical tube then abruptly tapering to slender tube terminally and connected to gametolytic sac (missing during dissection). Free oviduct short; oviduct compact and enlarged to form lobule alveoli (Fig. 14A). Internal wall of vagina possessing corrugated and deep crenelated ridges on nearly its entire vagina wall; ridges slightly smooth surface near genital orifice then becoming prominent vaginal pilasters in middle and close to free oviduct opening (Fig. 14C).

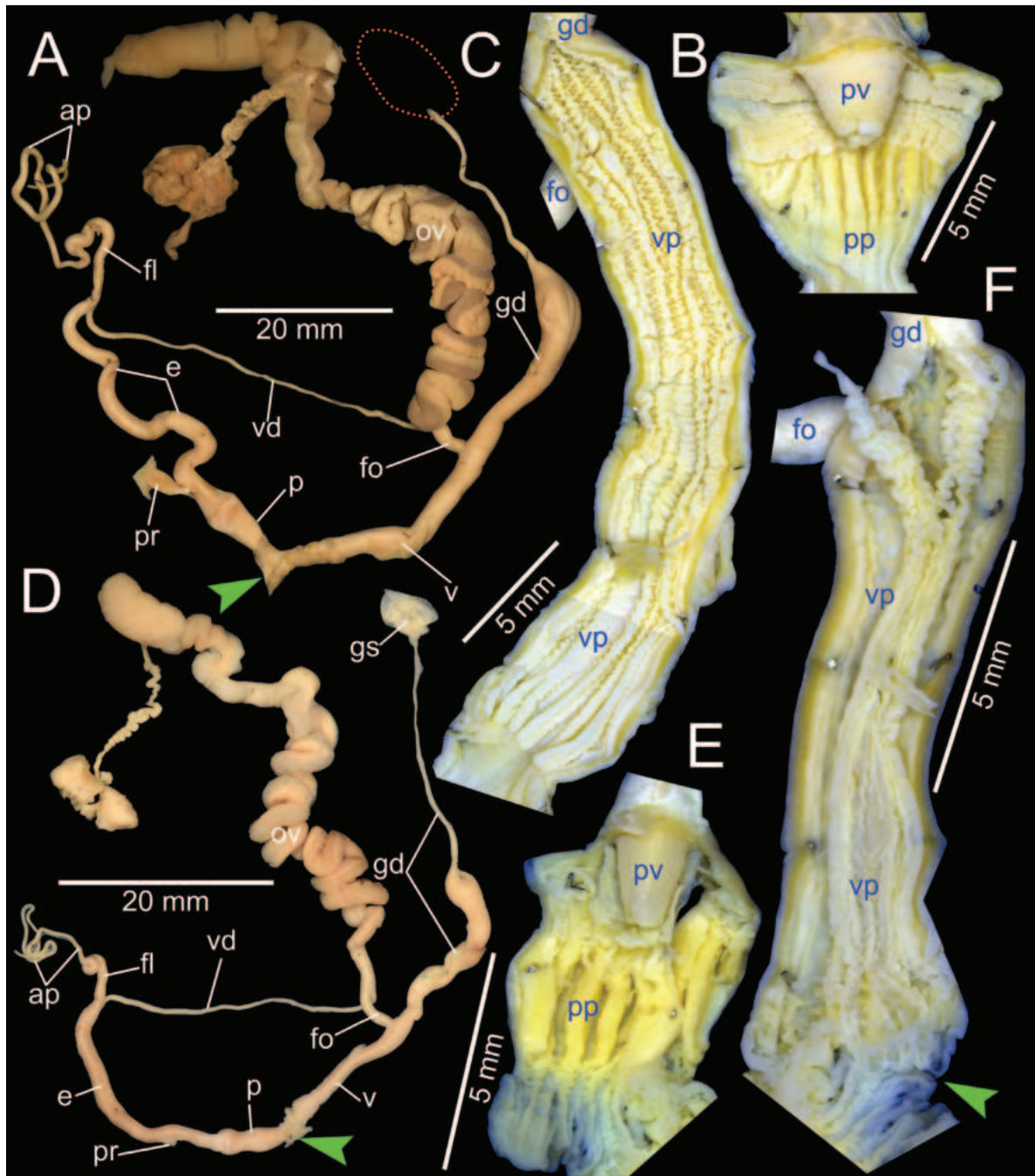


**Figure 14.** Genitalia of *Amphidromus* spp **A–C** *Amphidromus ingensoides* sp. nov. from Hon Ba, Khanh Son, Khanh Hoa, Vietnam (NMNS-8764-107), showing **A** general view of genitalia **B** interior structures of penis **C** interior structures of vagina chamber **D–F** *Amphidromus buelowi* Fruhstorfer, 1905 from Nha Trang, Khanh Hoa, Vietnam (NMNS-8764-031), showing **D** general view of genitalia **E** interior structures of penis **F** interior structures of vagina chamber. Red dots indicate the shape of the missing gametolytic sac. Green arrows indicate the genital openings. Abbreviations: ap, appendix; e, epiphallus; fl, flagellum; fo, free oviduct; gd, gametolytic duct; gs, gametolytic sac; ov, oviduct; p, penis; pp, penial pilaster; pr, penial retractor muscle; pv, penial verge; v, vagina; vd, vas deferens; vp, vaginal pilaster

**Living specimens** with soft body morphology generally similar to *A. ingens*. Animals with pale yellowish body covered with reticulated skin, anterior body usually with dark reticulated strip dorsally. Foot broad and long, and with narrow and orange colour stripe above foot margin. Head with orange patch covering tentacles. Upper and lower tentacles orange to paler in colour (Fig. 6E, F).

**Distribution.** This species is found in Dak Lak and Khanh Hoa provinces, Vietnam.

**Remarks.** As a small number of specimens were dissected, this new species seems to have a vagina shorter than penis + epiphallus length, while *A. ingens* and *A. bozhii* have a vagina almost as long as penis + epiphallus. In addition, *A. ingensoides* sp. nov. possesses a longer appendix than the geographically closer species *A. ingens* from M'drak District, Dak Lak Province.

### ***Amphidromus buelowi* Fruhstorfer, 1905**

Figs 6H, I, 12B, 14D–F, 15, 16

*Amphidromus (Goniodromus) buelowi* Fruhstorfer, 1905: 83–84, pl. 1, fig. 2. Type locality: West-Sumatra. Rolle 1908: 67. Laidlaw and Solem 1961: 587, 606, fig. 37.

*Amphidromus buelowi*. Dautzenberg and Fischer 1906: 365–366, pl. 8, figs 10–12. Degner 1928: 360. Benthem Jutting 1959: 165.

*Amphidromus (Goniodromus) asper* Haas, 1934: 96, figs 11, 12. Type locality: Süd-Annam, 120 km von der Küste, auf dem Wege zum Plateau von Lang-Bian, zw. 600–1000 m [South Annam, 120 km from the coast, on the way to the plateau of Lang-Bian, between 600–1000 m]. Laidlaw and Solem 1961: 588, 601. Zilch 1953: 138, pl. 25, fig. 44. syn. nov.

*Amphidromus asper*. Schileyko 2011: 49. Páll-Gergely et al. 2020: 49, 51, fig. 15. Thach 2020a: pl. 76, fig. 893 right.

*Amphidromus bulowi* [sic]. Huber 2015: figs 9, 10. Sutcharit et al. 2015: 61, fig. 4e.

*Amphidromus (Goniodromus) bulowi bulowi* [sic]. Parsons and Abbas 2016: 240–242, figs 4 bottom, 5, 6a, b, d, 7.

*Amphidromus franzhuberi* Thach, 2016: 64–65, fig. 42; pl. 23, figs 315–319. Type locality: along the border of Nha Trang outskirts and Khanh Vinh District, Khanh Hoa Province (Central Vietnam). Páll-Gergely et al. 2020: 50, fig. 14. Thach 2020a: 58, pl. 76, fig. 893 left. Thach 2021: 60 syn. nov.

*Amphidromus buelowi*. Páll-Gergely et al. 2020: fig. 16.

**Material examined.** INDONESIA: Sinistral, **lectotype** of “*Amphidromus buelowi*”, NHMUK 1910.12.30.98 (Fig. 15A). VIETNAM: Dextral, **holotype** of “*Amphidromus asper*”, SMF 7762 (Fig. 15B). Dextral, **holotype** of “*Amphidromus franzhuberi*”, MNHN-IM-2000-31892 (Fig. 15C).

**Other material examined.** INDONESIA: 2D specimens, Padang Sökeli, Singalang, RBINS I.G. 10591/1–2 (Fig. 15D); 4D specimens, Mount Singalang, Sepuluh Koto, Tanah Datar Regency, West Sumatra, NMNS-8764-022–NMNS-8764-025 (Fig. 15E).

VIETNAM: 2D specimens, Lang-Biang, Annam, RBINS I.G. 10591/3–4 (Fig. 15F); 2D specimens, Lang-Biang plateau, Lac Duong District, Lam Dong Province, NMNS-8764-026, NMNS-8764-027 (Fig. 15G); 6D + 1S specimens, Nha Trang, Khanh Hoa Province, NMNS-8764-028–NMNS-8764-034 (Fig. 15H, I).

**Diagnosis.** Shell large and chirally dimorphic. Shell colour with irregularly zigzag of dark radial streaks, and dark triangular blotches. Aperture elliptical ovate with more or less prominent anterior notch and umbilical hump; twisted columella plait. Genitalia with appendix.



**Figure 15.** Shells of *Amphidromus buelowi* Fruhstorfer, 1905 **A** lectotype of “*Amphidromus buelowi*” (NHMUK 1910.12.30.98) **B** holotype of “*Amphidromus asper*” (SMF 7762) **C** holotype of “*Amphidromus franzhuberi*” (MNHN-IM-2000-31892) **D** specimen from Padang Sökeli, Singalang, Indonesia (RBINS I.G. 10591) **E** specimen from Mount Singgalang, Sepuluh Koto, Tanah Datar Regency, West Sumatra, Indonesia (NMNS-8764-025) **F** specimen from Lang-Biang, Annam, Vietnam (RBINS I.G. 10591) **G** specimen from Lang-Biang plateau, Lac Duong, Lam Dong, Vietnam (NMNS-8764-027) **H, I** specimen from Nha Trang, Khanh Hoa, Vietnam (NMNS-8764-030, NMNS-8764-031). Credit: H. Taylor, NHM (**A**), M. Caballer, MNHN (**C**), RBINS (**D, F**).

**Differential diagnosis.** *Amphidromus buelowi* differs from the similar species *A. asperoides* sp. nov. in having a distinct twisted columella plait, a prominent umbilical hump encircling columellar area, and an apertural notch projecting anteriorly. In contrast, *A. asperoides* sp. nov. possesses a straight columella, and without apertural notch and umbilical hump. In addition, on the soft body of living snail, the entire body of *A. buelowi* is reddish orange, while *A. asperoides* sp. nov. exhibits a uniform brownish yellow to pale brown body. *Amphidromus buelowi* is also recognised by a distinct clade in the molecular phylogeny (Fig. 2), with the closest *p*-distance to *A. ingens* in COI (12.23%) and *A. asperoides* sp. nov. and *A. ingens* in 16S (4.61%) (Table 2).

**Description. Shell** large (height 45.3–51.1 mm, width 26.2–26.6 mm), chirally dimorphic, solid, and ovate conical. Spire conical with white or pale colour; apex acute without black spot on tip. Whorls 6–7 little convex to smooth; suture wide and shallow; last whorl well rounded to slightly elongated and with more or less prominent umbilical hump. Periostracum thin corneous; varices generally present. Shell ground colour pale yellowish, decorated with irregular zigzag of dark radial streaks, and dark triangular blotches connected with dark streaks. Parietal callus thickened, white and much thinner in central area. Aperture elliptical ovate; with more or less anterior notch; inner side of outer wall whitish colour; peristome thickened, expanded, and reflexed but not attached to last whorl; lip whitish. Columella white, straight and with distinct twisted plait. Umbilicus imperforate.

**Radula.** Teeth arranged in anteriorly pointed V-shaped rows. Central tooth monocuspid and slightly elongate-spatulate teeth with truncated cusp. Lateral teeth bicuspid; endocone curved with wide notch and blunt cusp; ectocone large with truncated cusp. Lateral teeth gradually transformed to asymmetric tricuspid marginal teeth. Outermost teeth with small and curved cusp on ectocone, and endocone and mesocone with curved cusps (Fig. 12B).

**Genital organs.** Atrium relatively short. Penis slender, conical, and nearly as long as vagina. Penial retractor muscle inserting on epiphallus close to penis. Epiphallus long, slender tube, and almost same diameter as penis. Flagellum short, extending from epiphallus and terminating in slightly enlarged folded coil. Appendix short, thin tube, 3× longer than flagellum, and approximately as long as epiphallus. Vas deferens slender tube passing from free oviduct and terminating at epiphallus-flagellum junction (Fig. 14D). Internal wall of penis corrugated, exhibiting series of thickened and swollen longitudinal penial pilasters forming fringe around penial wall, and with weaker folds around base of penial verge. Penial verge short conical with nearly smooth surface (Fig. 14E).

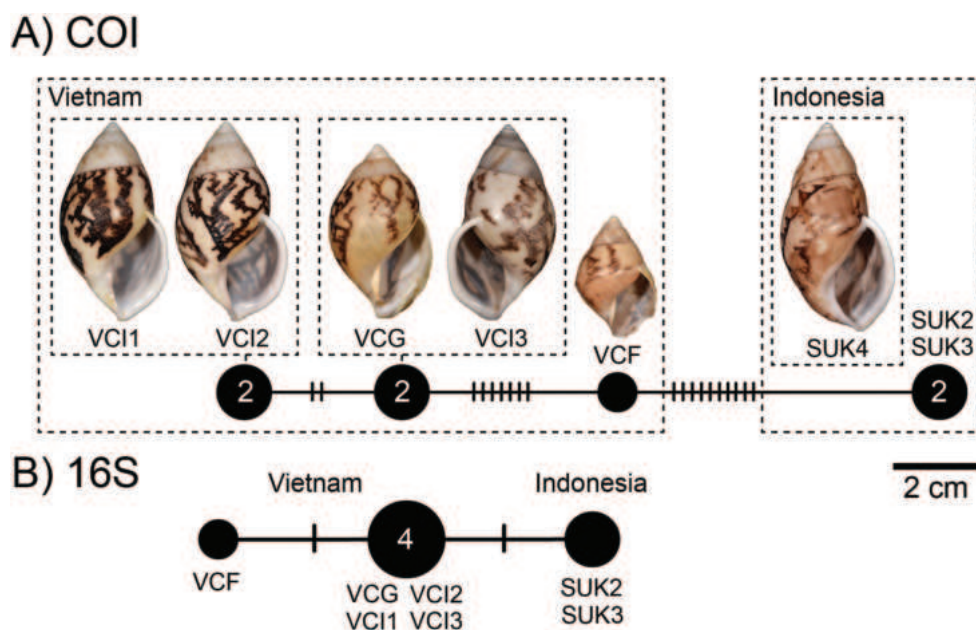


**Figure 16.** Mitochondrial haplotype minimum spanning networks of *Amphidromus buelowi* Fruhstorfer, 1905 **A** COI and **B** 16S rRNA. The size of each circle corresponds to the frequency of that haplotype, also shown as the number in that circle. The bars on the branches indicate the number of mutational steps between haplotypes. Specimen codes correspond to those in Table 1.

Vagina slender, long cylindrical, and  $\sim 2\times$  longer than penis. Gametolytic duct enlarged cylindrical tube then abruptly tapering to long, slender tube terminally, connected to elongate gametolytic sac. Free oviduct short; oviduct compact, enlarged to form lobule alveoli (Fig. 14D). Internal wall of vagina possessing corrugated ridges near genital orifice; ridges becoming thinner and smooth longitudinal vaginal pilasters in middle, swollen with irregularly shaped deep crenulations close to free oviduct opening (Fig. 14F).

**Living specimens** with soft body morphology generally similar to *A. ingens*. Animals with reddish orange body covered with reticulated skin. Lateral of body vary from yellowish (in younger specimen) to dark reddish orange colour (older specimens). Foot broad and long with reddish orange colour near foot sole margin. Head and dorsal of anterior body with reddish orange to dark colour. Upper tentacles pale reddish orange to brownish; lower tentacles short and paler in colour (Fig. 6H, I).

**Haplotype network.** There was a total of four COI haplotypes (Fig. 16A) and three 16S haplotypes (Fig. 16B) of *A. buelowi* in this study, and the highest numbers of mutational steps in the COI and 16S minimum spanning networks are ten and one, respectively.

**Distribution.** The species has a widely disjunct distribution: one in Mount Singgalang, West Sumatra, Indonesia, and some localities in Khanh Hoa and Lam Dong provinces, South Vietnam.

**Remarks.** This species was originally described by Fruhstorfer (1905) from four chirally dimorphic specimens from West Sumatra. Fruhstorfer (1905) also indicated that there was a similar species collected on the way to the Lang-Bian plateau,  $\sim 120$  km inland from the coast in southern Vietnam. He sent one specimen from this locality to O.F. von Möllendorff, who did not describe or taxonomically treat this specimen any further. Later, Haas (1934), recognising that there were some differences in shell characters to *A. buelowi*, described this particular specimen (now deposited in SMF) as a new species, *A. asper*. Thach (2016) also described a similar species, *A. franzhuberi* from the border of Nha Trang, Vietnam, which is described to differ from *A. buelowi* in having a broader shell shape, more swollen body whorls, a less excavated base, a more inflated spire, a rounded anterior end of the outer lip, and monomorphic dextrality (just from four type series). However, Thach (2016) did not compare with *A. asper* from the nearby area. In this study, the samples from Nha Trang exhibit dimorphic chirality (the specimen lot containing both sinistral and dextral shell coiling; Fig. 15H, I), and upon examining the type specimens of *A. asper* and *A. franzhuberi*, they agree well with the type specimen of *A. buelowi* in having the common diagnostic traits of a distinct twisted columella plait, a prominent umbilical hump, and a distinct apertural notch. The molecular phylogeny also revealed that all specimens from Mount Singgalang, West Sumatra, Indonesia, and Lang-Biang plateau and Nha Trang, Vietnam belong to the same clade. The mutational steps between Indonesian and Vietnamese specimens are only ten and one in the COI and 16S haplotype networks, respectively (Fig. 16). Based on the phylogenetic analyses and the common morphological diagnostics, we therefore treat *A. asper* and *A. franzhuberi* as junior subjective synonyms of *A. buelowi*.

Bülow (1905) introduced the monotypic subgenus *Goniodromus* to include *A. buelowi*, based on a less ovate aperture with an apertural notch projecting anteriorly. Later, Laidlaw and Solem (1961), although with doubt, listed *Go-*

*niodromus* as one of the three subgenera of *Amphidromus*, and included two more species, *A. asper* and *A. mirandus* Bavay & Dautzenberg, 1912. Another species, *A. thachi*, also possesses an aperture with prominent anterior notch (Fig. 17). However, these three species, *A. buelowi* (and its synonyms *A. asper* and *A. franzhuberi*), *A. thachi*, and *A. mirandus* did not together form a clade (Fig. 2; C-TL, unpublished data), revealing that an apertural anterior notch is not a shared derived character. Thus, the subgenus *Goniodromus* is regarded herein as a junior subjective synonym of the subgenus *Amphidromus*.

### ***Amphidromus thachi* Huber, 2015**

Figs 6J, 12C, 17, 18A–D, 19

*Amphidromus thachi* Huber, 2015: 29–30, figs 1–8. Type locality: outskirts of Nha Trang area, about 30 km southeast of Nha Trang city (Cam Lam District, Khanh Hoa Province, central Vietnam), at some distance from the village and the National Road No 1A. Thach 2017: 47–48, pl. 53, fig. 668. Thach 2018: pl. 70, figs 838, 839. Thach 2021: 79.

*Amphidromus thachi crisi* Thach, 2018: 63–64, pl. 70, figs 833–837. Type locality: Lac Duong District, Lam Dong Province, South Vietnam. Thach 2021: 79.

**Material examined.** VIETNAM: Dextral, **holotype** of “*Amphidromus thachi*”, RBINS MT.3381 (Fig. 17A).

**Other material examined.** VIETNAM: 1D + 1S specimens, fin de la route de Hon Ba (chalets de Yersin), Commune de Suoi Cat, Province de Khanh Hoa, Vietnam, MNHN- IM-214-6873 (Fig. 17B, C); 1D specimen, réserve de Hon Ba, près du chalet de Yersin, Commune de Suoi Cat, Province de Khanh Hoa, Vietnam, MNHN- IM-214-6874; 3D + 1S specimens, Vinh Thanh town, Binh Dinh Province, NMNS-8764-266–NMNS-8764-269 (Fig. 17D); 1D + 1S specimens, Buon Don District, Dak Lak Province, NMNS-8764-270, NMNS-8764-271 (Fig. 17E); 1S specimen, Da Lat city, Lam Dong Province, NMNS-8764-272 (Fig. 17F); 2D specimens, Krong Bong, Dak Lak Province, NMNS-8764-273, NMNS-8764-274; 2D specimens, Lac Duong District, Lam Dong Province, NMNS-8764-264, NMNS-8764-265 (Fig. 17G, H).

**Diagnosis.** Shell medium and chirally dimorphic. Aperture obliquely elliptical with prominent anterior notch; columella bending anteriorly. Parietal callus, lip and columella whitish or with dark brown. Genitalia with appendix.

**Differential diagnosis.** *Amphidromus thachi* is unique compared to all Vietnamese species reported by Schileyko (2011) in having a distinct shell shape, possessing an obliquely elliptical aperture with a prominent anterior notch, a columella bending anteriorly, and whitish or dark brown parietal callus, lip and columella. This type of shell form is similar to that of *Pseudopartula* Pfeiffer, 1856 (Bentham Jutting 1950). *Amphidromus thachi* is also recognised by a distinct clade in the molecular phylogeny (Fig. 2), with the closest *p*-distance to *A. asperoides* sp. nov. in both COI (12.69%) and 16S (6.22%) (Table 2).

**Description.** **Shell** medium (height 25.0–30.0 mm, width 17.0–18.5 mm), chirally dimorphic, thin to slightly thickened, and conical. Spire short conical with white or pale colouration; apex acute without black spot on tip. Whorls 6–7 little convex to smooth; suture wide and shallow; last whorl well

rounded to slightly elongated and with less prominent umbilical hump. Periostracum thin corneous; varices absent. Shell colour uniform whitish to pale cream; subsutural band opaque white. Parietal callus thickened, whitish and translucent or dark to dark brown. Aperture elliptical to obliquely elliptical with prominent anterior notch; inner side of outer wall whitish; peristome thickened, slightly expanded not reflected; lip whitish or with dark to dark brown. Columella whitish or dark, shortly straight then bending anteriorly. Umbilicus imperforate.

**Radula.** Teeth arranged in anteriorly pointed V-shaped rows. Central tooth monocuspid and spatulate with truncated cusp. Lateral teeth bicuspid; endocone slightly smaller than ectocone, curved, with wide notch and dull cusp; ectocone large with curved to dull cusp. Lateral teeth gradually transformed to asymmetric tricuspid marginal teeth. Outermost teeth with small and curved cusp on ectocone; endocone and mesocone with curved cusps (Fig. 12C).

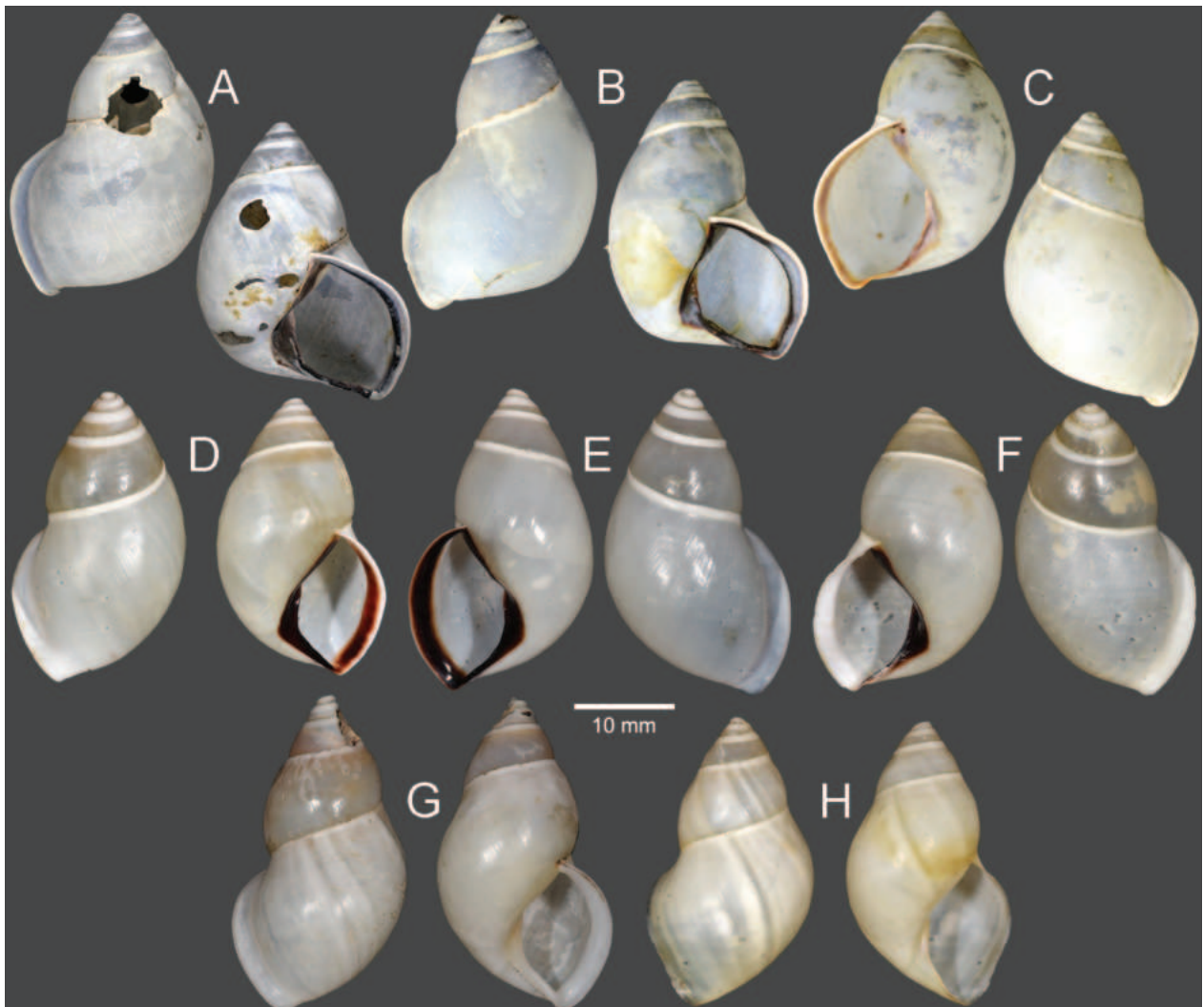


**Figure 17.** Shells of *Amphidromus thachi* Huber, 2015 **A** holotype of “*Amphidromus thachi*” (RBINS MT.3381) **B, C** specimens from fin de la route de Hon Ba (chalets de Yersin), Commune de Suoi Cat, Province de Khanh Hoa, Vietnam (MNHN-IM-214-6873) **D** specimen from Vinh Thanh, Binh Dinh, Vietnam (NMNS-8764-267) **E** Specimen from Buon Don, Dak Lak, Vietnam (NMNS-8764-271) **F** specimen from Da Lat, Lam Dong, Vietnam (NMNS-8764-272) **G, H** specimens from Lac Duong, Lam Dong, Vietnam (NMNS-8764-265, NMNS-8764-264). Credit: T. Backeljau and S. Yves, RBINS (**A**), B. Páll-Gergely (**B, C**).

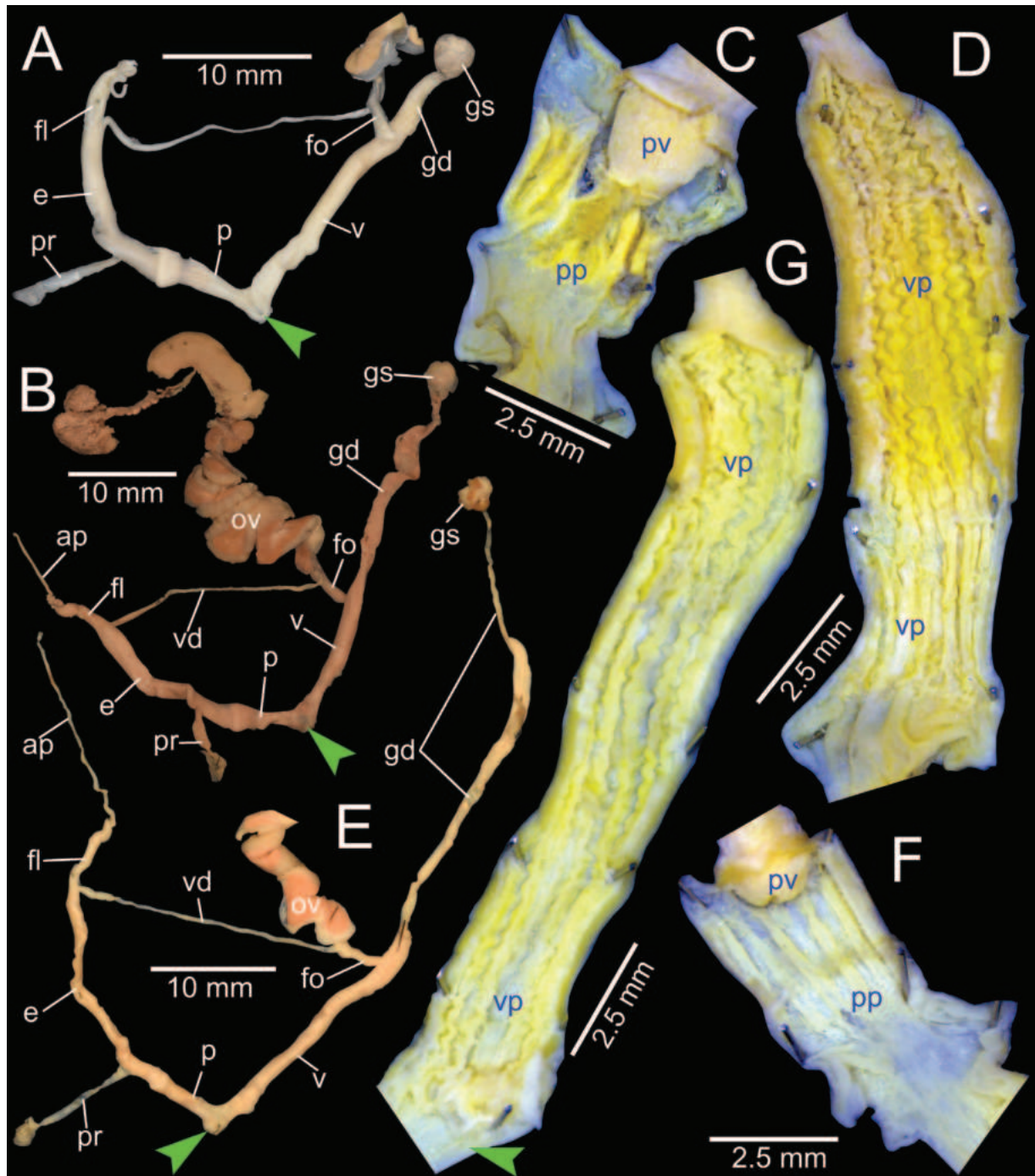


**Figure 18.** Genitalia of *Amphidromus* spp **A–D** *Amphidromus thachi* Huber, 2015 **A** general view of genitalia of specimen from Krong Bong, Dak Lak, Vietnam (NMNS-8764-274) **B–D** specimen from Buon Don, Dak Lak, Vietnam (NMNS-8764-271), showing **B** general view of genitalia **C** interior structures of penis **D** interior structures of vagina chamber **E–G** *Amphidromus metabletus* Möllendorff, 1900 from Nha Trang, Khanh Hoa, Vietnam (NMNS-8764-130), showing **E** general view of genitalia **F** interior structures of penis **G** interior structures of vagina chamber. Green arrows indicate the genital openings. Abbreviations: ap, appendix; e, epiphallus; fl, flagellum; fo, free oviduct; gd, gametolytic duct; gs, gametolytic sac; ov, oviduct; p, penis; pp, penial pilaster; pr, penial retractor muscle; pv, penial verge; v, vagina; vd, vas deferens; vp, vaginal pilaster.

**Genital organs.** Atrium relatively short. Penis slender, conical, and short, ~ 1/2 of vaginal length. Penial retractor muscle thickened and inserting on epiphallus close to penis. Epiphallus long, slender tube, almost same diameter as penis. Flagellum short, extending from epiphallus and terminating in weakly coiled.

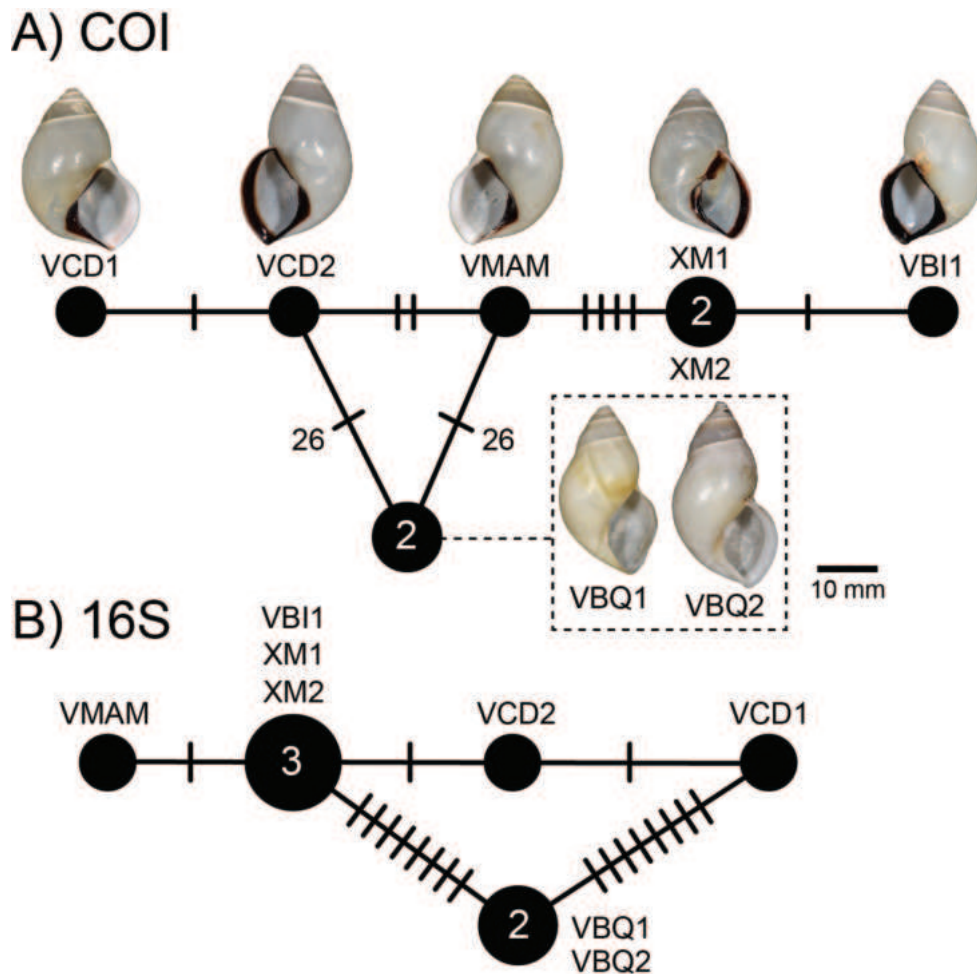


**Figure 19.** Mitochondrial haplotype minimum spanning networks of *Amphidromus thachi* Huber, 2015 **A** COI and **B** 16S rRNA. The size of each circle corresponds to the frequency of that haplotype, also shown as the number in that circle. The bars on the branches indicate the number of mutational steps between haplotypes. Specimen codes correspond to those in Table 1.

Appendix short, slender tube, similar length with flagellum, and ~ 1/2 of epiphallus length. Vas deferens slender tube passing from free oviduct and terminating at epiphallus-flagellum junction (Fig. 18A, B). Internal wall of penis corrugated, exhibiting series of thickened and smooth surfaced longitudinal penial pilasters forming fringe around penial wall, and with nearly smooth wall around base of penial verge. Penial verge short conical with smooth surface (Fig. 18C).

Vagina slender, cylindrical, and ~ 2× longer than penis. Gametolytic organ relatively short than other congeners: gametolytic duct shorter to slightly longer than vagina, cylindrical tube, then tapering to short, slender tube terminally; gametolytic sac globular shape. Free oviduct short; oviduct compact, enlarged to form lobule alveoli (Fig. 18A, B). Internal wall of vagina possessing smooth longitudinal ridges near genital orifice; ridges becoming stronger and corrugated vaginal pilasters with swollen, irregular shaped and deep crenulations (Fig. 18D).

**Living specimens** with soft body morphology generally similar to *A. ingens*. Animals with whitish to creamy body covered with reticulated skin. Foot broad and long with uniform whitish to creamy colouration to posterior tail. Head with whitish or sometimes with yellowish colour. Upper tentacles drumstick-shaped, greyish to brownish, with dark eyespots on tentacular tips; lower tentacles short and greyish in colour (Fig. 6J).

**Haplotype network.** There was a total of six COI haplotypes (Fig. 19A) and five 16S haplotypes (Fig. 19B) of *A. thachi* in this study, and the highest numbers of mutational steps in the COI and 16S minimum spanning networks are 26 and eight, respectively.

**Distribution.** The distribution range of this species covers Binh Dinh, Dak Lak, Khanh Hoa, and Lam Dong provinces, Vietnam.

**Remarks.** This species was originally described by Huber (2015) from outskirts of Nha Trang, Vietnam. Later, Thach (2018) described another subspecies from Lac Duong, Lam Dong, Vietnam as *A. thachi krisi*, which was different from the nominotypical subspecies in having a totally white lip. Based on this study, the specimens having a totally white lip from Lac Duong, Lam Dong constitutes a distinct clade from the remaining specimens with totally or partially dark lip, and the mutational steps between these two morphs with different lip colours are 26 and eight in the COI and 16S haplotype networks, respectively (Fig. 19). More specimens from wider distribution range will be needed to assess the taxonomic status of these *A. thachi* subspecies.

Two dissected specimens were found to have different lengths of the gametolytic duct. The specimen XM2 from Krong Bong, Dak Lak, Vietnam has a shorter gametolytic duct (Fig. 18A) than the specimen VCD2 from Buon Don, Dak Lak, Vietnam (Fig. 18B).

### ***Amphidromus metabletus* Möllendorff, 1900**

Figs 18E–G, 20, 21, 22A, 23

*Amphidromus metabletus* Möllendorff, 1900b: 22–23. Type locality: Berg “Mutter und Kind”, Annam [Vietnam]. Pilsbry 1900: 174–175. Möllendorff 1901: 48–49. Pilsbry 1901: 168–169, pl. 49, figs 1–4. Laidlaw and Solem 1961: 528, 640. Solem 1966: 102. Richardson 1985: 29. Thach 2005: 236. Schileyko 2011: 50.

*Amphidromus metabletus pachychilus* Möllendorff, 1901: 49. Type locality: Nha-trang, Süd-Annam [Nha Trang, Khanh Hoa Province, Vietnam]. Laidlaw and Solem 1961: 649. Richardson 1985: 30. Thach 2005: 236, pl. 73, figs 8, 13, 14, 18–21. Schileyko 2011: 50.

*Amphidromus metabletus insularis* Möllendorff, 1901: 49–50. Type locality: Insel Bai-min bei Nha-trang. Laidlaw and Solem 1961: 629–630. Richardson 1985: 30. Schileyko 2011: 50.

*Amphidromus metableta* [sic]. Fischer and Dautzenberg 1904: 406.

*Amphidromus metableta pachychilus* [sic]. Fischer and Dautzenberg 1904: 406.

*Amphidromus metableta insularis* [sic]. Fischer and Dautzenberg 1904: 406.

*Amphidromus (Amphidromus) metabletus metabletus*. Zilch 1953: 137, pl. 24, fig. 30.

*Amphidromus (Amphidromus) metabletus insularis*. Zilch 1953: 137, pl. 24, fig. 31.

*Amphidromus (Amphidromus) metabletus pachychilus*. Zilch 1953: 137, pl. 24, figs 32–36; pl. 25, figs 37, 38.

**Material examined.** VIETNAM: Dextral, **lectotype** of “*Amphidromus metabletus*”, SMF 7583/1 (Fig. 20A); 1S paralectotype of “*Amphidromus metabletus*”, SMF 122346/1 (Fig. 20B); 2D + 1S paralectotypes of “*Amphidromus metabletus*”, SMF 122347/3 (Fig. 20C); 2D + 1S paralectotypes of “*Amphidromus metabletus*”, SMF

7647/3 (Fig. 20D); 1D + 1S paralectotypes of "*Amphidromus metabletus*", SMF 82371/2 (Fig. 20E); 1S, paralectotype of "*Amphidromus metabletus*", ANSP 81428 (Fig. 20F). Sinistral, **lectotype** of "*Amphidromus metabletus insularis*", SMF 7585/1 (Fig. 20G). Dextral, **lectotype** of "*Amphidromus metabletus pachychilus*" forma *tritaeniata*, SMF 7587/1 (Fig. 20H); 1D, paralectotype of "*Amphidromus metabletus pachychilus*" forma *flava*, SMF 7588/1 (Fig. 20I); 1D, paralectotype of "*Amphidromus metabletus pachychilus*" forma *alba*, SMF 122348/1 (Fig. 20J); 1S, paralectotype of "*Amphidromus metabletus pachychilus*" forma *trizona*, SMF 122350/1 (Fig. 20K); 1S, paralectotype of "*Amphidromus metabletus pachychilus*" forma *interrupta*, SMF 122352/1 (Fig. 20L); 1D, paralectotype of "*Amphidromus metabletus pachychilus*" forma *confluens*, SMF 122354/1 (Fig. 21A); 1S, paralectotype of "*Amphidromus metabletus pachychilus*" forma *fusca*, SMF 122356/1 (Fig. 21B).

**Other material examined.** VIETNAM: 4D + 4S specimens, Nha Trang city, Khanh Hoa Province, NMNS-8764-123–NMNS-8764-130 (Fig. 21C–F); 15D + 4S specimens, Ninh Hoa, Khanh Hoa Province, NMNS-8764-131–NMNS-8764-149 (Fig. 21G–L).

**Diagnosis.** Shell medium to large, elongate conical, and chirally dimorphic. Spire elongate conical; aperture ovate. Genitalia with appendix.

**Differential diagnosis.** The monochromic form of the chirally dimorphic *A. metabletus* is similar to *A. cochinchinensis* (Pfeiffer, 1857) in having a monochrome whitish yellow shell, but *A. cochinchinensis* is distinct in having a very little expanded lip, elongate last whorl, and elliptical aperture (Sutcharit et al. 2015). The banded form is similar to the chirally dimorphic *Aegistohadra dautzenbergi* (Fulton, 1899), but *A. metabletus* has a shell ground colour varying from whitish, yellowish, to reddish brown, and the shell is without an umbilical hump, while *Ae. dautzenbergi* has a ground colour varying from whitish to yellowish and tinted pink, and the shell sometimes possesses an umbilical hump. *Aegistohadra dautzenbergi* also has a thinner shell, a more ovate last whorl with an expanded lip that is not thickened or reflected, a thin parietal callus and a straight columella, whereas *A. metabletus* has a thicker shell, a rounder last whorl with an expanded and usually reflected lip, a thick parietal callus and a curved columella. Moreover, the genitalia of *A. metabletus* lack a dart complex, while it is present in all *Aegistohadra* species (Jirapatrasilp et al. 2022). *Amphidromus metabletus* is also recognised by a distinct clade in the molecular phylogeny (Fig. 2), with the closest *p*-distance to *A. ingens* in COI (15.91%) and *A. thachi* in 16S (10.68%) (Table 2).

**Description.** **Shell** medium to large (height 36.5–46.5 mm, width 20.9–27.2 mm), chirally dimorphic, elongate conical, rather thick and glossy. Spire elongate conical to ovate conical; apex acute, without black spot on tip, and earlier whorls whitish to tinted pink. Whorls 6–7 convex to smooth; suture wide and shallow; last whorl well rounded. Periostracum thin corneous; varix usually absent. Shell ground colour varying from whitish, yellowish to reddish brown; banding pattern variable from non-banded (monochrome colour) to narrow to wide multiple reddish brown spiral bands on whitish or yellowish ground colour. Parietal callus slightly thickened, whitish or transparent. Aperture ovate; peristome expanded and not reflected; lip whitish. Columella straight, thick or thin. Umbilicus imperforate.

**Radula.** Teeth arranged in anteriorly pointed V-shaped rows. Central tooth monocuspid and short spatulate with truncated cusp. Lateral teeth bicuspid; endocone small, with wide notch and blunt cusp; ectocone large with blunt cusp. Lateral teeth gradually transformed to asymmetric tricuspid marginal teeth (Fig. 22A).



**Figure 20.** Shells of *Amphidromus metabletus* Möllendorff, 1900 **A** lectotype of “*Amphidromus metabletus*” (SMF 7583) **B–F** paralectotypes of “*Amphidromus metabletus*” **B** SMF 122346 **C** SMF 122347 **D** SMF 7647 **E** SMF 82371 **F** ANSP 81428 **G** lectotype of “*Amphidromus metabletus insularis*” (SMF 7585) **H** lectotype of “*Amphidromus metabletus pachy-chilus*” forma *tritaeniata* (SMF 7587) **I** paralectotype of “*Amphidromus metabletus pachy-chilus*” forma *flava* (SMF 7588) **J** paralectotype of “*Amphidromus metabletus pachy-chilus*” forma *alba* (SMF 122348) **K** paralectotype of “*Amphidromus metabletus pachy-chilus*” forma *trizona* (SMF 122350) **L** paralectotype of “*Amphidromus metabletus pachy-chilus*” forma *interrupta* (SMF 122352). Credit: ANSP (F).

**Genital organs.** Atrium relatively short. Penis slender, and short  $\sim \frac{1}{4}$  of vaginal length. Penial retractor muscle thin, long and inserting on epiphallus close to penis. Epiphallus long, slender tube, and almost same diameter as penis. Flagellum short, extending from epiphallus and terminating in slightly enlarged



**Figure 21.** Shells of *Amphidromus metabletus* Möllendorff, 1900 **A** paralectotype of "*Amphidromus metabletus pachy-chilus*" forma *confluens* (SMF 122354) **B** paralectotype of "*Amphidromus metabletus pachy-chilus*" forma *fusca* (SMF 122356) **C–F** specimens from Nha Trang, Khanh Hoa, Vietnam (NMNS-8764-123, NMNS-8764-125, NMNS-8764-127, NMNS-8764-129) **G–L** specimens from Ninh Hoa, Khanh Hoa, Vietnam (NMNS-8764-136, NMNS-8764-143, NMNS-8764-144, NMNS-8764-146, NMNS-8764-147, NMNS-8764-149).

folded coil. Appendix long, slender tube, ~ 3× longer than flagellum, and approximately as long as epiphallus. Vas deferens slender tube passing from free oviduct and terminating at epiphallus-flagellum junction (Fig. 18E). Internal wall of penis corrugated, exhibiting series of swollen and smooth surfaced longitudinal penial pilasters forming fringe around entire penial wall. Penial verge very short conical with smooth surface (Fig. 18F).

Vagina slender, long cylindrical, and ~ 4× longer than penis. Gametolytic duct very long cylindrical tube then abruptly tapering to slender tube terminally and connected to globular gametolytic sac. Free oviduct short; oviduct compact, forming lobule alveoli (Fig. 18E). Internal wall of vagina possessing corrugated ridges with wide crenulations on its entire vagina wall; ridges becoming stronger corrugated close to free oviduct opening (Fig. 18G).

**Haplotype network.** There were 12 COI haplotypes (Fig. 23A) and six 16S haplotypes (Fig. 23B) of *A. metabletus* in this study, and the highest numbers of mutational steps in the COI and 16S minimum spanning networks are seven and two, respectively.

**Distribution.** This species is found in Khanh Hoa Province, Vietnam.

**Remarks.** One species that was described earlier, *A. cochinchinensis* was originally described from “Cochin China”, the old geographic usage which is now interpreted as southern Vietnam, and this species was known only from the type materials (Sutcharit et al. 2015). This species is similar to *A. metabletus*, which is described from the same vicinity. The further inclusion of *A. cochinchinensis*-like specimens from southern Vietnam into the phylogenetic analyses will help clarify the taxonomic statuses of these two species.

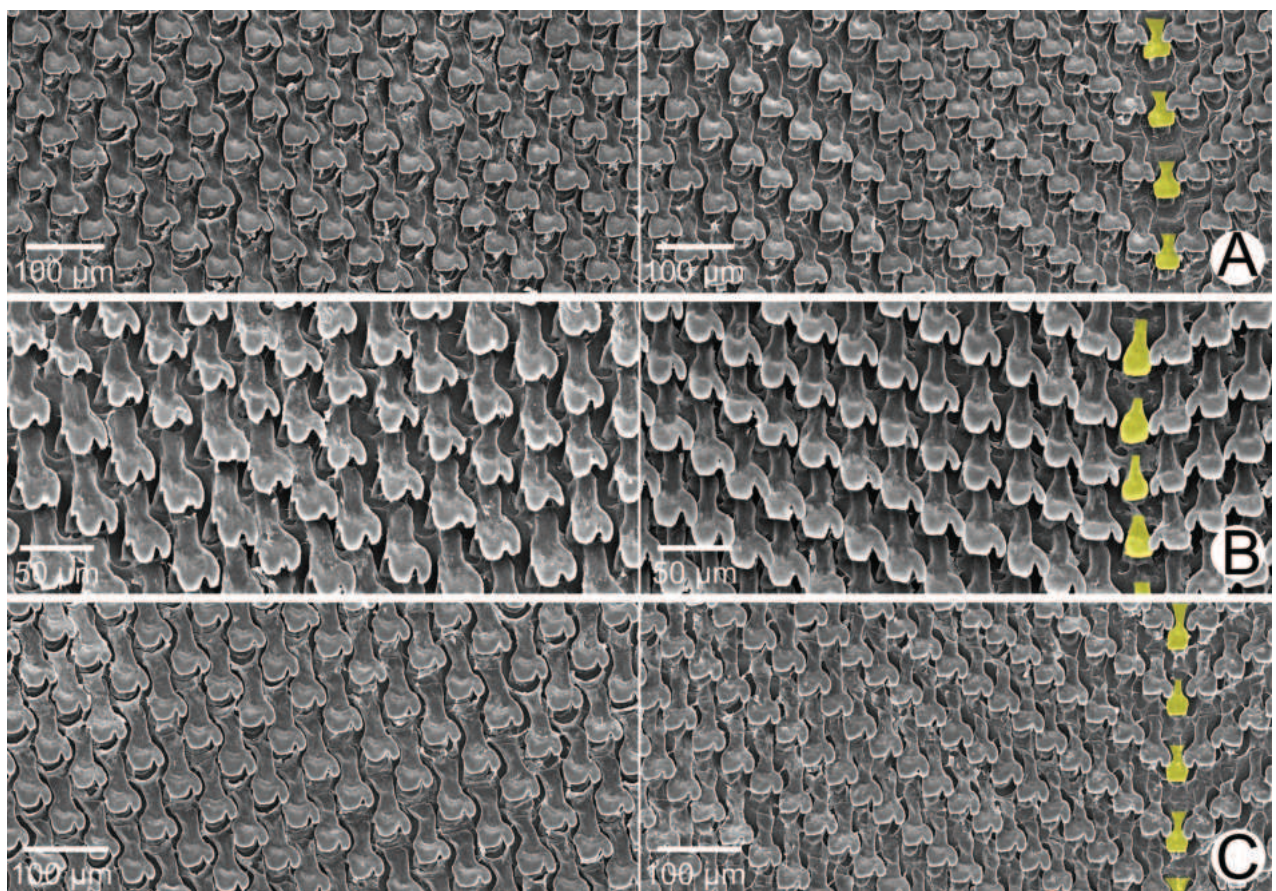


**Figure 22.** SEM images of the radula **A** *Amphidromus metabletus* Möllendorff, 1900 from Nha Trang, Khanh Hoa, Vietnam (NMNS-8764-130) **B** *Amphidromus madelineae* Thach, 2020 from Duy Xuyen, Quang Nam, Vietnam (NMNS-8764-110) **C** *Amphidromus costifer* Smith, 1893 from Ea Sup, Dak Lak, Vietnam (NMNS-8764-048). Central teeth are marked in yellow. The left and right images show the outer and inner sections of each radula, respectively.

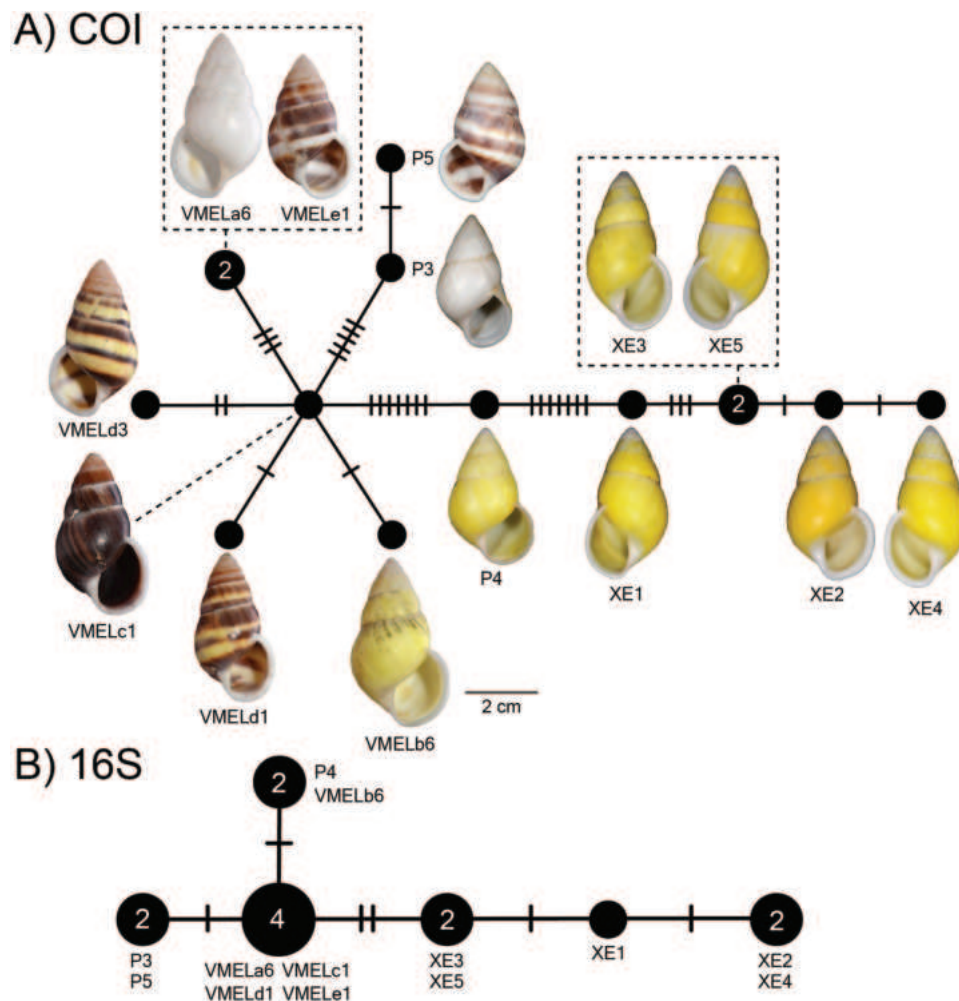


**Figure 23.** Mitochondrial haplotype minimum spanning networks of *Amphidromus metabletus* Möllendorff, 1900 **A** COI and **B** 16S rRNA. The size of each circle corresponds to the frequency of that haplotype, also shown as the number in that circle. The bars on the branches indicate the number of mutational steps between haplotypes. Specimen codes correspond to those in Table 1.

Möllendorff (1901) introduced several subspecies and shell forms. However, these forms could not be differentiated by mtDNA (COI and 16S rRNA) and some shell morphs with different colours and patterns belong to the same mtDNA haplotype (Fig. 23).

***Amphidromus haematostoma* Möllendorff, 1898**

Figs 24A–G, 25A, B, 26

*Amphidromus haematostoma* Möllendorff, 1898: 74–75. Type locality: Boloven [Boloven Plateau, Champasak, Laos]. Pilsbry 1900: 182–183. Möllendorff 1901: 50. Pilsbry 1901: 169. Fischer and Dautzenberg 1904: 406. Richardson 1985: 19. Schileyko 2011: 51. Inkhavilay et al. 2019: 91, figs 43f, 44a–c.

*Amphidromus haematostoma* var. *viridis* Möllendorff, 1898: 75. Type locality: Boloven. Pilsbry 1900: 183. Fischer and Dautzenberg 1904: 406.

*Amphidromus haematostoma* var. *varians* Möllendorff, 1898: 75. Type locality: Boloven. Pilsbry 1900: 183. Fischer and Dautzenberg 1904: 406.

- Amphidromus (Syndromus) haematostoma*. Zilch 1953: 132, pl. 22, figs 4, 5.  
Inkhavilay et al. 2017: 34–35, figs 13o–r.  
*Amphidromus haematostomus* [sic]. Laidlaw and Solem 1961: 527, 625.  
*Amphidromus haematostomus* [sic] *varians*. Laidlaw and Solem 1961: 668.  
*Amphidromus haematostomus* [sic] *viridis*. Laidlaw and Solem 1961: 670.  
*Amphidromus haematostoma varians*. Richardson 1985: 19.  
*Amphidromus haematostoma viridis*. Richardson 1985: 19.  
*Amphidromus (Syndromus) haematostomus* [sic]. Lehmann and Maassen 2004: 20.  
*Amphidromus attapeuensis* Thach & Huber in Thach, 2017: 37–38, figs 573–578. Type locality: Attapeu Province, southeast of Laos, close to Vietnam border. Thach 2020a: 51, 52. Thach 2021: 55.

**Material examined.** LAOS: Sinistral, **lectotype** of “*Amphidromus haematostoma* var. *viridis*”, SMF 7559/1 (Fig. 24A); sinistral, **lectotype** of “*Amphidromus haematostoma* var. *varians*”, SMF 7561/1 (Fig. 24B); sinistral, **holotype** of “*Amphidromus attapeuensis*”, NHMUK 20170278 (Fig. 24C).

**Other material examined.** LAOS: 5S specimens, Xe Pian village, Paksong District, Champasak Province, CUMZ 10217 (Inkhavilay et al. 2019: fig. 44a); two lots in W.J.M. Maassen Collection (8S specimens and 14S specimens), Boloven Plateau, Paksong District, Champasak; 4S specimens, Samphanh District, Phongsali Province, NMNS-8764-053–NMNS-8764-056 (Fig. 24D); 20S specimens, Ba Chien, Pakse District, Champasak Province, NMNS-8764-057–NMNS-8764-076 (Fig. 24E, F).

VIETNAM: 5S specimens, Kbang District, Gia Lai Province, NMNS-8764-077NMNS-8764-081 (Fig. 24G).

**Diagnosis.** Shell medium and sinistral. Parietal callus, lip and columella with bright to dark rose-pink. Varix sometimes present. Genitalia without appendix.

**Differential diagnosis.** *Amphidromus haematostoma* differs from the similar sinistral species *A. madelineae* in having a whitish apex, slightly thickened parietal callus with pale to dark rose-pink colouration, while *A. madelineae* has tinted pink ~ 1–2 whorls from apex, and thin transparent parietal callus. This species also differs from the similar *A. roseolabiatu*s in that the latter has a chirally dimorphic shell, a whitish apex and the genitalia with a very long appendix. The molecular phylogeny in this study reveals that *A. haematostoma* is a distinct clade from its sister *A. madelineae* (Fig. 2). The COI and 16S *p*-distances between *A. haematostoma* and *A. madelineae* are 13.93% and 6.04%, respectively (Table 2).

**Description.** **Shell** medium (height 23.8–35.4 mm, width 13.3–21.0 mm), sinistral, ovate conical, rather thin and glossy. Spire elongate conical; apex acute, without black spot on tip, and earlier whorls whitish. Whorls 6–7 convex to smooth; suture wide and depressed; last whorl well rounded. Periostracum thick corneous or with green to greenish yellow colour; varix occasionally present. Shell ground colour white or yellowish colour (without periostracum); dark yellow subsutural band and a band at around umbilicus usually present (rarely indistinguishable). Parietal callus thickened with bright to dark rose-pink colour. Aperture broadly ovate and inner side of outer wall whitish; peristome little thickened, expanded, and weakly reflexed but not attached to last whorl; lip bright to dark rose-pink colour and with little darker colour at the

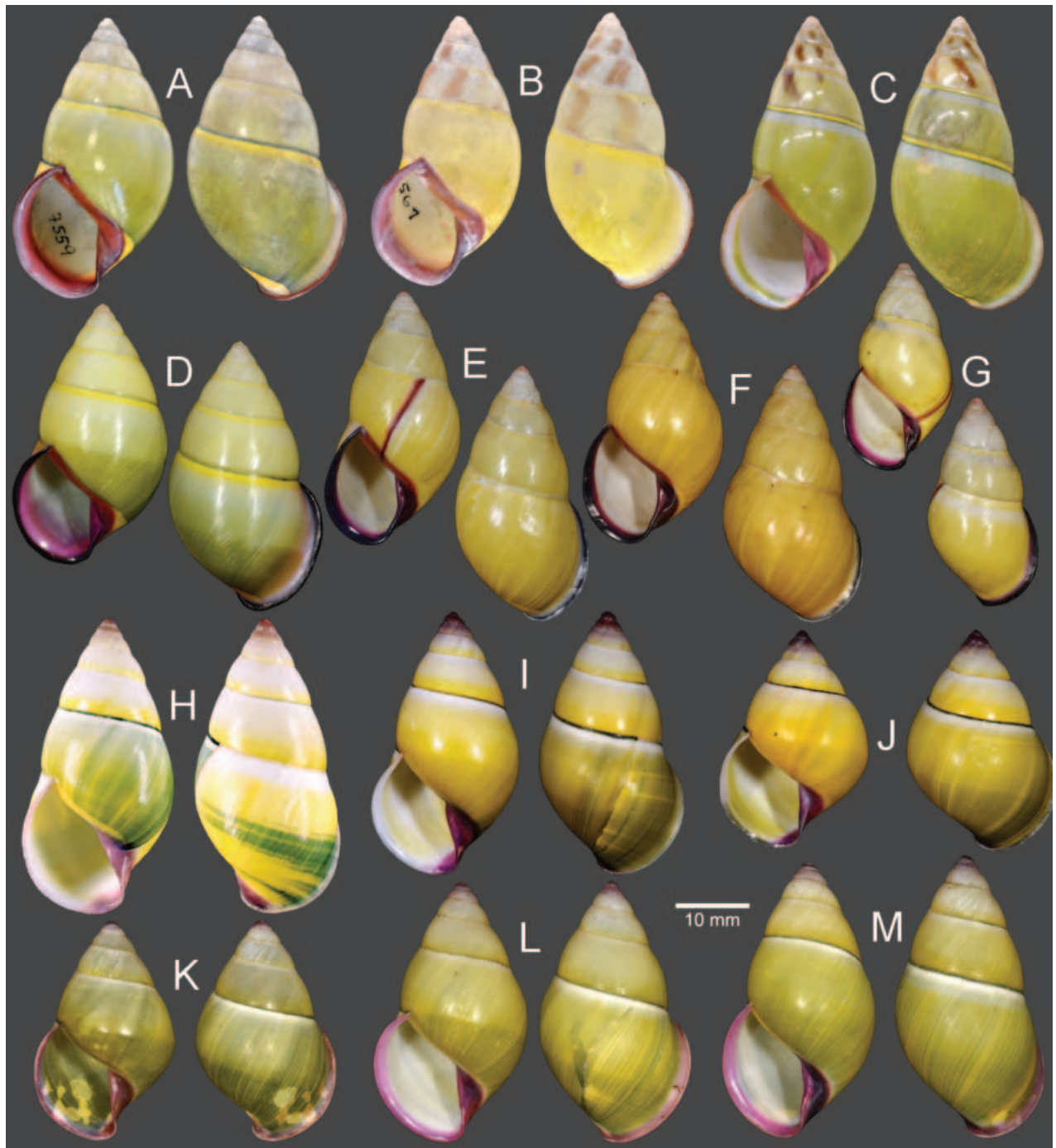


**Figure 24.** Shells of *Amphidromus* spp **A–G** *Amphidromus haematostoma* Möllendorff, 1898 **A** Lectotype of “*Amphidromus haematostoma* var. *viridis*” (SMF 7559) **B** lectotype of “*Amphidromus haematostoma* var. *varians*” (SMF 7561) **C** holotype of “*Amphidromus attapeuensis*” (NHMUK 20170278) **D** specimen from Samphanh, Phongsali, Laos (NMNS-8764-056) **E, F** specimens from Ba Chien, Pakse, Champasak, Laos (NMNS-8764-064, NMNS-8764-076) **G** specimen from Kbang, Gia Lai, Vietnam (NMNS-8764-080) **H–M** *Amphidromus madelineae* Thach, 2020 **H** holotype of “*Amphidromus madelineae*” (MNHN-IM-2000-35566) **I, J** Specimens from Duy Xuyen, Quang Nam, Vietnam (NMNS-8764-112, NMNS-8764-108) **K–M** specimens from Za Hung, Dong Giang, Quang Nam, Vietnam (NMNS-8764-114, NMNS-8764-118, NMNS-8764-122).

edge. Columella bright to dark rose-pink colour, straight, or little twisted. Umbilicus imperforate.

**Genital organs.** Atrium relatively short. Penis slender, conical, and short ~ 1/3 of vaginal length. Penial retractor muscle thickened, long and inserting on

epiphallus close to penis. Epiphallus stout tube and approximately as long as vagina. Flagellum short, extending from epiphallus and terminating in curved tip; appendix absent. Vas deferens slender tube passing from free oviduct and terminating at epiphallus-flagellum junction (Fig. 25A). Internal wall of penis corrugated, exhibiting prominent series of thickened and swollen longitudinal penial pilasters forming fringe around penial wall, and with fine and weak folds around base of penial verge. Penial verge very short, with smooth surface, and opening at the tip (Fig. 25B).

Vagina slender, long cylindrical, and ~2× longer than penis. Gametolytic duct cylindrical tube then gradually tapering to slender tube terminally and connected to gametolytic sac (missing during dissection). Free oviduct short; oviduct compact, forming lobule alveoli (Fig. 25A). Internal wall of vagina possessing corrugated ridges near genital orifice; ridges becoming smooth longitudinal vaginal pilasters in middle, swollen with irregularly shaped deep crenulations close to free oviduct opening (Fig. 25B).

**Distribution.** This species has a wide distribution range covering Attapeu, Champasak, and Phongsali provinces, Laos, and Gia Lai Province, Vietnam.

**Remarks.** A degree of shell colour variation occurs in the specimens from Pakse, Champasak, Laos (Fig. 24E, F) in having yellowish to golden-yellow periostracum, indistinct subsutural band and a dark rose-pink apertural lip. In addition, the type specimens and recently collected specimens from Kbang, Gia Lai, Vietnam (Fig. 24B, C, G) tend to have broad brownish radial bands on the earlier spire whorls.

This species also exhibits a prominent population genetic structure, where some clades constitute only the specimens from the same collecting locality (Fig. 26). The COI intraspecific distance among all *A. haematostoma* specimens is 10.03%, which is the highest distance of all *Amphidromus* species in this study. This value is higher than twice the optimum intra/interspecific threshold value of 4% for stylommatophoran land snails (Davison et al. 2009). However, as all specimens have congruent morphology as stated above, we refrain from treating each pool of samples from the same collecting locality as a distinct taxon, before more specimens from each locality are critically examined.

### ***Amphidromus madelineae* Thach, 2020**

Figs 22B, 24H–M, 25C, D, 26

*Amphidromus madelineae* Thach, 2020a: 68–69, pl. 48, figs 592, 593; pl. 49 figs 594–596. Type locality: Quang Nam Province, Central Vietnam. Thach 2021: 68.

**Material examined.** VIETNAM: Sinistral, **holotype** of “*Amphidromus madelineae*”, MNHN-IM-2000-35566 (Fig. 24H).

**Other material examined.** VIETNAM: 5S specimens, Duy Xuyen District, Quang Nam Province, NMNS-8764-108–NMNS-8764-112 (Fig. 24I, J); 10S specimens, Za Hung, Dong Giang District, Quang Nam Province, NMNS-8764-113–NMNS-8764-122 (Fig. 24K–M).

**Diagnosis.** Shell small to medium, sinistral; apex tinted pink to purplish pink. Parietal callus transparent; lip whitish to purplish pink; columella and inner side of outer wall around columella purplish pink. Genitalia without appendix.

**Differential diagnosis.** *Amphidromus madelineae* differs from the similar sinistral species *A. haematostoma* in having tinted-pink colour ~ 1–2 whorls from apex, and thin and transparent parietal callus, while *A. haematostoma* has a whitish apex, slightly thickened parietal callus with pale to dark rose-pink colour. This species also differs from the similar *A. roseolabiatus* in that the latter has a chirally di-

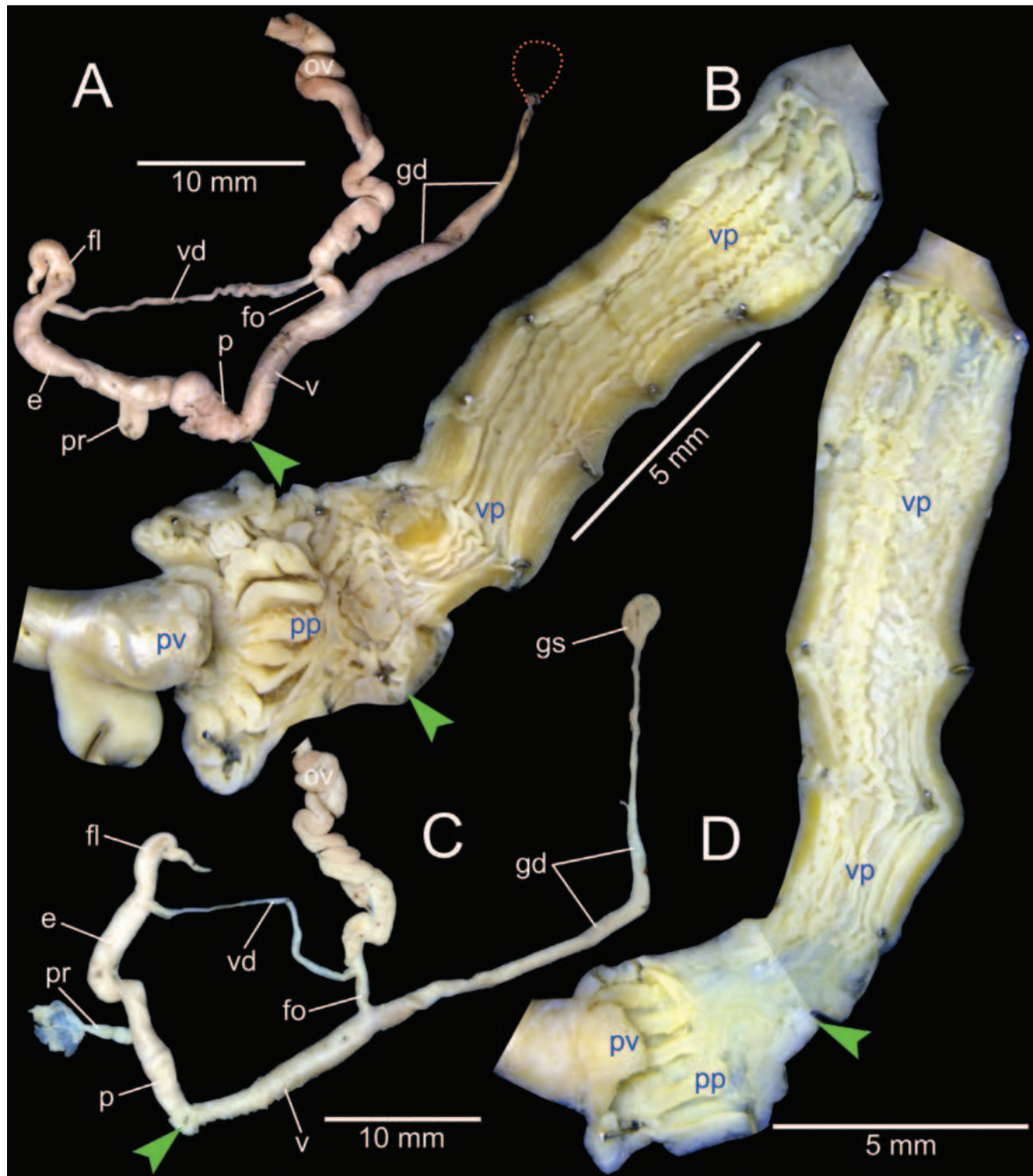


**Figure 25.** Genitalia of *Amphidromus* spp **A, B** *Amphidromus haematostoma* Möllendorff, 1898 from Ba Chien, Pakse, Champasak, Laos (NMNS-8764-061), showing **A** general view of genitalia **B** interior structures of penis and vagina chamber **C, D** *Amphidromus madelineae* Thach, 2020 from Duy Xuyen, Quang Nam, Vietnam (NMNS-8764-110), showing **C** general view of genitalia **D** interior structures of penis and vagina chamber. Red dots indicate the shape of the missing gametolytic sac. Green arrows indicate the genital openings. Abbreviations: e, epiphallus; fl, flagellum; fo, free oviduct; gd, gametolytic duct; gs, gametolytic sac; ov, oviduct; p, penis; pp, penial pilaster; pr, penial retractor muscle; pv, penial verge; v, vagina; vd, vas deferens; vp, vaginal pilaster.

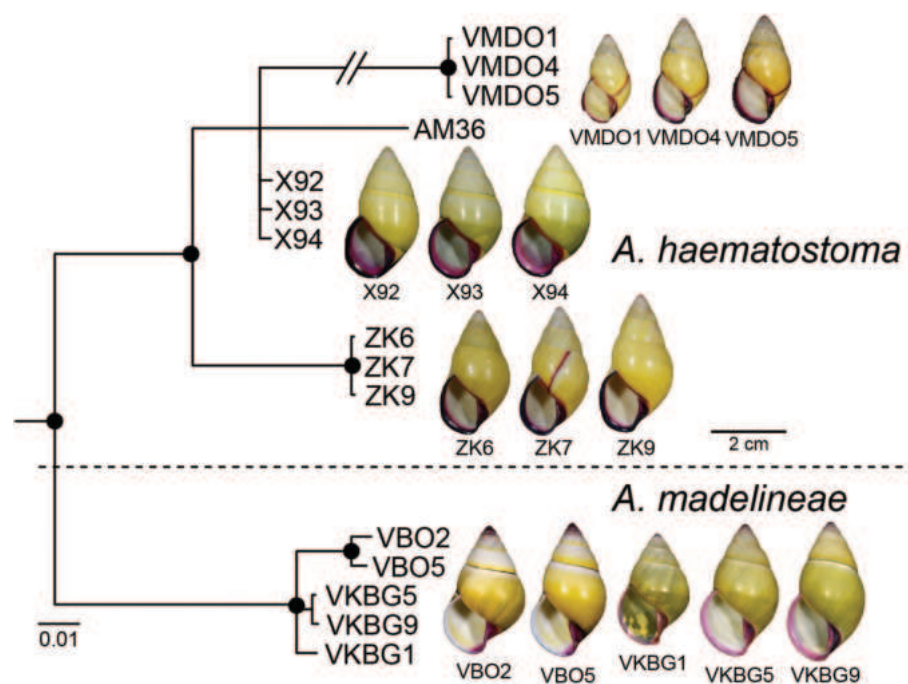


**Figure 26.** Bayesian phylogeny of *Amphidromus haematostoma* Möllendorff, 1898 and *Amphidromus madelineae* Thach, 2020 based on mitochondrial COI and 16S genes. Nodal support values are given as SH-aLRT/aBayes/ultra-fast bootstrap (IQ-TREE, ML)/posterior probability (MrBayes, BI). An asterisk on each branch indicates a clade with all well-supported values (SH-aLRT  $\geq$  80%, aBayes  $\geq$  0.95, BS  $\geq$  95%, PP  $\geq$  0.95).

morphic shell, a whitish apex and the genitalia with a very long appendix. The molecular phylogeny in this study reveals that *A. madelineae* is a distinct clade from its sister *A. haematostoma* (Figs 2, 26). The COI and 16S *p*-distances between *A. madelineae* and *A. haematostoma* are 13.93% and 6.04%, respectively (Table 2).

**Description. Shell** small to medium (height 27.7–38.0 mm, width 16.2–20.2 mm), sinistral, elongate to ovate conical, rather thin and glossy. Spire conical; apex acute, tinted pink to purplish pink and without black spot on tip. Whorls 5–6 nearly smooth; suture wide and shallow; last whorl rounded to nearly globose. Periostracum usually deciduous to yellowish green radial streaks, more conspicuous on last whorl and faded in earlier whorls. Last whorl with thin, dark green subsutural band, sometimes with irregular greenish spiral blotched bands below periphery; varix sometimes present. Parietal callus thin and transparent. Aperture ovate to elongate; peristome little thickened and expanded; lip generally whitish to purplish pink; inner side of outer wall whitish around columella with purplish pink colour. Columella straight, thickened and pale to dark purplish pink. Umbilicus imperforate.

**Radula.** Teeth arranged in anteriorly pointed V-shaped rows. Central tooth monocuspid and spatulate with truncated cusp. Lateral teeth bicuspid; endocone small, slightly elongate, with wide and deep notch, and dull cusp; ectocone large with slightly blunt to dull cusp. Lateral teeth gradually transformed to asymmetric tricuspid marginal teeth. Outermost teeth with small and multicuspid (Fig. 22B).

**Genital organs.** Atrium relatively short. Penis stout, cylindrical, and short,  $\sim$  1/2 as long as vagina. Penial retractor muscle thickened, short and inserting on epiphallus close to penis. Epiphallus stout tube and approximately as long as vagina. Flagellum short, extending from epiphallus and terminating in slightly curved tip; appendix absent. Vas deferens slender tube passing from

free oviduct and terminating at epiphallus-flagellum junction (Fig. 25C). Internal wall of penis corrugated, exhibiting prominent series of thickened and smooth surfaced longitudinal penial pilasters forming fringe around penial wall. Penial verge very short and with smooth surface (Fig. 25D).

Vagina long cylindrical, and ~ 2× longer than penis. Gametolytic duct long cylindrical tube then gradually tapering to slender tube terminally and connected to bulbus gametolytic sac. Free oviduct short; oviduct compact, forming lobule alveoli (Fig. 25C). Internal wall of vagina possessing slightly corrugated ridges near genital orifice; ridges becoming roughly irregular vaginal pilasters in middle and close to free oviduct opening (Fig. 25D).

**Distribution.** This species is found in Quang Nam Province, Vietnam.

**Remarks.** Specimens from Za Hung, Dong Giang, Quang Nam, Vietnam (Fig. 24L, M) are superficially similar to *A. haematostoma* in having greenish shell colour and a purplish pink lip.

### ***Amphidromus costifer* Smith, 1893**

Figs 22C, 27, 28A–C, 29

*Amphidromus costifer* Smith, 1893: 12, text fig. Type locality: dans les Montagnes boitées du Huyen de Tri-phuoc, Province Binh-dinh, An-nam [in the Huyen Mountains of Tri-phuoc, Binh-dinh Province, An-nam]. Fulton 1896: 91, pl. 7, fig. 6, 6a. Möllendorff 1898: 75. Pilsbry 1900: 176–177, pl. 59, figs 22, 23. Fischer and Dautzenberg 1904: 405. Laidlaw and Solem 1961: 590, 592, 613, fig. 40a, b. Schileyko 2011: 50. Sutcharit et al. 2015: 65, fig. 6c. Thach 2020a: pl. 46, figs 560, 561.

*Amphidromus costifer gemmalimae* Thach, 2020a: 55, pl. 45, figs 551–557. Type locality: Krong Nang, Dak Lak Province, Central Vietnam. Thach 2021: 58. syn. nov.

*Amphidromus nguyenkhoai* Thach, 2020a: 71, pl. 64, figs 776–784. Type locality: Krong Pa District, Gia Lai, Central Vietnam. Thach 2021: 71. syn. nov.

**Material examined.** VIETNAM: Dextral, **lectotype** of “*Amphidromus costifer*”, NHMUK 1893.2.26.4 (Fig. 27A); dextral, **holotype** of “*Amphidromus costifer gemmalimae*”, MNHN-IM-2000-35550 (Fig. 27B); dextral, **holotype** of “*Amphidromus nguyenkhoai*”, MNHN-IM-2000-35569 (Fig. 27C).

**Other material examined.** VIETNAM: 10D specimens, Tay Son District, Binh Dinh Province, NMNS-8764-035–NMNS-8764-044 (Fig. 27D, E); 6D specimens, Ea Sup District, Dak Lak Province, NMNS-8764-045–NMNS-8764-050 (Fig. 27F, G); 2D specimens, An Lao District, Binh Dinh Province, NMNS-8764-051, NMNS-8764-052 (Fig. 27H, I).

**Diagnosis.** Shell large, dextral, and spire ovate conical. Shell surface with prominent irregular growth lines or prominent crests of expanded lip. Aperture broadly ovate or truncate. Genitalia with appendix.

**Differential diagnosis.** *Amphidromus costifer* is unique among all reported Vietnamese species (Schileyko 2011) in having a large, dextral shell with an ovate conical spire, and the shell surface with prominent irregular growth lines or prominent crests of expanded lip. *Amphidromus costifer* is also recognised by a distinct clade in the molecular phylogeny (Fig. 2), with the closest *p*-distance to *A. metabletus* in COI (16.63%) and *A. buelowi* in 16S (13.44%) (Table 2).

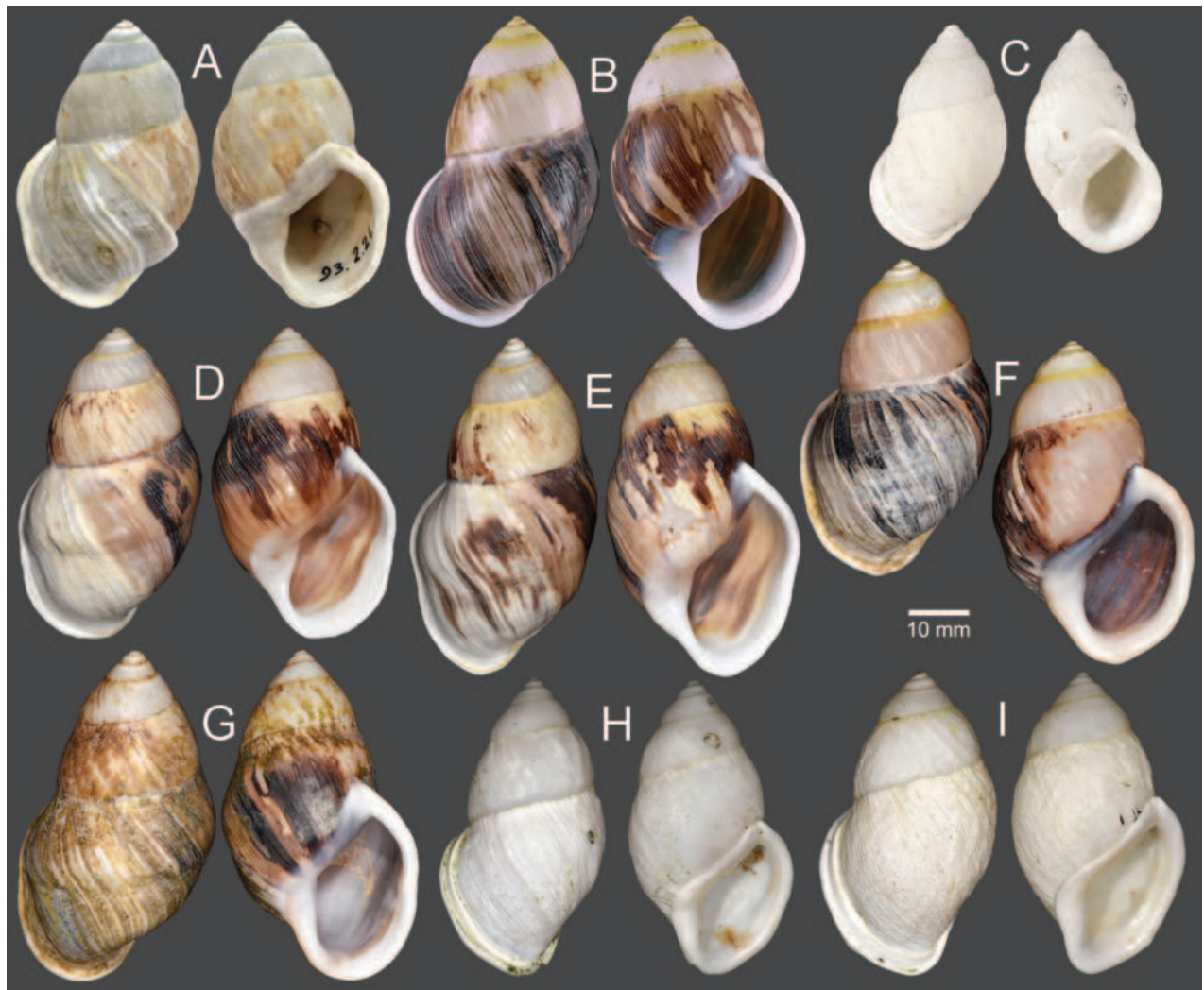


**Figure 27.** Shells of *Amphidromus costifer* Smith, 1893 **A** lectotype of “*Amphidromus costifer*” (NHMUK 1893.2.26.4) **B** holotype of “*Amphidromus costifer gemmalimae*” (MNHN-IM-2000-35550) **C** holotype of “*Amphidromus nguyenkhoai*” (MNHN-IM-2000-35569) **D, E** specimens from Tay Son, Binh Dinh, Vietnam (NMNS-8764-035, NMNS-8764-040) **F, G** specimens from Ea Sup, Dak Lak, Vietnam (NMNS-8764-047, NMNS-8764-048) **H, I** specimens from An Lao, Binh Dinh, Vietnam (NMNS-8764-051, NMNS-8764-052). Credit: H. Taylor, NHM (**A**), P. Bourguignon, MNHN (**B**), A. Lardeur (**C**).

**Description.** *Shell* large (height 48.9–59.7 mm, width 27.3–34.8 mm), dextral, solid, and ovate conical shape. Spire ovate conical; apex acute without black spot on tip. Whorls 5–7 little convex; suture wide and shallow; last whorl large, rounded to slightly ovate. Periostracum brownish to thin corneous; strong varix usually absent. Shell surface: spire generally with prominent irregular growth lines or with weak radial streak; last whorl with strong irregular growth lines, coarse or with prominent radial ridges, and usually prominent crest of expanded lip present. Shell colour highly variable: spire generally uniform whitish to yellowish (pale yellowish subsutural band detectable); last whorl has no pattern but usually stained with dark to dark brown blotches, smear or radial streaks. Parietal callus thickened and white, and broadly dilated at umbilical area. Aperture broadly ovate or truncate (sometimes irregular); inner side of outer wall generally whitish to yellowish. Peristome thickened, expanded, and slightly reflexed; lip whitish. Columella white and straight. Umbilicus imperforate.

**Radula.** Teeth arranged in anteriorly pointed V-shaped rows. Central tooth monocuspid and spatulate with truncated cusp. Lateral teeth bicuspid; endocone slightly curved with wide notch and curved cusp; ectocone large with truncated to blunt cusp. Lateral teeth gradually transformed to asymmetric tricuspid marginal teeth. Outermost teeth with tiny ectocone; endocone and mesocone large with curved cusps (Fig. 22C).

**Genital organs.** Atrium relatively short. Penis enlarged, conical, and nearly 1/2 as long as vagina. Penial retractor muscle thickened and inserting on epiphallus close to penis. Epiphallus long and slender tube. Flagellum short, extending from epiphallus, approximately as long as penis, and terminating in slightly enlarged coil. Appendix short, slender tube, 3× longer than flagellum and approximately as long as epiphallus. Vas deferens slender tube passing from free oviduct and terminating at epiphallus-flagellum junction (Fig. 28A). Internal wall of penis corrugated, exhibiting series of thickened longitudinal penial pilasters forming fringe around penial wall, and with smooth wall around base of penial verge. Penial verge short conical with thin longitudinal ridges surface, and with opening at the tip (Fig. 28B).

Vagina slender, long cylindrical, and ~ 2× longer than penis. Gametolytic duct cylindrical tube, extremely enlarged then abruptly tapering to slender tube terminally and connected to enlarged elliptical gametolytic sac. Free oviduct short; oviduct compact, enlarged to form lobule alveoli (Fig. 28A). Internal wall of vagina possessing corrugated ridges near genital orifice; ridges becoming swollen and smooth longitudinal vaginal pilasters in middle, and irregular shaped and deep crenulations close to free oviduct opening (Fig. 28C).

**Haplotype network.** There was a total of seven 16S haplotypes (Fig. 29) of *A. costifer* in this study, and the highest numbers of mutational steps in the 16S minimum spanning networks are 18.

**Distribution.** The distribution range of the species covers Binh Dinh, Dak Lak, and Gia Lai provinces, Vietnam.

**Remarks.** As Smith (1893) did not explicitly designate a type, and stated that a total of seven specimens were examined, the indication of the holotype in Sutcharit et al. (2015) is thus incorrect. Therefore, the syntype of “*Amphidromus costifer*” NHMUK 1893.2.26.4 is hereby designated as the lectotype.

Our recent specimens with a monochrome whitish shell identical to the holotype of *A. nguyenkhoai* were found to belong to the same clade as the typical *A. costifer*, with 14–18 mutational steps to the other specimens in the 16S haplotype network (Fig. 29). In addition, upon examining the type specimens of *A. costifer* and *A. nguyenkhoai*, except for the shell colour, the holotype of *A. nguyenkhoai* agrees well with the lectotype of *A. costifer* in terms of shell shape, shell surface, peristome, and apertural shape. Thus, *A. nguyenkhoai* is regarded herein as a junior subjective synonym of *A. costifer*.

The subspecies *A. costifer gemmalimae* was described as distinct from the nominotypical subspecies in having a stouter shell shape, smoother, not well-defined and not strongly calloused parietal wall, axial ribs with regular strength, a regularly convex outer rib, a completely closed umbilicus, and a columella not widening laterally (Thach 2020a). However, these characters fall within the intraspecific variations shown in *A. costifer* clade. Thus, *A. costifer gemmalimae* is also regarded herein as a junior subjective synonym of *A. costifer*.



**Figure 28.** Genitalia of *Amphidromus* spp **A–C** *Amphidromus costifer* Smith, 1893 from Ea Sup, Dak Lak, Vietnam (NMNS-8764-048), showing **A** general view of genitalia **B** interior structures of penis **C** interior structures of vagina chamber **D, E** *Amphidromus pankowskianus* Thach, 2020 from Khammouan Province, Laos, near Minh Hoa District, Quang Binh Province, Vietnam (NMNS-8764-152), showing **D** general view of genitalia **E** interior structures of penis and vagina chamber. Red dots indicate the shape of the missing gametolytic sac. Green arrows indicate the genital openings. Abbreviations: ap, appendix; e, epiphallus; fl, flagellum; fo, free oviduct; gd, gametolytic duct; gs, gametolytic sac; ov, oviduct; p, penis; pp, penial pilaster; pr, penial retractor muscle; pv, penial verge; v, vagina; vd, vas deferens; vp, vaginal pilaster.

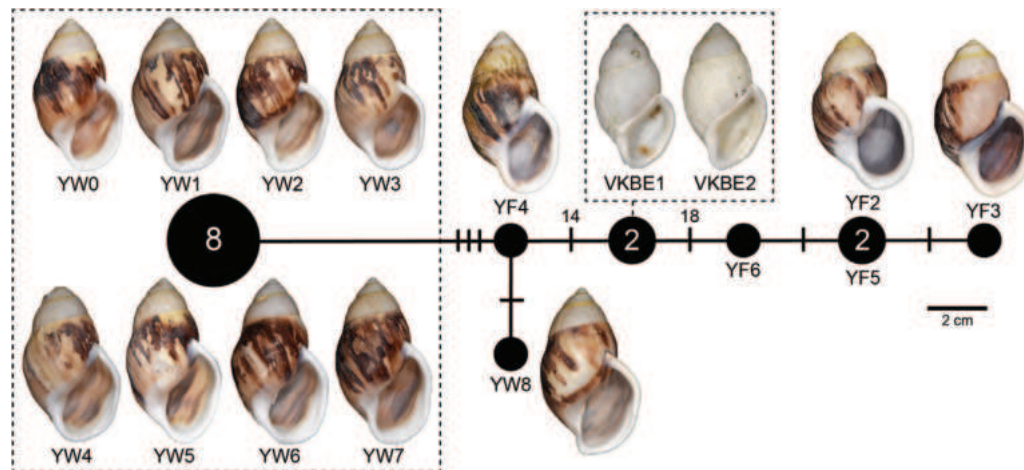


**Figure 29.** Mitochondrial 16S haplotype minimum spanning networks of *Amphidromus costifer* Smith, 1893. The size of each circle corresponds to the frequency of that haplotype, also shown as the number in that circle. The bars on the branches indicate the number of mutational steps between haplotypes. Specimen codes correspond to those in Table 1.

Additional shell variations, which occur in the monochrome whitish specimens from An Lao, Binh Dinh, Vietnam (Fig. 27C, H, I), are the occurrence of strongly thickened parietal callus, a thickened, multi-layered and broadly expanded apertural lip, and the shell surface much coarser with irregular growth lines and malleated pits.

The COI intraspecific distance among all *A. costifer* specimens is 7.84%, which is the second highest distance of all *Amphidromus* species in this study. This value is higher than the optimum intra/interspecific threshold value of 4% for stylommatophoran land snails (Davison et al. 2009). In addition, the 16S intraspecific distance among all *A. costifer* specimens is 3.39%, which is the highest distance of all *Amphidromus* species in this study, and the 16S haplotype network also exhibits a prominent population genetic structure (Fig. 29). However, as all specimens have congruent morphology as stated above, we refrain from treating each pool of samples from the same collecting locality as a distinct taxon, before more specimens from each locality are critically examined.

### ***Amphidromus roseolabiatatus* Fulton, 1896**

Figs 30A–F, 31

*Amphidromus roseolabiatatus* Fulton, 1896: 89, pl. 6, fig. 8. Type locality: Siam [Thailand]. Pilsbry 1900: 188, pl. 60, fig. 36. Fischer and Dautzenberg 1904: 407. Laidlaw and Solem 1961: 527, 655. Richardson 1985: 42. Schileyko 2011: 51. Sutcharit et al. 2015: 88, fig. 13j, k. Inkhavilay et al. 2019: 94, figs 45d–f, 58a. Páll-Gergely et al. 2020: 54. Thach 2020b: 360, fig. 7.

*Amphidromus (Amphidromus) roseolabiatatus*. Inkhavilay et al. 2017: 3, 6, 9, 10, figs 2a, b, 3a, b, 4a–f, 6a, b, 7a–c.

*Amphidromus phuonglinhae* Thach, 2017: 45, pl. 46, figs 581–584. Type locality: Bo Trach District, Quang Binh Province, Central Vietnam. Thach 2021: 76.

**Material examined.** THAILAND: Sinistral, **lectotype** of “*Amphidromus roseolabiatatus*”, NHMUK 19601462 (Fig. 30A); 1S, paralectotype of “*Amphidromus roseolabiatatus*”, NHMUK 19601463 (Fig. 30B).

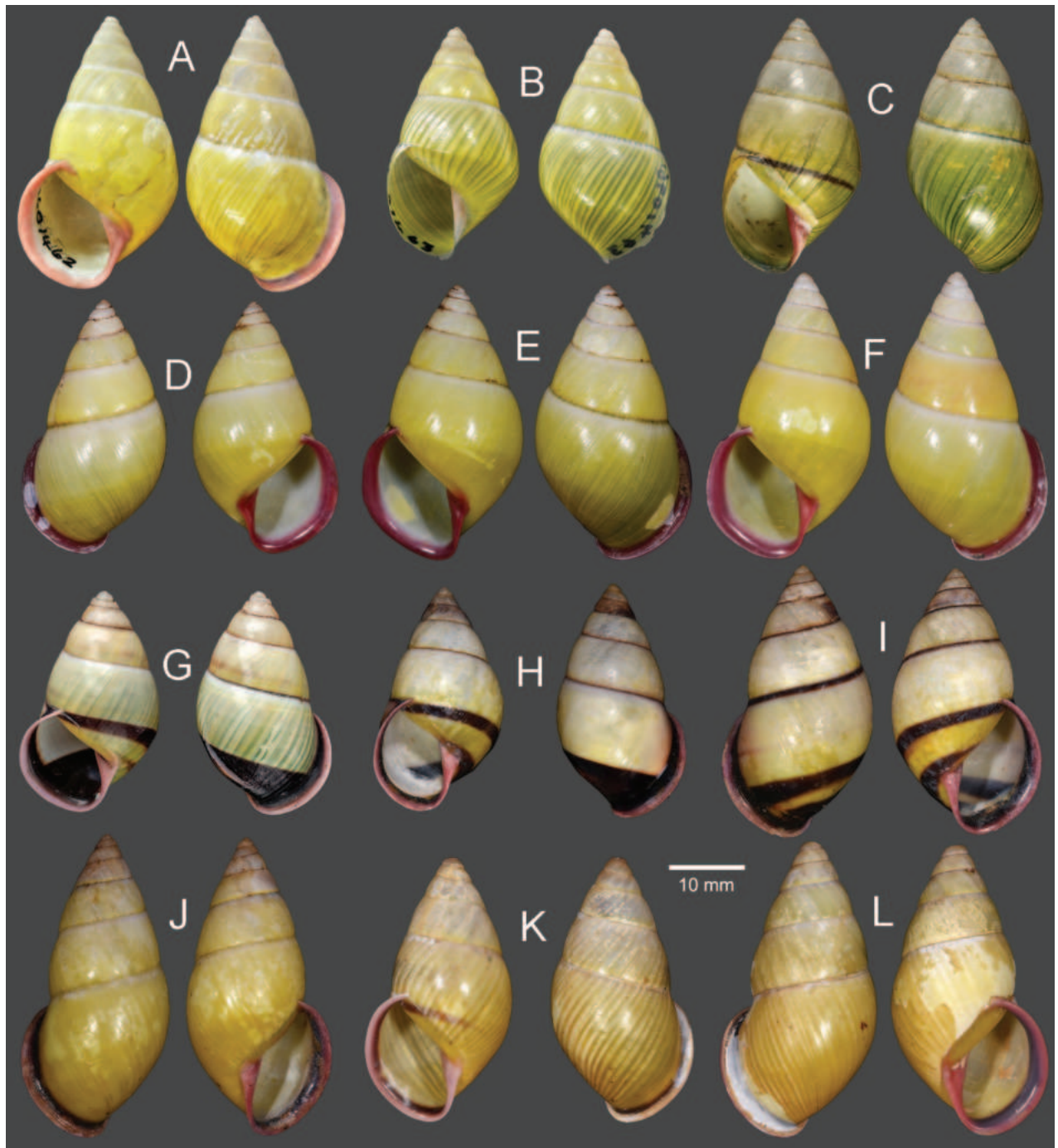


**Figure 30.** Shells of *Amphidromus* spp **A–F** *Amphidromus roseolabiatus* Fulton, 1896 **A** lectotype of “*Amphidromus roseolabiatus*” (NHMUK 19601462) **B** paralectotype of “*Amphidromus roseolabiatus*” (NHMUK 19601463) **C** holotype of “*Amphidromus phuonglinhae*” (MNHN-IM-2000-33200) **D–F** specimens from Kampong Siem, Kampong Cham, Cambodia (NMNS-8764-254, NMNS-8764-258, NMNS-8764-260) **G–L** *Amphidromus pankowskianus* Thach, 2020 **G** holotype (NHMUK 20200213) **H–J** specimens from Lak Sao, Khamkeut, Bolikhamesai, Laos (NMNS-8764-154, NMNS-8764-170, NMNS-8764-192) **K, L** specimens from Khammouan Province, Laos, near Minh Hoa District, Quang Binh Province, Vietnam (NMNS-8764-150, NMNS-8764-151). Credit: M. Caballer (C), K. Webb (G).

VIETNAM: Sinistral, **holotype** of “*Amphidromus phuonglinhae*”, MNHN-IM-2000-33200 (Fig. 30C).

**Other material examined.** CAMBODIA: 4D + 6S specimens, Kampong Siem District, Kampong Cham Province, NMNS-8764-254–NMNS-8764-263 (Fig. 30D–F).

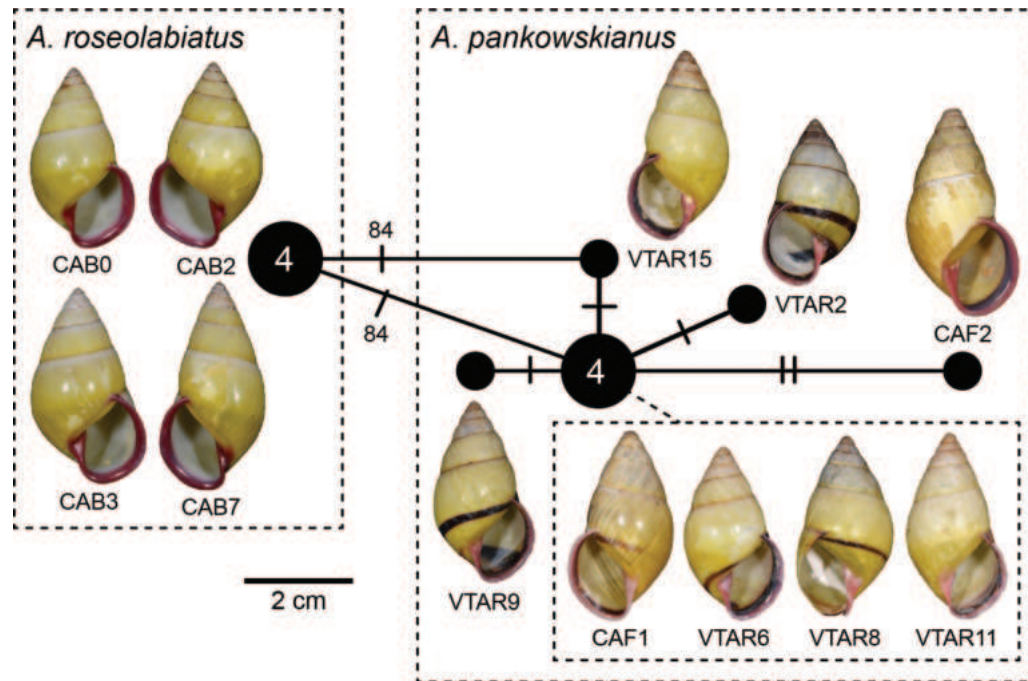


**Figure 31.** Mitochondrial COI haplotype minimum spanning networks of *Amphidromus roseolabiatus* Fulton, 1896 and *Amphidromus pankowskianus* Thach, 2020. The size of each circle corresponds to the frequency of that haplotype, also shown as the number in that circle. The bars on the branches indicate the number of mutational steps between haplotypes. Specimen codes correspond to those in Table 1.

**Diagnosis.** Shell medium and chirally dimorphic. Parietal callus transparent; lip and columella purplish pink. Genitalia with appendix.

**Differential diagnosis.** This species is very closely similar to *A. pankowskianus* in terms of shell morphology and colour pattern. However, this species lacks a dark radial band behind the reflected lip which is also visible in the inner side of the shell, and a dark spiral band below periphery, both of which are present in *A. pankowskianus*. *Amphidromus roseolabiatus* differs from the similar species *A. madelineae* and *A. haematostoma* in having a chirally dimorphic shell, and genitalia with a very long appendix, while both *A. madelineae* and *A. haematostoma* are exclusively sinistral, and the genitalia lacks an appendix. *Amphidromus roseolabiatus* also differs from both *A. smithi* Fulton, 1896 and *A. ventrosulus* Möllendorff, 1900 from Vietnam (Zilch 1953; Sutcharit et al. 2015) in having a chirally dimorphic shell, a purplish pink lip and fine green streaks. In contrast, *A. smithi* has a sinistral shell, a dark red to brownish lip with dark spot on the apex, and *A. ventrosulus* has a sinistral shell, uniform green colour, elongate spire and more depressed suture. The molecular phylogeny in this study reveals that *A. roseolabiatus* is a distinct clade from its sister *A. pankowskianus* (Fig. 2). The COI and 16S *p*-distances between *A. roseolabiatus* and *A. pankowskianus* are 13.02% and 6.14%, respectively (Table 2).

**Description. Shell** medium (height 33.1–38.6 mm, width 19.2–21.6 mm), chirally dimorphic, elongate to ovate conical, rather thin and glossy. Spire conical; apex acute, light brown and without black spot on tip. Whorls 6–7 nearly smooth; suture wide and depressed; last whorl rounded. Periostracum usually deciduous to yellowish green radial streaks, more conspicuous on last whorl and faded in earlier whorls. Last whorl with thin, whitish subsutural band; with or without reddish brown spiral band on periphery but usually not reaching ap-

ertural lip; varix absent. Parietal callus thin and transparent. Aperture ovate to elongate; peristome expanded and not reflected; lip usually purplish pink. Columella straight, thickened, purplish pink. Umbilicus narrowly opened.

**Haplotype network.** There was one COI haplotype of *A. roseolabiatus* in this study (Fig. 31).

**Distribution.** This species is found in Khammouan Province, Laos, Kampong Cham Province, Cambodia, and Quang Binh Province, Vietnam. The distribution of this species in Bolikhamxay, Laos according to Inkhavilay et al. (2017) is dubious (see below).

**Remarks.** Inkhavilay et al. (2017) also included the white-lipped morph from Bolikhamxay, Laos in *A. roseolabiatus*. However, in this study we only incorporated the typical purplish pink-lipped morph in the phylogenetic analyses. Therefore, the identification of the white-lipped morph from Bolikhamxay, Laos as *A. roseolabiatus* or another distinct species remains to be further investigated.

### ***Amphidromus pankowskianus* Thach, 2020**

Figs 28D, E, 30G–L, 31

*Amphidromus pankowskiana* [sic] Thach, 2020a: 72–73, pl. 48, figs 582–586.

Type locality: Northwestern District of Khanh Hoa Province, Central Vietnam.  
*Amphidromus pankowskianus*. Thach 2021: 72.

**Material examined.** VIETNAM: **Holotype**, NHMUK 20200213 (Fig. 30G).

**Other material examined.** LAOS: 2D + 1S specimens, Khammouan Province, near Minh Hoa District, Quang Binh Province, Vietnam, NMNS-8764-150–NMNS-8764-152 (Fig. 30K, L); 23D + 17S specimens, Lak Sao, Khamkeut District, Bolikhamsai Province, NMNS-8764-153–NMNS-8764-191, NMNS-8764-212 (Fig. 30H–J).

**Diagnosis.** Shell medium and chirally dimorphic. Last whorl without or with narrow to spiral band on periphery. Parietal callus transparent; lip and columella pale purplish pink; dark radial band on palatal wall. Genitalia with appendix.

**Differential diagnosis.** This species is very closely similar to *A. roseolabiatus* in terms of shell morphology and colour pattern. However, this species is distinct in having a dark radial band behind the reflected lip which is also visible in the inner side of the shell and sometimes with a dark spiral band below periphery. In addition, this species also differs from *A. haematostoma* and *A. madelineae* in having a chirally dimorphic shell, with dark radial bands behind the expanded lip, and the genitalia with a long flagellum. The molecular phylogeny in this study reveals that *A. pankowskianus* constitutes its own distinct clade which is sister to *A. roseolabiatus* (Fig. 2). The COI and 16S *p*-distances between *A. pankowskianus* and *A. roseolabiatus* are 13.02% and 6.14%, respectively (Table 2).

**Description.** **Shell** medium (height 30.8–39.9 mm, width 17.2–19.2 mm), chirally dimorphic, elongate to ovate conical, rather thin and glossy. Spire conical; apex acute, light brown and without black spot on tip. Whorls 6–7 nearly smooth; suture wide and depressed; last whorl rounded. Periostracum usually deciduous to yellowish green radial streaks, more conspicuous on last whorl and faded in earlier whorls. Last whorl without or with narrow to wide brownish spiral band on periphery; varix absent. Parietal callus thin and transparent.

Aperture ovate; peristome expanded and not reflected; lip pale purplish pink. Outer palatal wall with dark radial band just next to expanded lip (also visible on inner wall) and brownish radial band encircled umbilicus present (sometimes absent). Umbilicus narrowly opened.

**Genital organs.** Atrium relatively short. Penis enlarged, conical, and almost as long as vagina. Penial retractor muscle thin and inserting on epiphallus close to penis. Epiphallus thin and long slender tube, and approximately as long as penis. Flagellum short, extending from epiphallus, ~ 1/2 of penis length, and terminating in slightly enlarged coil. Appendix short, slender tube, nearly as long as epiphallus. Vas deferens slender tube passing from free oviduct and terminating at epiphallus-flagellum junction (Fig. 28D). Internal wall of penis corrugated, exhibiting series of weak longitudinal penial pilasters forming fringe around penial wall, and with smooth wall around base of penial verge. Penial verge very short conical with opening at the tip (Fig. 28E).

Vagina slender, cylindrical, and approximately as long as penis. Gametolytic duct cylindrical tube, similar diameter as vagina then tapering to slender tube terminally and connected to enlarged elliptical gametolytic sac (missing during dissection). Free oviduct short; oviduct forming lobule alveoli (Fig. 28D). Internal wall of vagina possessing smooth ridges near genital orifice; ridges becoming swollen and corrugated longitudinal vaginal pilasters in middle, and with deep crenulations close to free oviduct opening (Fig. 28E).

**Haplotype network.** There was a total of five COI haplotypes of *A. pankowskianus* in this study, and the highest number of mutational steps in the COI minimum spanning network is two (Fig. 31).

**Distribution.** This species is found in Bolikhamsai and Khammouan provinces, Laos, and Khanh Hoa Province, Vietnam.

**Remarks.** Empty shells from Phong Nha National Park, Quang Binh Province, Vietnam, identified as '*A. roseolabiatus*' in Inkhavilay et al (2017: CUMZ 7053; 2D+3S shells) possess a transparent parietal callus with a dark radial band on the palatal wall just next to the lip. This specimen lot could probably be assigned to *A. pankowskianus* instead. Future molecular evidence is needed to shed light on the systematic status of this population.

## Discussion

Arboreal snails in the genus *Amphidromus* exhibit high levels of variation in intraspecific shell colour and pattern (Haniel 1921; Lee et al. 2022), while shells of different species may be similar due to shared arboreal adaptations (Jirapatrasilp et al. 2022; Lee et al. 2022). Although conchological characters can be used to diagnose different *Amphidromus* species to some extent (Laidlaw and Solem 1961; Sutcharit and Panha 2006; Inkhavilay et al. 2019), the amount of intraspecific shell variability is most often not, or poorly, known. In this regard, DNA sequence data, especially the mitochondrial gene fragments referred to as "DNA barcodes," provide additional and solid evidence to delimit species and help to distinguish between intra- and interspecific shell differentiation (Pholyotha et al. 2021; Jirapatrasilp et al. 2022; Lee et al. 2022).

Apart from examining the reciprocal monophyly of each species, the use of interspecific genetic distances is another means to set the preliminary cut-off for each clade to become putative species, although the use of interspecific

genetic distances has been discussed as an unfavourable way to delimit species (Ferguson 2002). Davison et al. (2009) reported an optimal COI intra/interspecific threshold value for stylommatophoran land snails as 4%, although this value was associated with an overall false negative error (interspecific variation misdiagnosed as same species) of 32% and 44% for the longer (381 bp) and shorter (228 bp) sequences, respectively. In our study, the species retrieved from the reciprocal monophyly validated by this cut-off value are in accordance with the preliminarily retrieved morphospecies, and we identify a range of 9–12% as the COI interspecific threshold value for *Amphidromus* species in this study. Although Davison et al. (2009) did not conclusively identify a barcode gap in stylommatophoran land snails, our intraspecific distances of *Amphidromus* species typically fall below or hover around 5%. The notable exceptions are *A. haematostoma* (10.03%) and *A. costifer* (7.84%), in which these two species would be flagged for further examination of possible cryptic species. Therefore, we propose a COI barcode gap for *Amphidromus* of 5–9%, which could be used to delimit more *Amphidromus* species in further studies.

Although there is still no general 16S intra/interspecific threshold value for stylommatophoran land snails, we could estimate the threshold for the Camaenidae to some extent. In this study, we identify a range of 3–5% as the 16S interspecific threshold value for *Amphidromus*. This range is comparable to the lower boundary of 16S interspecific distances reported in other genera in the Camaenidae, e.g., *Aegistohadra* from China and Vietnam (5.97–11.86%; Jirapatrasilp et al. 2022), *Camaena* from China (5–15%; Ding et al. 2016), *Euhadra* from Bonin Islands, Japan (5.8–16.5%; Chiba 1999), and *Acusta* from East Asia (5.3–18.8% Hwang et al. 2021). The 16S barcode gap for *Amphidromus* in this study is less conspicuous, as the 16S intraspecific distances typically fall below or hover around 3%. Therefore, we suggest a 16S interspecific threshold range of 5–6% for the Camaenidae, which could be implemented to support the species delimited by the COI barcode gap. The phylogenetic tree constructed from 16S also yielded identical clades to those from the COI phylogeny.

Internal morphological characters, especially those of reproductive system such as penis and vagina, are often species-specific and therefore are interpreted as the prime species recognition characters (Gómez 2001). The differentiation of these characters has been assumed to promote speciation in land snails (Kameda et al. 2009; Sauer and Hausdorf 2009). In the present study we observed some modest differences among *Amphidromus* species with respect to the size, shape, and surface of the penial verge, and the inner wall sculpture of the penis and vagina. Further morphometric analyses of several parts of genitalia (Kameda et al. 2009; Sauer and Hausdorf 2009) will shed light on the extent of divergence in genital morphology of these *Amphidromus* species.

The non-monophyly of *Amphidromus* species exhibiting the same chirality state (exclusively sinistral or dextral, or chirally dimorphic) illustrates that the multiple origins of left–right coiling reversal are common in terrestrial snails (Schilthuizen and Davison 2005; Gittenberger et al. 2012). Within the family Camaenidae, shell coiling reversal has also been reported in *Satsuma* Adams, 1868 (Hoso et al. 2010) and *Aegistohadra* Wu, 2004 (Jirapatrasilp et al. 2022). *Amphidromus* is also well-known for a high number of species exhibiting dimorphic chirality (Schilthuizen et al. 2005; Sutcharit et al. 2007, 2013), and the

coexistence of both shell coiling directions in the same population has been assumed to be maintained by sexual selection (Schilthuizen et al. 2007, 2012). *Amphidromus* thus has an important role in chirality research, which would further support the importance of the systematic revision of this snail group.

## Acknowledgements

Special thanks go to Philippe Bouchet, Virginie Héros, Manuel Caballer, Philippe Maestrati, Alexandre Lardeur, and Priscillia Bourguignon (MNHN, Paris), Jonathan Ablett, Fred Naggs, Harold Taylor, and Kevin Webb (NHMUK, London), Thierry Backeljau and Yves Samyn (RBINS, Brussels), Jeroen Goud and the late Wim J.M. Maassen (RMNH, Leiden), and Ronald Janssen (SMF, Frankfurt) for allowing the authors to examine the type materials and photographs. We also thank Barna Páll-Gergely for comments, and the information and images of *A. thachi* specimens deposited in the MNHN, Arthit Polyotha for photographing SEM images, and Frank Köhler, Menno Schilthuizen, and Thor-Seng Liew for valuable comments that greatly improved the manuscript. Photographs of the type specimens from the Molluscs Collection (IM) of MNHN are credited to Virginie Héros and Philippe Maestrati taken under the project E-RECOLNAT: ANR-11-INBS-0004 unless stated otherwise. Images of the type specimens from the other museum collections are credited to each respective museum.

## Additional information

### Conflict of interest

The authors have declared that no competing interests exist.

### Ethical statement

No ethical statement was reported.

### Funding

This project is partially funded by the National Research Council of Thailand (NRCT-N35E660138) and Thailand Research Fund (grant no. DBG 6080011) to CS.

### Author contributions

Conceptualization: CS, PJ, CTL. Data curation: PJ, CS, CTL. Formal analysis: PJ. Funding acquisition: CS. Investigation: CWH, CTL, PJ, CS. Methodology: CS, CWH, PJ, CTL. Project administration: PJ. Resources: CS, CTL. Validation: CWH, CTL. Visualization: PJ. Writing - original draft: CS, PJ. Writing - review and editing: CWH, CTL.

### Author ORCIDs

Parin Jirapatrasilp  <https://orcid.org/0000-0002-5591-6724>

Chih-Wei Huang  <https://orcid.org/0000-0002-2921-4294>

Chirasak Sutcharit  <https://orcid.org/0000-0001-7670-9540>

Chi-Tse Lee  <https://orcid.org/0000-0003-2695-0680>

### Data availability

All of the data that support the findings of this study are available in the main text or Supplementary Information.

## References

- Albers JC (1850) Die Heliceen, nach natürlicher Verwandtschaft systematisch geordnet. Verlag von Th. Chr. Fr. Enslin, Berlin, 262 pp. <https://doi.org/10.5962/bhl.title.11507>
- Albers JC (1860) Die Heliceen nach natürlicher Verwandtschaft systematisch geordnet, ed. 2. Engelmann, Leipzig, 359 pp. <https://doi.org/10.5962/bhl.title.11218>
- Anisimova M, Gil M, Dufayard J-F, Dessimoz C, Gascuel O (2011) Survey of branch support methods demonstrates accuracy, power, and robustness of fast likelihood-based approximation schemes. *Systematic Biology* 60(5): 685–699. <https://doi.org/10.1093/sysbio/syr041>
- Bandelt HJ, Forster P, Röhl A (1999) Median-joining networks for inferring intraspecific phylogenies. *Molecular Biology and Evolution* 16(1): 37–48. <https://doi.org/10.1093/oxfordjournals.molbev.a026036>
- Bentham Jutting WSS van (1950) Systematic studies on the non-marine Mollusca of the Indo-Australian Archipelago. II. Critical revision of the Javanese pulmonate land-shells of the families Helicarionidae, Pleurodontidae, Fruticolidae and Streptaxidae. *Treubia* 20: 381–505. <https://doi.org/10.14203/treubia.v20i3.2634>
- Bentham Jutting WSS van (1959) Catalogue of the non-marine Mollusca of Sumatra and of its satellite islands. *Beaufortia* 7: 41–191. <https://repository.naturalis.nl/pub/504682>
- Bülow C (1905) Einige Seltenheiten aus meiner Sammlung. *Nachrichtenblatt der Deutschen Malakologischen Gesellschaft* 37: 78–83. <https://biostor.org/reference/190425>
- Chiba S (1999) Accelerated evolution of land snails *Mandarina* in the oceanic Bonin Islands: Evidence from mitochondrial DNA sequences. *Evolution* 53(2): 460–471. <https://doi.org/10.2307/2640782>
- Dautzenberg P, Fischer H (1906) Liste des mollusques récoltés par M.H. Mansuy en Indo-Chine et au Yunnan et description d'espèces nouvelles. *Journal de Conchyliologie* 53[1905]: 343–471. <https://biostor.org/reference/145632>
- Davison A, Blackie RLE, Scothern GP (2009) DNA barcoding of stylommatophoran land snails: A test of existing sequences. *Molecular Ecology Resources* 9(4): 1092–1101. <https://doi.org/10.1111/j.1755-0998.2009.02559.x>
- Degner E (1928) *Spolia mentaweisiana*: Binnen-Mollusken von den Mentawai-Inseln. *Treubia* 10: 319–354. <https://doi.org/10.14203/treubia.v10i2-3.1808>
- Ding H-L, Wang P, Qian Z-X, Lin J-H, Zhou W, Hwang C, Ai H-M (2016) Revision of sinistral land snails of the genus *Camaena* (Stylommatophora, Camaenidae) from China based on morphological and molecular data, with description of a new species from Guangxi, China. *ZooKeys* 584: 25–48. <https://doi.org/10.3897/zookeys.584.7173>
- Ferguson JWH (2002) On the use of genetic divergence for identifying species. *Biological Journal of the Linnean Society* 75(4): 509–516. <https://doi.org/10.1046/j.1095-8312.2002.00042.x>
- Fischer H, Dautzenberg P (1904) Catalogue des mollusques terrestres et fluviatiles de l'Indo-Chine orientale cités jusqu' à ce jour. In: Leroux E (Ed.) *Mission Pavie Indo-Chine 1879-1895, Études diverses III Recherches sur l'histoire naturelle de l'Indo-Chine orientale*. Leroux, E., Paris, 390–450. <https://doi.org/10.5962/bhl.title.50990>
- Fruhstorfer H (1905) Ein neuer *Amphidromus*. *Nachrichtenblatt der Deutschen Malakozoologischen Gesellschaft* 37: 83–84. <https://biostor.org/reference/190426>
- Fulton HC (1896) A list of the species of *Amphidromus*, Albers, with critical notes and descriptions of some hitherto undescribed species and varieties. *Annals & Magazine of Natural History* 17(97): 66–94. <https://doi.org/10.1080/00222939608680326>

- Gittenberger E, Hamann TD, Asami T (2012) Chiral speciation in terrestrial pulmonate snails. *PLOS ONE* 7(4): e34005. <https://doi.org/10.1371/journal.pone.0034005>
- Gómez BJ (2001) Structure and Functioning of the Reproductive System. In: Barker GM (Ed.) *The Biology of Terrestrial Molluscs*. CABI Publishing, New York, USA, 307–330. <https://doi.org/10.1079/9780851993188.0307>
- Haas F (1934) Neue Landschnecken des Senckenberg-Museums. *Senckenbergiana* 16: 94–98.
- Haniel CB (1921) Variationsstudie an timoresischen *Amphidromus* arten. *Zeitschrift für Induktive Abstammungs- und Vererbungslehre* 25: 1–88. <https://doi.org/10.1007/BF01808854>
- Hoang DT, Chernomor O, Haeseler A von, Minh BQ, Vinh LS (2018) UFBoot2: Improving the ultrafast bootstrap approximation. *Molecular Biology and Evolution* 35(2): 518–522. <https://doi.org/10.1093/molbev/msx281>
- Hoso M, Kameda Y, Wu S-P, Asami T, Kato M, Hori M (2010) A speciation gene for left–right reversal in snails results in anti-predator adaptation. *Nature Communications* 1(1): 133. <https://doi.org/10.1038/ncomms1133>
- Huber F (2015) *Amphidromus thachi*, a new species (Gastropoda: Camaenidae) from Vietnam. *Gloria Maris* 54: 29–31.
- Hwang C-C, Zhou W-C, Ger M-J, Guo Y, Qian Z-X, Wang Y-C, Tsai C-L, Wu S-P (2021) Biogeography of land snail genus *Acusta* (Gastropoda: Camaenidae): Diversification on East Asian islands. *Molecular Phylogenetics and Evolution* 155: 106999. <https://doi.org/10.1016/j.ympev.2020.106999>
- ICZN (1999) *International Code of Zoological Nomenclature*, 4<sup>th</sup> edn. International Trust for Zoological Nomenclature, London, 306 pp.
- Inkhavilay K, Sutcharit C, Panha S (2017) Taxonomic review of the tree snail genus *Amphidromus* Albers, 1850 (Pulmonata: Camaenidae) in Laos, with the description of two new species. *European Journal of Taxonomy* 330(330): 1–40. <https://doi.org/10.5852/ejt.2017.330>
- Inkhavilay K, Sutcharit C, Bantaowong U, Chanabun R, Siritwut W, Srisonchai R, Pholyotha A, Jirapatrasilp P, Panha S (2019) Annotated checklist of the terrestrial molluscs from Laos (Mollusca, Gastropoda). *ZooKeys* 834: 1–166. <https://doi.org/10.3897/zookeys.834.28800>
- Jirapatrasilp P, Huang C-W, Hwang C-C, Sutcharit C, Lee C-T (2022) Convergent evolution of *Amphidromus*-like colourful arboreal snails and phylogenetic relationship of East Asian camaenids, with description of a new *Aegistohadra* species (Helicoidei, Camaenidae, Bradybaeninae). *Invertebrate Systematics* 36(3): 244–290. <https://doi.org/10.1071/IS21015>
- Kalyaanamoorthy S, Minh BQ, Wong TKF, Haeseler A von, Jermin LS (2017) ModelFinder: Fast model selection for accurate phylogenetic estimates. *Nature Methods* 14(6): 587–589. <https://doi.org/10.1038/nmeth.4285>
- Kameda Y, Kawakita A, Kato M (2009) Reproductive character displacement in genital morphology in *Satsuma* land snails. *American Naturalist* 173(5): 689–697. <https://doi.org/10.1086/597607>
- Katoh K, Rozewicki J, Yamada KD (2017) MAFFT online service: Multiple sequence alignment, interactive sequence choice and visualization. *Briefings in Bioinformatics* 20(4): bbx108–bbx108. <https://doi.org/10.1093/bib/bbx108>
- Köhler F, Criscione F (2015) A molecular phylogeny of camaenid land snails from north-western Australia unravels widespread homoplasy in morphological characters

- (Gastropoda, Helicoidea). *Molecular Phylogenetics and Evolution* 83: 44–55. <https://doi.org/10.1016/j.ympev.2014.11.009>
- Kumar S, Stecher G, Tamura K (2016) MEGA7: Molecular Evolutionary Genetics Analysis version 7.0 for bigger datasets. *Molecular Biology and Evolution* 33(7): 1870–1874. <https://doi.org/10.1093/molbev/msw054>
- Laidlaw FF, Solem A (1961) The land snail genus *Amphidromus*: A synoptic catalogue. *Fieldiana. Zoology* 41: 507–677. <https://doi.org/10.5962/bhl.title.2832>
- Lee C-T, Huang C-W, Hwang C-C, Sutcharit C, Jirapatrasilp P (2022) Arboreal snail genus *Amphidromus* Albers, 1850 of Southeast Asia: Shell polymorphism of *Amphidromus cruentatus* (Morelet, 1875) revealed by phylogenetic and morphometric analyses. *PLOS ONE* 17(8): e0272966. <https://doi.org/10.1371/journal.pone.0272966>
- Lehmann H, Maassen WJM (2004) A new species of *Amphidromus* from Laos (Gastropoda, Pulmonata, Camaenidae). *Basteria* 68: 17–20. <https://natuurtijdschriften.nl/pub/597271/BAST2004068001003.pdf>
- Leigh JW, Bryant D (2015) POPART: Full-feature software for haplotype network construction. *Methods in Ecology and Evolution* 6(9): 1110–1116. <https://doi.org/10.1111/2041-210X.12410>
- Miller MA, Pfeiffer W, Schwartz T (2010) Creating the CIPRES Science Gateway for inference of large phylogenetic trees. *Proceedings of the Gateway Computing Environments Workshop (GCE)*, 14 Nov 2010, New Orleans, LA, 1–8. <https://doi.org/10.1109/GCE.2010.5676129>
- Möllendorff OF von (1898) Die Binnenmollusken Annams. *Nachrichtenblatt der Deutschen Malakozoologischen Gesellschaft* 30: 65–85. <https://www.biodiversitylibrary.org/item/89671>
- Möllendorff OF von (1900a) Zur Binnenmollusken-Fauna Annams III. *Nachrichtenblatt der Deutschen Malakozoologischen Gesellschaft* 32: 117–139. <https://www.biodiversitylibrary.org/page/15598462>
- Möllendorff OF von (1900b) Zwei neue *Amphidromus* aus Annam. *Nachrichtenblatt der Deutschen Malakozoologischen Gesellschaft* 32: 22–24. <https://www.biodiversitylibrary.org/page/15598365>
- Möllendorff OF von (1901) Zur Binnenmollusken-Fauna von Annam IV. *Nachrichtenblatt der Deutschen Malakozoologischen Gesellschaft* 33: 45–50. <https://www.biodiversitylibrary.org/page/15598588>
- MolluscaBase (2023) MolluscaBase taxon details: *Amphidromus* Albers, 1850. <https://www.molluscabase.org/aphia.php?p=taxdetails&id=818112> [Verified 20 July 2023]
- Nguyen L-T, Schmidt HA, Haeseler A von, Minh BQ (2015) IQ-TREE: A fast and effective stochastic algorithm for estimating maximum-likelihood phylogenies. *Molecular Biology and Evolution* 32(1): 268–274. <https://doi.org/10.1093/molbev/msu300>
- Páll-Gergely B, Hunyadi A, Auffenberg K (2020) Taxonomic vandalism in malacology: Comments on molluscan taxa recently described by N. N. Thach and colleagues (2014–2019). *Folia Malacologica* 28(1): 35–76. <https://doi.org/10.12657/folmal.028.002>
- Parsons J, Abbas J (2016) A new subspecies of *Amphidromus* (*Goniodromus*) *bulowi* Fruhstorfer, 1905 (Gastropoda: Pulmonata: Camaenidae) from Sumatra, Indonesia. *The Festivus* 48(4): 235–247. <https://doi.org/10.54173/F484235>
- Pholyotha A, Sutcharit C, Tongkerd P, Jeratthitikul E, Panha S (2021) Integrative systematics reveals the new land-snail genus *Taphrenalla* (Eupulmonata: Ariophantidae) with a description of nine new species from Thailand. *Contributions to Zoology* 90(1): 21–69. <https://doi.org/10.1163/18759866-BJA10013>

- Pilsbry HA (1900) Manual of Conchology, Second Series, Vol. 13. Academy of Natural Sciences of Philadelphia, Philadelphia, 253 pp. <https://www.biodiversitylibrary.org/item/16708>
- Pilsbry HA (1901) Manual of Conchology, Second Series, Vol. 14. Academy of Natural Sciences of Philadelphia, Philadelphia, 302 pp. <https://www.biodiversitylibrary.org/item/16294>
- Poppe GT (2020) Philippine *Amphidromus*. A taxonomic and nomenclatural puzzle. *Vivaya* (Supplement 15): 1–86.
- Richardson L (1985) Camaenidae: Catalogue of Species. *Tryonia* 12: 1–479. <https://www.biodiversitylibrary.org/item/262223>
- Rolle H (1908) Zur Fauna von West-Sumatra. *Nachrichtenblatt der Deutschen Malakozoologischen Gesellschaft* 40: 63–70. <https://biostor.org/reference/190496>
- Ronquist F, Teslenko M, van der Mark P, Ayres DL, Darling A, Höhna S, Larget B, Liu L, Suchard MA, Huelsenbeck JP (2012) MrBayes 3.2: Efficient Bayesian phylogenetic inference and model choice across a large model space. *Systematic Biology* 61(3): 539–542. <https://doi.org/10.1093/sysbio/sys029>
- San Mauro D, Agorreta A (2010) Molecular systematics: A synthesis of the common methods and the state of knowledge. *Cellular & Molecular Biology Letters* 15(2): 311–341. <https://doi.org/10.2478/s11658-010-0010-8>
- Sauer J, Hausdorf B (2009) Sexual selection is involved in speciation in a land snail radiation on Crete. *Evolution* 63(10): 2535–2546. <https://doi.org/10.1111/j.1558-5646.2009.00751.x>
- Schileyko AA (2011) Check-list of land pulmonate molluscs of Vietnam (Gastropoda: Stylommatophora). *Ruthenica* 21: 1–68. <https://www.biotaxa.org/Ruthenica/article/view/3603>
- Schilthuizen M, Davison A (2005) The convoluted evolution of snail chirality. *Naturwissenschaften* 92(11): 504–515. <https://doi.org/10.1007/s00114-05-0045-2>
- Schilthuizen M, Scott BJ, Cabanban AS, Craze PG (2005) Population structure and coil dimorphism in a tropical land snail. *Heredity* 95(3): 216–220. <https://doi.org/10.1038/sj.hdy.6800715>
- Schilthuizen M, Craze PG, Cabanban AS, Davison A, Stone J, Gittenberger E, Scott BJ (2007) Sexual selection maintains whole-body chiral dimorphism in snails. *Journal of Evolutionary Biology* 20(5): 1941–1949. <https://doi.org/10.1111/j.1420-9101.2007.01370.x>
- Schilthuizen M, Haase M, Koops K, Looijestijn SM, Hendrikse S, Gravendeel B (2012) The ecology of shell shape difference in chirally dimorphic snails. *Contributions to Zoology* 81(2): 95–101. <https://doi.org/10.1163/18759866-08102004>
- Smith EA (1893) Descriptions of six new species of land shells from Annam. *Proceedings of the Malacological Society of London* 1: 10–13. <https://doi.org/10.1093/oxfordjournals.mollus.a064066>
- Solem A (1965) Land snails of the genus *Amphidromus* from Thailand (Mollusca: Pulmonata: Camaenidae). *Proceedings of the United States National Museum* 117(3519): 615–627. <https://doi.org/10.5479/si.00963801.117-3519.615>
- Solem A (1966) Some non-marine mollusks from Thailand, with notes on classification of the Helicarionidae. *Spolia Zoologica Musei Hauniensis* 24: 1–110.
- Solem A (1983) First record of *Amphidromus* from Australia with anatomical note on several species (Mollusca: Pulmonata: Camaenidae). *Records of the Australian Museum* 35(4): 153–166. <https://doi.org/10.3853/j.0067-1975.35.1983.315>
- Sutcharit C, Panha S (2006) Taxonomic review of the tree snail *Amphidromus* Albers, 1850 (Pulmonata: Camaenidae) in Thailand and adjacent areas: subgenus

- Amphidromus*. Journal of Molluscan Studies 72(1): 1–30. <https://doi.org/10.1093/mollus/eyi044>
- Sutcharit C, Asami T, Panha S (2007) Evolution of whole-body enantiomorphy in the tree snail genus *Amphidromus*. Journal of Evolutionary Biology 20(2): 661–672. <https://doi.org/10.1111/j.1420-9101.2006.01246.x>
- Sutcharit C, Tongkerd P, Panha S (2013) First record on chiral dimorphic population of *Amphidromus inversus annamiticus* (Crosse and Fischer, 1863) from Thailand. Tropical Natural History 13: 53–57. <https://li01.tci-thaijo.org/index.php/tnh/article/view/103040>
- Sutcharit C, Ablett J, Tongkerd P, Naggs F, Panha S (2015) Illustrated type catalogue of *Amphidromus* Albers, 1850 in the Natural History Museum, London, and descriptions of two new species. ZooKeys 492: 49–105. <https://doi.org/10.3897/zookeys.492.8641>
- Sutcharit C, Naggs F, Ablett JD, Sang PV, Hao LV, Panha S (2021) Anatomical note on a tree snail *Amphidromus (Amphidromus) cambojiensis* (Reeve, 1860) from Vietnam (Eupulmonata: Camaenidae). Journal of Natural History 55(17–18): 1059–1069. <https://doi.org/10.1080/00222933.2021.1933230>
- Tanabe AS (2011) Kakusan4 and Aminosan: Two programs for comparing nonpartitioned, proportional and separate models for combined molecular phylogenetic analyses of multilocus sequence data. Molecular Ecology Resources 11(5): 914–921. <https://doi.org/10.1111/j.1755-0998.2011.03021.x>
- Thach NN (2005) Shells of Vietnam. Conchbooks, Hackenheim, 338 pp.
- Thach NN (2016) Vietnamese new mollusks with 59 new species. 48HrBooks Company, Ohio, USA, 205 pp.
- Thach NN (2017) New shells of Southeast Asia with 2 new genera and 85 new species. 48Hr-Books Company, Ohio, USA, 128 pp.
- Thach NN (2018) New shells of South Asia seashells-freshwater & land snails, 3 new genera, 132 new species & subspecies. 48HrBooks Company, Ohio, USA, 173 pp.
- Thach NN (2020a) New shells of South Asia. Vol. 2. Seashells\*Freshwater\*Land snails. With one New Genus and 140 New Species & Subspecies, Reply to comments made in error. 48HRBooks Company, Akron, Ohio, USA, 189 pp.
- Thach NN (2020b) Remarks on *Amphidromus reflexilabris* Schepman, 1892, *Amphidromus roseolabiatus* Fulton, 1896, *Amphidromus anhduongae* Thach, 2020 and correction of errors in “New Shells of South Asia, Volume 2”. The Festivus 52(4): 359–362. <https://doi.org/10.54173/F524359>
- Thach NN (2021) New shells of South Asia and Taiwan, China, Tanzania. Seashells\*-Freshwater\*Land snails. With 116 new species and subspecies and rejected synonyms, accepted species. 48HRBooks Company, Akron, Ohio, USA, 202 pp.
- Thach NN, Huber F (2014) A new *Amphidromus* (Gastropoda: Camaenidae) from Vietnam. Basteria 78: 35–37. <https://natuurtijdschriften.nl/pub/643896/BAST2014078001004.pdf>
- Thach NN, Simone LRL, Parsons J, Abbas J, Huber F (2020) Comments on “Vandalism” in Malacology. The Festivus 52(2): 184–190. <https://doi.org/10.54173/F522184>
- Trifinopoulos J, Nguyen L-T, Haeseler A von, Minh BQ (2016) W-IQ-TREE: A fast online phylogenetic tool for maximum likelihood analysis. Nucleic Acids Research 44(W1): W232–W235. <https://doi.org/10.1093/nar/gkw256>
- Verbinnen G, Segers L (2021) To the knowledge of *Amphidromus Mirandus* Bavay & Dautzenberg, 1912 and *Amphidromus heinrichhuberi* Thach & Huber in Thach, 2016 with comments on the publication by Barna Páll-Gergely et al (2020). Gloria Maris 60: 30–33.

- Wang YC (2019) Review on the synonymy concerning genus *Amphidromus* Albers, 1850 (Gastropoda: Camaenidae), with descriptions of new species. *The Festivus* 51(4): 297–305. <https://doi.org/10.54173/F514297>
- Zilch A (1953) Die Typen und Typoide des Natur-Museums Senckenberg, 10: Mollusca, Pleurodontidae (1). *Archiv für Molluskenkunde* 82: 131–140.

## Supplementary material 1

### Bayesian phylogenetic tree of *Amphidromus* spp.

Authors: Parin Jirapatrasilp, Chih-Wei Huang, Chirasak Sutcharit, Chi-Tse Lee

Data type: jpg

Copyright notice: This dataset is made available under the Open Database License (<http://opendatacommons.org/licenses/odbl/1.0/>). The Open Database License (ODbL) is a license agreement intended to allow users to freely share, modify, and use this Dataset while maintaining this same freedom for others, provided that the original source and author(s) are credited.

Link: <https://doi.org/10.3897/zookeys.1196.112146.suppl1>

# Complete mitochondrial genomes of the black corals *Alternatipathes mirabilis* Opresko & Molodtsova, 2021 and *Parantipathes larix* (Esper, 1788) (Cnidaria, Anthozoa, Hexacorallia, Antipatharia, Schizopathidae)

Brendan A. Cruz<sup>1\*</sup>, Anneau Cappelmann<sup>1\*</sup>, Hope Chutjian<sup>1\*</sup>, Jude C. Roman<sup>1\*</sup>, Mason A. Reid<sup>1\*</sup>, Jacob Wright<sup>1\*</sup>, Aydanni D. Gonzalez<sup>1\*</sup>, Taylor Keyman<sup>1\*</sup>, Kierstin M. Griffith<sup>1\*</sup>, Hannah J. Appiah-Madson<sup>2</sup>, Daniel L. Distel<sup>2</sup>, Vonda E. Hayes<sup>3</sup>, Jim Drewery<sup>4</sup>, D. Tye Pettay<sup>1</sup>, Joseph L. Staton<sup>1</sup>, Mercer R. Brugler<sup>1,5,6</sup>

1 Department of Natural Sciences, University of South Carolina Beaufort, 1100 Boundary St, Beaufort, SC 29902, USA

2 Ocean Genome Legacy Center, Northeastern University, 430 Nahant Road, Nahant, MA 01908, USA

3 Department of Fisheries & Oceans Canada, Northwest Atlantic Fisheries Centre, 80 East White Hills Road, St. John's, Newfoundland & Labrador, A1C 5X1, Canada

4 Marine Directorate of Scottish Government, Marine Laboratory, 375 Victoria Road, Aberdeen AB11 9DB, Scotland, UK

5 Division of Invertebrate Zoology, American Museum of Natural History, Central Park West at 79th Street, New York, NY 10024, USA

6 Department of Invertebrate Zoology, National Museum of Natural History, Smithsonian Institution, 10th St. & Constitution Ave. NW, Washington, DC 20560, USA

Corresponding author: Mercer R. Brugler ([mbrugler@uscb.edu](mailto:mbrugler@uscb.edu))

## Abstract

We describe the complete mitogenomes of the black corals *Alternatipathes mirabilis* Opresko & Molodtsova, 2021 and *Parantipathes larix* (Esper, 1790) (Cnidaria, Anthozoa, Hexacorallia, Antipatharia, Schizopathidae). The analysed specimens include the holotype of *Alternatipathes mirabilis*, collected from Derickson Seamount (North Pacific Ocean; Gulf of Alaska) at 4,685 m depth and a potential topotype of *Parantipathes larix*, collected from Secca dei Candelieri (Mediterranean Sea; Tyrrhenian Sea; Salerno Gulf; Italy) at 131 m depth. We also assemble, annotate and make available nine additional black coral mitogenomes that were included in a recent phylogeny (Quattrini et al. 2023b), but not made easily accessible on GenBank. This is the first study to present and compare two mitogenomes from the same species of black coral (*Stauropathes arctica* (Lütken, 1871)) and, thus, place minimum boundaries on the expected level of intraspecific variation at the mitogenome level. We also compare interspecific variation at the mitogenome-level across five different specimens of *Parantipathes* Brook, 1889 (representing at least two different species) from the NE Atlantic and Mediterranean Sea.

**Key words:** Antipatharian, genome skimming, holotype, intraspecific variation, Mitofinder, *Parantipathes*, *Stauropathes arctica*

## Introduction

Black corals (Cnidaria, Anthozoa, Hexacorallia, Antipatharia) are found in all oceans and hold the record for the deepest (*Schizopathes affinis* Brook, 1889 at 8,900 m; Molodtsova (2006)) and longest-lived (*Leiopathes glaberrima* (Esper,



Academic editor: James Reimer

Received: 4 December 2023

Accepted: 5 February 2024

Published: 22 March 2024

ZooBank: <https://zoobank.org/14A17856-7138-49D8-B73B-554F334AB858>

Copyright: © Brendan A. Cruz et al.  
This is an open access article distributed under the terms of the CCO Public Domain Dedication.

\* Undergraduate.

**Citation:** Cruz BA, Cappelmann A, Chutjian H, Roman JC, Reid MA, Wright J, Gonzalez AD, Keyman T, Griffith KM, Appiah-Madson HJ, Distel DL, Hayes VE, Drewery J, Pettay DT, Staton JL, Brugler MR (2024) Complete mitochondrial genomes of the black corals *Alternatipathes mirabilis* Opresko & Molodtsova, 2021 and *Parantipathes larix* (Esper, 1788) (Cnidaria, Anthozoa, Hexacorallia, Antipatharia, Schizopathidae). ZooKeys 1196: 79–93. <https://doi.org/10.3897/zookeys.1196.116837>

1792) at 4,265 years; Roark et al. (2009)) coral and serve as underwater hosts for a diverse and staggering number of epibionts (Love et al. 2007). Black corals have historically been considered a deep-water group; however, only 31.57% of the 285 currently-described species occur at depths greater than 800 m (Molodtsova et al. 2022, 2023). While the black coral community continues to wait for the first antipatharian nuclear genome, black coral mitogenomics is gaining in popularity due to the ease of bioinformatically extracting whole mitogenomes from genome-skimming data (Quattrini et al. 2023a), its informativeness, cost-effectiveness and the availability of comparative data (Brugler and France 2007; Sinniger and Pawlowski 2009; Kayal et al. 2013; Figueroa et al. 2019; Barrett et al. 2020; Asorey et al. 2021; Bledsoe-Becerra et al. 2022; Feng et al. 2023; Quattrini et al. 2023a, b; Ramos et al. 2023). Herein, we describe two additional black coral mitogenomes (*Alternatipathes mirabilis* Opresko & Molodtsova, 2021 and *Parantipathes larix* (Esper, 1790)), both from the family Schizopathidae and present them in a phylogenetic context. We analysed the holotype of *Alternatipathes mirabilis*, collected from Derickson Seamount (North Pacific Ocean; Gulf of Alaska) at 4,685 m depth and a potential topotype of *Parantipathes larix*, collected from Secca dei Candelieri (Mediterranean Sea; Tyrrhenian Sea; Salerno Gulf; Italy) at 131 m depth. According to Esper (1792), the type locality of *P. larix* is in the “ocean near Naples,” which is adjacent to the Gulf of Salerno.

The genus *Alternatipathes* was established by Molodtsova and Opresko (2017) with the type species of the genus as *Umbellapathes bipinnata* Opresko, 2005 (Opresko and Molodtsova 2021). Species assigned to the genus include *Umbellapathes bipinnata*, *Bathypathes alternata* Brook, 1889, *Alternatipathes venusta* Opresko & Wagner, 2020 and *Alternatipathes mirabilis*. *Alternatipathes mirabilis* is only known from a single specimen, which we analysed herein. The species name (*mirabilis*) is derived from Latin meaning “wonderful or strange.” The genus is broadly distributed in the Pacific, Indian, Atlantic and Southern Ocean basins at depths usually exceeding 2,500 m and often greater than 4,000 m (Opresko and Molodtsova 2021). DNA analysis of mitochondrial *nad5-nad1* from the holotype suggested a close relationship to *Schizopathes* Brook, 1889 (Chery et al. 2018); however, the full mitogenome of *Schizopathes* is not currently available to test this hypothesis more robustly. The genus *Parantipathes* was established by Brook (1889) with the type species of the genus as *Antipathes larix* Esper, 1790 (Opresko and Baron-Szabo 2001). In terms of its distribution, this species is only known from the Mediterranean Sea and eastern Atlantic Ocean.

In addition to describing the mitogenomes of *Alternatipathes mirabilis* and *Parantipathes larix*, we also assembled, annotated and made available nine additional black coral mitogenomes that were included in a recent phylogeny (Quattrini et al. 2023b), but not made easily accessible on GenBank (i.e. mtDNA reads are embedded in non-annotated bulk Illumina whole genome shotgun fastq files). The taxa include *Acanthopathes thyoides* (Pourtalès, 1880) (USNM1288453), *Aphanipathes pedata* (Gray, 1857) (USNM1288458), *Bathypathes alaskensis* Opresko & Molodtsova, 2021 (USNM1288462), *Elatopathes abietina* (Pourtalès, 1874) (USNM1288451), *Parantipathes* sp. (MSS29), *Stauropathes arctica* (Lütken, 1871) (DFONL ID #4089; Canadian Museum of Nature catalogue #CMNI 2023-0258), *Stauropathes* sp. Opresko, 2002 (USNM1404493), *Telopathes magna* MacIsaac & Best, 2013 (MacIsaac et al. 2013) (USNM1204049) and *Umbellapathes* sp. Opresko, 2005 (USNM1404092).

Herein, we also compare two mitogenomes from the same species of black coral (*Stauropathes arctica*) and determine the expected level of intraspecific variation at the mitogenome level, which has not been done previously. We compare the results of this intraspecific comparison to the unexpectedly low mitogenome-level variation found within the trigenic complex (*Dendrobathypathes*, *Lillipathes* and *Parantipathes* from the eastern North Pacific; Bledsoe-Becerra et al. (2022)). We also compare interspecific variation at the mitogenome-level across five different specimens of *Parantipathes* (representing at least two different species) from the northeast Atlantic and Mediterranean Sea.

## Materials and methods

### Specimen collection and species identification

The holotype of *Alternatipathes mirabilis* Opresko & Molodtsova, 2021 (USNM1070972) was collected by Dr. Amy Baco-Taylor on 20 July 2004, from Derickson Seamount (North Pacific Ocean; Gulf of Alaska; Station # JD-093) at 4,685 m depth using the Jason II ROV (Latitude, Longitude: 53.0419, -161.183). The holotype of *A. mirabilis* was deposited into the black coral collection at the Smithsonian Institution's National Museum of Natural History (NMNH). Specimens accessioned into the SI NMNH's Invertebrate Zoology collection are freely available to researchers to access and study. *A. mirabilis* was identified by Drs. Dennis Opresko and Tina Molodtsova, the leading authorities on black coral taxonomy and systematics. *Parantipathes larix* (Esper, 1788) (USNM1280881) was collected in July 2012 from Secca dei Candelieri (Mediterranean Sea; Tyrrhenian Sea; Salerno Gulf; Italy) at 131 m depth (Latitude, Longitude: 40.0744, 15.8765). *P. larix* was also deposited into the SI NMNH's Invertebrate Zoology collection. *P. larix* was identified by Dr. Marzia Bo of the Università di Genova in Italy, also an authority on black coral taxonomy and systematics.

### Specimen preparation and sequencing

Tissues from *Alternatipathes mirabilis* (OGL-E27108; USNM1070972) and *Parantipathes larix* (OGL-E27184; USNM1280881) were initially stored in 95% ethanol. DNA was isolated from these samples using a modified CTAB extraction protocol (France et al. 1996). Specifically, tissue samples were incubated in 750 µl of 2X-CTAB with 50 µl Proteinase K (Qiagen, Hilden, Germany) overnight before digestion at 56 °C for 3 hours. Ceramic beads (200 µl, 0.1 mm) were added to each sample and tubes were placed in a BeadBug microtube homogeniser (Benchmark Scientific, South Plainfield, NJ, USA) for two 30 second intervals at 2,800 rpm. Next, particulate material was precipitated by centrifugation at 17K RCF (Relative Centrifugal Force or g-force) for 5 minutes and the supernatants were transferred to new tubes with 750 µl of -20 °C chloroform, vortexed until cloudy and phases were separated by centrifugation at 17K RCF for 10 minutes. Supernatants were then transferred to tubes with 750 µl of -20 °C absolute ethanol, inverted and phases were separated by centrifugation at 17K RCF for 5 minutes. Supernatants were discarded and precipitated DNA was washed with 750 µl of 70% ethanol and then pelleted by centrifugation at 17K RCF for 5 min. Supernatants were again discarded and pellets were dried

using a Savant DNA 120 Speedvac Concentrator (Thermo Scientific, Waltham, MA, USA) before suspension in 50 µl of Buffer AE (Qiagen, Hilden, Germany). DNA extracts were subsequently treated with RNase A and purified using a Zymo Research DNA Clean & Concentrator (Irvine, CA, USA). To visualise DNA, 2 µl of each extract was loaded on to a horizontal slab gel (1% agarose, 1X TAE buffer containing 1% Biotium GelRed nucleic acid gel stain; Fremont, CA, USA) and separated at approximately 175 V for 5 min then 130 V for 30 min and visualised using a Bio-Rad Gel Doc XR + Molecular Imager and Image Lab software (Hercules, CA, USA). To quantify DNA present in each extract, 5 µl of each sample was analysed using a Promega QuantiFluor ONE dsDNA System with a Quantus Fluorometer (Madison, WI, USA). DNA extractions were sent to the New York Genome Center for whole genome shotgun (WGS) sequencing on an Illumina HiSeqX (2x150 bp). Library preparation utilised a TruSeq PCR-free kit (450 bp).

## Bioinformatics

Mitochondrial genomes were bioinformatically extracted from the WGS runs using MitoFinder v.1.4 (Allio et al. 2020). MitoFinder employed MEGAHIT v.3.0 (Li et al. 2015) for mitogenome assembly and tRNAscan-SE (Chan and Lowe 2019) for tRNA annotation. The following command was used to run MitoFinder on an iMac: `./mitofinder --megahit --override --new-genes -j [file name] -1 [left_reads.fastq.gz] -2 [right_reads.fastq.gz] -r [genbank_reference.gb] -o [genetic_code] -p [threads] -m [memory] -t trnscan. Stichopathes luetkeni (GenBank Accession # NC_018377) was used as the reference and translation table 4 (Mold, Protozoan and Coelenterate Mitochondrial Code and the Mycoplasma/Spiroplasma Code) was used as the genetic code. Newly-assembled mitogenomes were annotated using the MITOS Web Server (Bernt et al. 2013).`

## Phylogenetic analysis

The newly-obtained mitogenomes of *Alternatipathes mirabilis* (USNM1070972; GenBank Accession Number OR398473) and *Parantipathes larix* (USNM1280881; GenBank Accession Number OR398474) were added to the phylogeny presented in Bledsoe-Becerra et al. (2022) that contained 29 mitogenomes. We then assembled, annotated and added nine black coral mitogenomes that were included in a recent phylogeny (Quattrini et al. 2023b), but not made easily accessible on GenBank. We also included two newly-released black coral mitogenomes: *Myriopathes ulex* (Ellis & Solander, 1786) (NC\_071821) and *Cirrhopathes cf. anguina* (Dana, 1846) (ON653414; Shizuru et al. (2024)) for a total of 42 taxa. Each of the 13 protein-coding genes (*cox1-3*, *nad1-6*, *nad4L*, *atp6*, *atp8* and *cytb*) and two ribosomal RNAs (12S and 16S) from all 42 mitogenomes were placed in individual AliView v.1.23 (Larsson 2014) files, individually aligned using MAFFT LINS-i v.7 (Katoh et al. 2019) and subsequently concatenated into a single file using Seqotron v.1.0.1 (Fourment and Holmes 2016), treating the mitogenome as a single locus. Significant length variation was encountered within each of the 18 intergenic regions (IGRs) across the seven families, resulting in ambiguous alignments within these regions; thus, IGRs were not considered. The final dataset consisted of 42 taxa and 16,416 sites (alignment available upon re-

quest to co-author Brugler). The Akaike Information Criterion within jModelTest v.2.1.10 (Guindon and Gascuel 2003; Darriba et al. 2012) selected the GTR + I + G model of sequence evolution (p-inv: 0.4670; gamma: 1.0920). XSEDE on the CIPRES Science Gateway v.3.3 (Miller et al. 2011) was used to construct a Maximum Likelihood phylogeny using IQ-Tree v.2.2.2.5 with the GTR+I+G model of sequence evolution, a BioNJ starting tree and 1,000 ultrafast bootstrap replicates (Hoang et al. 2018; Minh et al. 2020). The resulting phylogenetic tree was visualised using FigTree v.1.4.4 (by Andrew Rambaut; <https://github.com/rambaut/figtree/releases>). The ML tree (Fig. 1) was rooted internally to the Leiopathidae. This decision was based on: 1) the mitogenome-based phylogeny presented in Barrett et al. (2020) that included nine hexacoral outgroups (4 actinarians, 3 zoantharians, 1 scleractinian and 1 corallimorpharian) and 2) a time-calibrated phylogeny by Horowitz et al. (2023), based on target-capture enrichment of 2,380 ultraconserved elements and exonic loci from 83 species of black coral and nine outgroups, both of which recovered the Leiopathidae as an early branching, monophyletic group sister to all other antipatharian families (but see DeSalle et al. (2023)). The number of variable sites (or single nucleotide polymorphisms; SNPs) and pairwise distance estimates were calculated using MEGA X (Kumar et al. 2018; Stecher et al. 2020) and included the Kimura 2-Parameter model (K2P), uniform rates amongst sites and pairwise deletion of gaps/missing data.

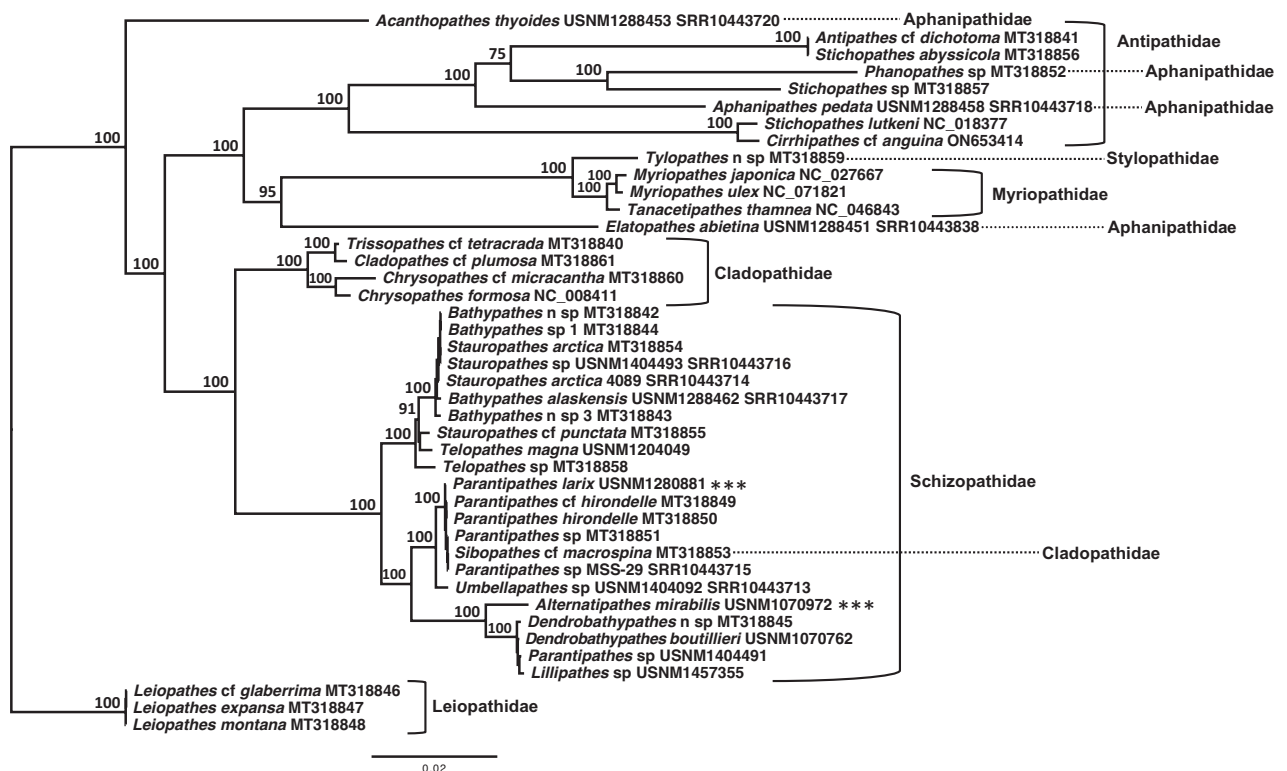


**Figure 1.** Maximum Likelihood phylogenetic tree, based on 13 protein-coding genes and two ribosomal RNAs (42 taxa and 16,416 sites). The mitogenomes of *Alternatipathes mirabilis* (USNM1070972; OR398473) and *Parantipathes larix* (USNM1280881; OR398474) are indicated with three asterisks. The families Aphanipathidae and Cladopathidae are polyphyletic with representatives indicated with a horizontal dotted line. The tree is rooted internally to the Leiopathidae. Node support values are based on 1,000 ultrafast bootstrap replicates. Species IDs are followed by museum voucher codes (e.g. USNM) and/or GenBank accession numbers (e.g. MT, NC, ON or SRR).

## Results

The *Alternatipathes mirabilis* mitogenome (OR398473) is 17,632 bp in length and contains the typical 13 protein-coding genes (*cox1-3*, *nad1-6*, *nad4L*, *atp6*, *atp8* and *cytb*), two ribosomal RNAs (12S and 16S) and two transfer RNAs (Met and Trp). Intergenic regions account for 8.72% (1,538 bp) of the mitogenome, with the longest IGR between *nad5*(5') and *nad1* (365 bp; Table 1). The *Parantipathes larix* mitogenome (OR398474) is 17,734 bp in length and contains the typical 13 protein-coding genes (*cox1-3*, *nad1-6*, *nad4L*, *atp6*, *atp8* and *cytb*), two ribosomal RNAs (12S and 16S) and two transfer RNAs (Met and Trp). Intergenic regions account for 9.41% (1,669 bp) of the mitogenome, with the longest IGR between *nad5*(5') and *nad1* (367 bp; Table 1). Both *A. mirabilis* and *P. larix* have the typical black coral mitochondrial gene order; thus, to date, one unique gene order has been observed within the Order Antipatharia. Base composition was similar between *A. mirabilis* (A: 5841, T: 4701, G: 3180, C: 3910) and *P. larix* (A: 5895, T: 4708, G: 3212, C: 3919) and both mitogenomes are AT-rich (59.79% each).

After assembling nine mitogenomes that were included in a phylogeny in Quattrini et al. (2023b), mitogenome sizes ranged from 17,699 (*Bathypathes alaskensis* USNM1288462) to 20,066 bp (*Acanthopathes thyoides* USNM1288453). Quattrini et al. (2023b) simply uploaded Illumina fastq files and each of the 13 protein-coding genes individually, but did not upload the two ribosomal RNAs (12S and 16S), two transfer RNAs (Met and Trp) or any of the intergenic regions. To make the data more easily accessible, we pulled data from the Illumina fastq files to assemble and annotate full mitogenomes. Complete nucleotide sequence data are now available in the Third Party Annotation (TPA) section of the DDBJ/ENA/GenBank databases under the following accession numbers: BK063761 (*Acanthopathes thyoides*; USNM1288453), BK063759 (*Aphanipathes pedata*; USNM1288458), BK063764 (*Bathypathes alaskensis*; USNM1288462), BK063760 (*Elatopathes abietina*; USNM1288451), BK063757 (*Parantipathes* sp.; MSS29), BK063763 (*Stauropathes arctica*; DFONL ID #4089; Canadian Museum of Nature catalogue #CMNI 2023-0258), BK063762 (*Stauropathes* sp.; USNM1404493), OR398475 (*Telopathes magna*; USNM1204049) and BK063758 (*Umbellapathes* sp.; USNM1404092). The two newly-released black coral mitogenomes ranged in size from 17,711 bp (*Myriopathes ulex* NC\_071821 [OP104910]; released 3 April 2023) to 20,452 bp (*Cirrhopathes* cf. *anguina* ON653414; released 24 December 2022; Shizuru et al. (2024)). *Elatopathes abietina* (BK063760) and *Myriopathes ulex* (NC\_071821) were the only taxa that contained a LAGLI-DADG homing endonuclease in the *cox1* gene (Beagley et al. 1996).

## Discussion

The Maximum Likelihood phylogeny (Fig. 1), consisting of 42 taxa and 16,416 sites, largely mirrors the phylogeny presented in Brugler et al. (2013) that was based on three mitochondrial gene regions (*igrW*, *igrN* and *cox3-cox1*); however, the mitogenome-based phylogeny, presented here, yields greater bootstrap support. In our new mitogenome-based phylogeny, the holotype of *Alternatipathes mirabilis* is sister to a clade containing *Dendrobathypathes* Opresko, 2002, *Parantipathes* (from the North Pacific Ocean) and *Lillipathes* Opresko, 2002 (bootstrap support: 100), while a putative topotype of *Parantipathes larix*

**Table 1.** Lengths of protein-coding genes, ribosomal RNAs, transfer RNAs and intergenic regions (IGRs) within the *Alternatipathes mirabilis* (17,632 bp; OR398473) and *Parantipathes larix* (17,734 bp; OR398474) mitogenomes.

Gene	<i>Parantipathes larix</i>	<i>Alternatipathes mirabilis</i>
12S	1141	1141
IGR	197	197
<i>nad2</i>	1518	1518
IGR	19	19
tRNA Trp	70	70
IGR	27	27
<i>nad5-3'</i>	1131	1131
IGR	115	115
<i>nad3</i>	357	357
IGR	48	32
<i>nad1</i>	984	984
IGR	367	365
<i>nad5-5'</i>	708	708
IGR	108	46
<i>atp6</i>	699	699
IGR	82	82
<i>atp8</i>	213	213
IGR	24	24
<i>nad6</i>	564	564
IGR	104	87
<i>nad4</i>	1476	1476
IGR	61	61
<i>cox2</i>	750	750
IGR	82	68
<i>nad4L</i>	300	300
IGR	92	92
<i>cox1</i>	1590	1590
IGR	34	34
<i>cox3</i>	789	789
IGR	96	74
16S	2561	2590
IGR	64	74
tRNA Met	71	71
IGR	49	40
<i>cytb</i>	1143	1143
IGR	100	101

is placed within a clade containing additional *Parantipathes* (all from the North-east Atlantic), *Sibopathes* van Pesch, 1914 and *Umbellapathes* (bootstrap support: 100). *Sibopathes* is currently classified in the family Cladopathidae yet falls within the Schizopathidae in our analyses. However, any potential reclassification of this genus should include data from the type specimen of *Sibopathes*. These data were not available at the time of this analysis.

According to our analyses, the family Aphanipathidae is polyphyletic with representatives forming a group sister to the majority of antipatharians (*Acanthopathes thyoides* USNM1288453; bootstrap support: 100), sister to the Myriopathidae (*Elatopathes abietina* USNM1288451; bootstrap support: 95) or

sister to different representatives of the Antipathidae (*Aphanipathes pedata* USNM1288458 and *Phanopathes* sp. Opresko, 2004 MT318852; bootstrap support: 100; taxon sampling within the Antipathidae is very limited as our phylogeny only includes five of 122+ species within the family).

In Brugler et al. (2013), *Acanthopathes thyoides* (USNM1288453) and *Elatopathes abietina* (USNM1288451) were considered “wandering taxa” as their phylogenetic relationship shifted depending on the dataset or tree-building algorithm. It appears that our new mitogenome-based phylogeny has stabilised their position and revealed more strongly-supported phylogenetic affiliations for both taxa.

Only one representative from the family Stylopathidae was included in the phylogeny (*Tylopathes* sp. nov. Brook, 1889 MT318859) and is sister to the Myriopathidae (bootstrap support: 100). Any potential reclassification of these genera within the Myriopathidae will require sequence data from the remaining genera within the Stylopathidae (*Stylopathes* Opresko, 2006 and *Triadopathes* Opresko, 2006). These data were not available at the time of this analysis.

To our knowledge, this study is the first to compare two mitogenomes from the same species of black coral (*Stauropathes arctica* MT318854 and CMNI 2023-0258) and thus we can, for the first time, place lower limits on the expected level of intraspecific variation at the mitogenome level. Both mitogenomes are 17,700 bp in length and a comparison revealed 12 SNPs (K2P distance: 0.0678%). *Stauropathes arctica* (MT318854) was collected at 1,446 m depth from North Porcupine Bank (NE Atlantic; Irish Margin). *Stauropathes arctica* (CMNI 2023-0258) was collected at 600 m depth from Treworgie Canyon (NW Atlantic; Grand Banks of Newfoundland). Bledsoe-Becerra et al. (2022) compared the mitogenomes of the trigenic complex (*Dendrobathypathes*, *Lillipathes* and *Parantipathes* from the eastern North Pacific) and only found 32 SNPs across 17,687 bp. Pairwise comparisons revealed 18 (*Dendrobathypathes* and *Parantipathes*) and 23 (*Lillipathes* and *Parantipathes*; *Lillipathes* and *Dendrobathypathes*) SNPs. If future mitogenomic studies show that approximately 12 SNPs are typical of intraspecific comparisons within the Antipatharia, then 18 and 23 SNPs may be indicative of interspecific variation and, thus, *Dendrobathypathes*, *Lillipathes* and *Parantipathes* (from the eastern North Pacific) could be consolidated into a single genus. However, a black coral nuclear genome is not available at this time, which could fundamentally change our understanding of species relationships within this group. Therefore, a major consolidation of multiple genera is not advised until nuclear genomes are also sequenced and analysed. It is also important to note that the mitogenome-level comparisons noted above (for *Stauropathes*, *Dendrobathypathes*, *Lillipathes* and *Parantipathes*) are all for taxa within the family Schizopathidae and, thus, variation within, or thresholds between, other families may differ given their different evolutionary histories. As per Horowitz et al. (2023), 95% of extant black corals were recovered in two distinct clades that diverged ~ 295 million years ago (during the Carboniferous-Permian) on the continental slope. The first clade contained members of the Antipathidae, Aphanipathidae, Myriopathidae and Stylopathidae with crown node at 242 My; these taxa largely stayed on the slope or moved up on to the shelf. The second clade contained members of the Schizopathidae and Cladopathidae with crown node at 202 My; these taxa are largely found at slope and abyssal depths.

We also had the unique opportunity to compare interspecific variation at the mitogenome-level across five different specimens of *Parantipathes* from the NE Atlantic

and Mediterranean Sea (*Parantipathes* cf. *hirondelle* MT318849; *Parantipathes hirondelle* Molodtsova, 2006 MT318850; *Parantipathes larix* USNM1280881; *Parantipathes* sp. MSS-29; *Parantipathes* sp. MT318851). We also included *Sibopathes* cf. *macrospina* (MT318853) in this analysis as it groups phylogenetically amongst these five *Parantipathes*. All six mitogenomes are 17,734 bp in length and a comparison revealed only 18 SNPs (K2P distances ranged from 0.00564% [*Sibopathes* cf. *macrospina* MT318853 vs. *Parantipathes* sp. MT318851 and *Parantipathes* sp. MSS-29 and *Parantipathes* cf. *hirondelle* MT318849 vs. *Parantipathes hirondelle* MT318850] to 0.0843% [*Parantipathes larix* USNM1280881 vs. *Parantipathes* sp. MSS-29]). These results also support consolidating *Dendrobathypathes*, *Lillipathes* and *Parantipathes* (from the eastern North Pacific) into a single genus. Again, obtaining sequence data from the type specimen of *Sibopathes* will be necessary prior to the potential reclassification of this genus.

We encourage future black coral mitogenomic studies to focus on obtaining mitogenomes from type species (where possible) and continue to fill in missing taxonomic gaps, particularly in the Antipathidae, Aphanipathidae, Myriopathidae and Stylopathidae.

While morphological characteristics are the gold standard for delineating relationships amongst organisms, the combined use of morphology and genetics is a powerful combination to better understand evolutionary relationships (e.g. Wagner et al. (2010); Horowitz et al. (2020)). In fact, many fields must entirely rely on genetics to characterise diversity at the family level and below because morphology is lacking (e.g. Blank and Trench (1985); LaJeu-nesse et al. (2014)) and/or morphological characteristics are problematic (e.g. Pinzón and Lajeunesse (2011); Pinzón et al. (2013); Rodríguez et al. (2014); Bledsoe-Becerra et al. (2022); Opresko et al. (2022); Molodtsova et al. (2023)). Based on the data presented here and clear ambiguities created when using morphological characteristics of black coral, we strongly advocate that the black coral community preferentially use diversity at the molecular level to delineate evolutionary relatedness between groups and morphology only be used to support relationships revealed by molecular analyses. We also urge the International Commission on Zoological Nomenclature (ICZN), which is responsible for producing the International Code of Zoological Nomenclature, to incorporate robust molecular comparisons into species descriptions to account for instances where morphology fails.

## Acknowledgements

We thank our reviewers, Anthony Montgomery and Jeremy Horowitz, for greatly improving an earlier version of the manuscript. Our ZooKeys subject editor, James Reimer, also deserves special recognition for providing a very positive experience for our team. MRB is a Research Associate at the American Museum of Natural History and the Smithsonian Institution's National Museum of Natural History and gratefully acknowledges these affiliations.

## Additional information

### Conflict of interest

The authors have declared that no competing interests exist.

## Ethical statement

An institutional animal care and use committee (IACUC) permit was not necessary as black corals are not vertebrates or cephalopods (Phylum Mollusca). Black corals are protected under appendix II of the Convention on International Trade of Endangered Species (CITES; [www.cites.org](http://www.cites.org)). Organisms listed in appendix II require an export permit as well as a Certificate of Scientific Exchange (COSE) on the receiving end. The Smithsonian Institution's National Museum of Natural History (NMNH) maintains an active COSE permit and, thus, can receive black corals that are shipped to them with the appropriate export permit. All black corals in the SI NMNH collection have been vetted for proper export permits. The SI NMNH is the institution from which the specimens studied herein were obtained.

## Funding

Sequencing was conducted at the New York Genome Center using funds provided to MRB through a Cycle 47 PSC-CUNY Research Award (#69191-00-47). Financial support was provided to MRB by the Port Royal Sound Foundation and to the Ocean Genome Legacy Center of Northeastern University by a grant from the National Fish and Wildlife Foundation. Resources purchased with funds from the NSF FSML programme (DBI 1722553, to Northeastern University) were used to generate data for this manuscript. Financial support was provided to BAC, HC, MR, JW and ADG through USCB's Summer Research Experience Scholarship Program and to JW and ADG through the University of South Carolina SMART Program.

## Author contributions

Conceptualisation: MRB. Provided samples and accessioned them into a museum: JD, VEWH. DNA extraction, DNA quantification, and shipping samples: HJAM, DLD. Data analysis: BAC, AC, HC, JCR, MAR, JW, ADG, JLS, MRB. Data interpretation: BAC, AC, HC, JCR, MAR, JW, ADG, TK, KG, DTP, JLS, MRB. Submitted data to GenBank: KG, JLS, MRB. Significant intellectual contributions: DTP. Wrote original draft of manuscript: BAC, AC, JCR, MAR, MRB. Revised manuscript: all authors.

## Author ORCIDs

Brendan A. Cruz  <https://orcid.org/0009-0008-4422-6489>

Anneau Cappelmann  <https://orcid.org/0009-0007-8700-5726>

Hope Chutjian  <https://orcid.org/0009-0008-5821-9335>

Jude C. Roman  <https://orcid.org/0009-0002-9297-8008>

Mason A. Reid  <https://orcid.org/0009-0009-6794-3947>

Jacob Wright  <https://orcid.org/0009-0007-3743-6181>

Aydanni D. Gonzalez  <https://orcid.org/0009-0007-7049-1019>

Taylor Keyman  <https://orcid.org/0009-0006-0844-8485>

Kierstin M. Griffith  <https://orcid.org/0009-0003-6800-4091>

Hannah J. Appiah-Madson  <https://orcid.org/0000-0001-8408-7729>

Daniel L. Distel  <https://orcid.org/0000-0002-3860-194X>

Vonda E. Hayes  <https://orcid.org/0000-0001-8153-5629>

Jim Drewery  <https://orcid.org/0000-0003-4308-1798>

D. Tye Pettay  <https://orcid.org/0000-0002-2060-3226>

Joseph L. Staton  <https://orcid.org/0009-0002-8695-5563>

Mercer R. Brugler  <https://orcid.org/0000-0003-3676-1226>

## Data availability

Mitogenomic data are available in GenBank under accession numbers OR398473 (*Alternatipathes mirabilis* USNM1070972), OR398474 (*Parantipathes larix* USNM1280881), BK063761 (*Acanthopathes thyoides* USNM1288453), BK063759 (*Aphanipathes pedata* USNM1288458), BK063764 (*Bathypathes alaskensis* USNM1288462), BK063760 (*Elatopathes abietina* USNM1288451), BK063757 (*Parantipathes* sp. MSS29), BK063763 (*Stauropathes arctica* CMNI 2023-0258), BK063762 (*Stauropathes* sp. USNM1404493), OR398475 (*Telopathes magna* USNM1204049) and BK063758 (*Umbellapathes* sp. USNM1404092). The phylogenetic tree can be found on figshare: <https://doi.org/10.6084/m9.figshare.25130414>.

## References

- Allio R, Schomaker-Bastos A, Romiguier J, Prosdocimi F, Nabholz B, Delsuc F (2020) MitoFinder: Efficient automated large-scale extraction of mitogenomic data in target enrichment phylogenomics. *Molecular Ecology Resources* 20(4): 892–905. <https://doi.org/10.1111/1755-0998.13160>
- Asorey CM, Sellanes J, Wagner D, Easton EE (2021) Complete mitochondrial genomes of two species of *Stichopathes* Brook, 1889 (Hexacorallia: Antipatharia: Antipathidae) from Rapa Nui (Easter Island). *Mitochondrial DNA, Part B, Resources* 6(11): 3226–3228. <https://doi.org/10.1080/23802359.2021.1990150>
- Barrett NJ, Hogan RI, Allcock AL, Molodtsova T, Hopkins K, Wheeler AJ, Yesson C (2020) Phylogenetics and mitogenome organisation in black corals (Anthozoa: Hexacorallia: Antipatharia): an order-wide survey inferred from complete mitochondrial genomes. *Frontiers in Marine Science* 7: 440. <https://doi.org/10.3389/fmars.2020.00440>
- Beagley CT, Okada NA, Wolstenholme DR (1996) Two mitochondrial group I introns in a metazoan, the sea anemone *Metridium senile*: One intron contains genes for subunits 1 and 3 of NADH dehydrogenase. *Proceedings of the National Academy of Sciences of the United States of America* 93(11): 5619–5623. <https://doi.org/10.1073/pnas.93.11.5619>
- Bernt M, Donath A, Jühling F, Externbrink F, Florentz C, Fritzsich G, Pütz J, Middendorf M, Stadler PF (2013) MITOS: Improved de novo metazoan mitochondrial genome annotation. *Molecular Phylogenetics and Evolution* 69(2): 313–319. <https://doi.org/10.1016/j.ympev.2012.08.023>
- Blank RJ, Trench RK (1985) Speciation and symbiotic dinoflagellates. *Science* 229(4714): 656–658. <https://doi.org/10.1126/science.229.4714.656>
- Bledsoe-Becerra YM, Whittaker IS, Horowitz J, Naranjo KM, Johnson-Rosemond J, Mullins KH, Cunningham KM, Shetty S, Messinides SN, Behney MS, Fehsal JA, Watson AN, McKnight KE, Nasiadka TW, Popa H, Pettay DT, Appiah-Madson HJ, Distel DL, Brugler MR (2022) Mitogenomics reveals low variation within a trigenic complex of black corals from the North Pacific Ocean. *Organisms, Diversity & Evolution* 22(2): 1–11. <https://doi.org/10.1007/s13127-021-00537-5>
- Brook G (1889) Report on the Antipatharia. Report on the scientific results of the Voyage Challenger. *Zoology: Analysis of Complex Systems, ZACS* 32: 5–222.
- Brugler MR, France SC (2007) The complete mitochondrial genome of the black coral *Chrysopathes formosa* (Cnidaria: Anthozoa: Antipatharia) supports classification of antipatharians within the subclass Hexacorallia. *Molecular Phylogenetics and Evolution* 42(3): 776–788. <https://doi.org/10.1016/j.ympev.2006.08.016>

- Brugler MR, Opresko DM, France SC (2013) The evolutionary history of the order Antipatharia (Cnidaria: Anthozoa: Hexacorallia) as inferred from mitochondrial and nuclear DNA: implications for black coral taxonomy and systematics. *Zoological Journal of the Linnean Society* 169(2): 312–361. <https://doi.org/10.1111/zoj.12060>
- Chan PP, Lowe TM (2019) tRNAscan-SE: searching for tRNA genes in genomic sequences. In: Kollmar M (Ed.) *Gene Prediction. Methods in Molecular Biology*, vol 1962. Humana, New York, 1–14. [https://doi.org/10.1007/978-1-4939-9173-0\\_1](https://doi.org/10.1007/978-1-4939-9173-0_1)
- Chery N, Parra K, Evankow A, Stein D, Distel D, Appiah-Madson H, Ross R, Sanon E, Alomari N, Johnson R, Vasovic A, Horowitz A, Popa H, Short B, Kourehjan D, Vasquez DM, Rodriguez E, Opresko DM, Brugler MR (2018) Partnering with the Ocean Genome Legacy to advance our understanding of black corals (Order Antipatharia). 15<sup>th</sup> Deep-Sea Biology Symposium, Monterey, California, 9–14 September 2018. Poster presentation. [preprint available at] <https://tidalmarshstaskforce.wixsite.com/uscb/publications>
- Darriba D, Taboada GL, Doallo R, Posada D (2012) jModelTest 2: More models, new heuristics and parallel computing. *Nature Methods* 9(8): 772–772. <https://doi.org/10.1038/nmeth.2109>
- DeSalle R, Narechania A, Tessler M (2023) Multiple outgroups can cause random rooting in phylogenomics. *Molecular Phylogenetics and Evolution* 184: 107806. <https://doi.org/10.1016/j.ympev.2023.107806>
- Esper EJC (1788–1830) *Die Pflanzenthiere in Abbildungen nach der Natur mit Farben erleuchtet nebst Beschreibungen*. Raspischen Buchhandlung, Nuremberg. 3 vols text, 2 vols pls.
- Feng H, Lv S, Li R, Shi J, Wang J, Cao P (2023) Mitochondrial genome comparison reveals the evolution of cnidarians. *Ecology and Evolution* 13(6): e10157. <https://doi.org/10.1002/ece3.10157>
- Figuroa DF, Hicks D, Figuroa NJ (2019) The complete mitochondrial genome of *Tanacetipathes thamnea* Warner, 1981 (Antipatharia: Myriopathidae). *Mitochondrial DNA, Part B, Resources* 4(2): 4109–4110. <https://doi.org/10.1080/23802359.2019.1692701>
- Fourment M, Holmes EC (2016) Seqotron: A user-friendly sequence editor for Mac OS X. *BMC Research Notes* 9(1): 1–4. <https://doi.org/10.1186/s13104-016-1927-4>
- France SC, Rosel PE, Ewann J (1996) DNA sequence variation of mitochondrial large-subunit rRNA. *Molecular Marine Biology and Biotechnology* 5(1): 15–28. <https://pubmed.ncbi.nlm.nih.gov/8869515/>
- Guindon S, Gascuel O (2003) A simple, fast, and accurate algorithm to estimate large phylogenies by maximum likelihood. *Systematic Biology* 52(5): 696–704. <https://doi.org/10.1080/10635150390235520>
- Hoang DT, Chernomor O, Von Haeseler A, Minh BQ, Vinh LS (2018) UFBoot2: Improving the ultrafast bootstrap approximation. *Molecular Biology and Evolution* 35(2): 518–522. <https://doi.org/10.1093/molbev/msx281>
- Horowitz J, Brugler MR, Bridge TC, Cowman PF (2020) Morphological and molecular description of a new genus and species of black coral (Cnidaria: Anthozoa: Hexacorallia: Antipatharia: Antipathidae: Blastopathes) from Papua New Guinea. *Zootaxa* 4821(3): 553–569. <https://doi.org/10.11646/zootaxa.4821.3.7>
- Horowitz J, Quattrini AM, Brugler MR, Miller DJ, Pahang K, Bridge TC, Cowman PF (2023) Bathymetric evolution of black corals through deep time. *Proceedings of the Royal Society B, Biological Sciences* 290(2008): 20231107. <https://doi.org/10.1098/rspb.2023.1107>
- Katoh K, Rozewicki J, Yamada KD (2019) MAFFT online service: Multiple sequence alignment, interactive sequence choice and visualization. *Briefings in Bioinformatics* 20(4): 1160–1166. <https://doi.org/10.1093/bib/bbx108>

- Kayal E, Roure B, Philippe H, Collins AG, Lavrov DV (2013) Cnidarian phylogenetic relationships as revealed by mitogenomics. *BMC Evolutionary Biology* 13(1): 1–18. <https://doi.org/10.1186/1471-2148-13-5>
- Kumar S, Stecher G, Li M, Knyaz C, Tamura K (2018) MEGA X: Molecular evolutionary genetics analysis across computing platforms. *Molecular Biology and Evolution* 35(6): 1547–1549. <https://doi.org/10.1093/molbev/msy096>
- LaJeunesse TC, Wham DC, Pettay DT, Parkinson JE, Keshavmurthy S, Chen CA (2014) Ecologically differentiated stress-tolerant endosymbionts in the dinoflagellate genus *Symbiodinium* (Dinophyceae) Clade D are different species. *Phycologia* 53(4): 305–319. <https://doi.org/10.2216/13-186.1>
- Larsson A (2014) AliView: A fast and lightweight alignment viewer and editor for large datasets. *Bioinformatics (Oxford, England)* 30(22): 3276–3278. <https://doi.org/10.1093/bioinformatics/btu531>
- Li D, Liu CM, Luo R, Sadakane K, Lam TW (2015) MEGAHIT: An ultra-fast single-node solution for large and complex metagenomics assembly via succinct de Bruijn graph. *Bioinformatics (Oxford, England)* 31(10): 1674–1676. <https://doi.org/10.1093/bioinformatics/btv033>
- Love MS, Yoklavich MM, Black BA, Andrews AH (2007) Age of black coral (*Antipathes dendrochristos*) colonies, with notes on associated invertebrate species. *Bulletin of Marine Science* 80(2): 391–399. <https://www.ingentaconnect.com/content/umrsmas/bullmar/2007/00000080/00000002/art00008#>
- Lütken C (1871) *Antipathes antarctica*, en ny Sortkoral fra Polarhavet. *Oversigt over det Kongelige Danske videnskabernes selskabs forhandlinger* 2: 18–26. <https://www.biodiversitylibrary.org/page/29561248>
- MacIsaac KG, Best M, Brugler MR, Kenchington ELR, Anstey LJ, Gordan T (2013) *Telopathes magna* gen. nov., spec. nov. (Cnidaria: Anthozoa: Antipatharia: Schizopathidae) from deep waters off Atlantic Canada and the first molecular phylogeny of the deep-sea family Schizopathidae. *Zootaxa* 3700(2): 237–258. <https://doi.org/10.11646/zootaxa.3700.2.3>
- Miller MA, Pfeiffer W, Schwartz T (2011) The CIPRES science gateway: a community resource for phylogenetic analyses. In: *Proceedings of the 2011 TeraGrid Conference: extreme digital discovery*, 1–8. <https://doi.org/10.1145/2016741.2016785>
- Minh BQ, Schmidt HA, Chernomor O, Schrempf D, Woodhams MD, Von Haeseler A, Lanfear R (2020) IQ-TREE 2: New models and efficient methods for phylogenetic inference in the genomic era. *Molecular Biology and Evolution* 37(5): 1530–1534. <https://doi.org/10.1093/molbev/msaa015>
- Molodtsova TN (2006) Black corals (Antipatharia: Anthozoa: Cnidaria) of North-East Atlantic. *Biogeography of the North Atlantic Seamounts*. KMK Press, Moscow, 141–151. [https://scholar.google.com/scholar?hl=en&as\\_sdt=0%2C41&q=Black+corals+%28Antipatharia%3A+Anthozoa%3A+Cnidaria%29+of+North-East+Atlantic.+&btnG=](https://scholar.google.com/scholar?hl=en&as_sdt=0%2C41&q=Black+corals+%28Antipatharia%3A+Anthozoa%3A+Cnidaria%29+of+North-East+Atlantic.+&btnG=)
- Molodtsova TN, Opresko DM (2017) Black corals (Anthozoa: Antipatharia) of the Clarion-Clipperton fracture zone. *Marine Biodiversity* 47(2): 349–365. <https://doi.org/10.1007/s12526-017-0659-6>
- Molodtsova TN, Opresko DM, Wagner D (2022) Description of a new and widely distributed species of *Bathypathes* (Cnidaria: Anthozoa: Antipatharia: Schizopathidae) previously misidentified as *Bathypathes alternata* Brook, 1889. *PeerJ* 10: e12638. <https://doi.org/10.7717/peerj.12638>
- Molodtsova TN, Opresko DM, O'Mahoney M, Simakova UV, Kolyuchkina GA, Bledsoe YM, Nasiadka TW, Ross RF, Brugler MR (2023) One of the Deepest Genera of

- Antipatharia: Taxonomic Position Revealed and Revised. *Diversity* 15(3): 436. <https://doi.org/10.3390/d15030436>
- Opresko DM (2002) Revision of the Antipatharia (Cnidaria: Anthozoa). Part II. Schizopathidae. *Zoologische Mededelingen* 76: 411–442. <https://repository.naturalis.nl/pub/217481>
- Opresko DM (2004) Revision of the Antipatharia (Cnidaria: Anthozoa). Part IV. Establishment of a new family, Aphanipathidae. *Zoologische Mededelingen, Leiden* 78(11): 209–240. <http://www.repository.naturalis.nl/document/51441>
- Opresko DM (2005) New genera and species of antipatharian corals (Cnidaria: Anthozoa) from the North Pacific. *Zoologische Mededelingen, Leiden* 79: 129–165. [https://repository.naturalis.nl/pub/210737/ZM79-02\\_129-166.pdf](https://repository.naturalis.nl/pub/210737/ZM79-02_129-166.pdf)
- Opresko DM (2006) Revision of the Antipatharia (Cnidaria: Anthozoa). Part V. Establishment of a new family, Stylopathidae. *Zoologische mededelingen, Leiden* 80-4(11): 109–138. [https://repository.si.edu/bitstream/handle/10088/6225/Opresko\\_2006\\_Part\\_5\\_Stylopathidae.pdf](https://repository.si.edu/bitstream/handle/10088/6225/Opresko_2006_Part_5_Stylopathidae.pdf)
- Opresko DM, Baron-Szabo RC (2001) Re-descriptions of the antipatharian coral described by EJC Esper with select English translations of the original German text. *Senckenbergiana Biologica* 81: 1–21. [http://miseryukyu.com/MISE@University\\_of\\_the\\_Ryukyus/Zoantharia\\_literature\\_files/Opresko\\_Baron-Szabo-2001.pdf](http://miseryukyu.com/MISE@University_of_the_Ryukyus/Zoantharia_literature_files/Opresko_Baron-Szabo-2001.pdf)
- Opresko DM, Molodtsova TN (2021) New species of deep-sea antipatharians from the North Pacific (Cnidaria: Anthozoa: Antipatharia), Part 2. *Zootaxa* 4999(5): 401–422. <https://doi.org/10.11646/zootaxa.4999.5.1>
- Opresko DM, Wagner D (2020) New species of black corals (Cnidaria: Anthozoa: Antipatharia) from deep-sea seamounts and ridges in the North Pacific. *Zootaxa* 4868(4): 543–559. <https://doi.org/10.11646/zootaxa.4868.4.5>
- Opresko DM, Stewart R, Voza T, Tracey DI, Brugler MR (2022) New genus and species of black coral from the SW Pacific and Antarctica (Cnidaria: Anthozoa: Antipatharia: Schizopathidae). *Zootaxa* 5169(1): 31–48. <https://doi.org/10.11646/zootaxa.5169.1.3>
- Pinzón JH, Lajeunesse TC (2011) Species delimitation of common reef corals in the genus *Pocillopora* using nucleotide sequence phylogenies, population genetics and symbiosis ecology. *Molecular Ecology* 20(2): 311–325. <https://doi.org/10.1111/j.1365-294X.2010.04939.x>
- Pinzón JH, Sampayo E, Cox E, Chauka LJ, Chen CA, Voolstra CR, LaJeunesse TC (2013) Blind to morphology: Genetics identifies several widespread ecologically common species and few endemics among Indo-Pacific cauliflower corals (*Pocillopora*, Scleractinia). *Journal of Biogeography* 40(8): 1595–1608. <https://doi.org/10.1111/jbi.12110>
- Quattrini AM, McCartin LJ, Easton EE, Horowitz J, Wirshing HH, Bowers H, Mitchell K, Sei M, McFadden CS, Herrera S (2023a) Skimming genomes for systematics and DNA barcodes of corals. *bioRxiv*. <https://doi.org/10.1101/2023.10.17.562770>
- Quattrini AM, Snyder KE, Purow-Ruderman R, Seiblit IG, Hoang J, Floerke N, Ramos NI, Wirshing HH, Rodriguez E, McFadden CS (2023b) Mito-nuclear discordance within Anthozoa, with notes on unique properties of their mitochondrial genomes. *Scientific Reports* 13(1): 7443. <https://doi.org/10.1038/s41598-023-34059-1>
- Ramos NI, DeLeo DM, Horowitz J, McFadden CS, Quattrini AM (2023) Selection in coral mitogenomes, with insights into adaptations in the deep sea. *Scientific Reports* 13(1): 6016. <https://doi.org/10.1038/s41598-023-31243-1>
- Roark EB, Guilderson TP, Dunbar RB, Fallon SJ, Mucciarone DA (2009) Extreme longevity in proteinaceous deep-sea corals. *Proceedings of the National Academy of Sciences*

- of the United States of America 106(13): 5204–5208. <https://doi.org/10.1073/pnas.0810875106>
- Rodríguez E, Barbeitos MS, Brugler MR, Crowley LM, Grajales A, Gusmão L, Häussermann V, Reft A, Daly M (2014) Hidden among sea anemones: The first comprehensive phylogenetic reconstruction of the order Actiniaria (Cnidaria, Anthozoa, Hexacorallia) reveals a novel group of hexacorals. PLOS ONE 9(5): e96998. <https://doi.org/10.1371/journal.pone.0096998>
- Shizuru LEK, Montgomery AD, Wagner D, Freel EB, Toonen RJ (2024) The complete mitochondrial genome of a species of *Cirripathes* de Blainville, 1830 from Kauaʻi, Hawaiʻi (Hexacorallia: Antipatharia). Mitochondrial DNA, Part B, Resources 9(2): 223–226. <https://doi.org/10.1080/23802359.2024.2310130>
- Sinniger F, Pawlowski J (2009) The partial mitochondrial genome of *Leiopathes glaberrima* (Hexacorallia: Antipatharia) and the first report of the presence of an intron in COI in black corals. Galaxea 11(1): 21–26. <https://doi.org/10.3755/galaxea.11.21>
- Stecher G, Tamura K, Kumar S (2020) Molecular evolutionary genetics analysis (MEGA) for macOS. Molecular Biology and Evolution 37(4): 1237–1239. <https://doi.org/10.1093/molbev/msz312>
- Wagner D, Brugler MR, Opresko DM, France SC, Montgomery AD, Toonen RJ (2010) Using morphometrics, in situ observations and genetic characters to distinguish among commercially valuable Hawaiian black coral species; a redescription of *Antipathes grandis* Verrill, 1928 (Antipatharia: Antipathidae). Invertebrate Systematics 24(3): 271–290. <https://doi.org/10.1071/IS10004>



# New species of redbait from the Philippines (Teleostei, Emmelichthyidae, *Emmelichthys*)

Matthew G. Girard<sup>1,2</sup>, Mudjekeewis D. Santos<sup>3</sup>, Katherine E. Bemis<sup>1,4</sup>

1 Department of Vertebrate Zoology, National Museum of Natural History, Smithsonian Institution, Washington, DC 20560, USA

2 Biodiversity Institute, University of Kansas, Lawrence, KS 66045, USA

3 Genetic Fingerprinting Laboratory, National Fisheries Research and Development Institute, Quezon City, 1103, Philippines

4 National Systematics Laboratory, Office of Science and Technology, NOAA Fisheries, Washington, DC, 20560, USA

Corresponding author: Matthew G. Girard ([GirardMG@si.edu](mailto:GirardMG@si.edu))

## Abstract

We describe a new species of redbait in the genus *Emmelichthys* collected from fish markets on Panay and Cebu islands in the Visayas region of the Philippines. The species is externally similar to *E. struhsakeri* but is diagnosable by two prominent fleshy papillae associated with the cleithrum and fewer pectoral-fin rays (18–19 vs. 19–21) and gill rakers (30–33 vs. 34–41). Additionally, mitochondrial DNA differentiates this taxon from other species of *Emmelichthys*. We generate mitochondrial genomes for two of the three type specimens and several other emmelichthyids to place the new taxon in a phylogenetic context. Analysis of the protein-coding mitochondrial loci calls into question the monophyly of two emmelichthyid genera (*Emmelichthys* and *Erythrocles*) and highlights the need for subsequent analyses targeting the intrarelationships of the Emmelichthyidae.

## Buod (Tagalog)

Dito pinakita namin ang isang kakaibang isda na may Tagalog name na Rebentador pula at English name na Redbait na kabilang sa genus *Emmelichthys* na nakuha sa mga pamilihan ng isda sa isla ng Panay at Cebu sa Visayas, Philippines. Ang isdang ito ay may panglabas na anyo kamukha ng *E. struhsakeri* pero naiba ito dahil meron itong dalawa (2) prominenteng fleshy papillae na parte ng cleithrum, may mas konting pectoral-fin rays na may bilang na 18–19 at gill rakers na may bilang na 30–33. Iniiba ng mitochondrial DNA ang taxon na ito mula sa iba pang mga species ng *Emmelichthys*. Binuo, sinuri at kinumpara namin ang mitochondrial genomes ng dalawang type specimens ng kakaibang isda at iba pang isda na kabilang sa emmelichthyids para malaman kung bago nga ba ito. Lumabas sa pagsusuri, gamit ang lahat ng protein-coding mitochondrial loci, na bago nga ang kakaibang isda. Pero napag-alaman din na mukhang isang grupo lang at malapit na mag kamag-anak ang 2 genus (*Emmelichthys* and *Erythrocles*) na kasama sa Family Emmelichthyidae kung kaya't kailangan pa ang ibayong pagsusuri sa pagkakakilanlan ng nasabing 2 genus.

**Key words:** COI, *Erythrocles*, identification key, mitochondrial genome, mitogenome, *Plagiogeneion*, rovers, rubyfishes, systematics, Visayas



Academic editor: Maria Elina Bichuette

Received: 14 August 2023

Accepted: 15 February 2024

Published: 22 March 2024

ZooBank: <https://zoobank.org/E264F69C-8FAD-4860-9AE7-7F6E43608BB6>

Citation: Girard MG, Santos MD, Bemis KE (2024) New species of redbait from the Philippines (Teleostei, Emmelichthyidae, *Emmelichthys*). ZooKeys 1196: 95–109. <https://doi.org/10.3897/zookeys.1196.111161>

Copyright: © Matthew G. Girard et al.  
This is an open access article distributed under the terms of the CC0 Public Domain Dedication.

## Introduction

The Emmelichthyidae is a small family of fishes found in all temperate and tropical oceans between depths of 100 and 400 m. Commonly known as rovers, redbaits, and rubyfishes, emmelichthyids are often bright red in color and can be distinguished from other fishes by their fusiform bodies, highly protrusible mouths, toothless or nearly toothless jaws, and large rostral cartilage (Heemstra and Randall 1977; Johnson 1980). Little is known about the life history of emmelichthyids, with a recent study documenting larvae and juveniles of some species feeding within and around pelagic tunicates (Pastana et al. 2022). The family currently includes 17 species in three genera: *Emmelichthys*, *Erythrocles* and *Plagiogeneion* (Fricke et al. 2023; Girard 2024). Among emmelichthyids, the genus *Emmelichthys* is diagnosed by a highly fusiform body and separation of the spinous and soft dorsal fins by a distinct gap that contains one or more isolated dorsal-fin spines (Heemstra and Randall 1977). Six species are included in the genus: *E. cyanescens* (Guichenot, 1848) [recognized as a species by Fricke et al. (2014) but see study by Oyarzún and Arriaza 1993], *E. elongatus* Kotlyar, 1982, *E. karnellai* Heemstra & Randall, 1977, *E. nitidus* Richardson, 1845, *E. ruber* (Trunov, 1976) and *E. struhsakeri* Heemstra & Randall, 1977. A seventh species was described by Fricke et al. (2014) but this taxon has been found to be a species of *Dipterygonotus* in the Lutjanidae [*Emmelichthys* *marisrubri* = *Dipterygonotus marisrubri* (Fricke, Golani & Appelbaum-Golani, 2014); see Girard 2024]. Although a phylogeny of *Emmelichthys* and the Emmelichthyidae has yet to be generated, Heemstra and Randall (1977) noted morphological similarities and suggested relationships among species. For example, they considered *E. cyanescens* and *E. nitidus* to be closely related based on the presence of prominent protuberances on the anterior margin of the cleithrum (hereafter referred to as cleithral papillae).

In 2011, a collaboration among researchers at the National Museum of Natural History, Smithsonian Institution (NMNH), the Bureau of Fisheries and Aquatic Resources–National Fisheries Research and Development Institute, Department of Agriculture, Philippines (BFAR–NFRDI), and United States Food and Drug Administration (FDA) was established to document the diversity of fishes in Philippine markets. The goal of this collaboration was to develop a voucher-based genetic reference library to advance consumer safety and biodiversity research (Bemis et al. 2023). The project has yielded descriptions of several new species (e.g., Williams and Carpenter 2015; Carpenter et al. 2017; Matsunuma et al. 2018) and discovered additional taxa that have yet to be described (see Bemis et al. 2023). Two emmelichthyid specimens were collected from a fish market on Cebu Island in 2013 that are externally similar to *E. struhsakeri*, but they have two prominent fleshy papillae associated with the cleithrum, fewer pectoral-fin rays, and fewer gill rakers. While reviewing additional specimens, we identified a third Philippine specimen purchased at a fish market on Panay Island in 2016 that has the same phenotype as the two specimens from 2013. Examination of both genotypic and phenotypic characters of these papillae-bearing specimens indicates they represent an undescribed species. We describe this species and generate a phylogeny based on mitochondrial loci to place the taxon in an evolutionary context.

## Materials and methods

### Specimen examination

Methods for counts and measurements follow Heemstra and Randall (1977). Standard length is abbreviated as SL; total length is abbreviated as TL. Museum abbreviations follow Sabaj (2020) except for NMNH, which refers to non-Fishes Division equipment and personnel at the National Museum of Natural History, Smithsonian Institution. All specimens examined in this study, along with their lengths and museum catalog numbers, are listed in Table 1.

### Specimen imaging

We used microcomputed tomography ( $\mu$ CT) to examine internal osteology. Specimens were scanned using a GE Phoenix v|tome|x M 240/180 kV Dual Tube  $\mu$ CT at NMNH. Scan settings were 120–130 kV, 150  $\mu$ A, 250 ms exposure time, and 34–60  $\mu$ m voxel size. Resulting scans are available through MorphoSource project ID 000553669 and media identifiers for individual specimens can be found in Table 1. Scans of additional species generated in a previous study (project ID 000553611; Girard 2024) were also downloaded from MorphoSource for examination. All scan data were visualized and segmented using the protocol in Girard et al. (2022a). All other specimen imaging was performed using equipment and protocols listed in Girard et al. (2020) and Bemis et al. (2023).

**Table 1.** Specimens examined in this study.

Species	Museum voucher	Count	Collection latitude, longitude	SL (mm)	MorphoSource
<i>Emmelichthys papillatus</i> sp. nov. holotype	PNM 15806	1	11.000, 123.000	130	554144
<i>Emmelichthys papillatus</i> sp. nov. paratype	USNM 424606	1	10.292, 123.892	122	553712
<i>Emmelichthys papillatus</i> sp. nov. paratype	KAUM-I. 193858	1	10.292, 123.892	119	553717
<i>Emmelichthys karnellai</i>	KAUM-I. 146310	1		212	
<i>Emmelichthys karnellai</i>	KAUM-I. 149380	1	28.467, 129.467	208	
<i>Emmelichthys karnellai</i> paratype	USNM 214689	1	21.260, -157.207	101	553688
<i>Emmelichthys nitidus</i>	CSIRO H4244-01	1	-38.188, 149.277	274	553698
<i>Emmelichthys nitidus</i>	NSMT P.125978	16	-32.355, 130.035	116–123	553651
<i>Emmelichthys struhsakeri</i> holotype	USNM 214690	1	20.722, -156.830	150	553667
<i>Emmelichthys struhsakeri</i> paratype	USNM 214691	10	20.722, -156.830	136–159	
<i>Emmelichthys struhsakeri</i> paratype	AMS I.17244-001	1	-34.330, 151.000	170	
<i>Emmelichthys struhsakeri</i>	KAUM-I. 149520	1	28.467, 129.467	216	
<i>Erythrocles microceps</i>	NSMT P.102428	10		68–80	
<i>Erythrocles schlegelii</i>	NSMT P.105302	1		119	
<i>Erythrocles schlegelii</i>	USNM 403355	1	9.199, 123.267	230	
<i>Erythrocles scintillans</i>	OCF-P. 3558	1			
<i>Erythrocles scintillans</i> holotype	USNM 51051	1		282	
<i>Plagiogeneion macrolepis</i>	CSIRO H8671-01	1	-41.177, 144.192	215	
<i>Plagiogeneion rubiginosum</i>	NZ P.045174	1	-44.178, -176.955	194	

### Extraction, sequencing, assembly, and annotation of genetic data

We extracted genomic DNA from 13 samples of the Emmelichthyidae. These include the new species described in this study, three species of *Emmelichthys* (*E. karnellai*, *E. nitidus*, and *E. struhsakeri*), three species of *Erythrocles* [*E. microceps* Miyahara & Okamura, 1998, *E. schlegelii* (Richardson, 1846), and *E. scintillans* (Jordan & Thompson, 1912)], and two species of *Plagiogeneion* [*P. macrolepis* McCulloch, 1914 and *P. rubiginosum* (Hutton, 1875)]. Protocols for DNA extraction follow the methods described in Weigt et al. (2012). For 12 samples, we sequenced whole mitochondrial genomes (hereafter, mitogenomes) using the library preparation and sequencing protocol described in Hoban et al. (2022). Demultiplexed sequence data received in compressed FASTQ format were cleaned of adapter contamination and low-quality bases using the parallel wrapper illumiprocessor version 2.10 (Faircloth 2013) around trimmomatic version 0.39 (Bolger et al. 2014). Cleaned reads were submitted to GenBank and assigned SRA accession numbers SRR27284234–SRR27284245 under BioProject PRJNA1052721 (see Table 2). We assembled mitogenomes using the ‘map to reference’ function in Geneious version 11.1.5 (Kearse et al. 2012) with the settings described in Girard et al. (2022b) and a reference mitogenome downloaded from GenBank (*E. struhsakeri*, GenBank NC\_004407; Miya et al. 2003). Assembled mitogenomes were annotated using MitoAnnotator (Iwasaki et al. 2013; Sato et al. 2018; Zhu et al. 2023). Annotated mitogenomes were submitted to GenBank and assigned accession numbers OR974326–OR974337 (see Table 2). For one paratype (KAUM-I. 193858 [ex. USNM 424607]) only the cytochrome oxidase I barcode sequence was generated following the methods described in Weigt et al. (2012) and using the primers from Baldwin et al. (2009). The sequence contig was built, edited, and assembled using Geneious and deposited in GenBank (OR961526; see Table 2).

**Table 2.** Genetic voucher and GenBank information for samples examined in this study.

Species	Museum voucher	GenBank SRA	GenBank mitogenome accession number	GenBank COI accession number
<i>Emmelichthys papillatus</i> sp. nov. holotype	PNM 15806	SRR27284241	OR974328	See mitogenome
<i>Emmelichthys papillatus</i> sp. nov. paratype	USNM 424606	SRR27284240	OR974329	See mitogenome
<i>Emmelichthys papillatus</i> sp. nov. paratype	KAUM-I. 193858			OR961526
<i>Emmelichthys karnellai</i>	KAUM-I. 146310	SRR27284245	OR974326	See mitogenome
<i>Emmelichthys karnellai</i>	KAUM-I. 149380	SRR27284244	OR974327	See mitogenome
<i>Emmelichthys nitidus</i>	CSIRO H4244-01	SRR27284239	OR974330	See mitogenome
<i>Emmelichthys struhsakeri</i>	KAUM-I. 149520	SRR27284238	OR974331	See mitogenome
<i>Emmelichthys struhsakeri</i>			NC_004407	See mitogenome
<i>Erythrocles microceps</i>	NSMT P.102428	SRR27284237	OR974332	See mitogenome
<i>Erythrocles schlegelii</i>	NSMT P.105302	SRR27284236	OR974333	See mitogenome
<i>Erythrocles schlegelii</i>	USNM 403355	SRR27284235	OR974334	See mitogenome
<i>Erythrocles scintillans</i>	OCF-P. 3558	SRR27284234	OR974335	See mitogenome
<i>Plagiogeneion macrolepis</i>	CSIRO H8671-01	SRR27284243	OR974336	See mitogenome
<i>Plagiogeneion rubiginosum</i>	NZ P.045174	SRR27284242	OR974337	See mitogenome

## Phylogenetic analysis

To generate a hypothesis of relationships for the taxa sampled in our study, we collated orthologous loci from the 13 protein-coding regions of the mitogenome into individual FASTA files and aligned them with MAFFT version 7 (Kato and Standley 2013). Lengths of alignments were as follows: ATPase6 683 base pairs (bps); ATPase8 168 bps; COI 1551 bps; COII 691 bps; COIII 785 bps; CytB 1141 bps; ND1 975 bps; ND2 1046 bps; ND3 349 bps; ND4 1381 bps; ND4L 297 bps; ND5 1839 bps; ND6 522 bps. Aligned matrices were concatenated for partitioning and phylogenetic inference. IQ-Tree version 2.2.0 (i.e., MFP + MERGE; Chernomor et al. 2016; Kalyaanamoorthy et al. 2017; Minh et al. 2020) recovered an optimal partitioning scheme of six groups based on 39 partitions designated for the three codon positions in each of the loci. Ten tree searches were performed in IQ-Tree using the optimal partitioning scheme and concatenated alignment. Support for the resulting topology was assessed by generating 500 standard bootstrap replicates (-bo). Analyses were rooted on *Plagiogeneion rubiginosum*.

## Results

### Species description

#### *Emmelichthys papillatus* sp. nov.

<https://zoobank.org/804D459E-72C9-458A-A347-6CD8D88B2E30>

**Etymology.** Named for the diagnostic fleshy cleithral papillae.

**English name.** Papillated redbait.

**Tagalog name.** Rebentador pula.

**Types. Holotype.** PNM 15806 (ex. KAUM-I. 91845); 154 mm TL; 130 mm SL; purchased 12 September 2016 from Oton Fish Market; likely captured off Iloilo, Panay Island, Philippines, 11°N, 123°E (Fig. 1, Tables 1–4). Collected by Y. Fukui and M. Matsunuma (Motomura et al. [2017: 128] identified as *E. struhsakeri*).

**Paratypes.** USNM 424606; 138 mm TL; 122 mm SL; purchased 1 June 2013 from Pasil Market, Cebu Island, Philippines, 10°17'30.1"N, 123°53'31.2"E (Fig. 2, Tables 1–4). Collected by J. T. Williams, K. E. Carpenter, A. Lizano, and A. Mascapac. KAUM-I. 193858 (ex. USNM 424607); 132 mm TL; 119 mm SL; same collection information as USNM 424606.

**Diagnosis.** *Emmelichthys papillatus* is distinguished from congeners in the Pacific Ocean by the presence of two fleshy papillae on the cleithrum (absent in *E. elongatus*, *E. karnellai*, *E. struhsakeri*; see Fig. 3) and fewer number of gill rakers (30–33 vs. 34+ in other species). It can be further differentiated from *E. cyanescens* and *E. nitidus*, which have bony cleithral papillae, by fewer pectoral-fin rays (18–19 vs. 22 in *E. cyanescens*, 20–23 in *E. nitidus*) and fewer lateral-line scales (69–74 vs. 100–105 in *E. cyanescens*, 87–93 in *E. nitidus*). It can also be differentiated from *Erythrocles schlegelii*, which also has fleshy cleithral papillae, by II isolated dorsal-fin spines between the spinous and soft dorsal fin.

**Description (See Tables 3, 4 for counts and measurements).** Dorsal fin with anterior VIII spines connected by membrane; penultimate II spines not connected to adjacent spines via membrane but with short membrane behind each spine;

membrane of last dorsal-fin spine connected to first soft dorsal-fin ray. Upper 2 pectoral-fin rays unbranched. Body and head, except for a narrow median region dorsal to upper lip, covered with ctenoid scales; 5–7 scales from middle of spinous dorsal fin to lateral line; 7–8 scales from dorsal-fin origin and 14–16 from anal-fin origin to lateral line; 26–28 circumpeduncular scales. Soft dorsal and anal fins with scaly sheath at base, broadening near last few rays; no scales on dorsal or anal fins beyond basal sheath; pectoral fins scaled proximally; caudal fin with small scales on basal fleshy region and proximally on rays. Nostrils small, subequal, close-set. Maxilla reaching vertical at front edge of pupil. Opercle with 2–3 flat spines. No teeth on vomer, palatines, or jaws. Shallow groove on rear margin of gill cavity at upper end of cleithrum; cleithrum with two pronounced fleshy papillae that lack underlying osteological support (Fig. 3A–B; compare with *E. struhsakeri* [Fig. 3C–D] and *E. nitidus* [Fig. 3E–F]). Pectoral fins reaching slightly posterior to vertical at tips of pelvic fins. Anal fin origin slightly posterior to vertical at first soft dorsal-fin ray. Anus well in advance of anal fin origin.

Color of market specimens dusky rose dorsally, becoming silver-pink ventrally (Figs 1–2). Indistinct wide lateral bar of yellowish pink below lateral-line canal. Indistinct dark mottling above the lateral-line canal. Centers of flank scales darker pink. Dorsal fin pinkish white; pelvic, anal, and caudal fins whitish, with rays pinker than membrane; pectoral fins pink, grading to white distally; lips red. In alcohol, uniformly tan, no distinct coloration remains (Fig. 1).

**Distribution.** All three specimens of *Emmelichthys papillatus* were collected from markets of the Visayas region of the Philippines (Fig. 2C). It is unknown if this species occurs beyond Philippine waters.



**Figure 1.** Holotype of *Emmelichthys papillatus* sp. nov. (PNM 15806 [ex. KAUM-I. 91845]) from the Philippines **A** before preservation. Photograph by the Kagoshima University Museum **B** preserved specimen.

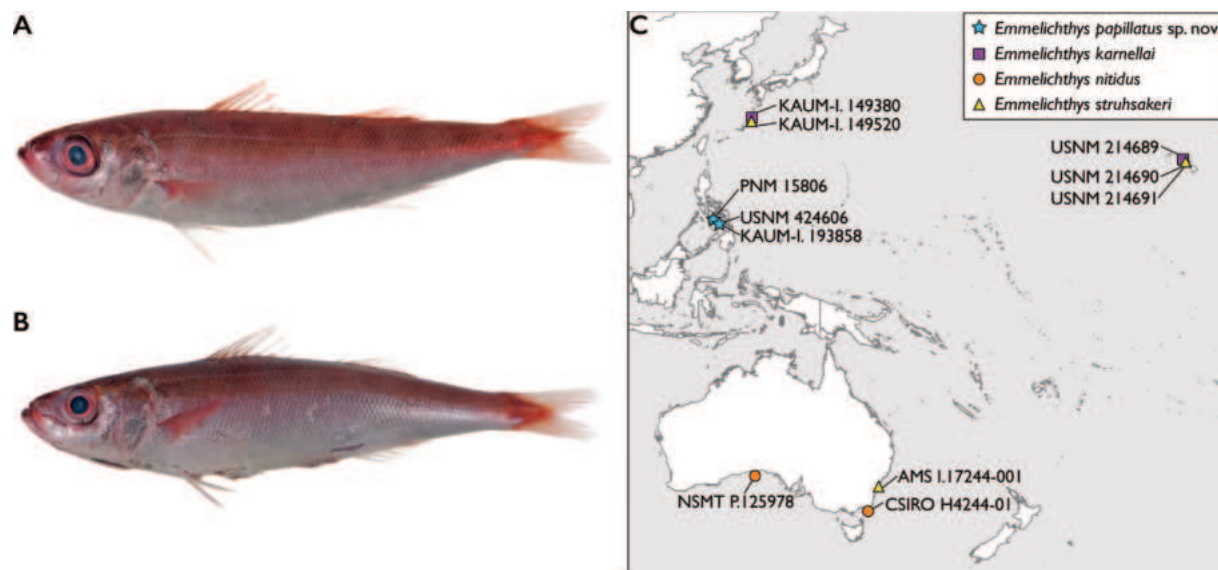


**Figure 2.** Paratypes of *Emmelichthys papillatus* sp. nov. and collection localities for specimens examined in this study **A** KAUM-I. 193858 (ex. USNM 424607) before preservation **B** USNM 424606 before preservation. Photographs by J. T. Williams **C** distribution of Pacific *Emmelichthys* spp. type materials examined.

**Table 3.** Counts and measurements of type specimens for *Emmelichthys papillatus* sp. nov. Dashes indicate data not collected because of specimen damage.

Characters	Holotype	Paratype	Paratype
	PNM 15806	USNM 424606	KAUM-I. 193858
Total length in mm	154	138	132
Standard length (SL) in mm	130	122	119
Dorsal-fin spines	XI	–	XI
Dorsal-fin spines connected by membrane	VIII	–	VIII
Isolated posterior dorsal-fin spines	II	II	II
Dorsal-fin rays	11	11	11
Pectoral-fin rays	18	19	19
Anal-fin rays	10	10	10
Gill rakers (Upper + Lower)	8+22	8+25	8+25
Lateral-line scales	74	74	69
Fleshy cleithral papillae	Present	Present	Present
Body depth in %SL	19.8	–	–
Body width in %SL	12.5	11.6	–
Head length in %SL	27.9	26.0	25.3
Orbit diameter in %SL	7.7	7.0	6.7
Interorbital width in %SL	7.4	6.3	7.1
Predorsal distance in %SL	36.2	34.4	35.3
Distance from snout to anus in %SL	60.9	–	–
Spinous dorsal-fin base in %SL	27.8	27.5	27.4
Pectoral-fin length in %SL	17.7	15.7	16.3
Pelvic-fin length in %SL	14.6	13.1	12.6
Caudal-peduncle depth in %SL	7.2	7.8	7.3
Caudal-peduncle width in %SL	3.5	3.0	4.1
Longest dorsal-fin spine in %SL	13.1	12.6	12.4
Penultimate dorsal-fin spine in %SL	2.1	2.8	1.9
Last dorsal-fin spine in %SL	–	3.2	3.2
First anal-fin spine in %SL	1.3	–	1.4
Third anal-fin spine in %SL	4.5	–	5.2
Pelvic base to anus in %SL	28.1	–	–

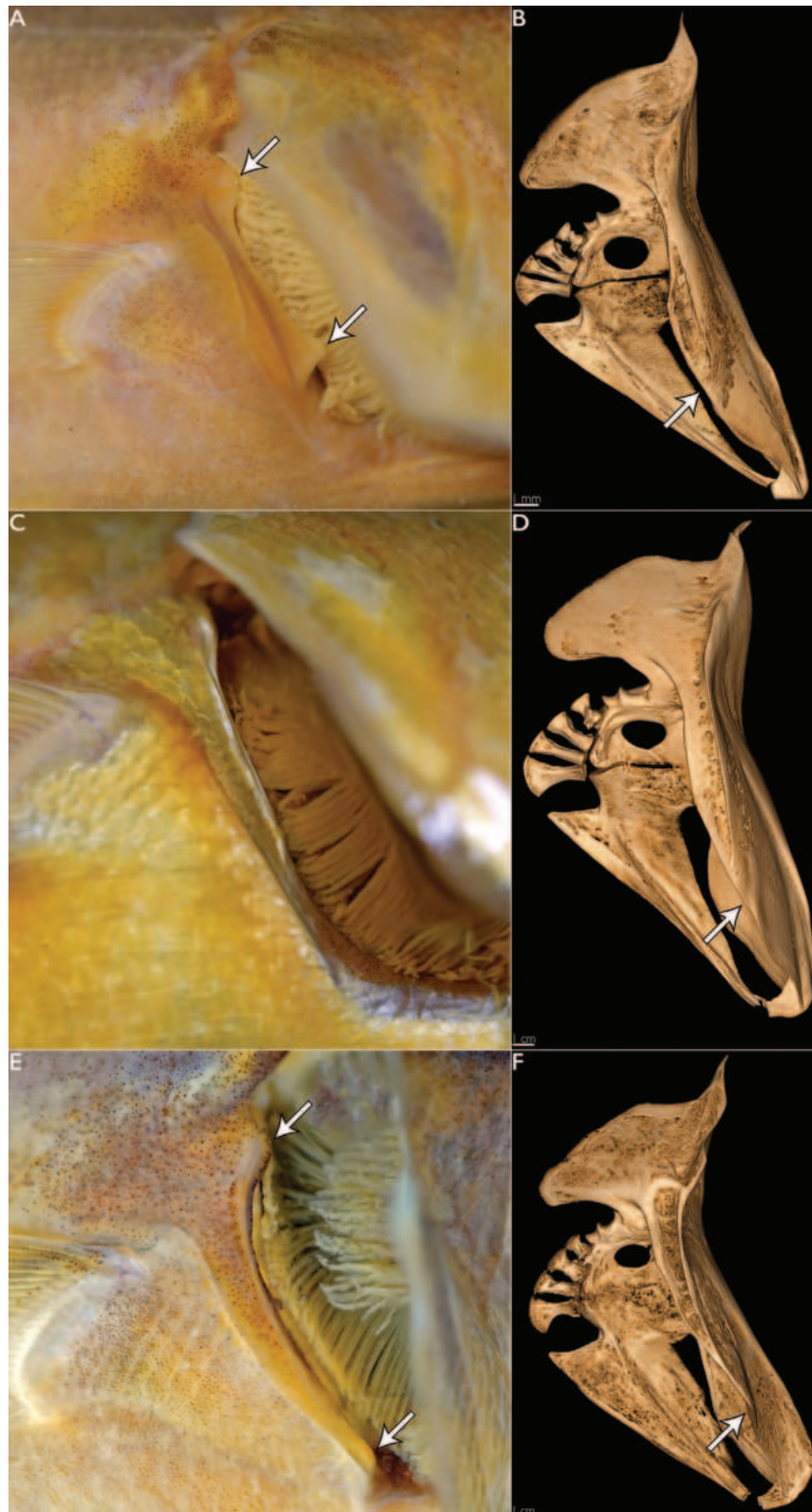


**Figure 3.** Pectoral girdle in species of *Emmelichthys* **A** fleshy cleithral papillae (arrows) in *E. papillatus* sp. nov. (PNM 15806 [ex. KAUM-I. 91845] holotype) **B**  $\mu$ CT scan of pectoral girdle in *E. papillatus* sp. nov. (PNM 15806 [ex. KAUM-I. 91845] holotype). Arrow indicates absence of anterior expansion of cleithrum **C** absence of cleithral papillae in *E. struhsakeri* (AMS I.17244-001) **D**  $\mu$ CT scan of pectoral girdle in *E. struhsakeri* (USNM 214690 holotype). Arrow indicates absence of anterior expansion of cleithrum **E** bony cleithral papillae (arrows) in *E. nitidus* (NSMT P.125978) **F**  $\mu$ CT scan of pectoral girdle in *E. nitidus* (CSIRO H 4244-01). Arrow indicates prominent anterior expansion of cleithrum that supports ventral cleithral papilla.

**Table 4.** Counts and measurements among species of *Emmelichthys*. Values for species not described in this study from Heemstra and Randall (1977), Kotlyar (1982) and Fricke et al. (2014). Dashes indicate data not available.

Characters	<i>E. papillatus</i> sp. nov.	<i>E. cyanescens</i>	<i>E. elongatus</i>	<i>E. karnellai</i>	<i>E. nitidus</i>	<i>E. ruber</i>	<i>E. struhsakeri</i>
Dorsal-fin spines	XI	XIII–XIV	XII	XII–XIII	XIII–XIV	XII–XIII	XI–XII
Dorsal-fin spines connected by membrane	VIII	XI–X	VIII	VIII–IX	IX–X	VII–IX	VIII–X
Isolated posterior dorsal-fin spines	II	II–III	III	IV–V	II–III	III–V	I–III
Length of posterior dorsal-fin spines	Protruding	Protruding	Protruding	Embedded	Protruding	Embedded	Protruding
Dorsal-fin rays	11	9–10	9–10	10–11	9–11	9–11	10–12
Pectoral-fin rays	18–19	22	18–20	21–23	20–23	19–20	19–21
Anal-fin rays	10	10–11	9–10	9–10	9–10	9–10	9–10
Gill rakers	30–33	39–42	34–38	37–43	37–43	33–38	34–41
Lateral-line scales	69–74	100–105	61–68	76–85	87–98	71–74	68–76
Cleithral papillae	Present - Fleshy	Present - Bony	Absent	Absent	Present - Bony	Absent	Absent
Body depth in %SL	19.8	18.0–22.0	15.0–19.0	19.0–22.0	19.0–24.0	19.0–28.0	20.0–25.0
Body width in %SL	11.6–12.5	–	11.0–13.0	14.0–17.0	11.0–17.0	11.0–16.0	13.0–16.0
Head length in %SL	25.3–27.9	25.0–27.0	26.0–27.0	25.0–27.0	25.0–30.0	25.0–32.0	26.0–30.0
Orbit diameter in %SL	6.7–7.7	7.1–8.7	6.5–9.6	8.8–9.6	7.0–11.0	8.6–12.9	9.0–11.1
Interorbital width in %SL	6.3–7.4	5.9–6.2	5.4–6.6	7.0–7.7	6.0–7.7	5.8–7.1	6.3–7.8
Predorsal distance in %SL	34.4–36.2	35.0–37.0	–	37.0–39.0	35.0–39.0	35.0–43.0	35.0–40.0
Distance from snout to anus in %SL	60.9	64.0–67.0	–	57.0–66.0	64.0–72.0	57.0–62.0	58.0–63.0
Spinous dorsal-fin base in %SL	27.4–27.8	30.0–31.0	28.0–36.0	32.0–34.0	30.0–36.0	25.0–31.0	26.0–30.0
Pectoral-fin length in %SL	15.7–17.7	18.0–20.0	16.0–20.0	17.0–19.0	19.0–24.0	16.0–20.0	18.0–21.0
Pelvic-fin length in %SL	12.6–14.6	13.0–14.0	10.0–14.0	11.0–15.0	13.0–17.0	12.0–20.0	14.0–16.0
Caudal-peduncle depth in %SL	7.2–7.8	6.0–7.1	5.8–7.5	5.7–7.7	6.5–8.5	6.3–11.6	6.4–8.3
Caudal-peduncle width in %SL	3.0–4.1	–	5.2–7.2	4.2–4.9	2.8–5.7	–	3.0–5.5
Longest dorsal-fin spine in %SL	12.4–13.1	12.0	–	12.0–16.0	12.0–15.0	12.0–15.0	13.0–16.0
Penultimate dorsal-fin spine in %SL	1.9–2.8	2.9	–	2.6–3.7	2.5–3.8	0.6–1.3	2.1–3.8
Last dorsal-fin spine in %SL	3.2	2.5	–	3.3–4.1	2.1–3.7	3.1–3.6	3.1–5.5
First anal-fin spine in %SL	1.3–1.4	1.5–1.9	1.1–2.4	1.0–1.9	1.0–2.9	1.2–3.8	1.4–2.8
Third anal-fin spine in %SL	4.5–5.2	4.2–5.3	2.7–6.0	4.1–6.4	3.1–6.7	4.8–7.1	4.7–7.3
Pelvic base to anus in %SL	28.1	–	25.0–30.0	8.0–11.0	15.0–27.0	–	9.0–14.0

### Mitochondrial data

Mitogenomes of two type specimens are circular and 16,614–16,616 bps in length (99.9% similar; 9 bps different total). Both encoded 37 mitochondrial loci (13 protein coding, 22 tRNAs, and 2 rRNAs) and one non-coding control region (D-loop). Of these, 26 loci are on the majority strand and the remaining nine are on the minority strand. The locus order matches that of previously sequenced species of *Emmelichthys* (Fig. 4; Miya et al. 2003). Sequences of *E. papillatus* are 82.5–87.5% similar (2046–2964 bps different total) to all other emmelichthyids sampled in this study. The COI barcode from the three types is 99.85–100% similar (1 bp different total), with sequences of *E. papillatus* 88.5–91.3% similar (130–184 bps different total) from all other emmelichthyids sampled in this study.

### Results of phylogenetic analysis

All ten tree searches resulted in a single optimal topology with slightly different branch lengths. The best-scoring topology (Ln  $L = -37445.526$ ) is shown in Fig. 4. High levels of support were recovered, with all but one node having a

value  $\geq 97\%$  (Fig. 4). We recovered all three specimens of *E. papillatus* in an independent lineage from other species of *Emmelichthys* sampled (i.e., *E. karnellai*, *E. nitidus* and *E. struhsakeri*). *Emmelichthys* is recovered as a non-monophyletic group, with species of *Erythrocles* nested among the species of *Emmelichthys*. *Emmelichthys nitidus* is the earliest-diverging species, with the remaining taxa

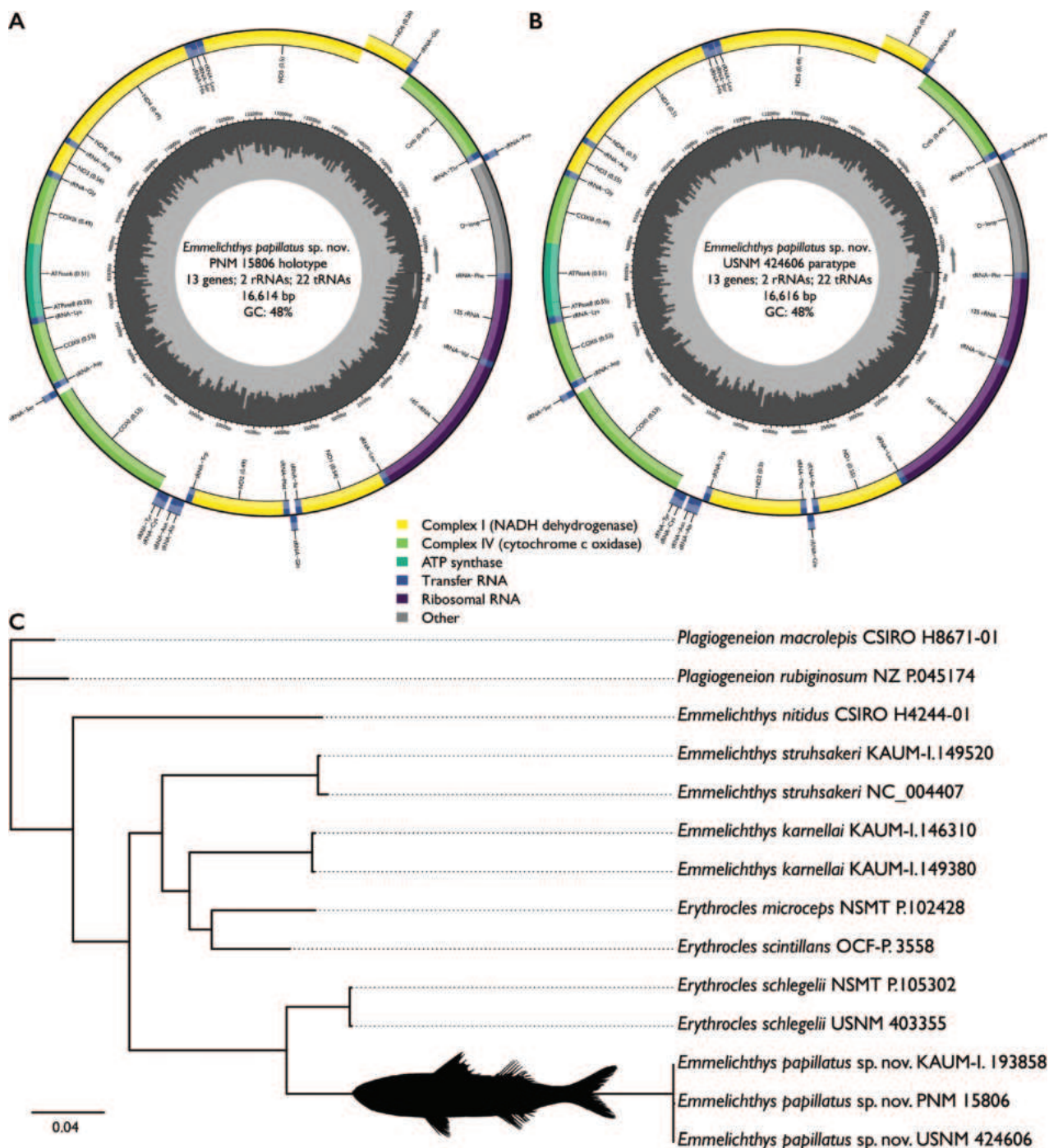


**Figure 4.** Mitogenome structure and placement of *E. papillatus* sp. nov. among species of *Emmelichthys* **A** mitogenome structure of *E. papillatus* sp. nov. (PNM 15806 [ex. KAUM-I. 91845] holotype) **B** mitogenome structure of *E. papillatus* sp. nov. (USNM 424606 paratype) **C** phylogeny of emmelichthyids based on 13 protein-coding mitochondrial loci. Bootstrap values not listed, see text.

sampled recovered in two clades. In one clade, *Emmelichthys struhsakeri* is the earliest-diverging species, with *Emmelichthys karnellai* sister to a clade of *Erythrocles microceps* and *Erythrocles scintillans*. In the other clade, all samples of *E. papillatus* are recovered sister to all samples of *Erythrocles schlegelii* (Fig. 4).

## Discussion

### Fishery implications

We did not identify additional specimens of *Emmelichthys papillatus* in collections beyond the three type specimens described in this study. This may be due, in part, to the rarity of emmelichthyids housed in museums, a lack of species-specific identification of freshly caught specimens, and/or the challenges of species-specific identifications for emmelichthyids broadly. In the Philippines, species of *Emmelichthys* are caught by bagnet, Danish seine, fish corrals, hook and line, otoshi ami, purse seine, ringnet, stationary liftnet, and trawl, but are not typically identified to species (Calvelo et al. 1991). Locally known as rebentador, sikwan and tuliloy, species of *Emmelichthys* are sold in markets, especially in Caraga, Cebu and Panay. It is unknown what percentage of *Emmelichthys* spp. catch in the Philippines is *E. papillatus*.

### Non-monophyly of *Emmelichthys* and *Erythrocles*

When compared with species of *Plagiogeneion*, species of *Emmelichthys* and *Erythrocles* have divided spinous and soft dorsal fins and more fusiform bodies (see Heemstra and Randall 1977). Along with the morphology of the dorsal fin, Heemstra and Randall (1977) further separated the genera of emmelichthyids by differences in head length and body depth; however, we lack a phylogenetic assessment targeting emmelichthyid intrarelationships. Rabosky et al. (2018) included one species of *Emmelichthys* (*E. nitidus*), two species of *Erythrocles* (*E. monodi* Poll & Cadenat, 1954 and *E. schlegelii*) and two species of *Plagiogeneion* (*P. macrolepis* and *P. rubiginosum*) in their study on the broad relationships among ray-finned fishes, recovering *Erythrocles* as non-monophyletic based on five overlapping loci (see their suppl. materials). Similarly, we recovered a non-monophyletic *Erythrocles* in our study as well as a non-monophyletic *Emmelichthys*. As the intrarelationships among emmelichthyids are beyond the scope of this study, we do not modify the classification of the family based on our dataset. Morphological convergence has caused confusion about the taxonomy and classification of the Emmelichthyidae for nearly 80 years (see Schultz 1945; Heemstra and Randall 1977; Johnson 1980; Girard 2024) and the dorsal-fin morphology and differences in head length and body depth that diagnose *Emmelichthys*, *Erythrocles* and *Plagiogeneion* may have repeatedly evolved within the family. Subsequent investigations into the intrarelationships of Emmelichthyidae are needed to understand the evolution of these and other morphological characters of rovers, redbaits and rubyfishes.

**Key to the species of *Emmelichthys* (modified from Heemstra and Randall [1977] and Fricke et al. [2014])**

- 1 Posterior dorsal-fin spines embedded within dorsal profile of body ..... **2**
- Posterior dorsal-fin spines protruding above dorsal profile of body..... **3**
- 2 Lateral-line scales 71–74; pectoral-fin rays 19–20; total gill rakers 33–38  
..... ***E. ruber* (Bermuda, Jamaica and St. Helena)**
- Lateral-line scales 76–85; pectoral-fin rays 21–23; total gill rakers 37–43  
..... ***E. karnellai* (Hawaiian Islands and Easter Island)**
- 3 Lateral-line scales 61–76..... **4**
- Lateral-line scales 87–105 ..... **6**
- 4 Lateral-line scales 61–68; body depth 15.0–19.0% SL.....  
..... ***E. elongatus* (Nazca Ridge and Southeastern Pacific Ocean)**
- Lateral-line scales 68–76; body depth 19.8–25.0% SL..... **5**
- 5 Pectoral-fin rays 18–19; gill rakers 30–33; fleshy cleithral papillae present.....  
..... ***E. papillatus* sp. nov. (Philippines)**
- Pectoral-fin rays 19–21; gill rakers 34–41; cleithral papillae absent .....  
..... ***E. struhsakeri* (Australia, Hawaiian Islands and Japan)**
- 6 Lateral-line scales 87–98..... ***E. nitidus* (Australia, New Zealand, St. Paul and Amsterdam Islands and South Africa)**
- Lateral-line scales 100–105 .....  
..... ***E. cyanescens* (Chile and Juan Fernandez Islands)**

**Acknowledgements**

We thank N. A. L. Flores (DA-NFRDI), J. R. Deeds (Food and Drug Administration), K. Carpenter (ODU), D. Pitassy, K. Murphy, J. T. Williams, A. Driskell, D. Kanner, K. S. Macdonald III, L. Weigt, D. DiMichele, and C. Huddleston (NMNH) for their commitment and expertise they brought to sampling and curating specimens collected as part of this project; D. Tyler (NMNH) for editing our manuscript; I. P. Cabacaba, A. M. Lizano, A. Macaspac, S. M. S. Nolasco, and S. L. Sanchez (DA-NFRDI), Y. Fukui and M. Matsunuma (KAUM), E. P. Abunal, U. B. Alama, R. P. Babaran, R. S. Cruz, A. C. Gaje, S. S. Garibay, A. M. T. Guzman, L. H. Mooc, C. J. N. Rubido, R. F. M. Traifalgar, V. G. Urbina, and the graduate students of the College of Fisheries, University of the Philippines Visayas, for their support of specimen collection; J. Baclayo, R.S. Gaerlan, J.P. Macuno, and S. Mesa (DA-BFAR) for providing additional fisheries data; J. Hill (NMNH) for assistance with  $\mu$ CT scanning; A. Graham (CSIRO), H. Motomura (KAUM), G. Shinohara and M. Nakae (NSMT), J. Barker and S. Kortet (NZ), A. Kaneko and K. Miyamoto (OCF), and A. Reft and L. Willis (National Systematics Laboratory, National Oceanic and Atmospheric Administration) for providing support and/or access to specimens and tissues in their care; and N. Redmond, J. Steier, and C. Craig (NMNH) for providing sequencing support. Memoranda of Agreements among the BFAR-NFRDI, NMNH Laboratories of Analytical Biology, USNM, and Food and Drug Administration provided support for the collection and study of specimens from Philippine fish markets. A Memorandum of Agreement between DA-NFRDI, the University of the Philippines Visayas, KAUM, and Research Institute for Humanity and Nature, and Tokai University allowed for collection of the holotype. Extractions and library preparation were conducted at the NMNH Laboratories of Analytical Biology.

## Additional information

### Conflict of interest

The authors have declared that no competing interests exist.

### Ethical statement

No ethical statement was reported.

### Funding

Research was funded by a Smithsonian Institution Barcode Network grant (to MGG and KEB) and an Interagency Agreement between Food and Drug Administration of the United States of America and NMNH. MGG was supported by the Herbert R. and Evelyn Axelrod Endowment for Systematic Ichthyology at NMNH, the NMNH Office of the Associate Director for Science, and the Food and Drug Administration of the United States of America.

### Author contributions

Matthew G. Girard: conceptualization, data curation, formal analysis, funding acquisition, investigation, methodology, resources, validation, visualization, writing – original draft, writing – review & editing. Mudjekeewis D. Santos: investigation, project administration, resources, supervision, writing – review & editing. Katherine E. Bemis: funding acquisition, investigation, project administration, resources, visualization, supervision, writing – review & editing.

### Author ORCIDs

Matthew G. Girard  <https://orcid.org/0000-0003-3580-6808>

Mudjekeewis D. Santos  <https://orcid.org/0000-0002-4770-1221>

Katherine E. Bemis  <https://orcid.org/0000-0002-7471-9283>

### Data availability

All of the data that support the findings of this study are available in the main text, on GenBank, and/or MorphoSource.

## References

- Baldwin CC, Mounts JH, Smith DG, Weigt LA (2009) Genetic identification and color descriptions of early life-history stages of Belizean *Phaeoptyx* and *Astrapogon* (Teleostei: Apogonidae) with comments on identification of adult *Phaeoptyx*. *Zootaxa* 2008(1): 1–22. <https://doi.org/10.11646/zootaxa.2008.1.1>
- Bemis KE, Girard MG, Santos MD, Carpenter KE, Deeds JR, Pitassy DE, Flores NAL, Hunter ES, Driskell AC, Macdonald KS III, Weigt LA, Williams JT (2023) Biodiversity of Philippine marine fishes: A DNA barcode reference library based on voucher specimens. *Scientific Data* 10(1): 411. <https://doi.org/10.1038/s41597-023-02306-9>
- Bolger AM, Lohse M, Usadel B (2014) Trimmomatic: A flexible trimmer for Illumina sequence data. *Bioinformatics* 30(15): 2114–2120. <https://doi.org/10.1093/bioinformatics/btu170>
- Calvelo RR, Ganaden SR, Tuazon LC (1991) Relative abundance of fishes caught by bagnet around Calagua Island (Lamon Bay) with notes on their biology. *The Philippine Journal of Fisheries* 22: 49–68.
- Carpenter KE, Williams JT, Santos MD (2017) *Acanthurus albimento*, a new species of surgeonfish (Acanthuriformes: Acanthuridae) from northeastern Luzon, Philippines,

- with comments on zoogeography. *Journal of the Ocean Science Foundation* 25: 33–46.
- Chernomor O, von Haeseler A, Minh BQ (2016) Terrace aware data structure for phylogenomic inference from supermatrices. *Systematic Biology* 65(6): 997–1008. <https://doi.org/10.1093/sysbio/syw037>
- Faircloth BC (2013) Illumiprocessor: A Trimmomatic wrapper for parallel adapter and quality trimming. <https://doi.org/10.6079/J9ILL>
- Fricke R, Golani D, Appelbaum-Golani B (2014) *Emmelichthys marisrubri*, a new rover from the southern Red Sea (Teleostei: Emmelichthyidae). *Cybium* 38(2): 83–87. <https://doi.org/10.26028/cybium/2014-382-001>
- Fricke R, Eschmeyer WN, Van der Laan R (2023) Eschmeyer's Catalog of Fishes: Genera, Species, References. <http://researcharchive.calacademy.org/research/ichthyology/catalog/fishcatmain.asp> [Electronic version accessed 14 December 2023.]
- Girard MG (2024) Convergent evolution and the Red Sea rover: *Emmelichthys marisrubri* (Teleostei: Emmelichthyidae) is a species of fusilier (Lutjanidae: *Dipterygonotus*). *Ichthyology & Herpetology* 112(1): 41–52. <https://doi.org/10.1643/i2023048>
- Girard MG, Davis MP, Smith WL (2020) The phylogeny of carangiform fishes: Morphological and genomic investigations of a new fish clade. *Copeia* 108(2): 265–298. <https://doi.org/10.1643/C1-19-320>
- Girard MG, Davis MP, Tan HH, Wedd DJ, Chakrabarty P, Ludt WB, Summers AP, Smith WL (2022a) Phylogenetics of archerfishes (Toxotidae) and evolution of the toxotid shooting apparatus. *Integrative Organismal Biology* 4: obac013. <https://doi.org/10.1093/iob/obac013>
- Girard MG, Davis MP, Baldwin CC, Dettai A, Martin RP, Smith WL (2022b) Molecular phylogeny of threadfin fishes (Polynemidae) using ultraconserved elements. *Journal of Fish Biology* 100(3): 793–810. <https://doi.org/10.1111/jfb.14997>
- Heemstra PC, Randall JE (1977) A revision of the Emmelichthyidae (Pisces: Perciformes). *Marine and Freshwater Research* 28(3): 361–396. <https://doi.org/10.1071/MF9770361>
- Hoban ML, Whitney J, Collins AG, Meyer C, Murphy KR, Reft AJ, Bemis KE (2022) Skimming for barcodes: Rapid production of mitochondrial genome and nuclear ribosomal repeat reference markers through shallow shotgun sequencing. *PeerJ* 10: e13790. <https://doi.org/10.7717/peerj.13790>
- Iwasaki W, Fukunaga T, Isagozawa R, Yamada K, Maeda Y, Satoh TP, Sado T, Mabuchi K, Takeshima H, Miya M, Nishida M (2013) MitoFish and MitoAnnotator: A mitochondrial genome database of fish with an accurate and automatic annotation pipeline. *Molecular Biology and Evolution* 30(11): 2531–2540. <https://doi.org/10.1093/molbev/mst141>
- Johnson GD (1980) The limits and relationships of the Lutjanidae and associated families. *Bulletin of the Scripps Institution of Oceanography* 24: 1–112.
- Kalyaanamoorthy S, Minh BQ, Wong TKF, von Haeseler A, Jermiin LS (2017) ModelFinder: Fast model selection for accurate phylogenetic estimates. *Nature Methods* 14(6): 587–589. <https://doi.org/10.1038/nmeth.4285>
- Katoh K, Standley DM (2013) MAFFT multiple sequence alignment software version 7: Improvements in performance and usability. *Molecular Biology and Evolution* 30(4): 772–780. <https://doi.org/10.1093/molbev/mst010>
- Kearse M, Moir R, Wilson A, Stones-Havas S, Cheung M, Sturrock S, Buxton S, Cooper A, Markowitz S, Duran C, Thierer T, Ashton B, Meintjes P, Drummond A (2012) Geneious basic: An integrated and extend-able desktop software platform for the organization and analysis of sequence data. *Bioinformatics* 28(12): 1647–1649. <https://doi.org/10.1093/bioinformatics/bts199>

- Kotlyar AN (1982) A new species of the genus *Emmelichthys* (Emmelichthyidae, Osteichthyes) from the south-western [sic, south-eastern] part of the Pacific Ocean. *Biulleten' Moskovskogo Obshchestva Ispytatelei Prirody. Otdel Biologicheskii* 87(1): 48–52. [Bulletin of the Moscow Society of Naturalists Biological Series]
- Matsunuma M, Yamakawa T, Williams JT (2018) *Chelidoperca tosaensis*, a new species of perchlet (Serranidae) from Japan and the Philippines, with geographic range extension of *C. stella* to the northwestern Pacific Ocean. *Ichthyological Research* 65(2): 210–230. <https://doi.org/10.1007/s10228-017-0604-5>
- Minh BQ, Schmidt HA, Chernomor O, Schrempf D, Woodhams MD, von Haeseler A, Lanfear R (2020) IQ-TREE 2: New models and efficient methods for phylogenetic inference in the genomic era. *Molecular Biology and Evolution* 37(5): 1530–1534. <https://doi.org/10.1093/molbev/msaa015>
- Miya M, Takeshima H, Endo H, Ishiguro NB, Inoue JG, Mukai T, Satoh TP, Yamaguchi M, Kawaguchi A, Mabuchi K, Shirai SM, Nishida M (2003) Major patterns of higher teleostean phylogenies: A new perspective based on 100 complete mitochondrial DNA sequences. *Molecular Phylogenetics and Evolution* 26(1): 121–138. [https://doi.org/10.1016/S1055-7903\(02\)00332-9](https://doi.org/10.1016/S1055-7903(02)00332-9)
- Motomura H, Alama UB, Muto N, Babaran RP, Ishikawa S (2017) Commercial and by-catch market fishes of Panay Island, Republic of the Philippines. The Kagoshima University Museum, Kagoshima, University of the Philippines Visayas, Iloilo, and Research Institute for Humanity and Nature, Kyoto, 246 pp. [911 figs]
- Oyarzún GC, Arriaza ZM (1993) *Emmelichthys nitidus nitidus* Richardson, 1845 and *Emmelichthys nitidus cyanescens* (Guichenot, 1848), (Perciformes; Emmelichthyidae). Are really different subspecies? *Revista de Biología Marina, Valparaíso* 28(2): 341–348.
- Pastana MNL, Girard MG, Bartick MI, Johnson GD (2022) A novel association between larval and juvenile *Erythrocles schlegelii* (Teleostei Emmelichthyidae) and pelagic tunicates. *Ichthyology & Herpetology* 110(4): 675–679. <https://doi.org/10.1643/i2022008>
- Rabosky DL, Chang J, Title PO, Cowman PF, Sallan L, Friedman M, Kaschner K, Garilao C, Near TJ, Coll M, Alfaro ME (2018) An inverse latitudinal gradient in speciation rate for marine fishes. *Nature* 559(7714):392–395. <https://doi.org/10.1038/s41586-018-0273-1>
- Sabaj MH (2020) Codes for natural history collections in ichthyology and herpetology. *Copeia* 108(3): 593–669. <https://doi.org/10.1643/ASIHCONDONS2020>
- Sato Y, Miya M, Fukunaga T, Sado T, Iwasaka W (2018) MitoFish and MiFish pipeline: A mitochondrial genome database of fish with an analysis pipeline for environmental DNA metabarcoding. *Molecular Biology and Evolution* 35(6): 1553–1555. <https://doi.org/10.1093/molbev/msy074>
- Schultz LP (1945) *Emmelichthyops atlanticus*, a new genus and species of fish (family Emmelichthyidae) from the Bahamas, with a key to related genera. *Journal of the Washington Academy of Sciences* 35(4): 132–136.
- Weigt LA, Driskell AC, Baldwin CC, Ormos A (2012) DNA barcoding fishes. In: Kress WJ, Erickson DL (Eds) *DNA barcodes: Methods and protocols* Humana Press, Totowa, NJ, 109–126. [https://doi.org/10.1007/978-1-61779-591-6\\_6](https://doi.org/10.1007/978-1-61779-591-6_6)
- Williams JT, Carpenter KE (2015) A new fish species of the subfamily Serraninae (Perciformes, Serranidae) from the Philippines. *Zootaxa* 3911(2): 287–293. <https://doi.org/10.11646/zootaxa.3911.2.10>
- Zhu T, Sato Y, Sado T, Iwasaka W (2023) MitoFish, MitoAnnotator, and MiFish pipeline: Updates in 10 years. *Molecular Biology and Evolution* 40(3): msad035. <https://doi.org/10.1093/molbev/msad035>



# Confirmation of the valid specific status of *Dolichovespula kuami* Kim & Yoon, 1996 (Hymenoptera, Vespidae) based on molecular and morphological evidence

Chang-Jun Kim<sup>1</sup>, Jiang-Li Tan<sup>2</sup>, Jeong Kyu Kim<sup>3</sup>, Moon Bo Choi<sup>4,5</sup>

<sup>1</sup> Division of Gardens and Education, Korea National Arboretum, Pocheon, 11186, Republic of Korea

<sup>2</sup> Key Laboratory for Animal Conservation / Key Laboratory of Resource Biology and Biotechnology in Western China, College of Life Sciences, Northwest University, Xi'an, Shaanxi 710069, China

<sup>3</sup> Department of Bio Environment Health, Dongnam Health University, Suwon, 16328, Republic of Korea

<sup>4</sup> Institute of Plant Medicine, Kyungpook National University, Daegu, 41566, Republic of Korea

<sup>5</sup> Department of R&D, Wild Beei, Chilgok, 39864, Republic of Korea

Corresponding authors: Moon Bo Choi ([kosinchoi@hanmail.net](mailto:kosinchoi@hanmail.net)); Jeong Kyu Kim ([hymjkk@dongnam.ac.kr](mailto:hymjkk@dongnam.ac.kr))

## Abstract

The taxonomic validity of *Dolichovespula kuami*, especially in relation to *D. flora*, has been the subject of a long-term debate. Herein, the valid specific status of the former was supported through an integrated analysis of morphological characters and DNA barcodes. The pronotal rugae and male genitalia of the two species are different, and partial mitochondrial genes (cytochrome oxidase subunit I, COI) indicate that they form significantly distinct lineages. The hitherto unknown male of *D. kuami* is described for the first time, and a brief discussion of the *D. maculata* species group is provided.

**Key words:** Description, DNA barcoding, *Dolichovespula flora*, male, mt-COI, taxonomy, Vespidae, wasp



Academic editor: Andreas Köhler

Received: 28 July 2023

Accepted: 15 February 2024

Published: 22 March 2024

ZooBank: <https://zoobank.org/0F3402DB-DD2D-4E62-9CB4-2C1E396025DB>

**Citation:** Kim C-J, Tan J-L, Kim JK, Choi MB (2024) Confirmation of the valid specific status of *Dolichovespula kuami* Kim & Yoon, 1996 (Hymenoptera, Vespidae) based on molecular and morphological evidence. ZooKeys 1196: 111–119. <https://doi.org/10.3897/zookeys.1196.110224>

**Copyright:** © Chang-Jun Kim et al.

This is an open access article distributed under terms of the Creative Commons Attribution License ([Attribution 4.0 International – CC BY 4.0](https://creativecommons.org/licenses/by/4.0/)).

## Introduction

To date, 19 species in the genus *Dolichovespula* Rohwer, 1916 (Hymenoptera: Vespidae) have been described from the Palearctic, Nearctic and Oriental regions (Archer 2012; Tan et al. 2014; Daglio 2020; Wang et al. 2022). Among these, the *Dolichovespula maculata* group includes a total of four species (*D. flora* Archer, 1987, *D. maculata* (Linnaeus, 1763), *D. media* (Retzius, 1783) and *D. kuami* Kim & Yoon, 1996), the members of which are characterized by the presence of pronotal striae (or furrows), the structure of the male aedeagus, and a strongly notched seventh gastral sternum (Archer 2012). Within this group, the taxonomic validity of *D. kuami* with respect to *D. flora* remains a matter of contention (Archer 1999, 2006, 2012). Whereas Tan et al. (2014) considered these to be conspecific taxa, Kim (2011) has presented evidence to indicate that *D. kuami* is a valid discrete species. This discrepancy can be attributed, at least in part, to a lack of information regarding male characteristics and differences in interpreting the related morphological variations.

In 2014, however, Tan et al. described the males of *D. flora* after discovering their nests. Recently, two of the authors of this study (JKK and MBC) identified two young and mature nests of *D. kuami* in Korea and obtained specimens of all relevant castes in 2018 and 2019, respectively.

In an attempt to resolve the longstanding debate surrounding the taxonomic validity of *D. kuami* and *D. flora*, in this study, we performed further morphological comparisons and DNA barcode analyses (using the partial mt-COI gene). We also thoroughly re-examined the orientation of the pronotal rugae and the structure of the male genitalia, and compared DNA barcodes of the two species to assess their genetic limits. A description of the previously unrecorded male of *D. kuami* is also provided.

## Materials and methods

### Morphological terminology

The terminology used in this study follows that described by Archer (1987, 1999).

### Illustrations

The images were captured using a Leica DFC 495 camera mounted on a Leica M205A stereozoom microscope (Leica Microsystems, Solms, Germany) and acquired by using LAS v.4.1.0 (Leica Microsystems, Switzerland). In addition, to observe the pronotal rugae of *D. kuami* and *D. flora*, scanning electron microscopy (SEM) images of specimens selected from each species were obtained. Subsequently, the head, metasoma, wings and legs were removed and only the mesosoma was retained. The separated mesosomes were immersed in 10% NaOCl to remove excess tissue. The detached mesosoma was washed with distilled water using a soft brush to remove the remaining tissues. After cleaning, the samples were dried and coated with gold ion particles for SEM observation (Hitachi SU8220 & SU8230, Tokyo, Japan). Image plates were prepared using Adobe Photoshop CS6 (Adobe Systems Inc., San Jose, CA, USA).

### DNA extraction and amplification

Genomic DNA was extracted from the hind legs of dried or 100% alcohol-preserved specimens using the DNeasy Blood and Tissue Kit (Qiagen) after incubating for 24 h at 56 °C in lysis buffer and Proteinase K, as per the manufacturer's instructions. A total of 26 specimens of *D. kuami*, eight specimens of *D. media*, and two specimens of *D. flora* were sequenced. The cytochrome c oxidase I barcoding region was amplified using the primer pair LepF1 and LepR1 (Hebert et al. 2004). PCR was performed using Solg™ 2X Taq PCR Pre-Mix (Solgent). We prepared 30 µL of reaction mixture containing 15 µL of PCR Pre-Mix, 11 µL of nuclease-free dH<sub>2</sub>O, 2 µL DNA template, and 1 µL of 10 pmol of each primer. A typical PCR program started with 4 min of initial denaturation at 94 °C, followed by 40 cycles of 30 s at 94 °C, 45 s of annealing at 45 °C, and 45 s of elongation at 72 °C, ending with a 6-min period of final elongation at 72 °C.

## Molecular phylogenetic analyses

Sequence reads were edited and assembled using Geneious 11 (Biomatters, Auckland, New Zealand). The optimal model (GTR+I+G) for each partition was selected using the Akaike information criterion in jModelTest (Posada 2008). The tree was constructed using the maximum-likelihood method with RAxML v.8.1.2 (Stamatakis 2014), with 1000 bootstrap replications. Successful sequences were submitted to the NCBI GenBank (accession numbers presented in Table 1).

In addition, for phylogenetic analysis, other *Dolichovespula* species and outgroups, excluding the *D. maculata* group (*D. flora*, *D. maculata*, *D. media* and *D. kuami*), included were as follows: KU874880 (*Dolichovespula norvegica*), KM568773 (*D. alpicola*), MG374965 (*D. norvegicoides*), KJ147234 (*D. saxonica*), KJ147233 (*D. pacifica*), KJ147230 (*D. arenaria*), KM567260 (*D. adulterina*), KJ147235 (*D. sylvestris*), KJ147244 (*Vespa crabro*) and LT977378 (*Formica fusca*) (Table 1). The latter two species, from Vespidae and Formicidae, respectively, were included to test the monophyly of the family and root the tree, respectively.

## Specimens

Thirty-five specimens were used in this study to review the taxonomic positions of the focus species, *D. kuami* (25) from the Korea National Arboretum (Pocheon, Republic of Korea) and *D. flora* (2) from Northwest University (Xi'an, China), and *D. media* (8).

## Results

### Comparison of the pronotal rugae and carina of *D. kuami* and *D. flora*

The pronotum rugae of *D. kuami* were generally very dull and faint (Fig. 1A), whereas those of *D. flora* were relatively more distinct (Fig. 1D). We found that *D. kuami* has faint longitudinal rugae on the pronotal lateral face next to the pronotal pit (Fig. 1B), and the remaining posterior area has fine rugae running vertically (Fig. 1C). On the other hand, *D. flora* has distinct longitudinal rugae (Fig. 1E) that run downward, except in the upper pronotal area (Fig. 1F). Thus, there is a clear difference between the pronotal rugae of these two species. Additionally, the pronotum carina was sharper in *D. kuami* than in *D. flora*.

### Comparison of the external genitalic features of male *D. kuami* and *D. flora*

Genitalia (Fig. 2A–F). The external features of the genitalia of *D. kuami* and *D. flora* are very similar (Fig. 2A, D; also refer to Tan et al. 2014 for *D. flora*). However, *D. kuami* had a triangular parameral spine (Fig. 2C, arrow), whereas that of *D. flora* is short and slender (Fig. 2F, arrow). In addition, *D. kuami* has a truncated dorsal terminal process (Fig. 2A, arrow), whereas it is somewhat edged or shortly rounded in *D. flora* (Fig. 2D, arrow).

**Table 1.** Specimens, vouchers and GenBank accession information of *Dolichovespula* species included in the molecular phylogenetic analysis.

Species	Specimens	Vouchers	GenBank Accession #
1. <i>Dolichovespula kuami</i> Kim & Yoon, 1996	Korea: Gyeonggi-do, Pocheon-si	20Ves0603	OR029465
	Korea: Gyeonggi-do, Pocheon-si	20Ves0604	OR029466
	Korea: Gyeonggi-do, Yangpyeong-si	20Ves0605	OR029467
	Korea: Gangwon-do, Hwacheon-gun	20Ves0606	OR029468
	Korea: Gangwon-do, Hwacheon-gun	20Ves0607	OR029469
	Korea: Gyeonggi-do, Cheorwon-gun	20Ves0608	OR029470
	Korea: Gyeonggi-do, Pocheon-si	20Ves0609	OR029471
	Korea: Gangwon-do, Hwacheon-gun	20Ves0610	OR029472
	Korea: Gyeonggi-do, Namyangju-si	20Ves0611	OR029473
	Korea: Gyeonggi-do, Yeosu-gun	20Ves0613	OR029474
	Korea: Gyeonggi-do, Namyangju-si	20Ves0614	OR029475
	Korea: Gyeonggi-do, Yangju-si	20Ves0615	OR029476
	Korea: Gangwon-do, Hwacheon-gun	20Ves0616	OR029477
	Korea: Gyeonggi-do, Yangpyeong-si	20Ves0617	OR029478
	Korea: Gyeonggi-do, Yangpyeong-si	20Ves0619	OR029479
	Korea: Gyeonggi-do, Pocheon-si	20Ves0621	OR029480
	Korea: Gyeonggi-do, Pocheon-si	20Ves0622	OR029481
	Korea: Gyeonggi-do, Paju-si	20Ves0623	OR029482
	Korea: Gyeonggi-do, Yangpyeong-si	20Ves0624	OR029483
	Korea: Gangwon-do, Yanggu-gun	20Ves0627	OR029484
	Korea: Gyeonggi-do, Yeosu-gun	20Ves0628	OR029485
	Korea: Gangwon-do, Yanggu-gun	20Ves0630	OR029486
	Korea: Gyeonggi-do, Pocheon-si	20Ves0631	OR029487
Korea: Gyeonggi-do, Pocheon-si	20Ves0632	OR029488	
Korea: Gyeonggi-do, Pocheon-si	20Ves0633	OR029489	
Korea: Gyeonggi-do, Pocheon-si	20Ves0635	OR029490	
2. <i>D. media</i> (Retzius, 1783)	Korea: Gangwon-do, Yanggu-gun	20Ves0594	OR029457
	Korea: Gangwon-do, Goseong-gun	20Ves0595	OR029458
	Korea: Gangwon-do, Yanggu-gun	20Ves0596	OR029459
	Korea: Gangwon-do, Goseong-gun	20Ves0597	OR029460
	Korea: Gangwon-do, Hwacheon-gun	20Ves0598	OR029461
	Korea: Gangwon-do, Yanggu-gun	20Ves0599	OR029462
	Korea: Gangwon-do, Yanggu-gun	20Ves0600	OR029463
	Korea: Gangwon-do, Goseong-gun	20Ves0601	OR029464
3. <i>D. flora</i> Archer, 1987	China: Shaanxi, Huangbaiyuan	20Ves0643	OR029491
	China: Shaanxi, Huaxian	China004	OR029492
4. <i>D. maculata</i> (Linnaeus, 1763)	GenBank search	GenBank	KU874876
	GenBank search	GenBank	KJ147231
5. <i>D. norvegica</i> (Fabricius, 1781)	GenBank search	GenBank	KU874880
6. <i>D. alpicola</i> (Wagner, 1978)	GenBank search	GenBank	KM568773
7. <i>D. norvegicoides</i> (Sladen, 1918)	GenBank search	GenBank	MG374965
8. <i>D. saxonica</i> (Fabricius, 1793)	GenBank search	GenBank	KJ147234
9. <i>D. pacifica</i> (Birula, 1930)	GenBank search	GenBank	KJ147233
10. <i>D. arenaria</i> (Fabricius, 1775)	GenBank search	GenBank	KJ147230
11. <i>D. adulterina</i> (Buysson, 1905)	GenBank search	GenBank	KM567260
12. <i>D. sylvestris</i> (Scopoli, 1763)	GenBank search	GenBank	KJ147235
13. <i>Vespa crabro</i> Linnaeus, 1758	GenBank search	GenBank	KJ147244
14. <i>Formica fusca</i> Linnaeus, 1758	GenBank search	GenBank	LT977378

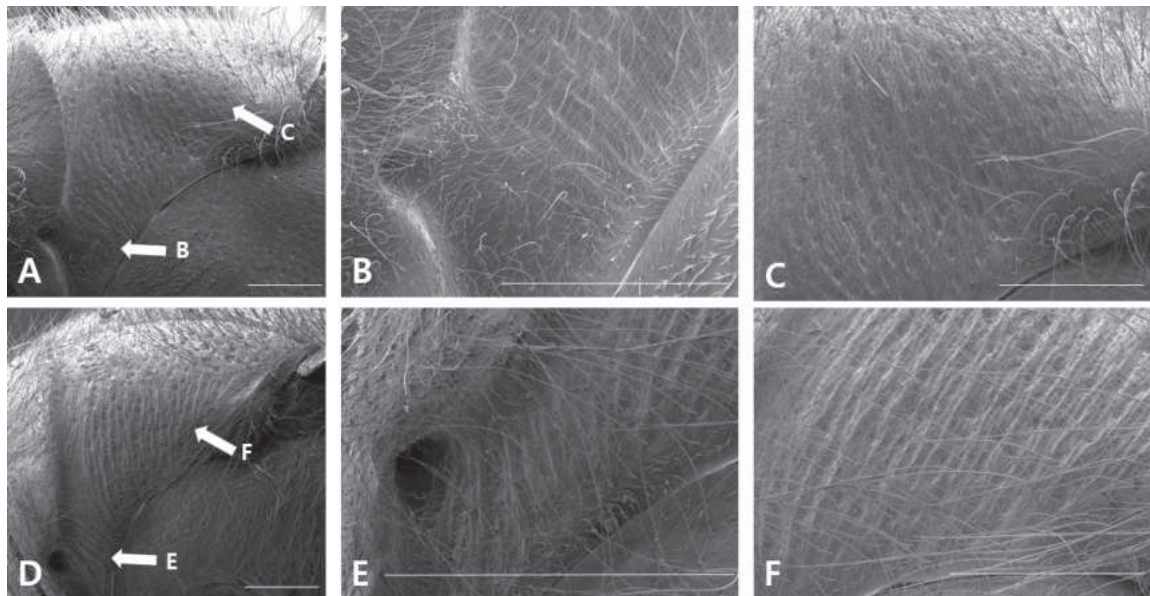


**Figure 1.** Comparison between the pronotal rugae and carinas of *D. kuami* and *D. flora*. Pronotum of *D. kuami* (A) and *D. flora* (D); rugae and carinas in the pronotal lateral part to the pronotal pit of *D. kuami* (B) and *D. flora* (E); rugae on the pronotum of *D. kuami* (C) and *D. flora* (F). Arrows in figures A, D indicate the enlarged parts in B, C, E, F. Scale bars: 0.5 mm.

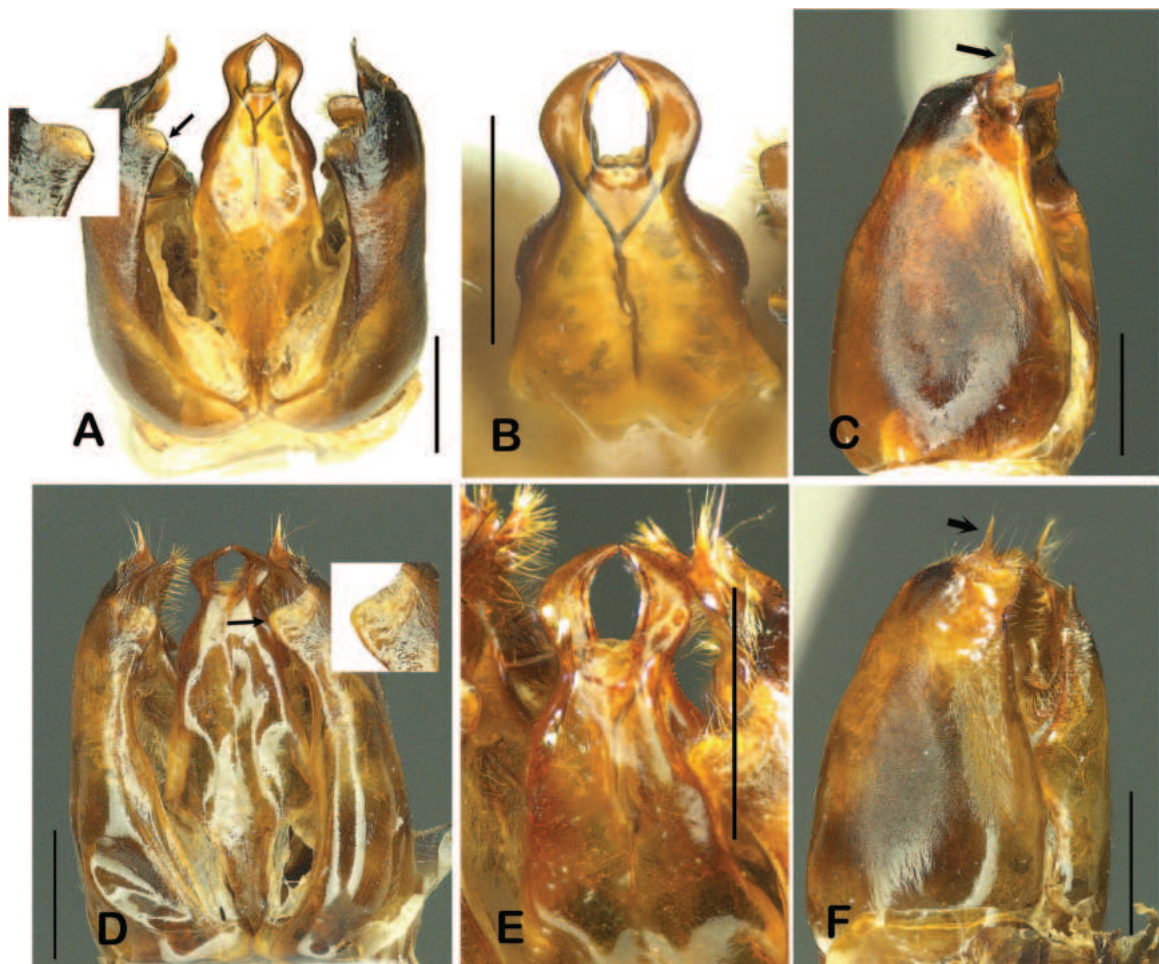


**Figure 2.** Genitalia of *Dolichovespula kuami* (A–C) and *D. flora* (D–F) A genitalic capsules, in dorsal view (truncated dorsal terminal process, arrow) B aedeagus C gonostipes and triangular parameral spine (arrow) D genitalic capsules, in dorsal view (shortly rounded terminal process, arrow) E aedeagal tip F gonostipes and slender parameral spine (arrow). Scale bars: 1 mm.

## DNA barcoding

Phylogenetically, *D. maculata* clearly clustered with other *Dolichovespula* spp. (Fig. 3). In the *D. maculata* group, *D. flora* was more closely related to *D. maculata* and *D. media*, whereas *D. kuami* clustered as a sister species to the clade that included these three species (Fig. 3). Thus, the two species *D. flora* and *D. kuami* stat. rev. were clearly separated into well-supported clusters, and the genetic distance between them was relatively high (average DNA barcode distance: 0.0996), suggesting that they represent two biological species. These results were further supported by those of the morphological examination.

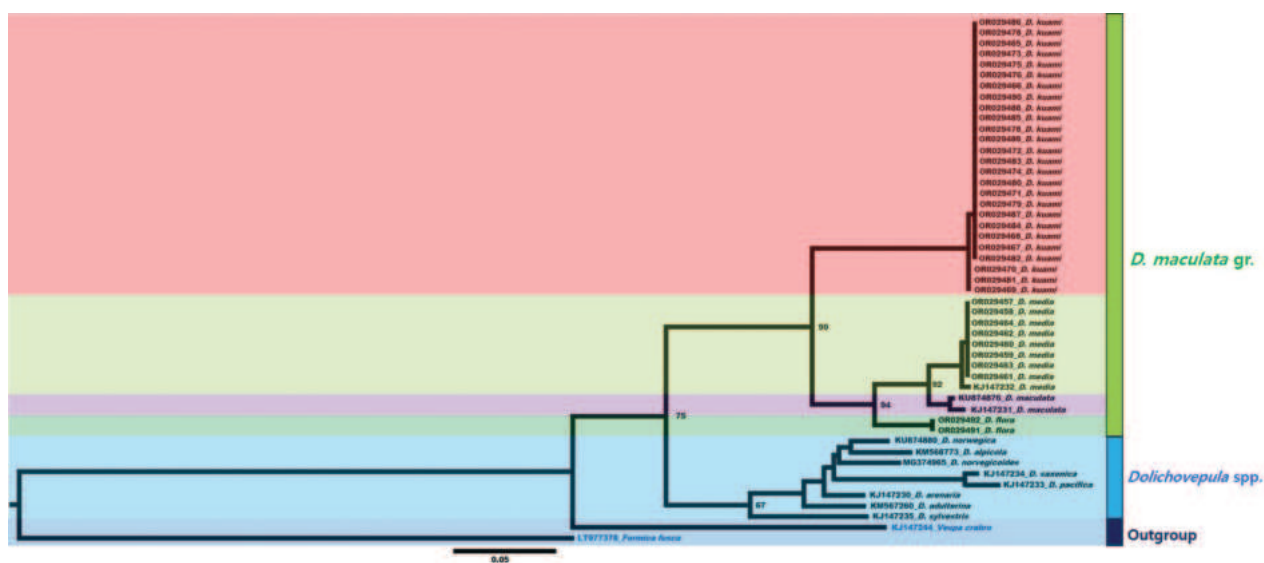


**Figure 3.** A maximum-likelihood phylogenetic tree of the successfully DNA barcoded *Dolichovespula* specimens. The numbers above the branches indicate bootstrap proportions.

## Discussion

According to Archer (1999), *D. kuami* was treated as a conspecific to *D. flora* because the orientation of the rugae in the lateral part of the pronotum is the same, and the observed differences in body color are a type of variation. Although Kim (2011) re-described this aspect with additional specimens, Archer (2012) consistently insisted that these two species were conspecific. In fact, as shown by Kim (2011) (Fig. 2), the rugae of the pronotum were not clearly distinguished under light microscopy because they are the same color as the base color. Therefore, in this study, we attempted to obtain very clear rugae images using SEM and observed that the pronotal rugae of the two species were clearly different. Despite these morphological differences, differences in male genitalia or DNA sequences are most critically needed to provide evidence of the difference between these two species (Archer 1999; Tan et al. 2014).

*Dolichovespula kuami* and *D. flora* are uncommon species in Korea and China, respectively, and their nests and males have not been recorded for many years. Tan et al. (2014) collected males of *D. flora* and described their genitalia. We collected males for the first time in 2018, when the first nest of *D. kuami* was discovered. This discovery enabled us to compare the male genitalia of

the two species. In general, their external morphologies were relatively similar, but there were clear differences in the parameral spine and dorsal terminal processes. None of the *D. kuami* strains were conspecific to *D. flora* based on evidence of their pronotal rugae, color patterns (Fig. 4), genitalia and DNA sequences. These results support the conclusion of the long-term conspecific debate and the specific status of *D. kuami*.

Additionally, DNA barcoding is an excellent tool for accelerating species identification and complementing species delimitation (Mo et al. 2021; Zhang and Wenjun 2022; Jafari et al. 2023). In particular, COI barcode information from the genus *Polistes*, a related genus of Vespidae, provides insight into the phylogenetic relationships within the group (Schmid-Egger et al. 2017). Based on the results of this study, morphological evidence and DNA barcoding in Vespidae will provide critical evidence to resolve species delimitations in the future.

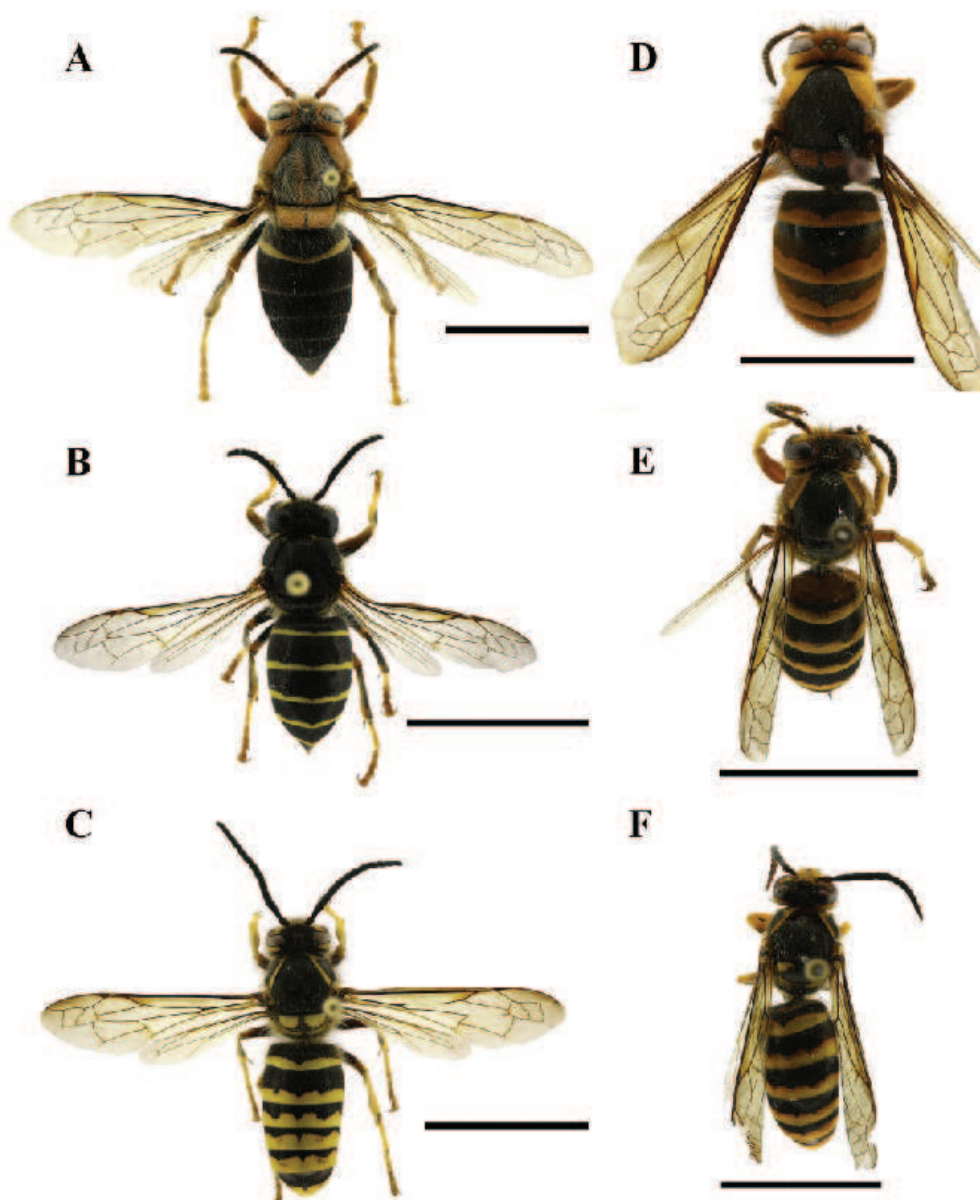


**Figure 4.** Comparison of the general habitus of *Dolichovespula kuami* and *D. flora* (**A, D** queen **B, E** worker **C, F** drone): *D. kuami* (**A–C**) *D. flora* (**D–F**). Scale bars: 1 cm.

## Additional information

### Conflict of interest

The authors have declared that no competing interests exist.

### Ethical statement

No ethical statement was reported.

### Funding

This study was supported by the Korea National Arboretum [project no. KNA1-1-20, 16-1].

### Author contributions

Conceptualization, MB Choi and JK Kim; data curation, CJ Kim, MB Choi and JL Tan; formal analysis, CJ Kim and MB Choi; funding acquisition, CJ Kim; investigation, MB Choi, JK Kim and JL Tan; methodology, CJ Kim and JK Kim; project administration, CJ Kim and MB Choi; supervision, MB Choi and JK Kim; writing—original draft, MB Choi, JK Kim and CJ Kim; writing—review and editing, JK Kim and JL Tan. All authors have read and agreed to the published version of the manuscript.

### Author ORCIDs

Chang-Jun Kim  <https://orcid.org/0000-0002-5823-8703>

Jeong Kyu Kim  <https://orcid.org/0000-0003-2175-5798>

### Data availability

All of the data that support the findings of this study are available in the main text.

## References

- Archer ME (1987) Three new species of *Dolichovespula* (Hym., Vespidae) from China. *Entomologist's Monthly Magazine* 123: 27–31.
- Archer ME (1999) Taxonomy and world distribution of the Euro-Asian species of *Dolichovespula* (Hym., Vespidae). *Entomologist's Monthly Magazine* 135: 153–160.
- Archer ME (2006) Taxonomy, distribution and nesting biology of species of the genus *Dolichovespula* (Hymenoptera, Vespidae). *Entomological Science* 9(3): 281–293. <https://doi.org/10.1111/j.1479-8298.2006.00174.x>
- Archer ME (2012) Vespine wasp of the world behavior, ecology, taxonomy of the Vespinae. Siri Scientific Press. Manchester, UK.
- Daglio A (2020) Yellowjackets of the World. LAP LAMBERT Academic Publishing. Mauritius.
- Hebert PDN, Penton EH, Burns JM, Janzen DH, Hallwachs W (2004) Ten species in one: DNA barcoding reveals cryptic species in the neotropical skipper butterfly *Astraptes fulgerator*. *Proceedings of the National Academy of Sciences of the United States of America* 101(41): 14812–14817. <https://doi.org/10.1073/pnas.0406166101>
- Jafari S, Müller B, Rulik B, Rduch V, Peters RS (2023) Another crack in the Dark Taxa wall: A custom DNA barcoding protocol for the species-rich and common Eurytomidae (Hymenoptera, Chalcidoidea). *Biodiversity Data Journal* 11: e101998. <https://doi.org/10.3897/BDJ.11.e101998>
- Kim JK (2011) *Dolichovespula kuami* (Vespidae, Hymenoptera): Taxonomic complement with newly found specimens. *Sociobiology* 57: 11–18.

- Kim JK, Yoon IB (1996) A new species of *Dolichovespula* (Insecta: Hymenoptera: Vespidae) from Korea. *Korean Journal of Systematic Zoology* 12: 199–202.
- Mo W-h, Chen H-y, Pang H, Liu J-x (2021) DNA barcoding for molecular identification of the genus *Oxyscelio* (Hymenoptera, Scelionidae) from southern China, with descriptions of five new species. In: Lahey Z, Talamas E (Eds) *Advances in the Systematics of Platygastroidea III*. *Journal of Hymenoptera Research* 87: 613–633. <https://doi.org/10.3897/jhr.87.7191>
- Posada D (2008) jModelTest: phylogenetic model averaging. *Molecular Biology & Evolution* 25(7): 1253–1256. <https://doi.org/10.1093/molbev/msn083>
- Schmid-Egger C, van Achterberg K, Neumeyer R, Morinière J, Schmidt S (2017) Revision of the West Palaearctic *Polistes* Latreille, with the descriptions of two species – an integrative approach using morphology and DNA barcodes (Hymenoptera, Vespidae). *ZooKeys* 713: 53–112. <https://doi.org/10.3897/zookeys.713.11335>
- Stamatakis A (2014) RAxML version 8: A tool for phylogenetic analysis and post-analysis of large phylogenies. *Bioinformatics* 30(9): 1312–1313. <https://doi.org/10.1093/bioinformatics/btu033>
- Tan JL, Chen X, van Achterberg C (2014) Description of the male *Dolichovespula flora* Archer (Hymenoptera: Vespidae). *Entomotaxonomia* 36(1): 75–80. <https://doi.org/10.3897/zookeys.391.6606>
- Wang H, Wen Q, Wang T, Ran F, Wang M, Fan X, Wei S, Li Z, Tan J (2022) Next-Generation Sequencing of Four Mitochondrial Genomes of *Dolichovespula* (Hymenoptera: Vespidae) with a Phylogenetic Analysis and Divergence Time Estimation of Vespidae. *Animals (Basel)* 12(21): 3004. <https://doi.org/10.3390/ani12213004>
- Zhang H, Wenjun B (2022) Exploring Large-Scale Patterns of Genetic Variation in the COI Gene among Insecta: Implications for DNA Barcoding and Threshold-Based Species Delimitation Studies. *Insects* 13(5): 425. <https://doi.org/10.3390/insects13050425>



# New synonymy among gall thrips of the Asian genus *Mesothrips*, with revision of species from China (Thysanoptera, Haplothripini)

Lihong Dang<sup>1,2,3,4</sup>, Xiaoli Tong<sup>5</sup>, Laurence A. Mound<sup>6</sup>

1 School of Bioscience and Engineering, Shaanxi University of Technology, Hanzhong, 723000, China

2 Shaanxi Province Key Laboratory of Bioresources, Hanzhong, 723000, China

3 Qinba Mountain Area Collaborative Innovation Center of Bioresources Comprehensive Development, Hanzhong, 723000, China

4 Qinba State Key Laboratory of Biological Resources and Ecological Environment (Incubation), Hanzhong, 723000, China

5 College of Plant Protection, South China Agricultural University, Guangzhou 510642, Guangdong Province, China

6 Australian National Insect Collection CSIRO, PO Box 1700, Canberra, ACT 2601, Australia

Corresponding author: Laurence A. Mound ([laurence.mound@csiro.au](mailto:laurence.mound@csiro.au))

## Abstract

Historical, nomenclatural, technical, and biological problems associated with the 42 species of *Mesothrips* are discussed. Type specimens have been re-examined of 14 of the 25 species that were described prior to 1930 and remain known only from imperfectly slide-mounted specimens. As a result, seven new synonyms are recognised. From China, six species of *Mesothrips* have been listed, but the records of *M. alluaudi* and *M. manii* are rejected, and three new species are described: *M. jianfengi* **sp. nov.**, *M. longistylus* **sp. nov.**, and *M. vernicia* **sp. nov.** These three species are divergent from other members of *Mesothrips* in lacking a prominent fore tarsal tooth and may indicate a possible generic relationship to the flower-living species in the Asian genus *Dolichothrips*. An illustrated key is provided to the seven *Mesothrips* species now known from China.

**Key words:** Key, *M. jianfengi*, *M. longistylus*, *M. vernicia*, new species



Academic editor: Elison F. B. Lima

Received: 3 January 2024

Accepted: 20 February 2024

Published: 22 March 2024

ZooBank: <https://zoobank.org/C1E809C2-1B1B-4AD0-8A2A-60836D2DD252>

Citation: Dang L, Tong X, Mound LA (2024) New synonymy among gall thrips of the Asian genus *Mesothrips*, with revision of species from China (Thysanoptera, Haplothripini). ZooKeys 1196: 121–138. <https://doi.org/10.3897/zookeys.1196.118131>

Copyright: © Lihong Dang et al.

This is an open access article distributed under terms of the Creative Commons Attribution License ([Attribution 4.0 International – CC BY 4.0](https://creativecommons.org/licenses/by/4.0/)).

## Introduction

The genus *Mesothrips* Zimmermann, 1900 continues to comprise one of the most misunderstood groups of leaf-feeding species in the subfamily Phlaeothripinae. The 42 species listed under this genus name are all presumed to be gall-living, with some of them almost certainly gall-inducing (ThripsWiki 2023). Publications referring to these thrips involve a series of problems. At least 25 of the species listed in the genus were described prior to 1930. They were based on specimens that were not mounted to modern standards and are difficult to study and compare (Fig. 1). Subsequent recordings of these named species by other authors are commonly based solely on published data, not on study of type specimens, and there are no studies on the life-history, host specificity, or dispersive activity of these species. As a result, much of the published taxonomy for this genus requires further verification, based on good field samples rather than just re-examination of the 100-year-old type specimens.

The problems began with the original description of the genus and the five new species that Zimmermann included and described. The first of these, *Mesothrips uzeli* Zimmermann, 1900 was also placed by Zimmermann as the only species of his second new genus, *Gynaikothrips* Zimmermann, 1900. In pointing this out, Priesner (1929a) indicated that three of the other five listed species should also probably be placed in *Gynaikothrips*, and so he recognised *Mesothrips jordani* Zimmermann, 1900, the fourth of Zimmermann's species, as the type species of *Mesothrips*. Priesner further listed 16 species that he considered likely to be members of this genus, of which *M. australiae* Hood, 1918 is now placed as a synonym of *M. jordani*. However, the 16 species did not include all the names available in this genus at the time Priesner was writing, with three species by Karny not mentioned: *M. armatus* Karny, 1913, *M. picticornis* Karny, 1913, and *M. lividicornis* Karny, 1923, nor *M. alluaudi* Vuillet, 1914 from Madagascar and *M. sus* (Priesner, 1921) from Java.

Ananthakrishnan (1976) is the only author to attempt an extensive revision of the members of *Mesothrips*, and he provided a key to 28 of the 37 species known at that date. The first couplet of the key appears to be clear; eight species have the fore wings either clear or with light shading around the margins distally, whereas all the other species have fore wings more or less shaded. But interpretation within the key of the first of these choices seems inconsistent, because of the eight species treated as having clear fore wings two actually have the distal half of the wing shaded, *M. constrictus* (Karny, 1912) and *M. leeuweni* Karny, 1913. A similar problem arises with decisions concerning wing colour in couplets 9 and 10. Certainly the fore wings of some species are fully shaded, such as *M. breviceps* Karny, 1913, but the fore wings of *M. jordani* are shaded only on the distal half, the fore wing basal half being pale and with no longitudinal markings. Unfortunately, in slide mounted specimens that have been cleared for critical study the fore wings may have lost much of their colour, and wing colour may vary between individuals in a population, in relation to maturity and body size. Head length has also been used to distinguish species in this genus, although this length is interpreted here as being variable within and between populations of *M. jordani*. Similarly, the relative lengths of the pronotal epimeral and postero-angular setae have been used to distinguish species, but these setae are also more variable than some authors have considered. The key to nine *Mesothrips* species from India (Ananthakrishnan and Sen 1980) includes similar problematic decisions. As a result, in the present study of *Mesothrips* from China, some species are newly placed into synonymy, based on examination of the original specimens.

Two further authors have produced identification keys to species of this genus from particular areas. Reyes (1994) recorded five species from the Philippines, although the first species in that key, *M. ignotus* Reyes, 1994, is now recognised as a member of the genus *Adelphothrips* Priesner, 1953 (ThripsWiki 2023). Moreover, the statement in the key that the compound eyes of *M. leeuweni* are prolonged ventrally is not correct. Some syntypes of that species certainly have the pigment of the eyes migrated posteriorly and somewhat distant from the eye structure, but the posterior margin of the eye itself is visible and the eye is slightly shorter ventrally than dorsally. Okajima (2006) provided a clear generic diagnosis together with a key to the two species known from Japan, *M. claripennis* Moulton, 1928 and *M. jordani*. The first of these has the fore

wings uniformly pale and lives on *Ardisia* [Primulaceae], whereas the second has the wings uniformly shaded on the distal half and lives on *Ficus* [Moraceae].

Interpreting the taxonomic significance of structural variation between populations of gall thrips involves problems. Previous authors have commonly stressed slight structural differences, considering that these distinguish species, although such hypotheses remain untested. An alternative hypothesis is equally valid, that small structural differences are intra-specific and reflect in gall-thrips populations a founder effect. This second hypothesis assumes that a population within a single gall is usually the progeny of a single, once-mated, female, and hence shows limited structural variation. Similarly, in the absence of evidence of dispersive activity by *Mesothrips* species, it can be assumed that the members of a population on a single tree are likely to be closely related and more similar to each other than to individuals from more distant populations. Earlier taxonomic work appears to have assumed that speciation in this genus has sometimes occurred on single plant species, such as the common *Ficus benjamina*. However, we suggest that speciation within the genus *Mesothrips* is related to differences between host plant species, although the available host data to support this suggestion remains inadequate. This dichotomy in hypotheses is involved here in interpreting variation among individuals of what we consider to be a single species, *M. jordani*.

### Notes on species diversity of *Mesothrips*

It is currently not possible to produce a revision of the species listed in this genus, as the type specimens are widely dispersed amongst various collections, and some are not available for study. For production of this account of *Mesothrips* species from China, type specimens (Fig. 1) of 12 nominal species were borrowed from Senckenberg Museum during a visit by LAM in 2023, and *M. pycetes* Karny, 1916 and *M. elaeocarpi* Ananthakrishnan, 1976 were previously studied by LHD in 2012 (Dang et al. 2014).

*Mesothrips breviceps* Karny (1913: 69) is the only species available for study with uniformly shaded fore wings. One syntype from Java on *Ardisia cymosa* [Primulaceae] has been studied (from SMF). Several species have been studied with the fore wings uniformly pale or with only the extreme margins slightly shaded. One of these, *M. longisetis* Priesner, 1929, has exceptionally long pronotal and postocular setae, and is known from *Melastoma malabathricum* [Melastomataceae] in Malaya. However, *Mesothrips sus* was described from two females as the only member of a new genus *Trichaplothrips* Priesner, 1921. These specimens were taken at Salatiga in central Java from *Melastoma polyanthemum*, and these two plant names are now considered to refer to the same plant species, *Melastoma affine*. A syntype male of *M. longisetis* has been studied and compared to the two syntype females of *M. sus* (Fig. 7) and these are here considered to represent the same species. *Mesothrips longisetis* is therefore considered a new synonym of *M. sus*.

*Mesothrips schouteniae* Priesner, 1929 has fore wings pale with margins slightly shaded and antennae largely yellow, but with pronotal setae less elongate than *M. sus*; it was described from Java on *Schoutenia ovata* [Malvaceae]. Also with pale fore wings is *M. vitripennis* Karny, 1922 (Fig. 19) from Vietnam on *Aporosa leptostachya* [Phyllanthaceae], and *M. moundi* Ananthakrishnan, 1976 (Figs 6, 11) from Hong Kong on *Bischofia trifoliata* [Phyllanthaceae] is consid-

ered below as a new synonym of *M. vitripennis*. Similarly, *M. elaeocarpi* (Figs 27, 29) is here considered a new synonym of *M. vitripennis*.

*Mesothrips mendax* (Karny, 1912) also has pale fore wings but is distinctive in having slender fore femora and the mouth cone pointed; this species was taken in central Java in leaf galls on *Mallotus repandus* [Euphorbiaceae]. Another species with similar fore wings is *M. ustulatus* Karny, 1912 from a leaf gall on *Memecylon* [Melastomataceae] in Vietnam, but the two available syntypes are too poorly preserved for serious comparisons with other species.

The published descriptions of three species from India, *M. extensivus* Ananthkrishnan & Jagadish, 1969, *M. acutus* Muraleedharan & Sen, 1981 and *M. ambasensis* Muraleedharan & Sen, 1981, also state that the fore wings are pale; the first was described from galls on *Anogeissus* [Combretaceae], but the other two merely from galls with no host plant record. In contrast, *M. manii* Ananthkrishnan, 1972 was described from southern India as having fore wings with a yellowish tinge, based on a long series of both sexes from leaf galls on *Santalum album* [Santalaceae]. The species *M. pyctes* (Figs 26, 28, 30, 31) from Java on *Eugenia* sp. [Myrtaceae] was described as having the fore wings "schwach graulich" (weakly greyish), and the type specimens of this species need to be compared to original specimens of *M. manii* to determine if these represent different species. *Mesothrips manii* has been recorded from China twice (Zhang 1984; Zhang et al. 1999), but the specimens on which these records were based, from Hainan and Fujian respectively, have now been re-examined and are here identified as *M. jordani* and *Bamboosiella* sp.



Figure 1. Type specimens of eight species that have been referred to the genus *Mesothrips*.

*Mesothrips jordani* is here considered to be widespread on the leaves of *Ficus benjamina* [Moraceae], and this species is interpreted here as having a characteristic fore wing colour - uniformly shaded on the distal half with the basal half pale and lacking any dark median line (Fig. 18). Three species are listed below as new synonyms of *M. jordani*. However, *M. apatelus* Karny, 1926 from India, known only from descriptions and the key by Ananthakrishnan and Sen (1980), is possibly a further synonym of this species.

*Mesothrips leeuweni* Karny has fore wings that are rather similar to those of *M. jordani* but with a more obvious median dark line on the basal half of the fore wing, also the antennal segments are more extensively pale than is usual in *M. jordani*. Karny recorded *M. leeuweni* at more than one site in Java in leaf galls on *Poikilospermum suaveolens* [Urticaceae], although he used the generic name *Conocephalus* that is now considered a synonym of *Poikilospermum*.

*Mesothrips picticornis* Karny, 1913 also has the distal half of the fore wing shaded but is distinctive in having antennal segments III–V extensively blackish brown with the base of each segment pale. Karny described this species from Java as taken in leaf galls on *Vitis papillosa* [Vitaceae].

Moulton (1942) described *M. guamensis* Moulton, 1942 from a single male, and *M. swezeyi* Moulton, 1942 from a single female, both specimens having been taken together under the bark of a tree in Guam. These specimens have now been re-examined and have broad maxillary stylets arranged in a V-shape and retracted almost to the postocular setae. Moreover, all the antennal segments are dark brown. These specimens are here recognised as members of the Idolothripinae genus *Ethiorthrips* Karny, 1925. Neither specimen has been cleared before slide mounting and they are thus difficult to study. However, the two species are here both considered to be new synonyms of the widespread species *Ethiorthrips stenomelas* (Walker, 1859), of which an excellent modern description is available (Okajima and Masumoto 2023).

## Generic relationships

The genus *Mesothrips* is a member of the tribe Haplothripini Priesner, as re-defined by Mound and Minaei (2007) from the *Haplothrips*-lineage of Mound and Marullo (1996). The species in this tribe have the fore wings with a median constriction, although this varies from being almost a pouch to being scarcely visible. The prosternum has a pair of basantral sclerites, and the metathoracic sternopleural sutures are not developed. In the males, tergite IX setae S2 are shorter than setae S1, and sternite VIII lacks a pore plate. Species of *Haplothrips* Amyot & Serville, 1843 (with very few exceptions) have either one or two sense cones on antennal segment III, whereas all species previously assigned to *Mesothrips* have three sense cones on this segment. The type species of *Mesothrips* has the head distinctly constricted at the base, but in other members of the genus this constriction is only weakly developed. As a result, these species share character states with *Dolichothrips* Karny, 1912, an Asian genus in which the species are not gall-living but are commonly found in flowers, often of the genera *Macaranga* and *Mallotus* (Mound and Okajima 2015). The distinction between these two genera becomes more confused by the description below of three new species in the genus *Mesothrips*, all of which lack a prominent tooth on the fore tarsus, and one of them has only two sense cones on the third an-

tennal segment. These three species share several character states and are presumably closely related to each other. However, their generic relationships are far from clear, and they are described here in the genus *Mesothrips* primarily because of the additional sigmoid setae on the tergites. It is possible that the forests of southwestern China have a previously unknown diversity of leaf-feeding Phlaeothripinae that will require future revisions of the generic classifications.

## Materials and methods

The descriptions and drawings were produced from slide-mounted specimens with a Nikon Eclipse 80i microscope. Images were prepared with a Leica DM2500 using DIC illumination, and processed with Automontage and Adobe Photoshop v.7.0. The abbreviations used for the pronotal setae are as follows: **am** – anteromarginal, **aa** – anteroangular, **ml** – midlateral, **epim** – epimeral, **pa** – posteroangular; **CPS** – campaniform sensilla. The unit of measurement in this study is the micrometre ( $\mu\text{m}$ ). Most specimens studied here are available in the School of Bioscience and Engineering, Shaanxi University of Technology (**SNUT**), Hanzhong, China, the Australian National Insect Collection (**ANIC**), CSIRO, Canberra, Australia, and South China Agricultural University (**SCAU**). Further slides were studied on loan from the Senckenberg Museum, Frankfurt (**SMF**).

## Taxonomy

### *Mesothrips* Zimmermann

*Mesothrips* Zimmermann, 1900: 12. Type species *Mesothrips jordani* Zimmermann, 1900, by subsequent designation of Priesner 1929a: 452.

**Note.** From China six species have been recorded in this genus (Dang et al. 2014), but the records of *M. alluaudi* and *M. manii* are here rejected. *Mesothrips alluaudi* was recorded from China by Moulton (1928b: 318), based on a single female collected from *Machilus* sp. at Taihoku, Taiwan by R. Takahashi on 27 June 1927. Subsequent authors in China have repeated this record, but apparently without checking the original Moulton paper. The specimen from Taiwan was identified by Moulton based only on Vuillet's original description of two specimens taken in Madagascar, and that original description is insufficient to place *M. alluaudi* with confidence into any genus. Moreover, it states that only two sense cones are present on the third antennal segment, in contrast to the three on *Mesothrips* species. The identity of the specimen from Taiwan that Moulton identified as this species remains unknown. *Mesothrips manii* was based on a holotype female taken with over 100 adults of both sexes in leaf galls on *Santalum album* in Tamil Nadu, southern India. The original description states that the body length of females was 1718–2215  $\mu\text{m}$ , and the head length 181–215  $\mu\text{m}$ , with the fore wings having a yellowish tinge, and tergite IX setae S1 slightly shorter than the tube. Zhang (1984: 17) recorded *M. manii* from China on Hainan Island and subsequently Zhang et al. (1999) recorded this species from Fujian Province. We have now re-examined these specimens; the four males from Hainan are here recognised as *M. jordani* and from Fujian the single female is considered a species of the genus *Bamboosiella*.

**Generic diagnosis.** small to medium sized, dark, macropterous Phlaeothripinae-Haplothripini. Head usually longer than wide, cheeks sharply constricted at base (Figs 2–7); postocular setae developed; maxillary stylets rather short, usually not reaching postocular setae, V-shaped (rarely reaching postocular setae, and parallel medially); maxillary bridge present. Antennae 8-segmented (Figs 8–11, 31); segment III with three (rarely two) sense cones, IV with four major sense cones; VIII usually short. Pronotum well developed, with five pairs of major setae (Figs 2–7, 26, 27); notopleural sutures complete. Prosternal basantra present; ferna well developed; mesopresternum usually divided into two lateral triangular plates; metathoracic sternopleural sutures absent. Fore tarsal tooth usually large in both sexes (Fig. 5), sometimes absent or scarcely visible (Figs 12, 13). Fore wings constricted medially, with duplicated cilia (Figs 18, 19). Pelta triangular, usually with a pair of CPS (Fig. 16); tergites II–VII each with two pairs of sigmoid wing-retaining setae, also usually with a pair of accessory sigmoid setae anterior to first pair (Figs 17, 21, 22); tergite IX setae S1 and S2 long and pointed (Figs 28, 29). Male tergite IX setae S2 short (Figs 24, 25); sternite VIII without pore plate.

### Taxonomic account

#### Key to *Mesothrips* species from China

- 1 Fore tarsal tooth absent or minute and visible only when tarsus rotated (Figs 12, 13) ..... **2**
  - Fore tarsal tooth present, usually large and pointed (Fig. 5) ..... **4**
- 2 Maxillary stylets parallel medially with transverse maxillary bridge, elongate and at full retraction extending to postocular setae (Fig. 2) ..... **M. longistylus sp. nov.**
  - Maxillary stylets wide apart, arranged in V-shape, short and not reaching to postocular setae (Figs 3–6) ..... **3**
3. Antennal segment III with only 2 sense cones (Fig. 9)..... **M. vernicia sp. nov.**
  - Antennal segment III with 3 sense cones (Fig. 10) ..... **M. jianfengi sp. nov.**
- 4 Tergite IX setae S1 and S2 approx. as long as or longer than tube (Fig. 29) ... **5**
  - Tergite IX setae shorter than tube (Fig. 28) ..... **6**
- 5 Fore wings distal 1/2 uniformly but sometimes weakly shaded, basal 1/2 pale without any dark longitudinal marks (Fig. 18) [on *Ficus*] ..... **M. jordani**
  - Fore wings uniformly pale (Fig. 19) ..... **M. vitripennis**
- 6 Anal setae slightly shorter than tube, ~ 0.9 × as long as tube (in Okajima 2006) ..... **M. claripennis**
  - Anal setae much shorter than tube, ~ 0.6 × as long as tube (Fig. 28) ..... **M. pycetes**

#### ***Mesothrips claripennis* Moulton**

Fig. 23

*Mesothrips claripennis* Moulton, 1928a: 315.

**Material examined.** 1♀, CHINA, Yunnan, Lincang, Cangyuan, from grasses, 8.vi.2021 (SNUT); 1♂, Guangdong (SCAU); 1♂, Hainan, Zhanxian, 11.vi.1981

(**SCAU**); 1♀, Hainan, Danzhou, from gall of *Aporosa dioica* [Phyllanthaceae], 2.xi.2014, Shulan Yang (**SCAU**); 1♀, Guangxi, Nanning, from *Ficus* sp. [Moraceae], 11.vii.1986, Weiqiu Zhang (**SCAU**); 1♂, Guangxi, Longzhou, 27.vii.1985, Weiqiu Zhang (**SCAU**).

**Comments.** Described from China on a single female taken on an unknown plant by Takahashi, 30.xii.1926 at “Kannonzan, Formosa”, it was subsequently taken by that collector from other localities and recorded rolling the leaves of *Bladhia sieboldia* (Takahashi 1936). *Bladhia* is now recognised as a synonym of the Primulaceae genus, *Ardisia*, and Okajima (2006) recorded the thrips from leaf rolls on this plant on the Ryukyu Islands, Japan. This species has a smaller body (~ 2.5 mm) in comparison to most *Mesothrips*, and the fore wings are entirely pale. The specimens listed above are identified as *M. claripennis* from the description in Okajima (2006).

***Mesothrips jianfengi* sp. nov.**

<https://zoobank.org/3166AB9E-F018-42B5-9E4A-DF97D03517A1>

Figs 3, 10, 13, 14

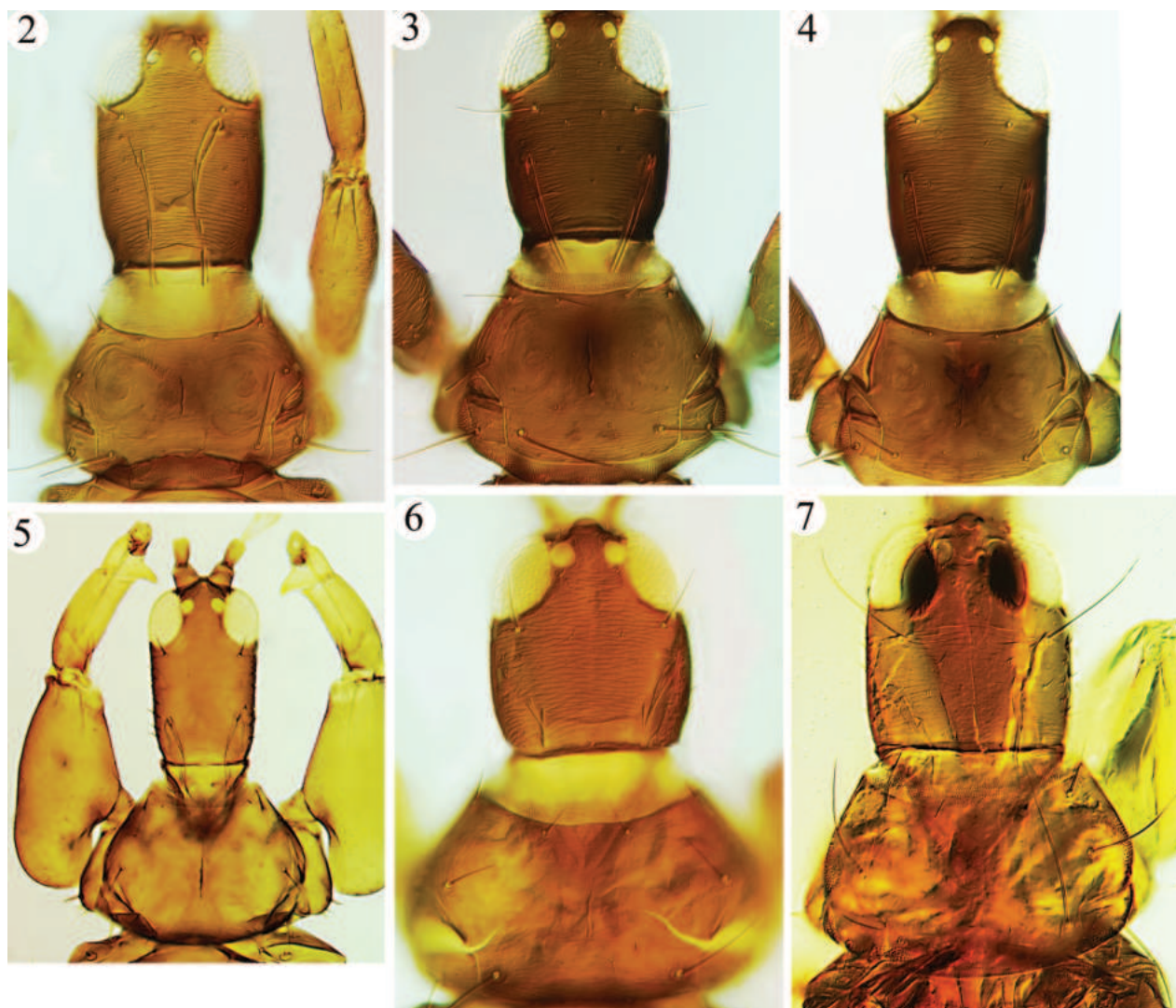
**Material examined. Holotype**, ♀, CHINA, Xizang, Zhangmu, taken on leaves of unknown plant, viii.2013, Jianfeng Wang (**SNUT**); **paratypes**, 2♀1♂, with same data as holotype (**SNUT**); 2♀1♂, Yunnan, Dali, on leaves of unknown plant, viii.2009, Lixin Su (**SNUT**).

**Description. Holotype. Female macroptera.** Body brown; all femora and tibiae brown, fore tarsi clear yellow, mid and hind tarsi brownish, slightly lighter than tibiae; antennal segments I and II brown, III clear yellow, IV–VI yellow but shaded on apical half, VII and VIII brown (Fig. 10); major setae pale; fore wing slightly greyish.

**Head.** Head ~ 1.3 × as long as wide (Fig. 3), constricted at base; postocular setae pointed or slightly blunt at apex, approx. as long as eyes (Fig. 3); eyes equal in length ventrally and dorsally; maxillary stylets V-shaped, retracted to median of head; mouth cone long, reaching to posterior margin of basantra. Antennal segments broad (Fig. 10), segment III ~ 2.1 × as long as apical width; III with three sense cones, IV with four major sense cones, VIII constricted at base.

**Thorax.** Pronotum with five pairs of setae, slightly blunt at apex, am and aa approx. equal in length (Fig. 3), epim and pa longer and equal in length; surface almost smooth, with weak sculpture near margins. All legs slender, fore tarsi with minute and scarcely visible tooth (Fig. 13). Fore wing with three sub-basal setae arising in straight line, S1 and S2 equal in length, blunt at apex, S3 slightly longer, acute at apex, with eight duplicated cilia. Mesonotum transversely reticulate, lateral setae well developed, blunt at apex. Metanotum longitudinally reticulate, major setae slender and acute (Fig. 14). Mesopresternum with paired lateral triangles, metathoracic sternopleural sutures absent.

**Abdomen.** Pelta broadly triangular, reticulate, with pair of CPS; tergites II–VII with two pairs of major wing-retaining setae, one pair of accessory sigmoid setae located anterior to first pair; tergite II with eight pairs of lateral setae; tergite IX setae S1 and S2 longer than tube, acute at apex, S3 approx. as long as tube, acute at apex; tube shorter than head, anal setae shorter than tube.



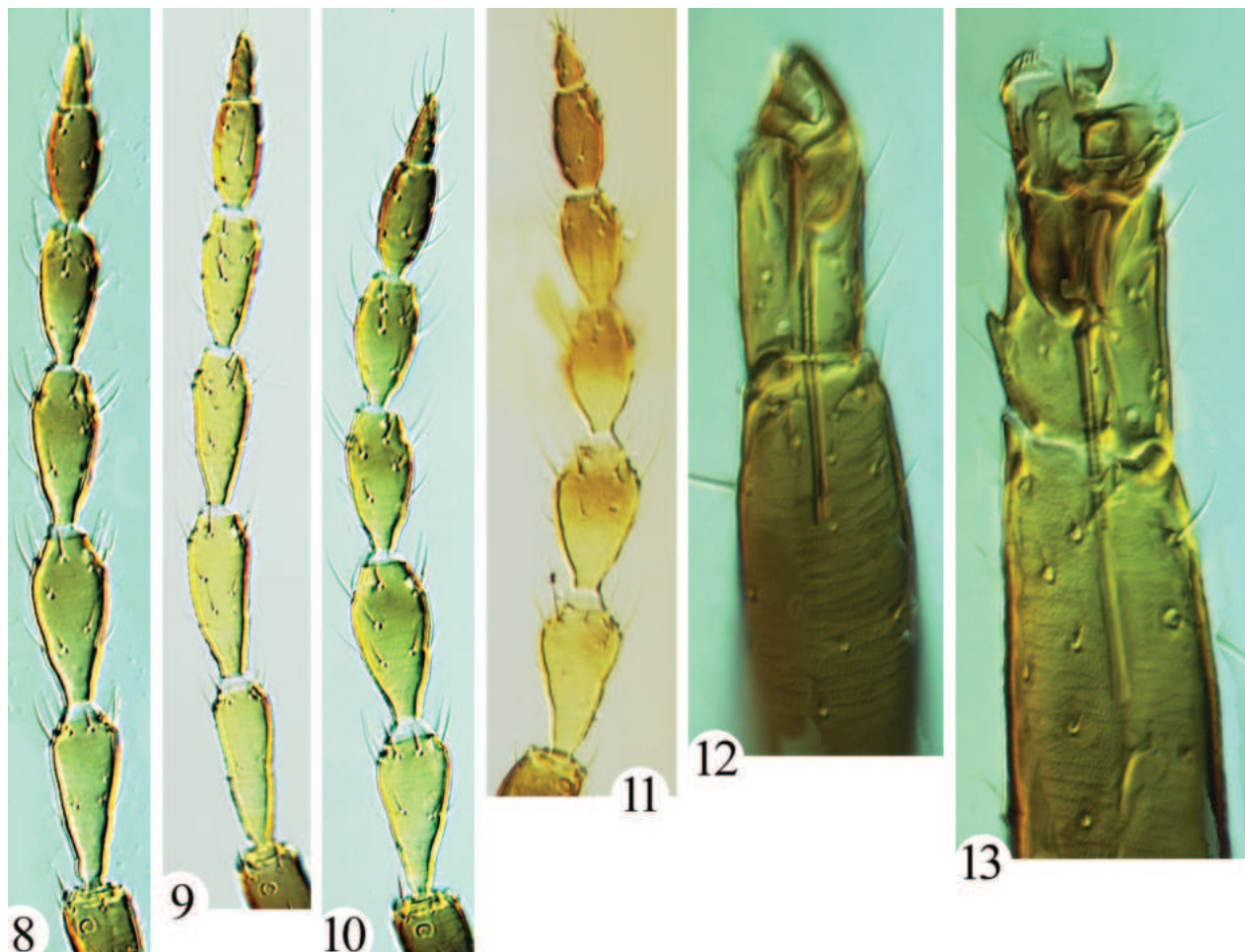
Figures 2–7. Head and pronotum 2 *M. longistylus* sp. nov. 3 *M. jianfengi* sp. nov. 4 *M. vernicia* sp. nov. 5 *M. jordani* 6 *M. vitripennis* (paratype female of *moundi*) 7 *M. sus* (syntype female).

**Measurements** (holotype female in  $\mu\text{m}$ ). Body length 2820. Head length (maximum width) 250 (190); distance between maxillary stylets (across bridge) 115; eye length dorsally 90; postocular setae length 90; antennal segments I–VIII length (width): 45 (35), 50 (35), 75 (35), 75 (40), 65 (30), 60 (25), 55 (25), 35 (15); sense cone on III length 30. Pronotum length (width) 190 (270); am 40, aa 45, ml 60, epim 100, pa 100. Fore wing length 1160; sub-basal setae S1 90, S2 90, S3 110. Tergite IX setae S1 270, S2 240, S3 180; tube length 220, basal width 75, apical width 50; anal setae length 220.

**Male macroptera.** Similar to female in colour and sculpture; fore tarsal tooth scarcely visible; fore wing with ~ 9 or 10 duplicated cilia; abdominal tergite IX setae S2 small and pointed; sternite VIII without pore plate.

**Measurements** (paratype male in  $\mu\text{m}$ ). Body length 2460. Head length (maximum width) 240 (175); eye length dorsally 85; postocular setae length 75. Pronotum length (width) 170 (230); am 35, aa 30, ml 40, epim 80, pa 85. Tergite IX setae S1 205, S2 25, S3 220; tube length 190; anal setae length 190.

**Etymology.** The species epithet refers to one of the collectors, Jianfeng Wang (Shenyang University).



Figures 8–13. *Mesothrips* spp. Antennae (8–11) 8 *M. longistylus* sp. nov. 9 *M. vernicia* sp. nov. 10 *M. jianfengi* sp. nov. 11 *M. vitripennis* (paratype female of *moundi*); fore tarsi (12–13) 12 *M. vernicia* sp. n. 13 *M. jianfengi* sp. nov.

**Comments.** This species is closely related to *M. longistylus* sp. nov., but it can be distinguished by the short V-shaped maxillary stylets (Fig. 3). The third new species described here, *M. vernicia* sp. nov., also has short stylets (Fig. 4), but *M. jianfengi* sp. nov. can be differentiated in antennal segment III with 3 sense cones (Fig. 10).

#### ***Mesothrips jordani* Zimmermann**

Figs 5, 18, 22

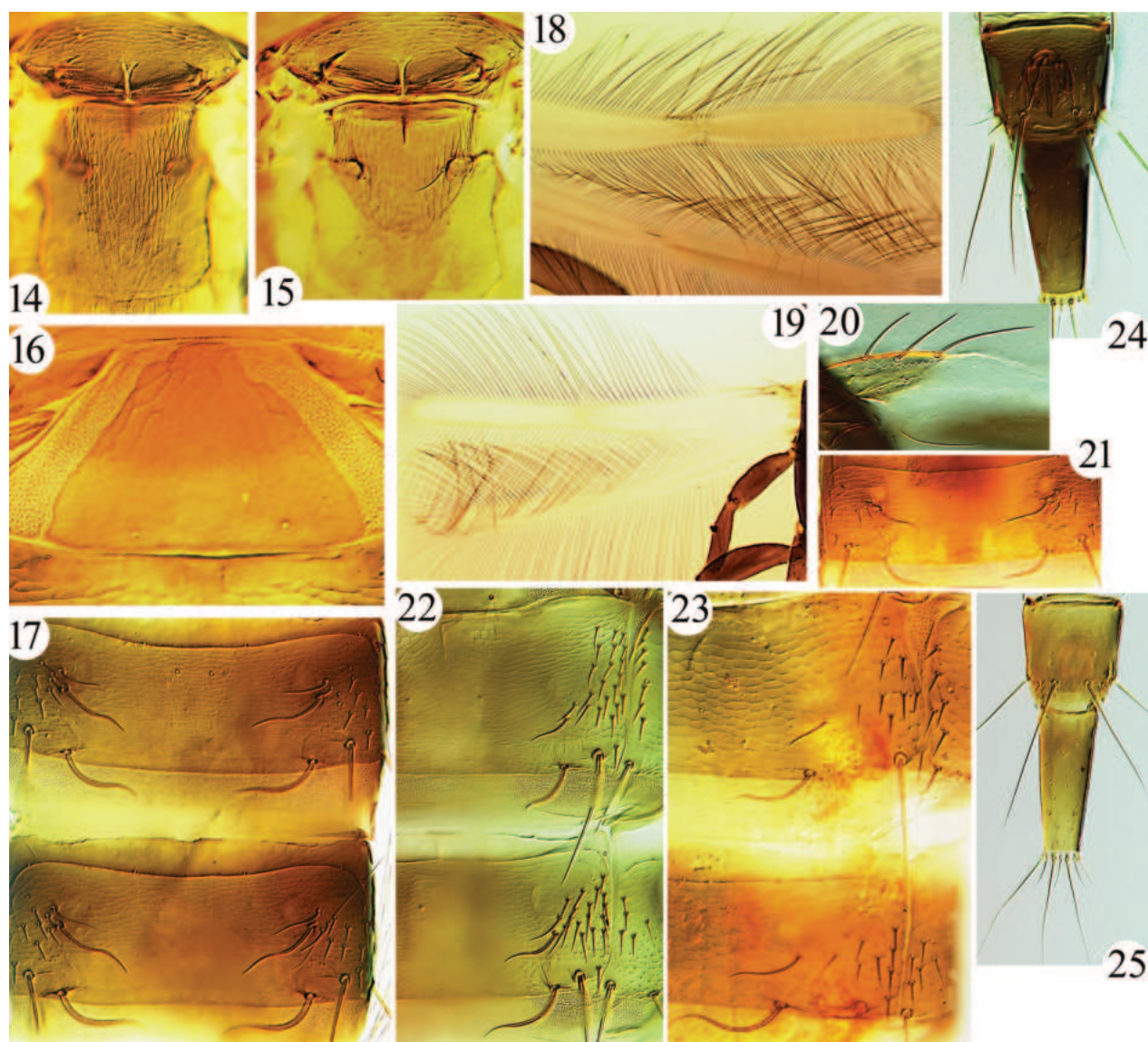
*Mesothrips jordani* Zimmermann, 1900: 16.

*Leptothrips angusticollis* Karny, 1915: 88. Syn. nov.

*Mesothrips annamensis* Priesner, 1929b: 215. Syn. nov.

*Leptothrips constrictus* Karny, 1912: 150. Syn. nov.

**Material examined.** 1♀, CHINA, Shaanxi, Hanzhong, 10.iv.2016, Kan Liu and Hui Lin (SNUT); 1♀, Fujian, Xiamen, from gall of *Ficus* sp. [Moraceae], 23.vi.2015, Lihong Dang (SNUT); 1♀1♂, Yunnan, Puer, from *Ficus concinna* [Moraceae], 11.vii.2022, Yanqiao Li (SNUT); 4♂, Hainan, Diaoluoshan, from *Ficus* sp. [Moraceae], 5.iv.1984, Weiqiu Zhang (SCAU); 1♀1♂, Guangxi, Nanning, from *Ficus* sp.



Figures 14–25. *Mesothrips* spp. Meso- and metanotum (14–15) 14 *M. jianfengi* sp. nov. 15 *M. longistylus* sp. nov.; *M. longistylus* sp. nov. (16–17) 16 pelta 17 tergites III–IV; fore wings (18–20) 18 *M. jordani* 19 *M. vitripennis* 20 *M. longistylus* sp. nov., sub-basal setae of forewing; tergites II–III (21–23) 21 *M. vernicia* sp. nov., tergite III 22 *M. jordani* 23 *M. claripennis*; tergites IX–X (24–25) 24 *M. longistylus* sp. nov. 25 *M. vernicia* sp. nov.

[Moraceae], 3.viii.1985, Weiqiu Zhang (SCAU); 1♀1♂, Guangdong, Guangzhou, Fanyu, from *Ficus microcarpa* [Moraceae], 17.v.2009, Jiaqian Gao (SCAU); 9♀, Yunnan, Simao, 9 females from *Ficus* [Moraceae], 4.viii.2010 (ANIC). **Syntypes**, 1♀1♂ of *annamensis*, VIETNAM, Vinh Tan, on *Citrus* sp. [Rutaceae], 7.iii.1925 (SMF). **Lectotype**, 1♀ of *angusticollis*, INDONESIA, Java, on Anonaceae sp., 1.ix.1912 (SMF). **Syntype**, 1♀ of *constrictus*, INDONESIA, Java, Semarang, in leaf galls of *Ficus benjamina* [Moraceae], 16.i.2012 (SMF). **Holotype** and **paratype**, 1♀1♂ of *bianchii*, AUSTRALIA, Queensland, Atherton, from *Ficus* leaves [Moraceae], 31.iii.68 (ANIC); 5♀1♂, Cairns, from *Ficus* leaves [Moraceae], 12.xi.2007 (ANIC); 4♀3♂, Noosa Heads, from *Ficus* leaves [Moraceae], 31.iii.1995 (ANIC); 12♀10♂, Brisbane, Mt Cootha, from *Ficus benjamina* [Moraceae], 13.v.1994 (ANIC). 3♀, TIMOR LESTE. Dili, from *Ficus microcarpa* leaves [Moraceae], 26.viii.2018 (ANIC). 1♀1♂, MALAYSIA, Kuala Lumpur, from *Ficus benjamina* leaf

gall [Moraceae], 4.x.1973 (ANIC). 1♀1♂, the PHILIPPINES, Quezon, from *Ficus* [Moraceae], 23.x.2011 (ANIC). 7♀3♂, THAILAND, Ang Thong, from *Ficus* leaf folds [Moraceae], 9.vi.2018 (ANIC). 2♀, ISRAEL, Tel Aviv, from *Ficus microcarpa* [Moraceae], i.2014 (ANIC).

**Comments.** This species was described from both sexes and larvae, and the author reported it to be common on *Ficus* leaves at the Botanic Gardens in Buitenzorg [= Bogor], Java. Priesner described *M. annamensis* from two males and one female taken at a coastal locality in Vietnam, and two of these specimens have been studied here. Karny described *M. angusticollis* from an unspecified number of specimens on Annonaceae in Java, without further details. The *M. angusticollis* specimen listed above bears this data as quoted by Priesner (1929a), and the slide is labelled 'Lectotype' but that designation apparently was never formally published. Karny (1912) described *M. constrictus* from both sexes taken in leaf galls on *Ficus benjamina* in northern Java and syntypes have been studied as listed above. These three species have the distinctive fore wing pattern that is here considered to be typical of *M. jordani*. A further slide labelled as *Leptothrips constrictus* with four specimens (in SMF) has been studied that was collected at the same site as that species. However, those four specimens have fully clear fore wings, are labelled as collected from *Schoutenia ovata*, and are here considered to represent *M. schouteniae*. As mentioned above, and judging from the description, *M. apatelus* from India is possibly the same species as *M. jordani*. In descriptions by Ananthakrishnan the lengths of the tergite IX setae and the pronotal epimeral setae are given considerable importance for distinguishing species. The tergite IX setae S1 in *M. jordani* are variable between samples, from slightly longer to slightly shorter than the tube. Similarly, in a single sample of six *M. longisetis* specimens from Java, these setae are usually distinctly longer than the tube but in one of two males they are shorter. Among specimens here identified as *M. jordani* on *Ficus* leaves from various sites, the pronotal posteroangular setae are commonly slightly longer than the epimeral setae. However, in two specimens from *Ficus benjamina* galls in Malaya they are only half as long as the epimerals. Arbitrary use of differences in lengths of these setae to distinguish species, without consideration of variation within and between populations, may be misleading.

***Mesothrips longistylus* sp. nov.**

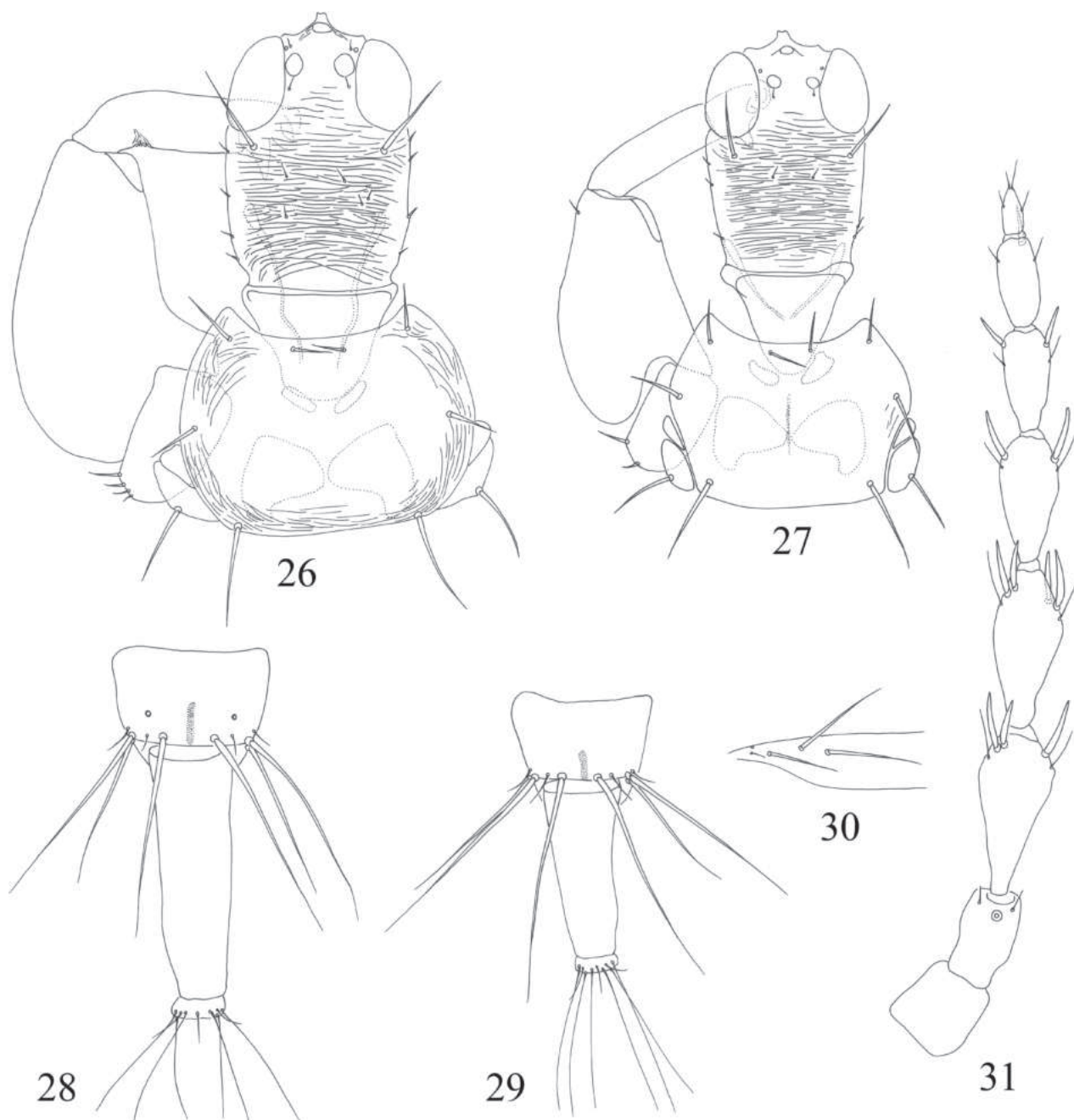
<https://zoobank.org/1DB00123-0CA9-419D-84C7-D65FFB5B33A7>

Figs 2, 8, 15–17, 20, 24

**Material examined. Holotype**, ♀, CHINA, Sichuan, Ganzi, on leaves of unknown plant, 27.vii. 2013, Jianfeng Wang (SNUT); **paratypes**, 4♀3♂, with same data as holotype (SNUT).

**Description. Holotype. Female macroptera.** Body brown; all femora and tibiae brown, all tarsi yellowish brown, slightly lighter than tibiae; antennal segments I and II brown, III clear yellow, IV–VI yellow but shaded on apical half, VII–VIII brown (Fig. 8); major setae pale; fore wing pale.

**Head.** Head ~ 1.4 × as long as wide (Fig. 2), constricted at base; postocular setae slightly blunt, shorter than eyes (Fig. 2); eyes equal in length ventrally and dorsally; maxillary stylets parallel medially with transverse maxillary bridge,



Figures 26–31. *Mesothrips* spp. Head, pronotum and foreleg (26–27) 26 *M. pyctes* 27 *M. vitripennis* (type specimens of *elaecarpi*); tergites IX–X (28–29) 28 *M. pyctes* 29 *M. vitripennis* (type specimens of *elaecarpi*); *M. pyctes* (30–31) 30 sub-basal setae of forewing 31 antennae.

elongate and at full retraction extending to postocular setae (Fig. 2); mouth cone long, reaching to ferna. Antennal segments broad (Fig. 8), segment III ~ 2.1 × as long as apical width; III with three sense cones, IV with four major sense cones, VIII broadly connected with VII.

**Thorax.** Pronotum with five pairs of well-developed setae, am, aa and ml blunt at apex (Fig. 2), epim and pa longer and equal in length, slightly expanded at apex; surface almost smooth, with weak sculpture near margins. All legs slender, fore tarsal tooth tiny, visible only when tarsi rotated. Fore wing with three sub-basal setae arising in straight line (Fig. 20), S1 and S2 equal in length,

slightly expanded at apex, S3 longest, acute at apex, with 9–12 duplicated cilia. Mesonotum transversely reticulate, lateral setae well-developed, blunt (Fig. 15). Metanotum longitudinally reticulate, major setae slender and acute (Fig. 15). Mesopresternum with paired lateral triangles, metathoracic sternopleural sutures absent.

**Abdomen.** Pelta broadly triangular, weakly reticulate, with pair of CPS (Fig. 16); tergites II–VII with two pairs of major wing retaining setae, one pair of accessory sigmoid setae located anterior to first pair (Fig. 17); tergite II with eight pairs of lateral setae; tergite IX setae S1 and S2 longer than tube, acute at apex (Fig. 17), S3 approx. as long as tube, acute at apex; tube shorter than head, anal setae approx. as long as tube.

**Measurements** (holotype female in  $\mu\text{m}$ ). Body length 2600. Head length (maximum width) 275 (195); distance between maxillary stylets (across bridge) 50; postocular setae length 70; antennal segments I–VIII length (width): 45 (35), 55 (30), 75 (35), 75 (40), 70 (30), 65 (30), 60 (25), 35 (20); sense cone on III length 15. Pronotum length (width) 170 (275); am 45, aa 35, ml ?, epim 90, pa 90. Fore wing length 1140; sub-basal setae S1 60, S2 85, S3 120. Tergite IX setae S1 185, S2 190, S3 140; tube length 170, basal width 75, apical width 50; anal setae length 170.

**Male macroptera.** Similar to female in colour and sculpture; postocular setae slightly shorter than eyes, slightly blunt at apex; fore tarsal tooth scarcely visible; abdominal tergite IX setae S2 small and pointed (Fig. 24); sternite VIII without pore plate.

**Measurements** (paratype male in  $\mu\text{m}$ ). Body length 2240. Head length (maximum width) 270 (200); postocular setae length 90. Pronotum length (width) 170 (270); am 53, aa 28, ml 75, epim 75, pa 85. Tergite IX setae S1 180, S2 20, S3 180; tube length 165; anal setae length 175.

**Etymology.** The species epithet refers to the elongate and parallel maxillary stylets.

**Comments.** The elongate and parallel maxillary stylets of this new species are unique in *Mesothrips*, most of which species have the stylets wide apart and arranged in a V-shape.

### ***Mesothrips pycetes* Karny**

Figs 26, 28, 30, 31

*Mesothrips pycetes* Karny, 1916: 191.

**Material examined. Syntypes**, 1♀1♂, INDONESIA, Java, on *Ficus* sp. [Moraceae], 1.iii.1914, Docters van Leeuwen (SMF).

**Comments.** This species was described from an unspecified number of adults taken in Java, Indonesia, from leaf galls on a species of *Eugenia* [Myrtaceae]. No further studies were published on this species until Wang (2002) listed it from Taiwan, presumably based only on the key to species by Ananthakrishnan (1976). Fortunately, one female and one male labelled as syntypes, but labelled as taken from *Ficus* sp., were checked during studies in 2013 (Dang et al. 2014). *Mesothrips* species usually have setae on tergite IX as long as or longer than tube, but these syntypes have these setae shorter than the tube

(Fig. 28), a condition that also occurs in *M. claripennis*. However, it seems that they can be distinguished by the length of the anal setae (Fig. 28), as indicated in the key.

***Mesothrips vernicia* sp. nov.**

<https://zoobank.org/4DEE6509-DB4E-4A71-8D2A-E233B77B6E4A>

Figs 4, 9, 12, 21, 25

**Material examined.** *Holotype*, ♀, CHINA, Sichuan, Guangyuan, on leaves of *Vernicia* sp. [Euphorbiaceae], 07.viii.2018, Lihong Dang, Yang Hu and Danle Xie (SNUT); *paratypes*, 2♀3♂, with same data as holotype (SNUT); ♀, Hubei, Luotian, on leaves of unknown tree, 03.vii.2014, Lixin Su (SNUT).

**Description.** *Holotype. Female macroptera.* Body brown; all femora and tibiae brown, fore tarsi clear yellow, mid and hind tarsi brownish, slightly lighter than tibiae; antennal segments I and II brown, III–VI uniformly yellow, VII yellow on basal 2/3, and light brown on apical 1/3, VIII lightly brown (Fig. 9); major setae pale; fore wing slightly greyish.

**Head.** Head ~ 1.5 × as long as wide (Fig. 4), constricted at base; postocular setae blunt, ~ 1/2 length of eyes (Fig. 4); eyes longer ventrally than dorsally; maxillary stylets V-shaped, retracted to median of head; mouth cone long, reaching to ferna. Antennae slender, segment III ~ 3.2 × as long as apical width; III with two sense cones, IV with four major sense cones, VIII broadly connected with VII (Fig. 9).

**Thorax.** Pronotum with five pairs of blunt setae, am, aa and pa equal in length (Fig. 4), epim and pa longer and equal in length; surface almost smooth, with weak sculpture near margins. All legs slender, fore tarsal tooth absent (Fig. 12). Fore wing with three blunt sub-basal setae arising in straight line, S1 and S2 equal in length, S3 longest, with seven duplicated cilia. Mesonotum transversely reticulate, lateral setae well-developed, blunt. Metanotum longitudinally reticulate, major setae slender and acute. Mesopresternum with paired lateral triangles, metathoracic sternopleural sutures absent.

**Abdomen.** Pelta broadly triangular, weakly reticulate, with pair of CPS; tergites II–VII with two major pairs of wing retaining setae, one pair of accessory sigmoid setae located anterior to first pair (Fig. 21); tergite II with four pairs of lateral setae; tergite IX setae S1 and S2 longer than tube, acute at apex, S3 approx. as long as tube, acute at apex; tube shorter than head, anal setae approx. as long as tube.

**Measurements** (holotype female in µm). Body length 2620. Head length (maximum width) 260 (175); distance between maxillary stylets (across bridge) 120; eye length dorsally 90, ventrally 120; postocular setae length 45; antennal segments I–VIII length (width): 40 (30), 50 (35), 80 (25), 80 (30), 75 (30), 65 (20), 50 (20), 25 (15); sense cone on III length 20. Pronotum length (width) 170 (240); am ?, aa 35, ml 25, epim 70, pa 55. Fore wing length 1000; sub-basal setae S1 45, S2 50, S3 95. Tergite IX setae S1 195, S2 185, S3 150; tube length 150, basal width 75, apical width 45; anal setae length 170.

**Male macroptera.** Similar to female in colour and sculpture; antennal segment VII largely brown; fore tarsal tooth absent; abdominal tergite IX setae S2 small and pointed (Fig. 25); sternite VIII without pore plate.

**Measurements** (paratype male in  $\mu\text{m}$ ). Body length 2100. Head length (maximum width) 240 (145); eye length dorsally 85, ventrally 85; postocular setae length 45. Pronotum length (width) 135 (185); am 25, aa 30, ml 20, epim 45, pa 25. Tergite IX setae S1 180, S2 15, S3 180; tube length 145; anal setae length 175.

**Etymology.** The species epithet refers to the genus name of the host plant.

**Comments.** As indicated above, the relationships of this species remain far from clear. It is similar in structure to the other two new species but differs sharply from the other *Mesothrips* species in lacking a prominent fore tarsal tooth (Fig. 12), and in the presence of only two sense cones on the third antennal segment (Fig. 9).

### ***Mesothrips vitripennis* Karny**

Figs 6, 11, 19, 27, 29

*Mesothrips vitripennis* Karny, 1922: 149.

*Mesothrips moundi* Ananthakrishnan, 1976: 195. Syn. nov.

*Mesothrips elaeocarpi* Ananthakrishnan, 1976: 192. Syn. nov.

**Material examined.** 1♂, CHINA, Guangxi, Chongzuo, from tree leaves, 25.vii.2021, Xia Wang (SNUT); **paratype**, 1♀ of *moundi*, Hongkong, Tai Ling, from leaves of *Bischofia trifoliata* [Phyllanthaceae], 5.v.1966 (ANIC). 1♀1♂, VIETNAM, Kha-Tin, from leaf gall on *Aporosa leptostachya* [Phyllanthaceae], 20.xi.1920, Docters v. Leeuwen-No. 86 (SMF). **Paratype**, 1♀ of *elaecarpi*, INDONESIA, Java, Bogor, from leaf gall of *Elaeocarpus stipularis* [Elaeocarpaceae], 28.v.1925 (SMF). 1♀, INDIA, Courtallam, on *Mallotus* sp. [Euphorbiaceae], 26.vii.1967, identified by Ananthakrishnan (SMF).

**Comments.** The original description states that this species was collected at Saigon from leaf galls on *Aporosa* on 19.x.1920, whereas the specimens studied here were labelled by Karny from a slightly different locality, collected 10.xi.1920 from leaf galls on *Aporosa leptostachya*. From a plant in the same family, Ananthakrishnan described *M. moundi* (Figs 6, 11) from 17 females and 3 males taken in Hong Kong, and a paratype female is listed below as studied here. This specimen cannot be distinguished as a separate species from the *M. vitripennis* specimens. The head of *M. vitripennis* is rather short, the tube is short and approx. as long as the head width, tergite IX setae S1 are longer than the tube and the fore wings are pale. The new synonymy of *M. elaeocarpi* is based on the paratype female listed below, also one female from India identified by Ananthakrishnan.

### **Acknowledgements**

We are grateful to Laura Marrero Palma of the Naturmuseum Senckenberg (SMF), Frankfurt, Germany for arranging the loan of many slides. And we also thank all collectors of thrips specimens.

### **Additional information**

#### **Conflict of interest**

The authors have declared that no competing interests exist.

## Ethical statement

No ethical statement was reported.

## Funding

This work was supported by the Natural Science Basic Research program of Shaanxi Province [2023-JC-QN-0178], the National Natural Sciences Foundation of China [No. 31702042], the Youth Innovation Team of Shaanxi University (2023-77), the Second Tibetan Plateau Scientific Expedition and Research (STEP) program [Grant No.2019QZ-KK0501], and Survey of Wildlife Resources in Key Areas of Tibet (ZL202203601).

## Author contributions

Lihong Dang: writing – original draft. Xiaoli Tong: data curation. Laurence A. Mound: writing – reviewing and editing.

## Author ORCIDs

Lihong Dang  <https://orcid.org/0000-0002-7571-8426>

Xiaoli Tong  <https://orcid.org/0000-0003-1731-229X>

Laurence A. Mound  <https://orcid.org/0000-0002-6019-4762>

## Data availability

All of the data that support the findings of this study are available in the main text.

## References

- Ananthkrishnan TN (1972) Further studies on Indian Gall Thrips II. *Marcellia* 37(5): 3–20.
- Ananthkrishnan TN (1976) Studies on *Mesothrips* (Thysanoptera: Tubulifera). *Oriental Insects* 10(2): 185–214. <https://doi.org/10.1080/00305316.1976.10434905>
- Ananthkrishnan TN, Sen S (1980) Taxonomy of Indian Thysanoptera. *Zoological Survey of India* 1: 1–234. [Handbook Series]
- Dang LH, Mound LA, Qiao GX (2014) Conspectus of the Phlaeothripinae genera from China and Southeast Asia (Thysanoptera, Phlaeothripidae). *Zootaxa* 3807(1): 001–082. <https://doi.org/10.11646/zootaxa.3807.1.1>
- Karny H (1912) Gallenbewohnende Thysanopteren aus Java. *Marcellia* 1: 115–169.
- Karny H (1914–1916) Beiträge zur Kenntnis der Gallen von Java. Zweite Mitteilung über die javanischen Thysanopterocecidien und deren Bewohner. *Zeitschrift für wissenschaftliche Insektenbiologie* 10 [1914]: 201–208, 288–296, 355–369; 11 [1915]: 32–39, 85–90, 138–147, 203–210, 249–256, 324–331; 12 [1916]: 15–22, 84–94, 125–132, 188–199.
- Karny H (1922) Thysanoptera from Siam and Indo-China. *The Journal of the Siam Society* 16: 91–153.
- Karny H (1923) Beiträge zur Malayischen Thysanopterenfauna. VI. Malayische Rindenthripse, gessammelt von Dr. N.A. Kemner. VII. Gallenbewohnende Thysanopteren von Celebes und den Inseln südlich davon, gesammelt von Herrn W. Docters v. Leeuwen. VIII. Ueber die tiergeographischen Beziehungen der malayischen Thysanopteren. *Treubia* 3: 277–380.
- Karny H, Docters van Leeuwen-Reijnvaan W and J (1913) Beiträge zur Kenntnis der Gallen von Java. 5. Über die javanischen Thysanopteren-ecidien und deren Bewohner. *Bulletin du Jardin Botanique de Buitenzorg* 10: 1–126.

- Moulton D (1928a) New Thysanoptera from Formosa. Transactions of the Natural History Society of Formosa 18: 287–328.
- Moulton D (1928b) Thysanoptera of Japan: New species, notes, and a list of all known Japanese species. Annotationes zoologicae Japonensis 11: 287–337.
- Moulton D (1942) Thrips of Guam. Bishop Museum Bulletin 172: 7–16.
- Mound LA, Marullo R (1996) The Thrips of Central and South America: An Introduction. Memoirs on Entomology. International 6: 1–488.
- Mound LA, Minaei K (2007) Australian insects of the *Haplothrips* lineage (Thysanoptera – Phlaeothripinae). Journal of Natural History 41: 2919–2978. <https://doi.org/10.1080/00222930701783219>
- Mound LA, Okajima S (2015) Taxonomic Studies on *Dolichothrips* (Thysanoptera: Phlaeothripinae), pollinators of *Macaranga* trees in Southeast Asia (Euphorbiaceae). Zootaxa 3956(1): 79–96. <https://doi.org/10.11646/zootaxa.3956.1.4>
- Okajima S (2006) The Suborder Tubulifera (Thysanoptera). The Insects of Japan 2: 1–720. [The Entomological Society of Japan, ToukaShobo Co. Ltd., Fukuoka.]
- Okajima S, Masumoto M (2023) Six genera of the subtribe Macrothripina from Southeast Asia to Taiwan (Thysanoptera, Phlaeothripidae, Idolothripinae). Zootaxa 5291(1): 001–074. <https://doi.org/10.11646/zootaxa.5291.1.1>
- Priesner H (1921) *Haplothrips*-Studien. Treubia 2: 1–20.
- Priesner H (1929a) Indomalayische Thysanopteren I. Treubia 10: 447–462.
- Priesner H (1929b) Eine neue *Mesothrips*-Art aus Annam. Bollettino del Laboratorio di Zoologia Generale e Agraria. Portici 21: 215–217.
- Reyes CP (1994) Thysanoptera (Hexapoda) of the Philippine Islands. The Raffles Bulletin of Zoology 42: 107–507.
- Takahashi R (1936) Thysanoptera of Formosa. Philippine Journal of Science 60: 427–459.
- ThripsWiki (2023) ThripsWiki – providing information on the World’s thrips. [http://thrips.info/wiki/Main\\_Page](http://thrips.info/wiki/Main_Page) [Accessed 30 Sept 2023]
- Vuillet A (1914) Description d’un *Mesothrips* nouveau de Madagascar (Thysanopt. Phlaeothripidae). Bulletin de la Société Entomologique de France 2014(7): 211–212. <https://doi.org/10.3406/bsef.1914.25555>
- Wang CL (2002) Thrips of Taiwan: Biology and Taxonomy. Special Publication 99. Taichung: Taiwan Agricultural Research Institute 328 pp. [in Chinese]
- Zhang WQ (1984) Preliminary note on Thysanoptera collected from Hainan Island, Guangdong, China. III Subfamily: Phlaeothripinae (Thysanoptera: Phlaeothripidae). Journal of the South China Agricultural College 5(3): 15–27.
- Zhang WQ, Tong XL, Luo XN, Zhuo WX (1999) Thysanoptera. In: Huang BK (Ed.) Fauna of Insects Fujian province of China. Vol. I. Science Technology of Fujian, Fuzhou, 479 pp.
- Zimmermann A (1900) Ueber einige javanische Thysanoptera. Bulletin de l’Institut botanique de Buitenzorg 7: 6–19.

# Back to the future: A preserved specimen validates the presence of *Molossus pretiosus* (Molossidae, Chiroptera) in Honduras

Manfredo A. Turcios-Casco<sup>1,2</sup>, Vinícius Cardoso Cláudio<sup>3</sup>, Thomas E. Lee Jr<sup>4</sup>

1 *Asociación para la Sostenibilidad e Investigación Científica en Honduras (ASICH), Barrio La Granja, entre 28 y 29 calle, Comayagüela M.D.C., Francisco Morazán, Tegucigalpa, Honduras*

2 *Laboratório de Etnoconservação e Áreas Protegidas, Universidade Estadual de Santa Cruz, Ilhéus, BA, Brazil*

3 *Fundação Oswaldo Cruz, Fiocruz Mata Atlântica, 22713-560, Rio de Janeiro, Brazil*

4 *Department of Biology, Box 27868, Abilene Christian University, Abilene, Texas, 79699, USA*

Corresponding author: Manfredo A. Turcios-Casco ([matcasco.ppgzoo@uesc.br](mailto:matcasco.ppgzoo@uesc.br))

## Abstract

*Molossus pretiosus* is a molossid bat that has been thought to exist in Honduras. While some authors have suggested its range extends all the way to Mexico, others have placed its northernmost distribution in Nicaragua. We present evidence, based on one specimen collected in 2005, confirming the presence of this species in the Caribbean of Honduras within the Islas de la Bahía department. This discovery increases the count of known species within this family to 18 in the country and raises the total bat species count for Honduras to 114. We recommend a detailed study of historical specimens to confirm the identification of species that may have been misidentified as well as a thorough examination of molossids distributed in northern Honduras.

**Key words:** Bat diversity, Caribbean islands, Central America, distribution, Islas de la Bahía, morphology



Academic editor: Nilton Cáceres

Received: 23 November 2023

Accepted: 19 February 2024

Published: 22 March 2024

ZooBank: <https://zoobank.org/C111A250-501C-44F9-AF85-AC280A0C312D>

**Citation:** Turcios-Casco MA, Cardoso Cláudio V, Lee Jr TE (2024) Back to the future: A preserved specimen validates the presence of *Molossus pretiosus* (Molossidae, Chiroptera) in Honduras. ZooKeys 1196: 139–148. <https://doi.org/10.3897/zookeys.1196.116144>

**Copyright:** © Manfredo A. Turcios-Casco et al. This is an open access article distributed under terms of the Creative Commons Attribution License ([Attribution 4.0 International – CC BY 4.0](https://creativecommons.org/licenses/by/4.0/)).

## Introduction

Currently, 113 bat species has been reported for Honduras (Turcios-Casco et al. 2020b; Mora et al. 2021), new records which include: *Lasiurus cinereus* (Palisot de Beauvois, 1796), *Lasiurus egregius* (Peters, 1870), *Neoptesicus brasiliensis* (Desmarest, 1819), *Balantiopteryx io* Thomas, 1904, *Vampyriscus nymphaeus* (Thomas, 1909), *Nyctinomops aurispinosus* (Peale, 1848), *N. macrotis* (Gray, 1840), *Hylonycteris underwoodi* Thomas, 1903, *Chiroderma gorgasi* Handley, 1960, *Diaemus youngii* (Jentink 1893), *Natalus lanatus* Tejedor, 2005, *Cynomops mexicanus* (Jones and Genoways 1967) and *Centronycteris centralis* Thomas, 1912 (Espinal and Mora 2012; Mora 2012; Divoll and Buck 2013; Mora et al. 2014; Espinal et al. 2016, 2021; Mora et al. 2016; Turcios-Casco and Medina-Fitoria 2019; Turcios-Casco et al. 2020a, b). One of the major issues with Honduran bat studies is that there are several historically-preserved specimens that have not been verified yet. For example, museum specimens of *Natalus lanatus* and *Cynomops mexicanus* reported by Turcios-Casco et al. (2020b) were collected in 1963 and 1967, respectively. Collecting and recording efforts have

increased in the past 15 years, raising the number of bat species to 113 (Turcios-Casco et al. 2020b). Turcios-Casco et al. (2020b) and Mora et al. (2021), expect additional species to occur based on their wide distributions in Central America these include: *Cormura brevirostris* (Wagner, 1843), *Lampronycotis brachyotis* (Dobson, 1879), *Trinycteris nicefori* (Sanborn, 1949), *Mesophylla macconnelli* (Thomas, 1901), *Molossus coibensis* J. A. Allen, 1904, *Molossus pretiosus* Miller, 1902 and *Thyroptera discifera* (Lichtenstein & Peters, 1855). Historical collections from Honduras in international museums remain poorly assessed, and verification of the identification of many species (e.g., in the genera *Natalus*, *Molossus*, *Eumops* and phyllostomines) not only of bats (e.g., rodents such as *Peromyscus*, shrews such as *Cryptotis*) remains unclarified.

One of the most contentious bat families in Central America is Molossidae, because their overlapping external characters [see diagnoses in Loureiro et al. (2018, 2019, 2020)] make field identification difficult, and also because most of their echolocation calls have not been verified within their distribution (B. Miller, pers. comm.). Therefore, taxonomic identification of Central American molossids remains problematic and unresolved.

Among molossids, the Miller's Mastiff Bat, *Molossus pretiosus*, has been considered widely distributed (Loureiro et al. 2019), and even though some authors consider it to be distributed far north as Mexico and southward to Brazil (e.g., Simmons 2005; Medina-Fitoria 2014; Cláudio et al. 2018; Díaz et al. 2021), the species was not included in Mexico by Ramírez-Pulido et al. (2014). Additionally, historical specimens in the Global Information Biodiversity Facility (GBIF.org 2023) database that have been identified as *M. pretiosus* were recorded from Belize and Mexico. The majority of the specimens identified as *M. pretiosus* in northern Central America, especially from Mexico and Belize, must be confirmed, as they could have been confused with other species of *Molossus* (B. Miller, pers. comm.). This occurrence was supported by Díaz et al. (2021) who included *M. pretiosus* in the bat checklist for Mexico and Costa Rica but not for Belize. Burgin et al. (2020) also confirm the species in Mexico and Belize. In contrast, other authors considered Nicaragua as the northernmost country within its range (e.g., Loureiro et al. 2019; Jennings et al. 2000; Simmons and Cirranello 2023). As described above, there is controversy over the distribution of *M. pretiosus* in northern Mesoamerica. As part of an effort to further investigate museum specimens from Honduras, we present evidence that confirms the occurrence of *M. pretiosus* on the Caribbean Island of Roatán in northern Honduras.

## Materials and methods

### Preserved specimens and description of the locality

On 6 March 2005, one specimen of *M. pretiosus* (ACUNHC 1034) was found on the beach shore of Fantasy Island Resort in Roatán, within the Islas de la Bahía department in northern Honduras. The skull and the skeleton were deposited in the Abilene Christian University Natural History Collection (ACUNHC-Mammal). Roatán is the largest island (40 km long and 8 km wide) within the Islas de la Bahía department; it reaches approximately 300 m a.s.l. in elevation and is mostly covered with tropical dry forests and mangroves along the shore; private properties are very common all along the island (Goode et al. 2020).

## Morphological description

For the identification of the specimen, we mainly followed Cláudio et al. (2018) to compare Latin American samples, as well as Nogueira et al. (2008) and Loureiro et al. (2018, 2019, 2020) for taking the following measurements: forearm length (FA), greatest length of skull including incisors (GLS), condylobasal length (CBL), condylocanine length (CCL), postorbital breadth (PB), zygomatic breadth (ZB), braincase breadth (BB), mastoid breadth (MB), maxillary toothrow length (MTL), breadth across molars (BM) and breadth across canines (BC). Calipers accurate to the nearest 0.01 mm were used to take the measurements. Additional publications were consulted to help us describe the qualitative and quantitative characteristics of ACUNHC 1034: DeBlase and Martin (1981), Dolan (1989), Gregorin and Taddei (2000), Jennings et al. (2000), Loureiro et al. (2018, 2019, 2020) and Díaz et al. (2021).

## Distribution

Data from the Global Biodiversity Information Facility (GBIF.org; accessed in September 2023) of all preserved *M. pretiosus* specimens was downloaded and analyzed to define the distribution of the species. These records included both verified specimens (Gregorin and Taddei 2000; Eger 2008; Cláudio et al. 2018; Loureiro et al. 2019, 2020) and specimens recorded in the GBIF that need to be further verified (Fig. 1). Additionally, the range of the species was contrasted with the data presented by the IUCN, International Union for Conservation of Nature (Solari 2019).

## Results

### *Molossus pretiosus* Miller, 1902

**Material examined.** HONDURAS • 1 ♀; Roatán, Fantasy Island Resort, Islas de la Bahía department; 16°21'30"N, 86°26'9"W; 4 m a.s.l.; 6 March 2005; Thomas Lee leg; dead specimen found on the ground; ACUNHC 1034.

**Description.** Given that the skin (ACUNHC 1034) was desiccated when discovered, no description is available for the fur. As a result, the identification of the specimen primarily relies on characteristics of the skull (Table 1). The rostrum is short and quadrangular in shape. There is no projection over the nasal cavity by the nasal process of the premaxilla; therefore, the nasal process is undeveloped. The skull presented a squarish occipital complex (Fig. 2A) because of the significant size and angling of the lambdoidal crests. The skull exhibits distinct features, including a well-developed bulging braincase and sagittal crest (Fig. 2B), as well as a deep basioccipital pit with a ridge. There is a noticeable crest between the basisphenoid and basioccipital pits. Infraorbital foramen opened laterally, when viewing from the front. Additionally, the M3 molars display cup-like structures with a V-shaped pattern (Fig. 2C). The elongated upper incisors extend beyond the canines and the tips and are not in contact. The forearm measurement in the dried skin of the ACUNHC 1034 specimen is recorded as 45.08 mm. This measurement matches the range observed in Central American specimens (44.3–45.9 mm) (Jennings et al. 2000).

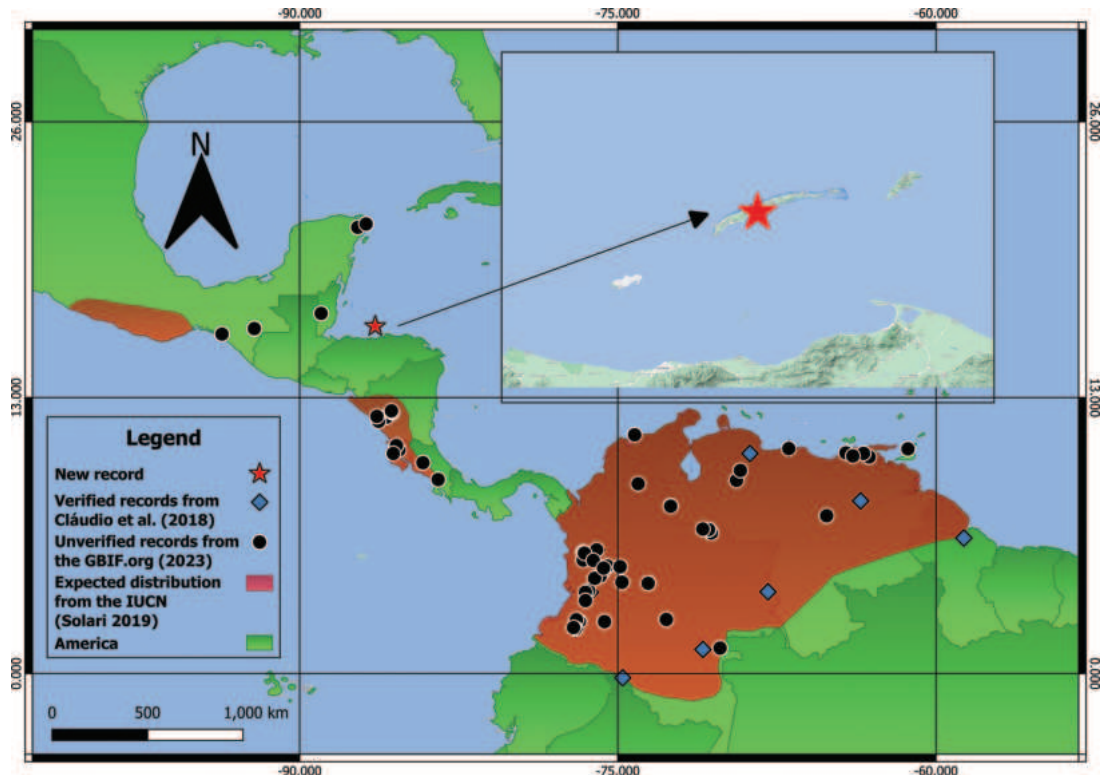
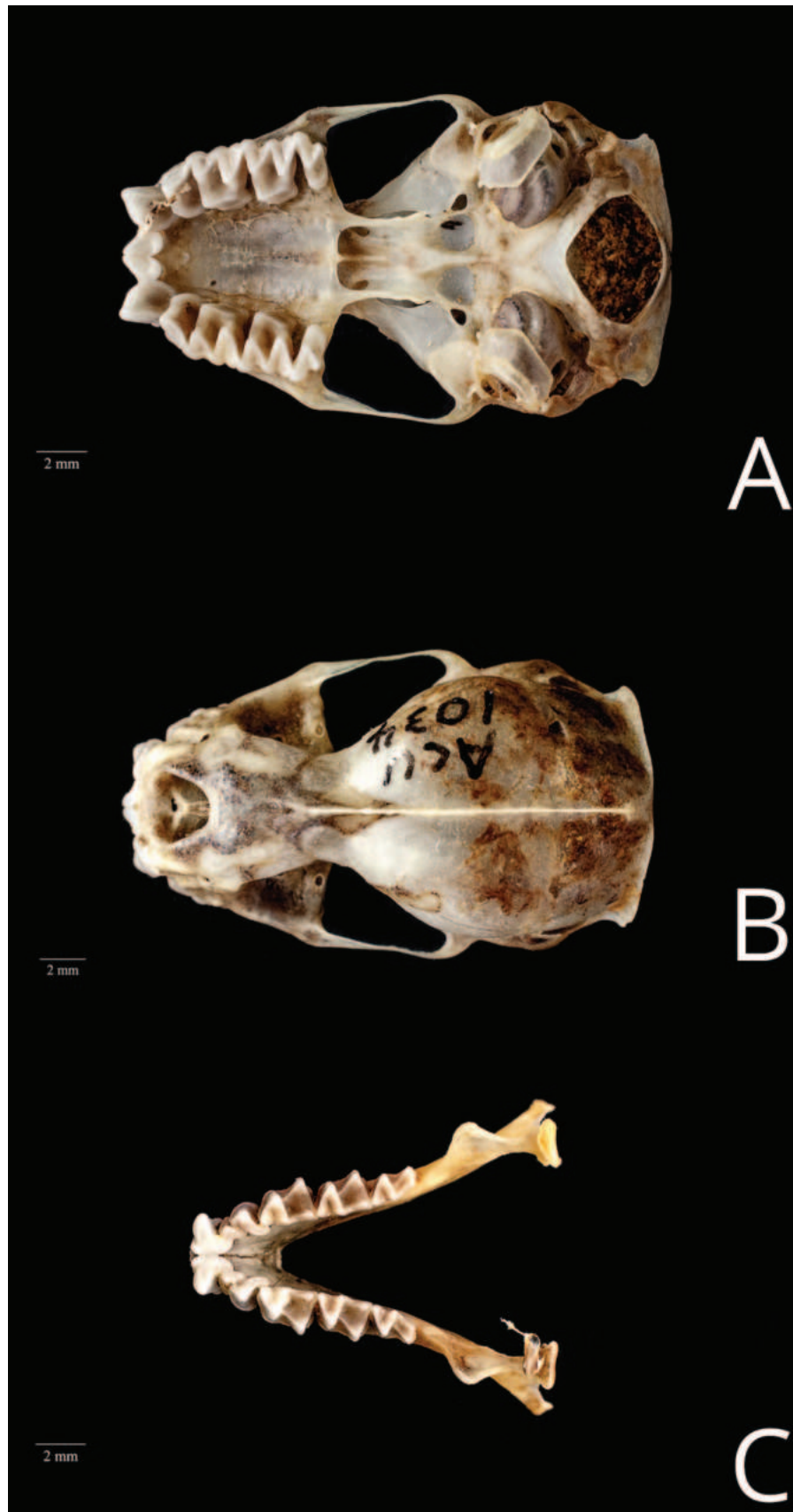


Figure 1. Distribution map of *Molossus pretiosus*. We considered the records mentioned by Cláudio et al. (2018) as verified, and we included in the distribution other records based on the GBIF.org (2023) database. In addition, we overlap these records with the expected distribution of the species based on the IUCN (Solari 2019).

Table 1. Comparison of cranial measurements (see Material and methods for abbreviations) and forearm length (FA) of *Molossus pretiosus* specimens along its distribution in Latin America. Specimens and locations as follow: 1. Cláudio et al. (2018), 2. Nogueira et al. (2008), 3. Gregorin and Taddei (2000) and 4. Dolan (1989).

Measurements	ACUNHC 1034 (this study)	Bahía, Brazil <sup>1</sup>	Minas Gerais, Brazil <sup>2</sup>	Mato Grosso do Sul, Brazil <sup>3</sup>	Costa Rica <sup>4</sup>	Nicaragua <sup>4</sup>
FA	45.0	46.3	43.6–47.2	42.6–45.5	43.4–46.0	41.6–45.9
GLS	18.3	19.8	19.1–20.4	19.2–19.6	19.7–20.9	18.8–20.8
CBL	17.4	18.2	17.5–18.5	–	17.5–18.1	16.4–18.6
CCL	17.1	18.1	–	–	–	–
PB	3.8	4.0	4.1–4.6	–	–	–
BB	9.0	10.0	9.8–10.5	9.7–9.9	9.6–10.6	9.7–10.6
ZB	10.9	12.3	–	–	–	–
MB	10.4	10.8	11.9–13.5	–	–	–
MTL	7.2	7.0	7.0–7.5	7.2–7.3	6.8–7.1	6.3–7.4
BM	8.1	8.8	8.5–9.7	8.8–9.2	8.3–9.0	8.5–9.3
BC	4.5	4.8	5.0–5.6	–	5.0–5.3	4.8–5.5

**Comparisons.** In comparison to the other species of *Molossus* that occur in Honduras, *Molossus nigricans* Miller, 1902 is larger than *M. pretiosus*, the FA of the former varies from 47.2–54.5 mm in females and GLS from 20.1–22.6 mm in females (Loureiro et al. 2019). *Molossus alvarezii* (González-Ruiz, Ramírez-Pulido & Arroyo-Cabrales, 2011) is medium-sized and may overlap in some measurements, but it does not have a well-developed sagittal crest; it



**Figure 2.** Skull (**A**, **B**) and mandible (**C**) of *Molossus pretiosus* (ACUNHC 1034) from Roatán Island. A ventral view (squarish occipital complex) B dorsal view (note the well-developed bulging braincase and sagittal crest C dorsal view of the upper mandible (M3 molars with a V-shaped pattern). Credits of the photos are to Nil Santana (ACUNHC 1034).

has pincer-like upper incisors converging at the tips, and the occipital region is triangular (González-Ruiz et al. 2011; Díaz et al. 2021). *Molossus molossus* (Pallas, 1766) is usually smaller with FA ranging from 36.4–42.6 mm in females and GLS from 15.6–18.6 mm in females (Loureiro et al. 2018). In addition to the other two species that occur in Honduras, *Molossus bondae* J. A. Allen, 1904 and *Molossus aztecus* Saussure, 1860 have upper incisors as pincer-like with convergent tips, but those of *M. pretiosus* are larger than those of *M. bondae* (FA <43 mm) (Loureiro et al. 2019; Jennings et al. 2000), and *M. aztecus* differs in having its basisphenoid pits with a moderate depth (Díaz et al. 2021), and is currently only known from western Honduras (McCarthy et al. 1993; Turcios-Casco et al. 2021).

## Discussion

In addition to *M. alvarezii*, *M. aztecus*, *M. bondae*, *M. molossus* and *M. nigricans*, we present the record of a sixth *Molossus* species to Honduras, *M. pretiosus*. This brings the total number of molossids known to occur in Honduras to 18 [*Cynomops greenhalli* Goodwin, 1958; *C. mexicanus*; *Eumops auripendulus* (Shaw, 1800); *Eumops ferox* (Gundlach, 1961); *Eumops hansae* Sanborn, 1932; *Eumops nanus* (Miller, 1900); *Eumops underwoodi* (Goodwin, 1940); *N. aurispinosus*; *Nyctinomops laticaudatus* (É. Geoffroy, 1805); *N. macrotis*; *Promops centralis* Thomas, 1915; and *Tadarida brasiliensis* (L. Geoffroy, 1824)]; and increases the current list of bat species for Honduras to 114 (see Turcios-Casco et al. 2020b). There are still poorly known molossids in the country; *T. brasiliensis*, one of the most common and widespread species of molossid (Kunz et al. 1995), is known from two official records, one in western Honduras in Ocotepeque and another in the central region of the country in Francisco Morazán (McCarthy et al. 1993; Turcios-Casco et al. 2021). In addition, *M. aztecus* is only known from historical records from La Paz in western Honduras, supported by the revision of McCarthy et al. (1993) of museum specimens misidentified as *M. bondae* by Goodwin (1942).

Molossidae is still an understudied mammalian group in Honduras. One of the major issues of studying the group in the country is that many of them lack a robust and verified database of their echolocation calls, besides the limited sampling that has been done on bat acoustics since 1999 in Honduras (B. Miller pers. comm.). Reasons for this lack of information also include the small number of researchers interested in the family in Honduras, acoustic research being a recent addition to bat monitoring, and the relatively new use of canopy nets (B. Miller. pers. comm.). The natural history and ecological behaviour of molossids, which typically forage above mist nets, also present challenges to their study (Simmons 2005; Cláudio et al. 2018; Díaz et al. 2021). The under-utilization and lack of revision of historical mammalian specimens from Honduras present significant obstacles to accurately describing the biogeography of these animals. Misidentifications resulting from outdated taxonomy can impede efforts to elucidate the historical ranges of species, hindering our understanding of past ecosystems and potentially influencing modern conservation strategies.

The record of *M. pretiosus* presented herein for Honduras fills the gap in the northern portion of its distribution (Fig. 1) and indicates that it may be present in other regions of northern Mesoamerica. Since there is still some uncertainty

about the northern limits of the distribution of the species, we strongly recommend revisiting museum specimens of *M. pretiosus* in northern Mesoamerica (e.g., Mexico and Belize) and verifying calls of molossids in Central America to identify other characteristics (e.g., bioacoustics) for molossid species identification as well as analysing molecular data whenever possible. Additionally, special attention must be given to the population in the Caribbean islands of Honduras because molossids in this region could probably be misidentified due to the overlap of external characters. To avoid the misidentification of specimens, we recommend the use of a larger set of morphological traits during field identification, such as forearm length, shape and length of upper indictors, fur colour and pattern of banding (see Loureiro et al. 2018, 2019, 2020; Díaz et al. 2021). Also, the collection and deposition of voucher specimens in scientific collections are encouraged in order to verify and confirm field identifications. Finally, the proper preparation of museum specimens such as skull, skeletons, skins, and tissues for further molecular studies is fundamental, especially for problematic groups like Molossidae.

## Acknowledgments

To Phaedra Kokkini and Paula Jenkins from the Mammal Section of the Natural History Museum of London for providing information and photos of the specimen NHMUK 1984.1634 and the collection made by B.H. Gaskell. To Bruce Miller for his comments on Central American bat calls. To Monica Díaz, Sergio Solari, Nilton Cáceres, Polina Petrakieva and Christopher Glasby for their useful comments that helped to improve this manuscript. Photos of the ACUNHC specimen were taken by Nil Santana. MATC has received a scholarship from CAPES for the Programa de Pós-Graduação em Zoologia da Universidade Estadual de Santa Cruz (UESC), edital UESC n° 176/2022. TL received financial support from the Clark Stevens Endowed Chair. VCC has received support from Fundação Carlos Chagas Filho de Amparo à Pesquisa do Estado do Rio de Janeiro (FAPERJ, E-26/205.820/2022 and 205.821/2022).

## Additional information

### Conflict of interest

The authors have declared that no competing interests exist.

### Ethical statement

No ethical statement was reported.

### Funding

Clark Stevens Endowed Chair. Fundação Carlos Chagas Filho de Amparo à Pesquisa do Estado do Rio de Janeiro (FAPERJ, E-26/205.820/2022 and 205.821/2022). CAPES, Universidade Estadual de Santa Cruz (edital UESC n° 176/2022).

### Author contributions

MATC orchestrated the study, reached out to the Natural History Museum of London to obtain information on the NHMUK 1984.1634 specimen information, made the distribution map, and composed the initial manuscript draft. VCC confirmed the taxonomic

identity of the individuals by examining skull descriptions and with MATC the verified records within the distribution of *M. pretiosus*. TL conducted measurements and gathered ACUNHC 1034; additionally, he sought funding for the publication and coordinated the specimen's photography. All authors actively contributed to both the writing and revision of this manuscript.

### Author ORCIDs

Manfredo A. Turcios-Casco  <https://orcid.org/0000-0002-3198-3834>

Vinicius Cardoso Cláudio  <https://orcid.org/0000-0002-3438-911X>

Thomas E. Lee Jr  <https://orcid.org/0000-0001-5185-5568>

### Data availability

All information pertaining to the validation of the findings in this study can be found in the main text.

### References

- Burgin CJ, Wilson DE, Mittermeier RA, Rylands AB, Lacher TE, Sechrest W [Eds] (2020) Illustrated Checklist of the Mammals of the World. Lynx Edicions, Barcelona, 1166 pp.
- Cláudio VC, Silveira GC, Farias SG, Lepenta MJ (2018) First record of *Molossus pretiosus* Miller, 1902 (Chiroptera, Molossidae), for the Cerrado of Bahia, northeastern Brazil. *Check List* 14(1): 177–182. <https://doi.org/10.15560/14.1.177>
- DeBlase AF, Martin RE (1981) A manual of mammalogy, with keys to the families of the World. William C. Brown Company Publishers, Dubuque Iowa, 458 pp.
- Díaz MM, Solari S, Aguirre LF, Aguiar LMS, Barquez RM (2021) Clave de Identificación de los murciélagos de Sudamérica. *Publicación Especial N° 2 PCMA (Programa de Conservación de los Murciélagos de Argentina)*.
- Divoll TJ, Buck DG (2013) Noteworthy field observations of cave roosting bats in Honduras. *Mastozoología Neotropical* 20(1): 149–151.
- Dolan PG (1989) Systematics of Middle American mastiff bats of the genus *Molossus*. *Special Publications, The Museum. Texas Tech University* 29: 1–79. <https://doi.org/10.5962/bhl.title.142636>
- Eger JL (2008 [2007]) Family Molossidae P. Gervais, 1856. In: Gardner AL (Ed.) *Mammals of South America, Volume I. Marsupials, Xenarthrans, Shrews, and Bats*. University of Chicago Press, Chicago, 399–439.
- Espinal M, Mora JM (2012) Noteworthy record of *Eptesicus brasiliensis* (Vespertilionidae) in Honduras. *Ceiba* 53(2): 77–80. <https://doi.org/10.5377/ceiba.v53i2.2433>
- Espinal M, Mora JM, O'Reilly CM (2016) The occurrence of the Peale's free-tailed bat (*Nyctinomops aurispinosus*, Molossidae) in Central America. *Caribbean Journal of Science* 49(1): 79–82. <https://doi.org/10.18475/cjos.v49i1.a8>
- Espinal MR, Miller BW, Mora JM (2021) First record of *Centronycteris centralis* (Chiroptera: Emballonuridae) from Honduras. *Notas sobre Mamíferos Sudamericanos* 3: 1–10. <https://doi.org/10.31687/saremNMS.21.11.1>
- GBIF.org (2023) GBIF Occurrence. <https://doi.org/10.15468/dl.hhmxat> [Accessed 28 September 2023]
- González-Ruiz N, Ramírez-Pulido J, Arroyo-Cabrales J (2011) A new species of mastiff bat (Chiroptera: Molossidae: *Molossus*) from Mexico. *Mammalian Biology* 76(4): 461–469. <https://doi.org/10.1016/j.mambio.2010.06.004>

- Goode ABC, Pasachnik SA, Maple TL (2020) Assessing the status of a threatened island endemic, *Ctenosaura oedirhina*, on Roatán, Honduras. *Wildlife Research* 47(2): 137–145. <https://doi.org/10.1071/WR18195>
- Goodwin GG (1942) Mammals of Honduras. *Bulletin of the American Museum of Natural History* 79: 111–119.
- Gregorin R, Taddei VA (2000) New records of *Molossus* and *Promops* from Brazil (Chiroptera: Molossidae). *Mammalia* 64(4): 471–476. <https://doi.org/10.1515/mamm.2000.64.4.471>
- Jennings JB, Best TL, Rainey JC, Burnett SE (2000) *Molossus pretiosus*. *Mammalian Species* 635: 1–3. [https://doi.org/10.1644/1545-1410\(2000\)635<0001:MP>2.0.CO;2](https://doi.org/10.1644/1545-1410(2000)635<0001:MP>2.0.CO;2)
- Kunz TH, Whitaker Jr JO, Wadanoli MD (1995) Dietary energetics of the insectivorous Mexican free-tailed bat (*Tadarida brasiliensis*) during pregnancy and lactation. *Oecologia* 101(4): 407–415. <https://doi.org/10.1007/BF00329419>
- Loureiro LO, Gregorin R, Perini FA (2018) Diversity, morphological phylogeny, and distribution of bats of the genus *Molossus* E. Geoffroy, 1805 (Chiroptera, Molossidae) in Brazil. *Zoosystema* 40(18): 425–452. <https://doi.org/10.5252/zoosystema2018v40a18>
- Loureiro LO, Engstrom M, Lim B, González CL, Juste J (2019) Not all *Molossus* are created equal: Genetic variation in the mastiff bat reveals diversity masked by conservative morphology. *Acta Chiropterologica* 21(1): 51–64. <https://doi.org/10.3161/15081109ACC2019.21.1.004>
- Loureiro LO, Engstrom MD, Lim BK (2020) Single nucleotide polymorphisms (SNPs) provide unprecedented resolution of species boundaries, phylogenetic relationships, and genetic diversity in the mastiff bats (*Molossus*). *Molecular Phylogenetics and Evolution* 143: 106690. <https://doi.org/10.1016/j.ympev.2019.106690>
- McCarthy TJ, Davis WB, Hill JE, Jones Jr JK, Cruz GA (1993) Bat (Mammalia: Chiroptera) records, early collectors, and faunal lists for Northern Central America. *Annals of the Carnegie Museum* 62(3): 191–228. <https://doi.org/10.5962/p.226650>
- Medina-Fitoria A (2014) Murciélagos de Nicaragua, guíade campo. Ministerio del Ambiente y los Recursos Naturales, Managua, 278 pp.
- Mora JM (2012) Big red bat *Lasiurus egregius* (Vespertilionidae) in Honduras. *The Southwestern Naturalist* 57(1): 104–105. <https://doi.org/10.1894/0038-4909-57.1.104>
- Mora JM, Marineros L, López LI (2014) First Record of the Striped Yellow-Eared Bat, *Vampyriscus nymphaea* (Stenodermatinae, Phyllostomidae) in Honduras. *Caribbean Journal of Science* 48(1): 49–51. <https://doi.org/10.18475/cjos.v48i1.a7>
- Mora JM, Espinal MR, Ruedas LA, López LI (2016) The big free-tailed bat, *Nyctinomops macrotis* (Gray, 1839), in central America. *Mastozoología Neotropical* 23(2): 551–556.
- Mora JM, López LI, Espinal MR (2021) Clave de campo para la identificación de los murciélagos de Honduras. *Notas sobre Mamíferos Sudamericanos* 3, 1–33. <https://doi.org/10.31687/saremNMS.21.6.1>
- Nogueira MR, Pol A, Monteiro LR, Peracchi AL (2008) First record of Miller's mastiff bat, *Molossus pretiosus* (Mammalia: Chiroptera), from the Brazilian Caatinga. *Chiroptera Neotropical* 14(1): 346–353.
- Ramírez-Pulido J, González-Ruiz N, Gardner AL, Arroyo-Cabrales J (2014) List of recent land mammals of Mexico, 2014. *Special Publications - the Museum, Texas Tech University*. Texas Tech University. *Museum* 63: 1–69. <https://doi.org/10.5962/bhl.title.142891>
- Simmons NB (2005) Order Chiroptera. In: Wilson DE, Reeder DM (Eds) *Mammal species of the world, a taxonomic and geographic reference*. The Johns Hopkins Press, Baltimore, 312–529.

- Simmons NB, Cirranello AL (2023) Bat Species of the World: A taxonomic and geographic database. Version 1.4. <https://batnames.org/home.html> [Accessed 21 November 2023]
- Solari S (2019) *Molossus pretiosus*. The IUCN Red List of Threatened Species 2019: e.T13649A22106312. <https://doi.org/10.2305/IUCN.UK.2019-1.RLTS.T13649A22106312.en>
- Turcios-Casco MA, Medina-Fitoria A (2019) Occurrence of *Hylonycteris underwoodi* (Chiroptera, Phyllostomidae) and *Thyroptera tricolor* (Chiroptera, Thyropteridae) in Honduras. *Studies on Neotropical Fauna and Environment* 54(1): 69–72. <https://doi.org/10.1080/01650521.2018.1544205>
- Turcios-Casco MA, Ávila-Palma HD, LaVal RK, Stevens RD, Ordoñez-Trejo EJ, Soler-Orellana JA, Ordoñez-Mazier DI (2020a) A systematic revision of the bats (Chiroptera) of Honduras: An updated checklist with corroboration of historical specimens and new records. *Zoosystematics and Evolution* 96(2): 411–429. <https://doi.org/10.3897/zse.96.51059>
- Turcios-Casco MA, Medina-Fitoria A, Estrada-Andino N (2020b) Northernmost record of *Chiroderma trinitatum* (Chiroptera, Phyllostomidae) in Latin America, with distributional comments. *Caribbean Journal of Science* 50(1): 9–15. <https://doi.org/10.18475/cjos.v50i1.a2>
- Turcios-Casco MA, LaVal RK, Wilson DE, Ávila-Palma HD (2021). Bats in time: Historical and geographic distribution in Honduras. *Museum of Texas Tech University* 375: 1–22. <https://www.depts.ttu.edu/nsrl/publications/downloads/OP375.pdf>

# A new species of terrestrial toad of the *Rhinella festae* group (Anura, Bufonidae) from the highlands of the Central Cordillera of the Andes of Colombia

Luis Santiago Caicedo-Martínez<sup>1,2</sup>, Jose J. Henao-Osorio<sup>1,2</sup>, Héctor Fabio Arias-Monsalve<sup>1,2,3</sup>, Julián Andrés Rojas-Morales<sup>1,2</sup>, Paula A. Ossa-López<sup>4</sup>, Fredy A. Rivera-Páez<sup>4</sup>, Héctor E. Ramírez-Chaves<sup>1,4</sup>

1 Natural History Laboratory, Integrative Zoological Biodiversity Discovery, Centro de Museos, Museo de Historia Natural, Universidad de Caldas, Carrera 23 # 58-65, Manizales 170004, Colombia

2 Programa de Biología, Facultad de Ciencias Exactas y Naturales, Universidad de Caldas, Calle 65 No. 26-10, Manizales 170004, Colombia

3 Fundación Ecológica Cafetera, Manizales, Caldas, Colombia

4 Grupo de Investigación en Genética, Biodiversidad y Manejo de Ecosistemas (GEBIOME), Departamento de Ciencias Biológicas, Facultad de Ciencias Exactas y Naturales, Universidad de Caldas, Calle 65 No. 26-10, Manizales 170004, Colombia

Corresponding author: Héctor E. Ramírez-Chaves ([hector.ramirez@ucaldas.edu.co](mailto:hector.ramirez@ucaldas.edu.co))



Academic editor: Miquéias Ferrão

Received: 28 October 2023

Accepted: 21 February 2024

Published: 25 March 2024

ZooBank: <https://zoobank.org/E7252895-B04A-4868-AABE-6EBEAB758073>

**Citation:** Caicedo-Martínez LS, Henao-Osorio JJ, Arias-Monsalve HF, Rojas-Morales JA, Ossa-López PA, Rivera-Páez FA, Ramírez-Chaves HE (2024) A new species of terrestrial toad of the *Rhinella festae* group (Anura, Bufonidae) from the highlands of the Central Cordillera of the Andes of Colombia. ZooKeys 1196: 149–175. <https://doi.org/10.3897/zookeys.1196.114861>

**Copyright:** © Luis S. Caicedo-Martínez et al. This is an open access article distributed under terms of the Creative Commons Attribution License ([Attribution 4.0 International – CC BY 4.0](https://creativecommons.org/licenses/by/4.0/)).

## Abstract

The genus *Rhinella* (Bufonidae) comprises 92 species of Neotropical toads. In Colombia, *Rhinella* is represented by 22 recognized species, of which nine belong to the *Rhinella festae* group. Over the past decade, there has been increasing evidence of cryptic diversity within this group, particularly in the context of Andean forms. Specimens of *Rhinella* collected in high Andean forests on both slopes of the Central Cordillera in Colombia belong to an undescribed species, *Rhinella kumanday* **sp. nov.** Genetic analyses using the mitochondrial 16S rRNA gene indicated that the individuals belong to the *festae* species group. However, they can be distinguished from other closely related species such as *Rhinella paraguas* and *Rhinella tenrec* by a combination of morphological traits including the presence of tarsal fold, a moderate body size, and substantial genetic divergence in the 16S rRNA gene (> 5%). Through this integrative approach, the specimens from the Central Cordillera of Colombia are considered an evolutionary divergent lineage that is sister to *R. paraguas*, and described as a new species. *Rhinella kumanday* **sp. nov.** is restricted to the Central Cordillera of Colombia inhabiting both slopes in the departments of Caldas and Tolima, in an elevational range between 2420 and 3758 m. With the recognition of this new species, the genus *Rhinella* now comprises 93 species with 23 of them found in Colombia, and ten species endemic to the country.

**Key words:** Andes, Central Cordillera, distribution, diversity, endemism, systematics

## Introduction

*Rhinella* Fitzinger, 1826 (Bufonidae) comprises 92 species of toads distributed mainly in the Neotropical region (Pereyra et al. 2021; Frost 2023). Over the past decades, several studies have delved into the taxonomic and phylogenetic complexity of the genus, resulting in the description of new species (Pramuk 2006;

Moravec et al. 2014; Castillo-Urbina et al. 2021; Lehr et al. 2021), and the systematics examination of specific species groups (Graybeal 1997; Maciel et al. 2006; Pramuk 2006; Chaparro et al. 2007; Fouquet et al. 2007; Narvaes and Rodrigues 2009; Pyron and Wiens 2011; Moravec et al. 2014; Pereyra et al. 2016; 2021; Rivera et al. 2021). In a more recent and comprehensive study of the systematics of *Rhinella*, Pereyra et al. (2021) defined eight distinct species groups based on a combination of osteological, muscular, external morphology, and molecular data: *R. arunco*, *R. crucifer*, *R. festae*, *R. granulosa*, *R. margaritifera*, *R. marina*, *R. spinulosa*, and *R. veraguensis*.

The *festae* group was first proposed based on genetic data by Moravec et al. (2014) and initially consisted of seven species. This group incorporated three species from the *acrolopha* group (including taxa previously considered within the genus *Ramphophryne* Trueb, 1971): *R. festae* (Peracca, 1904), *R. macrorrhina* (Trueb, 1971), and *R. rostrata* (Noble, 1920). Additionally, the *festae* group included four species from the paraphyletic *R. veraguensis* group: *R. manu* Chaparro, Pramuk & Gluesenkamp, 2007, *R. nesiotetes* Duellman & Toft, 1979, *R. chavin* Lehr, Köhler, Aguilar & Ponce, 2001, and *R. yanachaga* Lehr, Pramuk, Hedges & Córdova, 2007. More recently, Pereyra et al. (2021) redefined the *festae* group, which now comprises 20 species, including two yet-to-be described species from Colombia and Peru. The undescribed species from Colombia was identified based on a single specimen collected at the Central Cordillera in the Andean region of the Department of Tolima (Pereyra et al. 2021).

Pereyra et al. (2021) expanded the *festae* group by reclassifying ten species that were previously part of the *acrolopha* group from Colombia, Ecuador, Panama, and Peru. Furthermore, Pereyra et al. (2021) resolved the paraphyly of the *veraguensis* group by reassigning eight species from Bolivia and Peru in the *festae* group. As a result of these changes, together with the addition of recently described species have brought the *festae* group to a total of 22 species (two remaining undescribed) including: i) *R. acrolopha* (Trueb, 1971), ii) *R. arborescandens* (Duellman & Schulte, 1992), iii) *R. chavin*, iv) *R. chullachaki* Castillo-Urbina, Glaw, Aguilar-Puntriano, Vences & Köhler, 2021, v) *R. lilyrodriguezae* Cusi, Moravec, Lehr & Gvozdik, 2017, vi) *R. festae*, vii) *R. lindae* (Rivero & Castaño, 1990), viii) *R. macrorrhina*, ix) *R. manu*, x) *R. moralesi* Lehr, Cusi, Rodríguez, Venegas, García-Ayachi & Catenazzi, 2021, xi) *R. multiverrucosa* (Lehr, Pramuk & Lundberg, 2005), xii) *R. nesiotetes*, xiii) *R. nicefori* (Cochran & Goín, 1970), xiv) *R. paraguas* Grant & Bolívar-G., 2014, xv) *R. rostrata*, xvi) *R. ruizi* (Grant, 2000), xvii) *R. tacana* (Padial, Reichle, McDiarmid & De La Riva, 2006), xviii) *R. tenrec* (Lynch & Renjifo, 1990), xix) *R. truebae* (Lynch & Renjifo, 1990), xxi) *R. yanachaga*, and the two undescribed species, one each from Peru and Colombia in Pereyra et al. (2021).

In Colombia, *Rhinella* is represented by 22 recognized species, nine of which belong to the *festae* group (Pereyra et al. 2021). Most of these species are primarily found in restricted montane regions, in elevations ranging from moderate to highland altitudes (1400–3100 m a.s.l.) in the Andes. The exception to this pattern is *R. acrolopha* which is distributed in the Biogeographic Chocó Region (Trueb 1971; Lynch and Renjifo 1990; Grant and Bolívar-G 2014; Pereyra et al. 2021). Among the *festae* group, one of the two undescribed species occurs in the Central Cordillera of Colombia, along the road between the cities of Manizales in the Department of Caldas (Rojas-Morales et al. 2014), and

Murillo, Department of Tolima (Machado et al. 2016; Pereyra et al. 2021). In the last two decades, individuals tentatively assigned to this undescribed species have been recorded in the highlands of the municipality of Villamaría, Caldas, in close proximity to the previously reported localities (see Rojas-Morales et al. 2014; Rojas-Morales and Marín-Martínez 2019). After conducting a meticulous revision of the specimens from the Central Cordillera of the Department of Caldas using morphological and genetic analyses, we found that they possess distinct morphological and genetic characteristics that warrant their classification as a new species. This new species is exclusively found in Andean ecosystems that are highly threatened. Recognizing the taxonomic status of these populations is crucial for effective conservation planning. Therefore, in this study, we formally describe the specimens from the Central Andes in the departments of Caldas and Tolima, previously categorized within the *festae* group, based on genetic analyses and discrete external and osteological traits.

## Materials and methods

To morphologically diagnose the new species, we reviewed specimens of *Rhinella* from the Central Cordillera of Colombia, deposited in the Colección de Anfibios of the Museo de Historia Natural of the Universidad de Caldas (**MHN-UCa-Am**), and a collection of new specimens, which were euthanized with 5% lidocaine, fixed in 10% formalin and stored in 70% ethanol. The diagnosis follows the proposal by Trueb (1971) and Grant and Bolívar-G. (2014); the osteological description was carried out based on two double stained and cleared specimens (MHN-UCa-Am 1492, 1802). For this procedure, we followed the protocol proposed by Taylor and Van-Dyke (1985) and the modifications made by Fernández-Blanco and Witmer (2020); osteological terminology and characters were taken from Pramuk (2006) corrected by Pereyra et al. (2021), as well as those reported by Deforel et al. (2021). We also used the species description of Vélez-R and Ruiz-C (2002), Grant and Bolívar-G. (2014) and Castillo-Urbina et al. (2021) for comparison. We described the webbing formulae following to Savage and Heyer (1967) and the modifications by Myers and Duellman (1982) and Savage and Heyer (1997). Fingers were counted from pre-axial to post-axial side as I–IV in hand and I–V in foot; the comparative length of fingers I and II was taken by adpressing to each other, and adpressing toes III and V to toe IV (Castillo-Urbina et al. 2021). We took external measurements using a digital caliper ( $\pm 0.01$  mm) following Castillo-Urbina et al. (2021) and included: Snout-vent length (**SVL**); Head width (**HW**); Head length (**HL**); horizontal eye diameter (**ED**); interorbital distance (**IOD**); upper eyelid width (**EW**); upper eyelid length (**EL**); internarial distance (**IND**); Eye-nostril distance (**E-N**); Nostril-snout distance (**NSD**); snout length (**SL**); forearm length (**FL**); hand length (**HNDL**); femur length (**FEML**); tibia length (**TL**); foot length (**FOOTL**) and, parotoid length (**PL**).

To compare genetic affinities of the *Rhinella* from the Central Cordillera in the Department of Caldas, we extracted genomic DNA from two specimens from tissues preserved in 96% ethanol. DNA was extracted with a Wizard® Genomic DNA Purification kit (Promega Corporation) following the manufacturer's protocol, with modifications in the incubation time (24 h). We performed amplification of the mitochondrial 16S gene using primers 16S Ar-L 5'–CGCCTGTTTATCAAAAACAT–3' 16S Br-H 5'–CCGGTCTGAACTCAGATCACGT–3' which amplify

a fragment of  $\approx 520$  bp (Palumbi et al. 1991). The PCR products were sent to MacroGen Inc. (South Korea) for purification and sequencing. The sequences were analyzed in Geneious Prime® v. 2023.1.2 software.

A phylogenetic analysis was performed following the updated taxonomy by Pereyra et al. (2021), including the species of the *R. festae* group, except for species *R. moralesi* and *R. truebae* that lack sequences in GenBank. In total, 185 DNA sequences previously reported in GenBank were used for the analysis, with *Anaxyrus americanus* (Holbrook, 1836), *A. woodhousii* (Girard, 1854), and *A. quercicus* (Holbrook, 1840) used as the outgroup (Suppl. material 1). Sequence alignment was performed in MAFFT v. 7 (Kato and Standley 2013), ambiguously aligned fragments were removed using Gblocks (Talavera and Castresana 2007) included in PhyloSuite (Zhang et al. 2020). The best fit evolutionary model was selected across ModelFinder (Kalyaanamoorthy et al. 2017) using AIC criterion: TIM2+F+I+G4. Phylogenetic inferences were constructed using Maximum Likelihood (ML) in IQ-TREE v 2.2.0 (Nguyen et al. 2015) with 1000 ultrafast-bootstrap (UFB) (Minh et al. 2013), as well as the Shimodaira–Hasegawa–like approximate likelihood-ratio test (Guindon et al. 2010). We used FigTree v. 1.4.3 to visualize the phylogenetic tree (Rambaut 2007). Genetic distances were estimated using the *p-distance* method with the MEGA v. 11 program.

## Results

We reviewed nine specimens of the *R. festae* group deposited in the collections of the MHN-UCa-Am (including one specimen preserved as skeleton). The specimens exhibited morphological characteristics commonly associated with the *R. festae* group including the absence of the annulus tympanicus and tympanic membrane, a slightly exostosed skull; webbed fingers; a poorly developed preorbital crest, and a weak supratympanic crest. In addition to these typical traits, we also identified a set of unique morphological traits that set them apart from other *Rhinella* species distributed in the Central Cordillera and neighboring areas (i.e., *R. acrolopha*, *R. festae*, *R. lindae*, *R. macrorhina*, *R. nicefori*, *R. paraguas*, *R. rostrata*, *R. truebae*, and *R. tenrec*). The distinct traits included the presence of a tarsal fold, the extent of skull ornamentation, and the number of vertebrae (seven).

For the genetic comparisons, we generated two new mitochondrial 16S rDNA sequences [accession numbers: OR680126; OR680127] from two specimens (MHN-UCa-Am 1164 and 1462). Both sequences exhibit a 100% similarity with a single sequence [KT221613] identified as *Rhinella* sp. “gr. *acrolopha*” (Pereira et al. 2021: 112) or “*Rhinella* sp. 4” originating from a specimen collected at in Murillo, km 22 road Murillo-Manizales, Department of Tolima. The collection or museum in which the specimen from which the sequence KT221613 was obtained is deposited is unknown. The interspecific genetic distances (Table 1) between the specimens of *Rhinella* from the Central Cordillera and other species within the *R. festae* group (except for *R. moralesi* and *R. truebae*) ranged from 3.6% to 10.1% for the 16S gene (Table 1) and are within the ranges known for different species of the group. The phylogenetic relationships based on Maximum Likelihood (ML) recovered our sequences together with the one from the Department of Tolima with a support of 99.5/100% (Fig. 1, Table 1) within the species of *R. festae* group. Finally, the *R. festae* group clade is also supported by 100/100.

**Table 1.** Genetic distances between species of *R. festae* group. Intraspecific (on the diagonal) and interspecific (below the diagonal) distances based on *p-distance* method for the mitochondrial 16S rRNA gene.

Species	Accessions	1	2	3	4	5	6	7	8	9	10	11	12	13	14	15	16	17	18	19	20	21	
1 <i>Rhinella kumanday</i> sp. nov. MHN-Uca-Am 1164	[OR680126]	/																					
2 <i>Rhinella kumanday</i> sp. nov. MHN-Uca-Am 1492	[OR680127]	0.000	/																				
3 <i>Rhinella</i> sp. 4	[KT221613]	0.000	0.000	/																			
4 <i>Rhinella</i> cf. <i>nicefori</i>	[MW003543]	0.036	0.037	0.053	/																		
5 <i>Rhinella ruizi</i>	[MW003567; MW003568]	0.038	0.039	0.054	0.001	0.000																	
6 <i>Rhinella paraguas</i>	[MW003552; MW003553]	0.055–0.057	0.056–0.058	0.057–0.063	0.050–0.055	0.051–0.057	0.035																
7 <i>Rhinella acrolopha</i>	[MW003440; MW003441]	0.069–0.070	0.070–0.072	0.079–0.081	0.074–0.075	0.075–0.076	0.083–0.088	0.011															
8 <i>Rhinella macrorhina</i>	[MW003517; MW003518; MW003519; MW003520]	0.080–0.083	0.082–0.085	0.083–0.092	0.076–0.082	0.077–0.083	0.074–0.095	0.079–0.022	0.000–0.022														
9 <i>Rhinella tenrec</i>	[MW003593; MW003594]	0.099	0.101	0.095–0.099	0.090–0.092	0.092–0.093	0.090–0.099	0.076–0.088	0.064–0.066	0.000													
10 <i>Rhinella lindae</i>	[MW003514; MW003515; MW003516]	0.065	0.066	0.066–0.073	0.060–0.061	0.062–0.063	0.060–0.075	0.060–0.067	0.060–0.067	0.070–0.075	0.000–0.002												
11 <i>Rhinella arborescendens</i>	[MW003449; MW003450; MW003451]	0.063–0.066	0.064–0.067	0.073–0.075	0.066	0.067	0.068–0.077	0.066–0.071	0.063–0.068	0.079–0.081	0.053–0.060	0.000–0.018											
12 <i>Rhinella rostrata</i>	[AF375533]	0.066	0.069	0.080	0.080	0.082	0.096–0.099	0.083–0.084	0.075–0.094	0.094–0.098	0.074–0.083	0.079–0.080	/										
13 <i>Rhinella festae</i>	[KR012624; DQ158423]	0.066–0.067	0.068–0.069	0.074–0.078	0.064–0.070	0.065–0.071	0.074–0.080	0.075–0.083	0.054–0.076	0.077–0.087	0.052–0.067	0.060–0.070	0.017–0.019	0.000									
14 <i>Rhinella chullachaki</i>	[MW493261]	0.081	0.081	0.081	0.079	0.081	0.085–0.094	0.083–0.104	0.102–0.104	0.126	0.086	0.069–0.075	0.070	0.075–0.078	/								
15 <i>Rhinella lilyrodriguezae</i>	[MW003509; MW003510; MW003511]	0.082–0.085	0.084–0.088	0.080–0.083	0.078–0.082	0.079–0.083	0.084–0.091	0.088–0.094	0.080–0.094	0.097–0.109	0.073–0.083	0.061–0.064	0.089–0.096	0.077–0.083	0.058	0.001–0.023							
16 <i>Rhinella chavin</i>	[DQ158441]	0.079	0.081	0.091	0.084	0.085	0.086–0.090	0.081–0.082	0.087–0.099	0.091–0.094	0.075–0.082	0.074–0.078	0.090	0.076–0.085	0.070	0.068–0.072	/						
17 <i>Rhinella</i> cf. <i>multiverrucosa</i>	[MW003540]	0.072	0.074	0.086	0.080	0.082	0.083–0.089	0.080–0.081	0.084–0.095	0.086–0.091	0.072–0.079	0.071–0.077	0.090	0.074–0.083	0.065	0.067–0.071	0.000	/					
18 <i>Rhinella yanachaga</i>	[MW003603; MW003604]	0.064–0.066	0.066–0.068	0.085–0.087	0.078–0.080	0.079–0.081	0.077–0.090	0.079–0.085	0.086–0.097	0.094–0.096	0.064–0.081	0.068–0.071	0.092–0.094	0.078–0.083	0.059–0.061	0.067	0.043–0.046	0.040–0.042	0.002				
19 <i>Rhinella manu</i>	[MW003523]	0.089	0.091	0.085	0.073	0.075	0.092	0.090	0.097	0.102	0.084	0.072	0.074	0.072–0.074	0.085	0.088–0.091	0.084	0.082	0.079–0.082	0.000			
20 <i>Rhinella nesioties</i>	[MW003541; MW003542]	0.079–0.082	0.081–0.084	0.083–0.084	0.080–0.082	0.081–0.083	0.077–0.081	0.090–0.095	0.077–0.080	0.094–0.099	0.080–0.084	0.072–0.078	0.074–0.082	0.068–0.077	0.089–0.091	0.079–0.084	0.082–0.088	0.082–0.085	0.085–0.089	0.048–0.050	0.006		
21 <i>Rhinella tacana</i>	[MW003589; MW003590; MW003592]	0.076–0.084	0.078–0.084	0.085–0.088	0.080–0.083	0.082–0.085	0.081–0.106	0.090–0.094	0.079–0.096	0.097–0.102	0.088–0.092	0.072–0.081	0.072–0.085	0.072–0.081	0.074–0.081	0.085–0.091	0.087–0.093	0.083–0.090	0.079–0.058	0.050–0.058	0.022–0.025	0.001–0.009	

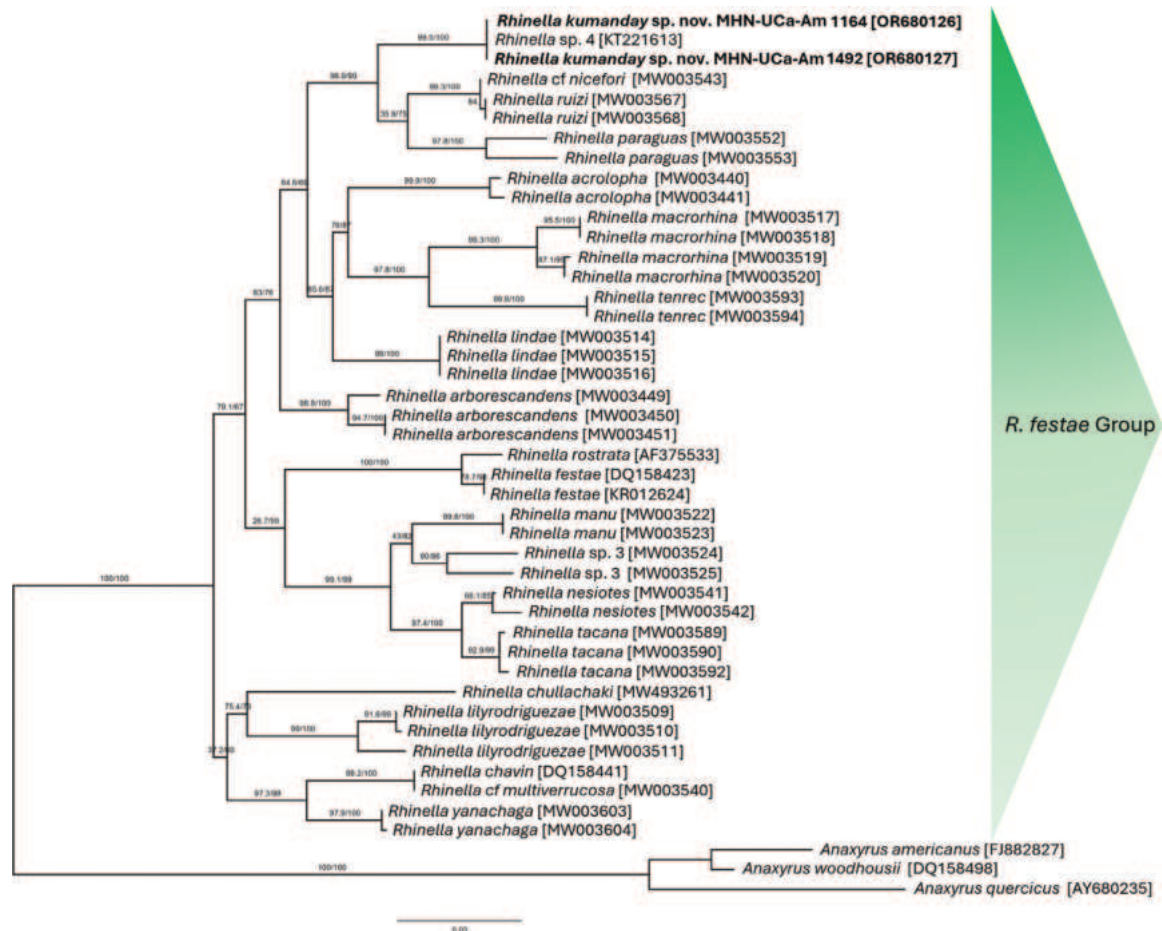


**Figure 1.** Phylogenetic tree of the partial sequences of the 16S gene of the species of *Rhinella*. The accessions in the present study (in bold), and of the sequences in GenBank (accession numbers in bracket), using maximum likelihood (ML) method under the TIM2+F+I+G4 model. Numbers at nodes are selbranch support analyses; from left to right: ultrafast bootstrap values, and Shimodaira–Haseglike approximate likelihood ratio test (SH-like aLRT). Three species of *Anaxyrus* sequences were used as outgroups.

Based on our analyses, we concluded that the specimens from the Central Cordillera of Colombia in the departments of Caldas and Tolima do not represent any of the described *Rhinella* species. Therefore, we assert that they belong to a new, undescribed species that we thoroughly document and describe in this study as *Rhinella kumanday* sp. nov.

## Systematics

### Family Bufonidae Gray, 1825

### Genus *Rhinella* Fitzinger, 1826

#### *Rhinella kumanday* sp. nov.

<https://zoobank.org/3392CAEB-0277-419E-ADAE-F03B1B1D697A>

Figs 2–6

Suggested English name: Kumanday Beaked Toad

Suggested Spanish name: Sapo picudo del Kumanday

*Rhinella* sp.: Rojas-Morales et al. 2014: 87, 89.

*Rhinella* sp. C.: Machado et al. 2016: 687, 688, 689, 690, 692, table 1.

*Rhinella* sp. C: Cusi et al. 2017: 26, 42, 43.

*Rhinella* sp. Gómez-Salazar et al. 2017: 78, table 1.

*Rhinella* sp. C (= *Rhinella* sp. *acrolopha* group sensu Grant and Bolívar-G. 2014): Cusi et al. 2017: 27, table 1.

*Rhinella* sp.: Rojas-Morales and Marín-Martínez 2019: 13266, 13269, 13270, 13271, 13274, image 4B, fig. 4, appendix 1

*Rhinella* sp. 4: Pereyra et al. 2021: 40, 63, 65, 112, 131, fig. 13, table 10, appendix 1, appendix suppl. data 2, suppl. data 3.5, suppl. data 4.5, map 7.

*R*[*hinella*]. sp. "gr. *acrolopha*": Pereyra et al. 2021: 112, 131, appendix 1, appendix 2.

*R*[*hinella*]. sp. 'C': Castillo-Urbina et al. 2021: 182, 184, fig. 1.

**Type material examined. Holotype.** MHN-UCa-Am 1164 (adult female, Fig. 2), from Torre 4, Reserva Forestal Protectora Bosques de la CHEC, municipality of Manizales, Department of Caldas, Colombia (5.0266, -75.39299), 2730 m collected by Jose J. Henao-Osorio (JJHO) on 24 October 2019. **Paratypes** ( $n = 6$ ): 3 females, 2 males, 1 indeterminate sex (Figs 3, 4). Two adult males (MHN-UCa-Am 196, 199) and one adult female (MHN-UCa-Am 198), from Reserva Forestal Protectora Bosques de la CHEC, municipality of Villamaría, Department of Caldas, Colombia (4.99833, -75.39194; 2954 m) collected by Oscar López-Castrillón (OLC-005), Luisa F. Galvis (LFG-009) and Juan M. Pérez (JMP-010) respectively, on 12 October 2012. An adult female (MHN-UCa-Am 1698) from El Cedral, Reserva Forestal Protectora Bosques de la CHEC, municipality of Villamaría, Department of Caldas (5.027671, -75.414618, 2695 m) collected by Héctor F. Arias-Monsalve on 5 March 2023. one female (MHN-UCa-Am 1718) from Reserva Ecológica Río Blanco, municipality of Manizales, Department of Caldas (5.074302, -75.43353, 2705 m,) collected by L. Santiago Caicedo-Martínez (SCM-139) on 25 May 2023. An individual with unknown sex (MHN-UCa-Am 1492, stained skeleton) from the Reserva Forestal Protectora Bosques de la CHEC in Gallinazo, municipality of Villamaría, Department of Caldas (4.99833, -75.39194, 2954 m) collected by Héctor F. Arias-Monsalve (HFA-364) on 23 February 2022.

**Other specimens examined.** Three females, the first (MHN-UCa-Am 421) from Vereda Montaña municipality of Villamaría, Department of Caldas (4.99213, -75.45565, 2433 m) collected by Gustavo Gonzales-Durán (GGD-055) on 18 May 2009; the second (MHN-UCa-Am 1717) from Reserva Ecológica Río Blanco, municipality of Manizales, Department of Caldas (5.074720, -75.434795, 2667 m) by SCM (138) on 25 May 2023; and the third (MHN-UCa-Am 1802) collected at the Reserva Ecológica Río Blanco.

**Diagnosis.** A moderate-sized species of the *Rhinella festae* group sensu Pereyra et al. (2021), and which can be distinguished from other members of the genus by the following combination of characters: males SVL 36.4–37.8 mm ( $\bar{x} = 37.1$ ;  $n = 2$ ); females SVL 32.5–40.1 mm ( $\bar{x} = 37.1$ ;  $n = 5$ ). (1) seven pre-sacral vertebrae; (2) sacral vertebrae no fused with the coccyx, but fused with the urostyle; (3) sagittal ridge present; (4) snout long, protuberant and directed anteroventrally; (5) canthal crest present but weak; (6) preorbital crest present; (7) supraorbital present; (8) postorbital crest weak; (9) pretympanic crests weak; (10) supratympanic crest distinct; (11) parietal crest present; (12) dorsal

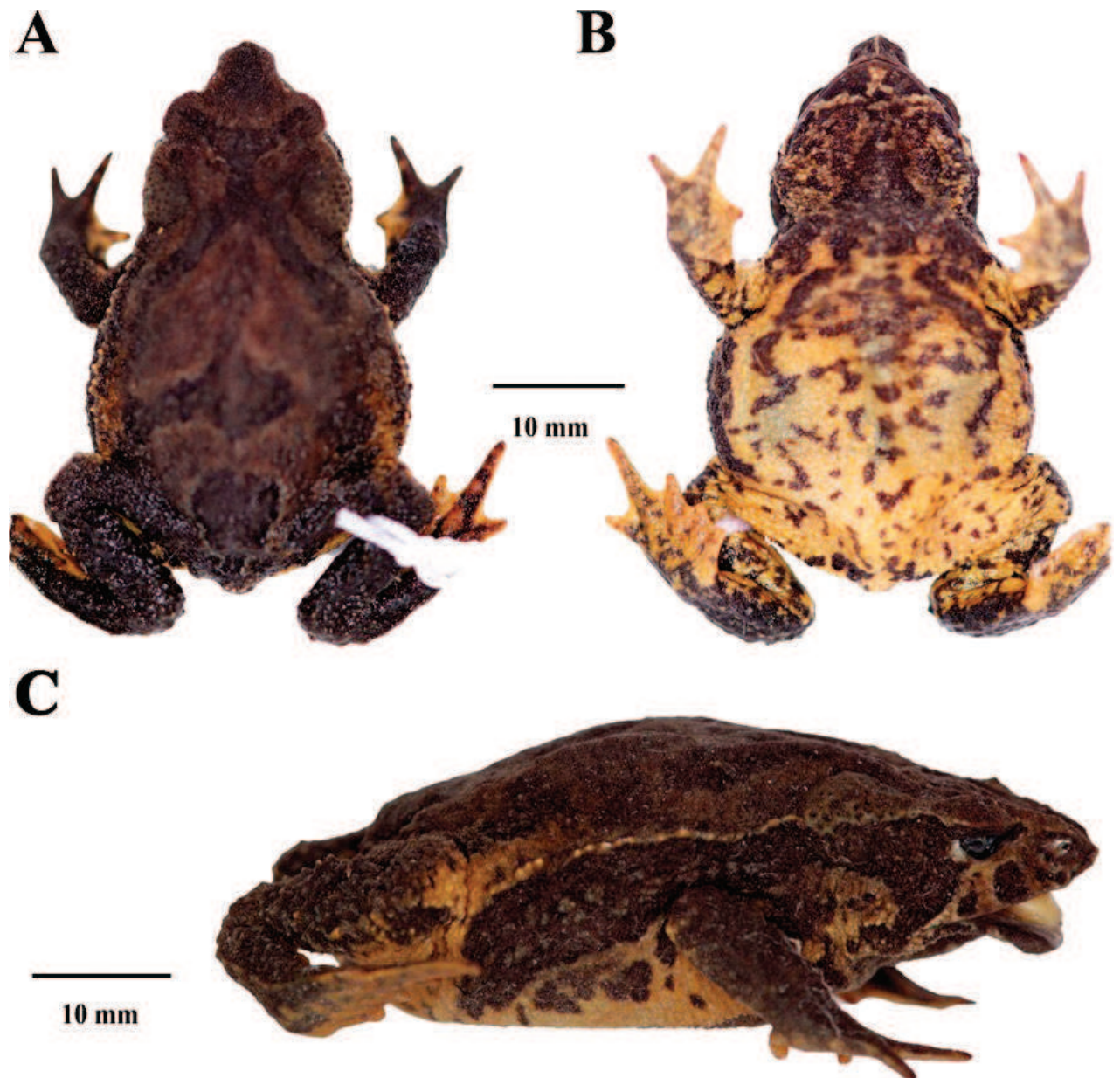


Figure 2. Holotype of *Rhinella kumanday* sp. nov. (MHN-UCa-Am 1164, adult female), SVL 39.4 mm, in preservative **A** dorsal view **B** ventral view **C** lateral view.

surface with scattered tubercles, small and round with some conical ones; (13) parotoid glands well developed and ovoid; (14) lateral row of tubercle variable from scattered conical tubercle from the posterior side of the parotoid gland until 2/3 of the lateral space to the groin, to a complete fold of conical tubercles from the posterior part of the parotoid glands to the groin; (15) skin on dorsal surface of limbs with many warts and conical tubercles; (16) finger I smaller than II; (17) fingers and toes moderate webbed, digits long; (18) subarticular tubercles diffuse, barely evident in some individuals (19) many supernumerary tubercles, small, round and low; (20) modal webbing in hand: I 1–2 II 1–2 III–2–2 IV; in foot: I 0–0 II 0–2 III 1–3 IV 3–1 V; (21) males without vocal slits; (22) nuptial pads absent in males; (23) testes small and black; (24) coloration in life: dorsum light brown, in some cases with few dark spots and/or cream



**Figure 3.** Female (MHN-UCa-Am 1698; paratype) of *Rhinella kumanday* sp. nov. in life (SVL 35.01 mm).

middorsal line; flanks dark yellow with many grey and dark mottling; venter creamy yellow with variable size marks dark brown; iris golden with irregular dark brown marks.

**Description of the Holotype (Figs 2, 4).** Adult female (SVL = 39.43 mm; Fig. 2), body robust; head triangular in dorsal view, protruding and sharp in lateral view; head wider than long (HW 1.5 times HL) narrower than body; HW and HL 34.1% and 22.8% of SVL, respectively. Snout acuminate, triangular in the tip; SL 59.9% of the HL; the distance from the nostril to the tip of the snout is equal to the distance from the anterior margin of the eye to the nostril (2.6 mm); snout protruding and sharp; upper jaw directed beyond the lower. Snout protruding with a sagittal ridge between the upper lip and the point of the snout. *Canthus rostralis* elevated forming a weak canthal crest, concave in dorsal view; loreal region concave; nostril round, small and protuberant, no visible from dorsal view; eye diameter more than half of the interorbital distance ( $ED/IOD = 0.53$ ); ED longer than the distance between eye and nostril ( $ED/E-N = 1.25$ ). Canthal crest present but weak; preorbital crest non evident but present; supraorbital crest present; postorbital crest weak; supratympanic crest present, distinct, expanded laterally; pretympanic crest present. Tympanic annulus and tympanic membrane absent. Parotoid glands subtriangular, large, almost two times ED ( $PL/ED = 1.88$ ). Skin of the eyelid with abundant small warts of different shapes and sizes, eyelid edge above the eye forming a thick fold. Forearm slender, 25.4% of SVL; forearm skin bearing abundant subconical warts and smaller

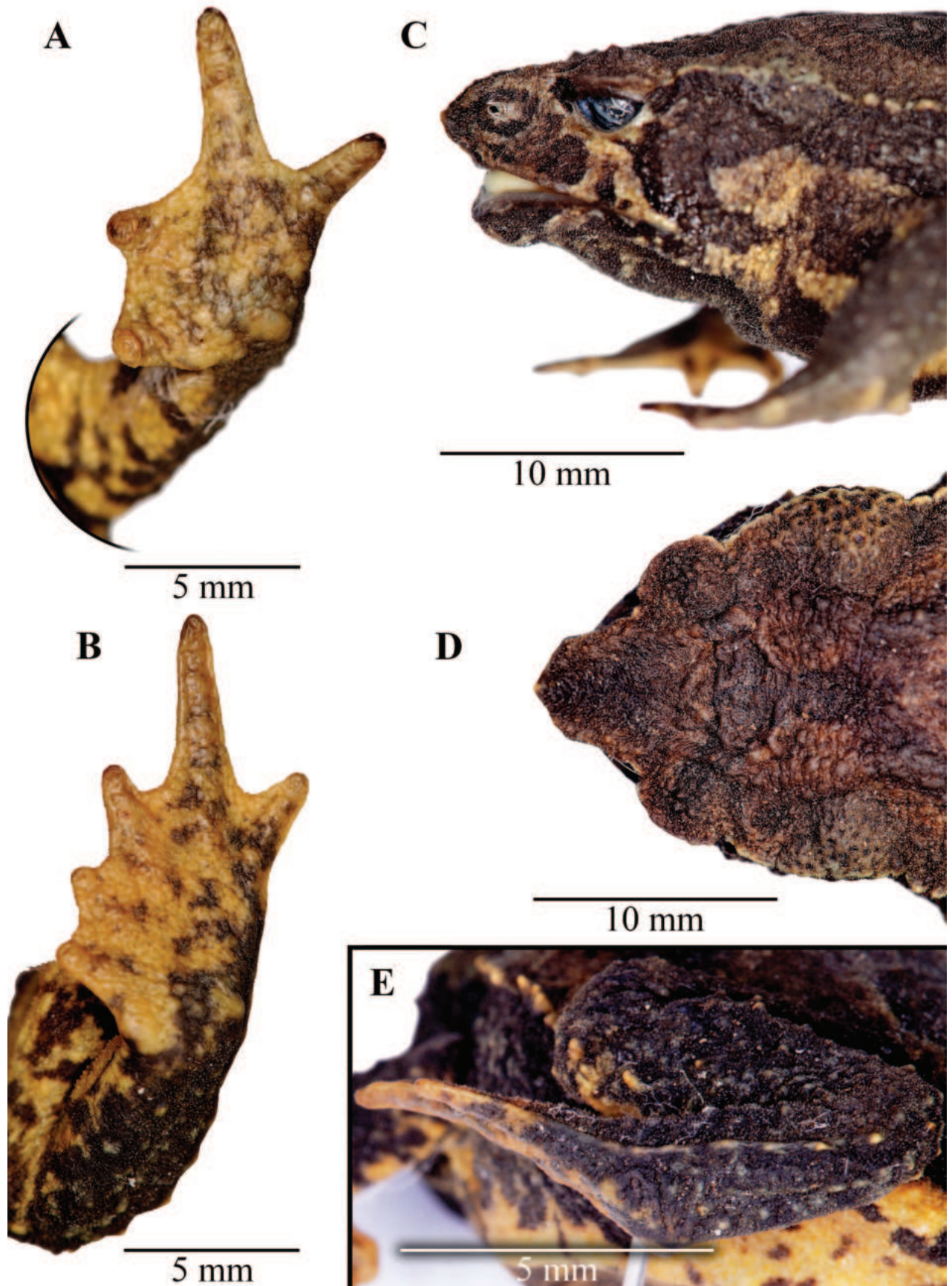


**Figure 4.** Head, hand, and foot of the holotype of *Rhinella kumanday* sp. nov. (MHN-UCa-Am 1164) **A** dorsal view of head **B** lateral view of head **C** ventral view of right hand **D** ventral view of right foot **E** tarsal fold on the left foot.

conical tubercles along the entire surface. Hands long, slender, hand length 25.1% of SVL; hands densely covered by minute tubercles in the entire dorsal surface; fingers slender and long; relative length of fingers  $I < II < IV < III$ ; finger tips round; basal webbing between fingers present, webbing formula: I 1–2 II 2–3 III 3–2<sup>+</sup>IV; fingers with lateral fringes; palmar and thenar tubercles distinct, small and ovoid; thenar less than a half of palmar tubercle; palmar surface of the hand with multiple accessory tubercles like warts and minute tubercles barely visible; supernumerary and subarticular tubercles diffuses. Hindlimbs short, robust; femur length and tibia length 33.7% and 34.6% of SVL, respectively; entire surface of the hindlimbs covered with abundant warts and conical and subconical tubercles of different sizes foot long, 33.2% of SVL; toes long and slender; relative length of toes  $I < II < III < V < IV$ ; toes tip round; toes with extensive webbing between toe I and II, moderate in toes III, IV and V, webbing formula: I 0–0 II 0<sup>+</sup>–2<sup>+</sup> III 1–3 IV 3–1<sup>+</sup> V; fingers bearing lateral fringes; tarsal fold present, formed from the postaxial lateral fringe of toe V, in the portion proximal to the heel the tarsal fold is replaced by tubercles; outer metatarsal tubercle barely visible, round, ~ 3× smaller than the round inner metatarsal tubercle; plantar surface with flat warts indistinct, accessory tubercles small, indistinct; supernumerary tubercles indistinct; subarticular tubercles diffuses, round.

Dorsum with scattered subconical, round warts with hard tips and densely covered with minute conical tubercles; lateral row of subconical tubercles from the posterior region of the parotoid gland to insertion of the groin, forming a discontinuous fold. Skin more granular in the flanks with more prominent warts densely distributed. Skin on venter with minute tubercles; chest and gular region more granular than venter. Cloacal opening protuberant, directed posteriorly at mid-level of the thighs. Tongue robust, ~ 2× longer than wide; notched anteriorly, one half free posteriorly. Choana small and ovoid, widely separated. Maxillary, premaxilla and vomerine teeth absent. Measurements of the holotype (mm). SVL: 39.4; HW: 13.4; HL: 9; ED: 3.3; IOD: 6.1; EW: 3.3; EL: 4.3; IND: 4.0; E-N: 3.1; NSD: 2.6; SL: 5.4; FL: 10.0; HNDL: 9.9; FEML: 13.3; TL: 13.6; FOOTL: 13.1; PL: 6.2.

**Coloration of Holotype in life.** Head mainly brown with some darker zones in the tympanic region; the pupil is circular and the iris appears golden, accompanied by black mottled spots that become more grouped near the sclera. The suborbital area is cream yellowish and extend in two lines of the same color, one ends in the mouth corner, and the second, reach the upper lip. The dorsal surface has a light brown background with a dark brown medial band that start at the interorbital space covering both eyelids and extend medially toward the cloacal sheath, becoming a discontinuous mark in the latter; at the level of the parotoid glands and the middle of the dorsum, the aforementioned band turns into an inverted V-shaped mark. The flanks of the body have a light brown coloration, in which highlights a cream yellowish line that extends from the upper eyelid to the groin that is cream yellowish with few black spots, crossing the parotoid glands and the fine lateral row of tubercles. The ventral surface of the body and posterior and anterior extremities have a cream yellowish background, with the presence of brown mottle marks that are more concentrated at gular region and turn diffuses towards the posterior region of venter. The cloacal opening has a divide coloration, in which the upper region is brown with yellow spots, and the lower region has a cream yellowish with brown marks. The tarsal fold is light yellow and extend from the keel to the distal point of the toe V.

**Coloration of holotype in preservative (Figs 2, 4).** The head has mainly a dark brown coloration; the tympanic region is dark brown; the suborbital region has a yellow mustard color and form two lines of the same color that extends to the mouth corner and the upper lip, respectively. The dorsum has a light brown background with a darker band that start in the interorbital space and covers both eyelids and extends to the cloaca turning in a diffuse mark in this region; at the level of the parotoid glands and the middle of dorsum this band forms an inverted V-shaped mark. The flanks are dark brown almost black with a cream yellowish line that start at the upper eyelid and extends to the groin that has a yellow background with black spotting, crossing the brown parotoid glands. The dorsal surfaces of the extremities are dark brown with cream yellowish marks at the webbing and the tips of the fingers and toes. The ventral surfaces of the body and extremities have brown mottled marks on a yellow mustard background; the brown marks are concentrated in the gular region turning into diffuse marks toward the cloaca. The cloaca has two different colorations, in which the upper region is brown with few yellow spots, and the lower region has a yellow background with brown marks. The tarsal fold is yellow.

**Variation.** There is variation in the measurements between females and males in which females have a longer size in some structures (Table 2). There is also variation in the degree of the dorsolateral row of prominent tubercles as follow: scattered conical tubercles that does not form a row (MHN-UCa-Am 198–199); lateral row of conical tubercles from the anterior part of the parotid glands to 2/3 of the lateral space to the groin (MHN-UCa-Am 196, 0412); complete lateral row of conical tubercles from the anterior part of the parotid glands to the groin (MHN-UCa-Am 1164). Head triangular in dorsal view pointed at the tip in females (MHN-UCa-Am 198, 421, 1164) or blunt at the tip in males (MHN-UCa-Am 196, 199). The color patterns vary among the type series from light brown with darker markings in the dorsum (MHN-UCa-Am 196), a darker brown dorsum with diffuse dark marks (MHN-UCa-Am 198, Am 421, Am 1717; Fig. 5B, H, I, respectively) to a dark brown, almost black dorsum with indistinct black marks (MHN-UCa-Am 199, Am 1698, Am 1718, Fig. 5A, C and G, respectively; and Am 1164, Fig. 2A). Three individuals have a cream/yellowish longitudinal line in the dorsum (MHN-UCa-Am 199, 421, 1718, Fig. 5A, G, I). The variability in the degree of the dark brown mottling and markings in the venter is high (Fig. 5D–F, J–L); the chest and gular region varies from a light cream yellowish background with diffuse and thin dark brown marks more abundant from chest to the gular region (MHN-UCa-Am 196, 421, 1698, 1717) to a cream colored background with thick and abundant dark brown to black markings along the entire venter and completely dark in chest and gular region (MHN-UCa-Am 198–199, 1718). Two individuals present two light cream lines, one longitudinal from the tip of lower lip to the cloacal opening and the second horizontal from the insertion of the arm (MHN-UCa-Am 199, 421). The females have large eggs with a cream-yellow color and lacking reticulations (Fig. 6A). The males lack nuptial excrescences and vocal slits, the testes are small and present black reticulations (Fig. 6B).

**Osteological description.** The following description is based on two stained and cleared adult female specimens (MHN-UCa-Am 1802, SVL = 35.98 mm; MHN-UCa-Am 1492, SVL = 35.01 mm).

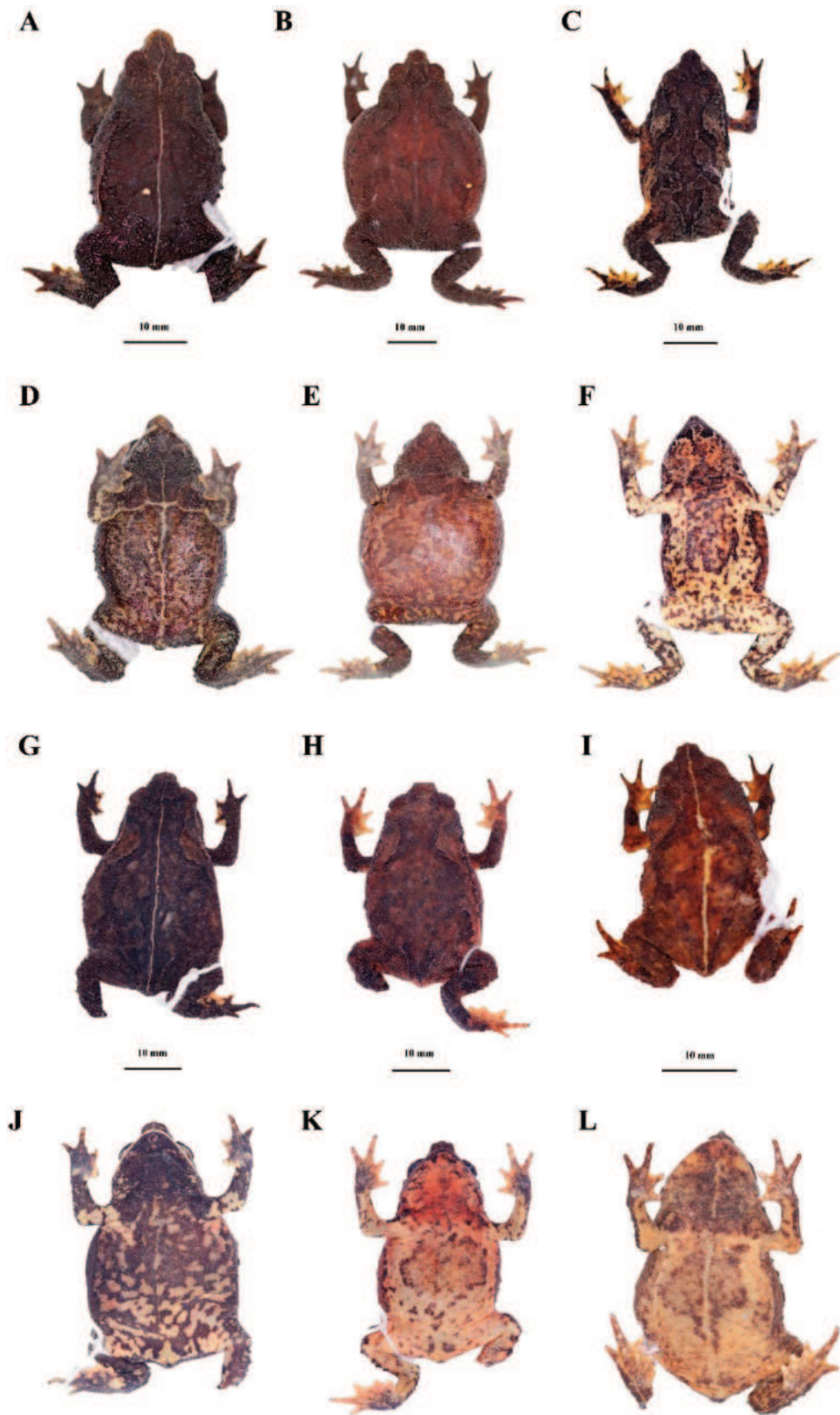


**Figure 5.** Paratypes and referred specimens of *Rhinella kumanday* sp. nov. in preservative **A, B, C, G–I** dorsal views (MHN-UCa-Am 199, 198, 1698, 1718, 1717, 421, respectively) and ventral views **D–F, J–L** (MHN-UCa-Am 199, 198, 1698, 1718, 1717, 421, respectively).

**Table 2.** Measurements taken to the nine individuals of *Rhinella kumanday* sp. nov. housed in the MHN-UCa-Am. For the measurements definitions see Materials and methods. MHN-UCa-Am 421, 1717, and 1802 are not part of the type series.

Measurements	Female holotype MHN-UCA-AM 1164	Female MHN-UCA-AM 198	Juvenile female MHN-UCA-AM 421	Female MHN-UCA-AM 1698	Female MHN-UCA-AM 1717	Female MHN-UCA-AM 1718	Female MHN-UCA-AM 1802	Male MHN-UCA-AM 196	Male MHN-UCA-AM 199
SVL	39.4	40.1	32.5	35.01	35.54	37.71	35.98	36.4	37.8
HW	13.4	13.7	12.1	12.36	12.51	13.26	11.08	11.6	11.5
HL	9	8.7	7.2	9.45	9.87	9.61	8.30	6.1	8.0
ED	3.3	3.2	3.5	3.12	3.87	3.59	3.92	3.1	3.2
IOD	6.1	5.5	4.4	4.23	4.56	4.84	3.85	5.7	2.8
EW	3.3	2.6	3.4	2	3.55	3.21	3.02	2.8	2.7
EL	4.3	3.7	4.3	3.19	4.71	4.42	3.35	4.8	4.2
IND	4.0	3.8	3.4	3.3	3.64	3.63	3.86	3.5	3.8
E-N	3.1	2.4	2.4	2.52	2.82	2.81	–	2.3	2.1
NSD	2.6	2.9	2.4	1.63	2.5	2.49	3.3	2.8	2.7
SL	5.4	5.2	4.5	4.96	4.93	5.06	–	5.6	5.2
FL	10.0	9.0	6.9	8.55	8.36	7.96	10.06	7.1	7.0
HNDL	9.9	9.6	7.4	9.39	9.06	8.33	4.59	8.6	8.5
FEML	13.3	10.9	9.9	12.6	12.69	12.79	13.32	8.2	9.0
TL	13.6	12.8	9.6	11.42	11.44	10.91	14.99	11.3	10.5
FOOTL	13.1	11.6	10	12.03	11.67	11.12	14.21	11.1	10.9
PL	6.2	5.9	5.7	4.84	4.35	4.7	–	5.8	5.4

**Cranium.** Shape of anterior margin of nasal bones are relatively blunt and in contact medially; the anterior margin of the frontoparietal bones are not completely articulated with the posterior margin of nasals making the dorsal surface of sphenethmoid visible; dermal roofing bones heavily ornamented with pits, striations and rugosities; canthal crest blunt; preorbital crest present; supraorbital crest blunt and thick; postorbital crest present but weak; supratympanic crest present, distinct, expanded laterally towards the postorbital crest, but the occipital artery pathway avoids connecting with the supraorbital crest; pretympanic crest weak; parietal crest weak; the occipital artery canal partially cover by bones; otic ramus enlarged in contact with the posterolateral margin of frontoparietal bones; anterior margins of the nasal bones extended beyond the dorsal margins of the alary processes of the premaxillae; alary processes of the premaxillae angled posteriorly to the anterior margin of the premaxillae; the anterior end of the septomaxilla is not developed; the zygomatic ramus of squamosal is free from the ventral ramus; the jaw articulation is opposite to the fenestra ovalis; columella is present but reduced in size and articulated with the palatoquadrate and squamosal; tympanic annulus is absent; frontoparietal extends beyond the lateral margins of the sphenethmoid; the sphenethmoid reaches the palatines; the anterior ramus of the pterygoid articulates along the margin of maxilla and does not contact the palatine; ventral ridge of the palatines absent; medial ramus of the pterygoid is fused with the anterolateral margin of the parasphenoid; the surface of contact is jagged between the medial ramus of pterygoid and parasphenoid alae; anterior margin of the cultriform process of the parasphenoid is broadly rounded anteriorly; bony protrusion at the angle of the jaw absent.

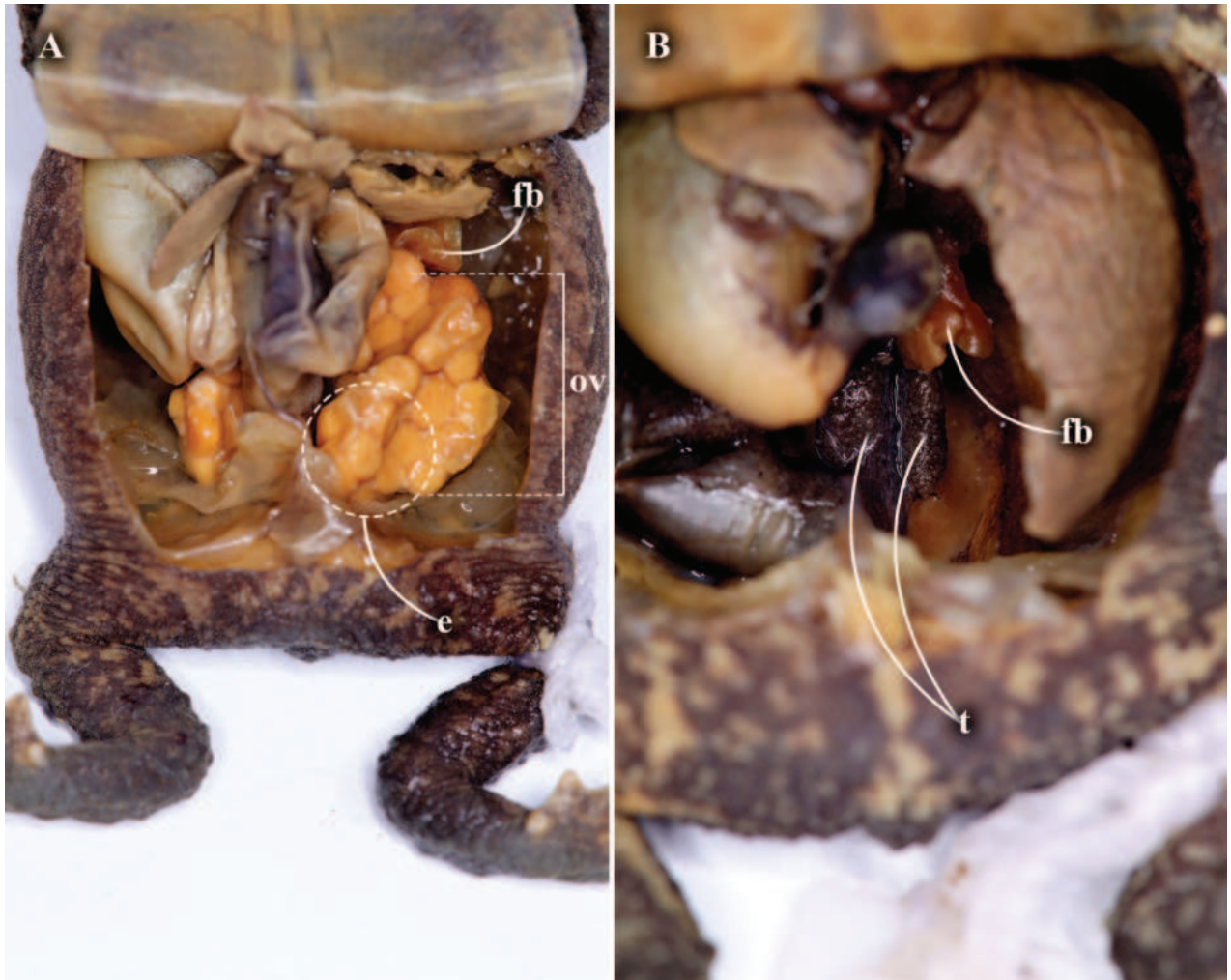


**Figure 6.** Internal sexual anatomy of *Rhinella kumanday* sp. nov. **A** female (MHN-UCa-Am 198) **B** male (MHN-UCa-Am 199). Abbreviations: **fb** fat bodies; **ov** ovary; **e** ovarian eggs; **t** testes.

**Vertebral column.** The axial column consists of seven presacral vertebrae with the neural spine flat or slightly elevated, and vertebrae I–II are fused. The decreasing lengths of the transverse processes and sacrum are: III>IV>Sacrum>V>VII>VI>II; the maximum width of the sacral diapophysis is smaller than the maximum length (maximum length and width of MHN-UCa-Am 1492: 5.36 mm and 3.85 mm, and MHN-UCa-Am 1802: 5.38 mm and 3.74 mm, respectively); the length of the transverse processes of III and VI vertebrae are larger than the length of the transverse process of vertebrae V (maximum length: 8.61 mm, 9.70 mm and 7.18 mm, respectively); transverse process of the VI vertebrae is parallel to the V vertebrae; transverse process of the VII vertebrae is orientated anteriorly in relation to the medial axis of the vertebral column. The anterior edge of the sacral diapophysis is oriented anteriorly to the midline axis of the vertebral column; posterior margin of the sacral diapophyses is relatively smooth; the fusion of the sacrum and the urostyle is distinguished; the urostyle present lateral fringes in dorsal view. Ilium presents a large dorsally directed protuberance and its dorsal crest is present but small; in lateral view, the anteroventral margin of the symphysis of the iliac bone with the iliac axis of the pelvic girdle is perpendicular to the plane of the iliac bone, forming an

angle of 90°; ilia shaft lacks the dorsal crest in medial view; in lateral view, the relative contribution of the ischium to the pelvic girdle is not evident, but the contribution of the ilium to the pelvic girdle is observed, indicating a possible fusion between the ischium and the pubis; the postventral crest of acetabular expansion of ischium is well developed.

**Pectoral girdle.** The pectoral girdle is composed of various bones and cartilaginous elements, which may exhibit different degrees of mineralization; sternum presents mesosternum and xiphisternum of reduced size, occupying a small lower portion of coracoid, where a degree of mineralization can also be observed; free epicoracoid, partially ossified on the closest edge to the coracoid; each protocoracoid continues through the epicoracoid, reaching the upper part of the clavicle, and it expands laterally until it reaches the distal end where the clavicle articulates with the scapula; the omosternum is absent; a moderate-sized foramen is observed in the upper part of the glenoid cavity, probably caused by the medial union of the scapula, clavicle, and coracoid; clavicle small (~ 5 mm in length in MHN-UCa-Am 1802); well-ossified scapula being 2/3× clavicle length; the scapulae are wider at their lateral ends; anterior and posterior margins of each scapula are concave; distal end of each scapula has a bicondylar articulation; the most distal region of the pectoral girdle is formed by the cleithrum and the suprascapula; degree of ossification between the cleithrum and the suprascapula can vary, making it difficult to establish a boundary between the structures; the cleithrum is more ossified towards the anterior margin and extends laterally forming an incomplete rectangle (3/4 of the plate); the posterior border is cartilaginous and lobulated.

**Forelimbs.** The humerus is the longest bone of the forelimb; the caput humeri (glenoid epiphysis) is rounded; the eminentia capitata is visible as is a large, rounded structure in the distal epiphysis; the shaft has a well-developed ventral ridge that originates near the proximal head of the humerus and extends to 2/3 of the humerus. A poorly developed proximo-medial ridge is observed; the fossa cubitalis ventralis is narrow and inconspicuous; the radius and ulna are completely fused medially into a single structure that shows a longitudinal sulcus (sulcus intermedius) from the distal head to the middle of diaphysis; olecranon (proximal head of the ulna), and capitulum (proximal head of the radius) are conspicuous and form a concave articulation surface with the eminentia capitata. The autopodium has a set of carpal bones (ulnare, radiale, element Y, distal carpal 2, distal carpal 5–4–3, four metacarpals and their corresponding phalanges (II to V) plus two ossified prehallical elements; elongated metacarpals (IV>V>III>II); relative length of fingers is IV>V>III>II; the ultimate phalanx of the manual digits is pointed; the phalangeal formula is 2–2–3–3; in ventral view, manus presents a pad-like ossified structure.

**Hind limbs.** The femur is ~ 35% of SVL, has a robust appearance and slightly sigmoidal shape, accompanied by a rounded caput femoralis that fits into the acetabulum of the pelvic girdle; in lateral view, a slight femoral crest is observed and occupies 1/4 of the femur length; tibia and fibula are fused, only distinguishable by the presence of the sulcus intermedius; femur (~ 12 mm) is slightly longer than the tibia-fibula (~ 11 mm); the tibia-fibula present equal length and are fused at the distal and proximal epiphyses. The autopodium consist of a series of tarsal elements (tibia-fibula, and two distal elements), five metatarsal elements with their corresponding phalanges (I–V), and two ossified prehallical elements;

element Y is located proximally to metatarsal I and articulating medially with the proximal elements of prehallux; two voluminous elements likely represent fused element Y + distal tarsal 1, and distal tarsals 2 and 3, or element Y and distal tarsals 1–3; the last phalanx of the toes of the hind leg is pointed; phalangeal formula is 2–2–3–4–3, and the relative length of the toes is IV>III>V>II>I.

**Distribution.** *Rhinella kumanday* sp. nov. is distributed in the Central Cordillera of Colombia in an elevational range from 2404 to 3690 m (Fig. 7). It inhabits Andean and high-Andean vegetation (Fig. 8) of the Cauca and Magdalena Montane Forests (sensu Dinerstein et al. 2017). Records of this toad are confined to the area adjacent to Los Nevados Natural Park, which is in the northernmost volcanic belt of the Central Cordillera.

**Etymology.** The name “kumanday” means “white beautiful”, a word given by the indigenous Quimbaya to the snow-covered volcano that towers over the Central Cordillera in the coffee growing region of Colombia.

**Comparisons with other species.** According to our genetic results (Fig. 1), the most related species of the *festae* group to *Rhinella kumanday* sp. nov. are *R. paraguas*, *R. ruizi*, and *R. nicefori* with which are grouped. However, *R. kumanday* sp. nov. differs from *R. paraguas* and *R. nicefori* by the presence of a well-defined tarsal fold; moreover, differs from *R. paraguas* by having a smaller body size (Table 3), the presence of a well-defined parietal crest, and the absence of nuptial excrescences in males (parietal crest absent, nuptial excrescences present in *R. paraguas*; Grant and Bolívar-G. 2014). Also, *R. kumanday* sp. nov. differs from *R. ruizi* by the presence of a well-defined sagittal ridge between the point of the snout and the superior lip (absent in *R. ruizi*; Grant 2000), and the number of presacral vertebrae (seven in *R. kumanday* sp. nov. vs eight in *R. ruizi*; Grant and Bolívar-G. 2014). Moreover, the new species differs from other species of the *festae* group such as *R. acrolopha*, *R. chullachaki*, *R. festae*, *R. lindae*, *R. macrorhina*, *R. rostrata*, and *R. truebae* by the aforementioned presence of the tarsal fold (absent in those species); from *R. acrolopha*, *R. festae* and *R. macrorhina* by the presence of low cranial crest (prominent cranial crest in the three species; Trueb 1971); from *R. tenrec*, *R. lindae* and *R. truebae* by having a smaller body size (Table 3; Lynch and Renjifo 1990; Rivero and Castaño 1990). Also, *Rhinella kumanday* sp. nov. differs from *R. tenrec* by the less acute snout (very acute in *R. tenrec*), less presacral vertebrae (seven vs eight in *R. tenrec*), the fusion between sacral and the urostyle (not fused in *R. tenrec*), and the elevational distribution (> 2000 m in *R. kumanday* sp. nov. vs ≤ 1300 m in *R. tenrec*). *Rhinella kumanday* sp. nov. also differs from *R. truebae*, *R. chavin*, *R. lilyrodriguezae*, *R. manu*, *R. multiverrucosa*, *R. nesiotes*, *R. tacana*, and *R. yanachaga* by the absence of the tympanum and annulus tympanic (present in those species).

**Conservation status.** *Rhinella kumanday* sp. nov. is only known from 12 localities in the montane forests of both slopes of the Central Cordillera in the departments of Caldas and Tolima, Colombia. The calculation of its extent of occurrence (EOO) using the minimum convex polygon method, as recommended by the International Union for the Conservation of Nature computed with GeoCAT (Bachman et al. 2011), results in an EOO of 208 km<sup>2</sup>. This limited distribution area strongly suggests that the species should be classified as Endangered; however, population dynamics are still unknown. The observed specimens of *R. kumanday* sp. nov. show irregular temporal occurrences and are typically associated with occasional encounters. This new species is

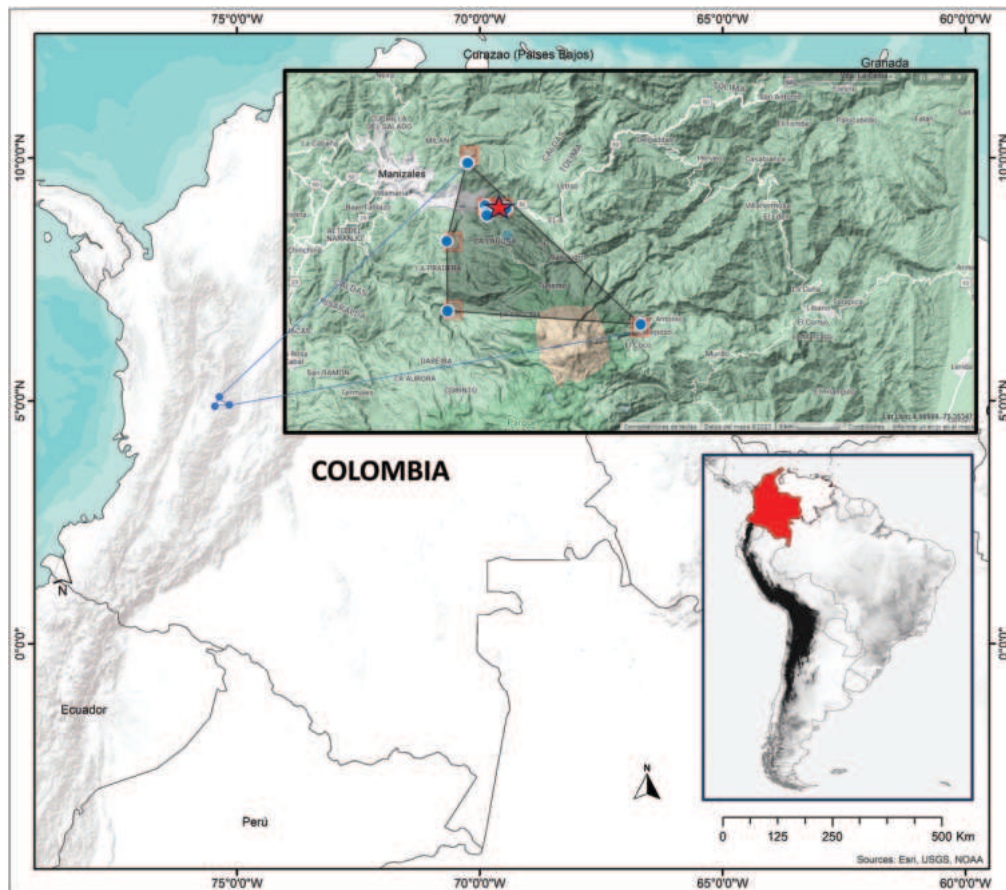


**Figure 7.** Distribution of *Rhinella kumanday* sp. nov. Records obtained from specimens deposited in the Colección de Anfibios of the Museo de Historia Natural of the Universidad de Caldas (MHN-UCa-Am) and the specimen (TG 2115) mentioned by Machado et al. (2016) and Pereyra et al. (2021). Red star indicates the type locality.

considered rare within its distribution area. Recent field surveys conducted in the type locality and surrounding areas have resulted in low capture success rates. Additionally, our knowledge of the species' natural history, distribution, and reproductive behavior remains incomplete, which raises concerns about its vulnerability. The Parque Nacional Natural Los Nevados and the Reserva Forestal Protectora Bosques de la CHEC, are likely protecting population of this species, but mining activities such as the Tolda Fría project might have adverse effects on the species. Records of *Rhinella* sp. from the departments of Quindío and Risaralda (e.g., Castaño et al. 2017), require further review to confirm whether or not they belong to *R. kumanday* sp. nov.

**Natural history.** *Rhinella kumanday* sp. nov. presents terrestrial and crepuscular habits. This species has been observed to be associated with leaf litter or under rotten log during early morning hours and twilight (Rojas-Morales and Marín-Martínez 2019 as *Rhinella* sp.). It has been recorded in secondary forests within the Andean ecosystems of the Central Cordillera in the departments of Caldas and Tolima (Fig. 8). The vegetation structure of the locations includes plants from genera such as *Brunellia* Ruiz & Pavón, 1794 (Brunelliaceae), *Chamaedorea* Willd., 1806 (Arecaceae), *Saurauia* Willdenow, 1801 (Actinidiaceae), *Oreopanax* Decaisne & J.E. Planchon, 1854 (Araliaceae), *Cyathea* Sm., 1793 (Cyatheaceae), *Juglans* L., 1753 (Juglandaceae), *Croton* L., 1753 (Euphorbiaceae), and *Ombrophytum* Poepp. ex Endl. (Balanophoraceae). *Rhinella kumanday* sp. nov. has

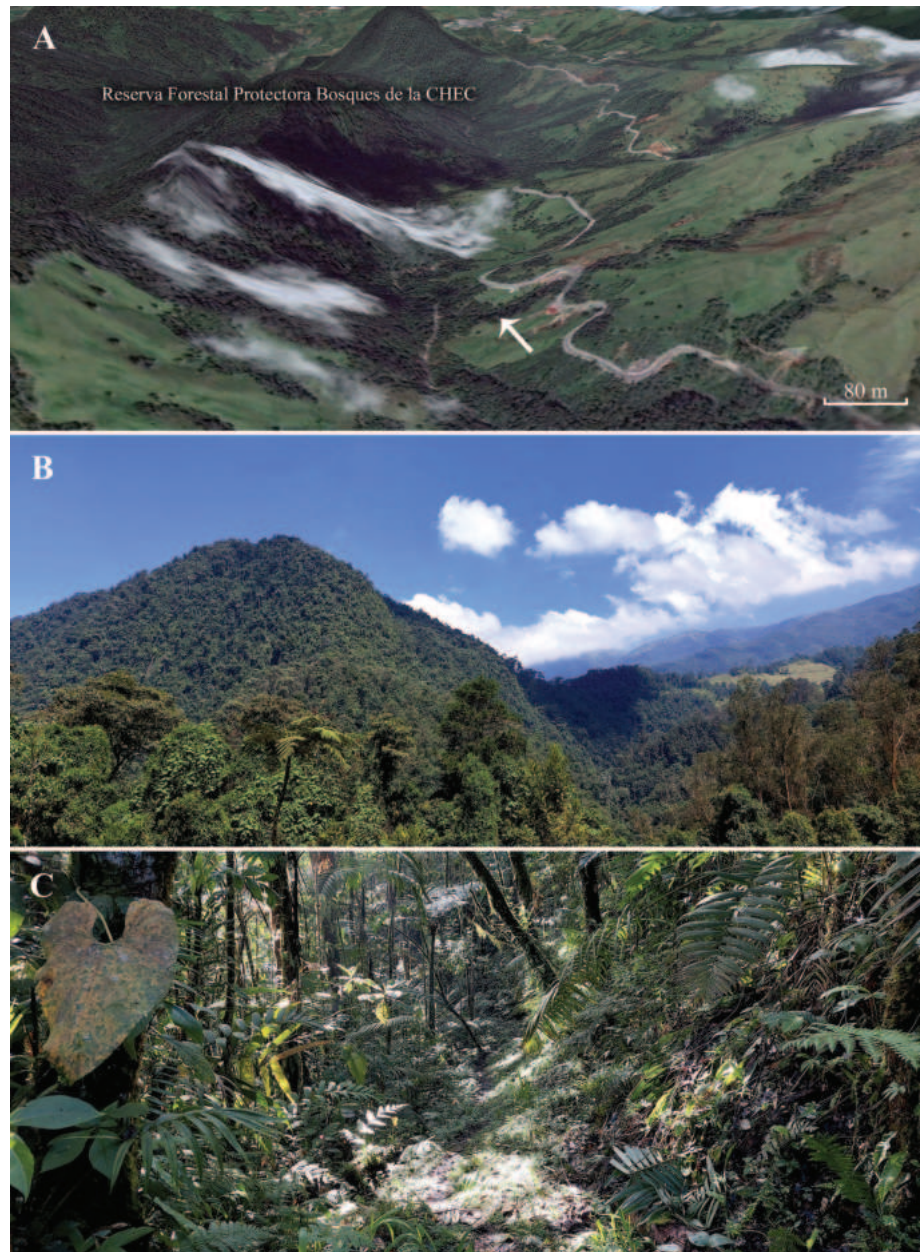


**Figure 8.** The Andean cloud forests of Manizales and Villamaría, Caldas **A** Google Earth® image with the type locality (arrow) of *Rhinella kumanday* sp. nov. **B** general landscape of the Reserva Forestal Protectora Bosques de la CHEC **C** collection site inside the forest.

been found at the edges of creeks and streams inside the forest, as well as near streams close to the Pan-American Road in Caldas. Based on observations of seven individuals, Escobar-Lasso and González-Duran (2012, as *Rhinella* sp.) described the defensive behavior of *R. kumanday* sp. nov. The behavior included thanatosis or death feigning. The only known natural predator of this species is the False-coral snake *Erythrolamprus lamona* (Dunn, 1944) (pers. obs.). *Rhinella kumanday* sp. nov. shares its habitat with other species, including the bufonid *Osornophryne percrassa* Ruiz & Hernández, 1976, in parts of its distribution. It is also likely to be sympatric with *Atelopus quimbaya* Ruiz & Osorno, 1994, which inhabits similar environments in the altitudinal band of the Los Nevados area. However, there have been no records of the latter species since 1997.

**Table 3.** Measurements (in mm) of some species of the *R. festae* group distributed in the Colombian Andes. The information was obtained from the literature and include minimum and maximum range, mean and standard deviation for *R. paraguas*. In the case of *R. kumanday*, the male data do not show the variation as there were only two males. For *R. tenrec* the complete dataset of measurements is given only for the female holotype, and for *R. truebae*, the species is only known from one female individual.

Measurements	<i>R. kumanday</i> females n = 5	<i>R. kumanday</i> males n = 2	<i>R. paraguas</i> females	<i>R. paraguas</i> males	<i>R. tenrec</i> females	<i>R. lindae</i> females	<i>R. lindae</i> males	<i>R. truebae</i> females	<i>R. macrorhina</i> females	<i>R. nicefori</i> females	<i>R. nicefori</i> males	<i>R. rostrata</i> males
SVL	35–40.1, (37.3, ± 2.1)	37.1	40.6–51.4, (45.1, ± 0.7)	31.3–41.7, (35.5, ± 0.8)	54.7–60.8, 56.7	62.2	26.9	65.9	51.4	32.9	31.9	42
HW	11.1–13.7, (12.7, ± 1.0)	11.6	13.1–16.7, (14.9, ± 0.2)	10.2–14.6, (11.8, ± 0.3)	22.3	–	–	20.5	18.8	11.4	11.1	14.3
HL	8.3–9.9, (9.2, ± 0.6)	7.1	12.2–14.4, (13.0, ± 0.1)	9.6–11.8, (10.6, ± 0.2)	20.1	23.8	9.0	20.8	18.2	10.1	10.0	13.6
ED	3.1–3.9, (3.5, ± 0.4)	3.2	–	–	5.00	–	–	6.6	4.8	3.2	3.3	4.6
IOD	3.9–6.1, (4.9, ± 0.8)	4.3	4.3–5.8, (5, ± 0.1)	3.1–5.0, (4.2, ± 0.2)	10.7	11.0	4.0	9.9	8.2	4	4	6.5
EW	2–3.6, (2.9, ± 0.6)	2.7	–	–	3.8	–	–	4.5	–	–	–	–
EL	3.2–4.7, (4.0, ± 0.6)	4.5	4.8–5.7, (5.3, ± 0.1)	3.9–4.7, (4.4, ± 0.1)	4.8	4.0	2.0	–	–	–	–	–
IND	3.3–4, (3.7, ± 0.24)	3.7	4.0–4.8, (4.5, ± 0.1)	3.5–4.3, (3.9, ± 0.1)	–	–	–	–	–	–	–	–
E–N	2.4–2.8, (2.7, ± 0.3)	2.2	2.6–3.5, (3.0, ± 0.1)	2.0–2.9, (2.5, ± 0.1)	6.0	6.1	3.0	6.5	4	2.2	1.9	3.3
NSD	1.6–3.3, (2.6, ± 0.6)	2.7	2.3–3.5, (3.1, ± 0.1)	2.3–3.1, (2.7, ± 0.1)	–	–	–	–	4	1.7	1.9	2.4
SL	4.9–5.4, (5.1, ± 0.2)	5.4	5.4–6.4, (6.1, ± 0.1)	4.7–5.8, (5.2, ± 0.1)	–	3	1.5	–	–	–	–	–
FL	7.9–10.1, (8.9, ± 0.9)	7.0	10.1–13.3, (11.2, ± 0.2)	7.4–10.6, (8.6, ± 0.2)	–	–	–	–	–	–	–	–
HNDL	4.6–9.9, (8.5, ± 1.9)	8.5	11.1–13.5, (12.1, ± 0.2)	7.3–10.2, (8.8, ± 0.2)	–	–	–	–	–	–	–	–
FEML	10.9–13.3, (12.6, ± 0.9)	8.6	–	–	–	23.25	10.0	–	–	–	–	–
TL	10.9–14.9, (12.5, ± 1.6)	10.9	13.3–16.9, (14.8, ± 0.2)	9.8–12.8, (11.4, ± 0.3)	21.3	23.35	10.5	23.8	16	9.0	10.2	15.3
FOOTL	11.1–14.21, (12.3, ± 1.2)	11	13.3–18.2, (15.8, ± 0.3)	9.5–13.5, (11.8, ± 0.3)	20.1	27.5	10.5	29.5	26	16.1	15.00	25.1
PL	4.4–6.2, (5.2, ± 0.8)	5.6	–	–	–	–	–	11.9	–	–	–	–

Regarding diet, based on dissection of three stomachs of preserved specimens (MHN-UCa-Am 198, 1492, 1802), we found three invertebrate prey items belonging to Coleoptera (Curculionidae and one unidentified) and Acari. The reproductive biology is not documented. We have not seen tadpoles or amplexant pairs; however, three preserved gravid females with an unknown gravity period (MHN-UCa-Am 198, 1802, and GGD-001) contained 96 (diameter  $1.82 \pm 0.19$ ;  $n = 10$ ), 38 ( $1.81 \text{ mm} \pm 0.21$ ;  $n = 10$ ), and 81 eggs ( $1.40 \text{ mm} \pm 1.50$ ;  $n = 10$ ), respectively. The eggs presented mostly a yellowish cream coloration in preservative. This color condition has also been reported in preserved specimens of *R. acrolopha*, *R. chavin*, *R. festae*, *R. macrorhina*, and *R. nicefori* (Trueb 1971; Lehr et al. 2001). The calls of *R. kumanday* sp. nov. are unknown, although we tried to record them in captivity without success.

## Discussion

We present compelling evidence encompassing morphological, genetic, and osteological traits supporting the recognition of a new species of *Rhinella* in the Central Andes of Colombia. Over the past decade, a series of studies conducted in montane and subparamo forests of the municipalities of Manizales and Villamaría, Department of Caldas, as well as in the municipality of Murillo, Department of Tolima, have consistently alluded to the presence of an undescribed species (Rojas-Morales et al. 2014; Machado et al. 2016; Gómez-Salazar et al. 2017; Rojas-Morales and Marín-Martínez 2019; Pereyra et al. 2021). Our results confirm these previous observations and, in addition, the affiliation of *R. kumanday* sp. nov. with the *R. festae* group. The formal description of *R. kumanday* sp. nov. underscores the remarkable diversity of the genus which now comprises 23 species in Colombia and 93 globally (Acosta-Galvis 2023; Frost 2023). However, the extent of diversity within the genus is still underestimated (Pereyra et al. 2021).

The small number of specimens deposited in biological collections, as well as paucity of collaborative research efforts among scientists interested in this group of toads may have been the cause of the delayed description of this species. Recognizing the vulnerability of many *Rhinella* species within the *festae* group (IUCN 2023), *R. kumanday* sp. nov. is key for the implementation of localized conservation initiatives, as previously undertaken or recommended for other Andean species (Burbano-Yandí et al. 2015). Of the 23 species of *Rhinella* distributed in Colombia, eight are listed as threatened (IUCN 2023), and seven of these threatened species belong to the *R. festae* group: *R. rostrata* (Critically Endangered - EN); *R. acrolopha*, *R. lindae*, *R. nicefori*, and *R. tenrec* (Endangered - EN); and *R. macrorrhina* and *R. ruizi* (Vulnerable – VU; IUCN 2023). Beyond Colombian borders, the species of this group face similar threats with four species listed as threatened: *R. nesiotes*: (VU); *R. arborescandens*, *R. chavin* and *R. yanachaga* (EN; IUCN 2023). This means that 50% of the group's recognized and named species (11 of 21) are considered threatened. Five additional species are included in the Data Deficient category. Increasing field efforts may reveal more threatened species within the genus. In the case of *R. kumanday* sp. nov., we suggest it should be assessed as Endangered due to the extent of its occurrence spanning only 208 km<sup>2</sup>. This species appears to be restricted to the Andean forests of both slopes of the Central Andes in the departments of Caldas and Tolima based on observations of our research team aimed at locating and evaluating the current status of other endangered species such as *Atelopus quimbaya*. During this ongoing project, new individuals of *R. kumanday* sp. nov. have been discovered (MHN-UCa-Am 1717-18).

Based on morphological traits including the snout projected, cranial crest relatively developed, tympanic membrane and annulus tympanic absent (Pereyra et al. 2021:11), *R. kumanday* sp. nov. aligns with the internal clade previously recognized as the *R. acrolopha* group but now part of the *R. festae* group. The lack of tympanic structures is a prevalent trait among species in the *R. festae* group and other *Rhinella* species (Pereyra et al. 2021; Castillo-Urbina et al. 2021). The absence of tympanic structures is linked to a communication mechanism based on the reception of environmental vibrations (Castillo-Urbina et al. 2021). Consequently, exploring the acoustics behavior of the earless *R. kumanday* sp. nov., and data on reproductive aspects such as mating and the morphological traits of the tadpoles are essential for a deeper understanding

of the natural history of this species. However, the high yolk concentration as suggested by the mostly yellowish cream coloration of the eggs could indicate that this species has direct development as observed in other amphibian species (de Lima et al. 2016). Reproductive ecology and behavior are important aspects to study in the near future for these poorly known toads. Lehr et al. (2021) stated that *R. manu* is often found far away from the water, suggesting they also may reproduce through direct development. Although *R. kumanday* sp. nov. inhabits near of creeks and streams within the Andean forest, it might also direct-development.

Finally, the Andes play a pivotal role in both the diversification and conservation of amphibians, with new species being discovered every year (Sepúlveda-Seguro et al. 2022). Nonetheless, the Andean and sub-Andean forests in Colombia are highly threatened with only ~ 25% of the original area remaining (Armenteras and Villareal 2003; Etter et al. 2017). Consequently, evaluating the effects of deforestation and the expansion of the agricultural-livestock frontier on small and restricted species such as those within the *R. festae* species group, including the new species described here, is imperative. Furthermore, phylogeographic studies including the Colombian species of this group are relevant for understanding the underlying dynamics influencing their current distribution.

## Acknowledgements

We thank the Central Hidroeléctrica de Caldas S.A. E.S.P. (CHEC) for supporting our research and allowing the access to the reserves in which a large part of the local diversity is protected. Edgar Lehr, Miquéias Ferrão, and one anonymous reviewer provided useful comments to improve early versions of the manuscript.

## Additional information

### Conflict of interest

The authors have declared that no competing interests exist.

### Ethical statement

This study was carried following the guidelines for use of live amphibians and reptiles in field research (Beaupre et al. 2004) compiled by the American Society of Ichthyologists and Herpetologists (ASIH), the Herpetologists' League (HL), and the Society for the Study of Amphibians and Reptiles (SSAR). All procedures with animals (see below) were reviewed by the Autoridad Nacional de Licencias Ambientales (ANLA), granted to the Universidad de Caldas as stipulated in resolution 02497 of December 31, 2018.

### Funding

The Mohamed Bin Zayed Fund (project No. 222529372) for supporting our field work activities in the Andes of Colombia. Vicerrectoría de Investigaciones, Universidad de Caldas.

### Author contributions

HERC, HFAM, SCM, JJHO, JARM collected specimens, performed morphological comparisons, and prepared figures. PAOL and FARP obtained genetic data and performed phylogenetic analyses. All authors analyzed the data and wrote the manuscript.

## Author ORCIDs

Luis Santiago Caicedo-Martínez  <https://orcid.org/0000-0002-9564-5703>

Jose J. Henao-Osorio  <https://orcid.org/0000-0002-8618-8539>

Héctor Fabio Arias-Monsalve  <https://orcid.org/0000-0003-0783-2611>

Julián Andrés Rojas-Morales  <https://orcid.org/0000-0002-3312-8022>

Paula A. Ossa-López  <https://orcid.org/0000-0002-9079-4988>

Fredy A. Rivera-Páez  <https://orcid.org/0000-0001-8048-5818>

Héctor E. Ramírez-Chaves  <https://orcid.org/0000-0002-2454-9482>

## Data availability

All of the data that support the findings of this study are available in the main text or Supplementary Information.

## References

- Acosta-Galvis AR (2023) Lista de los Anfibios de Colombia: An online reference. V.13.2023. Electronic Database. <http://www.batrachia.com> [Accessed 10 May 2023]
- Armenteras D, Villareal F (2003) Andean forest fragmentation and the representativeness of protected natural areas in the eastern Andes, Colombia. *Biological Conservation* 113(2): 245–256. [https://doi.org/10.1016/S0006-3207\(02\)00359-2](https://doi.org/10.1016/S0006-3207(02)00359-2)
- Bachman S, Moat J, Hill A, de la Torre J, Scott B (2011) Supporting Red List threat assessments with GeoCAT: geospatial conservation assessment tool. *ZooKeys* 150: 117–126. <https://doi.org/10.3897/zookeys.150.2109>
- Beaupre SJ, Jacobson ER, Lillywhite HB, Zamudio K (2004) Guidelines for use of live amphibians and reptiles in field and laboratory research. *American Society of Ichthyologists and Herpetologists*, Lawrence, 43 pp.
- Blanco MVF, Witmer L (2020) A clearing-and-staining procedure for the study of the chondrocranium and other aspects of skeletal development in crocodylian embryos. *Vertebrate Zoology* 70: 447–454.
- Burbano-Yandí CE, Bolívar-G W, Velásquez-Trujillo DA, González-Colorado AM, Ospina-Herrera O (2015) Plan de conservación de la especie endémica de Colombia Sapito de Páramo *Osornophryne percrassa*, en el departamento de Caldas. Corporación Autónoma Regional de Caldas (Corpocaldas), Manizales, 40 pp.
- Castaño JH, Carranza-Quinceno JA, Londoño E, Roa Cubillos MM (2017) Biodiversidad del Distrito de Conservación de Suelos Campoalegre. v2.3. Corporación Autónoma Regional de Risaralda - CARDER. Dataset/Checklist. <https://doi.org/10.15472/0jxeo4>
- Castillo-Urbina E, Claw F, Aguilar-Puntriano C, Vences M, Köhler J (2021) Genetic and morphologic evidence reveal another new toad of the *Rhinella festae* species group (Anura: Bufonidae) from the Cordillera Azul in Central Perú. *Salamandra (Frankfurt)* 57: 181–195. <https://doi.org/10.5281/zenodo.4767016>
- Chaparro JC, Pramuk JB, Gluesenkamp AG (2007) A new species of arboreal *Rhinella* (Anura: Bufonidae) from cloud forest of southeastern Perú. *Herpetologica* 63(2): 203–212. [https://doi.org/10.1655/0018-0831\(2007\)63\[203:ANSOAR\]2.0.CO;2](https://doi.org/10.1655/0018-0831(2007)63[203:ANSOAR]2.0.CO;2)
- Cochran DM, Goin CJ (1970) Frogs of Colombia. *Bulletin of the United States National Museum* 288: 1–655. <https://doi.org/10.5962/bhl.part.6346>
- Cusi JC, Moravec J, Lehr E, Gvoždík V (2017) A new species of semiarboreal toad of the *Rhinella festae* group (Anura, Bufonidae) from the Cordillera Azul National Park, Peru. *ZooKeys* 673: 21–47. <https://doi.org/10.3897/zookeys.673.13050>

- de Lima AV, Reis AH, Amado NG, Cassiano-Lima D, Borges-Nojosa DM, Oriá RB, Abreu JG (2016) Developmental aspects of the direct-developing frog *Adelophryne marangapensis*. *Genesis* (New York, N.Y.) 54(5): 257–271. <https://doi.org/10.1002/dvg.22935>
- Deforel F, Duport-Bru AS, Rosset SD, Baldo D, Candiotti FV (2021) Osteological Atlas of *Melanophryniscus* (Anura, Bufonidae): A Synthesis after 150 Years of Skeletal Studies in the Genus. *Herpetological Monograph* 35(1): 1–27. <https://doi.org/10.1655/HERPMONOGRAPHS-D-20-00002>
- Dinerstein E, Olson D, Joshi A, Vynne C, Burgess ND, Wikramanayake E, Hahn N, Palminteri S, Hedao P, Noss R, Hansen M, Locke H, Ellis EC, Jones B, Barber CV, Hayes R, Kormos C, Martin V, Crist E, Sechrest W, Price L, Baillie JEM, Weeden D, Suckling K, Davis C, Sizer N, Moore R, Thau D, Birch T, Potapov P, Turubanova S, Tyukavina A, de Souza N, Pinteá L, Brito JC, Llewellyn OA, Miller AG, Patzelt A, Ghazanfar SA, Timberlake J, Klöser H, Shennan-Farpón Y, Kindt R, Lillesø JPB, van Breugel P, Graudal L, Vogé M, Al-Shammari KF, Saleem M (2017) An ecoregion-based approach to protecting half the terrestrial realm. *Bioscience* 67(6): 534–545. <https://doi.org/10.1093/biosci/bix014>
- Duellman WE, Schulte R (1992) Description of a new species of *Bufo* from northern Peru with comments on phenetic groups of South American toads (Anura: Bufonidae). *Copeia* 1992(1): 162–172. <https://doi.org/10.2307/1446548>
- Duellman WE, Toft CA (1979) Anurans from the Serranía de Sira, Amazonian Perú: Taxonomy and biogeography. *Herpetologica* 35: 60–70. <https://www.jstor.org/stable/3891754>
- Dunn ER (1944) A revision of the Colombian snakes of the genera *Leimadophis*, *Lygophis*, *Liophis*, *Rhadinaea*, and *Pliocercus*, with a note on Colombian *Coniophanes*. *Caldasia* 2: 479–495. <https://www.jstor.org/stable/23640977>
- Escobar-Lasso S, González-Duran GA (2012) Strategies employed by three neotropical frogs (Amphibia: Anura) to avoid predation. *Herpetology Notes* 5: 79–84.
- Etter A, Andrade A, Saavedra K, Cortés J (2017) Actualización de la Lista Roja de los Ecosistemas Terrestres de Colombia: conocimiento del riesgo de ecosistemas como herramienta para la gestión: An online reference. Electronic Database. <http://reporte.humboldt.org.co/biodiversidad/2017/cap2/204/#seccion1> [Accessed 13 May 2023]
- Fouquet A, Gaucher P, Blanc M, Veléz-Rodríguez CM (2007) Description of two new species of (Anura: Bufonidae) from the lowlands of the Guiana Shield. *Zootaxa* 1663: 17–32.
- Frost DR (2023) Amphibian species of the world: An online reference. Version 6.1. An online reference. Electronic Database. <https://doi.org/10.5531/db.vz.0001> [Accessed 13 May 2023]
- Gómez-Salazar JC, Ramírez-Castaño VA, Guevara G (2017) Vertebrados terrestres de la Reserva Natural de la Central Hidroeléctrica de Caldas –CHEC– (Villamaría, Colombia): Estado del conocimiento. *Boletín Científico Museo de Historia Natural Universidad de Caldas* 21(1): 71–89. <https://doi.org/10.17151/bccm.2017.21.1.6>
- Grant T (2000) Una nueva especie de *Rhamphophryne* (Anura: Bufonidae) de la Cordillera Central de Colombia. *Revista de la Academia Colombiana de Ciencias Exactas, Físicas y Naturales* 23: 287–292. [https://www.accefyn.com/revista/Vol\\_23/supl/287-292.pdf](https://www.accefyn.com/revista/Vol_23/supl/287-292.pdf)
- Grant T, Bolívar-G. W (2014) A new species of semiarborescent toad with a salamander-like ear (Anura: Bufonidae: *Rhinella*). *Herpetologica* 70(2): 198–210. <https://doi.org/10.1655/HERPETOLOGICA-D-13-00082R1>
- Graybeal A (1997) Phylogenetic relationships of bufonid frogs and tests of alternate macroevolutionary hypotheses characterizing their radiation. *Zoological Journal of the Linnean Society* 119(3): 297–338. <https://doi.org/10.1111/j.1096-3642.1997.tb00139.x>
- Guindon S, Dufayard JF, Lefort V, Anisimova M, Hordijk W, Gascuel O (2010) New algorithms and methods to estimate maximum-likelihood phylogenies: Assessing

- the performance of PhyML 3.0. *Systematic Biology* 59(3): 307–321. <https://doi.org/10.1093/sysbio/syq010>
- IUCN (2023) The IUCN Red List of Threatened Species. Version 2022-2. An online reference. Electronic Database. <https://www.iucnredlist.org> [Accessed 14 May 2023]
- Kalyaanamoorthy S, Minh BQ, Wong TKF, von Haeseler A, Jermiin LS (2017) ModelFinder: Fast model selection for accurate phylogenetic estimates. *Nature Methods* 14(6): 587–589. <https://doi.org/10.1038/nmeth.4285>
- Katoh K, Standley DM (2013) MAFFT multiple sequence alignment software version 7: Improvements in performance and usability. *Molecular Biology and Evolution* 30(4): 772–780. <https://doi.org/10.1093/molbev/mst010>
- Lehr E, Köhler G, Aguilar C, Ponce E (2001) New species of *Bufo* (Anura: Bufonidae) from central Peru. *Copeia* 2001(1): 216–223. [https://doi.org/10.1643/0045-8511\(2001\)001\[0216:NSOBAB\]2.0.CO;2](https://doi.org/10.1643/0045-8511(2001)001[0216:NSOBAB]2.0.CO;2)
- Lehr E, Pramuk JB, Lundberg M (2005) A new species of *Bufo* (Anura: Bufonidae) from Andean Peru. *Herpetologica* 61(3): 308–318. <https://doi.org/10.1655/04-90.1>
- Lehr E, Pramuk JB, Hedges SB, Córdova JH (2007) A new species of arboreal *Rhinella* (Anura: Bufonidae) from Yanachaga-Chemillén National Park in central Peru. *Zootaxa* 1662: 1–14.
- Lehr E, Cusi JC, Rodríguez LO, Venegas PJ, García-Ayachi LA, Catenazzi A (2021) A new species of toad (Anura: Bufonidae: *Rhinella*) from northern Perú. *Taxonomy* 1(3): 210–225. <https://doi.org/10.3390/taxonomy1030015>
- Lynch JD, Renjifo JM (1990) Two new toads (Bufonidae: *Ramphophryne*) from the Northern Andes of Colombia. *Journal of Herpetology* 24(4): 364–371. <https://doi.org/10.2307/1565051>
- Machado JD, Lyra ML, Grant T (2016) Mitogenome assembly from genomic multiplex libraries: Comparison of strategies and novel mitogenomes for five species of frogs. *Molecular Ecology Resources* 16(3): 686–693. <https://doi.org/10.1111/1755-0998.12492>
- Maciel NM, Schwartz CA, Colli GR, Castro MS, Fontes W, Schwartz ENF (2006) A phylogenetic analysis of species in the *Bufo crucifer* group (Anura: Bufonidae), based on indolealkylamines and proteins from skin secretions. *Biochemical Systematics and Ecology* 34(6): 457–466. <https://doi.org/10.1016/j.bse.2006.01.005>
- Minh BQ, Nguyen MA, von Haeseler A (2013) Ultrafast approximation for phylogenetic bootstrap. *Molecular Biology and Evolution* 30(5): 1188–1195. <https://doi.org/10.1093/molbev/mst024>
- Moravec J, Lehr E, Cusi JC, Córdova JH, Gvodzík V (2014) A new species of the *Rhinella margaritifera* species group (Anura, Bufonidae) from the montane forest of the Selva Central, Perú. *ZooKeys* 371: 35–56. <https://doi.org/10.3897/zookeys.371.6580>
- Myers CW, Duellman WE (1982) A new species of *Hyla* from Cerro Colorado, and other tree frog records and geographical notes from western Panama. *American Museum Novitates* 2752: 1–32.
- Narvaes P, Rodrigues MT (2009) Taxonomic revision of *Rhinella granulosa* species group (Amphibia, Anura, Bufonidae) with a description of a new species. *Arquivos de Zoologia* 40(1): 1–73. <https://doi.org/10.11606/issn.2176-7793.v40i1p1-73>
- Nguyen LT, Schmidt HA, von Haeseler A, Minh BQ (2015) IQ-TREE: A fast and effective stochastic algorithm for estimating maximum-likelihood phylogenies. *Molecular Biology and Evolution* 32(1): 268–274. <https://doi.org/10.1093/molbev/msu300>
- Noble GK (1920) Two new batrachians from Colombia. *Bulletin of the American Museum of Natural History* 42: 441–446. <http://digitallibrary.amnh.org/handle/2246/1917>

- Padial JM, Reichle S, McDiarmid RW, De la Riva I (2006) A new species of arboreal toad (Anura: Bufonidae: *Chaunus*) from Madidi National Park, Bolivia. *Zootaxa* 1278(1): 57–58. <https://doi.org/10.11646/zootaxa.1278.1.3>
- Palumbi SR, Martin A, McMillan WO, Stice L, Grabowski G (1991). The simple fool's guide to PCR, Version 2.0: privately published document compiled by S. Palumbi, 45 pp.
- Peracca MG (1904) Viaggio del Dr. Enrico Festa nell' Ecuador e regioni vicine. Rettili ed anfibi. Bollettino dei Musei di Zoologia e Anatomia Comparata della R. Università di Torino 19: 1–41. <https://doi.org/10.5962/bhl.part.11596>
- Pereyra MO, Baldo D, Blotto BL, Iglesias PP, Thomé MTC, Haddad CFB, Barrios-Amorós C, Ibañez R, Faivovich J (2016) Phylogenetic relationships of toads of the *Rhinella granulosa*. (Anura: Bufonidae): a molecular perspective with comments on hybridization and introgression. *Cladistics* 32(1): 1–18. <https://doi.org/10.1111/cla.12110>
- Pereyra MO, Blotto BL, Baldo D, Chaparro JC, Ron SR, Elías-Costa AJ, Iglesias PP, Venegas PJ, Thomé MTC, Ospina-Sarria JJ, Maciel NM, Rada M, Kolenc F, Borteiro C, Rivera-Correa M, Rojas-Runjaic FJM, Moravec J, De La Riva I, Wheeler WC, Castroviejo-Fisher S, Grant T, Haddad CFB, Faivovich J (2021) Evolution in the genus *Rhinella*: A total evidence of phylogenetic analysis of neotropical True Toads (Anura: Bufonidae). *Bulletin of the American Museum of Natural History* 447: 1–155. <https://doi.org/10.1206/0003-0090.447.1.1>
- Pramuk JB (2006) Phylogeny of South American *Bufo* (Anura: Bufonidae) inferred from combined evidence. *Zoological Journal of the Linnean Society* 146(3): 407–452. <https://doi.org/10.1111/j.1096-3642.2006.00212.x>
- Pyron RA, Wiens JJ (2011) A large-scale phylogeny of Amphibia including over 2800 species and a revised classification of extant frogs, salamanders and caecilians. *Molecular Phylogenetics and Evolution* 61(2): 543–583. <https://doi.org/10.1016/j.ympev.2011.06.012>
- Rambaut A (2007) FigTree v1.4.3 (Version 1.4.3). A Graphical Viewer of Phylogenetic Trees. <http://tree.bio.ed.ac.uk/software/figtree>
- Rivera D, Prates I, Firneno Jr TJ, Rorigues MT, Caldwell JP, Fujita MK (2021) Phylogenomics, introgression, and demographic history of South American true toads (*Rhinella*). *Molecular Ecology* 31(3): 978–992. <https://doi.org/10.1111/mec.16280>
- Rivero JA, Castaño CJ (1990) A new and peculiar species of *Rhamphophryne* (Amphibia: Bufonidae) from Antioquia, Colombia. *Journal of Herpetology* 24(1): 1–5. <https://doi.org/10.2307/1564282>
- Rojas-Morales JA, Marín-Martínez M (2019) Diversity, structure and natural history of amphibian in upper Claro River basin, a buffer zone of the National Natural Park Los Nevados, Central Cordillera of Colombia. *Journal of Threatened Taxa* 11(3): 13261–13277. <https://doi.org/10.11609/jott.4075.11.3.13261-13277>
- Rojas-Morales JA, Arias-Monsalve HF, González-Durán GA (2014) Anfíbios y reptiles de la región centro-sur del departamento de Caldas. *Biota Colombiana* 15: 73–93. <https://www.redalyc.org/pdf/491/49140738005.pdf>
- Savage JM, Heyer WR (1967) Variation and distribution of the tree-frog genus *Phyllomedusa* in Costa Rica, Central America. *Beiträge zur Neotropischen Fauna* 5(2): 111–131. <https://doi.org/10.1080/01650526709360400>
- Savage JM, Heyer WR (1997) Digital webbing formulae for Anurans: A refinement. *Herpetological Review* 28(3): 131.
- Sepúlveda-Seguro AA, Marín CM, Amézquita A, García YA, Daza JM (2022) Phylogeographic structure suggests environmental gradient speciation in a montane frog from

- the northern Andes of Colombia. *Organisms, Diversity & Evolution* 22(3): 803–820. <https://doi.org/10.1007/s13127-022-00549-9>
- Talavera G, Castresana J (2007) Improvement of phylogenies after removing divergent and ambiguously aligned blocks from protein sequence alignments. *Systematic Biology* 56(4): 564–577. <https://doi.org/10.1080/10635150701472164>
- Taylor WR, Van Dyke GC (1985) Revised procedures for staining and clearing small fishes and other vertebrates for bone and cartilage study. *Cybio* 9: 107–109.
- Trueb L (1971) Phylogenetic relationships of certain neotropical toads with the description of a new genus (Anura: Bufonidae). *Contribution in Science. Contributions in Science* 216: 1–40. <https://doi.org/10.5962/p.241202>
- Vélez-R CM, Ruiz-C PM (2002) A new species of *Bufo* (Anura: Bufonidae) from Colombia. *Herpetologica* 58(4): 453–462. [https://doi.org/10.1655/0018-0831\(2002\)058\[0453:ANSOBA\]2.0.CO;2](https://doi.org/10.1655/0018-0831(2002)058[0453:ANSOBA]2.0.CO;2)
- Zhang D, Gao F, Jakovlić I, Zou H, Zhang J, Li WX, Wang GT (2020) PhyloSuite: An integrated and scalable desktop platform for streamlined molecular sequence data management and evolutionary phylogenetics studies. *Molecular Ecology Resources* 20(1): 348–355. <https://doi.org/10.1111/1755-0998.13096>

## Supplementary material 1

### Estimates of divergence between sequences based on *p-distance* method for the mitochondrial 16S rRNA gene

Authors: Luis Santiago Caicedo-Martínez, Jose J. Henao-Osorio, Héctor Fabio Arias-Monsalve, Julián Andrés Rojas-Morales, Paula A. Ossa-López, Fredy A. Rivera-Páez, Héctor E. Ramírez-Chaves

Data type: xlsx

Explanation note: Accessions in bold correspond to this study.

Copyright notice: This dataset is made available under the Open Database License (<http://opendatacommons.org/licenses/odbl/1.0/>). The Open Database License (ODbL) is a license agreement intended to allow users to freely share, modify, and use this Dataset while maintaining this same freedom for others, provided that the original source and author(s) are credited.

Link: <https://doi.org/10.3897/zookeys.1196.114861.suppl1>

## Supplementary material 2

### Phylogenetic tree of the partial sequences of the 16S gene of the species of *Rhinella*

Authors: Luis Santiago Caicedo-Martínez, Jose J. Henao-Osorio, Héctor Fabio Arias-Monsalve, Julián Andrés Rojas-Morales, Paula A. Ossa-López, Fredy A. Rivera-Páez, Héctor E. Ramírez-Chaves

Data type: png

Copyright notice: This dataset is made available under the Open Database License (<http://opendatacommons.org/licenses/odbl/1.0/>). The Open Database License (ODbL) is a license agreement intended to allow users to freely share, modify, and use this Dataset while maintaining this same freedom for others, provided that the original source and author(s) are credited.

Link: <https://doi.org/10.3897/zookeys.1196.114861.suppl2>



# Key to the North American tribes and genera of herb, rose, bramble, and inquiline gall wasps (Hymenoptera, Cynipoidea, Cynipidae *sensu lato*)

Louis F. Nastasi<sup>1</sup>, Matthew L. Buffington<sup>2</sup>, Charles K. Davis<sup>1</sup>, Andrew R. Deans<sup>1</sup>

1 Frost Entomological Museum, Department of Entomology, The Pennsylvania State University, 501 Agricultural Science & Industries Building, University Park, PA, 16802, USA

2 Systematic Entomology Laboratory, USDA-ARS, c/o National Museum of Natural History, Smithsonian Institution, PO Box 37012, MRC 168, Washington, DC, 20013, USA

Corresponding author: Louis F. Nastasi ([LFNastasi@gmail.com](mailto:LFNastasi@gmail.com))

## Abstract

Robust keys exist for the family-level groups of Cynipoidea. However, for most regions of the world, keys to genera are not available. To address this gap as it applies to North America, a fully illustrated key is provided to facilitate identification of the tribes and genera of rose gall, herb gall, and inquiline gall wasps known from the region. For each taxon covered, a preliminary diagnosis and an updated overview of taxonomy, biology, distribution, and natural history are provided.

**Key words:** Cecidology, identification, taxonomy



This article is part of:

**Global Taxon Reviews**

Edited by Michael Engel, Fedor Konstantinov

Academic editor: Michael S. Engel

Received: 9 January 2024

Accepted: 21 February 2024

Published: 25 March 2024

ZooBank: <https://zoobank.org/D10E0EA0-16D7-42B9-83D9-3871CBF06FE1>

Citation: Nastasi LF, Buffington ML, Davis CK, Deans AR (2024) Key to the North American tribes and genera of herb, rose, bramble, and inquiline gall wasps (Hymenoptera, Cynipoidea, Cynipidae *sensu lato*). ZooKeys 1196: 177–207. <https://doi.org/10.3897/zookeys.1196.118460>

Copyright: This is an open access article distributed under terms of the CC0 Public Domain Dedication.

## Introduction

Gall wasps (Hymenoptera: Cynipidae *sensu lato*) comprise a fascinating group of gall inducers and inquilines that are associated with a tremendous diversity of host plants, including at least eight families (Ronquist et al. 2015; Azmaz and Katilmiş 2020; Buffington et al. 2020). However, the taxonomy of these insects is poorly resolved, and few resources exist to enable their identification. Some recent keys (e.g., Buffington et al. 2020) stand as milestones within systematics of Cynipoidea, as they are heavily illustrated and feature images that highlight important diagnostic characters, but these products only address family-level taxa. Within the gall wasps in particular, no comparable keys exist for genera, and virtually no useful diagnostic tools exist for the North American fauna specifically. The last generic key broadly covering North American cynipids is that of Weld (1952), privately published more than 70 years ago. As a result, a new key is necessary to enable tribal and generic identification of North American cynipids.

Part and parcel to this dilemma is a general observation that the current limits of many cynipid genera themselves are in flux, leaving a difficult situation for providing effective keys. Towards this end, we have addressed this challenge by focusing herein on inquiline cynipids and those inducing galls on herbaceous and rosaceous plants, therein leaving the oak galling cynipids (tribe Cynipini) for future projects.

Recent revisionary works (e.g., Lobato-Vila and Pujade-Villar 2021) have made the North American cynipid fauna more approachable. Additionally, the cynipid fauna of the United States, Canada, and Mexico exclusive of Cynipini was recently cataloged by Nastasi and Deans (2021). An overview of North American cynipid taxonomy as treated therein is provided in Table 1.

## Materials and methods

Our taxonomic framework follows Nastasi and Deans (2021); nomenclatural, biological, and distributional data are provided therein for each species in the genera treated in the present work. The skeleton of this key was based on Buffington et al. (2020). Other characters in the present work follow Ronquist et al. (2015) or have been developed through the authors' taxonomic work on North American Cynipoidea.

For those unfamiliar with cynipoid morphology, we recommend consulting the line drawings of 'Hymenoptera of the World' (Goulet and Huber 1993) and Melika (2006). Those more advanced in their knowledge may opt to reference the Hymenoptera Anatomy Ontology (Yoder et al. 2010) or the Phenotype and Trait Ontology (PATO curators 2023), the former of which serves as the primary foundation of the morphological terminology applied herein (Table 2).

Each character is illustrated by color micrographs of museum specimens, which enables stronger recognition of relevant morphology. Images were captured using a Macroscopic Solutions 'microkit' (Tolland, CT) imaging station, stacked using Zerene Stacker LLC (Richland, WA), and edited using Adobe Photoshop and/or Adobe Illustrator (San Jose, CA).

**Table 1.** Overview of North American gall wasp fauna. Species numbers refer to those known from North America; taxonomy, species numbers, and biological data are based on Nastasi and Deans (2021) except for Cynipini, which is derived from Melika et al. (2021). \* = raised to subfamily Diplolepidinae in the family Diplolepididae by Hearn et al. (2023).

Taxon	Biology	Nr of spp.
<b>Tribe Aulacideini</b>	<b>Gall inducers on Asteraceae; Lamiaceae</b>	<b>21</b>
Genus <i>Antistrophus</i> Walsh	Gall inducers on <i>Chrysothamnus</i> , <i>Lygodesmia</i> , <i>Microseris</i> , <i>Silphium</i> (Asteraceae)	10
Genus <i>Aulacidea</i> Ashmead	Gall inducers on <i>Hieracium</i> , <i>Lactuca</i> , <i>Nabalus</i> , <i>Pilosella</i> , <i>Rhaponticum</i> (Asteraceae)	10
Genus <i>Liposthenes</i> Förster	Gall inducers on <i>Glechoma</i> (Lamiaceae)	1
<b>Tribe Ceroptresini</b>	<b>Inquiline of Cynipini</b>	<b>19</b>
Genus <i>Buffingtonella</i> Lobato-Vila & Pujade-Villar	Unknown; presumed inquiline of Cynipini as in <i>Ceroptres</i>	1
Genus <i>Ceroptres</i> Hartig	Inquiline of Cynipini	18
<b>Tribe Cynipini</b>	<b>Gall inducers on Fagaceae, especially <i>Quercus</i></b>	<b>~ 680</b>
<b>Tribe Diastrophini</b>	<b>Gall inducers on Rosaceae or inquiline of <i>Diastrophus</i> or Diplolepidini</b>	<b>25</b>
Genus <i>Diastrophus</i> Hartig	Gall inducers on <i>Fragaria</i> , <i>Potentilla</i> , <i>Rubus</i> (Rosaceae)	14
Genus <i>Periclistus</i> Förster	Inquiline in galls induced by <i>Diplolepis</i>	7
Genus <i>Synophromorpha</i> Ashmead	Inquiline in galls induced by <i>Diastrophus</i>	4
<b>Tribe Diplolepidini*</b>	<b>Gall inducers on <i>Rosa</i></b>	<b>34</b>
Genus <i>Diplolepis</i> Geoffroy	Gall inducers on <i>Rosa</i>	34
<b>Tribe Phanacidini</b>	<b>Gall inducers on Asteraceae</b>	<b>2</b>
Genus <i>Phanacis</i> Förster	Gall inducers on <i>Hypochaeris</i> , <i>Taraxacum</i> (Asteraceae)	2
<b>Tribe Synergini</b>	<b>Inquiline of Cynipini</b>	<b>69</b>
Genus <i>Saphonecrus</i> Dalla Torre & Kieffer	Inquiline of Cynipini	2
Genus <i>Synergus</i> Hartig	Inquiline of Cynipini	67

**Table 2.** Overview of morphological terminology employed in the key to genera. URLs link to entries in the Hymenoptera Anatomy Ontology (Yoder et al. 2010) or the Phenotype and Trait Ontology (PATO curators 2023).

Term	URL or definition
Areolet	<a href="http://purl.obolibrary.org/obo/HAO_0000147">http://purl.obolibrary.org/obo/HAO_0000147</a>
Carina (plural carinae)	<a href="http://purl.obolibrary.org/obo/HAO_0000188">http://purl.obolibrary.org/obo/HAO_0000188</a>
Coriaceous sculpture	<a href="http://purl.obolibrary.org/obo/HAO_0002379">http://purl.obolibrary.org/obo/HAO_0002379</a>
Eye	<a href="http://purl.obolibrary.org/obo/HAO_0000217">http://purl.obolibrary.org/obo/HAO_0000217</a>
Facial radiating striae	<a href="http://purl.obolibrary.org/obo/HAO_0001770">http://purl.obolibrary.org/obo/HAO_0001770</a>
Fore wing	<a href="http://purl.obolibrary.org/obo/HAO_0000351">http://purl.obolibrary.org/obo/HAO_0000351</a>
Frons	<a href="http://purl.obolibrary.org/obo/HAO_0001044">http://purl.obolibrary.org/obo/HAO_0001044</a>
Granular sculpture	<a href="http://purl.obolibrary.org/obo/PATO_0001759">http://purl.obolibrary.org/obo/PATO_0001759</a>
Hypopygium	<a href="http://purl.obolibrary.org/obo/HAO_0000410">http://purl.obolibrary.org/obo/HAO_0000410</a>
Mesopleural impression	<a href="http://purl.obolibrary.org/obo/HAO_0001952">http://purl.obolibrary.org/obo/HAO_0001952</a>
Mesopleuron	<a href="http://purl.obolibrary.org/obo/HAO_0000566">http://purl.obolibrary.org/obo/HAO_0000566</a>
Mesoscutum	<a href="http://purl.obolibrary.org/obo/HAO_0000575">http://purl.obolibrary.org/obo/HAO_0000575</a>
Metasoma	<a href="http://purl.obolibrary.org/obo/HAO_0000626">http://purl.obolibrary.org/obo/HAO_0000626</a>
Metasomal tergite 1	<a href="http://purl.obolibrary.org/obo/HAO_0000053">http://purl.obolibrary.org/obo/HAO_0000053</a>
Metasomal tergite 2	<a href="http://purl.obolibrary.org/obo/HAO_0000056">http://purl.obolibrary.org/obo/HAO_0000056</a>
Metasomal tergite 3	<a href="http://purl.obolibrary.org/obo/HAO_0000057">http://purl.obolibrary.org/obo/HAO_0000057</a>
Metatarsal claw	<a href="http://purl.obolibrary.org/obo/HAO_0001927">http://purl.obolibrary.org/obo/HAO_0001927</a>
Notaulus (plural notauli)	<a href="http://purl.obolibrary.org/obo/HAO_0000647">http://purl.obolibrary.org/obo/HAO_0000647</a>
Pronotal plate	<a href="http://purl.obolibrary.org/obo/HAO_0000838">http://purl.obolibrary.org/obo/HAO_0000838</a>
Pronotum	<a href="http://purl.obolibrary.org/obo/HAO_0000853">http://purl.obolibrary.org/obo/HAO_0000853</a>
Punctate-setigenous sculpture	The sculpture that consists of punctation in which each puncture contains a single seta.
Reticulate sculpture	The sculpture that is superficially net-like, consisting of a network of carinae or indentations enclosing polygonal cellules.
Sculpture	<a href="http://purl.obolibrary.org/obo/HAO_0000913">http://purl.obolibrary.org/obo/HAO_0000913</a>
Scutellar fovea (plural scutellar foveae)	<a href="http://purl.obolibrary.org/obo/HAO_0000916">http://purl.obolibrary.org/obo/HAO_0000916</a>
Seta (plural setae)	<a href="http://purl.obolibrary.org/obo/HAO_0002299">http://purl.obolibrary.org/obo/HAO_0002299</a>
Striate sculpture	<a href="http://purl.obolibrary.org/obo/PATO_0001410">http://purl.obolibrary.org/obo/PATO_0001410</a>
Suture	<a href="http://purl.obolibrary.org/obo/HAO_0000982">http://purl.obolibrary.org/obo/HAO_0000982</a>
Syntergite	<a href="http://purl.obolibrary.org/obo/HAO_0000987">http://purl.obolibrary.org/obo/HAO_0000987</a>
Torus (plural toruli)	<a href="http://purl.obolibrary.org/obo/HAO_0000908">http://purl.obolibrary.org/obo/HAO_0000908</a>
Wing cell	<a href="http://purl.obolibrary.org/obo/HAO_0001091">http://purl.obolibrary.org/obo/HAO_0001091</a>

Specimens referenced during the production of this key, including those photographed to produce figures, are housed in the Frost Entomological Museum (**PSUC**; University Park, PA) or the United States National Museum of Natural History (**USNM**; Washington, DC). Unique specimen identifiers in the form of catalog numbers (**USNMMENT** or **PSUC\_FEM** numbers with corresponding bar-codes) link each image to specimens housed at the corresponding collection.

## Results

### Key to the tribes and genera of herb, rose, bramble, and inquiline gall wasps of North America (Hymenoptera: Cynipoidea)

To verify the applicability of this key to a given specimen, first run unknown individuals through the superfamily key in Goulet and Huber (1993) to confirm

the specimen belongs to Cynipoidea, then Buffington et al. (2020) to confirm placement in Cynipidae. This process is critical in that a few North American Figitidae can superficially resemble Cynipidae. We recommend the use of good lighting, diffused through mylar, when using the key; this is especially essential for viewing patterns of cuticular sculpture and characters involving the pronotal plate.

Some North American genera are problematic with regard to their taxonomic status or their true occurrence in the region. Where applicable, these taxa are present in the key or otherwise mentioned in the systematic treatment below. Additionally, many undescribed taxa within the scope of these keys are known, and many taxonomic acts are necessary to stabilize the fauna covered here. Future iterations of the key in this work will address updated taxonomy as it is published, but the present key has been written to be as compatible as possible with all upcoming taxonomic changes known to the authors. We provide provisional taxon diagnoses in the below taxon treatments to facilitate identification of the tribes and genera as they are currently defined; these diagnoses are based only on North American members of each taxon. We expect these diagnoses to change as taxonomic work on the North American cynipid fauna progresses.

- 1 Pronotum distinctly short dorsomedially, forming a narrow strip behind head, with medial height (Figs 1–4, pmh) approximately 1/7 or less the lateral height (Figs 3, 4, plh). Pronotal submedial pits absent (Figs 1, 2). Gall inducers on *Rosa* (Rosaceae) or several genera of Fagaceae, especially *Quercus* .....2
- Pronotum taller and broader dorsomedially, with medial height (Figs 5, 6, pmh) usually approximately 1/3 the lateral height (Figs 7, 8, plh). Pronotal submedial pits usually present and well-impressed (mep, Fig. 6). Gall inducers on other plants or inquilines in galls.....3



**Figures 1–8.** 1 *Andricus quercuscalifornicus*, anterodorsal view (USNMENT01231839) 2 *Diplolepis bicolor*, anterodorsal view (USNMENT01231831) 3 *Dryocosmus kuriphilus*, lateral view (USNMENT01231861) 4 *Diplolepis bicolor*, lateral view (USNMENT01231831) 5 *Synergus atripennis*, anterodorsal view (USNMENT01231845) 6 *Antistrophus laciniatus*, anterodorsal view (USNMENT01448496) 7 *Phanacis* sp., lateral view (USNMENT01448498) 8 *Antistrophus laciniatus*, lateral view (USNMENT01448496). Abbreviations: mep = pronotal submedial pits, plh = pronotum lateral height, pmh = pronotum medial height.

- 2 Mesopleuron medially with broad, crenulate transverse impression (Fig. 9, mci). Female hypopygium always distinctly plowshare-shaped (Fig. 10, hyp). Scutellar foveae faint or absent (Fig. 11, scf). Fore wing vein 2r usually with distinct median vein stump projecting distally (Fig. 12, 2r). Gall inducers on *Rosa* ..... **Diplolepididae: *Diplolepis* Geoffroy**
- Mesopleuron usually without broad crenulate impression (Fig. 13). Female hypopygium usually not plowshare-shaped (Fig. 14, hyp); if plowshare-shaped (only in *Protobalandricus* Melika, Nicholls & Stone, 2018), then mesopleuron entirely smooth. Scutellar foveae usually distinct (Fig. 15, scf). Fore wing vein 2r usually without distinct stump (Fig. 16, 2r). Gall inducers on Fagaceae, especially *Quercus* ..... **Cynipini (not keyed further; see taxonomic treatment below)**

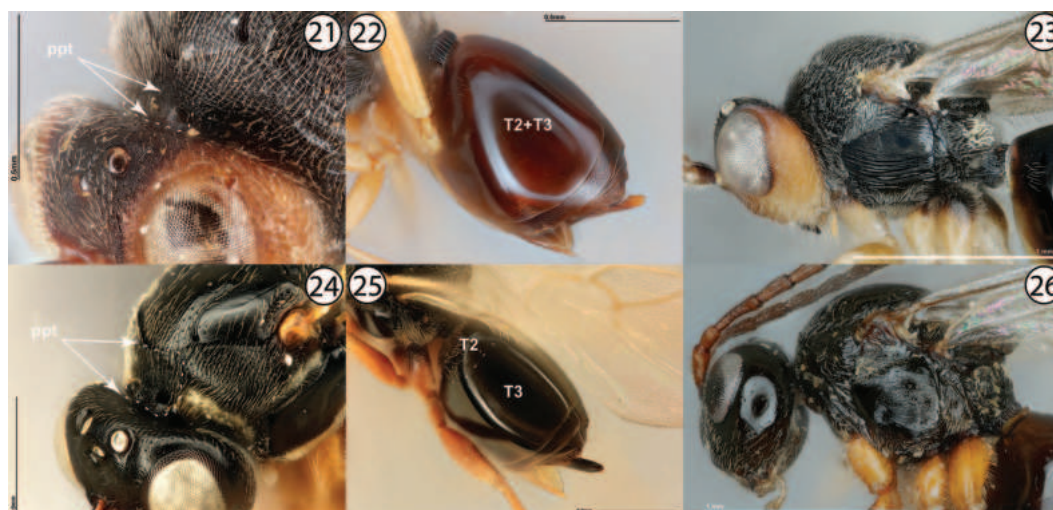


**Figures 9–16.** **9** *Diplolepis bicolor*, lateral view (USNMENT01231831) **10** *Diplolepis bicolor*, lateral view (USNMENT01231831) **11** *Diplolepis bicolor*, dorsal view (USNMENT01231831) **12** *Diplolepis rosae*, fore wing (USNMENT00655959) **13** *Dryocosmus kuriphilus*, lateral view (USNMENT01231861) **14** *Andricus quercuscalifornicus*, lateral view (USNMENT01231839) **15** *Dryocosmus kuriphilus*, dorsolateral view (USNMENT01231861) **16** *Andricus cornigerus*, fore wing (USNMENT00655954). Abbreviations: hyp = hypopygium, mci = mesopleural crenulate impression, scf = scutellar foveae.

- 3 Metasomal tergites 2 and 3 partially or completely fused into a syntergite, resulting in a metasoma composed of one or two segments (Figs 17, 18, arrows indicate length of syntergite). Inquilines in galls on *Quercus* or female inquilines in galls on Rosaceae ..... **4**
- Metasomal postpetiolar terga free and articulated, not forming syntergite and with no single segment especially enlarged (Figs 19, 20, arrows indicate length of longest tergite). Gall inducers on Rosaceae, Asteraceae, or Lamiaceae, or male inquilines in galls on Rosaceae ..... **8**
- 4 Metasomal tergites 2 and 3 entirely fused into syntergite (Fig. 22, T2+T3). Head and mesosoma generally roughly sculptured (Fig. 23). Pronotal plate incomplete, at most weakly defined dorsally, and with marginal sutures never reaching anterior margin of mesoscutum (Fig. 21, ppt). Inquilines in galls on *Quercus* ..... **Synergini: *Synergus* Hartig**
- Metasomal tergites 2 and 3 often delineated by a distinct suture, with tergite 2 much smaller than tergite 3 and appearing ligulate (Fig. 25), although occasionally entirely fused into syntergite. Body usually less roughly sculptured, often smooth and/or shining (Fig. 26). Pronotal plate complete, well-defined both dorsally and ventrally, and with marginal sutures reaching anterior margin of mesoscutum (Fig. 24, ppt.). Inquilines in galls on *Quercus* or female inquilines in galls on Rosaceae ..... **5**



**Figures 17–20.** **17** *Synergus* sp., metasoma, dorsolateral view (USNMENT01231858) **18** *Ceroptres* sp., metasoma, dorsolateral view (USNMENT00917016) **19** *Aulacidea* cf. *hieracii*, metasoma, lateral view (PSUC\_FEM 000253105) **20** *Antistrophus pisum*, metasoma, lateral view (PSUC\_FEM 000247264). Arrows indicate length of longest metasomal tergite.



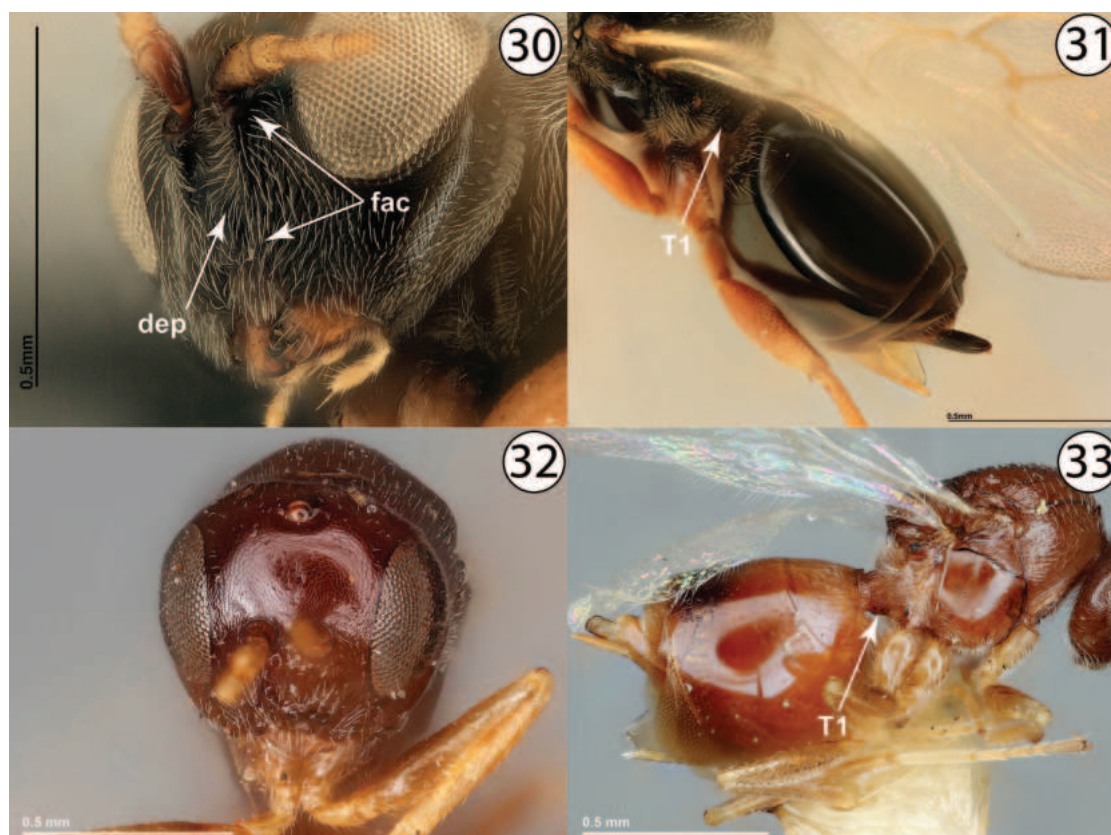
**Figures 21–26.** **21** *Synergus atripennis*, dorsolateral view (USNMENT01231845) **22** *Synergus* sp., metasoma, lateral view (USNMENT01231858) **23** *Synergus* sp., lateral view (PSUC\_FEM 000079457) **24** *Synophromorpha* sp., dorsolateral view (USNMENT01448499) **25** *Ceroptres* sp., metasoma, dorsolateral view (USNMENT00917016) **26** *Diastrophus kincaidii*, lateral view (PSUC\_FEM 000251280). Abbreviations: ppt = pronotal plate, T2 = second metasomal tergite, T2+3 = completely fused second and third metasomal tergites, T3 = third metasomal tergite.

- 5 Metasomal tergites 2 and 3 delineated by a distinct suture, with tergite 2 much smaller than tergite 3 and appearing ligulate (Fig. 27). Mesoscutum with or without abundant setigenous punctation. Female or male inquilines in galls on *Quercus* ..... **6 (Ceroptresini)**
- Metasomal tergites 2 and 3 entirely fused into syntergite, at most with a slight indication of a suture delimiting tergite 2 but never with tergites fully separated (Fig. 28). Mesoscutum with distinct setigenous punctation at least anteriorly (Fig. 29). Female inquilines in galls on Rosaceae ..... **7 (Diastrophini, in part)**



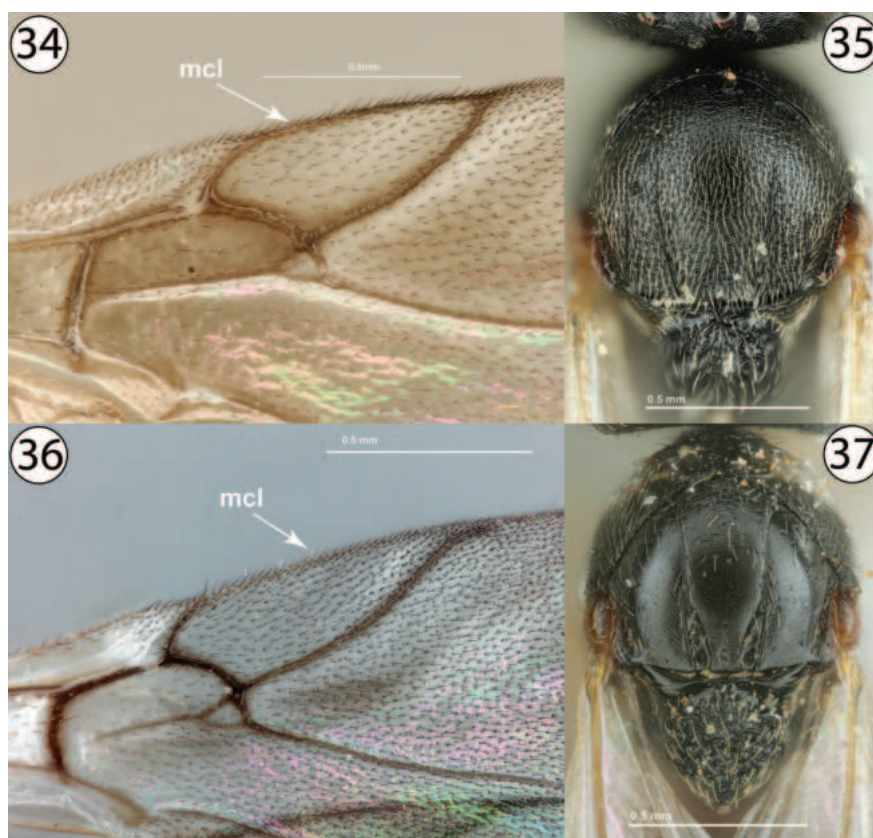
**Figures 27–29.** **27** *Ceroptres* sp., metasoma, dorsolateral view (USNMENT00917016) **28** *Diastrophus kincaidii*, metasoma, lateral view (PSUC\_FEM 000251280) **29** *Periclistus* sp., lateral view (PSUC\_FEM 000250920). Abbreviations: T2 = second metasomal tergite, T2+3 = completely fused second and third metasomal tergites.

- 6 Area between toruli depressed and often pubescent (Fig. 30, dep). Metasomal tergite 1 mostly concealed, smooth (Fig. 31, T1). Frons with distinct facial carinae ventral to toruli apparent at least as short ridges below toruli (Fig. 30, fac). Frequently collected ..... ***Ceroptres* Hartig**
- Area between toruli not depressed and not strongly pubescent (Fig. 32). Metasomal tergite 1 relatively large and ring-like, not concealed, and longitudinally striate (Fig. 33). Frons entirely without facial carinae ventral to toruli (Fig. 32). Very rarely collected ..... ***Buffingtonella* Lobato-Vila & Pujade-Villar**



**Figures 30–33.** **30** *Ceroptres* sp., head, anterior view (USNMENT00917016) **31** *Ceroptres* sp., metasoma, dorsolateral view (USNMENT00917016) **32** *Buffingtonella polita*, head, anterior view (USNMENT00892509) **33** *Buffingtonella polita*, lateral view (USNMENT00892509). Abbreviations: dep = depressed intratorular area, fac = facial carinae, T1 = first metasomal tergite.

- 7 Fore wing with marginal cell closed, with a distinct, complete vein along anterior wing margin (Fig. 34, mcl). Notauli incomplete, absent anteriorly, well developed posteriorly, not apparently widened posteriorly (Fig. 35). Mesoscutum (Fig. 35) coriaceous and punctate-setigenous throughout, and more densely pubescent. Inquelines in galls on *Rosa*...***Periclistus* Förster (females)**
- Fore wing with marginal cell open, without distinct vein along anterior wing margin (Fig. 36, mcl). Notauli usually complete, always distinctly widened posteriorly relative to anterior width (Fig. 37). Mesoscutum (Fig. 37) smooth to granulate and with fewer setigenous punctures, and less densely pubescent. Inquelines in galls on *Rubus*.....***Synophromorpha* Ashmead (females)**



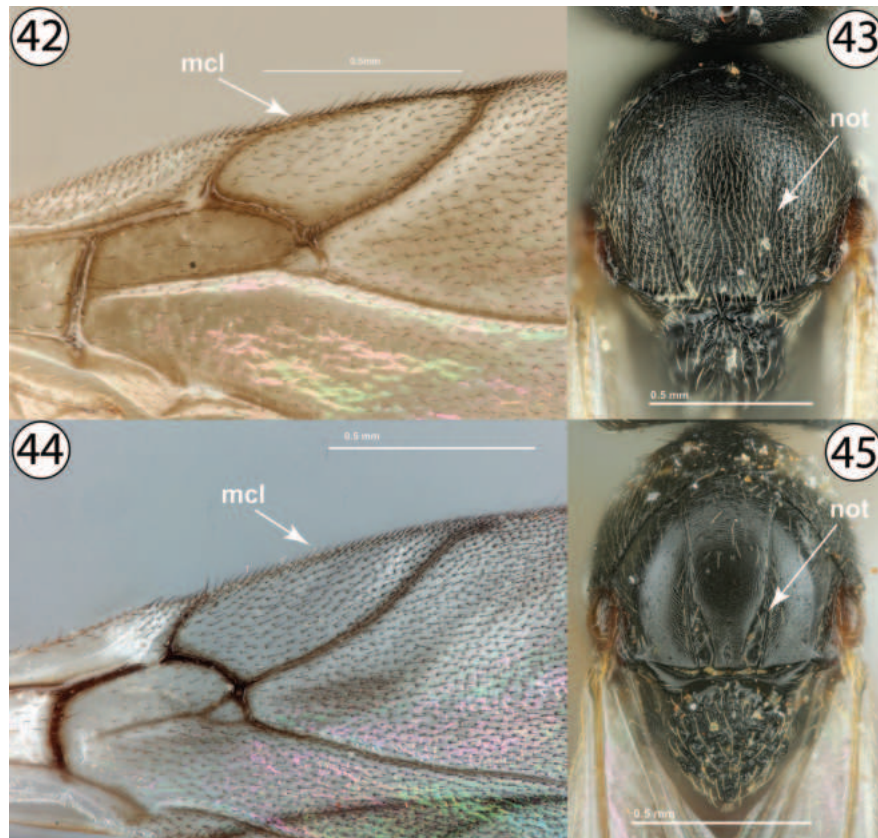
**Figures 34–37.** **34** *Synergus* sp., fore wing (PSUC\_FEM 000079457) **35** *Periclistus* sp., dorsal view (PSUC\_FEM 000250920) **36** *Synophromorpha* sp., fore wing (PSUC\_FEM 000250918) **37** *Synophromorpha* sp., dorsal view (PSUC\_FEM 000250918). Abbreviations: mcl = marginal cell.

- 8 Pronotal plate complete, well-defined both dorsally and ventrally, and with marginal sutures distinctly reaching anterior margin of mesoscutum (Fig. 38, ppt). Metatarsal claws with distinct basal lobe (Fig. 39, mtl). Gall inducers or male inquelines in galls on Rosaceae....**9 (Diastrophini, in part)**
- Pronotal plate usually poorly defined dorsally, never with marginal sutures clearly reaching anterior margin of mesoscutum (Fig. 40, ppt). Metatarsal claws simple and without distinct basal lobe (Fig. 41). Gall inducers on Asteraceae or Lamiaceae .....**11**



Figures 38–41. **38** *Synophromorpha* sp., dorsolateral view (USNMENT01448499) **39** *Diastrophus kincaidii*, tarsal claw (PSUC\_FEM 000251280) **40** *Antistrophus laciniatus*, anterodorsal view (USNMENT01448496) **41** *Antistrophus silphii*, tarsal claw (CYNANT0048). Abbreviations: mtl = metatarsal claw lobe, ppt = pronotal plate.

- 9 Fore wing with marginal cell closed, with a distinct, complete vein along anterior wing margin (Fig. 42, mcl). Notauli weakly developed, never distinctly complete, and not distinctly widened posteriorly (Fig. 43, not). Mesoscutum more or less densely pubescent throughout (Fig. 43). Male inquilines in galls on *Rosa* ..... ***Periclistus Förster (males)***
- Fore wing with marginal cell open, without distinct vein along anterior wing margin (Fig. 44, mcl). Notauli well-developed, usually distinctly complete, and always distinctly widened posteriorly relative to anterior width (Fig. 45, not). Mesoscutum much less pubescent (Fig. 45). Female or male gall inducers on Rosaceae or male inquilines in galls on *Rubus*..... **10**
- 10 Mesoscutum mostly to entirely coriaceous and with distinct setigenous punctures, especially medially (Fig. 46). Male inquilines of *Diastrophus* galls on *Rubus* (females with metasomal tergites 2 and 3 fused into a syntergite, causing metasoma to appear mostly as one large segment) ...  
..... ***Synophromorpha Ashmead (males)***
- Mesoscutum mostly smooth and shining, at most weakly coriaceous, and without abundant strong setigenous punctures (Fig. 47). Female or male gall inducers on Rosaceae (females with metasomal tergites 2 and 3 free and articulated and without syntergite)..... ***Diastrophus Hartig***

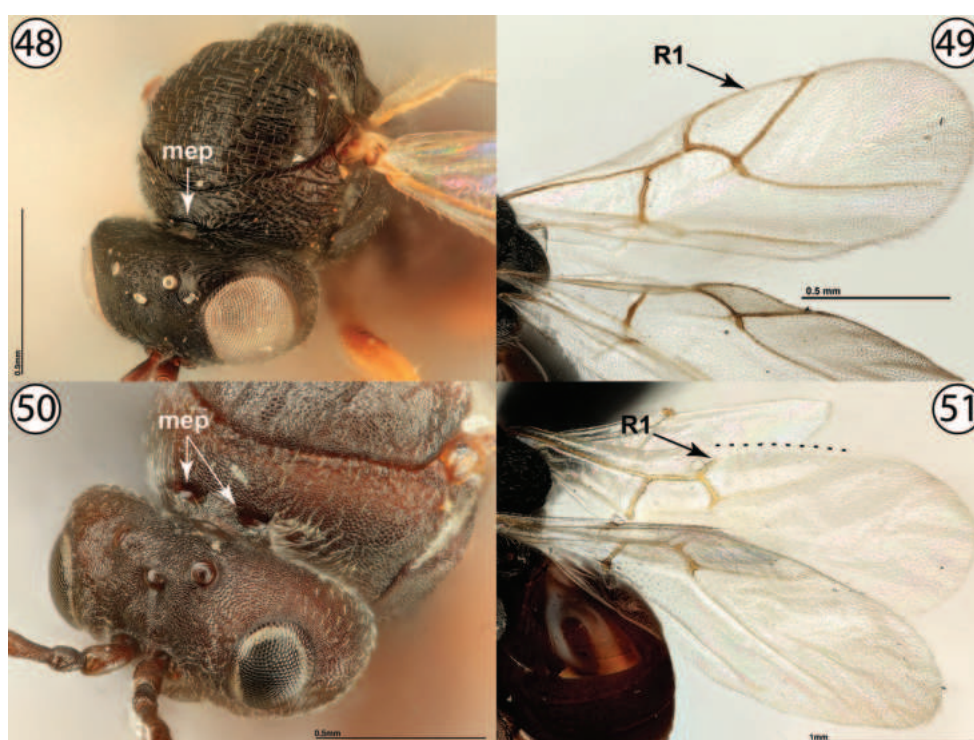


Figures 42–45. 42 *Synergus* sp., fore wing (PSUC\_FEM 000079457) 43 *Periclistus* sp., dorsal view (PSUC\_FEM 000250920) 44 *Synophromorpha* sp., fore wing (PSUC\_FEM 000250918) 45 *Synophromorpha* sp., dorsal view (PSUC\_FEM 000250918). Abbreviations: mcl = marginal cell, not = notauli.



Figures 46, 47. 46 *Synophromorpha* sp., dorsal view (PSUC\_FEM 000250918) 47 *Diastrophus kincaidii*, dorsal view (PSUC\_FEM 000251280).

- 11 Pronotum with submedial pits reduced, usually apparent as a continuous linear depression (Fig. 48). Fore wing with marginal cell partially open, with vein R1 reaching anterior margin of fore wing and continuing along wing margin but not meeting vein Rs (Fig. 49, arrow indicates end of vein R1). Gall inducers on *Taraxacum officinale* or *Hypochaeris radicata* (Asteraceae) ..... **Phanacidini: *Phanacis* Förster**
- Pronotum with submedial pits distinct and well-defined (Fig. 50, mep). Fore wing with marginal cell either entirely open (Fig. 51, arrow indicates end of vein R1 and dotted line indicates margin of fore wing along marginal cell), with vein R1 clearly not reaching wing margin, or entirely closed, with vein Rs reaching wing margin and distinctly reaching vein Rs to enclose cell. Gall inducers on several genera of Asteraceae, or *Glechoma hederacea* (Lamiaceae)..... **12 (Aulacideini)**



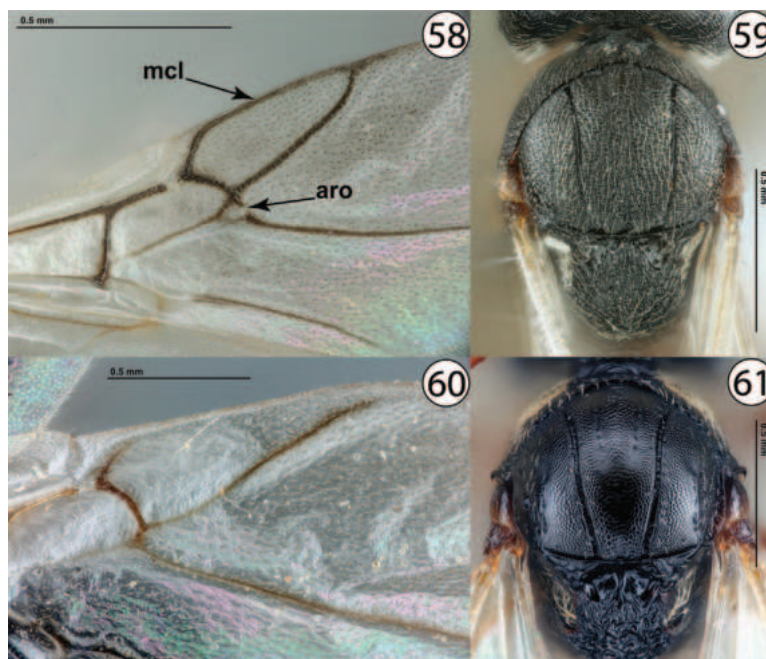
Figures 48–51. **48** *Phanacis* sp., anterodorsal view (USNMENT01448498) **49** *Phanacis* sp., wings (USNMENT01231855) **50** *Antistrophus laciniatus*, anterodorsal view (USNMENT01448496) **51** *Antistrophus laciniatus*, wings (USNMENT01448496); dotted line indicates margin of fore wing. Abbreviations: mep = pronotal submedial pits.

- 12 Mesopleuron with sculpture primarily or entirely reticulate (Fig. 52, msp), often with fine striae intermediate to rows of reticulate cells (Fig. 53, msp). Second metasomal tergite without distinct patch of setae, at most with a few scattered setae (Fig. 52, 53). Marginal cell of fore wing always open (Fig. 54, mcl). Gall inducers on *Chrysothamnus*, *Lygodesmia*, *Microseris*, or *Silphium* (Asteraceae) ..... ***Antistrophus* Walsh**
- Mesopleuron with sculpture primarily or entirely transversely striate (Fig. 55, msp). Second metasomal tergite usually with distinct anterolateral patch of pale setae (Fig. 56, T2p). Marginal cell of fore wing usually closed (Fig. 57, mcl), open only in *Liposthenes* Förster. Gall inducers on several genera of Asteraceae or on *Glechoma hederacea* (Lamiaceae) ..... **13**



Figures 52–57. 52 *Antistrophus pisum*, lateral view (PSUC\_FEM 000247286) 53 *Antistrophus meganae*, lateral view (PSUC\_FEM 000248165) 54 *Antistrophus laciniatus*, wings (USNMENT01448496) 55 *Aulacidea* sp., lateral view (PSUC\_FEM 000247286) 56 *Liposthenes glechomae*, lateral view (PSUC\_FEM 000248152) 57 *Aulacidea* sp., wings (PSUC\_FEM 000247286). Abbreviations: mcl = marginal cell, msp = mesopleuron, T2p = setose patch on second metasomal tergite.

- 13 Fore wing with marginal cell closed and usually with areolet distinct (Fig. 58, mcl and aro). Mesoscutum pubescent throughout, always with abundant, closely-set setae and often appearing densely silky (Fig. 59). Gall inducers primarily on Cichorieae (Asteraceae), especially *Lactuca* L. . . . . ***Aulacidea* Ashmead**
- Fore wing with marginal cell open and areolet indistinct (Fig. 60). Mesoscutum mostly bare, at most with a few scattered setae (Fig. 61). Gall inducers on *Glechoma hederacea* (Lamiaceae) . . . . . ***Liposthenes* Förster**



Figures 58–61. 58 *Aulacidea* sp., wings (PSUC\_FEM 000247286) 59 *Aulacidea* sp., dorsal view (PSUC\_FEM 000247286) 60 *Liposthenes glechomae*, wings (PSUC\_FEM 000248152) 61 *Liposthenes glechomae*, dorsal view (PSUC\_FEM 000248152). Abbreviations: aro = areolet, mcl = marginal cell.

## Systematic overview

### Aulacideini

Figs 62–67, 87–89

**Diagnosis.** Pronotum tall and broad dorsomedially. Pronotal submedial pits distinct and well-impressed. Pronotal plate present, usually only distinct in anterior half of pronotum. Mesopleuron sculpture striate, reticulate, or striate-reticulate. Mesoscutellar foveae distinct. Fore wing with marginal cell entirely open or entirely closed, never partially open. Wings always hyaline, never tinted or with darkened areas. Metatarsal claws without basal lobe. Metasomal tergites 2 and 3 free and articulate, never with a syntergite.

**Note.** The tribe Aulacideini is represented by approximately 90 species in ten genera worldwide (Nieves-Aldrey 2022), three of which are known from North America (Nastasi and Deans 2021): *Antistrophus* Walsh, 1869, *Aulacidea* Ashmead, 1897, and *Liposthenes* Förster, 1869. Monophyly of the tribe is rather well-established (e.g., Ronquist et al. 2015; Blaimer et al. 2020), but the generic taxonomy is somewhat unsettled (Nieves-Aldrey 2022), and many North American species await description (Nastasi, pers. comm.). The number of introduced described species established in North America is uncertain (see the treatment of *Aulacidea* Ashmead below), but Nastasi and Deans (2021) reported 21 described species.

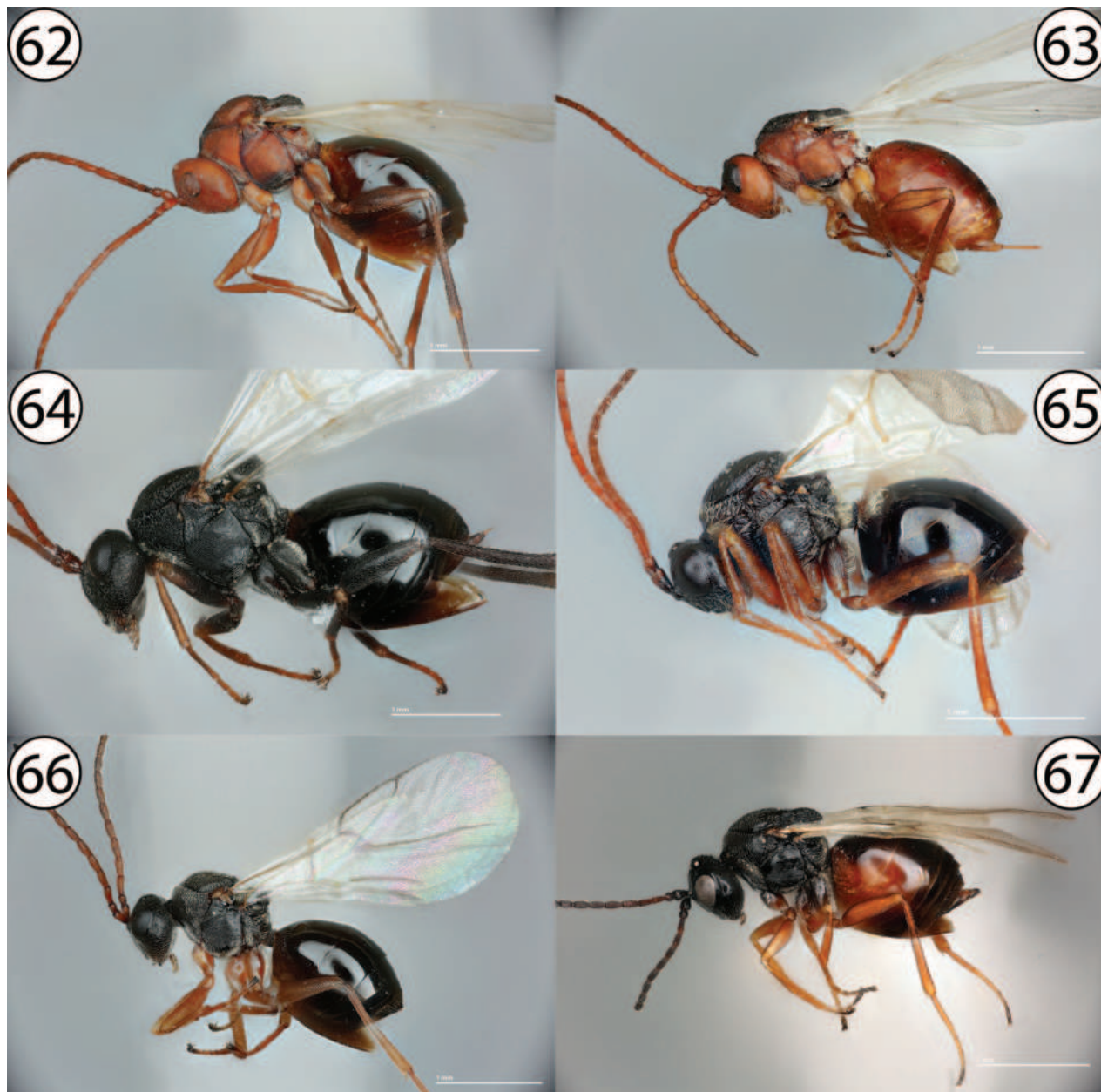
Globally, members of this tribe induce galls on five plant families (Azmaç and Katılmış 2020; Buffington et al. 2020; Nieves-Aldrey 2022), but the described North American taxa are restricted to host plants in the Asteraceae (tribes Astereae, Chicorieae, and Heliantheae) and Lamiaceae (*Glechoma hederacea* L.) (Nastasi and Deans 2021). Galls induced by wasps of this tribe (Figs 87–89) are most likely to yield adults when collected after host plants have senesced; adult wasps emerge in mid spring through late summer depending on the gall wasp species and collecting locality (Nastasi et al., in lit.). Many species induce cryptic galls that produce no externally discernable modification to the plant tissue; this phenomenon suggests that aulacideine herb gall wasps inducing cryptic galls are probably more diverse than currently known and have evaded detection due to their hidden galls.

### *Antistrophus* Walsh, 1869

**Type species.** *Antistrophus lygodesmiaepisum* Walsh, 1869 (= *Antistrophus pisum* Ashmead, 1885)

**Diagnosis.** Mesoscutum sparsely pubescent, at most with scattered setae throughout and never appearing silky. Notauli typically incomplete but complete in several species. Mesopleuron reticulate or striate-reticulate, never entirely transversely striate. Fore wing with marginal cell open, with R1 never reaching anterior wing margin, always without areolet, and with or without marginal setae. Second metasomal tergite without patch of setae.

**Note.** *Antistrophus* contains ten described species, all of which are known from America north of Mexico (Nastasi and Deans 2021). *Antistrophus* wasps are most commonly encountered in the Eastern and Midwestern United States,



Figures 62–67. **62** *Antistrophus pisum*, lateral view (PSUC\_FEM 000247286) **63** *Antistrophus meganae*, lateral view (PSUC\_FEM 000248165) **64** *Antistrophus silphii*, lateral view (CYNANT0048) **65** *Liposthenes glechomae*, lateral view (PSUC\_FEM 000248152) **66** *Aulacidea* sp., lateral view (PSUC\_FEM 000247286) **67** *Aulacidea hieracii*, lateral view (PSUC\_FEM 000253105).

although two species, *A. chrysothamni* (Beutenmüller) and *A. microseris* (McCracken & Egbert), are apparently restricted to Arizona and California respectively (Nastasi and Deans 2021). Unpublished records indicate that the genus is far more widely distributed than currently known and is likely common throughout the United States and adjacent parts of Canada (Nastasi, pers. obs.).

Species of *Antistrophus* induce galls on several genera of asteraceous plants: *Chrysothamnus* Nutt.; *Lygodesmia* D. Don; *Microseris* D. Don; and *Silphium* L. Additional plant genera are known to host undescribed species. *Antistrophus* associated with *Silphium* are especially diverse and primarily comprise undescribed species; each *Silphium* species appears to be galled by one or

more host-specific or narrowly oligophagous gall wasp species, and some *Antistrophus* are emerging as pests of cultivated *Silphium*.

*Antistrophus*, as currently circumscribed, is a heterogeneous assemblage. The genus contains all North American herb gall wasps that did not fit well within *Aulacidea* Ashmead, 1897 or *Diastrophus* Hartig, 1840, of which the latter is now placed in Diastrophini. Many undescribed species of this genus are known to us, and morphological and molecular data demonstrate that *Antistrophus* as currently defined is poorly circumscribed (unpublished data); the limits of *Antistrophus* will be revised by an ongoing study. Nevertheless, all described species currently placed in this genus as well as all undescribed species currently known to us correctly key to *Antistrophus* here.

### North American species (Nastasi and Deans 2021):

1. *Antistrophus bicolor* Gillette, 1891
2. *Antistrophus chrysothamni* (Beutenmüller, 1908)
3. *Antistrophus jeanae* Tooker & Hanks, 2004
4. *Antistrophus laciniatus* Gillette, 1891
5. *Antistrophus meganae* Tooker & Hanks, 2004
6. *Antistrophus microseris* (McCracken & Egbert, 1922)
7. *Antistrophus minor* Gillette, 1891
8. *Antistrophus pisum* Ashmead, 1885 (replacement name for *A. lygodesmi-aepisum* Walsh as given by Nieves-Aldrey [1994] but omitted from Nastasi and Deans [2021])
9. *Antistrophus rufus* Gillette, 1891
10. *Antistrophus silphii* Gillette, 1891

### *Aulacidea* Ashmead, 1897

**Type species.** *Aulax mulgediicola* Ashmead, 1896 (= *Aulacidea harringtoni* [Ashmead, 1897])

**Diagnosis** (based on North American taxa): Mesoscutum densely pubescent, often appearing silky but at least with rather abundant closely-set setae. Notauli almost always complete (incomplete only in an undescribed species from California). Mesopleuron transversely striate; with a small ventral patch of reticulate sculpture in *Aulacidea acroptilonica* Tyurebaev, 1972. Fore wing with marginal cell entirely closed, with R1 meeting Rs along anterior wing margin, always with areolet, and always with distinct marginal setae. Second metasomal tergite with a distinct patch of setae (absent in *Aulacidea acroptilonica* Tyurebaev, 1972 and sometimes appearing reduced in males of various species).

**Note.** *Aulacidea* contains some 40 described species (Azmaç and Katılmış 2020; Nieves-Aldrey 2022), 11 of which are known or suspected from North America (Nastasi and Deans 2021). Native species known from North America induce galls primarily on species of *Lactuca* L., although one species (*A. nabali* [Brodie, 1892]) induces galls on *Nabalis* Cass, and one species (*A. ambrosiae-cola* [Ashmead, 1896]) is doubtfully associated with *Ambrosia* L. Introduced or suspected species induce galls on *Hieracium* L., *Pilosella* Hill, and *Rhaponticum* Vaill. (Nastasi and Deans 2021).

The number of established exotic *Aulacidea* is problematic as several species have apparently been introduced (e.g., Moffat and Smith 2015), but few records indicate whether they have successfully established. *Aulacidea acroptilonica* Tyurebaev is definitively established in the Pacific Northwest, but it is unclear whether *A. subterminalis* Niblett, 1946 or *A. pilosellae* (Kieffer, 1901) are truly established (Nastasi and Deans 2021). A single *A. pilosellae* was collected via Malaise trap in Canada (Moffat and Smith 2015), but there appear to be no subsequent records indicating establishment of this species in North America. The only accessible evidence of establishment of *A. subterminalis* in North America is a government report detailing introduction attempts in Canada (Government of British Columbia 2018). Records appearing to represent *A. hieracii* (Linnaeus, 1758) on *Hieracium umbellatum* L. in North America have been confirmed since publication of the recent catalogue, although there are some disputes over whether the population present in the Nearctic is conspecific with those found in the Palearctic (unpublished data). Overall, more research is needed to substantiate the identity and establishment of the introduced taxa.

More generally, *Aulacidea* was erected by Ashmead for herb gall wasps (then, the tribe Aylacini) with a closed marginal cell; this conception of *Aulacidea* remains virtually unchanged at present. As with *Antistrophus*, *Aulacidea* is poorly circumscribed, and the limits of this genus require adjustment (Ronquist et al. 2015; Nieves-Aldrey 2022).

#### **North American species (Nastasi and Deans 2021):**

1. *Aulacidea abdita* Kinsey, 1920
2. *Aulacidea acroptilonica* Tyurebaev, 1972
3. *Aulacidea ambrosiaecola* (Ashmead, 1896)
4. *Aulacidea annulata* Kinsey, 1920
5. *Aulacidea harringtoni* (Ashmead, 1887)
6. *Aulacidea hieracii* (Linnaeus, 1758)
7. *Aulacidea nabali* (Brodie, 1892)
8. *Aulacidea pilosellae* (Kieffer, 1901)
9. *Aulacidea podagrae* (Bassett, 1890)
10. *Aulacidea subterminalis* Niblett, 1946
11. *Aulacidea tumida* (Bassett, 1890)

#### ***Liposthenes* Förster, 1869**

**Type species:** *Aulax glechomae* Hartig, 1841 (= *Cynips glechomae* Linnaeus, 1758).

**Diagnosis.** Mesoscutum sparsely pubescent, at most with a few scattered setae. Notauli complete. Mesopleuron mostly transversely striate, at most with slight indication of reticulate sculpture. Fore wing with marginal cell open, never with areolet distinct, and always with distinct marginal setae. Second metasomal tergite always with a distinct patch of setae.

**Note.** *Liposthenes* is known in North America from a single introduced species: *L. glechomae* (Linnaeus, 1758). This species was apparently introduced

from Europe along with its host plant, *Glechoma hederacea* L., and has since become widespread in the United States (Nastasi and Deans 2021). *Liposthenes glechomae* is the only known gall wasp associated with Lamiaceae in the Nearctic; all other known Nearctic Aulacideini, both described and known undescribed species, are associated with Asteraceae.

### North American species (Nastasi and Deans 2021):

1. *Liposthenes glechomae* (Linnaeus, 1758)

### Ceroptresini

Figs 68, 69

**Diagnosis.** Pronotum tall and broad dorsomedially. Pronotal submedial pits distinct and well-impressed. Pronotal plate present and complete. Mesoscutellar foveae distinct. Fore wing with marginal cell closed. Metatarsal claws with basal lobe. Metasoma with syntergite, with third tergite greatly enlarged and occupying most of metasoma and with second tergite reduced but free and articulating. First metasomal tergite usually more or less concealed between mesosoma and metasoma and without conspicuous sculpture (more visible and conspicuously striate in some taxa easily confused with *Ceroptres*). Body generally weakly sculptured.

**Note.** Ceroptresini includes 19 North American species: 18 species of *Ceroptres* Hartig and *Buffingtonella polita* (Ashmead, 1896) (Nastasi and Deans 2021).

### *Buffingtonella* Lobato-Vila & Pujade-Villar, 2019

**Type species.** *Ceroptres politus* Ashmead, 1896

**Diagnosis.** Area between toruli not depressed and without dense pubescence. Metasomal tergite 1 relatively large and ring-like, not concealed, and longitudinally striate. Frons entirely without facial carinae ventral to toruli.

**Note.** *Buffingtonella* is known only from Virginia from eight specimens collected in 1884 and 1885 (Lobato-Vila and Pujade-Villar 2019). These specimens were apparently ovipositing into the midribs of leaves of *Quercus rubra* L. at the time of collection, and as such, *B. polita* has been assumed to be an inquiline of an unidentified oak gall wasp (Lobato-Vila and Pujade-Villar 2019). However, the placement of this genus in Ceroptresini, its recognition as distinct from other related taxa, and its biology remain to be substantiated (Lobato-Vila and Pujade-Villar 2019). Upon examining the aforementioned material of this species in the National Museum of Natural History, we confirm the diagnostic characters for the genus as described by Lobato-Vila and Pujade-Villar (2019) and have included it in the above key.

### North American species (Nastasi and Deans 2021):

1. *Buffingtonella polita* (Ashmead, 1896)



Figures 68, 69. 68 *Buffingtonella polita*, lateral view (USNMENT00892509) 69 *Ceroptres* sp., lateral view (USNMENT00917016).

### ***Ceroptres* Hartig, 1840**

**Type species.** *Ceroptres clavicornis* Hartig, 1840.

**Diagnosis.** Area between toruli distinctly depressed and with abundant pubescence. Metasomal tergite 1 small, mostly concealed between mesosoma and following tergites, and dorsally smooth. Frons with distinct facial carinae ventral to toruli, apparent at least as short ridges (we strongly recommend careful positioning and light diffusion when assessing this character).

**Note.** *Ceroptres* are occasionally reared from galls induced on oaks by members of the tribe Cynipini (Lobato-Vila and Pujade-Villar 2019; Nastasi and Deans 2021), but are otherwise infrequently encountered. *Ceroptres* are presumed to be inquilines of Cynipini (Ronquist et al. 2015), although some theorize that they may actually be parasitoids due to observation of female *Ceroptres* ovipositing into mature galls rather than developing galls as is typical for gall inquilines (Z. Liu, in lit.). While 18 described species of *Ceroptres* are known from North America, the diversity of this genus has been sparsely surveyed, and many undescribed species are known in association with oak galls (S. Rollins and C. Tribull, pers. comm. 2023). *Ceroptres* have also been reared by several North American research groups in association with galls of cecidomyiid midges, although the exact nature of this association is unknown.

### **North American species (Nastasi and Deans 2021):**

1. *Ceroptres catesbaei* Ashmead, 1885
2. *Ceroptres confertus* (McCracken & Egbert, 1922)
3. *Ceroptres cornigera* Melika & Buss, 2002
4. *Ceroptres ensiger* (Walsh, 1864)
5. *Ceroptres frondosae* Ashmead, 1896
6. *Ceroptres junquerasi* Lobato-Vila & Pujade-Villar, 2019
7. *Ceroptres lanigerae* Ashmead, 1885
8. *Ceroptres lenis* Lobato-Vila & Pujade-Villar, 2019
9. *Ceroptres mexicanus* Lobato-Vila & Pujade-Villar, 2019
10. *Ceroptres minutissimi* Ashmead, 1885

11. *Ceroptres montensis* Weld, 1957
12. *Ceroptres nigricus* Lobato-Vila & Pujade-Villar, 2019
13. *Ceroptres petiolicola* (Osten Sacken, 1861)
14. *Ceroptres pisum* (Osten Sacken, 1861)
15. *Ceroptres quadratifacies* Lobato-Vila & Pujade-Villar, 2019
16. *Ceroptres rufiventris* Ashmead, 1896
17. *Ceroptres snellingi* Lyon, 1996

### Cynipini

Figs 70–72

**Diagnosis.** Pronotum distinctly short and narrow dorsomedially, without distinct plate or pits. Scutellar foveae usually distinct. Mesopleuron usually without broad crenulate impression. Female hypopygium only very rarely plow-share-shaped; only so in *Protobalandricus* Melika, Nicholls & Stone, 2018, in which the mesopleuron is entirely smooth and therein readily separable from *Diplolepis* Geoffroy, 1762 (Cuesta Porta, pers. comm. 13 Feb 2024).

**Note.** Cynipini is represented by an estimated 680 North American species that induce galls primarily on *Quercus* (Fagaceae) (Melika et al. 2021). Additional host genera known are *Castanea* Mill., *Chrysolepis* Hjelmq., and *Notholithocarpus* Manos, Cannon, & S.H. Oh (Buffington and Morita 2009). Genera belonging to Cynipini are not keyed in the present work due to the presence of several highly unstable genera that prohibit clear morphological recognition, although recent studies (e.g., Melika et al. 2021) have made taxonomic changes that greatly ease this burden. Further revisionary studies will continue to stabilize genera in the Cynipini, and a key to Cynipini will be published when possible. Relevant keys for Cynipini include Weld (1952), Zimmerman (2018), and Melika et al. (2021), but these works are partial in their taxon coverage or do not align well with current taxonomic hypotheses.

### Diastrophini

Figs 73–75, 92–94

**Diagnosis.** Pronotum tall and broad dorsomedially. Pronotal submedial pits distinct and well-impressed. Pronotal plate present and complete, distinct both dorsally and ventrally. Mesopleuron sculpture striate or smooth and shining. Mesoscutellar foveae distinct. Fore wing with marginal cell entirely open or entirely closed, never partially open. Wings often with darkened areas, especially around the marginal cell. Metatarsal claws always with basal lobe. Metasomal tergites 2 and 3 either free and articulate, or fused into a syntergite in some females.

**Note.** Diastrophini includes 25 described North American species in three genera: *Diastrophus* Hartig, 1840, *Periclistus* Förster, 1869, and *Synophromorpha* Ashmead, 1903 (Nastasi and Deans 2021). The North American members of this tribe are gall inducers on various Rosaceae or inquilines in the galls of *Diastrophus* Hartig, 1840 or *Diplolepis* Geoffroy, 1762 (Nastasi and Deans 2021).



Figures 70–72. 70 *Dryocosmus kuriphilus*, lateral view (USNMENT01231861) 71 *Andricus quercuscalifornicus*, lateral view (USNMENT01231839) 72 *Phylloteras* sp., lateral view (USNMENT01231835).



Figures 73–75. 73 *Diastrophus kincaidii*, lateral view (PSUC\_FEM 000251280) 74 *Periclistus* sp., lateral view (PSUC\_FEM 000250920) 75 *Synophromorpha* sp., lateral view (PSUC\_FEM 000250918).

### ***Diastrophus* Hartig, 1840**

**Type species.** *Cynips rubi* Bouché, 1834.

**Diagnosis.** Mesoscutum generally weakly sculptured and without abundant strong setigenous punctures. Notauli complete and strong throughout. Mesopleuron sculpture smooth to striate. Fore wing with marginal cell open. Metasoma never with syntergite.

**Note.** *Diastrophus* contains 14 North American species (Nastasi and Deans 2021). Many species induce galls on *Rubus* L., although the herbaceous genera *Fragaria* L. and *Potentilla* L. are also used. *Diastrophus smilacis* Ashmead, 1896 and its supposed inquiline, *Periclistus smilacis* Ashmead, 1896, were previously believed to be associated with *Smilax* L., making *D. smilacis* the only cynipid known to induce galls on a monocot plant (Gates et al. 2020). However, Gates et al. conclude that this association was erroneous, and the true gall inducer on *Smilax* is in fact a eulophid wasp (Chalcidoidea: *Aprostocetus smilax* Gates & Zhang). The biological associations of Diastrophini therein are still atypical as *Periclistus* inquilines are generally associated with the tribe Diplolepidini. Our own examination of the type material of *D. smilacis* and *P. smilacis* (deposited in the USNM) confirm that they are indeed placed in the appropriate genera, although the status of either species and their biological relationships remain suspect and require further investigation.

Galls of Diastrophini (Figs 92–94) can be collected for rearing in the fall, winter, or spring. As in Aulacideini, galls on herbaceous hosts are best collected after host plants have senesced, and adults of all *Diastrophus* emerge in spring and summer.

### **North American species (Nastasi and Deans 2021):**

1. *Diastrophus austrior* Kinsey, 1922
2. *Diastrophus bassettii* Beutenmüller, 1892
3. *Diastrophus cuscuteaeformis* Osten Sacken, 1863
4. *Diastrophus fragariae* Beutenmüller, 1915
5. *Diastrophus fusiformans* Ashmead, 1890
6. *Diastrophus kincaidii* Gillette, 1893
7. *Diastrophus nebulosus* (Osten Sacken, 1861)
8. *Diastrophus niger* Bassett, 1900
9. *Diastrophus piceus* Provancher, 1886
10. *Diastrophus potentillae* Bassett, 1864
11. *Diastrophus radicum* Bassett, 1870
12. *Diastrophus smilacis* Ashmead, 1896
13. *Diastrophus tumefactus* Kinsey, 1920
14. *Diastrophus turgidus* Bassett, 1870

### ***Periclistus* Förster, 1869**

**Type species.** *Aylax caninae* Hartig, 1840.

**Diagnosis.** Mesoscutum generally coarsely sculptured, usually densely pubescent, and with abundant strong setigenous punctures. Notauli incomplete, indistinct at least in anterior third, and weaker throughout. Fore wing with

marginal cell closed. Metasoma with syntergite in females but with all tergites free and articulating in males.

**Note.** *Periclistus* contains seven North American species, all of which are inquilines of *Diplolepis* Geoffroy inducing galls on species of *Rosa* L., except for *P. smilacis* Ashmead (see treatment of *Diastrophus* Hartig). The diversity of this genus is not well understood; Ritchie (1984) treated ten Nearctic species in his unpublished thesis including six new species, but a recent DNA barcoding study (Zhang et al. 2019) revealed the presence of two undescribed Nearctic species. More broadly, future study is needed to investigate host associations, especially given the presence of undescribed species.

#### **North American species (Nastasi and Deans 2021):**

1. *Periclistus arefactus* McCracken & Egbert, 1922
2. *Periclistus californicus* Ashmead, 1896
3. *Periclistus obliquus* Provancher, 1888
4. *Periclistus piceus* Fullaway, 1911
5. *Periclistus pirata* (Osten Sacken, 1863)
6. *Periclistus semipiceus* (Harris, 1841)
7. *Periclistus smilacis* Ashmead, 1896

#### ***Synophromorpha* Ashmead, 1903**

**Type species.** *Synophrus sylvestris* Osten Sacken, 1861.

**Diagnosis.** Mesoscutum generally less coarsely sculptured, appearing mostly or entirely coriaceous, less pubescent, and with some strong setigenous punctures. Notauli complete, strong throughout. Fore wing with marginal cell open. Metasoma with syntergite in females but with all tergites free and articulating in males.

**Note.** *Synophromorpha* is represented by four species in North America, all of which are inquilines of *Diastrophus* species associated with *Rubus* L. Ritchie and Shorthouse (1987) described the species *S. kaulbarsi* Shorthouse & Ritchie, 1987 from a single specimen collected in Mexico; they speculated that this species was evidence of undiscovered Mexican *Diastrophus* or represented the use of an alternative host such as an oak gall wasp.

#### **North American species (Nastasi and Deans 2021):**

1. *Synophromorpha kaulbarsi* Ritchie & Shorthouse, 1987
2. *Synophromorpha rubi* Weld, 1952
3. *Synophromorpha sylvestris* (Osten Sacken, 1861)
4. *Synophromorpha terricola* Weld, 1952

#### ***Diplolepis* Geoffroy, 1762 (Diplolepididae: Diplolepidinae)**

Figs 76–79, 90, 91

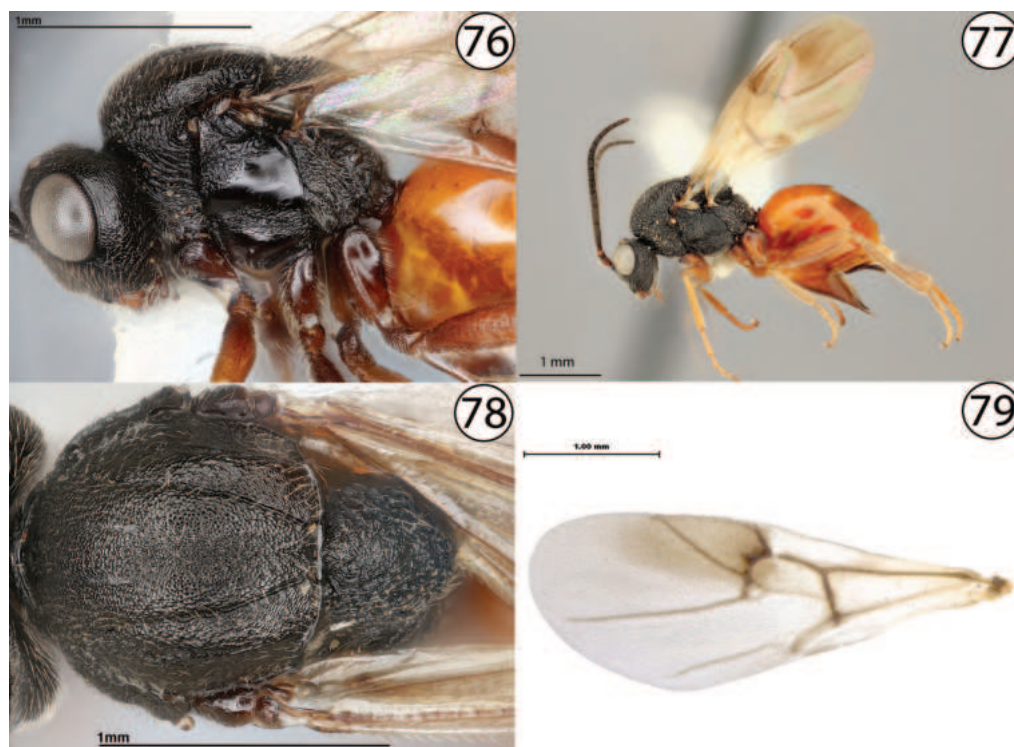
**Type species.** *Cynips rosae* Linnaeus, 1758.

**Diagnosis.** Pronotum distinctly short and narrow dorsomedially, without distinct plate or pits. Scutellar foveae faint or absent, never distinct and well impressed. Mesopleuron with broad crenulate medial impression. Female hypopygium plowshare-shaped.

**Note.** Diplolepidinae includes 34 described North American species in *Diplolepis* Geoffroy which induce structurally diverse galls (Figs 90, 91) on *Rosa* (Rosaceae) and are widely distributed in the US and Canada (Nastasi and Deans 2021). Recent phylogenomic studies (Blaimer et al. 2020; Hearn et al. 2023) showed that the tribe Diplolepidini clustered together with Pediaspidini outside of the core Cynipidae, causing Cynipidae to form a paraphyletic grade at the base of Cynipoidea. Hearn et al. (2023) raised the former tribe Diplolepidini to subfamily rank (Diplolepidinae) within the family Diplolepididae. All other taxa treated here remain in the Cynipidae.

### North American species (Nastasi and Deans 2021):

1. *Diplolepis arefacta* (Gillette, 1894)
2. *Diplolepis ashmeadi* (Beutenmüller, 1918)
3. *Diplolepis bassetti* (Beutenmüller, 1918)
4. *Diplolepis bicolor* (Harris, 1841)
5. *Diplolepis californica* (Beutenmüller, 1914)
6. *Diplolepis dichlocera* (Harris, 1841)
7. *Diplolepis fulgens* (Gillette, 1894)
8. *Diplolepis fusiformans* (Ashmead, 1890)
9. *Diplolepis gracilis* (Ashmead, 1897)
10. *Diplolepis ignota* (Osten Sacken, 1863)
11. *Diplolepis inconspicuis* Dailey & Campbell, 1973
12. *Diplolepis lens* Weld, 1952
13. *Diplolepis mayri* (Schlechtendal, 1877)
14. *Diplolepis nebulosa* (Bassett, 1890)
15. *Diplolepis neglecta* (Gillette, 1894)
16. *Diplolepis nervosa* (Curtis, 1838)
17. *Diplolepis nodulosa* (Beutenmüller, 1909)
18. *Diplolepis oregonensis* (Beutenmüller, 1918)
19. *Diplolepis ostensackeni* (Beutenmüller, 1918)
20. *Diplolepis polita* (Ashmead, 1890)
21. *Diplolepis pustulatoides* (Beutenmüller, 1914)
22. *Diplolepis radicum* (Osten Sacken, 1863)
23. *Diplolepis rosae* (Linnaeus, 1758)
24. *Diplolepis rosaefolii* (Cockerell, 1889)
25. *Diplolepis similis* (Ashmead, 1896)
26. *Diplolepis spinosa* (Ashmead, 1887)
27. *Diplolepis terrigena* Weld, 1952
28. *Diplolepis triforma* Shorthouse & Ritchie, 1984
29. *Diplolepis tuberculator* (Cockerell, 1888)
30. *Diplolepis tuberculosa* (Osten Sacken, 1861)
31. *Diplolepis tumida* (Bassett, 1890)
32. *Diplolepis variabilis* (Bassett, 1890)
33. *Diplolepis verna* (Osten Sacken, 1863)
34. *Diplolepis weldi* (Beutenmüller, 1913)



Figures 76–79. 76 *Diplolepis bicolor*, lateral view (USNMENT01231831) 77 *Diplolepis bicolor*, lateral view (USNMENT01231831) 78 *Diplolepis bicolor*, dorsal view (USNMENT01231831) 79 *Diplolepis rosae*, fore wing (USNMENT00655959).

### *Phanacis* Förster, 1860 (Phanacidini)

Figs 80–82, 95

**Type species.** *Parapanteliella eugeniae* Diakontschuk, 1981.

**Diagnosis.** Pronotum tall and broad dorsomedially. Pronotal submedial pits rather indistinct and poorly impressed, appearing as a narrow linear impression rather than distinct ovular pits. Pronotal plate present, usually only distinct in anterior half of pronotum. Mesopleuron sculpture reticulate. Mesoscutellar foveae distinct. Fore wing with marginal cell partially open, with vein R1 reaching anterior margin of fore wing and continuing along wing margin but not meeting vein Rs. Wings always hyaline, never tinted or with darkened areas. Metatarsal claws without basal lobe. Metasomal tergites 2 and 3 free and articulate, never with a syntergite.

**Note.** Phanacidini includes two North American species, both in *Phanacis* Förster, which have been introduced along with their host plants (Nastasi and Deans 2021). *Phanacis hypochoeridis* (Kieffer, 1887) induces galls on *Hypochoeris radicata* L. and is apparently restricted to the western United States (Nastasi and Deans 2021). The other species, *P. taraxaci* (Ashmead, 1897), induces galls on *Taraxacum officinale* F. H. Wigg. (Fig. 95) and is widespread in eastern North America (Nastasi and Deans 2021).

### North American species (Nastasi and Deans 2021):

1. *Phanacis hypochoeridis* (Kieffer, 1887)
2. *Phanacis taraxaci* (Ashmead, 1897)



Figures 80–82. **80** *Phanacis* sp., anterodorsal view (USNMENT01448498) **81** *Phanacis* sp., wings (USNMENT01231855) **82** *Phanacis* sp., lateral view (USNMENT01231855).

### **Synergus Hartig, 1840 (Synergini)**

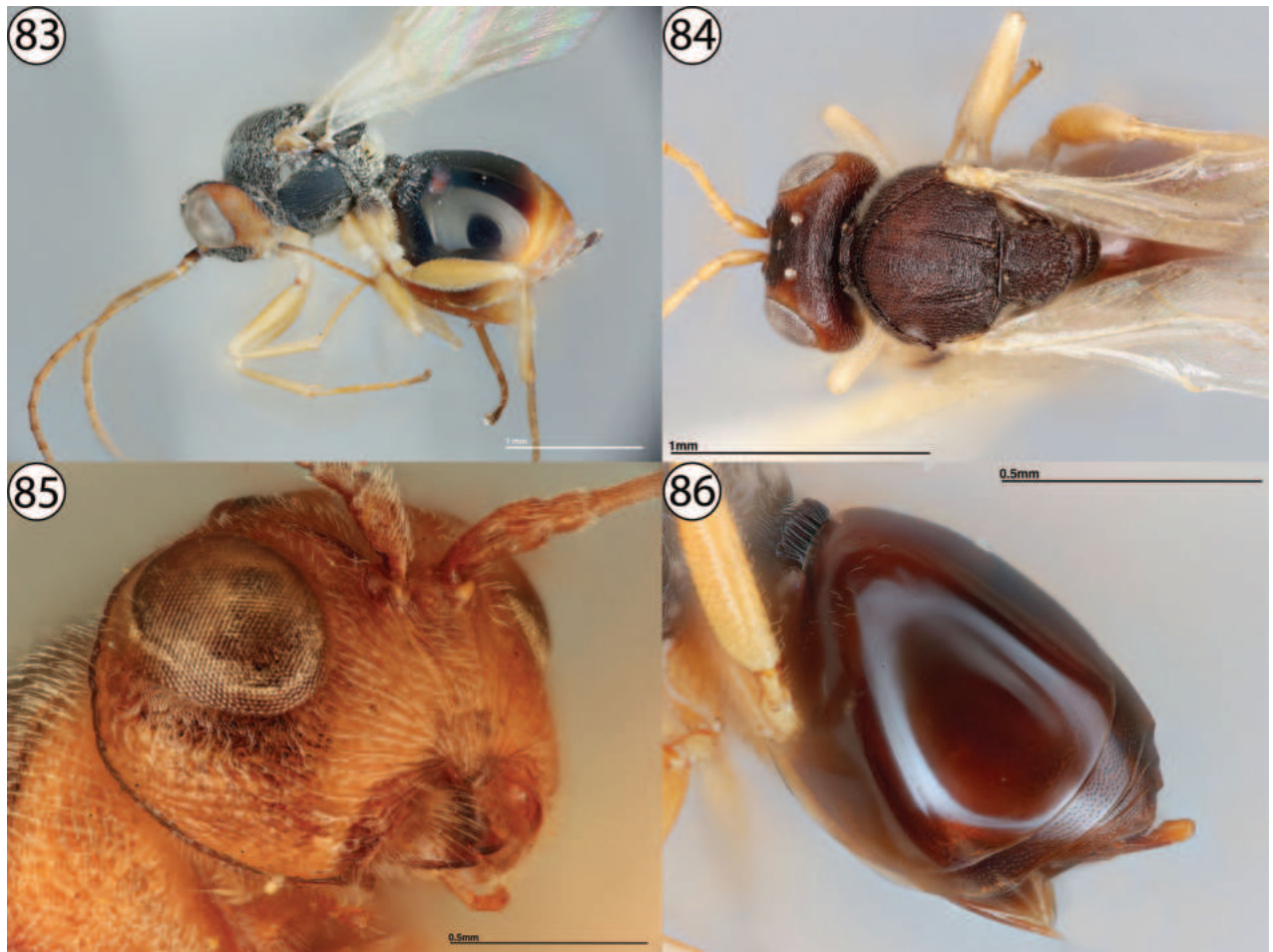
Figs 83–86

**Type species.** *Synergus vulgaris* Hartig, 1840.

**Diagnosis.** Pronotum tall and broad dorsomedially. Pronotal submedial pits distinct and well-impressed. Pronotal plate present but mostly indistinct. Mesoscutellar foveae usually distinct. Fore wing always with marginal cell closed (apparently only partly closed in *Synergus mexicanus* Gillette, 1896; see Pujade-Villar et al. 2015). Metatarsal claws with or without basal lobe. Metasoma with syntergite, with second and third tergites entirely fused, greatly enlarged, and occupying most of metasoma. Body generally strongly sculptured.

**Note.** Sixty-one species of *Synergus* are known from North America (Nastasi and Deans 2021). Members of *Synergus* Hartig are inquilines of galls induced by Cynipini on oaks (Buffington et al. 2020). *Synergus* are extremely commonly reared and are known in association with hundreds of oak gall wasps (Nastasi and Deans 2021; Ward et al. 2022). *Synergus* is demonstrably polyphyletic, with North American taxa forming as many as three independent clades and many undescribed species exist (Pénzes et al. 2012; Lobato-Vila and Pujade-Villar 2021; Lobato-Vila et al. 2022), meaning a great deal of revisionary work will be needed to resolve major questions within the genus and better understand its diversity.

The genus *Saphonecrus* Dalla Torre & Kieffer (Tribe Synergini) has long been considered present in North America, but recent taxonomic work refutes this idea. Nastasi and Deans (2021) reported two species: *S. favanus* Weld and *S. gemmariae* (Ashmead). *Saphonecrus gemmariae* was reported in error as the species was considered incertae sedis by Lobato-Vila et al. (2022) due to missing type material which was supposedly deposited in the National Museum of Natural History (USA, D.C.). Upon our own examination of the USNM collection, we were unable to locate the relevant type material. Similarly, the status of *S. favanus* is also questionable (Pénzes et al. 2009; Pénzes et al. 2012; Lobato-Vila and Pujade-Villar 2021); this species may represent a new genus distinct from other Synergini (Lobato-Vila et al. 2022). As such, we consider the presence of *Saphonecrus* in North America doubtful and have omitted *Saphonecrus* from the above key. We have examined type material of *S. favanus* deposited in USNM (specimen # USNMENT960420 and three additional individuals) and found that in the key to genera, the specimens key to *Synergus*, bearing no strong distinction from this genus. The taxonomy of the tribe Synergini as a whole is currently uncertain, and ongoing efforts to revise it will likely result in a stronger understanding of the North American fauna (Lobato-Vila et al. 2022).

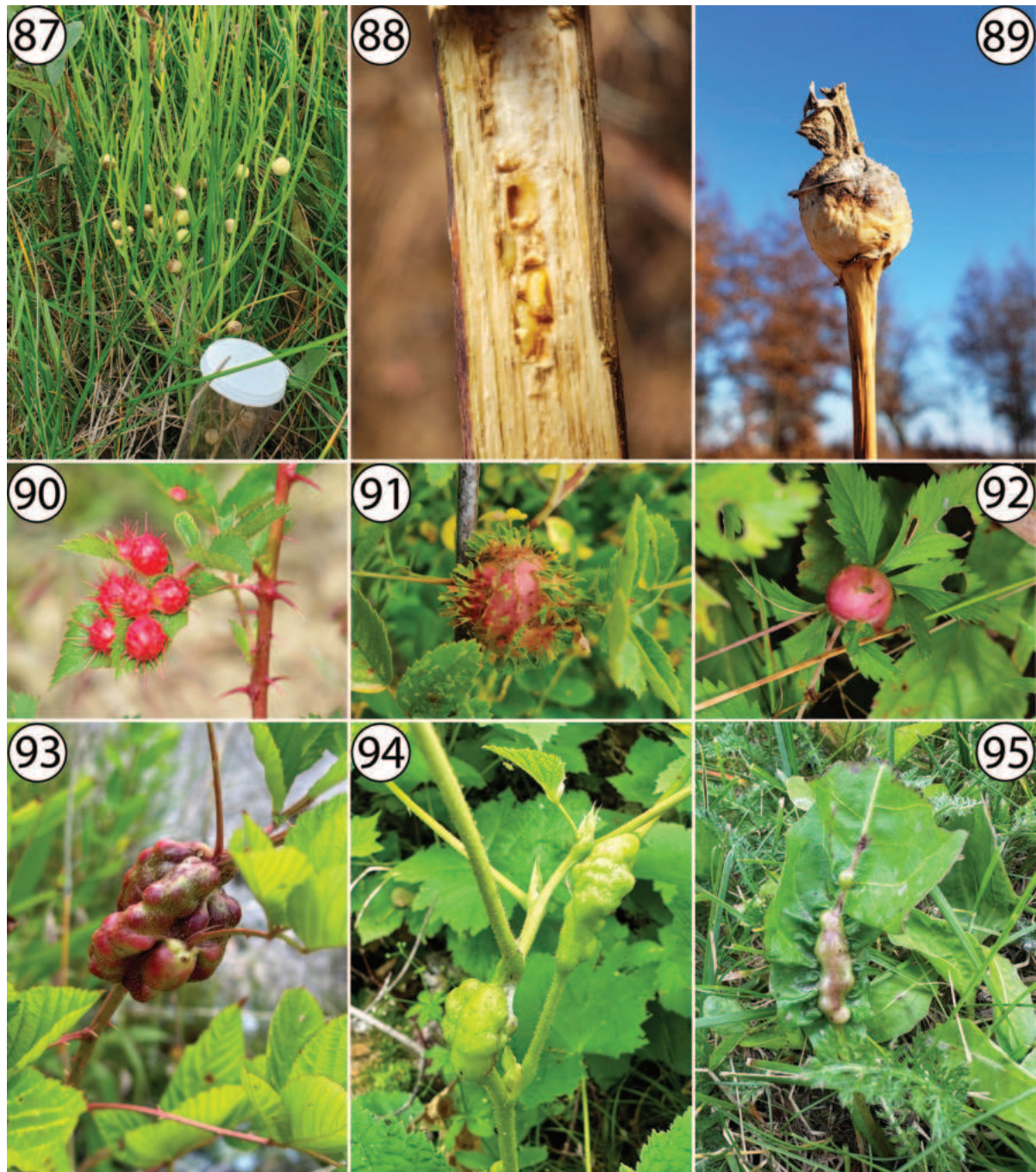


Figures 83–86. **83** *Synergus* sp., lateral view (PSUC\_FEM 000079457) **84** *Synergus incisus*, dorsal view (USNMENT01231859) **85** *Synergus lignicola*, anterior view (USNMENT01448497) **86** *Synergus* sp., metasoma, lateral view (USNMENT01231858).

#### North American species (Nastasi and Deans 2021):

1. *Synergus agrifoliae* Ashmead, 1896
2. *Synergus ashmeadi* Lobato-Vila & Pujade-Villar, 2021
3. *Synergus aurofacies* Lobato-Vila & Pujade-Villar, 2020
4. *Synergus atra* Gillette, 1896
5. *Synergus atripennis* Ashmead, 1896
6. *Synergus atripes* Gillette, 1896
7. *Synergus batatoides* Ashmead, 1885
8. *Synergus bellus* McCracken & Egbert, 1922
9. *Synergus beutenmulleri* Lobato-Vila & Pujade-Villar, 2021
10. *Synergus brevicornis* Ashmead, 1896
11. *Synergus bicolor* Ashmead, 1885
12. *Synergus campanula* Osten Sacken, 1865
13. *Synergus castanopsidis* (Beutenmüller, 1918)
14. *Synergus cibriani* Lobato-Vila & Pujade-Villar, 2017
15. *Synergus citriformis* (Ashmead, 1885)
16. *Synergus compressus* Lobato-Vila & Pujade-Villar, 2021
17. *Synergus confertus* McCracken & Egbert, 1922
18. *Synergus coniferae* Ashmead, 1885

19. *Synergus digressus* McCracken & Egbert, 1922
20. *Synergus dimorphus* Osten Sacken, 1865
21. *Synergus distinctus* McCracken & Egbert, 1922
22. *Synergus diversicolor* Lobato-Vila & Pujade-Villar, 2021
23. *Synergus dorsalis* (Provancher, 1888)
24. *Synergus duricorius* Gillette, 1896
25. *Synergus ebenus* Lobato-Vila & Pujade-Villar, 2021
26. *Synergus equihuai* Pujade-Villar & Lobato-Vila, 2016
27. *Synergus erinacei* Gillette, 1896
28. *Synergus estradae* Pujade-Villar & Lobato-Vila, 2016
29. *Synergus ficigerae* Ashmead, 1885
30. *Synergus filicornis* Cameron, 1883
31. *Synergus flavens* McCracken & Egbert, 1922
32. *Synergus forcadellae* Lobato-Vila & Pujade-Villar, 2020
33. *Synergus gilletti* Pujade-Villar & Lobato-Vila, 2017
34. *Synergus grahami* Lobato-Vila & Pujade-Villar, 2019
35. *Synergus incisus* Gillette, 1896
36. *Synergus laeviventris* (Osten Sacken, 1861)
37. *Synergus lignicola* (Osten Sacken, 1862)
38. *Synergus linnei* Lobato-Vila & Pujade-Villar, 2021
39. *Synergus longimalaris* Pujade-Villar & Lobato-Vila, 2017
40. *Synergus longiscapus* Pujade-Villar & Lobato-Vila, 2017
41. *Synergus macrackenae* Lobato-Vila & Pujade-Villar, 2021
42. *Synergus medullae* Ashmead, 1885
43. *Synergus mendax* Walsh, 1864
44. *Synergus mexicanus* Gillette, 1896
45. *Synergus nigroornatus* McCracken & Egbert, 1922
46. *Synergus oaxaquensis* Lobato-Vila & Pujade-Villar, 2021
47. *Synergus obtusilobae* (Ashmead, 1885)
48. *Synergus ochreus* Fullaway, 1911
49. *Synergus oneratus* (Harris, 1841)
50. *Synergus pacificus* McCracken & Egbert, 1922
51. *Synergus personatus* Lobato-Vila & Pujade-Villar, 2021
52. *Synergus pomiformis* Ashmead, 1885
53. *Synergus pseudofilicornis* Lobato-Vila & Pujade-Villar, 2018
54. *Synergus punctatus* Gillette, 1896
55. *Synergus quercuslana* (Fitch, 1859)
56. *Synergus reniformis* McCracken & Egbert, 1922
57. *Synergus ruficephalus* Lobato-Vila & Pujade-Villar, 2021
58. *Synergus rutulus* McCracken & Egbert, 1922
59. *Synergus shorthousei* Lobato-Vila & Pujade-Villar, 2019
60. *Synergus stelluli* Burnett, 1976
61. *Synergus stratifrons* Pujade-Villar & Lobato-Vila, 2017
62. *Synergus succinipedis* (Ashmead, 1885)
63. *Synergus tenebrosus* Lobato-Vila & Pujade-Villar, 2019
64. *Synergus villosus* Gillette, 1891
65. *Synergus virentis* (Ashmead, 1885)
66. *Synergus walshii* Gillette, 1896
67. *Synergus weldi* Lobato-Vila & Pujade-Villar, 2021



**Figures 87–95.** **87** galls of *Antistrophus pisum* on stem of *Lygodesmia juncea* (Asteraceae: Cichorieae), photographed by Chris Friesen (<https://www.inaturalist.org/observations/95588437>) **88** galls of *Antistrophus rufus* in dissected stem of *Silphium laciniatum* (Asteraceae: Heliantheae), photographed by Andy Deans (<https://www.inaturalist.org/observations/64708490>) **89** gall of *Antistrophus silphii* on apical stem of *Silphium integrifolium* (Asteraceae: Heliantheae), photographed by Andy Deans (<https://www.inaturalist.org/observations/64708191>) **90** galls of *Diplolepis polita* on leaves of *Rosa* sp. (Rosaceae: Roseae), photographed by Garth Harwood (<https://www.inaturalist.org/observations/165442438>) **91** gall of *Diplolepis californica* on *Rosa* sp. (Rosaceae: Roseae), photographed by Mary K. Hanson (<https://www.inaturalist.org/observations/115655737>) **92** gall of *Diastrophus potentillae* on *Potentilla simplex* (Rosaceae: Potentilleae), photographed by Tom Murray (<https://www.inaturalist.org/observations/134669544>) **93** gall of *Diastrophus nebulosus* on stem of *Rubus* sp. (Rosaceae: Rubeae), photographed by Pam Curtin (<https://www.inaturalist.org/observations/174007397>) **94** galls of *Diastrophus kincaidii* on stems of *Rubus parviflorus* (Rosaceae: Rubeae), photographed by Adam Heikkila (<https://www.inaturalist.org/observations/173314109>) **95** galls of *Phanacis taraxaci* on petiole of *Taraxacum officinale* (Asteraceae: Cichorieae), photographed by Nathan Earley (<https://www.inaturalist.org/observations/174118397>).

## Acknowledgments

We are indebted to Laura Porturas, Michael Skvarla, Codey Mathis, Anne Johnson, Cecil Smith, Jelani Alcorn, Sarah Kaniah, Abby Noel, and Michael Belt for assisting us in testing the key and providing valuable comments. We also thank Y. Miles Zhang for providing commentary on *Diplolepis*. Lastly, Victor Cuesta Porta and Stephanie Eskew reviewed the manuscript and provided valuable feedback.

Mention of trade names or commercial products in this publication is solely for the purpose of providing specific information and does not imply recommendation or endorsement by the USDA. USDA is an equal opportunity provider and employer.

## Additional information

### Conflict of interest

The authors have declared that no competing interests exist.

### Ethical statement

No ethical statement was reported.

## Funding

This material is based upon work supported by the National Science Foundation under Grant No. DEB-1856626. Any opinions, findings, and conclusions or recommendations expressed in this material are those of the authors and do not necessarily reflect the views of the National Science Foundation. The first author was generously supported by two awards from the Society of Systematic Biologists: Mini-ARTS and the Graduate Student Research Award.

## Author contributions

Conceptualization: LFFN. Funding acquisition: ARR. Investigation: LFFN, MLLB, CKD. Methodology: MLLB, LFFN. Project administration: LFFN. Resources: MLLB, ARR. Supervision: MLLB, ARR. Validation: MLLB. Visualization: CKD, LFFN. Writing - original draft: LFFN. Writing - review and editing: MLLB, CKD, ARR.

## Author ORCIDs

Louis F. Nastasi  <https://orcid.org/0000-0001-7825-480X>

Matthew L. Buffington  <https://orcid.org/0000-0003-1900-3861>

Charles K. Davis  <https://orcid.org/0000-0001-6056-3903>

Andrew R. Deans  <https://orcid.org/0000-0002-2119-4663>

## Data availability

All of the data that support the findings of this study are available in the main text.

## References

Azmaz M, Katılmış Y (2020) A new species of herb gall wasp (Cynipidae, Aulacideini, *Aulacidea*) from Turkey. *Zootaxa* 4747(2): 378–390. <https://doi.org/10.11646/zootaxa.4747.2.9>

- Blaimer BB, Gotzek D, Brady SG, Buffington ML (2020) Comprehensive phylogenomic analyses re-write the evolution of parasitism within cynipoid wasps. *BMC Evolutionary Biology* 20(1): 155. <https://doi.org/10.1186/s12862-020-01716-2>
- Buffington ML, Morita SI (2009) Not all oak gall wasps gall oaks: The description of *Dryocosmus rileypokei*, a new, apostate species of Cynipini from California. *Proceedings of the Entomological Society of Washington* 111(1): 244–253. <https://doi.org/10.4289/0013-8797-111.1.244>
- Buffington ML, Forshage M, Liljeblad J, Tang CT, van Noort S (2020) World Cynipoidea (Hymenoptera): A key to higher-level groups. *Insect Systematics and Diversity* 4(4): 1. <https://doi.org/10.1093/isd/ixaa003>
- Gates MW, Zhang YM, Buffington ML (2020) The great greenbriers gall mystery resolved? New species of *Aprostocetus* Westwood (Hymenoptera, Eulophidae) gall inducer and two new parasitoids (Hymenoptera, Eurytomidae) associated with *Smilax* L. in southern Florida, USA. *Journal of Hymenoptera Research* 80: 71–98. <https://doi.org/10.3897/jhr.80.59466>
- Goulet H, Huber JT (1993) *Hymenoptera of the World: An Identification Guide to Families*. Agriculture Canada, Ottawa, Ontario, 680 pp.
- Government of British Columbia (2018) *Aulacidea subterminalis* Niblett. [https://www2.gov.bc.ca/assets/gov/farming-natural-resources-and-industry/forestry/agents/aulacidea\\_subterminalis.pdf](https://www2.gov.bc.ca/assets/gov/farming-natural-resources-and-industry/forestry/agents/aulacidea_subterminalis.pdf) [accessed 01 May 2023]
- Hearn J, Gobbo E, Nieves-Aldrey JL, Branca A, Nicholls JA, Koutsovoulos G, Lartillot N, Stone GN, Ronquist F (2023) Phylogenomic analysis of protein-coding genes resolves complex gall wasp relationships. *Systematic Entomology* 49(1): 1–28. <https://doi.org/10.1111/syen.12611>
- Lobato-Vila I, Pujade-Villar J (2019) Revision of world Ceroptresini (Hymenoptera: Cynipidae) with the description of a new genus and five new species. *Zootaxa* 4685(1): 1–67. <https://doi.org/10.11646/zootaxa.4685.1.1>
- Lobato-Vila I, Pujade-Villar J (2021) The genus *Synergus* Hartig (Hymenoptera: Cynipidae: Synergini) in the New World: a complete taxonomic revision with a key to species. *Zootaxa* 4906(1): 1–121. <https://doi.org/10.11646/zootaxa.4906.1.1>
- Lobato-Vila I, Bae J, Roca-Cusachs M, Kang M, Jung S, Melika G, Péntzes Z, Pujade-Villar J (2022) Global phylogeny of the inquiline gall wasp tribe Synergini (Hymenoptera: Cynipoidea: Cynipidae): first insights and establishment of a new cynipid tribe. *Zoological Journal of the Linnean Society* 195(4): 1338–1354. <https://doi.org/10.1093/zoolinnean/zlab085>
- Melika G (2006) Gall wasps of Ukraine. Cynipidae, Vol. 1, Supplement 21, *Vestnik Zoologii*, Kiev, 300 pp.
- Melika G, Pujade-Villar J, Nicholls JA, Cuesta-Porta V, Cooke-McEwen C, Stone GN (2021) Three new Nearctic genera of oak cynipid gall wasps (Hymenoptera: Cynipidae: Cynipini): *Burnettweldia* Pujade-Villar, Melika & Nicholls, *Nichollesiella* Melika, Pujade-Villar & Stone, *Disholandricus* Melika, Pujade-Villar & Nicholls; and re-establishment of the genus *Paracraspis* Weld. *Zootaxa* 4993(1): 1–81. <https://doi.org/10.11646/zootaxa.4993.1.1>
- Moffat CE, Smith MA (2015) Pre-release detection of a biocontrol agent: combining independent and public DNA sequences to identify the first North American record of *Aulacidea pilosellae* (Hymenoptera: Cynipidae). *Canadian Entomologist* 147(4): 390–395. <https://doi.org/10.4039/tce.2014.48>
- Nastasi LF, Deans AR (2021) Catalogue of rose gall, herb gall, and inquiline gall wasps (Hymenoptera: Cynipidae) of the United States, Canada and Mexico. *Biodiversity Data Journal* 9: e68558. <https://doi.org/10.3897/BDJ.9.e68558>

- Nieves-Aldrey JL (2022) Description of *Fumariphilus* Nieves-Aldrey, gen. nov., a new genus of herb gall wasps, with a key to genera of the tribe Aulacideini (Hymenoptera: Cynipidae). *Zootaxa* 5155(3): 393–413. <https://doi.org/10.11646/zootaxa.5155.3.5>
- PATO curators (2023) Phenotype and Trait Ontology. <https://github.com/pato-ontology/pato/> [accessed 31 July 2023]
- Pénzes Z, Melika G, Bozsóki Z, Bihari P, Mikó I, Tavakoli M, Pujade-Villar J, Fehér B, Fülöp D, Szabó K, Bozsó M, Sipos B, Somogyi K, Stone GN (2009) Systematic re-appraisal of the gall-usurping wasp genus *Synophrus* Hartig, 1843 (Hymenoptera: Cynipidae: Synergini). *Systematic Entomology* 34(4): 688–711. <https://doi.org/10.1111/j.1365-3113.2009.00482.x>
- Pénzes Z, Tang CT, Bihari P, Bozsó M, Schwéger S, Melika G (2012) Oak associated inquilines (Hymenoptera, Cynipidae, Synergini). TISCIA monograph series 11: 1–76.
- Pujade-Villar J, Serrano-Muñoz M, Villecas-Guzmán GA, Roca-Cusachs M (2015) *Synergus mexicanus* Gillette, 1896: a species that increases the generic conflict (Hym., Cynipidae: Synergini). *Bulletí de la Institució Catalana d'Història Natural* 79: 145–148.
- Ritchie AJ (1984) A review of the higher classification of the inquiline gall wasps (Hymenoptera: Cynipidae) and a revision of the Nearctic species of *Periclistus* Forster. PhD Thesis, Carleton University, Ottawa, Ontario, Canada.
- Ritchie AJ, Shorthouse JD (1987) Revision of the genus *Synophrormorpya* Ashmead (Hymenoptera: Cynipidae). *Canadian Entomologist* 119(3): 215–230. <https://doi.org/10.4039/Ent119215-3>
- Ronquist F, Nieves-Aldrey JL, Buffington ML, Liu Z, Liljeblad J, Nylander JA (2015) Phylogeny, evolution and classification of gall wasps: The plot thickens. *PLoS ONE* 10(5): e0123301. <https://doi.org/10.1371/journal.pone.0123301>
- Ward AK, Busbee RW, Chen RA, Davis CK, Driscoe AL, Egan SP, Goldberg BAR, Hood GR, Jones DG, Kranz AJ, Meadely-Dunphy SA, Milks AK, Ott JR, Prior KM, Shiekh SI, Shzu S, Weinersmith KL, Zhang L, Zhang YM, Forbes AA (2022) The arthropod associates of 155 North American cynipid oak galls. *Zoological Studies (Taipei, Taiwan)* 61: e57. <https://doi.org/10.1101/2022.04.26.489445>
- Weld LH (1952) Cynipoidea (Hym.) 1905–1950 being a Supplement to the Dalla Torre and Kieffer monograph, the Cynipidae in *Das Tierreich*, Lieferung 24, 1910 and bringing the systematic literature of the world up to date, including keys to families and subfamilies and list of new generic, specific and variety names. Ann Arbor, Michigan, privately printed, 351 pp.
- Yoder MJ, Mikó I, Seltmann KC, Bertone MA, Deans AR (2010) A gross anatomy ontology for Hymenoptera. *PLoS ONE* 5(12): e15991. <https://doi.org/10.1371/journal.pone.0015991>
- Zhang YM, László Z, Looney C, Dénes AL, Hanner RH, Shorthouse JD (2019) DNA barcodes reveal inconsistent species boundaries in *Diplolepis* rose gall wasps and their *Periclistus* inquilines (Hymenoptera: Cynipidae). *Canadian Entomologist* 151(6): 717–727. <https://doi.org/10.4039/tce.2019.59>
- Zimmerman JR (2018) A synopsis of oak gall wasps (Hymenoptera: Cynipidae) of the southwestern United States with a key and comments on each of the genera. *Journal of the Kansas Entomological Society* 91(1): 58–70. <https://doi.org/10.2317/0022-8567-91.1.58>



# Two new species of the *Cnemaspis galaxia* complex (Squamata, Gekkonidae) from the eastern slopes of the southern Western Ghats

Akshay Khandekar<sup>1,2</sup>, Tejas Thackeray<sup>1</sup>, Ishan Agarwal<sup>1</sup>

<sup>1</sup> Thackeray Wildlife Foundation, Mumbai, 400051, India

<sup>2</sup> Department of Zoology, Shivaji University, Kolhapur, 416004, India

Corresponding author: Ishan Agarwal ([ishan.agarwal@gmail.com](mailto:ishan.agarwal@gmail.com))

## Abstract

Two new species allied to *Cnemaspis galaxia* are described from the eastern slopes of the south Western Ghats, Tamil Nadu, India. Both new species are members of the *ornata* subclade within the *beddomei* clade. The two new species can be easily distinguished from all other members of the *beddomei* clade and each other by a combination of non-overlapping morphological characters such as small body size, distinct colouration of both sexes, the number of dorsal tubercles around the body, the number or arrangement of paravertebral tubercles, the number of midventral scales across the belly and longitudinal ventral scales from mental to cloaca, besides uncorrected pairwise ND2 and 16S sequence divergence of  $\geq 7.4\%$  and  $\geq 2.7\%$ . The two new species are distributed from low elevation, deciduous forests of Srivilliputhur, and add to the five previously known endemic vertebrates from Srivilliputhur-Megamalai Tiger Reserve.

**Key words:** Asia, biodiversity hotspot, dwarf geckos, integrative taxonomy, phylogeny, species complex



Academic editor: Anthony Herrel

Received: 28 December 2023

Accepted: 26 February 2024

Published: 27 March 2024

ZooBank: <https://zoobank.org/4FCB2EDD-68BF-471D-AD38-108491E07909>

**Citation:** Khandekar A, Thackeray T, Agarwal I (2024) Two new species of the *Cnemaspis galaxia* complex (Squamata, Gekkonidae) from the eastern slopes of the southern Western Ghats. ZooKeys 1196: 209–242. <https://doi.org/10.3897/zookeys.1196.117947>

**Copyright:** © Akshay Khandekar et al. This is an open access article distributed under terms of the Creative Commons Attribution License ([Attribution 4.0 International – CC BY 4.0](https://creativecommons.org/licenses/by/4.0/)).

## Introduction

The *beddomei* clade is the only clade of South Asian *Cnemaspis* restricted to the southern Western Ghats (Cyriac et al. 2018; Sayyed et al. 2019, 2023a, b; Pal et al. 2021). All members of the *beddomei* clade are brightly coloured in life and the first two species were described more than 150 years ago (Beddome 1870; Theobald 1876; Cyriac et al. 2018; Sayyed et al. 2019, 2023a, b; Pal et al. 2021; Khandekar et al. 2022). However, this clade was only recently sampled and recognised in a molecular phylogeny of South Asian *Cnemaspis* (Pal et al. 2021). As currently understood, the *beddomei* clade began diversifying in the Eocene and includes 16 described species, distributed from scrub to evergreen forests on the eastern and western slopes of the Western Ghats south of the Palghat Gap (Cyriac et al. 2018; Sayyed et al. 2019, 2023a, b; Pal et al. 2021; Khandekar et al. 2022). The clade is made up of three deeply divergent, well-supported subclades – the *anamudiensis* subclade with three species, *C. anamudiensis* Cyriac, Johny, Umesh & Palot, 2018, *C. nimbus* Pal, Mirza, Dsouza & Shanker, 2021, and

*C. wallaceii* Pal, Mirza, Dsouza & Shanker, 2021; the *beddomei* subclade with four species, *C. beddomei* (Beddome, 1870), *C. maculicollis* Cyriac, Johny, Umesh & Palot, 2018, *C. smaug* Pal, Mirza, Dsouza & Shanker, 2021, and *C. rubraoculus* Pal, Mirza, Dsouza & Shanker, 2021; and the *ornata* subclade with nine species, *C. ornata* (Beddome, 1870), *C. aaronbaueri* Sayyed, Grismer, Campbell & Dileepkumar, 2019, *C. azhagu* Khandekar, Thackeray & Agarwal, 2022, *C. galaxia* Pal, Mirza, Dsouza & Shanker, 2021, *C. nairi* Inger, Marx & Koshy, 1984, *C. nigriventris* Pal, Mirza, Dsouza & Shanker, 2021, *C. regalis* Pal, Mirza, Dsouza & Shanker, 2021, *C. rashidi* Sayyed et al., 2023, and *C. sundara* Sayyed et al., 2023 (Cyriac et al. 2018; Sayyed et al. 2019, 2023a, b; Pal et al. 2021; Khandekar et al. 2022).

The most diverse of the three subclades of the *beddomei* clade is the *ornata* subclade which includes nine valid species distributed from low elevations on the eastern slopes to high elevations (~ 200–1000+ m a.s.l.) in the Western Ghats south of Srivilliputhur (Fig. 1). Most species are low to mid elevation (~ 200–700 m a.s.l.) and are distributed on the eastern slopes as well as through some low passes onto the western slopes, and only *C. ornata* and the recently described *C. rashidi* are high elevation species found at elevations > 1,000 m a.s.l. (Sayyed et al. 2023a, b). Members of the *ornata* subclade are all strongly sexually dichromatic, diurnal, and scansorial, found on rocks, buildings and occasionally trees (Sayyed et al. 2019, 2023a, b; Pal et al. 2021; Khandekar et al. 2022). Seven of these species have been described since 2019, suggesting the diversity of this subclade is still incompletely known (Sayyed et al. 2019, 2023a, b; Pal et al. 2021; Khandekar et al. 2022).

As part of a project on the lizards of Tamil Nadu, we surveyed the southern Western Ghats from 2018–2022, specifically targeting known species of *Cnemaspis* as well as potential habitats that had not been previously sampled. We were able to collect most described species of the *ornata* subclade as well as multiple unnamed divergent lineages, two of which were subsequently described as *C. rashidi* and *C. sundara* (Sayyed et al. 2023a, b). In this paper, we provide molecular data from new localities for *C. galaxia*, *C. nairi*, *C. nigriventris*, *C. rashidi*, and *C. sundara* and describe two new species allied to *C. galaxia*. We also provide a brief note on the Code of Ethics and how it is rarely followed in the Indian context, and call for more collaborative research.

## Materials and methods

### Taxon sampling

Surveys were conducted in the early morning until a few hours after dark, specimens were observed on rocks, tree trunks, and collected by hand, followed by euthanasia using isoflurane after taking colour photos in life. Liver or tail tissues of at least two individuals of each new species/per locality were collected in molecular grade ethanol and subsequently stored at –20 °C for genetic analysis. Specimens were fixed in 8% formalin for ~ 12–24 h, washed and kept in tap water for ~ 24 h, and transferred to 70% ethanol for long-term storage. Collection permit was issued by the Tamil Nadu Forest Department (see acknowledgements), and collection protocols cleared by an inhouse ethics committee. Specimens are deposited in the Museum and Research Collection Facility at National Centre for Biological Sciences, Bengaluru (NRC-AA).

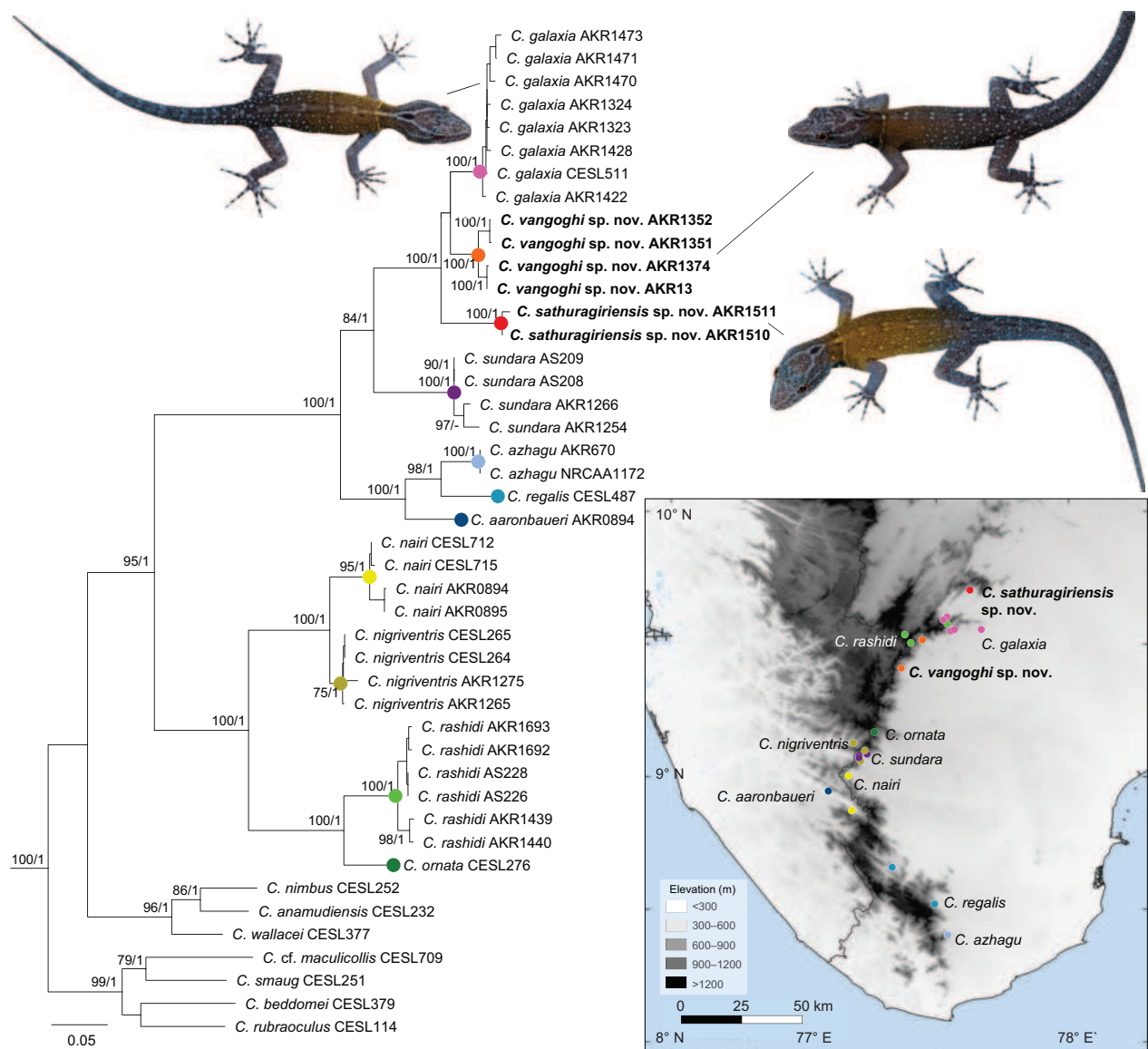


**Figure 1.** Maximum likelihood phylogeny of the *beddomei* clade (ND2 + 16S concatenated, 1610 base pairs) with photographs of the new species and *C. galaxia* (not to scale); numbers at nodes represent bootstrap support/ posterior probability > 70/0.99 (not shown close to terminal nodes). Inset, elevation map of the southern Western Ghats showing type and sampled localities for the *ornata* subclade.

## Molecular data and analyses

We generated new sequences for 25 individuals representing five known species and three divergent lineages of the *ornata* subclade from ~ 18 localities (Fig. 1, Table 1). We targeted two mitochondrial genes that have been used in Indian *Cnemaspis* phylogenies, the protein coding ND2 and the large ribosomal subunit (16S). We extracted DNA from liver or tail-tips using the Qia-gen DNeasy Blood and Tissue Extraction kit. We used the Macey et al. (1997) primers L4437 and H5934 to PCR amplify ND2 with L4437 and H5540 used for sequencing, and 16SA and 16SB (Palumbi et al. 1991) to amplify and sequence 16S; with PCR and sequencing outsourced to Barcode Biosciences, Bangalore. We combined the new sequences with published sequences for the *beddomei* clade using members of the *wynadensis* clade as outgroups (Table 1; Pal et al.

2021; Khandekar et al. 2022; Sayyed et al. 2023a, b). Sequences were aligned in MEGA 5.2 (Tamura et al. 2011) using CLUSTALW (Thompson et al. 1994) with default settings. The ND2 sequences were translated to amino acids to check for erroneous stop codons, which were absent, confirming we had sequenced the targeted mitochondrial protein coding gene. Pairwise uncorrected sequence divergence was calculated in MEGA 5.2 using the pairwise deletion option for each marker. We reconstructed phylogenetic relationships for the ND2 and 16S data separately (not shown as both mitochondrial markers were largely congruent) as well as in a concatenated analysis, using Maximum Likelihood (ML) in RaXML HPC 8.2.12 (Stamatakis 2014) and Bayesian Inference (BI) in MrBayes 3.2.7 (Ronquist and Huelsenbeck 2003). The best-fit models of sequence evolution and partitioning scheme were selected using the Bayesian Inference Criteria in PartitionFinder 2 (Lanfear et al. 2016) with the greedy algorithm (Lanfear et al. 2012) and RaxML (Stamatakis 2014). Three partitions were selected for each codon position of ND2 and one for 16S with the GTR+I+G model for codon position 1 and 16S and GTR+G for the other two codon positions. ML analyses employed 10 independent runs and 1000 non-parametric bootstraps (BS) to assess support. Partitioned BI analyses had parameters unlinked across partitions, four chains each (one cold and three hot) with two parallel runs with 1,000,000 generations sampled every 100 generations and convergence determined based on standard deviation of split frequencies ( $<< 0.01$ ) and examination of ESS scores ( $> 200$ ). The sumt function was used to build a consensus tree after removing the first 25% of trees as burn-in, with support assessed using posterior probability (PP) of each node.

**Table 1.** Sequences used in this study. Museum abbreviations are as follows: BNHS, Bombay Natural History Society, Mumbai; CESL, Centre for Ecological Sciences, Bangalore; NRCAA, National Centre for Biological Sciences, Bangalore; AK/ AK-R, Akshay Khandekar field series; AS, Amit Sayyed field series. All from India; KL = Kerala, MH = Maharashtra, TN = Tamil Nadu.

Species	Voucher	Locality	ND2	16S	Subclade
<i>Cnemaspis aaronbaueri</i>	AS 214	KL: Kollam District, Thenmala	OR714926	OR708521	<i>ornata</i>
<i>C. azhagu</i>	NRC-AA1171	TN: Tirunelveli District, Thirukurungudi range	–	PP382789	<i>ornata</i>
<i>C. azhagu</i>	NRC-AA1172	TN: Tirunelveli District, Thirukurungudi range	ON494554	PP382790	<i>ornata</i>
<i>C. galaxia</i>	AK-R 1323	TN: Virudhunagar District, Shenbaga Thopu	PP387688	PP382791	<i>ornata</i>
<i>C. galaxia</i>	AK-R 1324	TN: Virudhunagar District, Shenbaga Thopu	PP387689	PP382792	<i>ornata</i>
<i>C. galaxia</i>	AK-R 1422	TN: Virudhunagar District, Vyankateshpuram RF	PP387690	PP382793	<i>ornata</i>
<i>C. galaxia</i>	AK-R 1428	TN: Virudhunagar District, Shenbaga Thopu	–	PP382794	<i>ornata</i>
<i>C. galaxia</i>	AK-R 1470	TN: Virudhunagar District, Atti Kovil falls	PP387691	PP382795	<i>ornata</i>
<i>C. galaxia</i>	AK-R 1471	TN: Virudhunagar District, Atti Kovil falls	PP387692	PP382796	<i>ornata</i>
<i>C. galaxia</i>	AK-R 1473	TN: Virudhunagar District, Atti Kovil falls	PP387693	PP382797	<i>ornata</i>
<i>C. galaxia</i>	CESL 511	TN: Virudhunagar District, Shenbaga Thopu	MZ701818	MZ291589	<i>ornata</i>
<i>C. nairi</i>	AK-R 894	TN: Tenkasi District, Courtallam	PP387700	PP382804	<i>ornata</i>
<i>C. nairi</i>	AK-R 895	TN: Tenkasi District, Courtallam	PP387701	PP382805	<i>ornata</i>
<i>C. nairi</i>	CESL 712	KL: Kollam District, Shendurney	–	MZ291607	<i>ornata</i>
<i>C. nairi</i>	CESL 715	KL: Kollam District, Shendurney	–	MZ291608	<i>ornata</i>
<i>C. nigriventris</i>	AK-R 1265	TN: Tenkasi District, Courtallam	PP387702	PP382806	<i>ornata</i>
<i>C. nigriventris</i>	AK-R 1275	TN: Tenkasi District, Courtallam	PP387703	PP382807	<i>ornata</i>
<i>C. nigriventris</i>	CESL 264	KL: Kollam District, Achankovil RF	MZ291609	MZ701808	<i>ornata</i>
<i>C. nigriventris</i>	CESL 265	KL: Kollam District, Achankovil RF	MZ291610	–	<i>ornata</i>

Species	Voucher	Locality	ND2	16S	Subclade
<i>C. ornata</i>	CESL 276	TN: Tirunelveli District, Devarmalai Hills	MZ701809	MZ291613	<i>ornata</i>
<i>C. rashidi</i>	AK-R 1439	TN: Virudhunagar District, Srivilliputhur-Megamalai Tiger Reserve, higher elevations of Shenbaga Thopu	PP387704	PP382808	<i>ornata</i>
<i>C. rashidi</i>	AK-R 1440	TN: Virudhunagar District, Srivilliputhur-Megamalai Tiger Reserve, higher elevations of Shenbaga Thopu	PP387705	PP382809	<i>ornata</i>
<i>C. rashidi</i>	AK-R 1692	TN: Theni District, Srivilliputhur-Megamalai Tiger Reserve, Vellimalai	PP387706	PP382810	<i>ornata</i>
<i>C. rashidi</i>	AK-R 1693	TN: Theni District, Srivilliputhur-Megamalai Tiger Reserve, Vellimalai	PP387707	PP382811	<i>ornata</i>
<i>C. rashidi</i>	AS 226	TN: Virudhunagar District, Kottamalai estate	OR714921	–	<i>ornata</i>
<i>C. rashidi</i>	AS 228	TN: Virudhunagar District, Kottamalai estate	OR714922	–	<i>ornata</i>
<i>C. regalis</i>	CESL 487/ 488	TN: Tirunelveli District, Kalakad Mundanthurai Tiger Reserve	MZ701816/ MZ701817	MZ291615	<i>ornata</i>
<i>C. sathuragiriensis</i> sp. nov.	AK-R 1510	TN: Virudhunagar District, Sathuragiri Hills	PP387694	PP382798	<i>ornata</i>
<i>C. sathuragiriensis</i> sp. nov.	AK-R 1511	TN: Virudhunagar District, Sathuragiri Hills	PP387695	PP382799	<i>ornata</i>
<i>C. sundara</i>	AK-R 1254	TN: Tenkasi District, Mohan's resort	PP387708	–	<i>ornata</i>
<i>C. sundara</i>	AK-R 1266	TN: Tenkasi District, Mohan's resort	PP387709	–	<i>ornata</i>
<i>C. sundara</i>	BNHS 2916	TN: Tenkasi District, Mekkarai	OR714924	–	<i>ornata</i>
<i>C. sundara</i>	BNHS 2917	TN: Tenkasi District, Mekkarai	OR714925	–	<i>ornata</i>
<i>C. vangoghi</i> sp. nov.	AK-R 1351	TN: Virudhunagar District, Srivilliputhur-Megamalai Tiger reserve, Ayyanar Kovil,	PP387696	PP382800	<i>ornata</i>
<i>C. vangoghi</i> sp. nov.	AK-R 1352	TN: Virudhunagar District, Srivilliputhur-Megamalai Tiger reserve, Ayyanar Kovil,	PP387697	PP382801	<i>ornata</i>
<i>C. vangoghi</i> sp. nov.	AK-R 1373	TN: Virudhunagar District, Srivilliputhur-Megamalai Tiger reserve, Settur RF	PP387698	PP382802	<i>ornata</i>
<i>C. vangoghi</i> sp. nov.	AK-R 1374	TN: Virudhunagar District, Srivilliputhur-Megamalai Tiger reserve, Settur RF	PP387699	PP382803	<i>ornata</i>
<i>C. anamudiensis</i>	CESL 232	KL: Idukki District	MZ701805	MZ291574	<i>anamudiensis</i>
<i>C. nimbus</i>	CESL 252	KL: Idukki District, Mathikettan Shola NP	MZ701807	MZ291612	<i>anamudiensis</i>
<i>C. wallaceii</i>	CESL 377	TN: Coimbatore District, Anaimalai, Andiparai Shola	MZ701813	MZ291619	<i>anamudiensis</i>
<i>C. beddomei</i>	CESL 379	TN: Tirunelveli District, Kalakkad-Mundanthurai Tiger Reserve	MZ701814	MZ291581	<i>beddomei</i>
<i>C. cf. maculicollis</i>	CESL 709	KL: Kollam District, Shendurney WLS	MZ701825	MZ291582	<i>beddomei</i>
<i>C. rubraoculus</i>	CESL 114	KL: Idukki District, Periyar Tiger Reserve	ON494559	MZ291616	<i>beddomei</i>
<i>C. smaug</i>	CESL 251	KL: Idukki District, Mathikettan Shola NP	MZ701806	MZ291618	<i>beddomei</i>
<i>C. chengodumalaensis</i>	CESL 624	KL: Kozhikode District, Chengodumala	MZ701822	MZ291584	<i>wynadensis</i>
<i>C. kolhapurensis</i>	CESL 868	MH: Sindhudurg District, Amboli	MZ701829	MZ291599	<i>wynadensis</i>
<i>C. wynadensis</i>	CESL 630	KL: Wayanad District, Wayanad	MZ701823	MZ291620	<i>wynadensis</i>

## Morphological and meristic data

We restricted morphological comparisons to the *beddomei* clade (see Results). Morphological data were collected from 12 specimens of the two new species and from 42 specimens of the *beddomei* clade including type material of *C. azhagu*, *C. nimbus*, *C. smaug*, and *C. wallaceii*; type as well as topotypic and/or additional materials for *C. galaxia*, *C. nigriventris*, *C. regalis*, and *C. rubraoculus*; and additional materials for *C. beddomei*, *C. nairi*, *C. rashidi*, and *C. sundara* (all listed in Appendix 1). Data for remaining four species—*C. aaronbaueri*, *C. anamudiensis*, *C. maculicollis*, and *C. ornata* (as well as *C. boiei* which is incertae sedis within *Cnemaspis*) were obtained from published literature (Manamendra-Arachchi et al. 2007; Cyriac et al. 2018; Sayyed et al. 2019; Pal et al. 2021). Meristic counts and measurements were taken under a ZEISS Stemi 305 stereo dissecting microscope by AK on the right side of the body where possible. Colour pattern was recorded from photographs taken in life. All measurements were taken with a Mitutoyo digital vernier calliper (to the nearest 0.1 mm). Mensural, meristic,

and additional morphological character state evaluation is in accordance with Khandekar et al. (2019, 2024): snout vent length (SVL), tail length (TL), tail width (TW), forearm length (FL), crus length (CL), axilla to groin length (AGL), body height (BH), body width (BW), head length (HL), head width (HW), head depth (HD), eye diameter (ED), eye to ear distance (EE), eye to snout distance (ES), eye to nares distance (EN), internarial distance (IN), interorbital distance (IO), and ear length (EL); meristic data recorded for all specimens were number of supralabials (SL), infralabials (IL), supralabials at midorbital position (SL M), infralabials at midorbital position (IL M), paravertebral tubercles (PVT), dorsal tubercle rows (DTR), midventral scale rows across the belly (MVSR), ventral scales (VS), preloacal pores (PP), poreless scales between preloacal pores (SB PP), postloacal tubercles (PCT), traverse distal subdigital lamellae on manus: digit 1 (DLAMF1), digit 4 (DLAMF4), on pes: digit 1 (DLAMT1), digit 4 (DLAMT4), and digit 5 (DLAMT5); traverse basal subdigital LAMellae on manus: digit 1 (BLAMF1), digit 4 (BLAMF4), on pes: digit 1 (BLAMT1), digit 4 (BLAMT4), and digit 5 (BLAMT5); total LAMellae (TLAMF1, TLAMF4, TLAMT1, TLAMT4, and TLAMT5). We follow Agarwal et al. (2020) for body size categories (SVL) for South Asian *Cnemaspis* (small bodied < 40 mm, medium-bodied 40–49 mm, large-bodied ≥ 50 mm).

## Results

### Phylogenetic relationships

We recovered the three subclades of the *beddomei* clade, *anamudiensis*, *beddomei*, and *ornata*, each of which received high support (Fig. 2; BS > 95, PP 1; Fig. 1). The two undescribed lineages fall within the *ornata* subclade and form a well-supported clade (BS 100, PP 1) together with *C. galaxia*. The two lineages have an uncorrected ND2 p-distance of 10.7% between each other (2.7% on 16S), 7.4–10.1% (3.1–3.4% 16S) from *C. galaxia*, and ≥ 15.6% (≥ 7.8% 16S) from all other members of the clade (Table 2). The lowest uncorrected ND2 p-distance between previously described species of the *ornata* subclade is 6.3% (2.2% 16S) between *C. nairi* and *C. nigriventris*. We describe the two genetically divergent lineages as new species below.

**Table 2.** Uncorrected % sequence divergence within the *C. ornata* subclade of the *beddomei* clade. Above diagonal, 16S; below diagonal, ND2; along diagonal in bold, maximum intraspecific ND2 divergence; – indicates no data.

	1	2	3	4	5	6	7	8	9	10	11
1 <i>C. sathuragiriensis</i> sp. nov.	–	2.7	–	7.3	3.4	12.8	12.0	12.6	14.2	8.1	–
2 <i>C. vangoghi</i> sp. nov.	10.7	<b>2.3</b>	–	8.4	3.1	12.9	12.4	12.7	14.2	9.0	–
3 <i>C. aaronbaueri</i>	19.4	17.6	–	–	–	–	–	–	–	–	–
4 <i>C. azhagu</i>	20.4	17.5	12.3	–	8.8	15.0	14.6	14.5	15.6	2.8	–
5 <i>C. galaxia</i>	10.1	7.4	19.6	18.2	<b>1.7</b>	12.7	12.1	12.5	14.7	9.0	–
6 <i>C. nairi</i>	31.1	30.3	28.7	29.8	30.9	<b>0.1</b>	2.2	7.2	10.0	15.3	–
7 <i>C. nigriventris</i>	31.2	29.8	28.8	29.9	30.1	6.3	<b>0.6</b>	7.7	9.7	15.0	–
8 <i>C. ornata</i>	29.4	28.4	28.1	28.8	29.0	21.6	19.0	–	4.8	15.2	–
9 <i>C. rashidi</i>	31.6	30.4	30.3	30.2	29.8	20.3	17.7	10.8	<b>3.0</b>	16.5	–
10 <i>C. regalis</i>	21.3	20.0	13.1	11.1	20.6	27.8	28.2	26.6	28.0	–	–
11 <i>C. sundara</i>	17.5	15.6	16.9	18.0	15.6	28.5	28.7	28.4	29.5	19.1	<b>3.0</b>

## Systematics

### *Cnemaspis vangoghi* sp. nov.

<https://zoobank.org/A27D1DEC-6E26-47A4-AEDC-69C139A6FE51>

Figs 2–6, Tables 3–5

**Type material examined. Holotype.** NRC-AA-8342 (AK-R 1356), adult male, from near Neer Katha Ayyanar Kovil (9.5108°N, 77.4529°E; ca 250 m a.s.l.), Sri-villiputhur-Meghamalai Tiger Reserve, Virudhunagar district, Tamil Nadu state, India; collected by Akshay Khandekar, Ishan Agarwal, Swapnil Pawar and team on 16 April 2022. **Paratypes.** NRC-AA-8343 (AK-R 1351), NRC-AA-8344 (AK-R 1352), adult males, same data as holotype; NRC-AA-8345 (AK-R 1358), adult female, from near Ayyanar Kovil waterfalls (9.5200°N, 77.4478°E; ca 400 m a.s.l.), same data as holotype; NRC-AA-8346 (AK-R 1373), NRC-AA-8347 (AK-R 1374), NRC-AA-8348 (AK-R 1380), adult males, from Settur Reserve Forest (9.4036°N, 77.3721°E; ca 350 m a.s.l.), same data as holotype except collected on 17 April 2022.

**Diagnosis.** A small-sized *Cnemaspis*, snout to vent length  $\leq 34$  mm ( $n = 7$ ). Dorsal pholidosis heterogeneous; smooth to weakly keeled granular scales intermixed with fairly regularly arranged rows of enlarged, weakly keeled, conical tubercles; 10 rows of dorsal tubercles at midbody, 7–14 tubercles in paravertebral rows; ventral scales subequal from chest to vent, smooth, subcircular and subimbricate with rounded end; 29–31 midventral scales across belly, 125–140 longitudinal ventral scales from mental to cloaca; subdigital scansors smooth, unnotched, some divided and others entire, a distinct enlarged metacarpal scale below digit I; 11–14 lamellae under digit I of manus and 11–13 under digit I of pes, 19–22 lamellae under digit IV of manus and 18–25 lamellae under digit IV of pes; males with continuous series of six or seven precloacal pores ( $n = 6$ ); scales on non-regenerated tail dorsum heterogeneous; small, smooth, subcircular, flattened, subimbricate scales intermixed on anterior one third portion with enlarged, weakly keeled, and weakly conical tubercles forming seven whorls; six tubercles on first three whorl, four tubercles on fourth to seventh whorls, only a pair of paravertebral tubercles each on eighth to 11<sup>th</sup> whorls; rest of the tail lacking enlarged tubercles; median row of subcaudals smooth, roughly rectangular, distinctly enlarged, with condition of two enlarged scales alternating with a divided scale. Males with ochre anterior 1/2 of body, single central black dorsal ocellus on neck, a white ocellus on ventrolateral side of neck and one on throat posterior to jaw, venter off-white with dark throat, tail unbanded, females and juveniles brown, juveniles with indistinct mid-dorsal streak.

**Comparisons with members of *beddomei* clade.** *Cnemaspis vangoghi* sp. nov. can be easily distinguished from all 16 members of the *beddomei* clade as well as from *C. boiei* by a combination of the following differing or non-overlapping characters: A small-sized *Cnemaspis*, snout to vent length  $\leq 34$  mm (vs medium-sized *Cnemaspis*, snout to vent length 40–49 mm in *C. nairi*, *C. nimbus*, *C. ornata*, *C. rashidi*, *C. rubraoculus*, and *C. wallaceii*; large-sized *Cnemaspis*, snout to vent length  $> 50$  mm in *C. anamudiensis*, *C. beddomei*, *C. maculicollis*, and *C. smaug*; snout to vent length  $\leq 38$  mm in *C. azhagu*, *C. boiei*, and *C. nigriventris*); ten rows of dorsal tubercles at midbody (vs only a few enlarged scattered tubercles at midbody dorsum in *C. anamudiensis*, two or three rows of

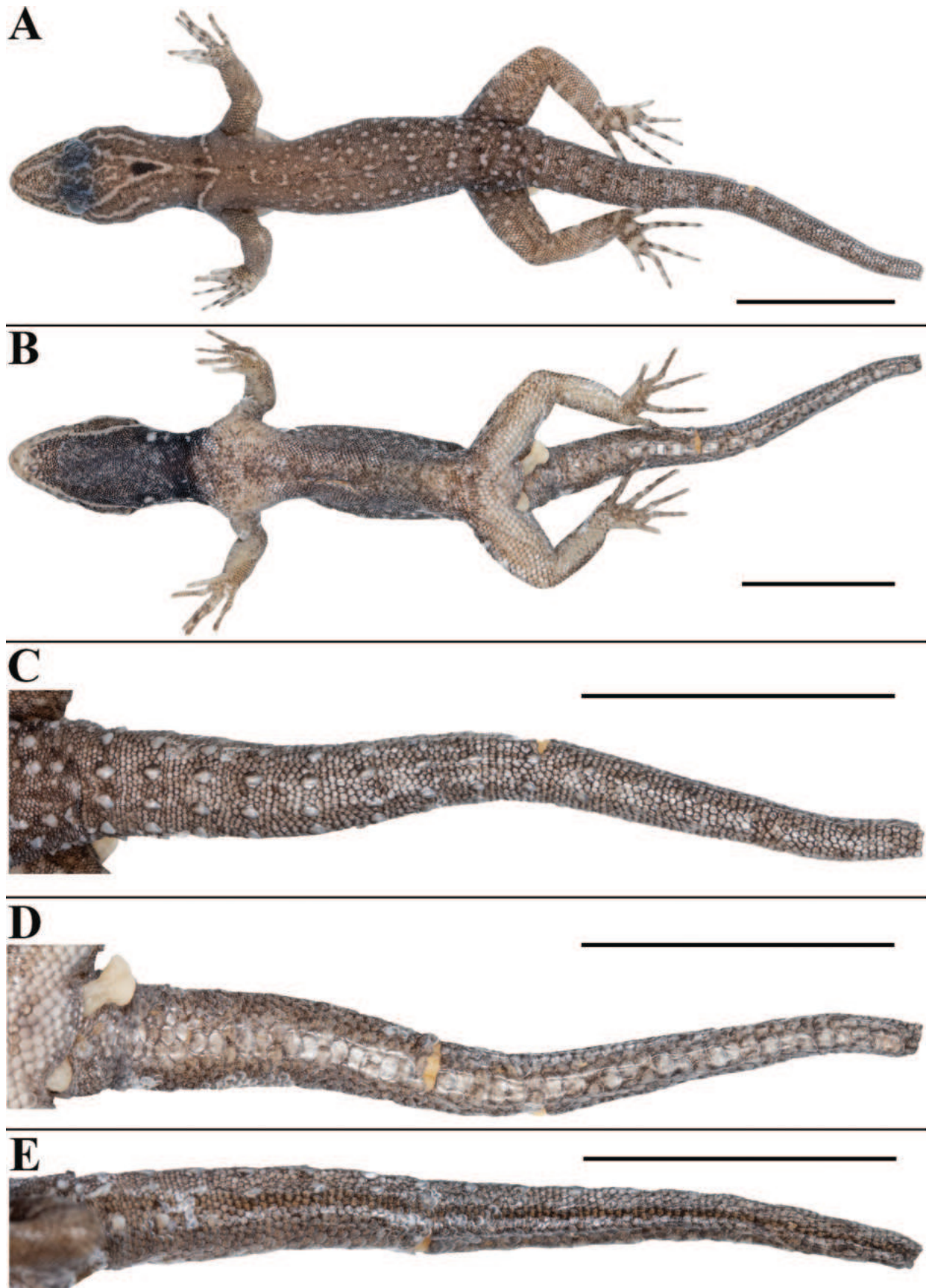


**Figure 2.** *Cnemaspis vangoghi* sp. nov. (holotype, NRC-AA-8342) **A** dorsal view of body **B** ventral view of body **C** dorsal view of tail **D** ventral view of tail **E** lateral view of tail. Photos by Akshay Khandekar. Scale bars: 10 mm.

dorsal tubercles at midbody in *C. azhagu*, eight in *C. galaxia*, 16–18 in *C. nairi*, 13 or 14 in *C. nigriventris*, 12–14 in *C. nimbus* and *C. ornata*, 7–9 in *C. regalis*, 19–22 in *C. smaug*, six in *C. sundara*, 14 or 15 in *C. wallaceii*); 125–140 longitudinal ventral scales from mental to cloaca (vs 151–171 longitudinal ventral scales from mental to cloaca in *C. azhagu*, 154–161 in *C. beddomei*, 153–159 in *C. galaxia*, 143–147 in *C. nairi*, 154–159 in *C. nigriventris*, 157–165 in *C. ornata*, 170–172 in *C. rashidi*, 148–154 in *C. regalis*, 142–150 in *C. smaug*, 156–160 in *C. sundara*, 154–156 in *C. wallaceii*); 7–14 tubercles in paravertebral rows (vs paravertebral tubercles either absent or irregular in *C. anamudiensis*, *C. azhagu*, and *C. sundara*, 18 or 19 tubercles in paravertebral rows in *C. aaronbaueri* and *C. beddomei*, 16 or 17 in *C. nimbus*, 21–23 in *C. ornata*, 27–30 in *C. smaug*, 18–20 in *C. wallaceii*); 29–31 midventral scales across belly (vs 34–44 midventral scales across belly in *C. azhagu*, 32 or 33 in *C. nairi*, 38–40 in *C. nigriventris*, 26 or 27 in *C. nimbus*, 40–44 in *C. regalis*, 33–37 in *C. rubraoculus*, 35 or 36 in *C. sundara*); a distinct white ocellus on ventrolateral sides of neck present in males (vs white ocellus on ventrolateral sides of neck absent in *C. aaronbaueri*, *C. anamudiensis*, *C. azhagu*, *C. beddomei*, *C. maculicollis*, *C. nimbus*, *C. nimbus*, *C. regalis*, *C. rubraoculus*, *C. smaug*, *C. wallaceii*); tail unbanded (tail distinctly banded in *C. nairi*, *C. nigriventris*, *C. ornata*, *C. rashidi*, *C. smaug*, *C. sundara*). *Cnemaspis vangoghi* sp. nov. is diagnosed against the other new species as part of its description below.

**Description of the holotype.** Adult male in good state of preservation except tail marginally bent towards left and tip is missing, hemipenis partially everted on right and fully on left side, and a 3.1 mm long incision in sternal region for tissue collection (Fig. 2A, B); SVL 32.1 mm, head short (HL/SVL 0.25), wide (HW/HL 0.68), not strongly depressed (HD/HL 0.40), distinct from neck. Loreal region marginally inflated, canthus rostralis indistinct. Snout 1/2 head length (ES/HL 0.48), 2.5× eye diameter (ES/ED 2.5); scales on snout and canthus rostralis sub-circular to elongate, subequal, smooth, weakly conical, much larger than those on forehead and interorbital region; scales on forehead similar to those on snout and canthus rostralis except almost 2× smaller and elongate; scales on interorbital region, occipital, and temporal region even smaller, granular (Fig. 3A). Eye small (ED/HL 0.19); with round pupil; supraciliaries short, larger anteriorly; eight interorbital scale rows across narrowest point of frontal bone; 27 scale rows between left and right supraciliaries at mid-orbit level (Fig. 3A). Ear-opening deep, oval, small (EL/HL 0.06); eye to ear distance much greater than diameter of eye (EE/ED 1.60) (Fig. 3C). Rostral slightly > 2× as wide (1.5 mm) as high (0.7 mm), incompletely divided dorsally by a strongly developed rostral groove for > 1/2 of its height; a single enlarged, roughly rectangular supranasal on each side, almost 3× larger than upper postnasal, and strongly in contact with each other on snout; a pair of enlarged scales on snout behind internasals, separated from each other by two much smaller, granular scales; rostral in contact with supralabial I, nostril, and supranasal on either side; nostrils oval, surrounded by four postnasals, supranasal, rostral and supralabial I on either side; four roughly circular postnasals on either side, the one touching supranasal largest, gradually decreasing in size posteriorly; two single row of scales separate orbit from supralabials (Fig. 3C). Mental enlarged, subtriangular, marginally wider (2.0 mm) than high (1.6 mm); two pairs of postmentals, inner pair roughly rectangular, shorter (0.9 mm) than mental, separated from each other below mental by a single enlarged median chin shield; inner pair bordered by mental, infralabial I,

outer postmental, median chin shield and a single enlarged chin shields on either side; outer postmentals roughly rectangular, slightly smaller (0.6 mm) than inner pair, bordered by inner postmentals, infralabial I and II, and four enlarged chin shields on either side; three enlarged gular scales between left and right outer postmentals; all chin scales bordering postmentals more or less flattened, subcircular, smooth, and smaller than outermost postmentals; scales on rest of throat, much smaller, smooth, subcircular, and subimbricate (Fig. 3B). Infralabials bordered below by a row or two of slightly enlarged, much elongated scales, decreasing in size posteriorly. Nine supralabials up to angle of jaw and five at midorbital position on each side; supralabial I largest, gradually decreasing in size posteriorly; eight infralabials on left and seven on right side up to angle of jaw, four at midorbital position on left and five on right side; infralabial I largest, gradually decreasing in size posteriorly (Fig. 3C).

Body relatively slender (BW/AGL 0.37), trunk < 1/2 of SVL (AGL/SVL 0.42) without spine-like tubercles on flank (Fig. 4A–C). Dorsal pholidosis heterogeneous; smooth to weakly keeled granular scales intermixed with a fairly regularly arranged rows of enlarged, weakly keeled, conical tubercles; granular scales gradually increasing in size towards each flank, largest on mid-flank; granular scales on occiput and nape slightly smaller than paravertebral granules; enlarged tubercles in approximately 10 longitudinal rows at midbody; 12 (left) and 14 (right) tubercles in paravertebral rows (Fig. 4A, C). Ventral scales much larger than granular scales on dorsum, subequal from chest to vent, smooth, subcircular and subimbricate with rounded end; scales on precloacal region and four or five rows on femur distinctly enlarged; midventral scale rows across belly 31; 138 ventral scales from mental to anterior border of cloaca (Fig. 4B). A continuous series of six precloacal pores, femoral pores absent (Fig. 3D).

Scales on palm and soles granular, smooth, rounded, and flattened, a distinct enlarged metacarpal scale on palm below digit I; scales on dorsal aspects of limbs heterogeneous in shape and size; scales on upper arm and thigh much larger than granular scales on body dorsum, elongate, subimbricate with pointed ends; scales on lower arm and shank granular, similar in size to granular scales on body dorsum, smooth, rounded, gradually becoming larger, flattened and subimbricate anterolaterally and posteriorly, largest on anterolateral aspect of the hands and feet; scales on ventral aspect of upper arm smooth, granular, much smaller than granular scales on body dorsum, scales on ventral aspect of lower arm with much larger scales than those on upper arm, smooth, subcircular and flattened scales; ventral aspect of thigh and shank with enlarged, smooth, flattened, subimbricate scales, much larger than midventrals (Fig. 2A, B). Forelimbs and hindlimbs slightly long, slender (LAL/SVL 0.14); (CL/SVL 0.19); digits long, with a strong, recurved claw, distinctly inflected, distal portions laterally compressed conspicuously. Digits with both paired and unpaired lamellae, separated into a basal and narrower distal series by single enlarged lamella at inflection; one or two most basal paired on basal series and 1–4 paired lamellae above the inflection; basal lamellae series: (1-5-5-6-5 right manus, 2-7-7-7-4 right pes), (2-6-5-6-5 left manus, Fig. 3E; 2-7-7-8-3 left pes, Fig. 3F); distal lamellae series: (11-12-16-15-12 right manus, 10-12-16-16-16 right pes), (11-12-15-15-12 left manus, Fig. 3E; 10-12-16-16-16 left pes, Fig. 3F). Relative length of digits (measurements in mm in parentheses): IV (3.2) > III (3.1) > II (2.9) > V (2.7) > I (2.1) (left manus); IV (4.1) > V (3.9) = III (3.6) > II (2.9) > I (1.9) (left pes).

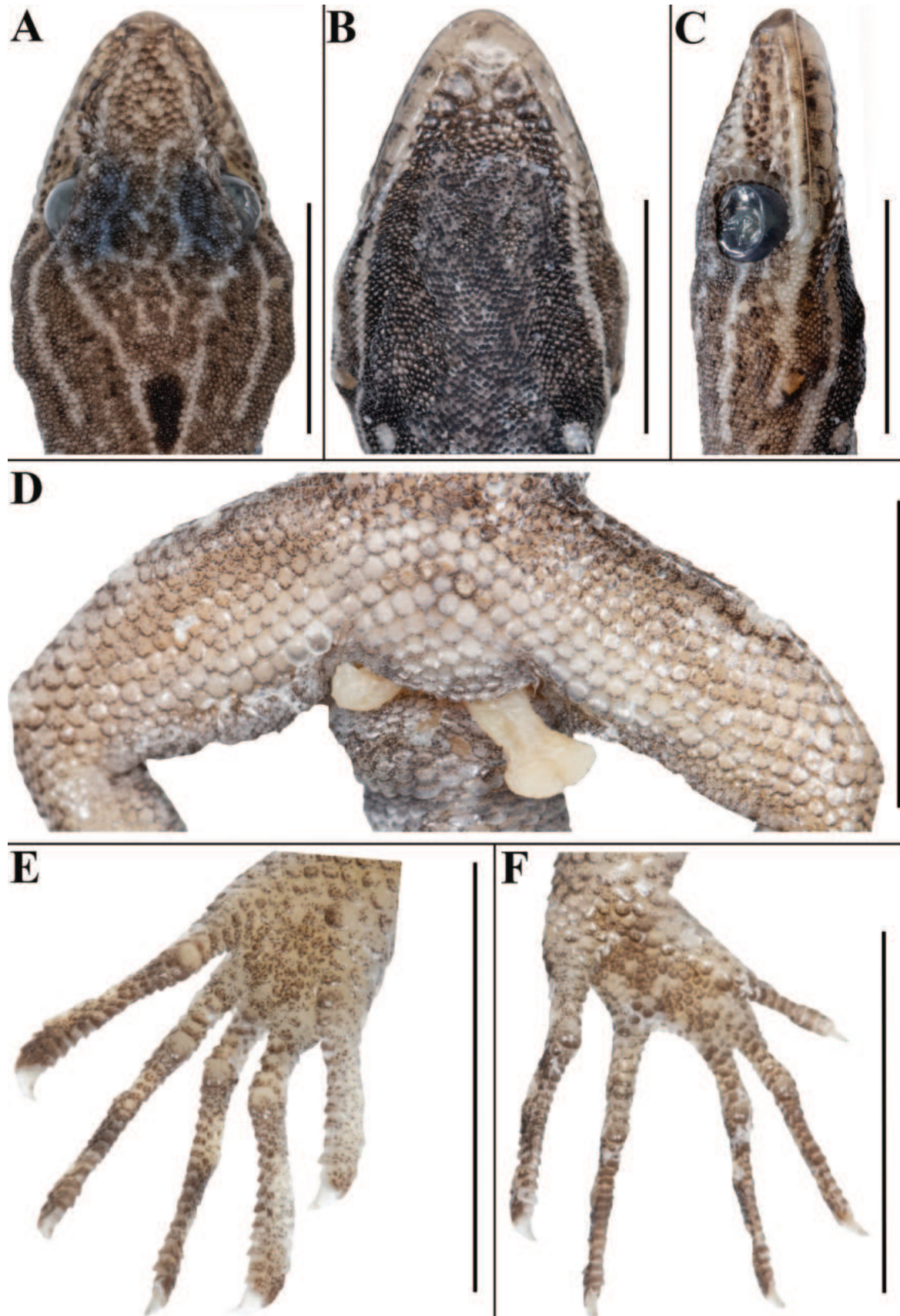


**Figure 3.** *Cnemaspis vangoghi* sp. nov. (holotype, NRC-AA-8342) **A** dorsal view of head **B** ventral view of head **C** lateral view of head on right **D** view of femoral region showing femoral pores **E** ventral view of left manus **F** ventral view of left pes. Photos by Akshay Khandekar. Scale bars: 5 mm.

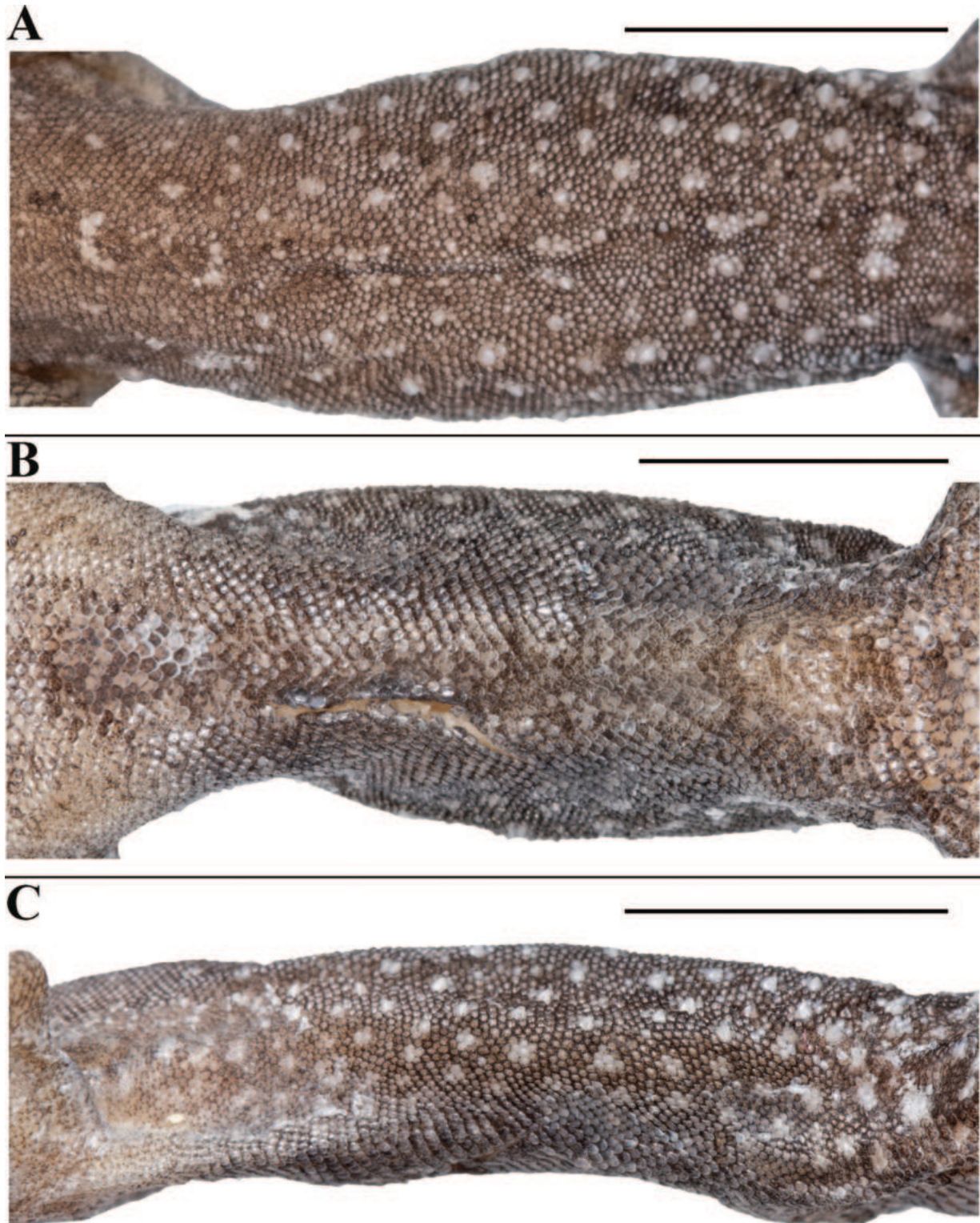


**Figure 4.** *Cnemaspis vangoghi* sp. nov. (holotype, NRC-AA-8342) **A** dorsal view of midbody **B** ventral view of midbody **C** lateral view of midbody. Photos by Akshay Khandekar. Scale bars: 5 mm.

Tail original, subcylindrical, slender, not entire, tail tip is detached and missing, TL = 27.2 mm (Fig. 2C–E). Dorsal pholidosis on tail heterogeneous; small, smooth, subcircular, flattened, subimbricate scales intermixed on anterior one third portion with enlarged, weakly keeled, and weakly conical tubercles forming seven whorls; six tubercles on first three whorl, four tubercles on fourth to sev-

enth whorls, only a pair of paravertebral tubercles on 8<sup>th</sup> to 11<sup>th</sup> whorls; rest of the tail lacking enlarged tubercles (Fig. 2C, E). Scales on tail venter much larger than those on dorsal aspect, smooth, roughly subcircular, flattened, subimbricate; median series smooth, roughly rectangular, distinctly enlarged than rest, with condition of two enlarged scales alternating with a divided scale (Fig. 2D). Scales on tail base much smaller, smooth, imbricate; a single enlarged, smooth and weakly conical postcloacal tubercle on each side (Fig. 2D, E).

**Colouration in life (Fig. 5A).** Dorsal ground colour of body, limbs and tail light grey; neck to mid-body ochre, fading slightly at mid-body. Light blue-grey preorbital streak runs from nostril to orbit; three light postorbital streaks, uppermost on either side meeting in parietal region forming an inverted chevron enclosing a single large elongate black ocellus on occiput, middle terminating on neck and lowermost continuing until ear opening. Head finely reticulated with pale blue-grey, a white ocellus on a black patch of scales on each side of ventrolateral aspect of neck just anterior to forelimb insertions; a fine yellow collar at anterior edge of forelimb insertions, just divided by indistinct continuation of chevron on neck, two small black spots anterior to the division. No distinct dorsal spots or bands, tubercles and a few adjacent scales at mid-body and posterior 1/2 of body pale blue-grey; similar spots on femur and bands on tibia; forelimbs with some ochre near insertions, otherwise whitish-grey with dark outlines of scales; digits with white and dark markings. Original tail without bands, blue-grey with dark outlines of scales. Ventral ground colouration grey-white; throat strongly marked with black up to forelimb insertions except for a fine pale border just below infralabials; a white spot on either side of the throat posterior to jaw; belly with dark markings and blue-grey scales toward the lateral margins; underside of limbs and tail with few dark markings; precloacal, femoral and tibial regions with almost no dark markings. Pupil black, iris reddish with a pale orange ring lining pupil.

**Variation and additional information from type series (Figs 5B, C, 6).** Mensural, meristic and additional character state data for the type series is given in Tables 3–5, respectively. There are four adult males, a single subadult male, and a single adult female ranging in size from 28.6–33.6 mm (Fig. 6A, B). All paratypes resemble the holotype except as follows: three postnasals on either side in NRC-AA-8344, NRC-AA-8346, and NRC-AA-8348. Inner postmentals bordered by mental, infralabial I, outer postmental, enlarged median chin shield in all paratypes, additionally, bordered by two small chin scales on either side in NRC-AA-8343, single chin scale on left and two on right side in NRC-AA-8344. Outer postmentals bordered by inner pair, infralabial I and II in all paratypes, additionally, bordered by five chin scales on left and four on right side in NRC-AA-8344, NRC-AA-8345, NRC-AA-8347; four on left and five on right side in NRC-AA-8348; outer postmental separated from each other by five chin scales including median chin shield in NRC-AA-8343, four chin scales in NRC-AA-8344. NRC-AA-8348 with original and complete tail, slightly longer than body (TL/SVL 1.23); three paratypes, NRC-AA-8344, NRC-AA-8346, and NRC-AA-8347, with original partially broken tails; NRC-AA-8343 with small and partially regenerated tail, and NRC-AA-8345 with complete regenerated tail, detached from the body (Fig. 6A, B). NRC-AA-8347 with damaged skink on the snout; NRC-AA-8343 with fully everted hemipenis on either side, NRC-AA-8347 with fully everted hemipenis only on left side.

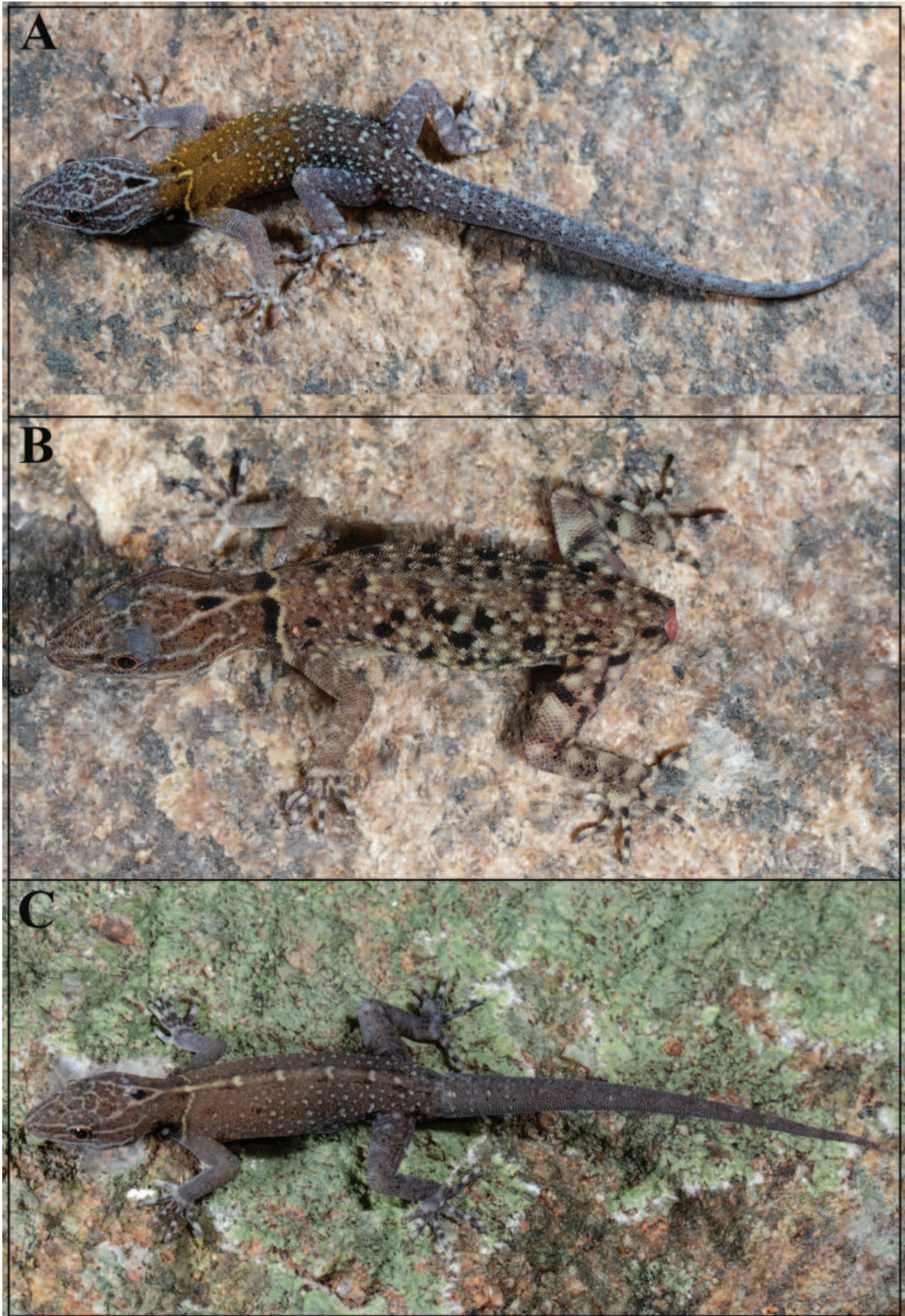


Figure 5. *Chemaspis vangoghi* sp. nov., in life **A** adult male (holotype, NRC-AA-8342) **B** adult female (paratype, NRC-AA-8345), and **C** subadult male (paratype, NRC-AA-8348). Photos by Akshay Khandekar.



**Figure 6.** Paratype series of *Cnemaspis vangoghi* sp. nov., from left to right, NRC-AA-8343–8348 **A** dorsal view, and **B** ventral view. Photos by Akshay Khandekar. Scale bar: 10 mm.

The new species is strongly sexually dimorphic and also shows ontogenetic colour variation (Fig. 5A–C): females brown with numerous black and pale blotches, collar pale brown, flanked anteriorly by thick black, divided by an extension of the neck chevron; distinct black ocellus on occiput; white ocelli on side of neck absent; forelimbs brown, hindlimbs with scattered dark and pale markings, digits banded. Regenerated tail grey, without bands. Ventral ground colouration of gular, body and tail grey-white; underside of limbs with few dark markings. Subadult male brown with an indistinct, cream mid-dorsal streak formed by the extension of the neck chevron, five or six spots in the streak; black ocellus on occiput and white ocelli on side of neck distinct; forelimbs brown, hindlimbs with scattered dark and pale markings, digits banded. Original tail without bands, grey with dark outlines of scales, regenerated portion brown. Ventral ground colouration of gular, body and tail grey-white; a white spot on either side of the throat posterior to jaw; belly without dark markings; underside of limbs and tail with few dark markings.

**Table 3.** Mensural (mm) data for the new species. Abbreviations are listed in Materials and methods, \* = tail incomplete.

Museum number	<i>Cnemaspis vangoghi</i> sp. nov.							<i>Cnemaspis sathuragiriensis</i> sp. nov.				
	Holotype	Paratypes						Holotype	Paratypes			
	NRC-AA-8342	NRC-AA-8343	NRC-AA-8344	NRC-AA-8345	NRC-AA-8346	NRC-AA-8347	NRC-AA-8348	NRC-AA-8349	NRC-AA-8350	NRC-AA-8351	NRC-AA-8352	NRC-AA-8353
Sex	Male	Male	Male	Female	Male	Male	Subadult male	Male	Male	Male	Male	Subadult female
SVL	32.1	33.6	33.6	32.9	31.3	32.8	28.6	32.8	32.9	31.2	33.0	26.7
TL	27.2*	16.9*	29.8*	33.7*	22.2*	26.9*	35.4	37.6	38.6	32.1*	3.1*	1.9*
TW	3.2	3.1	3.2	3.4	3.3	3.0	2.7	3.0	2.7	3.6	3.2	2.3
FL	4.7	4.6	5.0	5.2	4.9	4.7	4.6	4.8	4.9	4.9	5.1	4.0
CL	6.2	5.9	6.3	6.2	6.3	6.2	5.3	6.5	6.2	6.0	6.7	4.9
AGL	13.7	13.0	12.8	13.2	12.6	13.6	11.5	12.9	14.2	12.4	12.7	11.1
BH	3.5	3.7	3.4	4.2	3.6	3.4	3.7	3.6	3.5	3.3	4.2	3.9
BW	5.2	7.0	5.9	6.3	6.2	5.7	5.6	6.5	5.6	6.1	6.9	5.1
HL	8.2	8.5	8.8	9.1	8.4	8.8	7.0	9.0	8.1	8.5	8.9	6.6
HW	5.6	6.1	5.9	5.9	5.8	5.7	5.4	6.7	5.9	6.1	5.9	4.7
HD	3.3	3.5	3.7	4.6	3.78	3.7	3.3	4.7	3.4	3.7	3.8	2.7
ED	1.6	1.6	1.9	1.8	1.6	1.5	1.4	1.8	1.7	1.8	1.9	1.5
EE	2.6	2.9	2.7	2.8	2.8	2.9	2.3	2.9	2.6	2.7	2.7	2.3
ES	4.0	3.9	4.3	4.3	3.9	4.2	3.3	4.0	4.0	4.0	4.3	3.1
EN	3.1	3.1	3.4	3.2	3.1	3.3	2.6	3.2	3.0	3.2	3.5	2.5
IN	1.1	1.1	1.1	1.2	1.1	1.0	0.8	1.1	1.0	1.1	1.2	1.0
IO	2.1	2.3	2.5	2.6	2.5	2.1	2.1	2.4	2.4	1.8	2.3	1.9
EL	0.5	0.6	0.5	0.6	0.8	0.5	0.5	0.5	0.7	0.6	0.7	0.4

**Etymology.** The specific epithet is a patronym for Dutch painter Vincent Van Gogh (1853–1890). The colouration of the new species is reminiscent of one of Van Gogh’s most iconic paintings, *The Starry Night*. Suggested common name is Van Gogh’s starry dwarf gecko.

**Distribution and natural history.** *Cnemaspis vangoghi* sp. nov. is known only from two closely spaced localities (Ayyanar Kovil and Settur Reserve Forest, both in Meghamalai-Srivilliputhur Tiger Reserve, Tamil Nadu) within < 15 km straight line distance (Fig. 1). The new species was recorded in seasonally dry tropical forest with a mix of evergreen and deciduous species between elevations of 250–400 m a.s.l. on eastern slopes of the Western Ghats (Fig. 7A). Individuals of the new species were observed active during the daytime (0830–1400 hrs) on rocks and tree trunks < 2 m high from the base (Fig. 7B). A large number of individuals ( $n \geq 25/\text{hr}$ ) were observed at both the locations indicating high abundance. At Ayyanar Kovil, a few individuals were observed inactive, resting on rocks during evening and night time (1800–2030 hrs). We also observed Giant wood spider (*Nephila* sp.) feeding on an adult female individual of the new species. Sympatric lizards at the type locality include *Cnemaspis* cf. *gracilis*, *Hemidactylus* cf. *frenatus*, *H.* cf. *leschenaultii*, *H. vanam* Chaitanya, Lajmi & Giri, 2018, *Dravidoseps srivilliputhurensis* Agarwal, Thackeray & Khandekar, 2024, *Eutropis carinata* (Schneider, 1801), *E. macularia* (Blyth, 1853), and *Psammophilus* cf. *blanfordanus*.



**Figure 7.** Habitat of *Cnemaspis vangoghi* sp. nov. **A** general view at Settur Reserve Forest (paratype locality), and **B** microhabitat at type locality. Photos by Akshay Khandekar.

***Cnemaspis sathuragiriensis* sp. nov.**

<https://zoobank.org/5C640413-8B2F-417F-AD1C-A867AFE5A7B5>

Figs 8–12, Tables 3–5

**Type material examined. Holotype.** NRC-AA-8349 (AK-R 1510), adult male, from near Sathuragiri entry point (9.7093°N, 77.6307°E; ca 250 m a.s.l.), Sathuragiri, Virudhunagar district, Tamil Nadu state, India; collected by Akshay Khandekar, Ishan Agarwal, Swapnil Pawar and team on 26 April 2022. **Paratypes.** NRC-AA-8350 (AK-R 1511), NRC-AA-8351 (AK-R 1512), adult males, same data as

holotype; NRC-AA-8352 (AK-R 1513), adult male, NRC-AA-8353 (AK-R 1515), subadult female, from near Vazhukkuparai Saptur Reserve Forest (9.7174°N, 77.6244°E; ca 400 m a.s.l.), Sathuragiri; same data as holotype.

**Diagnosis.** A small-sized *Cnemaspis*, snout to vent length  $\leq 33$  mm ( $n = 5$ ). Dorsal pholidosis heterogeneous; smooth to weakly keeled granular scales intermixed with irregularly arranged rows of enlarged, weakly keeled, conical tubercles; 6–8 rows of dorsal tubercles at midbody, paravertebral tubercles either absent or irregular; ventral scales subequal from chest to vent, smooth, subcircular and subimbricate with rounded end; 28–30 midventral scales across belly, 130–137 longitudinal ventral scales from mental to cloaca; subdigital scansors smooth, unnotched, some divided and others entire, a distinct enlarged metacarpal scale below digit I; 11–13 lamellae under digit I of manus and 11 or 12 under digit I of pes, 18–21 lamellae under digit IV of manus and 23 or 24 lamellae under digit IV of pes; males with continuous series of seven or eight precloacal pores ( $n = 4$ ); scales on non-regenerated tail dorsum heterogeneous; small, smooth, subcircular, flattened, subimbricate scales intermixed on anterior one third portion with enlarged, weakly keeled, and weakly conical tubercles forming eight whorls; six tubercles on first whorl, four tubercles on second to fourth whorls, only a pair of paravertebral tubercles each on fifth to eighth whorls; rest of the tail lacking enlarged tubercles; median row of subcaudals smooth, roughly subcircular, distinctly enlarged than rest, with condition of two enlarged scales alternating with a divided scale. Males with ochre dorsum, single central black dorsal ocellus on neck, a white ocellus on ventrolateral side of neck and one on throat posterior to jaw, venter off-white with dark throat, tail unbanded, females and juveniles brown with a prominent mid-dorsal streak.

**Comparisons with members of *beddomei* clade.** *Cnemaspis sathuragiriensis* sp. nov. can be easily distinguished from all 16 members of the *beddomei* clade as well as from *C. boiei* by a combination of the following differing or non-overlapping characters: A small-sized *Cnemaspis*, snout to vent length  $\leq 33$  mm (vs medium-sized *Cnemaspis*, snout to vent length 40–49 mm in *C. nairi*, *C. nimbus*, *C. ornata*, *C. rashidi*, *C. rubraoculus* and *C. wallaceii*); large-sized *Cnemaspis*, snout to vent length  $> 50$  mm in *C. anamudiensis*, *C. beddomei*, *C. maculicollis*, and *C. smaug*; snout to vent length  $\leq 38$  mm in *C. azhagu*, *C. boiei*, and *C. nigriventris*); 6–8 rows of dorsal tubercles at midbody (vs only a few enlarged scattered tubercles at midbody dorsum in *C. anamudiensis*, two or three rows of dorsal tubercles at midbody in *C. azhagu*, 16–18 in *C. nairi*, 13 or 14 in *C. nigriventris*, 12–14 in *C. nimbus* and *C. ornata*, 19–22 in *C. smaug*, 10 in *C. vangoghi* sp. nov., 14 or 15 in *C. wallaceii*); 130–137 longitudinal ventral scales from mental to cloaca (vs 151–171 longitudinal ventral scales from mental to cloaca in *C. azhagu*, 154–161 in *C. beddomei*, 153–159 in *C. galaxia*, 143–147 in *C. nairi*, 154–159 in *C. nigriventris*, 157–165 in *C. ornata*, 170–172 in *C. rashidi*, 148–154 in *C. regalis*, 142–150 in *C. smaug*, 156–160 in *C. sundara*, 154–156 in *C. wallaceii*); paravertebral tubercles either absent or irregular (vs 18 or 19 tubercles in paravertebral rows in *C. aaronbaueri* and *C. beddomei*, 16 or 17 in *C. nimbus*, 21–23 in *C. ornata*, 27–30 in *C. smaug*, 7–14 in *C. vangoghi* sp. nov., 18–20 in *C. wallaceii*); 28–30 midventral scales across belly (vs 34–44 midventral scales across belly in *C. azhagu*, 32 or 33 in *C. nairi*, 38–40 in *C. nigriventris*, 26 or 27 in *C. nimbus*, 40–44 in *C. regalis*, 33–37 in *C. rubraoculus*, 35 or 36 in *C. sundara*); a distinct white ocellus on ventrolateral sides of neck present in

**Table 4.** Meristic data for the new species. Abbreviations are listed in Materials and methods, \* = lamellae damaged, L&R = left & right, A = absent.

Museum number	<i>Cnemaspis vangoghi</i> sp. nov.							<i>Cnemaspis sathuragiriensis</i> sp. nov.				
	Holotype	Paratypes						Holotype	Paratypes			
	NRC-AA-8342	NRC-AA-8343	NRC-AA-8344	NRC-AA-8345	NRC-AA-8346	NRC-AA-8347	NRC-AA-8348	NRC-AA-8349	NRC-AA-8350	NRC-AA-8351	NRC-AA-8352	NRC-AA-8353
SL L&R	9&9	9&8	9&9	8&8	7&7	9&10	8&7	8&8	8&8	8&8	8&8	8&8
IL L&R	8&7	6&7	7&7	8&7	6&7	7&7	8&8	7&7	7&7	7&7	7&7	7&7
SL M L&R	5&5	5&5	6&5	5&6	5&5	5&6	5&5	5&5	5&5	5&5	5&5	5&5
IL M L&R	4&5	4&4	5&5	4&5	5&4	4&5	4&4	5&5	4&4	4&4	4&4	5&4
PVT L&R	12&14	7&7	7&8	7&9	12&12	11&13	7&7	A	A	irr	A	irr
DTR	10	10	10	10	10	10	10	6	7	8	6	7
MVSR	31	31	30	30	29	29	31	30	28	30	28	29
VS	138	125	137	126	134	140	134	132	131	137	130	131
DLAMF1 L&R	11&11	10&10	11&11	9&10	10&11	12&12	12&12	10&10	10&10	10&10	10&10	11&12
BLAMF1 L&R	2&1	2&2	2&2	2&2	2&2	2&2	2&1	1&1	1&1	3&3	2&2	1&1
DLAMF4 L&R	15&15	13&13	14&15	13&14	14&14	16&10*	15&15	14&14	15&14	15&15	13&13	15&15
BLAMF4 L&R	6&6	6&6	6&6	6&6	6&6	6&6	7&6	6&6	3&4	6&6	6&6	6&5
DLAMT1 L&R	10&10	9&9	10&10	9&9	10&10	11&11	11&10	10&10	10&10	9&9	9&9	10&10
BLAMT1 L&R	2&2	2&2	2&2	2&2	2&2	2&2	2&2	1&1	2&2	2&2	2&2	2&2
DLAMT4 L&R	16&16	15&15	15&15	14&15	14&14	17&16	16&17	15&16	16&16	16&16	14&14	16&16
BLAMT4 L&R	8&7	7&6	6&6	4&6	6&7	8&8	7&7	8&8	7&7	8&8	9&9	7&7
DLAMT5 L&R	16&16	15&14	15&15	15&14	15&15	17&16	16&17	15&16	15&16	15&16	13&14	16&16
BLAMT5 L&R	3&4	2&2	2&2	2&2	3&3	2&2	2&2	2&2	2&2	2&2	2&3	2&2
TLAMF1 L&R	13&12	12&12	13&13	11&12	12&13	14&14	14&13	11&11	11&11	13&13	12&12	12&13
TLAMF4 L&R	21&21	19&19	20&21	19&20	20&20	22&16*	22&21	20&20	18&18	21&21	19&19	21&20
TLAMT1 L&R	12&12	11&11	12&12	11&11	12&12	13&13	13&12	11&11	12&12	11&11	11&11	12&12
TLAMT4 L&R	24&23	22&21	21&21	18&21	20&21	25&24	23&24	23&24	23&23	24&24	23&23	23&23
TLAMT5 L&R	19&20	17&16	17&17	17&16	18&18	19&18	18&19	17&18	17&18	17&18	15&17	18&18
PP	6	7	7	A	7	7	7	7	8	7	8	A
SB PP	A	A	A	A	A	A	A	A	A	A	A	A
PCT L&R	1&1	1&1	1&1	1&1	1&1	1&1	1&1	1&1	1&1	1&1	1&1	1&1

males (vs white ocellus on ventrolateral sides of neck absent in *C. aaronbaueri*, *C. anamudiensis*, *C. azhagu*, *C. beddomei*, *C. maculicollis*, *C. nimbus*, *C. regalis*, *C. rubraoculus*, *C. smaug*, *C. wallaceii*); tail unbanded (tail distinctly banded in *C. nairi*, *C. nigriventris*, *C. ornata*, *C. rashidi*, *C. smaug*, *C. sundara*).

**Description of the holotype.** Adult male in good state of preservation except tail marginally bent towards right, hemipenis fully everted on right, and a 4.1 mm long incision in sternal region for tissue collection (Fig. 8A–E); SVL 32.1 mm, head short (HL/SVL 0.27), wide (HW/HL 0.74), not strongly depressed (HD/HL 0.52), distinct from neck. Loreal region marginally inflated, canthus rostralis indistinct. Snout almost 1/2 of head length (ES/HL 0.44), 2× eye diameter (ES/ED 2.2); scales on snout and canthus rostralis subcircular to elongate, subequal, smooth, weakly conical, much larger than those on forehead and interorbital region; scales on forehead similar to those on snout and canthus rostralis except almost 2× smaller and elongate; scales on interorbital region, occipital, and temporal region even smaller, granular (Fig. 9A). Eye small (ED/HL 0.20);

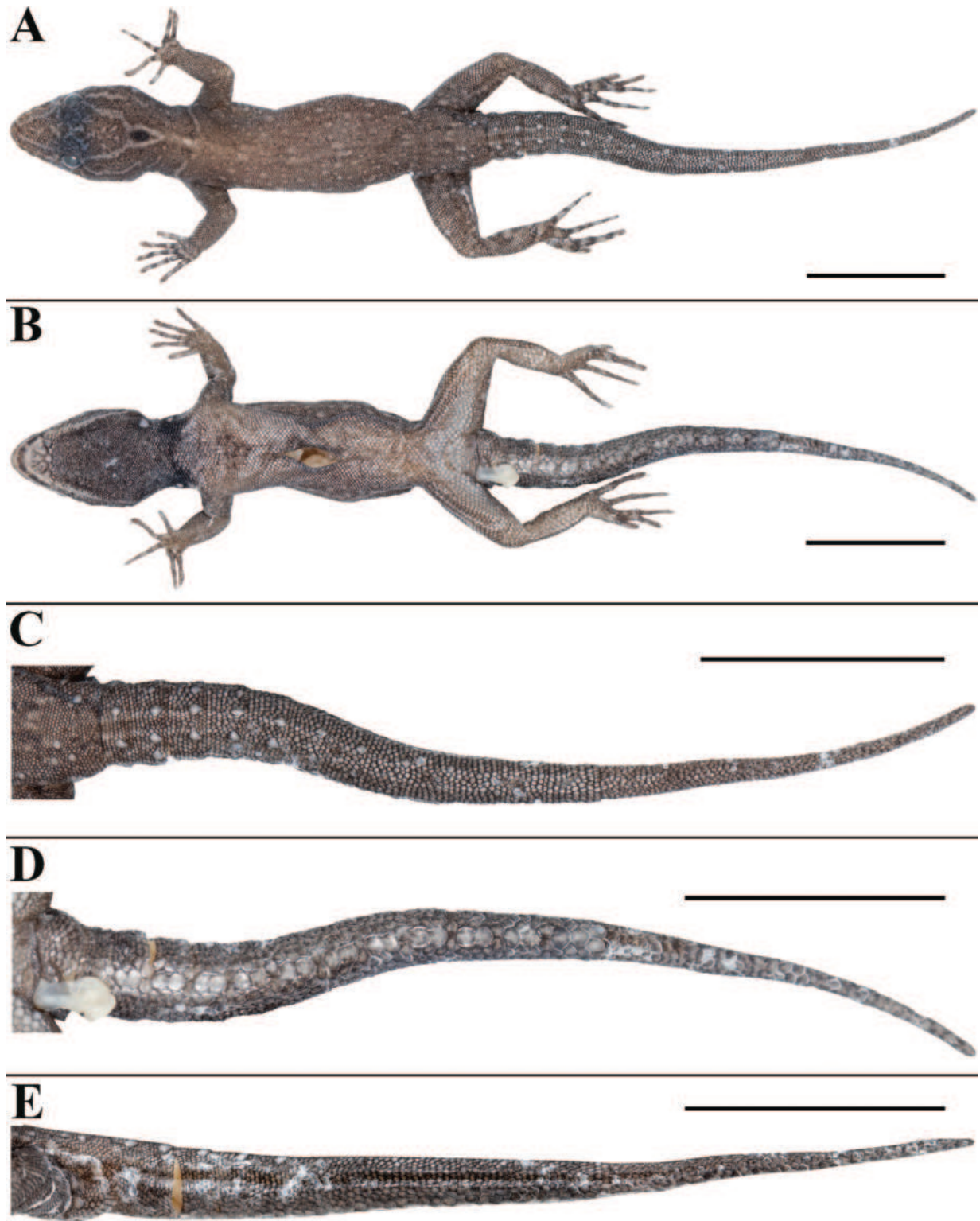


Figure 8. *Chemaspis sathuragiriensis* sp. nov. (holotype, NRC-AA-8349) **A** dorsal view of body **B** ventral view of body **C** dorsal view of tail **D** ventral view of tail **E** lateral view of tail. Photos by Akshay Khandekar. Scale bars: 10 mm.

with round pupil; supraciliaries short, larger anteriorly; seven interorbital scale rows across narrowest point of frontal bone; 29 scale rows between left and right supraciliaries at mid-orbit level (Fig. 9A, C). Ear-opening deep, oval, small (EL/HL 0.05); eye to ear distance much greater than diameter of eye

(EE/ED 1.61) (Fig. 9C). Rostral slightly  $> 2\times$  as wide (1.7 mm) as high (0.8 mm), incompletely divided dorsally by a strongly developed rostral groove for  $> 1/2$  of its height; a single enlarged, roughly rectangular supranasal on each side, almost  $3\times$  larger than upper postnasal, and strongly in contact with each other on snout; a pair of enlarged scales on snout behind internasals, separated from each other by a single smaller, granular scale; rostral in contact with supralabial I, nostril, and supranasal on either side; nostrils oval, surrounded by three postnasals, supranasal, rostral and supralabial I on either side; three postnasals on either side, the one touching supranasal largest, roughly rectangular, gradually decreasing in size posteriorly; two single row of scales separate orbit from supralabials (Fig. 9C). Mental enlarged, subtriangular, marginally wider (2.1 mm) than high (1.9 mm); two pairs of postmentals, inner pair roughly rectangular, shorter (1.0 mm) than mental, separated from each other below mental by a single enlarged median chin shield; inner pair bordered by mental, infralabial I, outer postmental, median chin shield and a single enlarged chin shields on either side; outer postmentals roughly rectangular, slightly smaller (0.6 mm) than inner pair, bordered by inner postmentals, infralabial I and II, and five enlarged chin shields on either side; three enlarged gular scales (including median chin shield) between left and right outer postmentals; all chin scales bordering postmentals more or less flattened, subequal, subcircular, smooth, and smaller than outermost postmentals; scales on rest of throat granular, smooth, subcircular, and juxtaposed scales (Fig. 9B). Infralabials bordered below by a row or two of slightly enlarged, much elongated scales, decreasing in size posteriorly. Eight supralabials up to angle of jaw and five at midorbital position on each side; supralabial I largest, gradually decreasing in size posteriorly; seven infralabials up to angle of jaw and five at midorbital position on either side; infralabial I largest, gradually decreasing in size posteriorly (Fig. 9C).

Body relatively slender (BW/AGL 0.50), trunk  $< 1/2$  of SVL (AGL/SVL 0.39) without spine-like tubercles on flank (Fig. 10A–C). Dorsal pholidosis heterogeneous; smooth to weakly keeled granular scales intermixed with irregularly arranged rows of enlarged, weakly keeled, conical tubercles; granular scales gradually increasing in size towards each flank, largest on mid-flank; granular scales on occiput and nape slightly smaller than paravertebral granules; enlarged tubercles in approximately six longitudinal rows at midbody; enlarged tubercles in paravertebral rows absent, (Fig. 10A, C). Ventral scales much larger than granular scales on dorsum, subequal from chest to vent, smooth, subcircular and subimbricate with rounded end; scales on precloacal region and four or five rows on femur distinctly enlarged; midventral scale rows across belly 30; 132 ventral scales from mental to anterior border of cloaca (Fig. 10B). A continuous series of seven precloacal pores, femoral pores absent (Fig. 9D).

Scales on palm and soles granular, smooth, rounded, and flattened, a distinct enlarged metacarpal scale on palm below digit I; scales on dorsal aspects of limbs heterogeneous in shape and size; scales on upper arm and thigh much larger than granular scales on body dorsum, smooth and a few feebly keeled, slightly elongate, subimbricate with weakly pointed ends; scales on lower arm and shank granular, similar in size to granular scales on body dorsum, smooth, rounded, gradually becoming larger, flattened and subimbricate anterolaterally and posteriorly, largest on anterolateral aspect of the hands and feet; scales on ventral aspect of upper arm smooth, granular, much smaller than granular

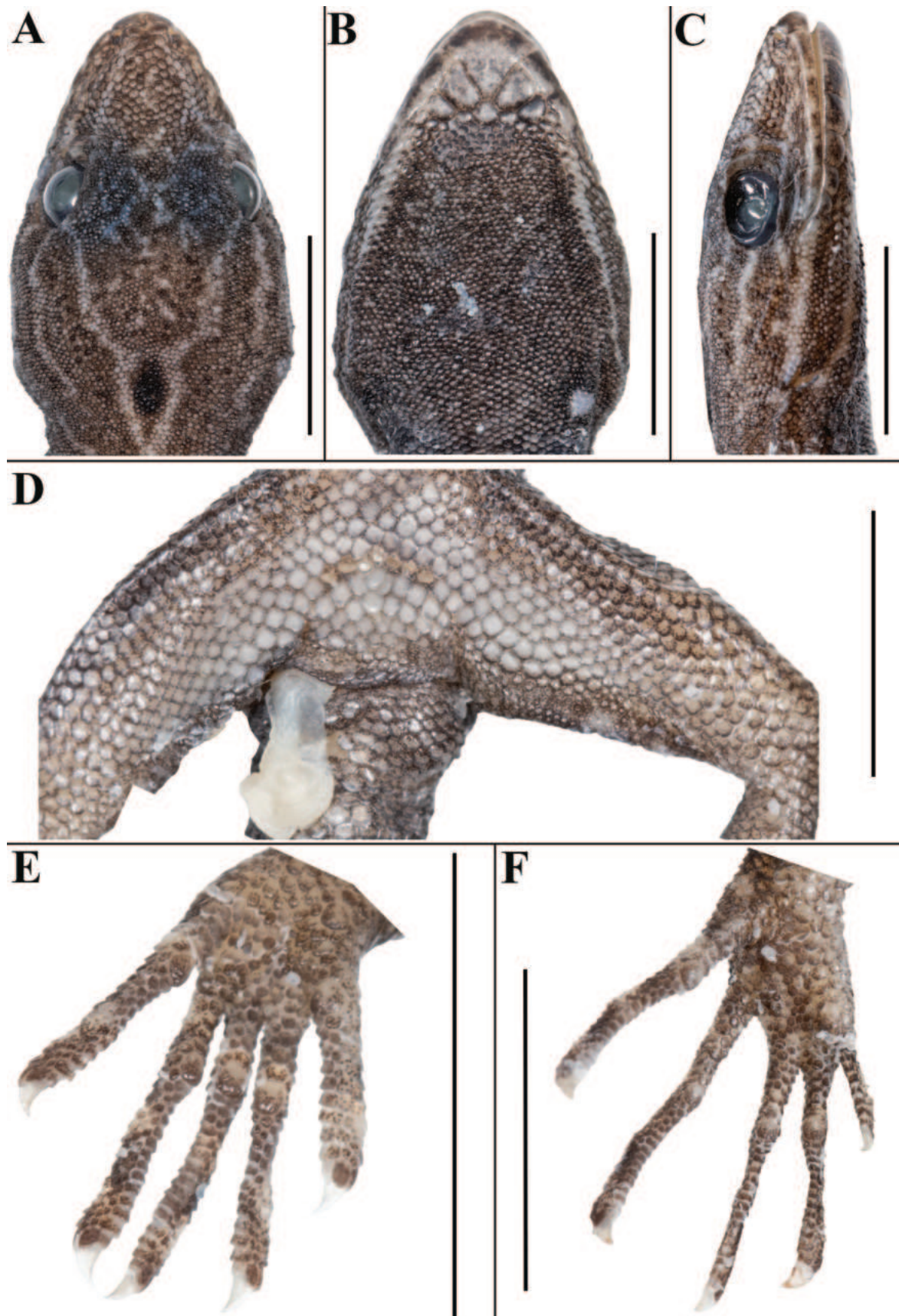


**Figure 9.** *Cnemaspis sathuragiriensis* sp. nov. (holotype, NRC-AA-8349) **A** dorsal view of head **B** ventral view of head **C** lateral view of head on right **D** view of femoral region showing femoral pores **E** ventral view of left manus **F** ventral view of left pes. Photos by Akshay Khandekar. Scale bars: 5 mm.

scales on body dorsum, scales on ventral aspect of lower arm with much larger scales than those on upper arm, smooth, subcircular and flattened scales; ventral aspect of thigh and shank with enlarged, smooth, flattened, subimbricate scales, much larger than midventrals (Fig. 8A, B). Forelimbs and hindlimbs slightly long, slender (LAL/SVL 0.14); (CL/SVL 0.19); digits long, with a strong, recurved claw, distinctly inflected, distal portions laterally compressed conspicuously. Digits with both paired and unpaired lamellae, separated into a basal and narrower distal series by single enlarged lamella at inflection; one or two most basal paired on basal series and 1–4 paired lamellae above the inflection; basal lamellae series: (1-5-4-6-3 right manus, 1-6-7-8-2 right pes), (1-5-4-6-4 left manus, Fig. 9E; 1-6-7-8-2 left pes, Fig. 9F); distal lamellae series: (10-12-14-14-12 right manus, 10-12-16-16-16 right pes), (10-12-15-14-12 left manus, Fig. 9E; 10-13-16-15-15 left pes, Fig. 9F). Relative length of digits (measurements in mm in parentheses): IV (3.4) = III (3.4) > II (3.1) > V (3.0) > I (2.2) (left manus); IV (4.1) = III (4.1) > II (3.4) = II (3.3) > I (2.2) (left pes).

Tail mostly original with regenerated tip, entire, subcylindrical, slender, marginally longer than body (TL/SVL = 1.14) (Fig. 8C–E). Dorsal pholidosis on tail heterogeneous; small, smooth, subcircular, flattened, subimbricate scales intermixed on anterior one third portion with enlarged, weakly keeled, and weakly conical tubercles forming eight whorls; six tubercles on first whorl, four tubercles on second to fourth whorls, only a pair of paravertebral tubercles each on fifth to eighth whorls; rest of the original and regenerated tail lacking enlarged tubercles (Fig. 8C, E). Scales on tail venter much larger than those on dorsal aspect, smooth, roughly subcircular, flattened, subimbricate; median series smooth, roughly subcircular, distinctly enlarged than rest, with condition of two enlarged scales alternating with a divided scale (Fig. 8D). Scales on tail base much smaller, smooth, imbricate; a single enlarged, smooth, and weakly conical postcloacal tubercle on each side (Fig. 8D, E).

**Colouration in life (Fig. 11A).** Dorsal ground colour of body, limbs, and tail pale grey; neck and trunk ochre, fading slightly near hindlimb insertions. Pale blue-grey preorbital streak runs from nostril to orbit; three pale postorbital streaks, uppermost on either side meeting in parietal region forming an inverted chevron enclosing a single large elongate black ocellus on occiput, middle terminating on neck and lowermost continuing until ear opening. Head finely reticulated with pale blue-grey, a white ocellus on a black patch of scales on each side of ventrolateral aspect of neck just anterior to forelimb insertions; a fine yellow collar at anterior edge of forelimb insertions, broken in the centre, two fine black spots anterior to and a yellow spot on the division. Fine black spots and paler blotches on dorsum, tubercles and a few adjacent scales around hindlimb insertions and on tail pale blue-grey; similar spots on posterior flank, femur and bands on tibia; upper 1/2 of upper arm ochre, otherwise whitish-grey with dark outlines of scales; digits with white and dark markings. Original tail without bands, blue with dark outlines of scales and darker markings. Ventral ground colouration grey-white; throat fairly strongly marked with black up to forelimb insertions except for a fine pale border just below infralabials, a white spot on either side of the throat posterior to jaw; belly with scattered dark markings and blue-grey scales toward the lateral margins; underside of limbs and tail with few dark markings; precloacal and femoral region with almost no dark markings. Pupil black, iris dark red with a pale orange ring lining pupil.

**Table 5.** Additional morphological characters of the new species. A = absent, / = data unavailable.

Museum number	<i>Cnemaspis vangoghi</i> sp. nov.						<i>Cnemaspis sathuragiriensis</i> sp. nov.					
	Holotype	Paratypes					Holotype	Paratypes				
	NRC-AA-8342	NRC-AA-8343	NRC-AA-8344	NRC-AA-8345	NRC-AA-8346	NRC-AA-8347	NRC-AA-8348	NRC-AA-8349	NRC-AA-8350	NRC-AA-8351	NRC-AA-8352	NRC-AA-8353
Anterior extra-brillar fringe scales enlarged (0) or not enlarged (1)	0	0	0	0	0	0	0	0	0	0	0	0
Occipital ocellus present (0) or absent (1)	0	0	0	0	0	0	0	0	0	0	0	0
Dorsal pholidosis homogeneous (0) or heterogeneous (1)	1	1	1	1	1	1	1	1	1	1	1	1
Dorsal tubercles weakly keeled (0) or smooth (1)	0	0	0	0	0	0	0	0	0	0	0	0
Tubercles linearly arranged (0) or more random (1)	0	0	0	0	0	0	0	1	1	1	1	1
Spine-like tubercles on flank present (0) or absent (1)	1	1	1	1	1	1	1	1	1	1	1	1
Gular scales keeled (0) or smooth (1)	1	1	1	1	1	1	1	1	1	1	1	1
Pectoral scales keeled (0) or smooth (1)	1	1	1	1	1	1	1	1	1	1	1	1
Ventral scales keeled (0) or smooth (1)	1	1	1	1	1	1	1	1	1	1	1	1
Precloacal pores continuous (0) or separated (1)	0	0	0	A	0	0	0	0	0	0	0	A
Precloacal pores elongate (0) or round (1)	0	0	0	A	0	0	0	0	0	0	0	A
Enlarged femoral scales present (0) or absent (1)	0	0	0	0	0	0	0	0	0	0	0	0
Subtibial scales keeled (0) or smooth (1)	1	1	1	1	1	1	1	1	1	1	1	1
Lateral caudal furrows present (0) or absent (1)	1	/	1	/	1	1	1	1	1	1	/	/
Caudal tubercles encircle tail (0) or not (1)	1	/	1	/	1	1	1	1	1	1	/	/
Subcaudals keeled (0) or smooth (1)	1	/	1	/	1	1	1	1	1	1	/	/
Median subcaudal scale row not enlarged (0) or enlarged (1)	1	/	1	/	1	1	1	1	1	1	/	/

**Variation and additional information from type series (Figs 11B, C, 12).**

Mensural, meristic, and additional character state data for the type series is given in Tables 3–5, respectively. There are three adult males, and a single subadult female ranging in size from 26.7–33.0 mm (Fig. 12). All paratypes resemble the holotype except as follows: inner postmentals bordered by mental, infralabial I, outer postmental, enlarged median chin shield in all paratypes, additionally, bordered by two small chin scales on left and a single scale on right side in NRC-AA-8351. Outer postmentals bordered by inner pair, infralabial I & II in all paratypes, additionally, bordered by four chin scales on left and five on right side in NRC-AA-8350, four on left and five on right side in NRC-AA-8351 and NRC-AA-8353, four on either side in NRC-AA-8352; outer postmental separated from each other by four chin scales including median chin shield in NRC-AA-8351. NRC-AA-8350 with almost original tail with tip regenerated, marginally longer than body (TL/SVL 1.17), NRC-AA-8351 with original tail with missing tail tip, equal to body (TL/SVL 1.02); Two paratypes, NRC-AA-8352 and NRC-AA-8353 with completely missing tails; NRC-AA-8351 with damaged skink on the tail base; NRC-AA-8350 with fully everted hemipenis only on left side.

The new species is strongly sexually dichromatic and shows ontogenetic colour variation (Fig. 11A–C): subadult female pale brown with a cream mid-dorsal streak that continues onto tail formed by the extension of the neck chevron, dorsum with scattered black and pale blotches, collar pale brown, flanked anteriorly by a few black spots; distinct black central ocellus on occiput, white ocelli on side of neck absent; forelimbs brown, hindlimbs with scattered dark and pale markings, digits banded. Original tail grey, without bands, regenerated portion blue in male paratypes. Ventral ground colouration of gular, body and tail

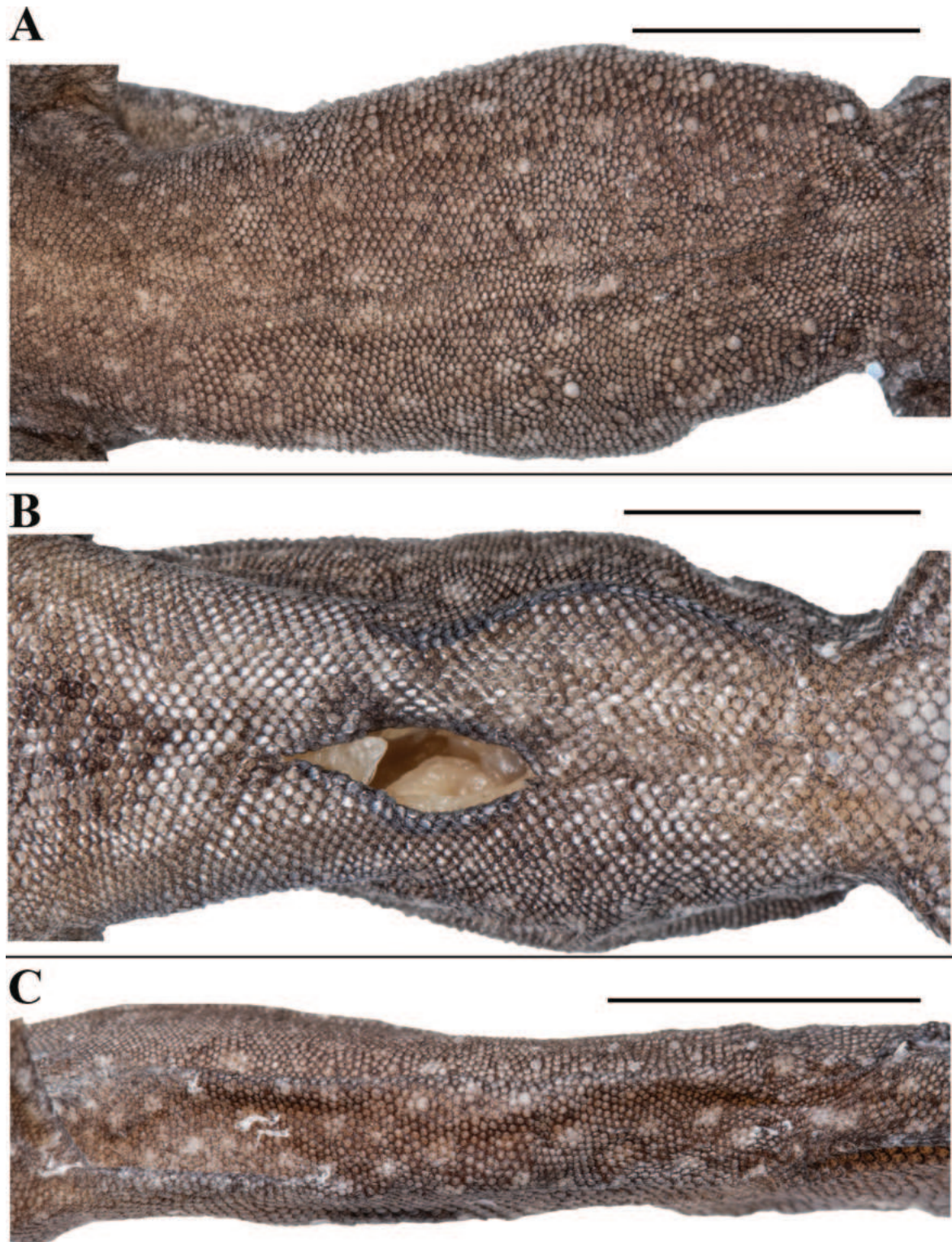


**Figure 10.** *Cnemaspis sathuragiriensis* sp. nov. (holotype, NRC-AA-8349) **A** dorsal view of midbody **B** ventral view of midbody **C** lateral view of midbody. Photos by Akshay Khandekar. Scale bars: 5 mm.

grey-white; underside of limbs with few dark markings. Juveniles brown with a cream mid-dorsal streak that continues onto tail where it is orange formed by the extension of the neck chevron; distinct black central ocellus on occiput, white ocelli on side of neck absent; forelimbs brown, hindlimbs with scattered dark and pale markings, digits banded. Original tail grey, without bands, regen-

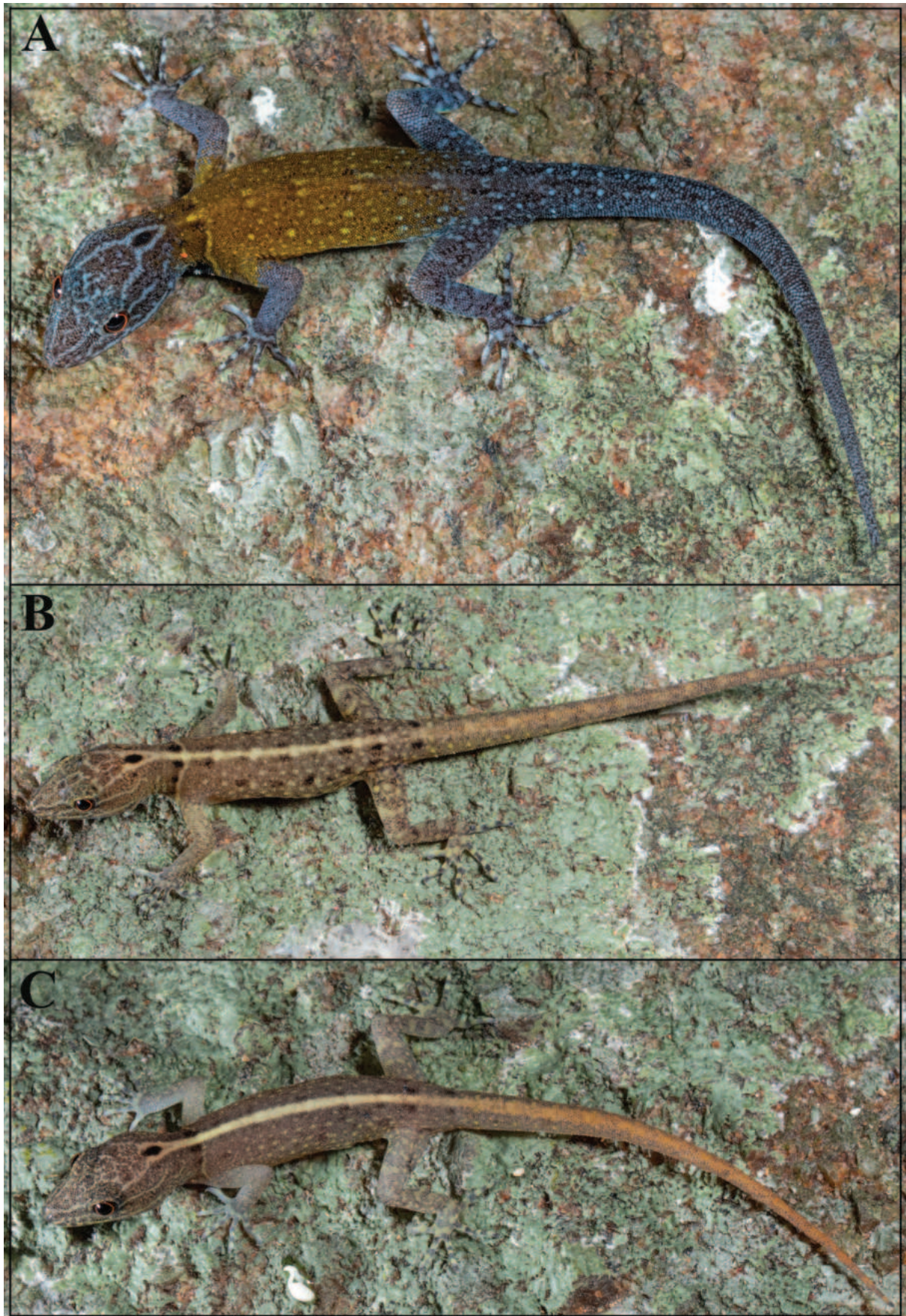


**Figure 11.** *Cnemaspis sathuragiriensis* sp. nov., in life **A** adult male (holotype, NRC-AA-8349) **B** subadult female (paratype, NRC-AA-8353), and **C** juvenile (uncollected). Photos by Akshay Khandekar.

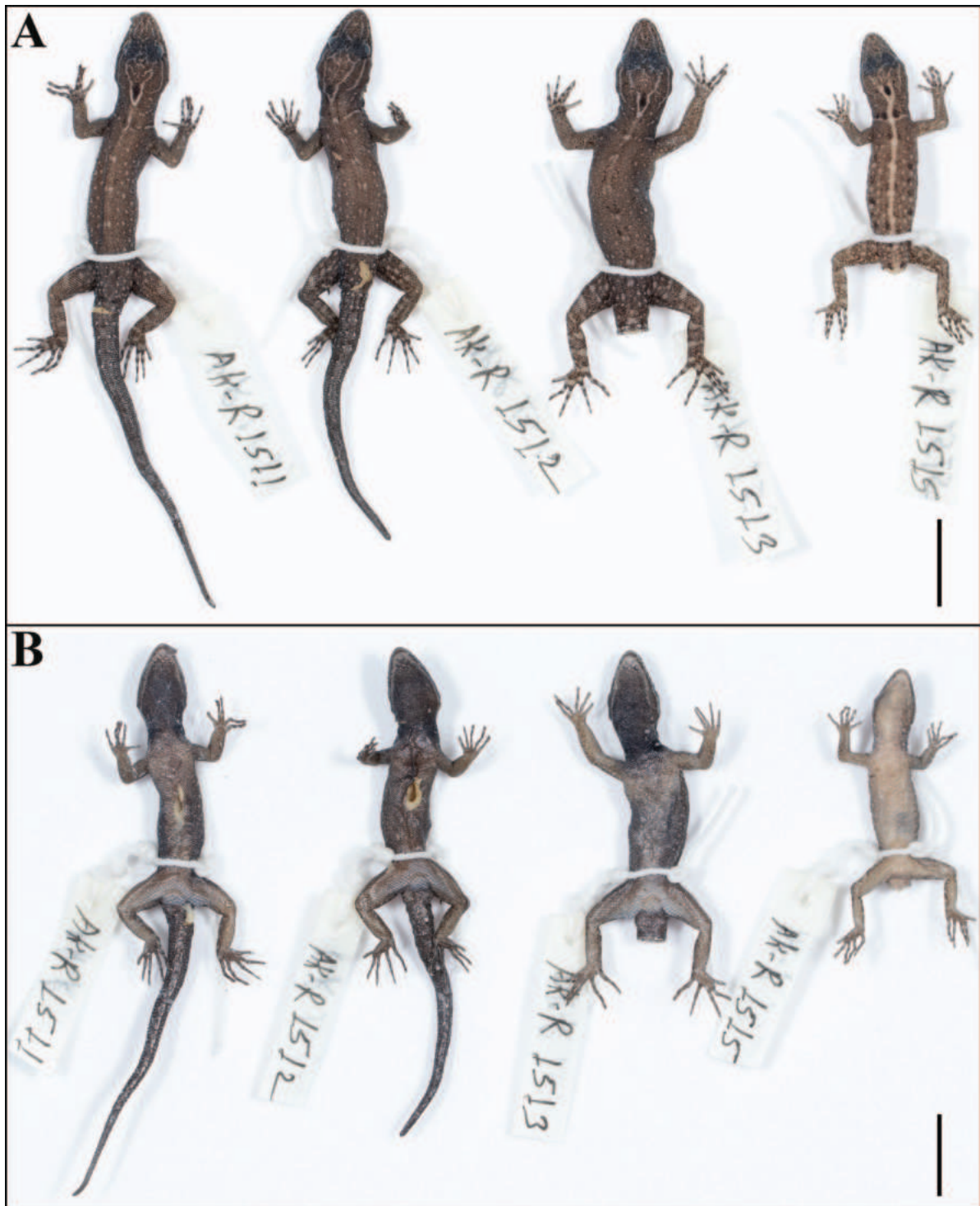


Figure 12. Paratype series of *Cnemaspis sathuragiriensis* sp. nov., from left to right, NRC-AA-8350–8353 **A** dorsal view, and **B** ventral view. Photos by Akshay Khandekar. Scale bars: 10 mm.

erated portion blue in male paratypes (Fig. 12A, B). Ventral ground colouration of gular, body and tail grey-white; underside of limbs with few dark markings.

**Etymology.** The specific epithet is a toponym for the type locality of the new species, Sathuragiri mountain in Srivilliputhur-Megamalai Tiger Reserve (SMTR), Virudhunagar District, Tamil Nadu. Suggested Common name is Sathuragiri dwarf gecko.

**Distribution and natural history.** *Cnemaspis sathuragiriensis* sp. nov. is known only from its type locality (Sathuragiri hills in Virudhunagar district, Tamil Nadu) between elevations of 250–400 m a.s.l. on eastern slopes of the Western Ghats (Fig. 1). Individuals of the new species were observed active during the daytime (0830–1100 hrs) on rocks and tree trunks < 2 m high from the base in seasonally dry tropical forest with a mix of evergreen and deciduous species (Fig. 13A). The species was observed in high abundance ( $n \geq 20/\text{hr}$ ), more commonly on boulders in shaded areas than tree trunks (Fig. 13B). Sympatric lizards at the type locality include *Cnemaspis* cf. *gracilis*, *Hemidactylus* cf. *frenatus*, *H.* cf. *leschenaultii*, *H. vanam*, *Dravidoseps srivilliputhurensis*, *Eutropis carinata*, *E. macularia*, and *Psammophilus* cf. *blanfordanus*.

### Key to the *ornata* subclade within the *beddomei* clade of South Asian *Cnemaspis*

- |   |  |                                     |
|---|--|-------------------------------------|
| 1 | White ocellus on ventrolateral sides of neck in males.....     | 2                                   |
| – | No white ocellus on ventrolateral sides of neck in males ..... | 7                                   |
| 2 | Original tail unbanded .....                                   | 3                                   |
| – | Original tail banded .....                                     | 5                                   |
| 3 | $\leq 140$ longitudinal scales from mental to cloaca .....     | 4                                   |
| – | 153–159 longitudinal scales from mental to cloaca .....        | <i>C. galaxia</i>                   |
| 4 | Entire dorsum ochre in adult males .....                       | <i>C. sathuragiriensis</i> sp. nov. |
| – | Anterior 1/2 of dorsum ochre in adult males .....              | <i>C. vangoghi</i> sp. nov.         |
| 5 | 150–165 longitudinal scales from mental to cloaca .....        | 6                                   |
| – | 143–147 longitudinal scales from mental to cloaca .....        | <i>C. nairi</i>                     |
| – | 170–172 longitudinal scales from mental to cloaca .....        | <i>C. rashidi</i>                   |
| 6 | Paravertebral tubercles absent .....                           | <i>C. sundara</i>                   |
| – | 15 or 16 paravertebral tubercles .....                         | <i>C. nigriventris</i>              |
| – | 21–23 paravertebral tubercles .....                            | <i>C. ornata</i>                    |
| 7 | Paravertebral tubercles irregular or absent .....              | <i>C. azhagu</i>                    |
| – | 18 or 19 paravertebral tubercles .....                         | <i>C. aaronbaueri</i>               |
| – | 15 or 16 paravertebral tubercles .....                         | <i>C. regalis</i>                   |

### Discussion

The *ornata* subclade now has 11 known valid species (including the two new species described in this paper) in a small geographic area spanning < 1° longitude and 1.5° latitude. At the southern extreme of the Western Ghats, the region is incredibly heterogeneous, with altitudinal variation from close to sea level to > 1,500 m a.s.l. and strong east-west gradients in total annual precipitation and seasonality. Habitats range from thorny scrub forest on the lower eastern slopes of the mountains to evergreen forest at higher elevations and on the western slopes. This subclade is distributed across the Shencottah Gap (SG), a relatively low elevation pass through the Western Ghats. All 11 members of the clade are strongly sexually dichromatic, and sexual selection may at least in part be a driver of the high diversity in this clade, as has been speculated for members of the *C. gracilis* clade (Agarwal et al. 2022). The two new species add to the five previously known endemic vertebrates from Srivilliputhur-Megamalai Tiger Reserve – the geckos *Cnemaspis galaxia*, *C. rashidi*,

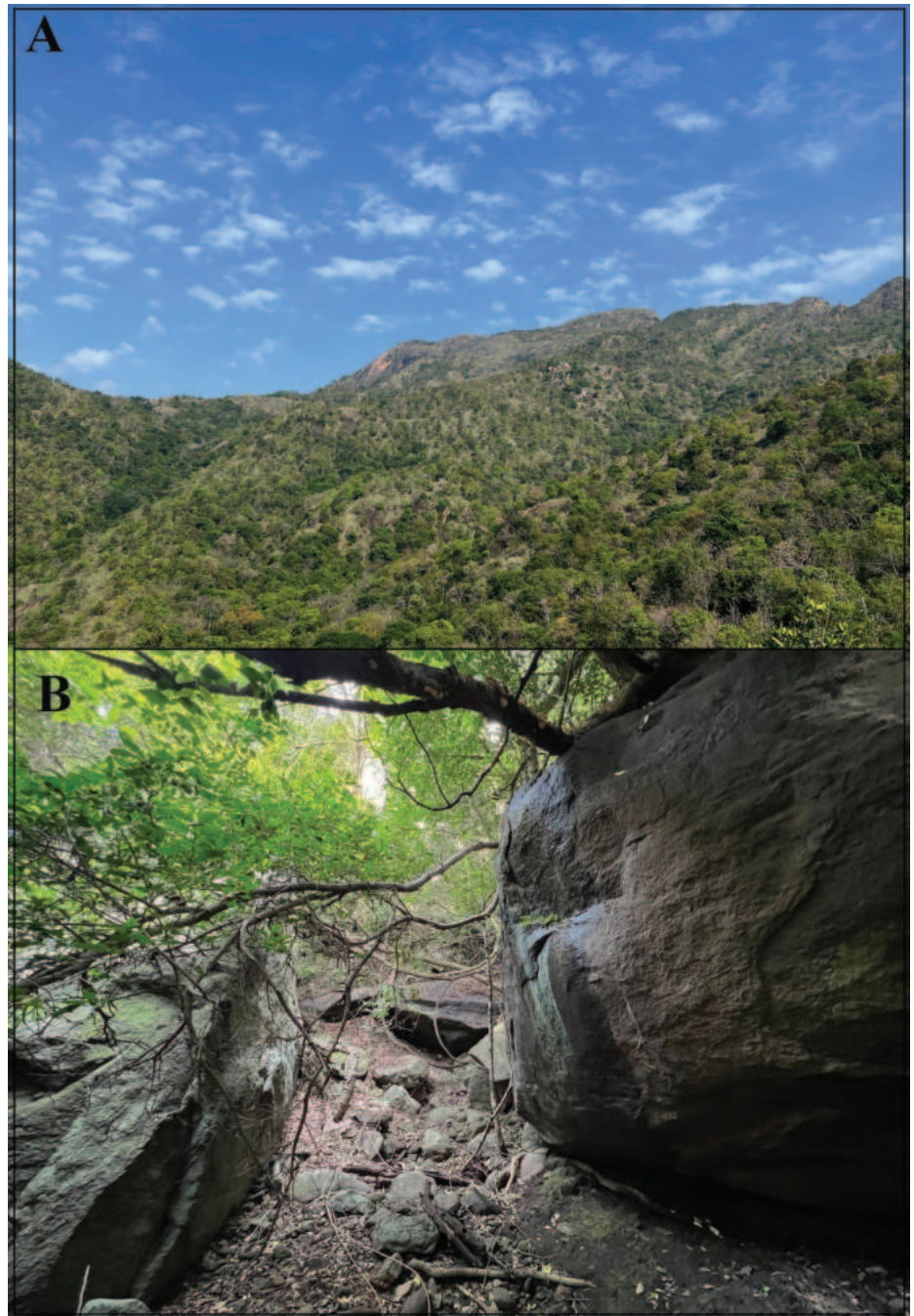


**Figure 13.** Habitat of *Cnemaspis sathuragiriensis* sp. nov. at the type locality **A** general view, and **B** microhabitat from where types were collected. Photos by Akshay Khandekar.

*Hemidactylus vanam*; the skink *Dravidoseps srivilliputhurensis* and the anuran *Nasikabatrachus bhupathyi* Janani, Vasudevan, Prendini, Dutta & Aggarwal, 2017 (Janani et al. 2017; Chaitanya et al. 2018; Pal et al. 2021; Sayyed et al. 2023a, b; Agarwal et al. 2024).

Though sampling of the *ornata* subclade likely remains incomplete as this vast mountainous landscape has a number of higher elevations we could not access in our rapid surveys, there are some geographic patterns that emerge based on available data. The only two high elevation species are the sister pair *C. ornata* + *C. rashidi* that are distributed north of the SG, together forming

the sister taxon to the low elevation species *C. nairi* + *C. nigriventris* that are distributed around the SG. These two sister pairs are deeply divergent from one another, indicative of potentially more undiscovered species in the intervening areas. The subclade containing *C. aaronbaueri*, *C. azhagu* and *C. regalis* is distributed entirely south of the SG and mainly on the eastern slopes, while the final subclade includes the low to mid elevation *C. sundara* which is distributed close to the SG, and the *galaxia* complex with three low elevation species in Srivilliputhur. Large sampling gaps exist between the distribution of *C. sundara* and *C. galaxia* as well as between *C. nairi* and *C. regalis*. Pal et al. (2021) considered the pairs *C. galaxia* + *C. regalis* and *C. nairi* + *C. nigriventris* to be separated by the Shencottah Gap – although we now know that each member of the former pair represents a cluster of closely related species, and at least *C. nigriventris* spans the Shencottah Gap. It is unclear what the northern boundary of the *ornata* subclade is, and we sampled areas north of Srivilliputhur including the Anaimalai and Palani Hills but failed to locate any species of the *ornata* subclade.

This last section is a note on violations of Principle 2 of the Code of Ethics prescribed by The Code (appendix A; Anonymous 1999) which states

“A zoologist should not publish a new name if he or she has reason to believe that another person has already recognized the same taxon and intends to establish a name for it (or that the taxon is to be named in a posthumous work). A zoologist in such a position should communicate with the other person (or their representatives) and only feel free to establish a new name if that person has failed to do so in a reasonable period (not less than a year).”

One of the authors of *Cnemaspis rashidi* accompanied us in the field in 2022 when we collected the then unnamed and distinctively coloured species, and multiple co-authors including the first author were aware that we were working in Tamil Nadu on *Cnemaspis* among other lizards (Sayyed et al. 2023a, b). While it is not unexpected that multiple workers may find the same undescribed species, what happens next is important. This is a matter of concern for the scientific community at large, and the Indian herpetological community in particular. In two other cases, even after we (AK, IA) explicitly initiated discussions with two groups whom we knew had collected the same species we were in the process of describing, the other teams went ahead with their descriptions without consultation, of *Eublepharis pictus* Mirza & Gnaneswar, 2022 and *Cyrtodactylus (Geckoella) aravindi* Narayanan et al., 2022 (Mirza and Gnaneswar 2022; Narayanan et al. 2022). While there are more than enough species to go around, it is in contravention of the Code of Ethics, besides being a waste of time, effort, and resources when teams compete against one another instead of coming together to collaborate and increase the amount of data available in a species description.

## Acknowledgements

We thank the Tamil Nadu Forest Department for permits to carry out this study (permit no. 53/2018), Teja Bhargava (former DFO, Jawadhu) for his help and co-ordination throughout fieldwork, and the then Field Director SMTR Deepak

Bilgi. Fieldwork assistance was provided by Swapnil Pawar, Vaibhav Patil, Satpal Gangalmale, Vivek Waghe, and Satheesh Kumar. We are thankful to Tarun Karmakar (NCBS field station and museum facility, Bengaluru for help with specimen registration, Uma Ramakrishnan for lab support at NCBS, Navendu Page for help with forest classification, R. Chaitanya for edits in the discussion, and Azhar Hotel Devaki for sustaining us on a high protein diet through our time at Srivilliputhur.

## Additional information

### Conflict of interest

The authors have declared that no competing interests exist.

### Ethical statement

The research project was cleared by an in-house animal ethics committee and was carried out with permits from the Tamil Nadu Forest Department.

### Funding

We thank the Tamil Nadu Forest Department for permits to carry out this study (permit no. 53/2018).

### Author contributions

Conceptualization: AK, TT, IA. Data curation: AK, IA. Formal analysis: AK, IA. Funding acquisition: TT. Investigation: IA, AK. Resources: TT. Software: IA. Writing - original draft: AK, IA. Writing - review and editing: AK, TT, IA.

### Author ORCIDs

Akshay Khandekar  <https://orcid.org/0000-0002-7956-089X>

Tejas Thackeray  <https://orcid.org/0000-0002-9981-8763>

Ishan Agarwal  <https://orcid.org/0000-0001-9734-5379>

### Data availability

All of the data that support the findings of this study are available in the main text.

## References

- Agarwal I, Thackeray T, Pal S, Khandekar A (2020) Granite boulders act as deep-time climate refugia: a Miocene divergent clade of rupicolous *Cnemaspis* Strauch, 1887 (Squamata: Gekkonidae) from the Mysore Plateau, India, with descriptions of three new species. *Journal of Zoological Systematics and Evolutionary Research* 58(4): 1234–1261. <https://doi.org/10.1111/jzs.12391>
- Agarwal I, Thackeray T, Khandekar A (2022) A multitude of spots! Five new microendemic species of the *Cnemaspis gracilis* group (Squamata: Gekkonidae) from massifs in the Shevaroy landscape, Tamil Nadu, India. *Vertebrate Zoology* 72: 1137–1186. <https://doi.org/10.3897/vz.72.e94799>
- Agarwal I, Thackeray T, Khandekar A (2024) A non-adaptive radiation of viviparous skinks from the seasonal tropics of India: systematics of *Subdoluseps* (Squamata: Scincidae), with description of a new genus and five cryptic new species. *Vertebrate Zoology* 74: 23–83. <https://doi.org/10.3897/vz.74.e110674>

- Anonymous [International Commission of Zoological Nomenclature] (1999) International code of zoological nomenclature. 4<sup>th</sup> edn. London (International Trust for zoological Nomenclature): i–xxix + 1–306.
- Beddome RH (1870) Descriptions of some new lizards from the Madras Presidency. Madras Monthly Journal of Medical Science 1: 30–35.
- Chaitanya R, Lajmi A, Giri VB (2018) A new cryptic, rupicolous species of *Hemidactylus* Oken, 1817 (Squamata: Gekkonidae) from Meghamalai, Tamil Nadu, India. Zootaxa 4374(1): 49–70. <https://doi.org/10.11646/zootaxa.4374.1.3>
- Cyriac VP, Johny A, Umesh PK, Palot MJ (2018) Description of two new species of *Cnemaspis* Strauch, 1887 (Squamata: Gekkonidae) from the Western Ghats of Kerala, India. Zootaxa 4459(1): 085–100. <https://doi.org/10.11646/zootaxa.4459.1.3>
- Janani SJ, Vasudevan K, Prendini E, Dutta SK, Aggarwal RK (2017) A new species of the genus *Nasikabatrachus* (Anura, Nasikabatrachidae) from the eastern slopes of the Western Ghats, India. Alytes 34(1–4): 1–19.
- Khandekar A, Gaitonde N, Agarwal I (2019) Two new *Cnemaspis* Strauch, 1887 (Squamata: Gekkonidae) from the Shevaroy massif, Tamil Nadu, India, with a preliminary ND2 phylogeny of Indian *Cnemaspis*. Zootaxa 4609(1): 68–100. <https://doi.org/10.11646/zootaxa.4609.1.3>
- Khandekar A, Thackeray T, Agarwal I (2022) Three more novel species of South Asian *Cnemaspis* Strauch, 1887 (Squamata, Gekkonidae) from Kalakad Mundanthurai Tiger Reserve, Tamil Nadu, India. Vertebrate Zoology 72: 385–422. <https://doi.org/10.3897/vz.72.e82343>
- Khandekar A, Gaikwad SM, Thackeray T, Gangalmale S, Agarwal I (2024) A preliminary taxonomic revision of the *girii* clade of South Asian *Cnemaspis* Strauch, 1887 (Squamata: Gekkonidae) with the description of four new species from southern Maharashtra, India. Zootaxa. [in press]
- Lanfear R, Calcott B, Ho SY, Guindon S (2012) PartitionFinder: Combined selection of partitioning schemes and substitution models for phylogenetic analyses. Molecular Biology and Evolution 29(6): 1695–1701. <https://doi.org/10.1093/molbev/mss020>
- Lanfear R, Frandsen PB, Wright AM, Senfeld T, Calcott B (2016) PartitionFinder 2: New methods for selecting partitioned models of evolution for molecular and morphological phylogenetic analyses. Molecular Biology and Evolution 34(3): 772–773. <https://doi.org/10.1093/molbev/msw260>
- Macey JR, Larson A, Ananjeva NB, Fang Z, Papenfuss TJ (1997) Two novel gene orders and the role of light-strand replication in rearrangement of the vertebrate mitochondrial genome. Molecular Biology and Evolution 14(1): 91–104. <https://doi.org/10.1093/oxfordjournals.molbev.a025706>
- Manamendra-Arachchi K, Batuwita S, Pethiyagoda R (2007) A taxonomic revision of the Sri Lankan day-geckos (Reptilia: Gekkonidae: *Cnemaspis*), with description of new species from Sri Lanka and southern India. Zeylanica 7(1): 9–122.
- Mirza Z, Gnaneswar C (2022) Description of a new species of leopard geckos, *Eublepharis* Gray, 1827 from Eastern Ghats, India with notes on *Eublepharis hardwickii* Gray, 1827. Evolutionary Systematics 6(1): 77–88. <https://doi.org/10.3897/evolsyst.6.83290>
- Narayanan S, Das S, Balan A, Tom R, Divakar N, Kp R, Deepak V (2022) A new species of *Cyrtodactylus* (Reptilia: Gekkonidae) from the southern Western Ghats of India. Vertebrate Zoology 72: 729–743. <https://doi.org/10.3897/vz.72.e89660>
- Pal S, Mirza ZA, Dsouza P, Shanker K (2021) Diversifying on the Ark: Multiple new endemic lineages of dwarf geckos from the Western Ghats provide insights into the sys-

- tematics and biogeography of South Asian *Cnemaspis* (Reptilia: Squamata). *Zoological Research* 42(6): 675–691. <https://doi.org/10.24272/j.issn.2095-8137.2021.074>
- Palumbi SR, Martin A, Romano S, Owen MacMillan W, Stice L, Grabowski G (1991) *The simple fool's guide to PCR*. Honolulu: Department of Zoology and Kewalo Marine Laboratory.
- Ronquist F, Huelsenbeck JP (2003) MrBayes 3: Bayesian phylogenetic inference under mixed models. *Bioinformatics* 19(12): 1572–1574. <https://doi.org/10.1093/bioinformatics/btg180>
- Sayyed A, Grismer LL, Campbell PD, Dileepkumar R (2019) Description of a cryptic new species of *Cnemaspis* Strauch, 1887 (Squamata: Gekkonidae) from the Western Ghats of Kerala State of India. *Zootaxa* 4656(3): 501–514. <https://doi.org/10.11646/zootaxa.4656.3.7>
- Sayyed A, Kirubankaran S, Khot R, Thanigaivel A, Satheeshkumar M, Sayyed A, Sayyed M, Purkayastha J, Deshpande S, Sulakhe S (2023a) A new species of the genus *Cnemaspis* Strauch, 1887 (Squamata: Gekkonidae) from the higher elevations of Tamil Nadu, India. *Asian Journal of Conservation Biology* 12(2): 179–188. <https://doi.org/10.53562/ajcb.83427>
- Sayyed A, Kirubankaran S, Khot R, Harsan S, Adhikari O, Sayyed A, Sayyed M, Fazil A, Jerith A, Deshpande S, Purkayastha J, Sulakhe S (2023b) Two new species of *Cnemaspis* Strauch, 1887 (Squamata: Gekkonidae) from southern India. *Zootaxa* 5374(3): 301–332. <https://doi.org/10.11646/zootaxa.5374.3.1>
- Stamatakis A (2014) Raxml version 8: A tool for phylogenetic analysis and post-analysis of large phylogenies. *Bioinformatics* 30(9): 1312–1313. <https://doi.org/10.1093/bioinformatics/btu033>
- Tamura K, Peterson D, Peterson N, Stecher G, Nei M, Kumar S (2011) MEGA5: Molecular evolutionary genetics analysis using maximum likelihood, evolutionary distance, and maximum parsimony methods. *Molecular Biology and Evolution* 28(10): 2731–2739. <https://doi.org/10.1093/molbev/msr121>
- Theobald W (1876) *Descriptive catalogue of the reptiles of British India*. Thacker, Spink & Co., Calcutta, 238 pp. <https://doi.org/10.5962/bhl.title.5483>
- Thompson JD, Higgins DG, Gibson TJ (1994) CLUSTAL W: Improving the sensitivity of progressive multiple sequence alignment through sequence weighting, position-specific gap penalties and weight matrix choice. *Nucleic Acids Research* 22(22): 4673–4680. <https://doi.org/10.1093/nar/22.22.4673>

## Appendix 1

### Material examined.

Institutional and field series abbreviations are as follows: National Centre for Biological Sciences, Bengaluru (NCBS-AU/ NCBS-BH/NRC-AA); Bombay Natural History Society, Mumbai (BNHS); Zoological Survey of India, Western Ghats regional station Kozhikode (ZSI/WGRC), and Akshay Khandekar field series (AK-R).

*Cnemaspis azhagu*: holotype, NRC-AA-1170 (adult male); paratypes, NRC-AA-1171, NRC-AA-1172, NRC-AA-1174, BNHS 2818, BNHS 2819, BNHS 2820 (adult males), BNHS 2821, (adult female), NRC-AA-1173 (subadult female),

- from Thirukurungudi forest range, Kalakad Mundanthurai Tiger Reserve, Tirunelveli District, Tamil Nadu state, India.
- Cnemaspis beddomei*: AK-R 578, AK-R 579, AK-R 581–583 (adult males), AK-R 580 (adult female), from Kakachi, Kalakkad-Mundanthurai Tiger Reserve, Tirunelveli District, India.
- Cnemaspis galaxia*: holotype, BNHS 2626 (adult male), from low elevation riparian forest, Srivilliputhur, Tamil Nadu; AK-R 1422, AK-R 1323, AK-R 1324, AK-R 1428, AK-R 1470, AK-R 1471, AK-R 1473 (all adults) from near Shenbaga Thoppu, Srivilliputhur, Virudhunagar District, Tamil Nadu, India.
- Cnemaspis nairi*: AK-R 894, AK-R 895 (adults), from Thenmala, Courtallam, Tenkasi District, Tamil Nadu, India.
- Cnemaspis nigriventris*: holotype, BNHS 2619 (adult male), from Achankovil Reserve Forest, Kollam District, Kerala; AK-R 1265 and AK-R 1275 (adults), from Mohan's resort, Tenkasi District, Tamil Nadu, India.
- Cnemaspis nimbus*: holotype, BNHS 2614 (adult male), from Mathikettan Shola National Park, Cardamom Hills, Idukki District, Kerala, India.
- Cnemaspis rashidi*: AK-R 1439 and AK-R 1440 (adults), from high elevation of Shenbaga Thoppu; AK-R 1692 and AK-R 1693, from Vellimalai, Srivilliputhur-Megamalai Tiger Reserve, Virudhunagar and Theni Districts, Tamil Nadu, India.
- Cnemaspis regalis*: holotype, BNHS 2617 (adult male); AK-R 453, AK-R 454, AK-R 453 (adults), from Mundanthurai, Kalakkad-Mundanthurai Tiger Reserve, Tirunelveli District, Tamil Nadu, India.
- Cnemaspis rubraoculus*: holotype, BNHS 2612 (adult male) from Upper Manalar, Periyar Tiger Reserve, Megamalai; AK-R 1728, AK-R 1729 (adults), from Vellimalai, AK-R 1777 (adults), from Megamalai, Srivilliputhur-Megamalai Tiger Reserve, Theni District, Tamil Nadu, India.
- Cnemaspis smaug*: holotype, BNHS 2615 (adult male) from Mathikettan Shola National Park, Cardamom Hills, Idukki District, Kerala, India.
- Cnemaspis sundara*: AK-R 1254 and AK-R 1266 (adults), from Mohan's resort, Tenkasi District, Tamil Nadu, India.
- Cnemaspis wallaceii*: holotype, BNHS 2613 (adult male), from Andiparai Shola, Anamalai Hills, Coimbatore District, Tamil Nadu, India.

# Revalidation of the jumping spider genus *Cheliceroides* Żabka, 1985 based on molecular and morphological data (Araneae, Salticidae)

Long Lin<sup>1,2</sup>, Zhiyong Yang<sup>1,2</sup>, Junxia Zhang<sup>1,2</sup>

<sup>1</sup> Key Laboratory of Zoological Systematics and Application, College of Life Sciences, Hebei University, Baoding, Hebei 071002, China

<sup>2</sup> Hebei Basic Science Center for Biotic Interaction, Hebei University, Baoding, Hebei 071002, China

Corresponding author: Junxia Zhan ([jxzhang1976@163.com](mailto:jxzhang1976@163.com))

## Abstract

The monotypic genus *Cheliceroides* Żabka, 1985 is revalidated based on both molecular sequence data (ultra-conserved elements and protein coding genes of mitochondrial genomes) and morphological evidence. Our molecular phylogenetic analyses show that *Cheliceroides* is not closely related to *Colopsus* Simon, 1902, not even in the same tribe, and a comparative morphological study also demonstrates significant differences in the genital structures (i.e. in the shape of embolus, and with or without pocket on epigynum) of the two genera. Therefore, we remove *Cheliceroides* from the synonymy of *Colopsus*, and its generic status is revalidated.

**Key words:** *Colopsus*, mitogenome, morphology, phylogeny, ultra-conserved element



Academic editor: Ingi Agnarsson

Received: 28 December 2023

Accepted: 5 March 2024

Published: 27 March 2024

ZooBank: <https://zoobank.org/CC8D78B1-82F5-424B-9801-9EDC10B79748>

Citation: Lin L, Yang Z, Zhang J (2024) Revalidation of the jumping spider genus *Cheliceroides* Żabka, 1985 based on molecular and morphological data (Araneae, Salticidae). ZooKeys 1196: 243–253. <https://doi.org/10.3897/zookeys.1196.117921>

Copyright: © Long Lin et al.

This is an open access article distributed under terms of the Creative Commons Attribution License ([Attribution 4.0 International – CC BY 4.0](https://creativecommons.org/licenses/by/4.0/)).

## Introduction

The jumping spider genus *Cheliceroides* Żabka, 1985 originally contained only the type species, *Cheliceroides longipalpis* Żabka, 1985, which has been commonly collected from Vietnam and southern China (World Spider Catalog 2024). A second species, *Cheliceroides brevipalpis* Roy, Saha & Raychaudhuri, 2016, was later reported from India (Roy et al. 2016), but it has been transferred to the genus *Bathippus* Thorell, 1892 (tribe Euophryini Simon, 1901; see Logunov 2021). Based on the results of a molecular phylogenetic study using Sanger-sequenced data (Maddison et al. 2014), Maddison (2015) included *Cheliceroides* in the tribe Hasariini Simon, 1903 in the phylogenetic classification of jumping spiders. Later, Logunov (2021) synonymized *Cheliceroides* with *Colopsus* Simon, 1902 based on similarities of morphological characters, such as the modified and elongate male chelicerae and male palpal characteristics, and transferred its type species to *Colopsus*, as *Colopsus longipalpis* (Żabka, 1985). *Colopsus* has been placed in the tribe Plexippini Simon, 1901 based on other molecular phylogenetic results (Kanesharatnam and Benjamin 2021). However, in a recent comparative mitogenomic study of jumping spiders, *Colopsus longipalpis* was not clustered with the other members of the tribe Plexippini on the phylogeny (Zhang et al. 2023a), which challenged Logunov's taxonomic treatment of *Cheliceroides*.

Here we thoroughly investigate the phylogenetic placement of *Cheliceroides* in relation to *Colopsus* and other putatively related genera using both ultra-conserved element (UCE) and mitochondrial genome datasets. Comparative morphological study on the type species of both *Cheliceroides* and *Colopsus* is carried out to further clarify the taxonomic status of *Cheliceroides*. The implication of phylogenomic results on the classification of salticids is also discussed.

## Materials and methods

All specimens are preserved in 85–100% ethanol and stored at  $-20^{\circ}\text{C}$ . The photographs of genitalia were taken under a Leica M205A stereomicroscope. Photographs of palp, epigyne, and spiders were stacked using Helicon Focus v. 7 and retouched in the Adobe Photoshop CC 2022. Specimens were measured by the measuring tool of Leica LAS v. 4.3. Female vulvae were cleared with Pancreatin (BBI Life Sciences) or macerated in clove oil. All specimens studied are deposited in the Museum of Hebei University, Baoding, China (**MHBU**). Abbreviations used in the study: **CD**, copulatory duct; **CO**, copulatory opening; **E**, embolus; **FD**, fertilization duct; **P**, pocket; **S**, spermatheca; **SD**, sperm duct; **RTA**, retrolateral tibial apophysis.

Molecular data were obtained for ultra-conserved elements (UCEs) and mitogenomes to compose the UCE and mitogenomic datasets, each with 46 species (see Table 1 for detailed information). Genomic DNA extraction was performed using the QIAGEN dNeasy Blood & Tissue Kit, and the RNA was removed with 4  $\mu\text{L}$  of rNase A (Solarbio) followed by a 2-minute incubation at room temperature. The library preparation was conducted using the NEXTFLEX Rapid DNA-Seq Kit 2.0 and the NEXTFLEX Unique Dual Index Barcodes (Set C) (Bioo Scientific) following the protocols by Zhang et al. (2023b). UCE enrichment followed the myBaits protocol 5.01 (Daicel Arbor Biosciences) using a modified version of the RTA probes, the “RTA\_v3” probe set (42,213 probes targeting 3818 UCE loci) that was proposed by Zhang et al. (2023b). The enriched UCE libraries were then sent to Novogene Co. Ltd for sequencing using the Illumina NovaSeq platform with 150-bp paired-end reads. The UCE loci were extracted from the empirically enriched and sequenced raw reads following the protocols applied in Zhang et al. (2023b) with the PHYLUCE (Faircloth 2016) workflow. For ten species with whole genome sequencing data, the genomes were first assembled using the Phylogenomics from Low-coverage Whole-genome Sequencing (PLWS) pipeline (Zhang et al. 2019), and then the UCEs were harvested using the “RTA\_v3” probes and the PHYLUCE workflow (see Zhang et al. 2023b for details).

The UCEs extracted from genomes and target enrichment data were combined and organized by locus, and then aligned using Mafft v. 7.313 (Katoh and Standley 2013) with the L-INS-I strategy. Poorly aligned regions were initially trimmed by the heuristic method “-automated1” in Trimal v. 1.4.1 (Capella-Gutiérrez et al. 2009). We then applied Spruceup v. 2020.2.19 (Borowiec 2019) to convert the remaining obviously misaligned fragments to gaps in each alignment (cutoff as 0.75). The gappy regions in each alignment were later masked using Seqtools (PASTA; Mirarab et al. 2014) with “masksites = 23”. Loci with trimmed alignment length less than 200 bp or less than 50% of taxon occupancy were removed, which resulted in 2593 loci in the final dataset for phylogenetic inference. All remaining UCE loci were concatenated by FASconCAT v. 1.0 (Kück and Meusemann 2010).

**Table 1.** Information of the representative taxa used in the phylogenetic analyses. Accession numbers with an asterisk (\*) indicate newly obtained sequences in this study.

Subfamily	Tribe	DNA Voucher Code	Species	UCE SRA accession number	Mitogenomes		
					Number of PCGs	GenBank accession number	SRA accession number
Salticinae	Aelurillini	JXZ714	<i>Langona</i> sp.	*SRR27541575	13	*OR965550	*SRR27726447
Salticinae	Aelurillini	JXZ730	<i>Phlegra</i> aff. <i>amitaii</i>	*SRR27541574	13	*OR965551	*SRR27726446
Salticinae	Agoriini	JXZ424	<i>Synagelides agoriformis</i>	SRR22908234	13	*OR965543	*SRR27726435
Salticinae	Baviini	JXZ585	<i>Bavia capistrata</i>	*SRR27541623	12	*OR965559	*SRR27726427
Salticinae	Baviini	JXZ695	<i>Maripanthus menghaiensis</i>	*SRR27541622	13	*OR965549	*SRR27726426
Salticinae	Chrysillini	JXZ741	<i>Chrysilla acerosa</i>	*SRR27541611	13	*OR965534	*SRR27726425
Salticinae	Chrysillini	JXZ574	<i>Epicilla</i> sp.	*SRR27541600	13	*OR965531	*SRR27726424
Salticinae	Chrysillini	JXZ745	<i>Menemerus bivittatus</i>	*SRR27541596	12	*OR965557	*SRR27541596
Salticinae	Chrysillini	JXZ740	<i>Phintella cavaleriei</i>	*SRR27541595			
Salticinae	Chrysillini		<i>Phintella cavaleriei</i>		13	NC060328	
Salticinae	Chrysillini	JXZ738	<i>Siler semiglaucus</i>	*SRR27541594	13	*OR965552	*SRR27726423
Salticinae	Dendryphantini	JXZ425	<i>Marpissa milleri</i>	SRR22908225	13	*OR965544	*SRR27726422
Salticinae	Dendryphantini	JXZ419	<i>Mendoza nobilis</i>	SRR22908224	13	*OR965541	*SRR27726421
Salticinae	Dendryphantini	JXZ582	<i>Rhene</i> sp.	*SRR27541593	13	*OR965545	*SRR27541593
Salticinae	Euophryini	JXZ358	<i>Agobardus cordiformis</i>	*SRR27541592	13	*OR965558	*SRR27541592
Salticinae	Euophryini	JXZ051	<i>Cobanus extensus</i>	*SRR27541591	13	*OR965529	*SRR27726445
Salticinae	Euophryini	JXZ418	<i>Corythalia opima</i>	SRR22908229	13	OQ281589	
Salticinae	Euophryini	JXZ417	<i>Parabathippus shelfordi</i>	SRR22908237	13	OQ429315	
Salticinae	Hasariini	JXZ743	<i>Bristowia heterospinosa</i>	*SRR27541621			
Salticinae	Hasariini		<i>Bristowia heterospinosa</i>		13	*PP083709	DRR297628
Salticinae	Hasariini	JXZ584	<i>Cheliceroides longipalpis</i>	*SRR27541620	13	*OR965546	*SRR27726444
Salticinae	Hasariini		<i>Chinattus ogatai</i>		13	*PP083710	DRR297852
Salticinae	Hasariini	JXZ935	<i>Chinattus tibialis</i>	*SRR27541619			
Salticinae	Hasariini	JXZ587	<i>Gedea pinguis</i>	*SRR27541618	13	*OR965547	*SRR27726443
Salticinae	Hasariini	JXZ693	<i>Hasarina</i> sp.	*SRR27541617	13	*OR965548	*SRR27726442
Salticinae	Hasariini	JXZ823	<i>Hasarina</i> sp.	*SRR27541616	10	*OR987883	*SRR27541616
Salticinae	Leptorchestini	JXZ940	<i>Yllenus</i> aff. <i>Arenarius</i>	*SRR27541615	13	*OR965556	*SRR27541615
Salticinae	Myrmarachnini	JXZ414	<i>Myrmarachne formicaria</i>	SRR22908238	13	*OR965539	*SRR27726441
Salticinae	Myrmarachnini	JXZ775	<i>Myrmarachne gisti</i>	*SRR27541614	13	*OR965555	*SRR27726440
Salticinae	Nannenini	JXZ578	<i>Langerra</i> cf. <i>oculina</i>	*SRR27541613	13	*OR965560	*SRR27541613
Salticinae	Plexippini	JXZ774	<i>Bianor maculatus</i>	*SRR27541612			
Salticinae	Plexippini	NZ19_9864	<i>Bianor maculatus</i>		13	*OR965536	SRR27728369
Salticinae	Plexippini	JXZ568	<i>Burmattus pococki</i>	*SRR27541610			
Salticinae	Plexippini		<i>Burmattus pococki</i>		13	*PP083711	DRR297354
Salticinae	Plexippini	JXZ795	cf. <i>Colopsus</i> sp.	*SRR27541609	7	*OR987884	*SRR27541609
Salticinae	Plexippini	JXZ412	<i>Evarcha albaria</i>	SRR22908228	13	*OR965538	*SRR27726439
Salticinae	Plexippini	JXZ807	<i>Harmochirus brachiatus</i>	*SRR27541608			
Salticinae	Plexippini		<i>Harmochirus insulanus</i>		13	*PP083708	DRR297138
Salticinae	Plexippini	JXZ766	<i>Pancorius crassipes</i>	*SRR27541607			
Salticinae	Plexippini		<i>Pancorius crassipes</i>		11	*PP060008	DRR297706
Salticinae	Plexippini		<i>Plexippoides doenitzi</i>		13	*PP083712	DRR297761
Salticinae	Plexippini	JXZ423	<i>Plexippoides regius</i>	SRR22908236			
Salticinae	Plexippini	JXZ436	<i>Plexippus setipes</i>	*SRR27541606	13	*OR965530	*SRR27726438

Subfamily	Tribe	DNA Voucher Code	Species	UCE SRA accession number	Mitogenomes		
					Number of PCGs	GenBank accession number	SRA accession number
Salticinae	Plexippini	JXZ742	<i>Ptocasius strupifer</i>	*SRR27541605	13	*OR965553	*SRR27726437
Salticinae	Plexippini	JXZ748	<i>Sibianor pullus</i>	*SRR27541604	13	*OR965554	*SRR27726436
Salticinae	Plexippini	JXZ734	<i>Yaginumaella cf. medvedevi</i>	*SRR27541603	13	*OR965533	*SRR27726434
Salticinae	Salticini	JXZ811	<i>Carrhotus sannio</i>	*SRR27541602			
Salticinae	Salticini		<i>Carrhotus xanthogramma</i>		13	NC027492	
Salticinae	Salticini	JXZ950	<i>Salticus latidentatus</i>	*SRR27541601			
Salticinae	Salticini	YHD043	<i>Salticus potanini</i>		13	*OR965537	*SRR27726433
Salticinae	Sitticini	JXZ416	<i>Attulus fasciger</i>	SRR22908231	13	*OR965540	*SRR27726432
Salticinae	Sitticini	JXZ421	<i>Attulus sinensis</i>	SRR22908230	13	*OR965542	*SRR27726431
Salticinae	Vicirini	JXZ762	<i>Irura cf. mandarina</i>	*SRR27541599	13	*OR965535	*SRR27726430
Salticinae	Vicirini	JXZ576	<i>Nungia epigynalis</i>	*SRR27541598	13	*OR965532	*SRR27726429
Spartaeinae	Spartaeini	JXZ415	<i>Portia heteroidea</i>		13	*OR655300	*SRR27726428
Spartaeinae	Spartaeini	JXZ573	<i>Portia wui</i>	*SRR27541597			
Spartaeinae	Spartaeini		<i>Spartaeus bani</i>		11	*PP083707	DRR297090
Spartaeinae	Spartaeini	JXZ588	<i>Spartaeus jaegeri</i>	SRR22796423			

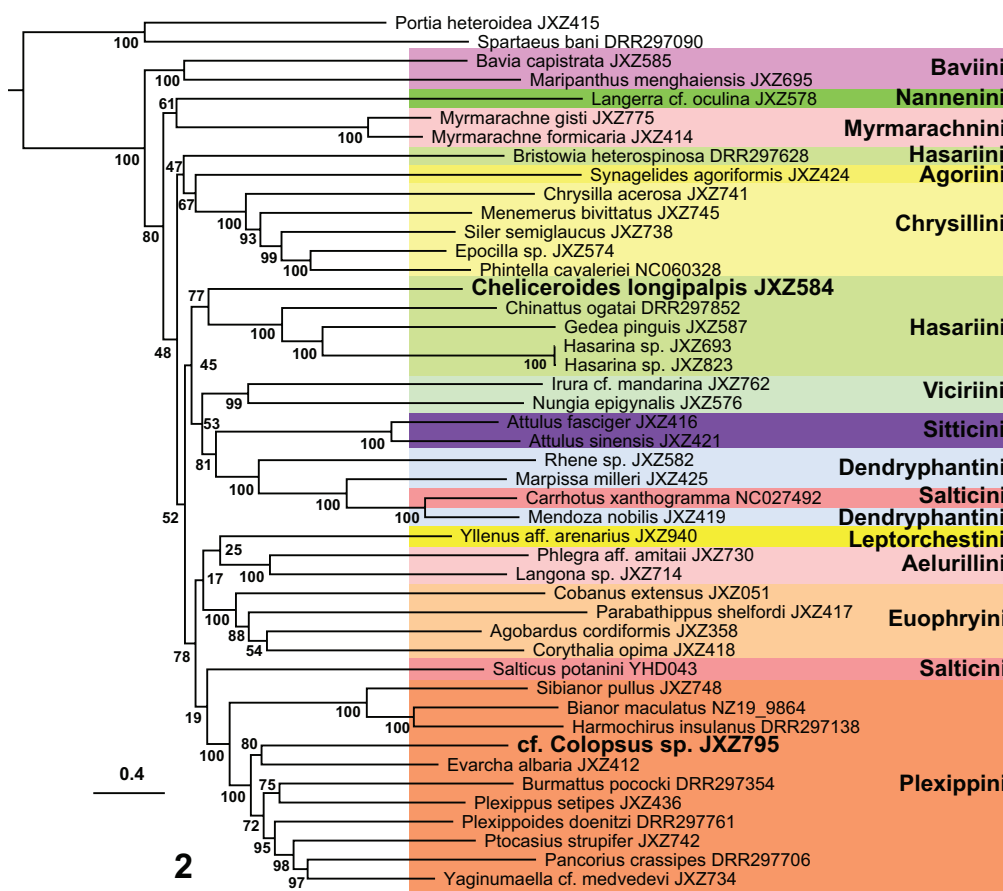
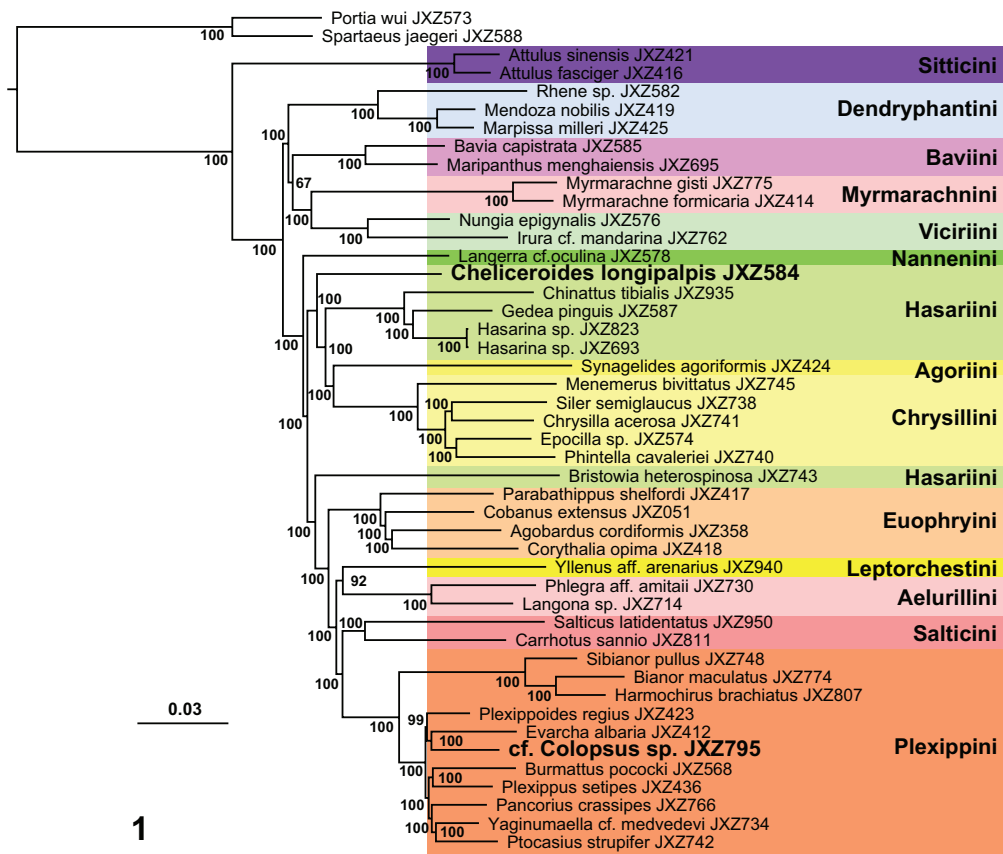
The maximum-likelihood (ML) analyses were conducted in IQ-TREE v. 2.0.6 (Minh et al. 2020) with the best-fitting model and optimized partition scheme inferred using the option “-m MF+MERGE”. Ten independent ML tree searches (five with random starting trees and five with parsimonious starting trees) were run with the optimized model and partition scheme, and 5,000 replicates of ultrafast bootstrap analysis was conducted to assess the node supports.

Mitochondrial genomes were assembled and annotated using MitoZ v. 3.4 (Meng et al. 2019) and MITOchondrial genome annotation Server (MITOS; Bernt et al. 2013) from the raw reads of UCEs, WGS (whole genome sequencing), or transcriptomes following the protocols described by Ding et al. (2023) and Zhang et al. (2023b). In addition, two mitochondrial genomes were downloaded from the GenBank. Thirteen mitochondrial protein-coding genes (PCGs) were extracted for phylogenetic analysis. Each of the 13 PCGs was aligned using Mafft v. 7.505 (Kato and Standley 2013) with the L-INS-i strategy, and then the gaps and misaligned sites were trimmed in Trimal v. 1.2rev57 (Capella-Gutiérrez et al. 2009) with the “automated1” mode. The trimmed alignments were concatenated in PhyloSuite v. 1.2.3 (Zhang et al. 2020), and PartitionFinder2 was used to select the best partition and model. ML analyses were performed in IQ-TREE v. 2.2.0 (Minh et al. 2020) using the optimized model and partition scheme, and an ultrafast bootstrap analysis with 1,000 replicates was conducted to assess the node support.

## Results

### Molecular phylogeny

The newly sequenced raw reads and assembled mitogenomes were submitted to the GenBank with accession numbers provided in Table 1. The phylogenies resulted from the UCE and 13-mitochondrial-PCG datasets are presented in Figs 1, 2. Both results show that *Cheliceroides longipalpis* (JXZ584) is distantly related to Plexippini, including a potential species of *Colopsus* (JXZ795).



Figures 1, 2. Phylogenetic results **1** maximum-likelihood tree from the UCE dataset **2** maximum-likelihood tree from the 13-mitochondrial-PCG dataset; numbers along the branches indicate bootstrap support.

In the UCE phylogeny, *Cheliceroides longipalpis* is recovered as sister to the clade with Hasariini (excluding *Bristowia* Reimoser, 1934), Agoriini, and Chry-sillini (Fig. 1), whereas in the mitogenomic phylogeny it is clustered as sister to other Hasariini (excluding *Bristowia*; Fig. 2). Therefore, the molecular phylogenetic results support removing *Cheliceroides* from the synonymy of *Colopsus*. Other implications of the molecular phylogenetic results are addressed in the discussion.

## Taxonomy

### *Cheliceroides* Żabka, 1985, stat. rev.

*Cheliceroides* Żabka, 1985: 209.

**Type species.** *Cheliceroides longipalpis* Żabka, 1985, by monotypy.

### *Cheliceroides longipalpis* Żabka, 1985

Figs 3–18

*Cheliceroides longipalpis* Żabka, 1985: 210, figs 76–80; Peng and Xie 1993: 81, figs 5–10; Peng 2020: 62, fig. 25a–h.

*Colopsus longipalpis*: Logunov 2021: 1024, figs 2–16 (transferred from *Cheliceroides*).

**Diagnosis.** *Cheliceroides longipalpis* differs from members of Hasariini by the presence of iridescent scales on the body (Figs 4, 6, 7, 12), the elongate male chelicera, the male palp with long and whip-like embolus originating at 2 o'clock (left palp) and coiling around the rounded tegulum (Figs 9–11, 16), and the female epigynum with anterior window-like structure and relatively long and coiled copulatory ducts (Figs 14, 15, 17, 18). It is similar to *Colopsus* species in having modified and elongate male chelicera and a relatively long male palpal tibia (equal to or longer than the cymbium) (Żabka 1985: 210; Logunov 2021: 1023–1024; Kanesharatnam and Benjamin 2021: 54; Fig. 3), but it can be distinguished by the S-shaped trajectory of the sperm duct on the tegulum of the male palp (vs C-shaped in *Colopsus*; compare Figs 16, 19), the longer embolus coiling in a circle around the tegulum (vs shorter and coiling in half a circle at most in *Colopsus*; compare Figs 16, 19), the absence of epigynal coupling pocket on epigynum (vs with two pockets in *Colopsus*; compare Figs 17, 20), and the long, coiled copulatory ducts (vs short and not obviously coiled in *Colopsus*; compare Figs 18, 21).

**Description.** See the detailed descriptions by Żabka (1985: 210) and Logunov (2021: 1024–1026).

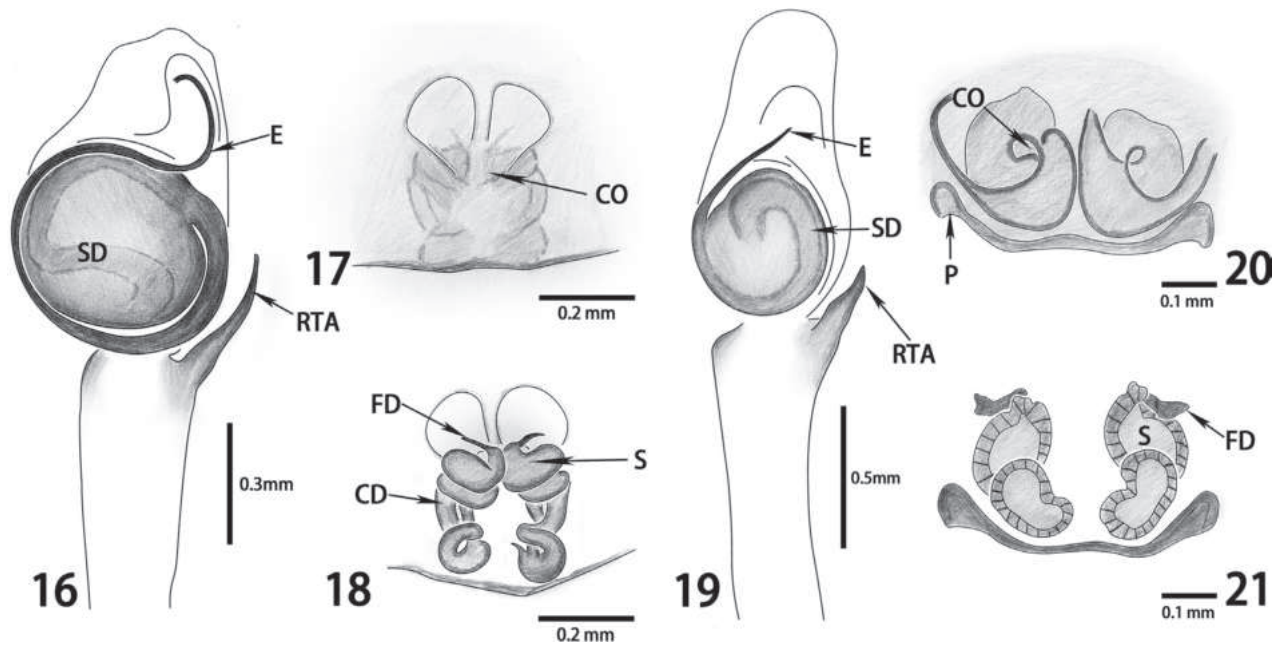
**Material examined.** CHINA • 4 ♂, 2 ♀; MHBU-ARA-00025627, MHBU-ARA-00025633; Guizhou, Shiqian County; 27.3342°N, 108.1519°E; 650 m elev.; 8 May 2023; Zhang et al. leg., HBUARA#2023-67.

**Distribution.** China, Vietnam.

**Natural history.** Arboreal, living on low vegetation.



Figures 3–15. *Cheliceroides longipalpis* Żabka, 1985 3–6 living photos of male (3–4) and female (5–6) 7–8 male habitus, dorsal (7) and ventral (8) view 9–11 left male palp, prolateral (9), ventral (10) and retrolateral (11) view 12–13 female habitus, dorsal (12) and ventral (13) view 14–15 epigynum, ventral (14) and dorsal (15) view.



Figures 16–21. Comparison of genital structures of *Cheliceroides longipalpis* Żabka, 1985 (16–18) and the type species of *Colopsus*, *Colopsus cancellatus* Simon, 1902 (19–21, modified from Kanesharatnam and Benjamin 2021) 16, 19 left palp, ventral view 17, 20 epigynum, ventral view 18, 21 epigynum, dorsal view.

## Discussion

Logunov (2021) synonymized *Cheliceroides* with *Colopsus* due to their similarities in body coloration, male chelicerae, and palp features (see Diagnosis above). The type species of *Colopsus*, *C. cancellatus* Simon, 1902, as well as two other *Colopsus* species (*C. ferruginus* Kanesharatnam & Benjamin, 2021 and *C. magnus* Kanesharatnam & Benjamin, 2021), were included in the molecular phylogenetic analyses using four gene regions (cytochrome c oxidase subunit I, 18S rRNA, 28S rRNA, and histone H3), and the results strongly supported the monophyly of *Colopsus* and its placement within the tribe Plexippini (Kanesharatnam and Benjamin 2021). The genitalia structures of *Colopsus* show clear similarities to those of *Evarcha* Simon, 1902 and *Pancorius* Simon, 1902, both typical plexippine genera, which also supports the placement of *Colopsus* within Plexippini (Kanesharatnam and Benjamin 2021). However, the molecular phylogenetic analyses on both UCE and mitogenomic datasets show that *Cheliceroides* is not a member of Plexippini, and is therefore not closely related to *Colopsus* (Figs 1, 2). Comparison of the genital features of *Cheliceroides longipalpis* (type species of *Cheliceroides*) and *Colopsus cancellatus* Simon, 1902 (type species of *Colopsus*) reveals significant differences in the trajectory of sperm duct and the shape of embolus of the palp in males, and the pockets and copulatory ducts of the epigynum in females (see Diagnosis above; Figs 16–21). Therefore, both molecular phylogeny and comparative morphology support removing *Cheliceroides* from the synonymy of *Colopsus*. The similarities of these genera represent an example of parallel evolution of morphological traits in separate lineages likely due to the adaptation to a similar microhabitat, which is commonly known in jumping spiders.

*Cheliceroides* was considered to be a member of Hasariini in the phylogenetic classification of jumping spiders (Maddison 2015), which was supported by the mitogenomic phylogeny but with poor support (bootstrap = 77%; Fig. 2). The UCE phylogeny recovered *Cheliceroides* as sister to the clade containing Hasariini (excluding *Bristowia*), Agoriini, and Chrysillini with strong support (bootstrap = 100%; Fig. 1). This indicates the placement of *Cheliceroides* within Hasariini is questionable. Another interesting finding from our study is the phylogenetic placement of *Bristowia*, which was also earlier included in the tribe Hasariini (Maddison 2015). We included the type species, *Bristowia heterospinosa* Reimoser, 1934 (JXZ743 and DRR297628), in our phylogenetic analyses, and the results show that it is not closely related to other Hasariini. The UCE phylogeny suggests it is sister to the clade containing Euophryini, Leptorchestini, Aelurillini, Salticini, and Plexippini (bootstrap = 100%; Fig. 1), and the mitogenomic phylogeny recovered it as sister to the clade composed of Agoriini and Chrysillini, but with low support (bootstrap = 44%; Fig. 2). Further phylogenetic study with an extended taxon sampling of major lineages of jumping spiders is needed to further clarify their phylogenetic placement.

## Acknowledgements

We thank Weihang Wang for providing living spider photographs of *Cheliceroides longipalpis*, Dr Wayne P. Maddison for helpful discussion on this topic and sharing UCE raw reads for mitogenome assembly, the reviewers (Dr Cheng Wang, Dr Kiran Marathe, Dr Wayne P. Maddison, Dr Tamás Szűts, and one anonymous reviewer), and editor (Dr Ingi Agnarsson) for valuable comments to improve the manuscript, and the Hebei Basic Science Center for Biotic Interaction for support.

## Additional information

### Conflict of interest

The authors have declared that no competing interests exist.

### Ethical statement

No ethical statement was reported.

### Funding

This work was funded by the National Natural Science Foundation of China to Junxia Zhang (grant no. 32070422), and the Post-graduate's Innovation Fund Project of Hebei University to Long Lin (grant no. HBU2024SS017).

### Author contributions

Conceptualization: JZ. Formal analysis: LL, JZ. Resources: ZY. Supervision: JZ. Visualization: ZY. Writing – original draft: LL. Writing – review and editing: JZ.

### Author ORCIDs

Long Lin  <https://orcid.org/0009-0006-0108-4463>

Zhiyong Yang  <https://orcid.org/0000-0002-7610-6843>

Junxia Zhang  <https://orcid.org/0000-0003-2179-3954>

## Data availability

The sequenced raw reads and annotated mitogenomes were submitted to the GenBank with accession numbers provided in Table 1. The alignments of UCE loci and mitochondrial protein-coding genes, the final concatenated UCE and 13-mitochondrial-PCG datasets, and the resulted phylogenetic trees are deposited in the Dryad Data Repository at <https://doi.org/10.5061/dryad.x3ffbg7sp>.

## References

- Bernt M, Donath A, Jühling F, Externbrink F, Florentz C, Fritzscht G, Pütz J, Middendorf M, Peter F (2013) MITOS: Improved de novo metazoan mitochondrial genome annotation. *Molecular Phylogenetics and Evolution* 69(2): 313–319. <https://doi.org/10.1016/j.ympev.2012.08.023>
- Borowiec ML (2019) Spruceup: Fast and flexible identification, visualization, and removal of outliers from large multiple sequence alignments. *Journal of Open Source Software* 4(42): 1635. <https://doi.org/10.21105/joss.01635>
- Capella-Gutiérrez S, Silla-Martínez JM, Gabaldón T (2009) trimAl: A tool for automated alignment trimming in large-scale phylogenetic analyses. *Bioinformatics* 25(15): 1972–1973. <https://doi.org/10.1093/bioinformatics/btp348>
- Ding Y, Zhang F, Zhang J (2023) Applicability and advantage of mitochondrial metagenomics and metabarcoding in spider biodiversity survey. *Diversity* 15(6): 711. <https://doi.org/10.3390/d15060711>
- Faircloth BC (2016) PHYLUCE is a software package for the analysis of conserved genomic loci. *Bioinformatics* 32(5): 786–788. <https://doi.org/10.1093/bioinformatics/btv646>
- Kanesharatnam N, Benjamin SP (2021) Phylogenetic relationships and systematics of the jumping spider genus *Colopsus* with the description of eight new species from Sri Lanka (Araneae: Salticidae). *Journal of Natural History* 54(43–44): 2763–2814. <https://doi.org/10.1080/00222933.2020.1869335>
- Katoh K, Standley DM (2013) MAFFT multiple sequence alignment software version 7: Improvements in performance and usability. *Molecular Biology and Evolution* 30(4): 772–780. <https://doi.org/10.1093/molbev/mst010>
- Kück P, Meusemann K (2010) FASconCAT: Convenient handling of data matrices. *Molecular Phylogenetics and Evolution* 56(3): 1115–1118. <https://doi.org/10.1016/j.ympev.2010.04.024>
- Logunov DV (2021) Jumping spiders (Araneae: Salticidae) of the Na Hang Nature Reserve, Tuyen Quang Province, Vietnam. *Arachnology* 18(9): 1021–1055. <https://doi.org/10.13156/arac.2021.18.9.1021>
- Maddison WP (2015) A phylogenetic classification of jumping spiders (Araneae: Salticidae). *The Journal of Arachnology* 43(3): 231–292. <https://doi.org/10.1636/arac-43-03-231-292>
- Maddison WP, Li D, Bodner M, Zhang J, Xu X, Liu Q, Liu F (2014) The deep phylogeny of jumping spiders (Araneae, Salticidae). *ZooKeys* 440: 57–87. <https://doi.org/10.3897/zookeys.440.7891>
- Meng G, Li Y, Yang C, Liu S (2019) MitoZ: A toolkit for animal mitochondrial genome assembly, annotation and visualization. *Nucleic Acids Research* 47(11): e63–e63. <https://doi.org/10.1093/nar/gkz173>

- Minh BQ, Schmidt HA, Chernomor O, Schrempf D, Woodhams MD, Von Haeseler A, Lanfear R (2020) IQ-TREE 2: New models and efficient methods for phylogenetic inference in the genomic era. *Molecular Biology and Evolution* 37(5): 1530–1534. <https://doi.org/10.1093/molbev/msaa015>
- Mirarab S, Nguyen N, Warnow T (2014) PASTA: ultra-large multiple sequence alignment. In: Sharan R (Ed.) *Research in Computational Molecular Biology. RECOMB 2014. Lecture Notes in Computer Science*. Springer, Cham, 177–191. [https://doi.org/10.1007/978-3-319-05269-4\\_15](https://doi.org/10.1007/978-3-319-05269-4_15)
- Peng XJ (2020) *Fauna Sinica, Invertebrata* 53, Arachnida: Araneae: Salticidae. Science Press, Beijing, 612 pp.
- Peng XJ, Xie LP (1993) A new species of the genus *Pellenese* and a description of the female spider of *Cheliceroides longipalpis* Żabka, 1985 from China (Araneae: Salticidae). *Acta Arachnologica Sinica* 2: 80–83.
- Roy TK, Saha S, Raychaudhuri D (2016) A treatise on the jumping spiders (Araneae: Salticidae) of tea ecosystem of Dooars, West Bengal, India. *World Scientific News* 53(1): 1–66.
- World Spider Catalog (2024) *World Spider Catalog. Version 25.0*. Natural History Museum Bern. <https://doi.org/10.24436/2> [Accessed on 21 February 2024]
- Żabka M (1985) Systematic and zoogeographic study on the family Salticidae (Araneae) from Viet-Nam. *Annales Zoologici* 39(11): 197–485.
- Zhang F, Ding Y, Zhu CD, Zhou X, Orr MC, Scheu S, Luan YX (2019) Phylogenomics from low-coverage whole-genome sequencing. *Methods in Ecology and Evolution* 10(4): 507–517. <https://doi.org/10.1111/2041-210X.13145>
- Zhang D, Gao F, Jakovlić I, Zou H, Zhang J, Li WX, Wang GT (2020) PhyloSuite: An integrated and scalable desktop platform for streamlined molecular sequence data management and evolutionary phylogenetics studies. *Molecular Ecology Resources* 20(1): 348–355. <https://doi.org/10.1111/1755-0998.13096>
- Zhang J, Li Z, Lai J, Zhang Z, Zhang F (2023b) A novel probe set for the phylogenomics and evolution of RTA spiders. *Cladistics* 39(2): 116–128. <https://doi.org/10.1111/cla.12523>
- Zhang W, Lin L, Ding Y, Zhang F, Zhang J (2023a) Comparative mitogenomics of jumping spiders with first complete mitochondrial genomes of Euophryini (Araneae: Salticidae). *Insects* 14(6): 517. <https://doi.org/10.3390/insects14060517>



# Three new species of the leafhopper genus *Arboridia* Zachvatkin (Hemiptera, Cicadellidae, Typhlocybinae), with a key and checklist to known species of China

Chang Han<sup>1</sup>, Bin Yan<sup>1</sup>, Xiaofei Yu<sup>2</sup>, Maofa Yang<sup>1,2</sup>, Michael D. Webb<sup>3</sup>

<sup>1</sup> Institute of Entomology, Guizhou Provincial Key Laboratory for Agricultural Pest Management of the Mountainous Region, Guizhou University, Guiyang 550025, China

<sup>2</sup> College of Tobacco Science, Guizhou University, Guiyang 550025, China

<sup>3</sup> Department of Entomology, The Natural History Museum, Cromwell Road, London, SW7 5BD, UK

Corresponding authors: Maofa Yang ([gddgly@126.com](mailto:gddgly@126.com)); Michael D. Webb ([M.Webb@nhm.ac.uk](mailto:M.Webb@nhm.ac.uk))

## Abstract

Three new species of the leafhopper genus *Arboridia* Zachvatkin 1946, *Arboridia* (*Arboridia*) *furcata* Han, **sp. nov.**, *Arboridia* (*Arboridia*) *rubrovittata* Han, **sp. nov.**, and *Arboridia* (*Arboridia*) *robustipenis* Han, **sp. nov.**, are described and illustrated from fruit trees in Southwest China. A key and checklist to known species from China are provided.

**Key words:** *Arboridia*, Hemiptera, identification key, new species, taxonomy, Typhlocybinae



Academic editor: Ilija Gjonov

Received: 15 January 2024

Accepted: 27 February 2024

Published: 28 March 2024

ZooBank: <https://zoobank.org/91F2B2E0-AC9E-4FA1-8487-BFB3BF86CF21>

**Citation:** Han C, Yan B, Yu X, Yang M, Webb MD (2024) Three new species of the leafhopper genus *Arboridia* Zachvatkin (Hemiptera, Cicadellidae, Typhlocybinae), with a key and checklist to known species of China. ZooKeys 1196: 255–269. <https://doi.org/10.3897/zookeys.1196.118829>

Copyright: © Chang Han et al.

This is an open access article distributed under terms of the Creative Commons Attribution License ([Attribution 4.0 International – CC BY 4.0](https://creativecommons.org/licenses/by/4.0/)).

## Introduction

The leafhopper genus *Arboridia* Zachvatkin, 1946 belongs to the tribe Erythroneurini of the subfamily Typhlocybinae (Hemiptera: Auchenorrhyncha: Cicadellidae) and includes two subgenera, *Arboridia* Zachvatkin, 1946 and *Arborifera* Sohi & Sandhu, 1971. Species feed on a variety of plants including fruit trees, hawthorn, maple, honeysuckle, dogwood and several other plants (Song and Li 2013). So far, 84 species have been described in this large genus, distributed throughout the Palaearctic and Oriental regions, including 25 valid species from China (Song et al. 2016; Cao et al. 2019).

In this study, three new species are described from Guizhou, China. Photographs of the whole body, illustrations of male genitalia, and biological information such as host plants and distributional records are provided. In addition, an updated key to the *Arboridia* species from China is provided.

## Materials and methods

Specimens used in this study were collected from grape, kiwi and walnut trees in Guizhou, China using a sweep net. A Nikon SMZ 1270 microscope was used to dissect the specimens and an Olympus CX41 microscope for observing and drawing the male genitalia. A KEYENCE VHX-6000 digital microscope was used to take pictures of the male habitus. Morphological terminology used in this

work follows Dietrich (2005) and Dworakowska (1993). All specimens examined in this study are deposited in the Institute of Entomology, Guizhou University, China (GUGC).

## Taxonomy

### *Arboridia* Zachvatkin

*Arboridia* Zachvatkin, 1946: 153. Type species. *Typhlocyba parvula* Boheman, 1845. *Khoduma* Dworakowska, 1972: 403. Synonymised by Dworakowska and Virak-tamath (1975: 529). Type species. *Khoduma jacobii* Dworakowska, 1972.

**Diagnosis.** Head slightly narrower than pronotum, crown weakly produced with fore margin rounded. Head and thorax yellow; vertex usually with pair of dark subapical spots; pronotum usually with irregular brown symmetric markings; scutellum with brown basal triangles. Forewing either without marking, with oblique vittae or with dark spots. Ventral abdominal apodemes small and extended to or beyond posterior margin of 3<sup>rd</sup> sternite. Male pygofer with wide-spread microtrichia and several small rigid setae on inner surface of hind margin; dorsal appendage present, free from pygofer side; ventral appendage absent; phragma lobe with spine-like setae present on each side of aedeagus, attached to dorsal apodeme of aedeagus by ligaments (Fig. 51). Subgenital plate upturned apically with lateral margin basally expanded triangular shaped with 2–4 lateral macrosetae in an oblique row slightly basad of midlength; lateral margin with short spine-like setae. Style apex usually with 3 points, sometimes 2<sup>nd</sup> point absent. Aedeagus with shaft laterally compressed, usually with processes, gonopore apical on ventral surface; dorsal apodeme and preatrium present or absent. Connective U- or V- shaped with median anterior lobe absent.

**Distribution.** Palaearctic and Oriental regions.

### Checklist of Chinese species of *Arboridia*

1. *Arboridia agrillacea* (Anufriev, 1969b: 182–183, fig. 13: 1–6, *Erythroneura*); Anufriev, 1978a: 87, transferred to *Arboridia*; Song & Li, 2013: 243–244, figs J, j, jj, 63–69; *Arboridia koreana* Oh & Jung, 2015: 447–448, figs 1, 3, 5, 7, 9–15, synonym. Distribution: Gansu, Guangxi, Guizhou, Henan, Shaanxi, Sichuan.
2. *Arboridia anteoculara* Song & Li, 2013: 230–233, figs A, a, 1–7. Distribution: Guizhou.
3. *Arboridia apicalis* (Nawa, 1913a: 480–486, Pl. 24, *Zygina*); Cockerell, 1920a: 247, *Erythroneura*; *Erythroneura sandagouensis* Vilbaste, 1968a: 108, synonym; Anufriev, 1969b: 185–186, fig. 15: 8–13; Dworakowska, 1970g: 607–608, fig. 18, transferred to *Arboridia*. Distribution: Anhui, Guizhou, Hebei, Henan, Hubei, Jiangsu, Liaoning, Shannxi, Shandong, Taiwan, Zhejiang.
4. *Arboridia baiyunensis* Song & Li, 2013: 233–234, figs B, b, 8–14. Distribution: Henan.
5. *Arboridia (Arborifera) changlingensis* Jiang, Luo & Song, 2021: 354–355, figs 5–8, 27–34. Distribution: Guizhou.

6. *Arboridia cincta* Song & Li, 2015: 585–587, figs A–C, 1–7. Distribution: Henan.
7. *Arboridia cuihuashana* Song & Li, 2013: 237–238, figs E, e, 29–35. Distribution: Shaanxi.
8. *Arboridia echinata* Song & Li, 2013: 239–240, figs G, g, gg, 42–48. Distribution: Guizhou.
9. *Arboridia furcata* Han, sp. nov. Distribution: Guizhou.
10. *Arboridia huajiangensis* Jiang, Luo & Song, 2021: 351–353, figs 1–4, 9–26. Distribution: Guizhou.
11. *Arboridia jinghongensis* Pu, Wang & Song, 2023: 296–297, figs 1a–f, 2a–h. Distribution: Yunnan.
12. *Arboridia kakogawana* (Matsumura, 1932: 113, *Zygina*); Ishihara, 1953b: 33, *Erythroneura*; Dworakowska, 1970g: 610, figs 25–29, transferred to *Arboridia*. Distribution: Beijing, Guizhou, Shandong, Xinjiang.
13. *Arboridia lunula* Song & Li, 2013: 234–236, figs D, d, 22–28. Distribution: Guizhou.
14. *Arboridia luojishangensis* Zhang, Jiang & Song, 2022: 6–8, figs 21–32. Distribution: Guizhou.
15. *Arboridia maculifrons* (Vilbaste, 1968a: 107, *Erythroneura*); Dworakowska, 1970g: 611, figs 19–22, transferred to *Arboridia*. Distribution: Guizhou, Hebei.
16. *Arboridia ochracea* Song & Li, 2015: 587–588, figs D–F, 8–15. Distribution: Henan.
17. *Arboridia paraprocessa* Song & Li, 2013: 239, figs F, f, 36–41. Distribution: Guizhou, Henan.
18. *Arboridia reniformis* Song & Li, 2013: 234, figs C, c, cc, 15–21. Distribution: Yunnan.
19. *Arboridia remmi* (Vilbaste, 1968a: 103, *Erythroneura*); Anufriev, 1969b: 183–184, figs 15: 1–7; Dworakowska, 1970g: 613, transferred to *Arboridia*. Distribution: Guizhou.
20. *Arboridia robustipenis* Han, sp. nov. Distribution: Guizhou.
21. *Arboridia rubrovittata* Han, sp. nov. Distribution: Guizhou.
22. *Arboridia sinensis* Guglielmino, Xu, Buckle & Dong, 2012: 878–881, figs 1: A–F, 2: A–B. Distribution: Yunnan.
23. *Arboridia suputinkaensis* (Vilbaste, 1968a: 109, *Erythroneura*); Dworakowska, 1970g: 613, transferred to *Arboridia*. Distribution: Henan, Zhejiang. <https://hoppers.speciesfile.org/otus/43920/overview> (Dmitriev et al. 2022)
24. *Arboridia (Arborifera) surstyli* Cai & Xu, 2006: 75–76, figs 1: 1–10. Distribution: Henan, Zhejiang.
25. *Arboridia suzukii* (Matsumura, 1916b: 396, *Zygina*); Ishihara, 1953b: 34, *Erythroneura*; *Erythroneura arboricola* Vilbaste, 1968a: 101, synonym; Dworakowska, 1970g: 613, transferred to *Arboridia*. Distribution: Gansu, Guizhou, shannxi, shanxi, Taiwan. <https://hoppers.speciesfile.org/otus/43922/overview>.
26. *Arboridia tridentata* Song & Li, 2013: 240–241, figs H, h, 49–55. Distribution: Yunnan.
27. *Arboridia xiaotungensis* Zhang, Jiang & Song, 2022: 2–5, figs 1–20. Distribution: Guizhou.
28. *Arboridia zhenyuana* Song & Li, 2013: 242–243, figs I, i, 56–62. Distribution: Gansu.

### Key to species (males) of *Arboridia* species from China

(modified from Jiang et al. 2021)

- 1 Preatrium of aedeagus short or absent (*Arborifera*) ..... 2
- Preatrium of aedeagus well developed (Figs 24, 39, 55) (*Arboridia*) ..... 3
- 2 Aedeagal shaft with pair of sharp inverted processes on dorsal margin ..... *A. surstyli*
- Aedeagal shaft with one broad triangular process on dorsal margin ..... *A. changlingensis*
- 3 Aedeagus without process, shaft with pair of lateral flanges ..... 4
- Aedeagus with processes, shaft without pair of lateral flanges ..... 6
- 4 Aedeagal shaft with lateral flanges serrate ..... *A. zhenyuana*
- Aedeagal shaft with lateral flanges not serrate ..... 5
- 5 Aedeagal shaft with lateral flanges narrow, entire ..... *A. agrillacea*
- Aedeagal shaft with larger lateral flanges partly wrapped around shaft ..... *A. jinghongensis*
- 6 Aedeagus with one process ..... 7
- Aedeagus with more than one process ..... 9
- 7 Aedeagus with process arising from preatrium ..... *A. apicalis*
- Aedeagus with process arising from midlength of shaft ..... 8
- 8 Aedeagus with dorsal apodeme extremely expanded in lateral view ..... *A. sinensis*
- Aedeagus with dorsal apodeme narrow in lateral view ..... *A. tridentata*
- 9 Aedeagus with one or two pairs of processes ..... 10
- Aedeagus with three or more processes ..... 19
- 10 Aedeagal shaft with two pairs of processes, one at apex and one at base .. *A. ochracea*
- Aedeagal shaft with one pair of processes arising from apex or base ..... 11
- 11 Aedeagus with processes arising from base of shaft ..... 12
- Aedeagus with processes arising from apex of shaft ..... 15
- 12 Aedeagus with two pairs of basal processes ..... *A. anteoculara*
- Aedeagus with one pair of basal processes ..... 13
- 13 Aedeagus with processes slender and bent basad apically (Figs 17, 24) ..... *A. furcata* sp. nov.
- Aedeagus with processes stout and straight ..... 14
- 14 Aedeagus with dorsal apodeme narrow in lateral view ..... *A. lunula*
- Aedeagus with dorsal apodeme extremely expanded in lateral view ..... *A. maculifrons*
- 15 Aedeagus with apical processes directed basally ..... 16
- Aedeagus with apical processes directed distally ..... 18
- 16 Apex of aedeagal shaft acuminate in ventral view ..... *A. cincta*
- Apex of aedeagal shaft truncate in ventral view ..... 17
- 17 Aedeagus without subapical bifurcation in ventral view ..... *A. reniformis*
- Aedeagus with subapical bifurcation in ventral view ..... *A. xiaotungensis*
- 18 Aedeagal shaft without spines ..... *A. cuihuashana*
- Aedeagal shaft with numerous short spines ..... *A. echinata*
- 19 Aedeagal shaft with two or three processes at midlength ..... 20
- Aedeagal shaft with one pair of apical processes ..... 22

- 20 Aedeagal shaft with three processes subbasally, a pair of upper bifurcate processes and a slightly more ventral process (Figs 35, 40) ..... ***A. rubrovittata* sp. nov.**
- Aedeagal shaft with two processes at midlength ..... **21**
- 21 Aedeagal shaft with two processes fused for 2/3 of their length (Figs 50–51, 55–56) ..... ***A. robustipenis* sp. nov.**
- Aedeagal shaft with two processes one above the other... ***A. luojiashangensis***
- 22 Apical processes of aedeagal shaft directed basally ..... **23**
- Apical processes of aedeagal shaft directed distally ..... **24**
- 23 Aedeagal shaft with slender apical processes, without ventral protrusion...  
..... ***A. suputinkaensis***
- Aedeagal shaft with short apical processes, with small ventral protrusion..  
..... ***A. huajiagensis***
- 24 Preatrium of aedeagus longer than shaft ..... **25**
- Preatrium of aedeagus shorter than shaft ..... **26**
- 25 Aedeagal shaft with numerous short spines ..... ***A. suzukii***
- Aedeagal shaft without spines ..... ***A. remmi***
- 26 Aedeagal shaft with distinct extension at midlength ..... ***A. baiyunensis***
- Aedeagal shaft without extension at midlength ..... **27**
- 27 Aedeagus with dorsal apodeme and shaft narrow in lateral view; preatrium with a long ventral process ..... ***A. paraprocessa***
- Aedeagus with dorsal apodeme and shaft expanded in lateral view; preatrium with a short ventral process ..... ***A. kakogawana***

***Arboridia (Arboridia) furcata* Han, sp. nov.**

<https://zoobank.org/92B51DA2-4F3F-40E6-9F01-D8D34BAD4884>

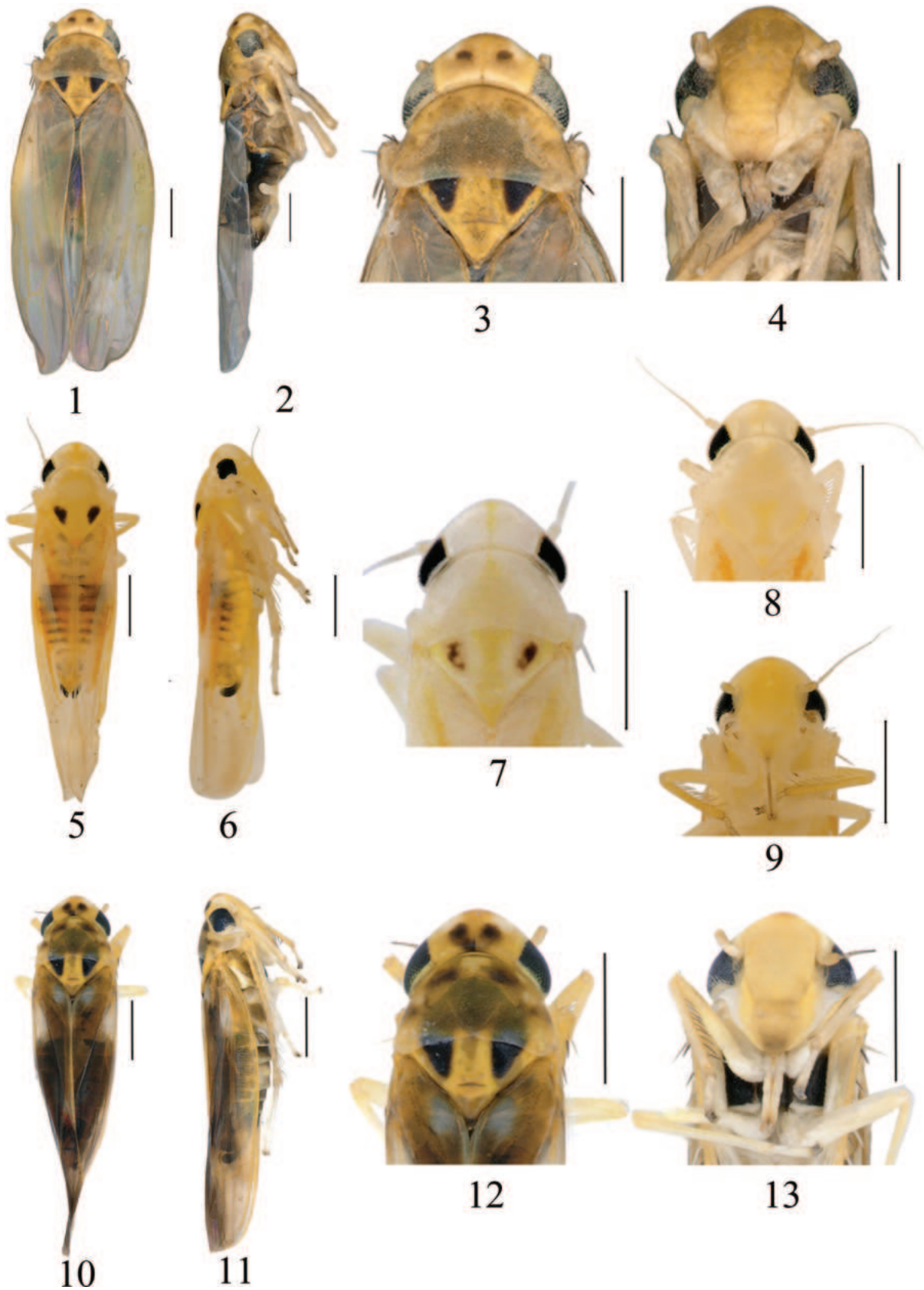
Figs 1–4, 14–28

**Description.** Dorsum yellowish brown; eyes grey with posterior margin beige; vertex with a pair of black spots subapically; coronal suture indistinct distally, pale brown basally (Figs 1–3). Face yellowish brown with median area of frontoclypeus and anteclypeus brighter towards apex; lorum and gena whitish (Fig. 4). Pronotum yellowish brown with brownish spots at anterior margin. Scutellum yellow with lateral triangles dark brown (Fig. 3). Forewing hyaline, veins brown. Abdominal tergites black; sternites milky white; subgenital plate dark apically (Figs 2, 14).

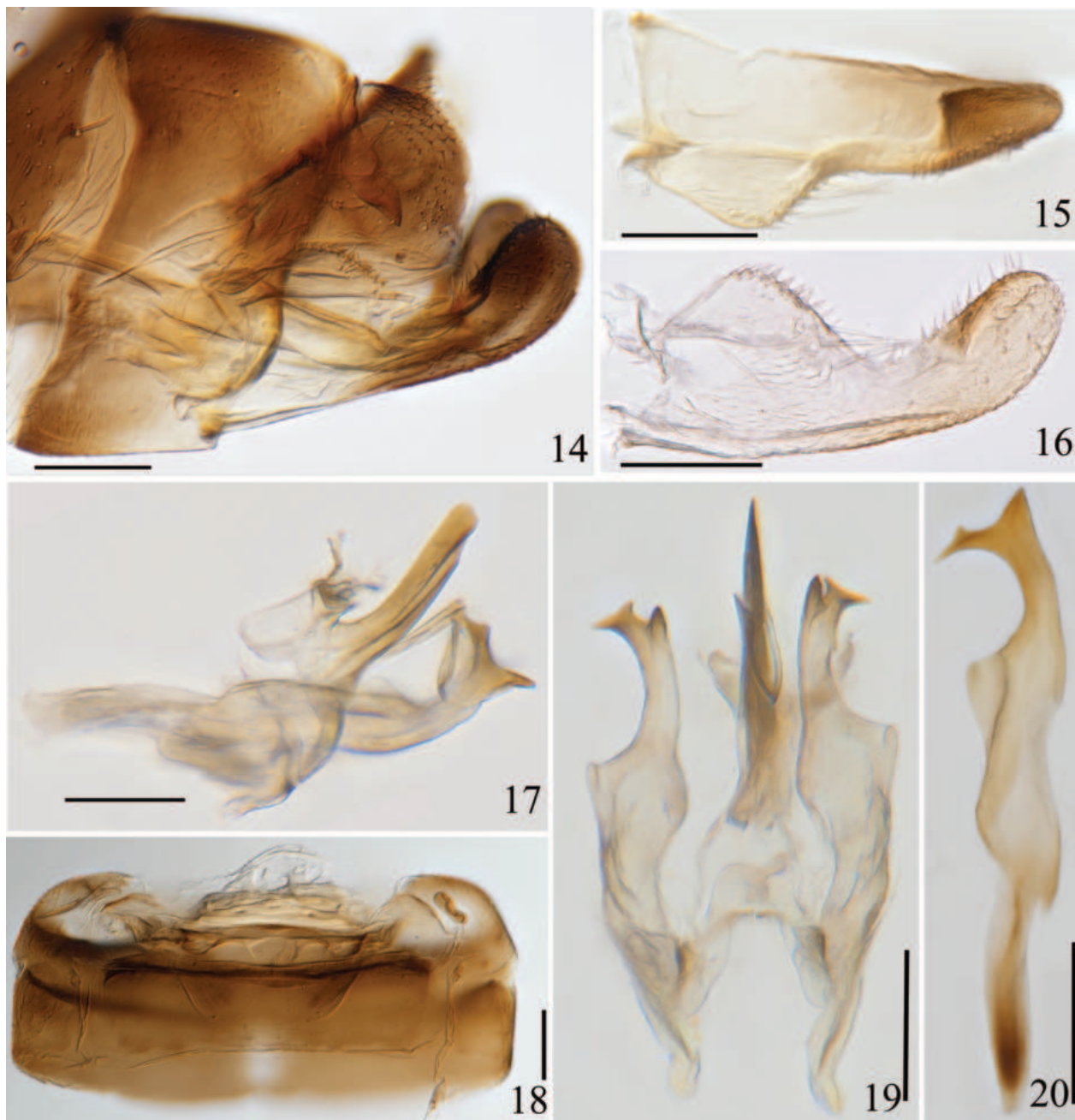
Ventral abdominal apodemes small, extended to 4<sup>th</sup> sternite (Figs 18, 27).

**Male genitalia.** Pygofer dorsal appendage simple, slender and wavy, with the apex obliquely truncate (Figs 14, 21). Subgenital plate with 3 lateral macrosetae in an oblique row slightly basad of midlength laterally (Figs 15, 16, 22, 23). Style long and slender, apex with 3 points; preapical lobe well developed; several small tubercles subapically and at midlength (Figs 20, 26). Aedeagal shaft long and stout, slightly laterally compressed, a pair of long slender basal processes on ventral surface of the shaft, parallel to the shaft in their basal half, then sharply turned in proximal direction in their distal half (Figs 17, 19, 24, 25); dorsal apodeme short and robust, expanded laterally at apex; preatrium short (Figs 17, 24). Connective U-shaped, with lateral arms long and stem broad (Figs 19, 28).

**Measurement.** Body length males 3.0–3.2 mm, females 3.2–3.3 mm.



Figures 1–13. External morphology of *Arboridia* species 1–4 *Arboridia furcata* Han, sp. nov. 1 habitus, dorsal view 2 habitus, lateral view 3 head and thorax, dorsal view 4 face 5–9 *Arboridia rubrovittata* Han, sp. nov. 5 habitus, dorsal view 6 habitus, lateral view 7, 8 head and thorax, dorsal view 9 face 10–13 *Arboridia robustipenis* Han, sp. nov. 10 habitus, dorsal view 11 habitus, lateral view 12 head and thorax, dorsal view 13 face. Scale bars: 0.5 mm.



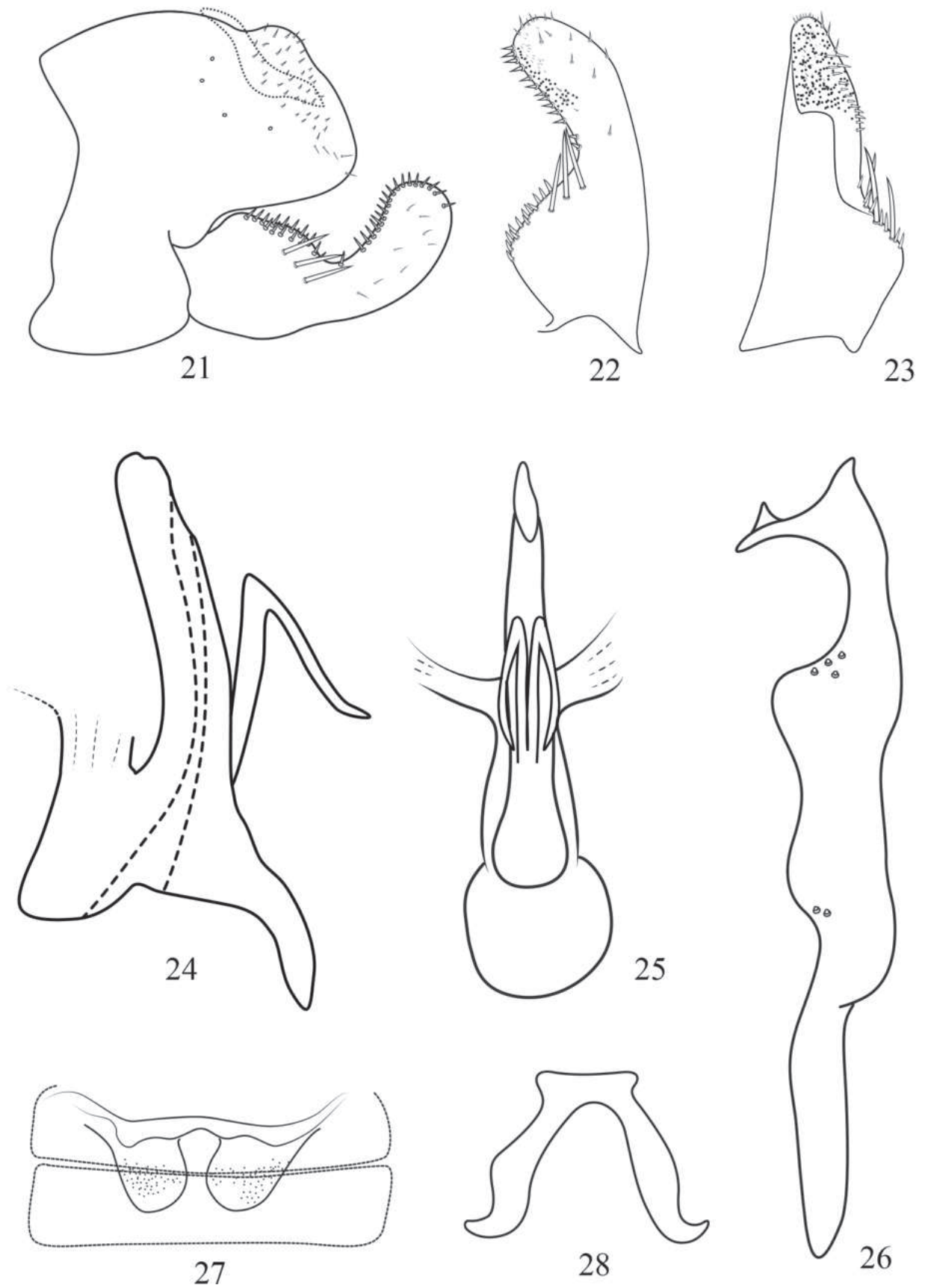
Figures 14–20. *Arboridia* (*A.*) *furcata* Han, sp. nov. 14 male genitalia, lateral view 15 subgenital plate, dorsal view 16 subgenital plate, ventral view 17 aedeagus, connective and style, lateral view 18 abdominal apodemes 19 aedeagus, connective and style, ventral view 20 style, lateral view. Scale bars: 0.1 mm.

**Specimen examined.** *Holotype* ♂: CHINA, Guizhou Prov., Dejiang, 22.VII.2017, coll. Chang Han and Bin Yan, on grape (GUGC). *Paratypes*: 5♂♂, 5♀♀, same data as holotype.

**Etymology.** The new species is named from the Latin word “*furcatus*”, referring to the forked aedeagal process.

**Remarks.** The new species is similar to *Arboridia* (*A.*) *anteoculara* Song & Li, 2013, but differs in only having a pair of processes on the ventrobasal surface of aedeagal shaft (Figs 17, 24); the latter species having two pairs of processes and arising from both sides of the aedeagal shaft.

**Host.** *Vitis vinifera* L. (grape).



**Figures 21–28.** *Arboridia (A.) furcata* Han, sp. nov. **21** male pygofer, lateral view **22** subgenital plate, ventral view **23** subgenital plate, dorsal view **24** aedeagus, lateral view **25** aedeagus, ventral view **26** style, lateral view **27** abdominal apodemes **28** connective.

***Arboridia (Arboridia) rubrovittata* Han, sp. nov.**

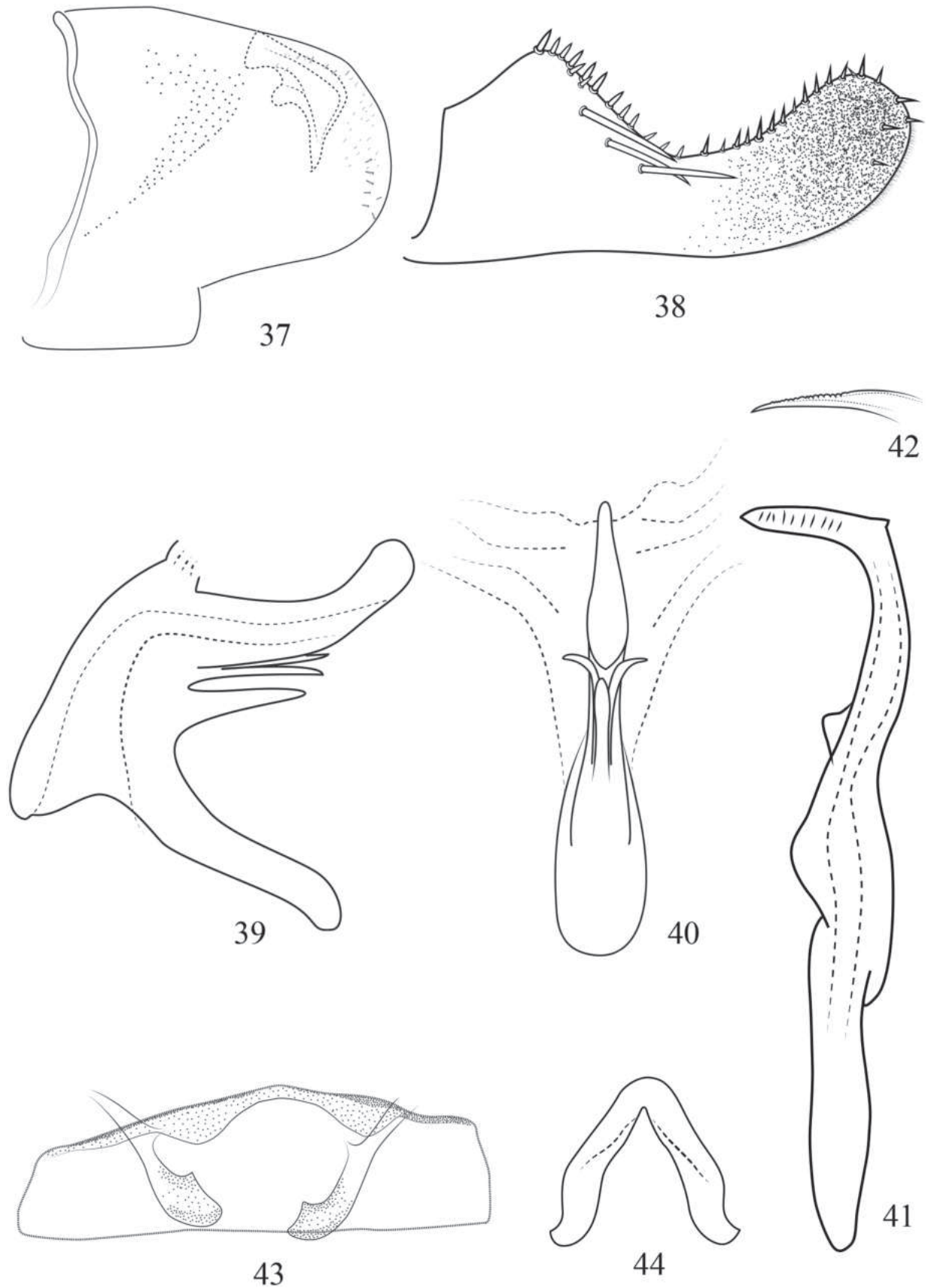
<https://zoobank.org/AE69B8DF-EB76-4CB8-A0EA-B9EB4D1FCB43>

Figs 5–9, 29–44

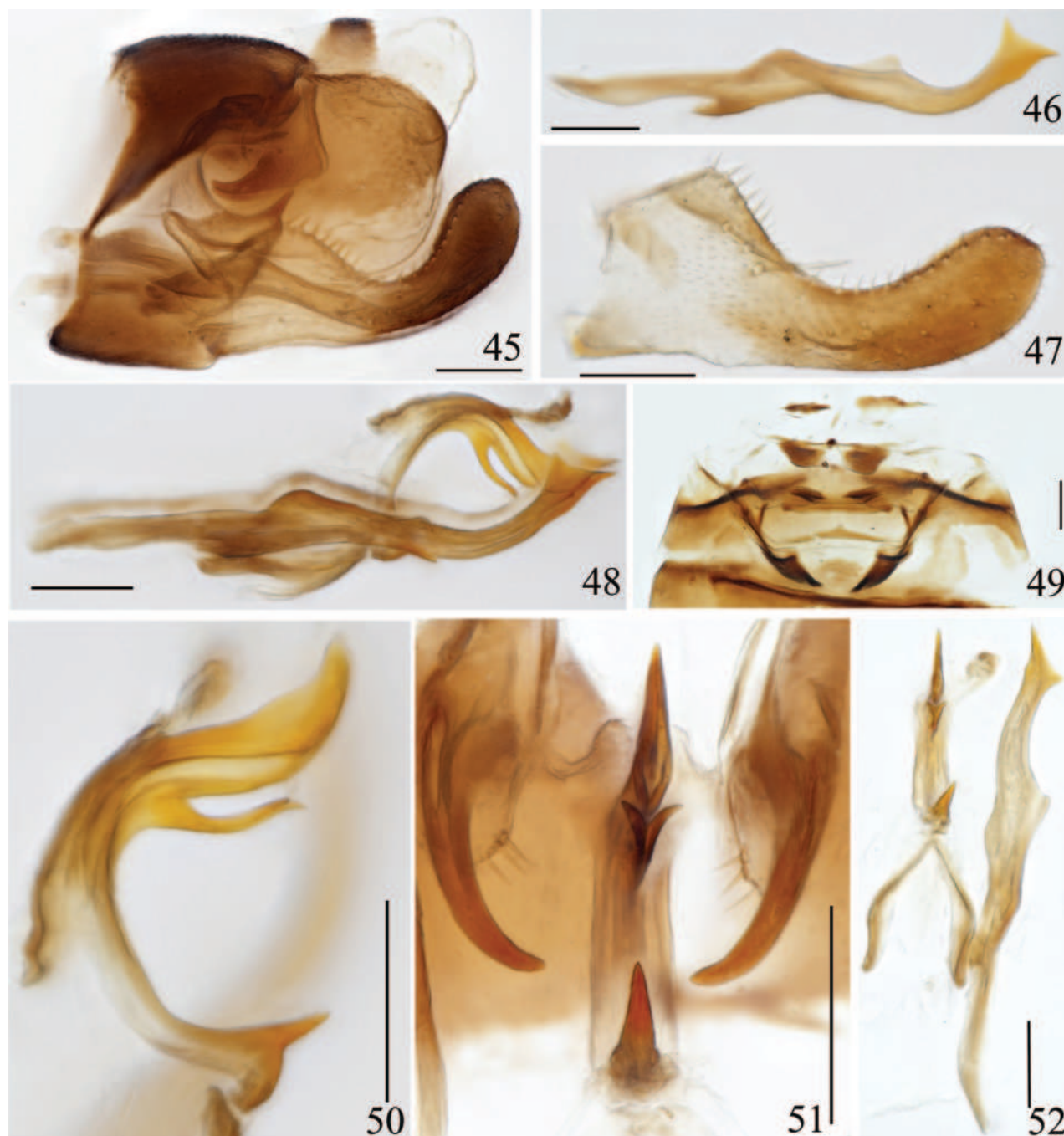
**Description.** Dorsum orange, yellow or beige. Eyes black, inner and posterior margins white (Figs 5, 6). Vertex without pair of dark spots, with a white patch each side of midline basally; coronal suture orange yellow (Figs 5, 7, 8). Face orange yellow. Pronotum with ivory or pale white streaks situated laterad of anterior margin.



**Figures 29–36.** *Arboridia (Arboridia) rubrovittata* Han, sp. nov. **29** male genitalia, lateral view **30** style, lateral view **31** subgenital plate **32** abdominal apodemes **33** aedeagus, connective and style, lateral view **34** aedeagus, lateral view **35** aedeagus, ventral view **36** aedeagus, connective and style, ventral view. Scale bars: 0.1 mm.



**Figures 37–44.** *Arboridia (Arboridia) rubrovittata* Han, sp. nov. **37** male pygofer, lateral view **38** subgenital plate **39** aedeagus, lateral view **40** aedeagus, ventral view **41** style, lateral view **42** style apex, ventral view **43** abdominal apodemes **44** connective.



**Figures 45–52.** *Arboridia (Arboridia) robustipennis* Han, sp. nov. **45** male genitalia, lateral view **46** style, lateral view **47** subgenital plate **48** aedeagus, connective and style, lateral view **49** abdominal apodemes **50** aedeagus, lateral view **51** aedeagus & pygofer dorsal appendage, ventral view **52** aedeagus, connective and style, ventral view. Scale bars: 0.1 mm.

Scutellum pale or whitish yellow with lateral triangles dark to pale brown (Figs 5, 7, 8). Forewing with oblique pale reddish-orange vittae in clavus and adjacent area of wing. Abdominal segments milky yellow, tergites with segment margins brown. Subgenital plate with nearly 2/3 apically dark (Figs 5, 6).

Ventral abdominal apodemes small, extended to posterior margin of 3<sup>rd</sup> sternite (Figs 32, 43).

**Male genitalia.** Pygofer dorsal appendage claw-like (Figs 29, 37). Subgenital plate with 3 lateral macrosetae in an oblique row slightly basad of midlength

(Figs 31, 38). Style slender, with 2 points, heel point small; sword-like apically with transverse wrinkles in lateral view (Figs 30, 41), serrated in ventral view (Fig. 42). Aedeagus relatively small, shaft laterally compressed, digitate and slightly upturned in lateral view; subbasally with three processes, two basal processes and a single unpaired spike basad, the distal paired processes divergent with branches slender, the proximal process slightly shorter and more robust, finger-like in ventral view (Figs 34, 35, 39, 40); preatrium long. Connective V-shaped (Figs 36, 44).

**Measurement.** Body length males 2.7–2.9 mm, females 2.9–3.0 mm.

**Specimen examined.** *Holotype* ♂: CHINA, Guizhou Prov., Jianhe, 26.V.2017, coll. Chang Han and Yaowen Zhang, on kiwi (GUGC). *Paratypes*: 23♂♂, 25♀♀, same data as holotype on kiwi; 3♂♂, 6♀♀, CHINA, Guizhou Prov., Wujiang, 19.V.2017, coll. Chang Han and Bin Yan, on walnut (GUGC).

**Etymology.** The new species name is derived from the Latin words “*ruber*” (red) and “*vittatus*” (banded), referring to the reddish-orange oblique stripes on the forewings.

**Remarks.** The new species can be distinguished from most *Arboridia* species by its vertex and pronotum without dark spots (Figs 5, 7, 8) and reddish-orange stripes on the forewing. Its male genitalia is similar to *A. (A.) lunula* Song & Li, 2013, but can be distinguished by the sword-like apex of the style and aedeagus with three basal ventral processes, the upper paired processes slender (Figs 34, 39).

**Host.** *Actinidia chinensis* Planch (kiwi fruit); *Juglans regia* L. (walnut).

***Arboridia (Arboridia) robustipenis* Han, sp. nov.**

<https://zoobank.org/C2F0CB93-2BA0-498A-878F-F91A7FE2D8DD>

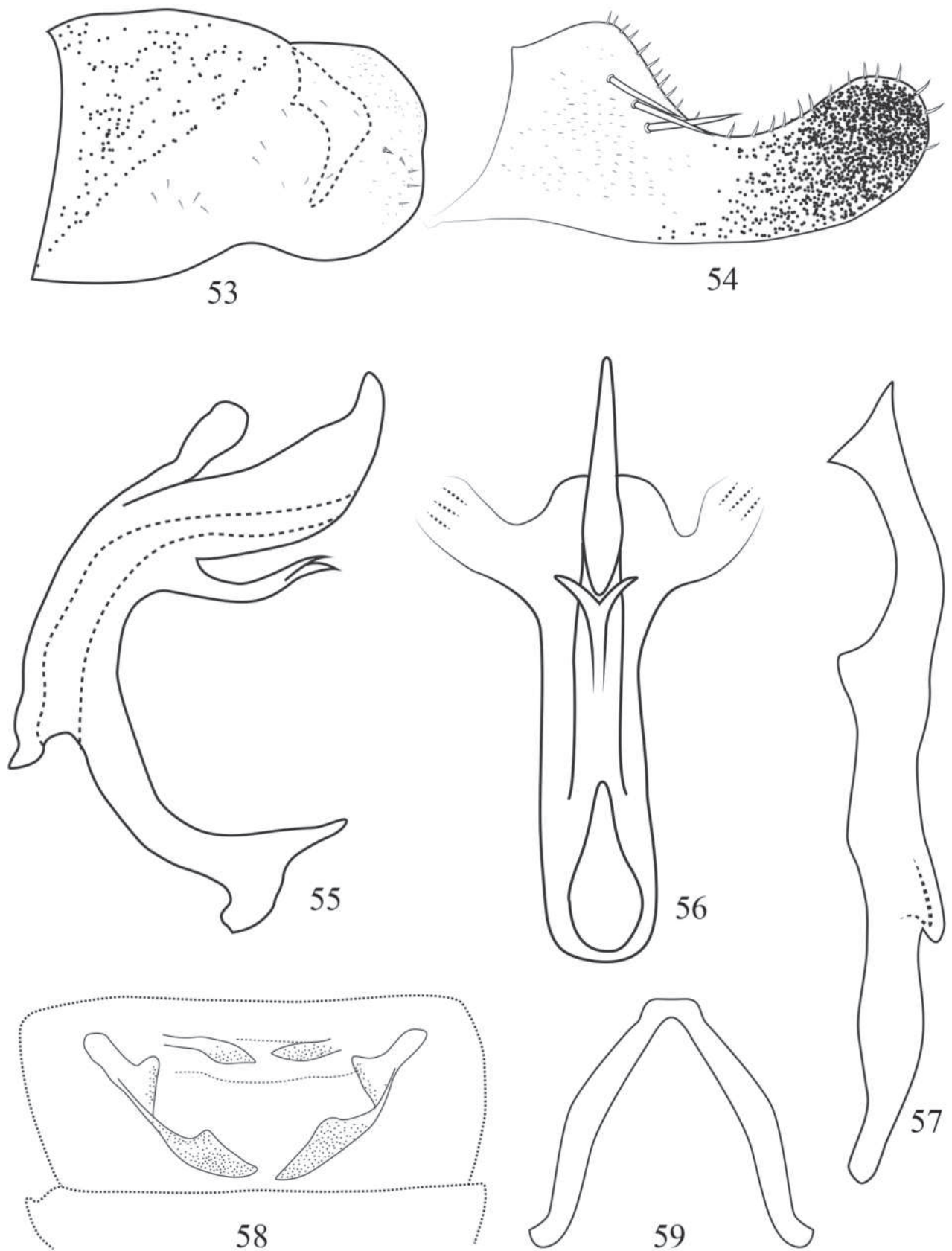
Figs 10–13, 45–59

**Description.** Head with eyes black with posterior margin pearl white; crown yellow with a dark yellow spot at apex, an adjacent brown spot posteriorly on each side of midline and a brown patch at base of coronal suture (Figs 10–12). Face pale yellow, with anteclypeus brown apically; gena whitish yellow (Fig. 13). Pronotum semitransparent with brown markings (Fig. 12). Scutellum yellow with lateral triangles dark brown (Fig. 12). Forewing brownish hyaline with off-white patch in clavus and brochosome region. Abdominal segments dark brown, sternites with yellow hind margins of segments; subgenital plates black apically (Figs 10, 11).

Abdominal apodemes small, not exceeding posterior margin of 3<sup>rd</sup> sternite (Figs 49, 58).

**Male genitalia.** Pygofer dorsal appendage tapering and curved ventrad (Figs 45, 53). Subgenital plate with 3 lateral macrosetae in an oblique row slightly basad of midlength (Figs 47, 54). Style apex with two triangular points; preapical lobe well developed (Figs 46, 57). Aedeagal shaft strongly laterally compressed and “C” shaped with apex upturned in lateral view, with two basal processes fused for 2/3 of their length at midlength of ventral margin; preatrium long, with a thorn-like basal projection (Figs 50–51, 55–56). Connective V-shaped with stem reduced (Figs 52, 59).

**Measurement.** Body length males 2.9–3.2 mm, females 3.0–3.3 mm.



**Figures 53–59.** *Arboridia (Arboridia) robustipenis* Han, sp. nov. **53** male pygofer, lateral view **54** subgenital plate **55** aedeagus, lateral view **56** aedeagus, ventral view **57** style, lateral view **58** abdominal apodemes **59** connective.

**Specimen examined. Holotype:** ♂, CHINA, Guizhou Prov., Wujiang, 19.V.2017, coll. Chang Han and Bin Yan, on walnut (GUGC). **Paratypes:** 5♂♂, 7♀♀, same data as holotype on walnut; 50♂♂61♀♀, CHINA, Guizhou Prov., Xiuwen, 19.VII.2017, coll. Chang Han and Bin Yan, on kiwi (GUGC)

**Etymology.** The new species name is derived from the Latin words “robustus” and “penis”, and refers to the robust aedeagal shaft in lateral view.

**Remarks.** The new species can be distinguished from *A. (A.) luojishangensis* Zhang & Song, 2022 by the aedeagus with strongly laterally compressed shaft “C” shaped; the paired basal processes fused for 2/3 of their length like a forked tongue (Figs 50–51, 55–56); and the preatrium with a thorn-like basal projection.

**Host.** *Actinidia chinensis* Planch (kiwi fruit); *Juglans regia* L. (walnut).

## Additional information

### Conflict of interest

The authors have declared that no competing interests exist.

### Ethical statement

No ethical statement was reported.

### Funding

The study was supported by the Program of Natural Science Foundation of China (No. 32360393, 31802002), Guizhou Province Science and Technology Innovation Talent Team Project (Qian Ke He Pingtai Rencai-CXTD [2021]-004) and the Basic Research Program (the natural science projects) of Guizhou Province (ZK[2022]-125).

### Author contributions

Conceptualization: XY, CH. Data curation: CH. Formal analysis: CH. Funding acquisition: XY, MY. Investigation: CH, BY. Methodology: CH. Project administration: CH. Writing - original draft: CH. Writing - review and editing: MW, XY, MY.

### Author ORCIDs

Bin Yan  <https://orcid.org/0000-0002-5290-4576>

Maofa Yang  <https://orcid.org/0000-0002-5523-6825>

Michael D. Webb  <https://orcid.org/0000-0000-0000-0000>

### Data availability

All of the data that support the findings of this study are available in the main text.

## References

- Cao YH, Dmitriev DA, Dietrich CH, Zhang YL (2019) New taxa and new records of Erythroneurini from China (Hemiptera: Cicadellidae: Typhlocybinae). *Acta Entomologica Musei Nationalis Pragae* 59(1): 189–210. <https://doi.org/10.2478/aemnp-2019-0017>
- Dietrich CH (2005) Keys to the families of Cicadomorpha and subfamilies and tribes of Cicadellidae (Hemiptera: Auchenorrhyncha). *The Florida Entomologist* 88(4): 502–517. [https://doi.org/10.1653/0015-4040\(2005\)88\[502:KTTFOC\]2.0.CO;2](https://doi.org/10.1653/0015-4040(2005)88[502:KTTFOC]2.0.CO;2)
- Dmitriev DA, Anufriev GA, Bartlett CR, Blanco-Rodríguez E, Borodin OI, Cao YH, Deitz LL, Dietrich CH, Dmitrieva MO, El-Sonbati SA, Evangelista de Souza O, Gjonov IV,

- Gonçalves AC, Hendrix S, McKamey S, Kohler M, Kunz G, Malenovský I, Morris BO, Novoselova M, Pinedo-Escatel JA, Rakitov RA, Rothschild MJ, Sanborn AF, Takiya DM, Wallace MS, Zahniser JN (2022) [onward] World Auchenorrhyncha Database. Taxon-Pages. <https://hoppers.speciesfile.org> [Retrieved on 2024-02-21]
- Dworakowska I (1972) On some Oriental Erythroneurini (Auchenorrhyncha, Cicadellidae, Typhlocybinae). Bulletin de l'Académie Polonaise des Sciences. Série des Sciences Biologiques 20(6): 395–405.
- Dworakowska I (1993) Remarks on *Alebra* Fieb. And Eastern Hemisphere Alebrini (Auchenorrhyncha: Cicadellidae: Typhlocybinae). Entomotaxonomia 15(2): 91–121.
- Dworakowska I, Viraktamath CA (1975) On some Typhlocybinae from India (Auchenorrhyncha, Cicadellidae). Bulletin de l'Académie Polonaise des Sciences. Série des Sciences Biologiques 23(8): 521–530.
- Jiang J, Luo GM, Song YH (2021) Two new species of the genus *Arboridia* Zachvatkin from China (Hemiptera: Cicadellidae: Typhlocybinae). Zootaxa 3(3): 349–357. <https://doi.org/10.11646/zootaxa.5005.3.9>
- Matsumura S (1932) A revision of the Palaearctic and Oriental Typhlocybid-genera with descriptions of new species and new genera. Insecta Matsumurana 6(3): 93–120.
- Pu TY, Wang JQ, Song YH (2023) Two new species of Erythroneurini from China (Hemiptera: Cicadellidae: Typhlocybinae). Zootaxa 5374(2): 295–300. <https://doi.org/10.11646/zootaxa.5374.2.8>
- Sohi AS, Sandhu PK (1971) *Arborifera* - a new subgenus of *Arboridia* Zachv. (Typhlocybinae, Cicadellidae) from Punjab, India, with description of its immature stages. Bulletin de l'Académie Polonaise des Sciences. Série des Sciences Biologiques 19(6): 401–406.
- Song YH, Li ZZ (2013) Some new species and new record of the genus *Arboridia* Zachvatkin (Hemiptera: Cicadellidae: Typhlocybinae) from six provinces of China. Zootaxa 3613(3): 229–244. <https://doi.org/10.11646/zootaxa.3613.3.2>
- Song YH, Li ZZ, Dietrich CH (2016) Contribution to knowledge of Typhlocybinae (Hemiptera: Cicadellidae) in Thailand: first record of genus *Arboridia* Zachvatkin with description of three new species and a new synonymy. Zootaxa 4171(2): 357–364. <https://doi.org/10.11646/zootaxa.4171.2.8>
- Zachvatkin AA (1946) Studies on the Homoptera of Turkey. I–VII. Transactions of the Royal Entomological Society of London 97(6): 149–176. <https://doi.org/10.1111/j.1365-2311.1946.tb00278.x>
- Zhang N, Jiang J, Song YH (2022) Two new species of the genus *Arboridia* Zachvatkin from karst area of southwestern China (Hemiptera: Cicadellidae: Typhlocybinae). Journal of Asia-Pacific Entomology 25(3): 101970. <https://doi.org/10.1016/j.aspen.2022.101970>



# A new species of freshwater snail of *Fenouilia* (Gastropoda, Pomatiopsidae) from northern Guangxi, China, based on morphological and DNA evidence

Hui Chen<sup>1</sup>, Yue Ming He<sup>2</sup>, Chong Rui Wang<sup>2</sup>, Da Pan<sup>1</sup>

<sup>1</sup> Jiangsu Key Laboratory for Biodiversity and Biotechnology, College of Life Sciences, Nanjing Normal University, Nanjing, 210023, China

<sup>2</sup> Hunan Fisheries Science Institute, 728 Shuanghe Road, Changsha, 410153, China

Corresponding authors: Da Pan ([dapan@njnu.edu.cn](mailto:dapan@njnu.edu.cn)); Chong Rui Wang ([hunanfish@163.com](mailto:hunanfish@163.com))

## Abstract

A new species of pomatiopsid freshwater snail, *Fenouilia undata* Chen & He, **sp. nov.**, is described from Guangxi, China, based on morphological and molecular evidence. The new species can be distinguished from its congeners by the following combination of characters: shell with low, prosocline, rounded axial ribs and fine spiral striae, broader than high; aperture broader than shell height; radula with lateral teeth have only two or three faint, wavy ridges on inner side. A molecular analysis of partial mitochondrial COI and 16S DNA sequences supports the systematic position of the new taxon.

**Key words:** Diversity, southern China, taxonomy, Triculinae



Academic editor: Frank Köhler

Received: 9 October 2023

Accepted: 17 February 2024

Published: 28 March 2024

ZooBank: <https://zoobank.org/OCA6C4A7-1E47-45FF-9D44-2422AE8B0A68>

**Citation:** Chen H, He YM, Wang CR, Pan D (2024) A new species of freshwater snail of *Fenouilia* (Gastropoda, Pomatiopsidae) from northern Guangxi, China, based on morphological and DNA evidence. ZooKeys 1196: 271–283. <https://doi.org/10.3897/zookeys.1196.113856>

Copyright: © Hui Chen et al.

This is an open access article distributed under terms of the Creative Commons Attribution License ([Attribution 4.0 International – CC BY 4.0](https://creativecommons.org/licenses/by/4.0/)).

## Introduction

Pomatiopsidae Stimpson, 1865 is a family of minute snails with shells usually 1–10 mm high. However, a few species can reach up to 20 mm in high. Typically, pomatiopsids inhabit rivers and streams, while some species also occur in brackish water or even in damp places on land (Liu et al. 1993; Lydeard and Cummings 2019). Shells of pomatiopsids vary in shape from spherical to oval, conical, or tower-shaped (Liu et al. 1979a). The Pomatiopsidae is widely distributed in Asia, South America, North America, Africa, and Australia. It is one of the most species-rich freshwater gastropod families, with approximately 36 recognized genera (Gerlach 2003; Ho and Dang 2010; Lydeard and Cummings 2019). There two main hypotheses about the origin of the Pomatiopsidae are that they originated in either Gondwanaland origin (Davis 1979) or Australia (Attwood 2009); neither of these hypotheses has been completely rejected yet by multilocus phylogenetic analyses (Kameda and Kato 2011; Wilke et al. 2013). The genus and species-level classification are poorly understood (Lydeard and Cummings 2019).

The tropical hills and rivers of China have rich biodiversity and are home to many species of freshwater snails. With at least 18 genera, China has the highest species richness of Pomatiopsidae in the world (Fulton 1904; Kang 1983; Davis et al. 1984; Davis et al. 1990; Davis et al. 1992; Zhang et al. 1997; Xiong and Li 2008; Lydeard and Cummings 2019).

In China, Pomatiopsidae are mainly distributed in the southwestern region (Shu et al. 2014), but the biodiversity of these freshwater snails is likely underestimated, especially in remote regions. Guangxi Province is in southwestern China, and 44 species of freshwater gastropods have been recorded from there (Liang 2023). However, only two genera of Pomatiopsidae have been recorded so far; *Oncomelania* (Gredler, 1881) and *Tricula* (Benson, 1843) occur in mountainous streams in the north of the province (Liu et al. 1979b).

In a recent survey in the Longjiang River, Hechi City, Guangxi, China, a new species of freshwater snail belonging to the genus *Fenouilia* Heude, 1889 was discovered. On comparison of its morphological traits with those of other freshwater snails known from this area, we conclude that this species is indeed undescribed. The new species can be distinguished from its congener *Fenouilia kreitneri* (Neumayr, 1880) by having low, rounded axial ribs on its shell, which is unique to this species. Molecular phylogenetic analyses, based on partial sequences of the mitochondrial 16S rRNA (16S) and COI genes, provide additional evidence supporting the novelty of this species. Our study contributes to a better understanding of pomatiopsid diversity in China and encourages the further exploration of freshwater gastropods in the region.

## Materials and methods

### Materials and morphological examination

All specimens were collected by hand in August 2022 and March 2023 on the Longjiang River, Yizhou District, Hechi City, Guangxi Province, China (Fig. 1). They were preserved in 95% ethanol and have been deposited in the Jiangsu Key Laboratory for Biodiversity and Biotechnology, Nanjing Normal University (NNU), Nanjing, China.

Before taking any action, preserved samples were soaked overnight in a saline solution. The tissue was extracted using anatomical needles. The shell and operculum were cleaned with a fine brush and then flushed with distilled water and photographed under a Nikon SMZ645 stereomicroscope. For traditional morphometrics, we measured five shell characteristics to the nearest 0.01 mm

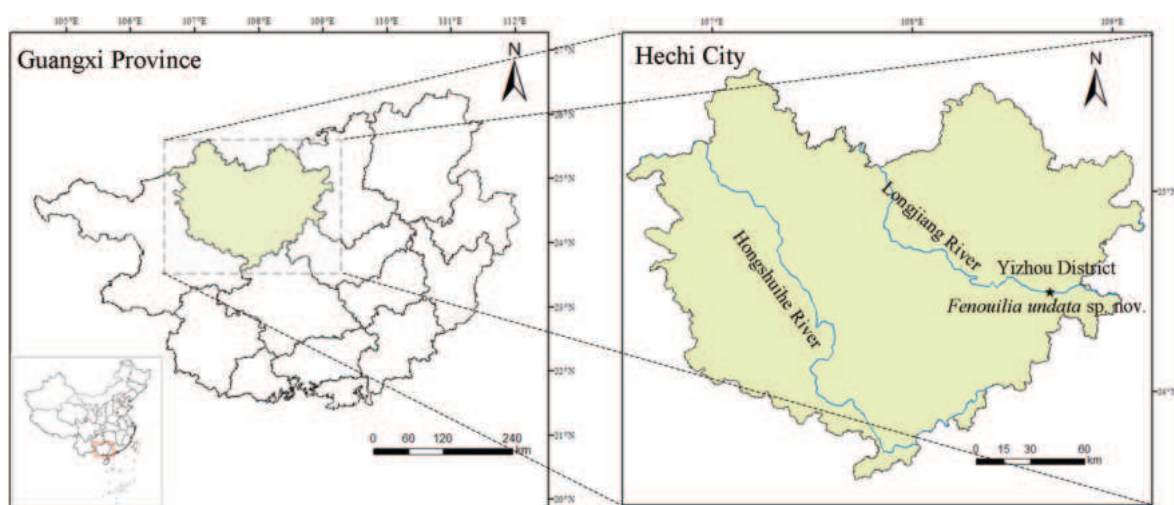


Figure 1. Known distribution of *Fenouilia undata* sp. nov. (Hechi City), and collection site (Longjiang River).

for each individual using digital calipers as follows: (1) shell height (**H**), which is the maximum dimension parallel to the axis of coiling; (2) shell width (**W**), the maximum dimension perpendicular to H; (3) length of aperture (**LA**), the maximum dimension from the junction of the outer lip with the penultimate whorl to the anterior lip; (4) width of aperture (**WA**), the maximum dimension perpendicular to LA; and (5) height of the body whorl (**BW**), the dimension from the lower margin of the aperture to the upper suture delimiting the first whorl. Other terminology used follows Liu et al. (1979a), Strong (2011), and Du et al. (2019).

Radulae were dissected from the buccal masses of three specimens and cleaned enzymatically with proteinase K following Du and Yang (2023); they were sonicated, mounted on aluminum specimen stubs with adhesive pads, and then observed using a JEOL JSM5610LV scanning electron microscope (**SEM**).

### DNA extraction, PCR amplification, and phylogenetic analyses

Total genomic DNA was extracted from foot tissue of three ethanol-preserved specimens using a Trelief TM Animal Genomic DNA kit (Tsingke®). Partial sequences of 16S rDNA were amplified using the universal primer set 16Sar CG-CCTGTTTATCAAAAACAT and 16Sbr CCGGTCTGAACTCAGATCACGT (Kessing et al. 1989). Partial sequences of COI were amplified using LCO1490 GCTCAA-CAAATCATAAAGATATT (Folmer et al. 1994) and HCO2198 TAWACTTCTGGT-GKCCAAARAAAT (Glaubrecht and Rintelen von 2003).

Each PCR reaction was performed in a total volume of 20 µL, including 9 µL of PCR mix, 8 µL of double distilled water, 1 µL of each primer and 1 µL of the DNA template. The PCR conditions were as follows: initial denaturation at 95 °C for 3 min; 35 cycles of denaturation at 95 °C for 40 s, annealing at 55 °C for 30 s and extension at 72 °C for 30 s; and final extension at 72 °C for 7 min. Both ends of sequences were obtained by automated sequencing using Applied Biosystems 3730 in Sangon Biotech Co. Ltd (Shanghai, China). In addition, two individuals of *Lithoglyphopsis modesta* (Gredler, 1886) and one of *Fenouilia kreitneri* (Neumayr, 1880) had their 16S rDNA extracted in this study.

To clarify the generic relationship of the new species, we included 16 sequences generated in this study with addition of 16S and COI gene sequences of 49 specimens representing 26 genera and 41 species, which were downloaded from GenBank (Table 1); *Lithoglyphus naticoides* (L. Pfeiffer, 1828) was used as the outgroup. Sequences obtained in the present study have been deposited in GenBank (for accession numbers, see Table 1). Sequences were aligned using MAFFT v. 7.505 based on the L-INS-i method (Kato and Toh 2008). Pairwise distances between species were calculated using MEGA X (Kumar et al. 2018). The 16S rDNA and COI were concatenated in PHYLOSUITE v. 2.3 (Zhang et al. 2020).

The best-substitution model was selected using the corrected Bayesian information criterion (BIC) in MODELFINDER v. 2.2.0 (Kalyaanamoorthy et al. 2017). For Bayesian analysis, two runs were performed simultaneously with four Markov chains starting from a random tree. Bayesian-inference and maximum-likelihood analyses were performed using MrBayes v. 3.2.7 (Ronquist et al. 2012) and IQTREE v. 2.2 (Minh et al. 2020), respectively, with reference to the selected model of sequence evolution. Bayesian posterior probabilities (BPPs) of nodes were determined using Metropolis-coupled Markov chains (one cold chain) for 2 million generations, with sampling every 1,000 generations. The first 25% of sampled trees were

**Table 1.** Nucleotide compositions of partial 16S rDNA and COI sequences of specimens investigated in this study.

Genus	Species	GenBank		References
		16S	COI	
<i>Lithoglyphus</i>	<i>Lithoglyphus naticoides</i>	AF445341	AF445332	Hausdorf et al. 2003
<i>Bythinella</i>	<i>Bythinella austriaca</i>	FJ028832	FJ028942	Benke et al. 2009
	<i>Bythinella austriaca</i>	FJ028831	FJ028943	
	<i>Bythinella carinulata</i>	FJ028884	FJ029100	
<i>Paludinella</i>	<i>Paludinella minima</i>	AB822685	AB822663	Wada et al. 2013
	<i>Paludinella minima</i>	AB822686	AB822664	
	<i>Paludinella kuzuensis</i>	AB822695	AB822675	
<i>Erhaia</i>	<i>Erhaia jianouensis</i>	AF212894	AF213340	Wilke et al. 2000
	<i>Erhaia wangchuki</i>	KY798003	MT237715	Gittenberger et al. 2020
<i>Akiyoshia</i>	<i>Akiyoshia kobayashii</i>	AB611822	AB611823	Kameda and Kato 2011
<i>Bithynia</i>	<i>Bithynia tentaculata</i>	FJ160288	JX970605	Wilke et al. 2013
<i>Pomatiopsis</i>	<i>Pomatiopsis lapidaria</i>	AY676118	AF367636	Wilke et al. 2001
<i>Robertsia</i>	<i>Robertsia</i> sp.	AF531548	AF531550	Attwood et al. 2003
<i>Pachydrobia</i>	<i>Pachydrobia munensis</i>	KC832721	KC832700	Liu et al. 2014
	<i>Pachydrobia</i> sp.	KC832711	KC832690	
<i>Jullienia</i>	<i>Jullienia rolfbrandti</i>	KC832718	KC832697	
<i>Hubendickia</i>	<i>Hubendickia schuetti</i>	KC832709	KC832688	
	<i>Hubendickia spiralis</i>	KC832710	KC832689	
<i>Jinghongia</i>	<i>Jinghongia jinghongensis</i>	KC832728	KC832707	
<i>Manningiella</i>	<i>Manningiella velimirovici</i>	KC832716	KC832695	
	<i>Manningiella conica</i>	KC832719	KC832698	
	<i>Manningiella polita</i>	KC832715	KC832694	
<i>Tricula</i>	<i>Tricula bamboensis</i>	KC832720	KC832699	
	<i>Tricula ludongbini</i>	KC832717	KC832696	
	<i>Tricula hudiequanensis</i>	KC832712	KC832691	
	<i>Tricula hongshanensis</i>	EF394876	EF394896	Guan et al. 2008
<i>Oncomelania</i>	<i>Oncomelania hupensis robertsoni</i>	DQ212900	DQ212855	Wilke et al. 2006
	<i>Oncomelania hupensis robertsoni</i>	DQ212901	DQ212856	
	<i>Oncomelania minima</i>	AB611790	AB611795	Kameda and Kato 2011
<i>Blanfordia</i>	<i>Blanfordia integra</i>	AB611722	AB611723	
	<i>Blanfordia japonica japonica</i>	AB611726	AB611727	
<i>Cecina</i>	<i>Cecina manchurica</i>	AB611746	AB611747	
	<i>Cecina manchurica</i>	AB611742	AB611743	
<i>Neotricula</i>	<i>Neotricula burchi</i>	AF531542	AF531544	Attwood et al. 2003
	<i>Neotricula aperta</i>	MF663277	MF663265	Attwood et al. 2019
<i>Gammatricula</i>	<i>Gammatricula fujianensis</i>	AF212896	AF213342	Wilke et al. 2000
	<i>Gammatricula shini</i>	AB611798	AB611799	Kameda and Kato 2011
	<i>Gammatricula chinensis</i>	EU573993	AF253067	Wilke et al. 2000
<i>Lacunopsis</i>	<i>Lacunopsis munensis</i>	KC832726	KC832705	Liu et al. 2014
<i>Delavaya</i>	<i>Delavaya dianchiensis</i>	KC832713	KC832692	
<i>Paraprososthenia</i>	<i>Paraprososthenia levayi</i>	KC832708	KC832687	
<i>Lithoglyphopsis</i>	<i>Lithoglyphopsis modesta</i>	OR515659	PP327217	This study
	<i>Lithoglyphopsis modesta</i>	OR515660	PP327222	
<i>Fenouilia</i>	<i>Fenouilia kreitneri</i>	OR515658	PP340173	
	<i>Fenouilia undata</i> sp. nov.	OR515661	PP333612	
	<i>Fenouilia undata</i> sp. nov.	OR515662	PP333613	
	<i>Fenouilia undata</i> sp. nov.	OR515663	PP333614	
<i>Kunmingia</i>	<i>Kunmingia kunmingensis</i>	OR784230	OR780554	
	<i>Kunmingia kunmingensis</i>	OR784231	OR780555	

discarded as burn-in when the standard deviation of split frequencies of the two runs was less than 0.01; the remaining trees were then used to create a 50% majority-rule consensus tree and to estimate BPPs. Node support for the maximum-likelihood analysis was determined using 1000 rapid bootstrap (BS) replicates.

Furthermore, to investigate the behavior of the new species, six individuals were maintained in an artificial field environment within the laboratory of Hunan Fisheries Science Institute for one year.

## Results

### Family Pomatiopsidae Stimpson, 1865

### Subfamily Pomatiopsinae Stimpson, 1865

### Genus *Fenouilia* Heude, 1889

#### *Fenouilia undata* Chen & He, sp. nov.

<https://zoobank.org/fffc0cf5-3700-45fe-8905-c9b9698358e0>

**Materials examined. Holotype:** CHINA • Guangxi Province, Hechi City, Yizhou District, Longjiang River; 24.4927°N, 108.6851°E; August 2022; Xu Cheng Wei & Yue Ming He leg.; NNU230701 (Fig. 2A–D), shell height 3.39 mm. **Paratypes:** CHINA • 2 specimens; same locality data as holotype; August 2022; NNU230702–03 • \_2\_ specimens; same locality data as holotype; March 2023; NNU230704–05. Shell height of all paratypes: 3.04–3.44 mm (Fig. 2E–P, Table 2).

**Diagnosis.** Shell small, thin but solid, with rounded, rather flattened shape, and width greater than height; sculptured with low, rounded axial ribs and fine spiral striae; whorls 4–5; body whorl swollen and large. Suture shallow; umbilicus narrow, crescent-shaped or closed. Aperture large, its length greater than shell height. Operculum ovate, corneous, slightly transparent, yellowish.

**Description.** Shell small, 3.04–3.44 mm high, thin but solid, with a rounded, rather flattened shape; whorls 4–5; body whorl swollen and large, taking up most (about 84–94%) of shell; whorls of spire rapidly expanding. Shell width longer than shell height (Fig. 2). Apex obtuse, usually eroded. Suture low. Shell amber-yellow, with low, prosocline, rounded axial ribs and fine spiral striae. Aperture round, large, broader than shell height. Lip slightly thickened; inner lip smooth, white; outer lip white or yellowish and slightly rolled outward. Umbilicus narrowly crescent-shaped or closed; base white (Fig. 2A–N).

Operculum ovate, smaller than aperture, corneous, thin, slightly transparent, yellowish, length 1.86–2.12 mm, width 1.53–1.72 mm; surface, including nucleus, of operculum smooth; nucleus located at bottom left third (Fig. 2O, P).

**Table 2.** Measurements of *Fenouilia undata* sp. nov. (in mm). Abbreviations: W, shell width; BW, height of the body whorl; H, shell height; LA, length of aperture; WA, width of aperture.

	Number	H	W	LA	WA	BW
Holotype	NNU230701	3.39	4.95	3.63	2.64	2.84
Paratype 1	NNU230702	3.25	4.67	3.44	2.43	3.07
Paratype 2	NNU230703	3.44	4.68	3.49	2.61	2.92
Paratype 3	NNU230704	3.07	4.37	3.22	2.49	2.81
Paratype 4	NNU230705	3.04	4.01	3.06	2.26	2.74

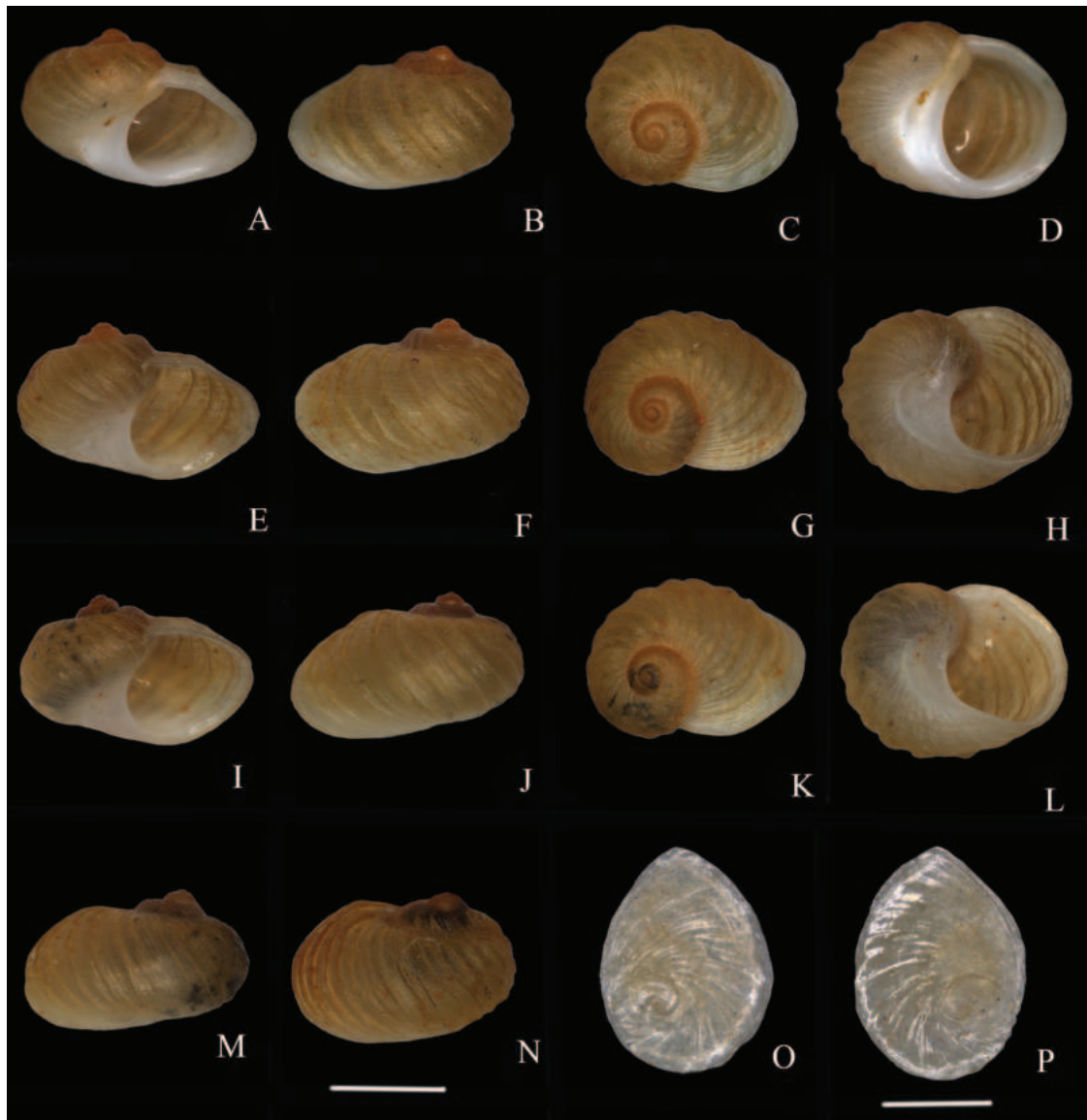


**Figure 2.** *Fenouilia undata* sp. nov. shells and operculum **A–D** holotype, NNU230701 **E–H** paratype, NNU230702 **I–L** paratype, NNU230703 **M** paratype, NNU230704 **N** paratype, NNU230705 **O, P** operculum, holotype, NNU230701. Scale bars: 2 mm (**A–N**); 1 mm (**O–P**).

Radula small; ribbon approximately 0.88 mm long. Central tooth with one large, triangular, pointed major cusp without serrations, with two small, sharp cusps on either side at base. Inner side of lateral teeth with two or three faint, wavy ridges; outer side smooth. Inner marginal teeth with five or six small cusps. Outer marginal teeth with 6–8 small cusps (Fig. 3).

Tentacles short, white; snout stubby, white, black pigmented. Mantle smooth, light gray, with small black spots. Intestine wider than base of tentacle; digestive gland milky white. Penis translucent white, thin, coiled, located behind right tentacle in neck area (Fig. 4).

**Habitat and distribution.** The new species was discovered in the Longjiang River, where the depth of the water was less than 5 m, water flow is variable, and the substrate is composed of large stones (Fig. 5).

**Biology.** In the laboratory aquarium, the new species fed on algae present on the surface of stones or watergrass. Snails reproduced many times during their

year in captivity. Each brownish egg was laid 1.5 mm from the next. Eggs were affixed to the surfaces of rocks with a secretion. In some months, some individuals were observed to occasionally perform a “dance” in which they repeatedly twisted their shells clockwise or counterclockwise. They were more active at night.

**Remarks.** The genus *Fenouilia* was established by Heude (1889) for *Fenouilia bicingulata* (Heude, 1889) from Dali, Yunnan, China; this species has a trochoidal shell, with rough, raised prosocline growth lines and no umbilicus. Subsequently, Davis et al. (1983) considered *F. bicingulata* to be a synonym of *F. kreitneri* (Neumayr, 1880); thus, the genus was thought to contain only a single species, until now. With prosocline axial ribs, triangular central tooth, and narrowly crescent-shaped or absent umbilicus, the new species is similar to *F. kreitneri*. However, the new species can be distinguished by its broader shell. In addition, *F. undata* sp. nov. has shorter tentacles (vs longer tentacles in *F. kreitneri*), and there are three ridges only on the inner side (vs. lateral teeth with obvious ridges on both sides). The adult shell of *F. undata* sp. nov. is similar to that of *Lacunopsis munensis* (Brandt, 1968) and *Lithoglyphopsis modesta* (Gredler, 1886). These species differ in the relative length of the aperture to shell height (the aperture is longer than shell height in *F. undata*, but shorter in *L. munensis*) and in relative shell width (the shell is broader than height in *F. undata*, but narrower in *L. modesta*).

**Molecular results.** The concatenation of COI and 16S rDNA yielded 1229 sites. The GTR+F+R5 model was selected as the best-fit of nucleotide substitution by BIC. Phylogenetic analyses revealed BI and ML trees with largely consistent topologies (Figs 6, 7). The average 16S genetic distance (uncorrected

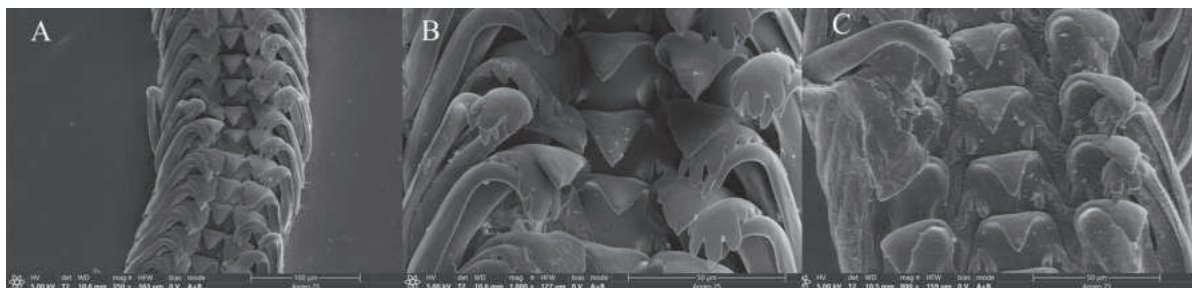


Figure 3. Radula of *Fenouilia undata* sp. nov. **A** frontal view of radula **B, C** magnified view of radula.

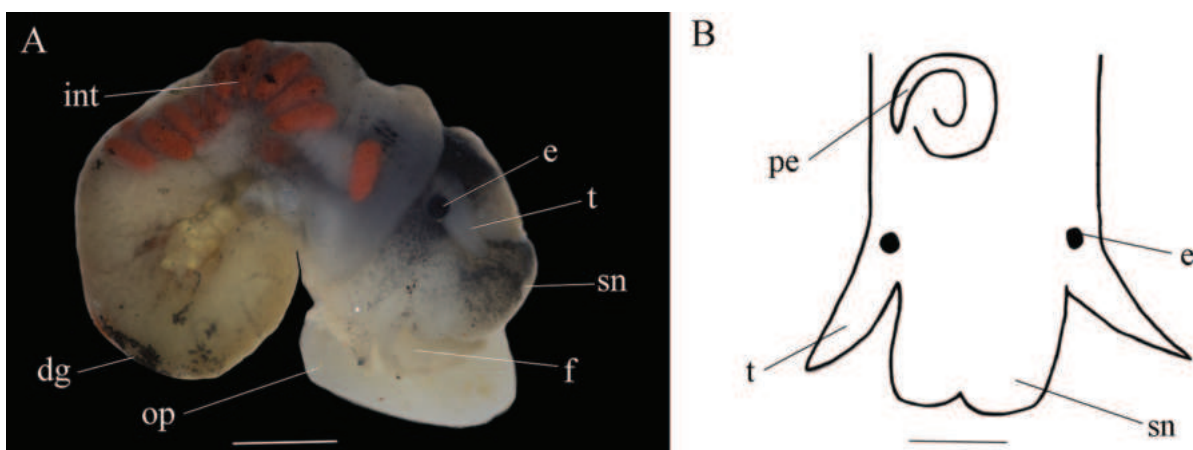


Figure 4. *Fenouilia undata* sp. nov. **A** dissection with labelled structures of female **B** head of male. Abbreviations: e, eye; t, tentacle; sn, snout; f, foot; op, operculum; dg, digestive gland; int, intestine; pe, penis. Scale bars: 1 mm (**A**); 0,5 mm (**B**).

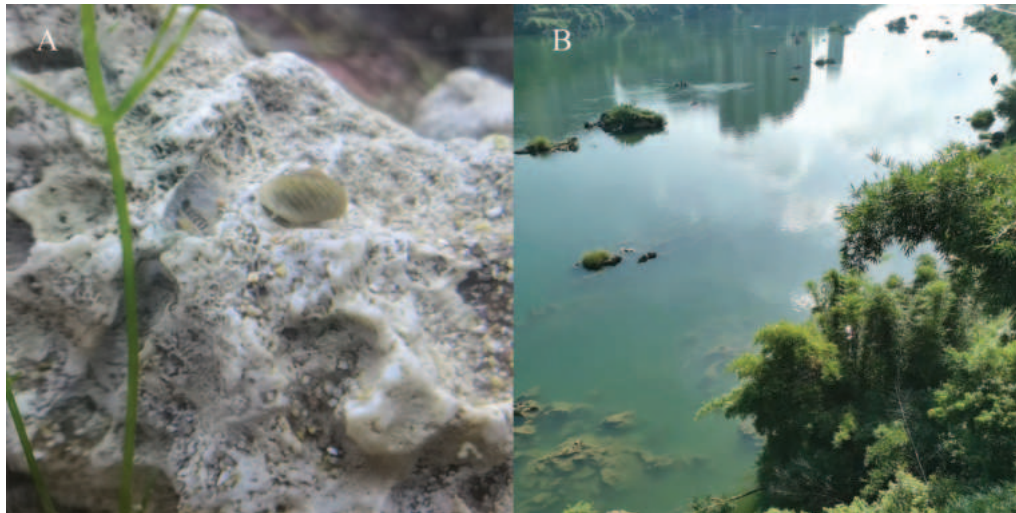


Figure 5. *Fenouilia undata* sp. nov. A color in life B natural habitat. Photographs by Xu Cheng Wei and Yue Ming He.

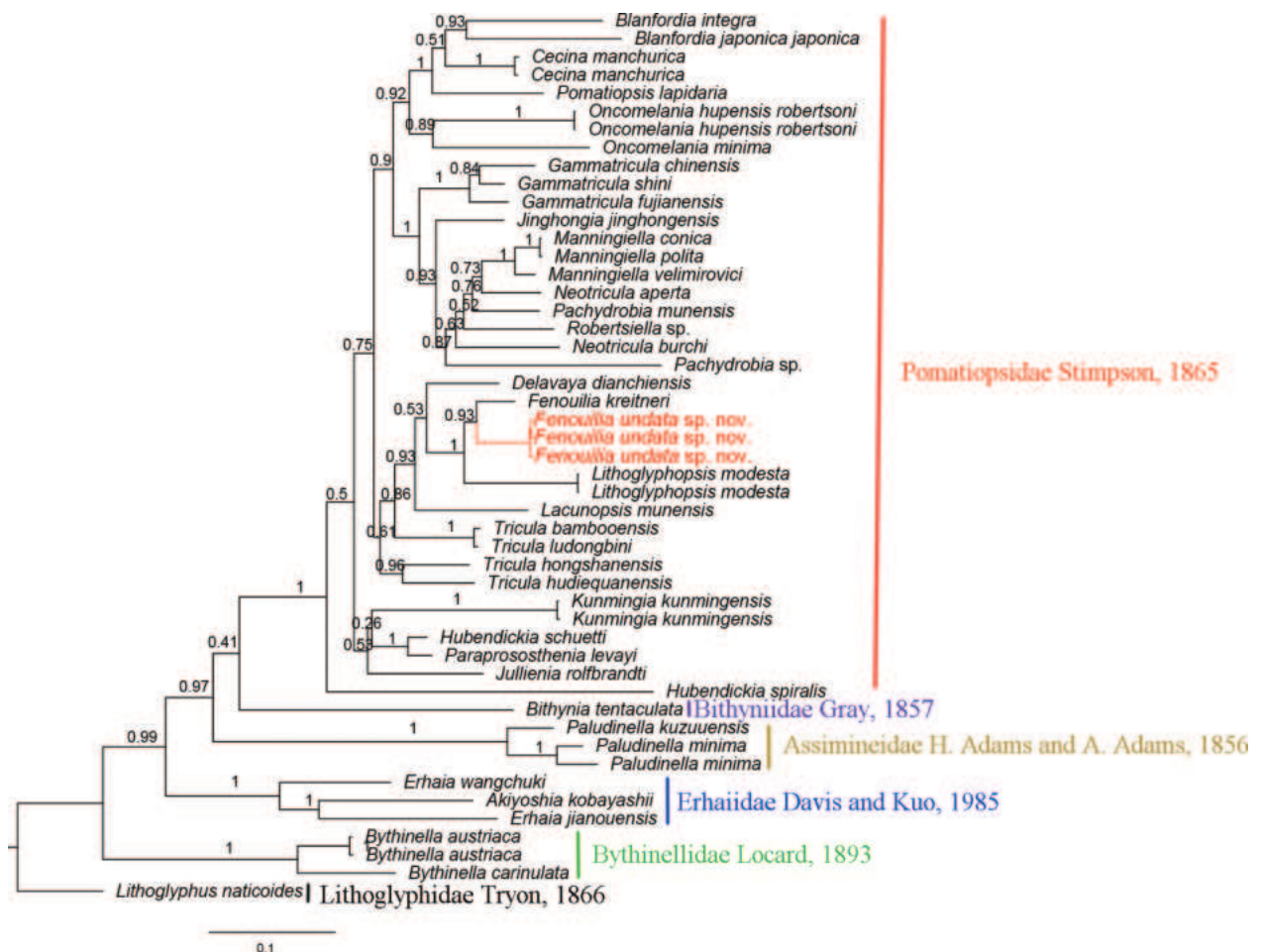
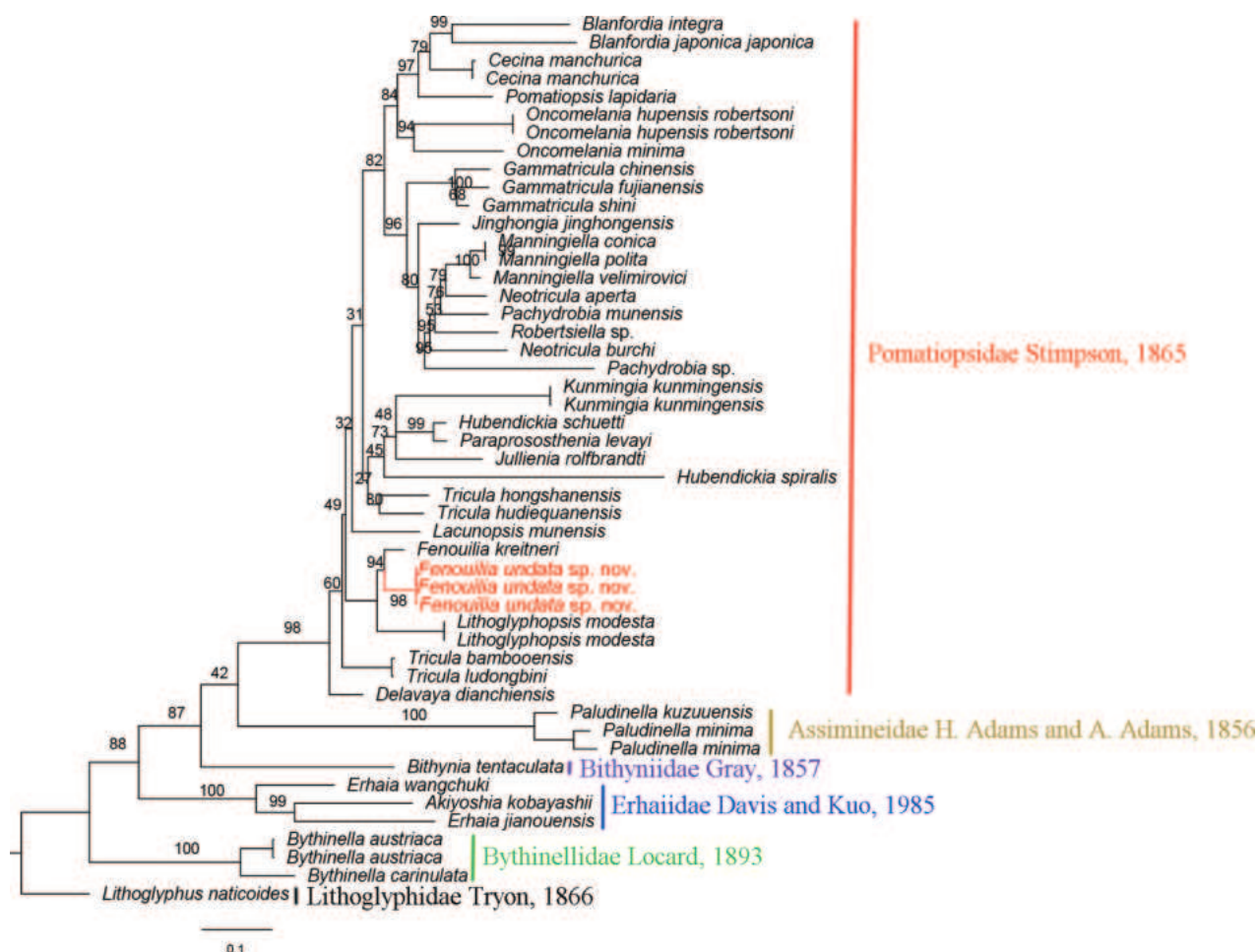


Figure 6. Bayesian-inference (BI) tree inferred from concatenated 16S and COI gene sequences. Posterior probabilities are shown on the left of nodes on the tree.

*p*-distance) between the *F. undata* sp. nov. and *F. kreitneri* is 1.04%; the COI *p*-distance is 6.96%.

**Etymology.** From the Latin adjective *undata* (wavy or wave-like form). We suggest the Chinese common name 波浪龙骨螺.



**Figure 7.** Maximum-likelihood (ML) tree inferred from concatenated 16S and COI gene sequences. Bootstrap supports are shown on the left of nodes on the tree.

## Discussion

The phylogenetic relationships and morphological traits found in this study support the placement of the new species in the genus *Fenouilia*. The prosocline axial ribs on the shell of the new species resemble the prominent, rough, raised prosocline growth lines present in *F. kreitneri*, and the radular of both species has a triangular central tooth without serrated cusps. The molecular phylogenies based on ML and BI analyses show that *Fenouilia undata* sp. nov. and *F. kreitneri* are nested in a monophyletic group with strong support (BS = 94%, BPP = 0.93) and sister to *Lithoglyphopsis modesta*.

Our phylogenetic tree includes all the genera in China except *Guoia* Davis & Chen, 1992, *Wuconchona* Kang, 1983, and *Parapyrgula* Annandale & Prashad, 1919. The new species can be distinguished from *Wuconchona niuzhuangensis* (Kang, 1983) and *Parapyrgula cogginii* (Annandale & Prashad, 1919) by the rounded, flattened shell with its width greater than height. The new species can be distinguished from *Guoia viridulula* (Möllendorff, 1888) by the presence of axial ribs on the shell and the aperture being longer than the shell height.

The hydrological environment is complex and heterogeneous in southern China. There are still many gaps in surveys for freshwater snails, and more new species have to be discovered. However, the freshwater-snail fauna has been

given little attention, especially the small species. With the environmental destruction and habitat modifications, many freshwater snails are gradually disappearing or becoming extinct (Du et al. 2011). Our study highlights the necessity and importance of further field surveys of freshwater snails which will help promote the conservation of freshwater ecosystems. We suggest that further intensified survey efforts are urgently required for accurate understanding of the freshwater snail diversity in southern China.

## Acknowledgements

We acknowledge Xu Cheng Wei from Guangxi for assistance in obtaining samples for this study. We are grateful to Kai Rui Jiao and Long Jie Xia from Nanjing Normal University for their help in image processing. We also extend our thanks to Yang Yang Li from Nanjing Normal University for assistance in DNA extraction.

## Additional information

### Conflict of interest

The authors have declared that no competing interests exist.

### Ethical statement

No ethical statement was reported.

### Funding

This research was funded by the Jiangsu Key Laboratory for Biodiversity and Biotechnology, College of Life Sciences, Nanjing Normal University, and the Hunan Fisheries Science Institute. Financial support from the National Natural Science Foundation of China (No. 32200356 to PD) and from the Natural Science Foundation of the Jiangsu Higher Education Institutions (No. 22KJB180018 to PD) is acknowledged.

### Author contributions

All authors have contributed equally.

### Author ORCIDs

Hui Chen  <https://orcid.org/0009-0004-5222-3975>

Yue Ming He  <https://orcid.org/0009-0002-9849-7977>

Chong Rui Wang  <https://orcid.org/0009-0009-2315-6941>

Da Pan  <https://orcid.org/0000-0001-5445-6423>

### Data availability

All of the data that support the findings of this study are available in the main text.

## References

Attwood SW (2009) Chapter 11 - Mekong schistosomiasis: Where did it come from and where is it going? In: Campbell IC (Ed.) *The Mekong: Biophysical Environment of an International River Basin*. Academic Press, New York, 276–297. <https://doi.org/10.1016/B978-0-12-374026-7.00011-5>

- Attwood SW, Ambu S, Meng XH, Upatham ES, Xu FS, Southgate VR (2003) The Phylogenetics of Triculine Snails (Rissooidea: Pomatiopsidae) from South-East Asia and Southern China: Historical biogeography and the transmission of human schistosomiasis. *The Journal of Molluscan Studies* 69(3): 263–271. <https://doi.org/10.1093/mollus/69.3.263>
- Attwood SW, Liu L, Huo GN (2019) Population genetic structure and geographical variation in *Neotricula aperta* (Gastropoda: Pomatiopsidae), the snail intermediate host of *Schistosoma mekongi* (Digenea: Schistosomatidae). *PLOS Neglected Tropical Diseases* 13(1): e0007061. <https://doi.org/10.1371/journal.pntd.0007061>
- Benke M, Brändle M, Albrecht C, Wilke T, BENKE M (2009) Pleistocene phylogeography and phylogenetic concordance in cold-adapted spring snails (*Bythinella* spp.). *Molecular Ecology* 18(5): 890–903. <https://doi.org/10.1111/j.1365-294X.2008.04073.x>
- Davis GM (1979) The origin and evolution of the gastropod family Pomatiopsidae, with emphasis on the Mekong River Triculinae. *Academy of Natural Sciences of Philadelphia Monograph* 20: 1–120. <https://doi.org/10.2307/2992315>
- Davis GM, Kuo YH, Hoagland KE, Chen PL, Yang HM, Chen DJ (1983) Advances in the systematics of the Triculinae (Gastropoda: Prosobranchia): The genus *Fenouilia* of Yunnan, China. *Proceedings. Academy of Natural Sciences of Philadelphia* 135: 177–199. <https://www.jstor.org/stable/4064803>
- Davis GM, Kuo YH, Hoagland KE, Chen PL, Yang HM, Chen DJ (1984) *Kunmingia*, a new genus of Triculinae (Gastropoda: Pomatiopsidae) from China: Phenetic and cladistic relationships. *Proceedings. Academy of Natural Sciences of Philadelphia* 136: 165–193. <https://www.jstor.org/stable/4064826>
- Davis GM, Liu YY, Chen YG (1990) New genus of *Triculinae* (Prosobranchia: Pomatiopsidae) from China: Phylogenetic relationships. *Proceedings of the Academy of Natural Sciences of Philadelphia* 142: 143–165. <https://www.jstor.org/stable/4064975>
- Davis GM, Chen CE, Wu C, Kuang TF, Xing XG, Li L, Liu WJ, Yan YL (1992) The Pomatiopsidae of Hunan, China (Gastropoda: Rissoacea). *Malacologia* 34(1–2): 143–342. <https://biostor.org/reference/100970>
- Du LN, Yang JX (2023) *Colored Atlas of Chinese Melani*. Henan Science and Technology Press, Zhengzhou, 10–15. [In Chinese]
- Du LN, Li Y, Chen XY, Yang JX (2011) Effect of eutrophication on molluscan community composition in the Lake Dianchi (China, Yunnan). *Limnologica* 41(3): 213–219. <https://doi.org/10.1016/j.limno.2010.09.006>
- Du LN, Chen J, Yu GH, Yang JX (2019) Systematic relationships of Chinese freshwater semisulcospirids (Gastropoda, Cerithioidea) revealed by mitochondrial sequences. *Zoological Research* 40(6): 541–551. <https://doi.org/10.24272/j.issn.2095-8137.2019.033>
- Folmer O, Black M, Hoeh W, Lutz R, Vrijenhoek R (1994) DNA primers for amplification of mitochondrial cytochrome c oxidase subunit I from diverse metazoan invertebrates. *Molecular Biotechnology* 3: 294–299. <https://pubmed.ncbi.nlm.nih.gov/7881515/>
- Fulton H (1904) On some species of *Melania* and *Jullienia* from Yunnan and Java. *The Journal of Malacology* 11: 51–52.
- Gerlach J (2003) New terrestrial Gastropoda (Mollusca) from the Seychelles. *Environmental Science and Biology* 11: 39–51. <https://api.semanticscholar.org/CorpusID:197409478>
- Gittenberger E, Leda P, Wangchuk J, Gyeltshen C, Bjorn ST (2020) The genera *Erhaia* and *Tricula* (Gastropoda, Rissooidea, Amnicolidae and Pomatiopsidae) in Bhutan and

- elsewhere in the eastern Himalaya. *ZooKeys* 929: 1–17. <https://doi.org/10.3897/zookeys.929.49987>
- Glaubrecht M, Rintelen von T (2003) Systematics and zoogeography of the pachychilid gastropod *Pseudopotamis* Martens, 1894 (Mollusca: Gastropoda: Cerithioidea): a limnic relict on the Torres Strait Islands, Australia? *Zoologica Scripta* 32: 415–435. <https://doi.org/10.1046/j.1463-6409.2003.00127.x>
- Guan F, Niu AO, Attwood SW, Li YL, Zhang B, Zhu YH (2008) Molecular phylogenetics of Triculine snails (Gastropoda: Pomatiopsidae) from southern China. *Molecular Phylogenetics and Evolution* 48(2): 702–707. <https://doi.org/10.1016/j.ympev.2008.04.021>
- Hausdorf B, Röpstorff P, Riedel F (2003) Relationships and origin of endemic Lake Baikal gastropods (Caenogastropoda: Risssooidea) based on mitochondrial DNA sequences. *Molecular Phylogenetics and Evolution* 26(3): 435–443. [https://doi.org/10.1016/S1055-7903\(02\)00365-2](https://doi.org/10.1016/S1055-7903(02)00365-2)
- Heude PM (1889) Diagnoses molluscorum novorum in Sinis collectorum. *Journal de Conchyliologie* 37(1): 40–50.
- Ho TH, Dang NT (2010) Contribution to the study on Triculinae snail group (Pomatiopsidae Mollusca) in Tay Nguyen Highland, Vietnam. *Tap Chi Sinh Vat Hoc* 32(4): 14–18. <https://doi.org/10.15625/0866-7160/v32n4.715>
- Kalyaanamoorthy S, Minh BQ, Wong TK, Von Haeseler A, Jermiin LS (2017) ModelFinder: Fast model selection for accurate phylogenetic estimates. *Nature Methods* 14(6): 587–589. <https://doi.org/10.1038/nmeth.4285>
- Kameda Y, Kato M (2011) Terrestrial invasion of pomatiopsid gastropods in the heavy-snow region of the Japanese Archipelago. *BMC Evolutionary Biology* 11(1): 118. <https://doi.org/10.1186/1471-2148-11-118>
- Kang ZB (1983) A new genus and three new species of the family Hydrobiidae (Gastropoda: Prosobranchia) from Hubei Province, China. *Oceanologia et Limnologia Sinica* 14(5): 499–505. <https://doi.org/10.5852/ejt.2017.328>
- Katoh K, Toh H (2008) Recent developments in the MAFFT multiple sequence alignment program. *Briefings in Bioinformatics* 9(4): 286–298. <https://doi.org/10.1093/bib/bbn013>
- Kessing B, Croom H, Martin A, McIntosh C, Owen Mcmillan W, Palumbi S (1989) *The simple fools guide to PCR*. University of Hawaii, Honolulu, 45 pp.
- Kumar S, Stecher G, Li M, Knyaz C, Tamura K (2018) MEGA X: Molecular evolutionary genetics analysis across computing platforms. *Molecular Biology and Evolution* 35(6): 1547–1549. <https://doi.org/10.1093/molbev/msy096>
- Liang M (2023) Biodiversity and Spatial Distribution of Freshwater Gastropods in Guangxi. Master's thesis, Guangxi Normal University, China. [in Chinese]
- Liu YY, Zhang WZ, Wang EY (1979a) Freshwater molluscs. In: YY Liu, WZ Zhang, YX Wang, EY Wang (Eds) *Economic Fauna of China*. Science press, Peking, 134 pp.
- Liu YY, Zhang WZ, Wang EY (1979b) Studies on *Tricula* (Prosobranchia: Hydrobiidae) from China. *Acta Zootaxonomica Sinica* 02: 135–140. [In Chinese]
- Liu YY, Zhang WZ, Wang YX (1993) *Medical malacology*. China Ocean Press, Beijing, 30–46. [In Chinese]
- Liu L, Huo GN, He HB, Zhou B, Attwood SW (2014) A phylogeny for the pomatiopsidae (Gastropoda: Risssooidea): a resource for taxonomic, parasitological and biodiversity studies. *BMC Evolutionary Biology* 14(1): 29. <https://doi.org/10.1186/1471-2148-14-29>
- Lydeard C, Cummings KS (2019) *Freshwater Mollusks of the world*. Johns Hopkins University Press, Baltimore, 242 pp. <https://doi.org/10.1353/book.66164>

- Minh BQ, Schmidt HA, Chernomor O, Schrempf D, Woodhams MD, von Haeseler A, Lanfear R (2020) IQ-TREE 2: New models and efficient methods for phylogenetic inference in the genomic era. *Molecular Biology and Evolution* 37(5): 1530–1534. <https://doi.org/10.1093/molbev/msaa015>
- Ronquist F, Teslenko M, van der Mark P, Ayres DL, Darling A, Höhna S, Larget B, Liu L, Suchard MA, Huelsenbeck JP (2012) MrBayes 3.2: Efficient Bayesian phylogenetic inference and model choice across a large model space. *Systematic Biology* 61(3): 539–542. <https://doi.org/10.1093/sysbio/sys029>
- Shu FY, Wang HJ, Cui YD, Wang HZ (2014) Species diversity and distribution patterns of freshwater molluscs in the Yangtze River Basin. *Acta Hydrobiologica Sinica* 30: 19–26. [In Chinese]
- Strong EE (2011) More than a gut feeling: utility of midgut anatomy and phylogeny of the Cerithioidea (Mollusca: Caenogastropoda). *Zoological Journal of the Linnean Society* 162(3): 585–630. <https://doi.org/10.1111/j.1096-3642.2010.00687.x>
- Wada S, Kameda Y, Chiba S (2013) Long-term stasis and short-term divergence in the phenotypes of microsnails on oceanic islands. *Molecular Ecology* 22(18): 4801–4810. <https://doi.org/10.1111/mec.12427>
- Wilke T, Davis GM, Gong X, Liu HX (2000) Erhaia (Gastropoda: Rissoidae): phylogenetic relationships and the question of Paragonimus coevolution in Asia. *The American Journal of Tropical Medicine and Hygiene* 62(4): 453–459. <https://doi.org/10.4269/ajtmh.2000.62.453>
- Wilke T, Davis GM, Falniowski A, Giusti F, Bodon M, Szarowska M (2001) Molecular systematics of Hydrobiidae (Mollusca: Gastropoda: Rissoidae): testing monophyly and phylogenetic relationships. *Proceedings of the Academy of Natural Sciences of Philadelphia* 151(1): 1–21. [https://doi.org/10.1635/0097-3157\(2001\)151\[0001:MSOHMG\]2.0.CO;2](https://doi.org/10.1635/0097-3157(2001)151[0001:MSOHMG]2.0.CO;2)
- Wilke T, Davis GM, Qiu D (2006) Extreme mitochondrial sequence diversity in the intermediate schistosomiasis host *Oncomelania hupensis robertsoni*: Another case of ancestral polymorphism? *Malacologia* 48(1): 143–157.
- Wilke T, Haase M, Hershler R, Liu LP, Misof B, Ponder WF (2013) Pushing short DNA fragments to the limit: Phylogenetic relationships of ‘hydrobioid’ gastropods (Caenogastropoda: Rissoidae). *Molecular Phylogenetics and Evolution* 66(3): 715–736. <https://doi.org/10.1016/j.ympev.2012.10.025>
- Xiong F, Li W (2008) Community structure and diversity of macrozoobenthos in Fuxian Lake, a deep plateau lake in Yunnan. *Biodiversity Science* 16(3): 288–297. <https://doi.org/10.3724/SP.J.1003.2008.07307>
- Zhang NG, Hao TX, Wu CY, Chen YX, Zhang W, Li JF, Zhang Y (1997) Primary investigation of freshwater Gastropoda in Yunnan Province. *Studia Marina Sinica* 39: 15–26. [In Chinese]
- Zhang D, Gao F, Jakovlić I, Zou H, Zhang J, Li WX, Wang GT (2020) PhyloSuite: An integrated and scalable desktop platform for streamlined molecular sequence data management and evolutionary phylogenetics studies. *Molecular Ecology Resources* 20(1): 348–355. <https://doi.org/10.1111/1755-0998.13096>



# A new loach species of the genus *Oreonectes* (Teleostei, Cypriniformes, Nemacheilidae) from Guangxi, China

Xue-Ming Luo<sup>1,2</sup>, Rui-Gang Yang<sup>3</sup>, Li-Na Du<sup>1,2</sup>, Fu-Guang Luo<sup>4</sup>

1 Key Laboratory of Ecology of Rare and Endangered Species and Environmental Protection (Guangxi Normal University), Ministry of Education Guilin 541004, China

2 Guangxi Key Laboratory of Rare and Endangered Animal Ecology, College of Life Science, Guangxi Normal University, Guilin 541004, China

3 Scientific Research Academy of Guangxi Environmental Protection, Nanning, Guangxi 530022, China

4 Liuzhou Aquaculture Technology Extending Station, Liuzhou 545006, China

Corresponding authors: Li-Na Du ([dulina@mailbox.gxnu.edu.cn](mailto:dulina@mailbox.gxnu.edu.cn)); Fu-Guang Luo ([luofuguang3563@163.com](mailto:luofuguang3563@163.com))

## Abstract

A new loach species, *Oreonectes andongensis* **sp. nov.** is described from the Guangxi Zhuang Autonomous Region, China. The new species can be differentiated from other members of the genus by combinations of characters: a developed posterior chamber of the swim bladder, 13–14 branched caudal-fin rays, 8–16 lateral-line pores, body width 12–15% of standard length (SL), interorbital width 42–47% of head length (HL), and caudal peduncle length 11–16% of SL. Bayesian inference phylogenetic analysis based on mitochondrial Cyt *b* provided strong support for validity of *O. andongensis* **sp. nov.** (uncorrected *p*-distance 6.0–7.5%).

**Key words:** New species, morphology, phylogeny, taxonomy, Xijiang River



Academic editor: Nina Bogutskaya

Received: 20 July 2023

Accepted: 12 February 2024

Published: 28 March 2024

ZooBank: <https://zoobank.org/3218C5F9-C9A4-4A57-BB82-67800B9F48F3>

**Citation:** Luo X-M, Yang R-G, Du L-N, Luo F-G (2024) A new loach species of the genus *Oreonectes* (Teleostei, Cypriniformes, Nemacheilidae) from Guangxi, China. ZooKeys 1196: 285–301. <https://doi.org/10.3897/zookeys.1196.109810>

**Copyright:** © Xue-Ming Luo et al.

This is an open access article distributed under terms of the Creative Commons Attribution License ([Attribution 4.0 International – CC BY 4.0](https://creativecommons.org/licenses/by/4.0/)).

## Introduction

The freshwater fish genus *Oreonectes* Günther, 1868, which belongs to the family Nemacheilidae, exhibits notable adaptations to the karst geomorphic environment. These small fish are predominantly distributed in southern China (Xijiang River system of Guangxi Zhuang Autonomous Region, Pearl River system of Guangdong Province, and Pearl River system of Hong Kong) and Kalong River of northern Vietnam (Quảng Ninh Province in northeast Vietnam) (Kottelat 2012). The genus was first established by Günther in 1868, designating *Oreonectes platycephalus* Günther, 1868 as the type species, collected from a small stream in Hong Kong within the Pearl River system. The diagnosis of the genus included a slightly compresses body, a markedly depressed head, and the origin of the dorsal fin much closer to the base of the caudal fin than to the operculum Günther (1868). Later, till 2006 a number of species have been added to the genus: *O. anophthalmus* Zheng, 1981 (an underground river in Taiji Cave, Wuming County, Guangxi, Youjiang River, China), *O. furco-caudalis* Zhu & Cao, 1987 (a subterranean water outlet in the suburbs of Rongshui County, Guangxi, Liujiang River, China), *O. retrodorsalis* Lan, Yang & Chen, 1995 (an underground river outlet in Longli Village, Nandan County, Guangxi, Hongshui River, China), and *O. translucens* Zhang, Zhao & Zhang, 2006 (Xia'ao

Town, Du'an County, Guangxi, Hongshui River, China) (Zheng 1981; Zhu 1989; Lan et al. 1995; Zhang et al. 2006). Subsequently, a revision of *Oreonectes* was published with description of two new species *O. microphthalmus* Du, Chen & Yang, 2008 (Du'an County, Guangxi, Hongshui River, China) and *O. polystigmus* Du, Chen & Yang, 2008 (Dabu Village, Guilin City, Guangxi, Lijiang River, China) (Du et al. 2008). Meanwhile, Du et al. (2008) subdivided the genus into two groups based on the caudal fin morphology: the round caudal fin group (*O. platycephalus* group), containing *O. anophthalmus*, *O. platycephalus*, *O. polystigmus*, and *O. retrodorsalis*, and the forked caudal fin group (*O. furcocaudalis* group), including *O. furcocaudalis* and *O. microphthalmus*. After 2009, various species were described, including *O. macrolepis* Huang, Du, Chen & Yang, 2009 (an underground river in Dacai Town, Huanjiang County, Guangxi, Xijiang River system, China), *O. luochengensis* Yang, Wu, Wei & Yang, 2011 (a cave near Tianhe Town, Luocheng County, Guangxi, Xijiang River system, China), *O. guananensis* Yang, Wei, Lan & Yang, 2011 (an underground karst cave outlet near Guan'an Village, Changmei Town, Huanjiang County, Guangxi, Xijiang River system, China), *O. elongatus* Tang, Zhao & Zhang, 2012 (Mulun Town, Huanjiang County, Guangxi, Longjiang River, China), *O. acridorsalis* Lan, 2013 (a cave near Bamu Town, Tian'e County, Guangxi, Hongshui River, China), *O. barbatus* Gan, 2013 (first described from a cave near Lihu Town, Nandan County, Guangxi, Hongshui River, China), *O. donglanensis* Wu, 2013 (a cave near Simeng Town, Donglan County, Guangxi, Hongshui River, China), *O. duanensis* Lan, 2013 (a cave near Chengjiang Town, Du'an County, Guangxi, Hongshui River, China), *O. daqikongensis* Deng, Xiao, Hou & Zhou, 2016 (Seven Big Scenic Spot, Libo County, Guizhou, Hongshui River, China), *O. shuilongensis* Deng, Wen, Xiao & Zhou, 2016 (a cave near Shuilong Town, Sandu County, Guizhou, Duliu River, China), *O. guilinensis* Huang, Yang, Wu & Zhao, 2020 (Shigumen Village, Xingping Town, Yangshuo County, Guilin City, Guangxi, Lijiang River, China), and *O. damingshanensis* Yu, Luo, Lan, Xiao & Zhou, 2023 (Waminggu Scenic Area, Leping Village, Guling Town, Mashan County, Guangxi, Xijiang River system, China) (Huang et al. 2009, 2020; Yang et al. 2011a, b; Tang et al. 2012; Lan et al. 2013; Deng et al. 2016a, b; Yu et al. 2023). Zhang et al. (2016) established the genus *Troglonectes* Zhang, Zhao & Tang, 2016, designating *O. furcocaudalis* as the type species, with *O. barbatus*, *O. elongatus*, *O. macrolepis*, *O. microphthalmus*, and *O. translucens*, characterized by a forked caudal fin, a developed adipose crest of the caudal fin, and the dorsal-fin origin above the pelvic-fin origin. Later studies added *O. daqikongensis*, *O. donglanensis*, *O. duanensis*, *O. retrodorsalis*, and *O. shuilongensis* to *Troglonectes* (Huang et al. 2020; Du et al. 2023), while *O. anophthalmus* and *O. acridorsalis* were assigned to a new genus, *Karstsinnectes* Zhou, Luo, Wang, Zhou & Xiao, 2023 based on morphological and molecular evidence (Luo et al. 2023).

Until now, the genus of *Oreonectes* contains six valid species, namely, *O. damingshanensis*, *O. guananensis*, *O. guilinensis*, *O. luochengensis*, *O. platycephalus*, and *O. polystigmus*. In July 2022, ten loach specimens were collected from Laibin City in the Hongshui River system, Guangxi Zhuang Autonomous Region, China. Morphological features and molecular data suggest that the specimens under consideration represent a previously undescribed species within the genus *Oreonectes*, which are described herein.

## Materials and methods

Field collections followed the Guide to Collection, Preservation, Identification, and Information Share of Animal Specimens (Xue 2010) and Implementation Rules of Fisheries Law of the People's Republic of China. All activities followed the Laboratory Animal Guidelines for the Ethical Review of Animal Welfare (GB/T 35892–2018). Specimens of the new species were collected by FGL. Samples were collected using a hand net and mesh traps. Freshly caught fish were euthanized using eugenol. After death, the pectoral fins from the right side were taken and preserved in ethanol for molecular analysis. Specimens used for morphological studies were preserved in 10% formalin, before being transferred to 75% ethanol for long-term storage at the collection of the Key Laboratory of Ecology of Rare and Endangered Species and Environmental Protection (Guangxi Normal University), Ministry of Education.

## Phylogenetic analyses

Mitochondrial cytochrome *b* gene (*Cyt b*) sequences were sequenced by the Science Corporation of Gene (China) following standard Illumina protocols. Genome sequencing data were submitted to GenBank (Accession No. OR188128, OR712240, OR712241). We retrieved 36 *Cyt b* sequences of Nemacheilidae species from the NCBI GenBank database (Appendix 1) for phylogenetic tree reconstruction to test the phylogenetic positions of *Oreonectes andongensis* sp. nov. All sequences were aligned in MEGA v. 11.0 (Tamura et al. 2021) by the MUSCLE (Edgar 2004) algorithm with default parameters, and then sequences were executed in PartitionFinder v. 2.1.1 (Lanfear et al. 2017) in order to select the most appropriate model of evolution to be used for phylogenetic analyses. The model selection for each codon position of the complete mitochondrial genes indicated that the best fit models were K80+I+G for the first codon, HKY+I+G for the second codon, and TRN+I+G for the third codon. Bayesian inference (BI) analysis was performed using MRBAYES v. 3.2.6 (Ronquist et al. 2012). The chains were run for two million generations and sampled every 1000 generations. The first 25% of the sampled tree was discarded as burn-in, and the remaining trees were used to create a consensus tree and to estimate Bayesian posterior probabilities (BPP). Nodes in the trees were considered well-supported at BPP  $\geq$  0.95.

## Morphological examination

Methods used for counts and measurements followed Du et al. (2021) and characteristics of the cephalic lateral line system were examined following Kottelat (1990) and Tang et al. (2012). All measurements were taken point-to-point with dial calipers to the nearest 0.1 mm. Abbreviations used in the text are as follows: **AFBL** for anal-fin base length, **AFL** for anal-fin length, **BD** for body depth, **BW** for body width, **CPL** for caudal peduncle length, **CPD** for caudal peduncle depth, **DAPN** for distance between anterior and posterior nostrils, **DAN** for distance between anterior nostrils, **DFBL** for dorsal-fin base length, **DFL** for dorsal-fin length, **DPN** for distance between posterior nostrils, **ED** for

eye diameter, **HD** for head depth, **HL** for head length, **HW** for head width, **ISBL** for inrostral barbel length, **IW** for interorbital width, **MBL** for maxillary barbel length, **OSBL** for outrostral barbel length, **PANL** for preanus length, **PAL** for pre-anal length, **PDL** for predorsal length, **PFBL** for pectoral-fin base length, **PFL** for pectoral-fin length, **PPL** for prepectoral length, **PVL** for prepelvic length, **STL** for snout length, **SL** for standard length, **TL** for total length, **VFBL** for pelvic-fin base length, and **VFL** for pelvic-fin length.

## Results

### Genetic evidence from phylogenetic analysis

BI analyses were performed to construct a phylogenetic tree, revealing consistent topologies based on Cyt *b* sequences spanning 1141 bp. The phylogenetic tree affirmed the validity of the new species with high nodal support (BPP  $\geq$  0.95). Additionally, members of the *Oreonectes* genus constituted a monophyletic group, which was phylogenetically sister to the *Guinemachilus* Du et al., 2023 and *Micronemacheilus* clade (Fig. 1). *Oreonectes andongensis* sp. nov. formed a highly supported clade with *O. damingshanensis*, *O. guilinensis*, *O. platycephalus*, and *O. polystigmus*.

The uncorrected *p*-distances of Cyt *b* between *Oreonectes andongensis* sp. nov. and the other six species ranged from 6.0% (for *O. polystigmus*) to 7.5% (for *O. guananensis*) (Table 2).

### Taxonomy

#### *Oreonectes andongensis* Luo, Yang, Du & Luo, sp. nov.

<https://zoobank.org/31E2362E-71AF-4E1F-B78A-53DFB1980F33>

Table 1, Figs 1–5

**Type material. Holotype.** GXNU20220601, 74.9 mm standard length (SL), Andong Town, Xincheng County, Laibin City, Hongshui River system, Guangxi Zhuang Autonomous Region, China, 24°18.57'N, 108°59.61'E, 179 m a.s.l., collected by F.G.L., 20 July 2022. **Paratypes.** GXNU20220602–10, 9 specimens, 45.9–68.7 mm SL, same data as holotype.

**Diagnosis.** The new species is assigned to the genus *Oreonectes* based on Cyt *b* phylogenetic analysis and morphological characters. The new species can be distinguished from other members of *Oreonectes* by the following combination of characters: posterior chamber of swim bladder developed (vs reduced in *O. platycephalus*), color pattern present (vs colorless in *O. luochengensis*), tip of pelvic fin not reaching anus (vs exceeding anus in *O. polystigmus* and *O. guilinensis*), dorsal-fin origin slightly posterior to pelvic-fin origin (vs opposite in *O. guananensis*), six branched pelvic-fin rays (vs 7 or 8 in *O. damingshanensis*, *O. guananensis*, *O. luochengensis*). *Oreonectes andongensis* sp. nov. can be further differentiated from *O. damingshanensis* by more numerous, better developed inner gill rakers on the first gill arch (11–12 vs 9).

**Description.** The morphometric data of the holotype and paratypes are in Table 1. Three unbranched and seven branched dorsal-fin rays, one unbranched and nine or ten branched pectoral-fin rays, one unbranched and six

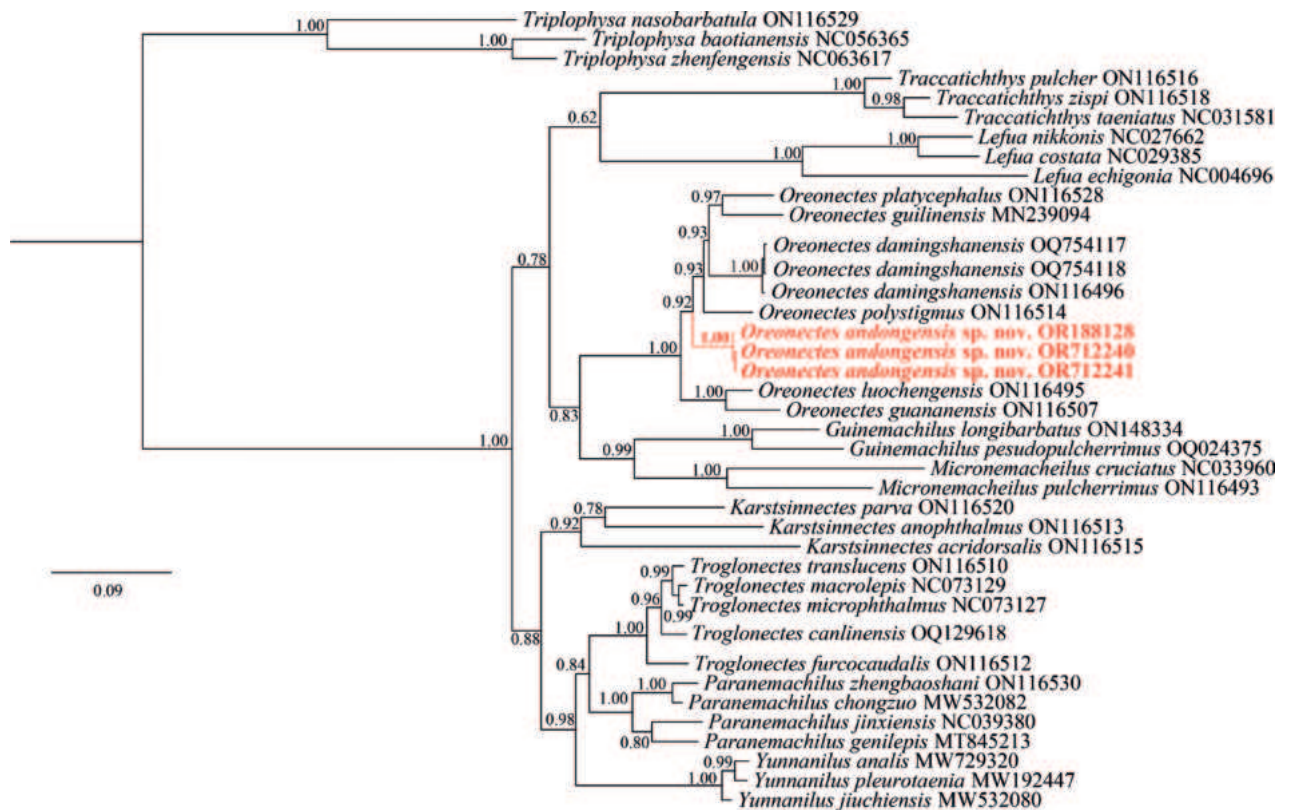


Figure 1. Bayesian phylogenetic tree of *Oreonectes* based on mitochondrial *Cyt b*. Numbers above branches are BPPs.

Table 1. Morphological data and habitat types of the genus *Oreonectes*. Data of *O. damingshanensis* is from the original description (Yu et al. 2023).

	<i>O. andongensis</i> sp. nov.	<i>O. damingshan-</i> <i>ensis</i>	<i>O. guananensis</i>	<i>O. guilinensis</i>	<i>O. luochengensis</i>	<i>O. platycephalus</i>	<i>O. polystigmus</i>
	Range (Mean ± SD)	Range (Mean ± SD)	Range (Mean ± SD)	Range (Mean ± SD)	Range (Mean ± SD)	Range (Mean ± SD)	Range (Mean ± SD)
TL (mm)	45.9–74.9 (57.1 ± 9.9)	63.7–98.9 (78.8 ± 8.8)	62.9–90.2 (75.7 ± 10.5)	63.2–89.7 (80.4 ± 7.6)	77.2–92.1 (84.2 ± 4.8)	49.6–82.5 (65.2 ± 11.7)	41.8–67.8 (52.2 ± 8.0)
SL (mm)	36.5–60.2 (46.2 ± 8.4)	52.5–81.8 (64.9 ± 7.3)	51.0–71.5 (60.9 ± 8.3)	52.0–73.5 (65.9 ± 6.1)	62.2–74.7 (68.1 ± 4.3)	38.7–64.2 (51.2 ± 9.3)	33.7–54.7 (42.5 ± 6.7)
Percentage of SL (%)							
BD	15.7–17.9 (16.7 ± 0.7)	14.2–18.1 (15.5 ± 1.3)	16.2–19.6 (17.6 ± 1.3)	16.7–18.5 (18.0 ± 0.5)	16.0–18.3 (17.3 ± 0.7)	14.8–19.3 (17.2 ± 1.4)	12.5–19.5 (16.3 ± 2.2)
BW	11.5–15.2 (12.7 ± 1.0)	10.4–12.5 (11.3 ± 0.6)	9.5–13.1 (11.3 ± 1.3)	12.7–14.8 (13.9 ± 0.6)	9.8–12.1 (10.8 ± 0.8)	9.5–11.5 (10.5 ± 0.5)	7.4–11.8 (8.7 ± 1.2)
HW	14.7–17.2 (15.7 ± 0.7)	14.4–17.8 (16.1 ± 1.0)	14.8–16.9 (15.9 ± 0.7)	15.4–19.0 (17.0 ± 1.1)	13.7–16.9 (14.9 ± 0.9)	14.6–17.5 (15.7 ± 0.8)	13.7–17.5 (15.5 ± 1.2)
HD	11.4–12.8 (12.1 ± 0.5)	10.8–12.9 (12.0 ± 0.7)	10.9–11.9 (11.4 ± 0.4)	12.0–15.2 (13.3 ± 1.0)	10.0–12.4 (11.1 ± 0.7)	10.3–13.5 (11.3 ± 0.9)	11.1–13.1 (12.1 ± 0.7)
HL	21.1–24.5 (22.3 ± 0.9)	20.2–23.0 (21.7 ± 0.9)	21.8–23.2 (22.6 ± 0.5)	20.3–24.2 (21.7 ± 1.1)	20.7–24.2 (22.4 ± 1.0)	20.8–25.4 (22.8 ± 1.4)	22.3–24.5 (23.6 ± 0.6)
PDL	57.7–62.4 (60.0 ± 1.7)	59.5–62.4 (60.7 ± 0.8)	57.2–59.5 (58.4 ± 0.8)	57.4–60.4 (58.9 ± 0.9)	58.0–63.3 (60.0 ± 1.5)	60.0–64.7 (62.0 ± 1.9)	59.2–63.9 (60.9 ± 1.6)
DFL	16.8–19.2 (18.1 ± 0.7)	17.2–21.7 (18.9 ± 1.2)	17.6–18.6 (18.0 ± 0.3)	16.6–19.0 (17.4 ± 0.8)	16.9–19.2 (18.2 ± 0.7)	15.7–21.1 (19.4 ± 1.6)	16.8–19.8 (18.1 ± 1.0)
DFBL	8.9–11.6 (10.4 ± 0.8)	9.0–11.3 (10.3 ± 0.7)	9.5–11.0 (10.1 ± 0.6)	7.2–10.4 (8.8 ± 0.9)	6.6–7.3 (7.0 ± 0.3)	9.4–11.1 (10.1 ± 0.5)	8.9–12.1 (10.0 ± 1.0)
PPL	19.4–23.7 (21.2 ± 1.2)	19.1–22.7 (21.4 ± 1.0)	21.4–23.0 (22.0 ± 0.5)	16.9–20.4 (19.1 ± 1.2)	19.0–21.8 (20.3 ± 0.7)	18.1–22.4 (21.1 ± 1.6)	19.2–25.2 (22.0 ± 1.6)
PFL	15.1–18.9 (16.7 ± 1.0)	15.5–18.7 (16.9 ± 1.1)	14.5–17.1 (16.1 ± 0.9)	14.2–16.0 (15.3 ± 0.6)	15.3–18.5 (17.1 ± 1.0)	15.1–22.1 (19.3 ± 1.8)	13.5–19.4 (15.6 ± 1.7)

	<i>O. andongensis</i> sp. nov.	<i>O. damingshanensis</i>	<i>O. guananensis</i>	<i>O. guilinensis</i>	<i>O. luochengensis</i>	<i>O. platycephalus</i>	<i>O. polystigmus</i>
	Range (Mean ± SD)	Range (Mean ± SD)	Range (Mean ± SD)	Range (Mean ± SD)	Range (Mean ± SD)	Range (Mean ± SD)	Range (Mean ± SD)
PFBL	3.2–4.3 (3.9 ± 0.3)	3.6–4.5 (4.0 ± 0.3)	3.4–4.5 (3.9 ± 0.4)	3.1–4.5 (3.9 ± 0.5)	4.0–5.6 (4.6 ± 0.5)	3.9–5.2 (4.5 ± 0.6)	2.7–4.5 (3.9 ± 0.5)
PVL	54.3–58.2 (56.1 ± 1.4)	48.6–52.2 (50.6 ± 1.0)	55.4–57.4 (56.5 ± 0.9)	53.8–55.8 (55.1 ± 0.8)	55.3–60.3 (56.3 ± 2.1)	52.2–56.4 (54.4 ± 1.7)	53.4–57.1 (55.1 ± 1.2)
VFL	11.1–13.6 (12.5 ± 0.8)	14.7–17.2 (15.8 ± 0.9)	14.5–17.1 (16.1 ± 0.9)	10.9–12.5 (11.8 ± 0.6)	11.9–14.7 (13.4 ± 0.9)	15.5–22.1 (19.3 ± 1.8)	12.1–15.7 (13.6 ± 1.2)
VFBL	3.0–4.0 (3.5 ± 0.4)	3.2–4.3 (3.8 ± 0.3)	3.0–4.2 (3.6 ± 0.4)	2.6–3.5 (3.2 ± 0.3)	3.1–3.9 (3.3 ± 0.2)	3.8–5.4 (4.5 ± 0.6)	2.7–4.0 (3.2 ± 0.4)
PAL	78.6–82.6 (80.0 ± 1.1)	74.6–77.9 (75.6 ± 1.0)	77.3–81.6 (80.6 ± 1.5)	78.4–81.2 (79.6 ± 0.9)	80.1–83.0 (81.3 ± 1.0)	77.6–80.5 (79.1 ± 1.0)	76.7–81.7 (79.9 ± 1.4)
AFL	14.3–17.7 (15.7 ± 1.1)	16.1–18.1 (16.9 ± 0.6)	14.2–16.1 (15.0 ± 0.6)	14.3–15.6 (14.6 ± 0.6)	14.0–16.8 (15.6 ± 0.8)	14.4–19.2 (17.8 ± 1.5)	14.9–17.2 (16.1 ± 1.0)
AFBL	6.8–8.1 (7.4 ± 0.5)	7.3–9.4 (8.4 ± 0.6)	6.7–7.5 (7.1 ± 0.3)	5.9–7.6 (6.8 ± 0.5)	6.6–7.3 (7.0 ± 0.3)	7.5–9.0 (8.1 ± 0.5)	7.1–11.0 (8.4 ± 1.2)
PANL	72.2–77.4 (74.1 ± 1.6)	78.6–82.8 (80.1 ± 1.2)	73.3–76.6 (74.6 ± 1.2)	71.7–74.2 (73.5 ± 0.9)	72.0–78.6 (74.1 ± 2.0)	71.2–76.1 (73.5 ± 1.6)	68.5–76.2 (73.8 ± 2.4)
CPL	11.2–15.5 (13.1 ± 1.3)	14.3–17.8 (15.7 ± 1.0)	11.5–13.4 (12.4 ± 0.6)	11.6–14.1 (12.2 ± 0.8)	10.1–12.5 (11.0 ± 0.8)	11.0–14.5 (12.6 ± 1.0)	10.2–14.3 (11.5 ± 1.2)
CPD	9.7–11.7 (10.6 ± 0.8)	10.0–11.6 (10.8 ± 0.5)	10.1–11.3 (10.8 ± 0.4)	9.5–11.3 (10.2 ± 0.6)	9.8–12.0 (10.7 ± 0.8)	12.2–14.8 (13.0 ± 0.9)	8.5–13.4 (10.9 ± 1.5)
Percentage of HL (%)							
ED	13.6–19.5 (15.9 ± 1.7)	11.2–15.2 (12.4 ± 1.2)	10.4–14.9 (12.9 ± 1.7)	9.2–13.5 (10.9 ± 1.3)	9.0–14.2 (11.9 ± 1.6)	11.1–19.7 (15.1 ± 2.3)	12.5–16.8 (14.7 ± 1.7)
IW	41.8–47.3 (43.9 ± 1.7)	34.6–44.6 (41.3 ± 2.5)	42.3–47.9 (44.9 ± 2.1)	44.1–51.9 (48.1 ± 2.7)	39.9–45.2 (42.2 ± 2.1)	41.1–49.9 (46.1 ± 2.5)	34.5–45.6 (40.3 ± 3.2)
STL	30.2–34.7 (32.8 ± 1.6)	37.7–43.3 (40.7 ± 1.8)	31.2–40.2 (36.0 ± 3.3)	30.3–40.5 (35.1 ± 3.3)	33.5–40.5 (36.4 ± 2.0)	34.4–40.9 (37.3 ± 2.4)	31.2–37.9 (34.0 ± 2.0)
DAN	29.6–36.4 (33.0 ± 2.2)	23.6–39.2 (29.7 ± 3.9)	30.6–36.5 (34.1 ± 1.9)	29.1–35.6 (32.5 ± 2.3)	31.4–35.1 (32.8 ± 1.4)	31.6–38.0 (35.0 ± 2.6)	26.4–37.1 (30.4 ± 2.9)
DPN	34.0–39.1 (37.2 ± 1.8)	33.8–38.9 (36.5 ± 1.5)	34.5–40.5 (37.7 ± 1.9)	34.0–37.8 (36.0 ± 1.3)	33.8–38.2 (36.0 ± 1.7)	37.6–42.8 (39.3 ± 1.6)	34.3–41.6 (36.7 ± 2.3)
DAPN	8.0–11.1 (9.6 ± 0.9)	6.3–10.6 (7.7 ± 1.3)	8.2–13.2 (10.6 ± 2.0)	7.5–11.9 (10.5 ± 1.4)	8.0–13.0 (9.9 ± 1.7)	10.1–12.3 (11.0 ± 0.7)	8.1–12.4 (10.3 ± 1.6)
MBL	43.3–55.9 (48.0 ± 4.4)	36.4–50.8 (43.3 ± 4.7)	52.9–61.7 (56.1 ± 2.7)	37.3–55.4 (45.5 ± 5.3)	41.5–55.6 (46.0 ± 4.5)	38.3–56.3 (48.7 ± 5.3)	33.9–55.9 (45.5 ± 8.0)
OSBL	50.0–69.6 (59.4 ± 6.6)	47.4–58.7 (54.4 ± 4.4)	64.8–71.6 (68.8 ± 2.6)	41.3–52.5 (48.2 ± 5.6)	43.9–60.7 (51.5 ± 6.4)	47.2–66.5 (57.4 ± 5.8)	39.2–61.4 (53.9 ± 7.1)
ISBL	25.5–48.5 (38.2 ± 8.6)	25.6–37.4 (33.1 ± 3.4)	30.6–51.5 (42.1 ± 6.4)	28.8–36.9 (33.1 ± 2.9)	28.7–40.8 (33.1 ± 4.6)	35.9–40.6 (37.8 ± 2.6)	21.1–47.9 (33.1 ± 7.4)
Percentage of CPL (%)							
CPD	67.2–98.7 (81.6 ± 8.9)	63.4–78.0 (68.7 ± 5.1)	75.1–97.5 (87.7 ± 6.8)	74.7–90.6 (83.3 ± 4.6)	95.2–118.2 (98.5 ± 10.1)	95.0–125.0 (103.4 ± 10.2)	73.8–131.0 (96.7 ± 20.5)
Habitat types	Small pools on surface where groundwater overflowed	Karst cave under mountain	Water outlet of underground karst cave	Open stream	Water of underground karst cave	Surface stream	Underground karst cave

branched pelvic-fin rays, three unbranched and five branched anal-fin rays, 13 or 14 branched caudal-fin rays, and 11 or 12 inner-gill rakers on first gill arch (in 3 specimens).

Body elongated and cylindrical, deepest body depth in front of dorsal-fin origin, deepest body depth 16–18% of standard length (SL). Head slightly depressed and flattened, maximum head width greater than deepest head height. Anterior

**Table 2.** Uncorrected *p*-distances (%) between seven species in the genus *Oreonectes* based on mitochondrial *Cyt b* genes.

ID	Species	1	2	3	4	5	6
1	<i>Oreonectes andongensis</i> sp. nov.						
2	<i>Oreonectes damingshanensis</i>	6.1					
3	<i>Oreonectes guananensis</i>	7.5	8.7				
4	<i>Oreonectes guilinensis</i>	7.0	7.2	8.8			
5	<i>Oreonectes luochengensis</i>	6.4	7.5	4.8	8.1		
6	<i>Oreonectes platycephalus</i>	6.6	6.7	8.7	6.5	7.9	
7	<i>Oreonectes polystigmus</i>	6.0	6.0	8.3	7.3	7.4	6.4

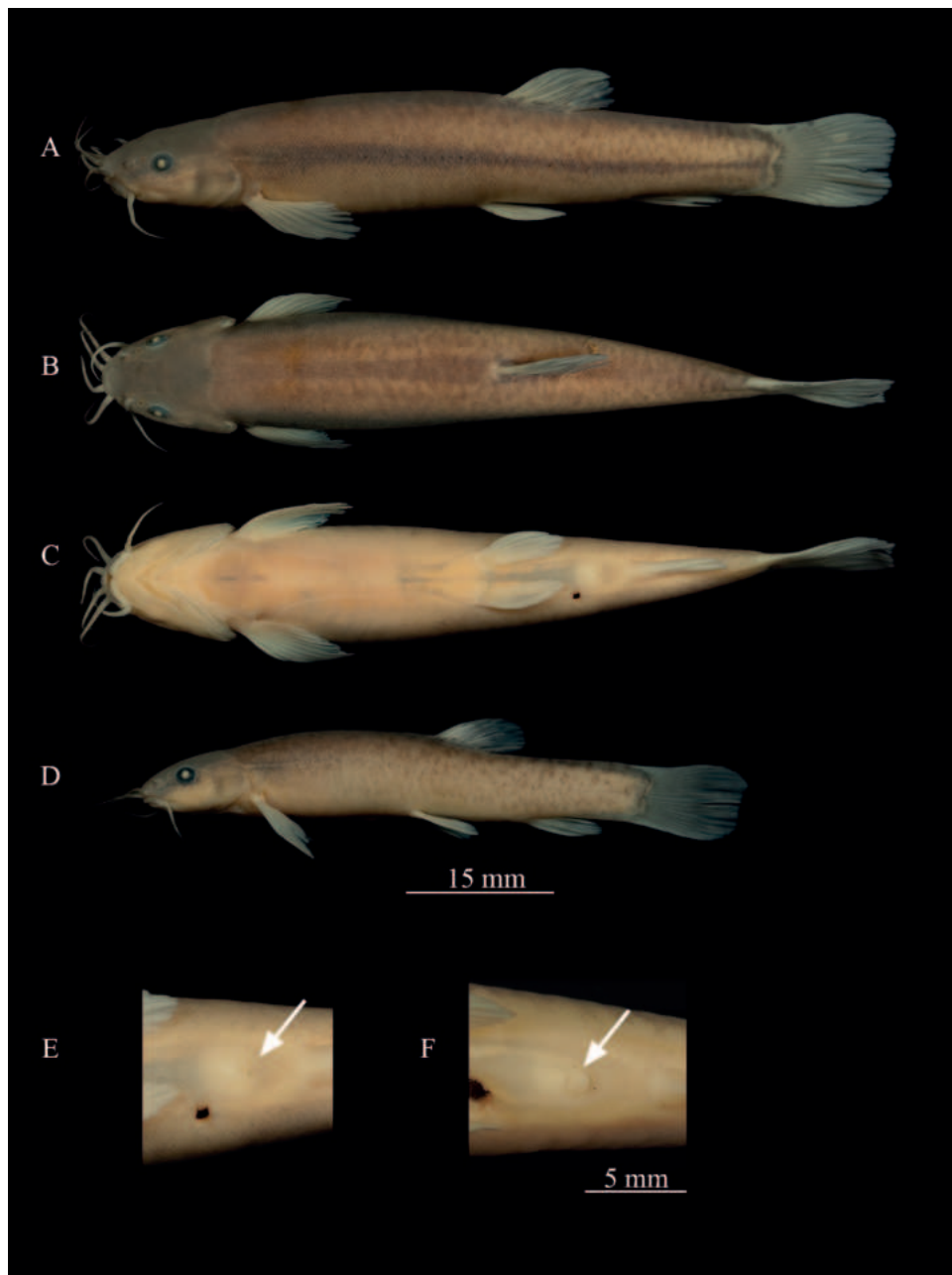


**Figure 2.** *Oreonectes andongensis* sp. nov. **A–C** lateral, dorsal and ventral views of holotype GXNU20220601 (♀), **D** lateral view of paratype GXNU20220610 (♂), **E, F** gonadal structure of female (**E**) and male (**F**).

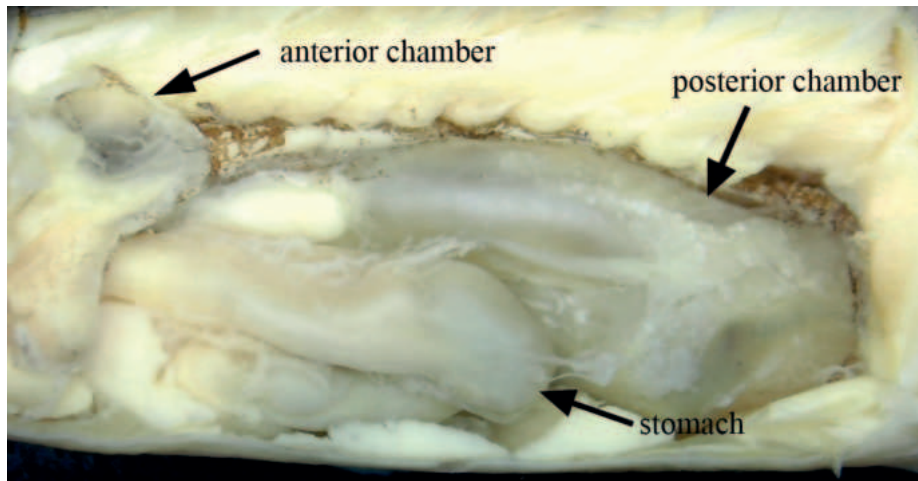


Figure 3. Stomach, anterior chamber, and posterior chamber of *Oreonectes andongensis* sp. nov.

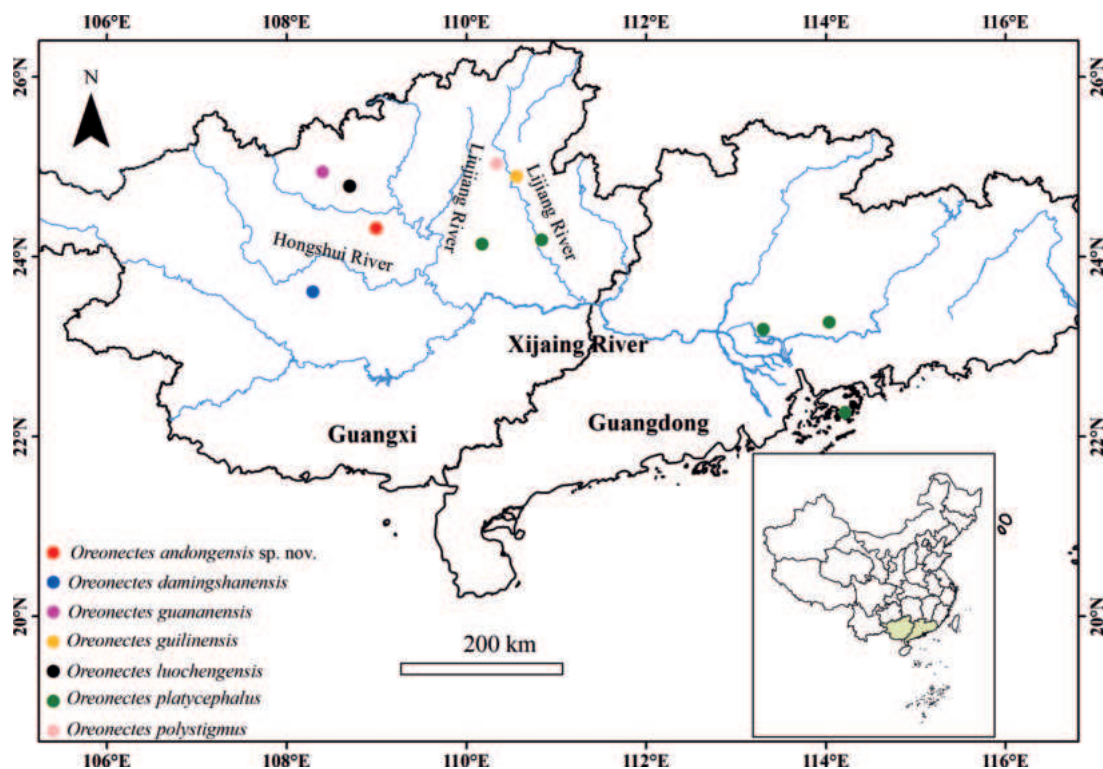


Figure 4. Distribution of *Oreonectes* in southern China.

and posterior nostrils adjacent, distance shorter than diameter of posterior nostril. Base of anterior nostril tube-shaped with elongated barbel-like tip; barbel longer than anterior nostril tube. Eyes normal, eye diameter 14–20% of head length (HL). Snout obtuse, snout length shorter than postorbital length. Mouth inferior, lips smooth, center of lower lip with notch. Three pairs of barbels, inner rostral barbel length 23–49% of HL, extending to the anterior margin of eye; outer rostral barbel length 50–70% of HL, extending to the posterior margin of eye; maxillary barbel length 43–56% of HL, not reaching to posterior margin of opercula.

Dorsal-fin origin slightly posterior to pelvic-fin origin. Predorsal length 58–62% of SL. Tip of pectoral fin not reaching half of distance between origin of pectoral and pelvic fins. Tip of pelvic fin not reaching anus. Short distance (two times eye diameter) between anal-fin origin and anus. Caudal fin straight.



Figure 5. Habitat of *Oreonectes andongensis* sp. nov.

Caudal peduncle without adipose crests along both dorsal and ventral sides. Caudal peduncle depth 67–99% of caudal peduncle length. Whole body covered by scales except head. Lateral line incomplete, with 8–16 pores. Cephalic lateral line system developed, with 6–9 supraorbital pores, 3 + 8–10 infraorbital pores, three or four canal pores, and 6–8 pre-operculo-mandibular canal pores.

Stomach U-shaped. Swim bladder divided into two chambers, anterior chamber covered by dumbbell-shaped bony capsule, and posterior chamber developed with posterior extremely reaching below dorsal-fin origin.

**Coloration.** In formalin-fixed specimens, dorsal surface and trunk of body yellowish, while abdomen appears grayish. Additionally, dorsal surface and flank with small spots or short bars. Dorsal and caudal fins with black speckles. Longitudinal stripe extending from gill opening to caudal peduncle in female, lacking in males.

**Sexual dimorphism.** In reproductive season, males possess large genital papilla located immediately posterior to anus, unclear in females; gonad opens at end of fleshy prominence.

**Distribution and habitat.** *Oreonectes andongensis* sp. nov. was collected from Andong Township, Xincheng County, Laibin City, Guangxi Zhuang Autonomous Region, China, a tributary of the Hongshui River in Xijiang River basin. During the rainy season, specimens were gathered from small pools on the surface where groundwater had overflowed. *Troglonectes canlinensis* Li et al., 2023 specimens were also collected from the same pool.

**Etymology.** The nomenclature of this species is derived from the Chinese pinyin of Andong, the name of the village where the specimens were obtained. We suggest the Chinese common name as “安东岭鳅”.

**Remarks.** *Oreonectes andongensis* sp. nov. can be distinguished from *O. damingshanensis* by the six branched pelvic-fin rays (vs 7), a dorsal-fin origin slightly posterior to pelvic-fin origin (vs posterior to pelvic-fin origin obviously), and 11 or 12 inner gill rakers on the first gill arch (vs 9), from *O. guananensis* by six branched pelvic-fin rays (vs 7 or 8), dorsal-fin origin slightly posterior to pelvic-fin origin (vs opposite to pelvic-fin origin), caudal with irregular black markings (vs without irregular black markings), and maxillary barbel not reaching to the gill cover (vs reaching to the gill cover), from *O. guilinensis* by lateral line pores 8–16 (vs 4–6), tip of pelvic fin not reaching to anus (vs exceeding to anus), and maxillary barbel not reaching to the opercula (vs reaching to posterior margin of the eye), from *O. luochengensis* by cephalic lateral line system present (vs absent), abdomen between pectoral-fin origin to pelvic-fin origin scaled (vs scaleless), from *O. platycephalus* by posterior chamber of swim bladder developed (vs reduced), dorsal-fin origin slightly posterior to pelvic-fin origin (vs posterior to pelvic-fin origin obviously), seven branched dorsal-fin rays (vs 8 or 9), and six branched pelvic-fin rays (vs 8), from *O. polystigmus* by tip of pelvic fin not reaching to anus (vs exceeding to anus), and maxillary barbel not reaching to the opercula (vs reaching to the pectoral-fin origin).

### Key to species of the genus *Oreonectes*

- |   |   |   |
|---|---|---|
| 1 | Body colorless .....  | <b><i>O. luochengensis</i></b>                |
| – | Color pattern present .....   | <b>2</b>                                      |
| 2 | Dorsal-fin origin opposite to pelvic-fin origin .....                             | <b><i>O. guananensis</i></b>                  |
| – | Dorsal-fin origin posterior to pelvic-fin origin .....                            | <b>3</b>                                      |
| 3 | Tip of pelvic fin exceeding anus .....  | <b>4</b>                                      |
| – | Tip of pelvic fin not reaching anus .....   | <b>5</b>                                      |
| 4 | Six branched dorsal-fin rays .....  | <b><i>O. guilinensis</i></b>                  |
| – | Seven branched dorsal-fin rays .....  | <b><i>O. polystigmus</i></b>                  |
| 5 | Posterior chamber of swim bladder reduced .....                                   | <b><i>O. platycephalus</i></b>                |
| – | Posterior chamber of swim bladder developed .....                                 | <b>6</b>                                      |
| 6 | Six branched pelvic fin rays, 11 or 12 inner gill rakers on first gill arch ..... | <b><i>Oreonectes andongensis</i> sp. nov.</b> |
| – | Seven branched pelvic fin rays, 9 inner gill rakers on first gill arch .....      | <b><i>O. damingshanensis</i></b>              |

### Discussion

The distinct lineage of *Oreonectes andongensis* sp. nov. marked by an uncorrected *p*-distance of 6.0% from *O. polystigmus*, along with notable morphological differences, substantiates its validity as a new species. With the addition of the new species, the genus *Oreonectes* now comprises seven species: *Oreonectes andongensis* sp. nov., *O. damingshanensis*, *O. guananensis*, *O. guilinensis*, *O. luochengensis*, *O. platycephalus*, and *O. polystigmus*.

*Oreonectes andongensis* sp. nov. exhibited sexual dimorphism. Notably, males contained larger genital papilla located immediately posterior to the anus, with the gonads opening at the end of a fleshy prominence. Zhu (1989) noted that this structure may be related to the special breeding habits of *Oreonectes*. Additionally, most species of *Oreonectes* possess that developed

posterior chamber of swim bladder except *O. platycephalus*. Zhu (1989) speculated that the posterior chamber of swim bladder related to adapting to habitat. *Oreonectes andongensis* sp. nov. and other congeneric species (except *O. platycephalus*) possess developed posterior chamber of swim bladder, and mainly habitat in pools surround subterranean river, but *O. platycephalus* inhabit in running water of upper reaches of the river.

Within the genus *Oreonectes*, *O. platycephalus* has a broader distribution, both within and beyond Guangxi, whereas the other species are exclusively found in Guangxi. In areas within Guangxi, *O. platycephalus* coexists with the other species, with their distribution overlapping along certain routes of *O. platycephalus* (Tang 2012). Wang (2022) suggested that the ancestors of the Nemacheilidae family in southwest China emerged around 26.19 million years ago (approximately the Late Oligocene). The uplift of the Tibetan Plateau led to the development of the Pearl River occurred concurrently (Zhang et al. 2022). This expansion towards the Pearl River Delta area likely facilitated the spread of *Oreonectes*. As the caves in southwest China continued to develop, some fish species entered these habitats, evolving traits suited to cave living, such as eye degeneration, loss of scales, and lack of pigmentation.

### Comparative material

All specimens were collected from Guangxi; their measurements are given in Appendix 2.

*Oreonectes guananensis*, KIZ2010003067, holotype, 71.5 mm SL, KIZ2010003068–072, paratypes, 5 ex., 51.0–71.9 mm SL, Guan'an Village, Changmei Town, Huanjiang County, Guangxi.

*Oreonectes guilinensis*, ASIZB208001, holotype, 73.5 mm SL, ASIZB208002–007, paratypes, 6 ex., 52.0–68.3 mm, Shigumen Village Xingping Town, Yangshuo County, Guilin City, Guangxi.

*Oreonectes luochengensis*, KIZ2010003073, holotype, 71.2 mm SL, KIZ2010003074–077, KIZ2010003242–244, paratypes, 7 ex., 61.3–74.7 mm SL, Tianhe Town, Luocheng County, Guangxi.

*Oreonectes platycephalus*, KIZ2003007105–106, 63.2–64.2 mm SL, KIZ2003007110, 60.9 mm SL, KIZ2005006211–212, 38.7–43.1 mm SL, KIZ2005006214–216, 45.6–47.7 mm SL, 8 ex., Fenzhan Village, Jinxiu County, Guangxi.

*Oreonectes polystigmus*, KIZ2001004626, holotype, 54.7 mm SL, KIZ2002004627–634, paratypes, 9 ex., 33.7–52.4 mm SL, Dabu Village, Guilin City, Guangxi.

### Acknowledgements

We are grateful to Ying-Nan Wang, Institute of Zoology, Chinese Academy of Sciences, Beijing (ASIZB) and Rui Min, Kunming Institute of Zoology, Chinese Academy of Sciences (KIZ) for providing *Oreonectes* specimens, Jun-Kai Huang for taking photographs of the new species, and Christine Watts for English correction and suggestions.

## Additional information

### Conflict of interest

The authors have declared that no competing interests exist.

### Ethical statement

No ethical statement was reported.

### Funding

This study was funded by the Guangxi Natural Science Foundation Project (2022GXNS-FAA035563 and 2020GXNSFAA238031), Key Laboratory of Ecology of Rare and Endangered Species and Environmental Protection (Guangxi Normal University), Ministry of Education, China (ERESEP2022Z05), and Biodiversity Survey and Assessment Project Conducted in the Nanling Biodiversity Conservation Priority Area (Liuzhou area), Guangxi (11N00760329320231202).

### Author contributions

XML measured the specimens, analyzed the data, constructed the phylogenetic tree, and prepared the manuscript; RGY provided the funding for the field survey; LND conceived and designed the study and reviewed the manuscript before submission; FGL conducted field surveys and provided funding for complete mitochondrial genomes. All authors have read and agreed to the published version of the manuscript.

### Author ORCIDs

Xue-Ming Luo  <https://orcid.org/0000-0001-6441-4817>

Li-Na Du  <https://orcid.org/0000-0002-2246-643X>

### Data availability

All of the data that support the findings of this study are available in the main text or Supplementary Information.

## References

- Deng HQ, Wen HM, Xiao N, Zhou J (2016a) A new blind species of the cave genus *Oreonectes* from Guizhou, China (Nemacheilinae). *ZooKeys* 637: 47–59. <https://doi.org/10.3897/zookeys.637.10202>
- Deng HQ, Xiao N, Hou XF, Zhou J (2016b) A new species (Cypriniformes: Nemacheilidae) from Guizhou, China. *Zootaxa* 4132(1): 143–150. <https://doi.org/10.11646/zootaxa.4132.1.13>
- Du LN, Chen XY, Yang JX (2008) A review of the Nemacheilinae genus *Oreonectes* Günther with descriptions of two new species (Teleostei: Balitoridae). *Zootaxa* 1729(1): 23–36. <https://doi.org/10.11646/zootaxa.1729.1.3>
- Du LN, Yang J, Min R, Chen XY, Yang JX (2021) A review of the Cypriniform tribe Yunnaniini Prokofiev, 2010 from China, with an emphasis on five genera based on morphologies and complete mitochondrial genomes of some species. *Zoological Research* 42(3): 310–334. <https://doi.org/10.24272/j.issn.2095-8137.2020.229>
- Du LN, Li SJ, Xu F, Luo T, Luo FG, Yu GH, Zhou J (2023) Clarification of phylogenetic relationships among Chinese Nemacheilids with tube-shaped anterior nostrils, with a description of a new genus and two new species. *Journal of Zoo-*

- logical Systematics and Evolutionary Research 2023: e3600085. <https://doi.org/10.1155/2023/3600085>
- Edgar RC (2004) MUSCLE: Multiple sequence alignment with high accuracy and high throughput. *Nucleic Acids Research* 32(5): 1792–1797. <https://doi.org/10.1093/nar/gkh340>
- Günther A (1868) *Catalogue of the Fishes in the British Museum*. Trustees of the British Museum, London, 369 pp.
- Huang AM, Du LN, Chen XY, Yang JX (2009) *Oreonectes macrolepis*, a new nemacheiline loach of genus *Oreonectes* (Balitoridae) from Guangxi, China. *Zoological Research* 30(4): 445–448. <https://doi.org/10.3724/SP.J.1141.2009.04445>
- Huang JQ, Yang J, Wu ZQ, Zhao YH (2020) *Oreonectes guilinensis* (Teleostei, Cypriniformes, Nemacheilidae), a new loach species from Guangxi, China. *Journal of Fish Biology* 96(1): 111–119. <https://doi.org/10.1111/jfb.14191>
- Kottelat M (1990) *Indochinese Nemacheilines: A Revision of Nemacheiline Loaches (Pisces, Cypriniformes) of Thailand, Burma, Laos, Cambodia and Southern Vietnam*. München, United Germany, 262 pp.
- Kottelat M (2012) *Conspectus cobitidum: An inventory of the loaches of the world (Teleostei: Cypriniformes: Cobitoidei)*. *The Raffles Bulletin of Zoology* 26(6): 1–199. <https://doi.org/10.1016/j.sleep.2014.01.018>
- Lan JH, Yang JX, Chen YR (1995) Two new species of the subfamily Nemacheilinae from Guangxi, China (Cypriniformes: Cobitidae). *Dong Wu Fen Lei Xue Bao* 20(3): 366–372. [in Chinese]
- Lan JH, Gan X, Wu TJ, Yang J (2013) *Cave Fishes of Guangxi, China*. Science Press, Beijing, 68–83. [in Chinese]
- Lanfear R, Frandsen PB, Wright AM, Senfeld T, Calcott B (2017) PartitionFinder 2: New methods for selecting partitioned models of evolution for molecular and morphological phylogenetic analyses. *Molecular Biology and Evolution* 34(3): 772–773. <https://doi.org/10.1093/molbev/msw260>
- Li SJ, Ge JK, Bao CY, Du LN, Luo FG, Zhou TX (2023) *Troglonectes canlinensis* sp. nov. (Teleostei: Nemacheilidae), A new troglomorphic loach from Guangxi, China. *Animals* 13(10): e1712. <https://doi.org/10.3390/ani13101712>
- Liu X, Deng HQ, Liu ZJ, Zhou J (2019) Reassignment of *Triplophysa jiarongensis* (Cypriniformes: Nemacheilidae) to *Oreonectes* Günther, 1868. *Zootaxa* 4565(3): 398–406. <https://doi.org/10.11646/zootaxa.4565.3.6>
- Luo T, Yang Q, Wu L, Wang YL, Zhou JJ, Deng HQ, Xiao N, Zhou J (2023) Phylogenetic relationships of Nemacheilidae cavefish (*Heminoemacheilus*, *Oreonectes*, *Yunnanilus*, *Paranemachilus*, and *Troglonectes*) revealed by analysis of mitochondrial genome and seven nuclear genes. *Zoological Research* 44(4): 693–697. <https://doi.org/10.24272/j.issn.2095-8137.2022.266>
- Ronquist F, Teslenko M, Van DMP, Ayres DL, Darling A, Höhna S, Larget B, Liu L, Suchard MA, Huelsenbeck JP (2012) MrBayes 3.2: Efficient Bayesian phylogenetic inference and model choice across a large model space. *Systematic Biology* 61(3): 539–542. <https://doi.org/10.1093/sysbio/sys029>
- Tamura K, Stecher G, Kumar S (2021) MEGA11: Molecular Evolutionary Genetics Analysis Version 11. *Molecular Biology and Evolution* 38(7): 3022–3027. <https://doi.org/10.1093/molbev/msab120>
- Tang L, Zhao YH, Zhang CG (2012) A new blind loach, *Oreonectes elongatus* sp. nov. (Cypriniformes: Balitoridae) from Guangxi, China. *Environmental Biology of Fishes* 93(4): 483–449. <https://doi.org/10.1007/s10641-011-9943-7>

- Tang L (2012) Study on Taxonomy and Distribution Patterns of the Genera *Oreonectes* and *Troglonectes* gen. nov. (Cypriniformes: Balitoridae) (Master's thesis). University of Chinese Academy of Sciences, Beijing. [in Chinese]
- Wang YL (2022) Systematic taxonomy of the genus *Oreonectes* (Master's thesis). Guizhou Normal University, Guiyang. [In Chinese]
- Xue D (2010) Guide to collection, preservation, identification and information share of animal specimens. Standard Press of China, Beijing, 103–125. [in Chinese]
- Yang J, Wu TJ, Wei RF, Yang JX (2011a) A new loach, *Oreonectes luochengensis* sp. nov. (Cypriniformes: Balitoridae) from Guangxi, China. *Zoological Research* 32(2): 208–211. <https://doi.org/10.3724/SP.J.1141.2011.02208> [in Chinese]
- Yang Q, Wei ML, Lan JH, Yang Q (2011b) A new species of the genus *Oreonectes* (Balitoridae) from Guangxi, China. *Guangxi Shifan Daxue Xuebao. Ziran Kexue Ban* 29(1): 72–75. <https://doi.org/10.16088/j.issn.1001-6600.2011.01.037>
- Yu J, Luo T, Lan CT, Zhou JJ, Deng HQ, Xiao N, Zhou J (2023) *Oreonectes damingshanensis* (Cypriniformes, Nemacheilidae), a new species of stream fish from Guangxi, Southwest China. *ZooKeys* 1180: 81–104. <https://doi.org/10.3897/zookeys.1180.104645>
- Zhang CG, Zhao YH (2016) Species Diversity and Distribution of Inland Fishes in China. Science Press, Beijing, 130–148. [in Chinese]
- Zhang ZL, Zhao YH, Zhang CG (2006) A new blind loach, *Oreonectes translucens* (Teleostei: Cypriniformes: Nemacheilinae), from Guangxi, China. *Zoological Studies* 45(4): 611–615.
- Zhang XT, Xiang XH, Zhao M, Cui YC, Zhang H (2022) Coupling relationship between Pearl river water system evolution and East Asian Terrain inversion. *Earth Science* 47(7): 2410–2420. <https://doi.org/10.3799/dqkx.2022.002>
- Zheng BS (1981) Freshwater Fishes of Guangxi Province. Guangxi People's Publishers, Nanning, 93–94. [in Chinese]
- Zhu SQ (1989) The Loaches of the Subfamily Nemacheilinae in China (Cypriniformes: Cobitidae). Jiangsu Science and Technology Publishing House, Nanjing, China, 22–26. [in Chinese]

## Appendix 1

**Table A1.** Localities, voucher information, and GenBank numbers for all samples used in this paper.

Species	Locality	Voucher	GenBank number
<i>Triplophysa nasobarbatula</i>	Libo County, Guizhou, China	GZNU20190114001	ON116529
<i>Triplophysa baotianensis</i>	Nanpanjiang River, Panzhou City, Guizhou, China	GZNU20180421005	NC056365
<i>Triplophysa zhenfengensis</i>	Xingren County, Guangxi, China	GZNU20180419002	NC063617
<i>Traccaticthys pulcher</i>	Daxin County, Guangxi, China	Tissue ID: GX1	ON116516
<i>Traccaticthys zispi</i>	Hainan, China	Tissue ID: HN01	ON116518
<i>Traccaticthys taeniatus</i>	N/A	N/A	NC031581
<i>Lefua nikkonis</i>	N/A	N/A	NC027662
<i>Lefua costata</i>	N/A	N/A	NC029385
<i>Lefua echigonia</i>	N/A	N/A	NC004696
<i>Oreonectes platycephalus</i>	Shenzhen City, Guangdong, China	GZNU2020112501	ON116528
<i>Oreonectes guilinensis</i>	Xingping Town, Yangshuo County, Guangxi, China	N/A	MN239094
<i>Oreonectes damingshanensis</i>	Leping Village, Guling Town, Mashan County, Guangxi, China	GZNU20230216011	OQ754117
<i>Oreonectes damingshanensis</i>	Leping Village, Guling Town, Mashan County, Guangxi, China	GZNU20230216012	OQ754118
<i>Oreonectes damingshanensis</i>	Damingshan Mountain, Shanglin County, Guangxi, China	GZNU 2020112502	ON116496
<i>Oreonectes polystigmus</i>	Dabu Town, Yanshan District, Guilin, Guangxi, China	GZNU2020011501	ON116514
<i>Oreonectes andongensis</i> sp. nov.	Andong Town, Xincheng County, Laibin City, Guangxi, China	N/A	OR188128

Species	Locality	Voucher	GenBank number
<i>Oreonectes andongensis</i> sp. nov.	Andong Town, Xincheng County, Laibin City, Guangxi, China	N/A	OR712240
<i>Oreonectes andongensis</i> sp. nov.	Andong Town, Xincheng County, Laibin City, Guangxi, China	N/A	OR712241
<i>Oreonectes luochengensis</i>	Tianhe Town, Luocheng County, Guangxi, China	GZNU2020011502	ON116495
<i>Oreonectes guananensis</i>	Changmei Town, Huanjiang County, Guangxi, China	GZNU2020073102	ON116507
<i>Guinemachilus longibarbus</i>	Hechi City, Guangxi, China	GZNU20210823001	ON148334
<i>Guinemachilus pseudopulcherrimus</i>	Dongmiao Village, Du'an County, Hechi City, Guangxi, China	D1925	OQ024375
<i>Micronemacheilus cruciatus</i>	N/A	N/A	NC033960
<i>Micronemacheilus pulcherrimus</i>	Duan County, Hechi City, Guangxi, China	GZNU20210609004	ON116493
<i>Karstsinnectes parva</i>	Ande Town, Jingxi City, Guangxi, China	Tissue ID: JTQ02	ON116520
<i>Karstsinnectes anophthalmus</i>	Leiping Town, Daxin County, Guangxi, China	GZNU2019011310	ON116513
<i>Karstsinnectes acridorsalis</i>	Bamu Town, Tiane County, Guangxi, China	GZNU2020	ON116515
<i>Troglonectes translucens</i>	Xiaao Town, Duan County, Guangxi, China	GZNU 2020082302	ON116510
<i>Troglonectes macrolepis</i>	Dacai Town, Huanjiang County, Guangxi, China	GZNU2019122202	NC073129
<i>Troglonectes microphthalmus</i>	Tianhe Town, Luocheng County, Guangxi, China	GZNU2020041601	NC073127
<i>Troglonectes canlinensis</i>	Andong Town, Xincheng County, Liuzhou City, Guangxi, China	c FFL-2023	OQ129618
<i>Troglonectes furcocaudalis</i>	Yongle Town, Rongshui County, Guangxi, China	GZNU2020042701	ON116512
<i>Paranemachilus zhengbaoshani</i>	Duan County, Guangxi, China	GZNU20210526001	ON116530
<i>Paranemachilus chongzuo</i>	Daxin County, Chongzuo City, Guangxi, China	N/A	MW532082
<i>Paranemachilus jinxiensis</i>	N/A	N/A	NC039380
<i>Paranemachilus genilepis</i>	N/A	N/A	MT845213
<i>Yunnanilus analis</i>	N/A	N/A	MW729320
<i>Yunnanilus pleurotaenia</i>	N/A	QT95	MW192447
<i>Yunnanilus jiuchiensis</i>	Jiuchi County, Penzhou City, Sichuan, China	N/A	MW532080

## Appendix 2

**Table A2.** Measurements of the eight species of *Oreonectes*. All units are in mm.

Species	Voucher number	TL	SL	BD	BW	HL	HD	HW	ED	IW	STL	PDL	PPL	PVL	PAL	PANL	CPL
<i>O. andongensis</i> sp. nov.	GXNU20220601	74.9	60.2	10.8	9.1	13.3	7.5	10.3	2.0	5.9	4.6	37.5	12.6	35.0	49.7	46.6	6.8
	GXNU20220602	68.7	56.4	10.0	7.5	12.7	7.0	8.8	2.1	5.3	3.9	35.0	10.9	32.4	46.2	42.1	7.0
	GXNU20220603	67.2	54.4	9.4	6.5	12.2	6.2	8.3	1.8	5.1	3.9	31.4	10.8	30.2	44.2	40.6	6.4
	GXNU20220604	61.4	50.9	8.0	6.7	10.8	5.8	7.8	1.6	5.1	3.6	29.7	10.6	27.6	41.3	36.9	6.5
	GXNU20220605	57.3	47.5	7.6	6.1	10.2	5.6	7.1	1.4	4.6	3.5	28.0	10.7	26.8	38.3	34.9	6.4
	GXNU20220606	52.3	40.8	6.8	5.2	8.9	5.2	6.5	1.4	3.9	3.1	23.7	8.8	22.4	32.5	29.4	4.9
	GXNU20220607	45.9	36.7	6.4	4.5	9.0	4.5	6.1	1.3	4.0	2.9	22.7	8.7	21.3	29.8	27.9	4.9
	GXNU20220608	49.6	40.4	6.4	4.7	9.0	4.8	5.9	1.8	3.8	2.9	24.0	8.5	22.2	32.4	29.3	5.4
	GXNU20220609	48.1	38.4	6.4	4.7	8.4	4.9	6.1	1.4	3.8	2.9	22.9	7.7	21.0	30.2	27.9	5.8
	GXNU20220610	46.1	36.5	5.9	4.2	8.5	4.5	5.6	1.5	3.7	2.6	22.4	8.0	20.7	29.6	27.3	5.7
<i>O. guananensis</i>	KIZ2010003067	90.2	71.5	11.8	8.7	16.6	8.3	11.3	1.8	7.4	5.2	41.6	15.7	41.0	58.3	52.8	9.6
	KIZ2010003068	76.8	61.4	10.1	7.1	13.9	7.2	9.7	1.8	6.4	4.4	36.0	13.5	35.3	49.6	47.1	7.8
	KIZ2010003069	69.6	56.3	9.9	5.3	12.3	6.3	8.3	1.7	5.9	5.0	33.5	12.2	31.2	45.7	41.3	6.8
	KIZ2010003070	66.2	53.3	10.5	5.2	12.3	6.4	9.0	1.8	5.2	4.6	30.5	11.8	29.7	43.5	39.9	6.4
	KIZ2010003071	62.9	51.0	9.7	6.1	11.2	5.8	8.4	1.6	5.2	4.2	29.3	10.9	28.3	39.4	37.7	6.5
	KIZ2010003072	88.5	71.9	11.7	9.4	16.6	7.8	11.3	1.7	7.0	6.2	42.6	16.6	41.3	58.5	54.4	8.3
<i>O. guilinensis</i>	ASIZB208001	89.7	73.5	12.3	9.3	16.0	10.3	12.2	1.6	7.8	6.1	43.4	38.6	39.9	39.7	40.0	31.4
	ASIZB208002	81.4	67.3	12.3	9.1	14.1	8.1	10.7	1.3	7.0	5.0	15.0	12.9	13.8	12.0	11.4	10.2
	ASIZB208003	82.8	68.3	12.4	10.1	14.8	9.1	12.1	2.0	7.5	6.0	40.4	37.0	38.1	37.5	36.4	29.1
	ASIZB208004	83.8	67.1	12.4	9.7	14.5	9.0	11.7	1.5	6.7	4.4	59.7	54.2	53.7	53.2	53.0	41.3
	ASIZB208005	82.2	67.6	12.4	9.3	14.3	8.2	10.4	1.7	6.3	4.5	54.4	49.8	49.0	48.7	49.7	38.6
	ASIZB208006	63.2	52.0	9.5	7.4	12.6	7.9	9.9	1.3	5.7	4.4	8.8	7.8	8.5	7.9	9.5	6.3
	ASIZB208007	79.6	65.5	11.8	9.1	13.3	8.6	11.0	1.5	6.9	4.6	7.3	6.4	7.7	6.9	7.1	5.1

Species	Voucher number	TL	SL	BD	BW	HL	HD	HW	ED	IW	STL	PDL	PPL	PVL	PAL	PANL	CPL
<i>O. luochengensis</i>	KIZ2010003073	86.0	71.2	11.4	7.4	14.7	11.6	10.7	2.1	6.0	5.5	42.5	14.4	39.4	58.2	52.8	7.3
	KIZ2010003074	83.9	67.0	11.5	6.6	15.5	12.0	9.2	2.0	6.2	5.2	39.6	13.2	36.4	53.7	48.7	6.9
	KIZ2010003075	86.3	68.8	11.8	7.8	15.3	12.5	10.4	1.8	6.7	5.8	41.8	14.2	38.4	55.7	50.3	7.8
	KIZ2010003076	87.0	71.2	13.0	8.6	15.9	12.4	10.0	1.6	6.9	5.5	42.4	14.3	39.7	57.2	51.6	7.4
	KIZ2010003077	77.2	62.2	10.7	6.7	15.1	11.7	10.5	2.0	6.7	5.4	37.8	13.6	37.5	51.3	48.9	7.0
	KIZ2010003242	84.9	68.6	12.6	6.9	15.3	11.6	10.1	1.8	6.2	5.5	40.2	13.1	37.2	55.3	49.4	6.9
	KIZ2010003243	92.1	74.7	12.9	8.9	16.6	13.1	11.5	1.5	7.5	6.1	47.2	15.2	44.4	62.0	55.5	8.7
	KIZ2010003244	76.4	61.3	10.3	6.2	13.3	10.9	9.1	1.6	5.4	5.4	35.5	12.4	33.9	49.6	46.2	7.6
<i>O. platycephalus</i>	KIZ2003007105	82.5	64.2	12.4	6.8	16.3	12.5	11.2	2.4	6.7	6.1	41.5	14.1	36.2	51.3	48.8	7.1
	KIZ2003007106	80.1	63.2	12.0	6.0	13.2	11.0	9.9	1.9	5.9	4.6	41.1	14.4	35.7	50.6	46.5	7.7
	KIZ2003007110	75.9	60.9	10.9	6.2	13.0	10.7	9.7	1.4	5.9	5.0	38.3	11.6	34.1	47.2	45.7	7.8
	KIZ2005006211	56.7	43.1	7.2	4.6	10.5	8.6	7.0	1.5	5.0	4.3	26.7	9.6	22.8	34.5	31.7	6.3
	KIZ2005006212	49.6	38.7	6.2	4.5	9.0	7.5	6.1	1.8	4.0	3.3	23.3	8.5	21.6	30.4	28.8	5.1
	KIZ2005006214	56.9	46.5	6.9	4.7	10.4	8.5	7.2	1.7	5.0	4.2	28.4	8.4	24.6	36.3	33.3	5.6
	KIZ2005006215	61.6	47.7	7.8	5.1	10.9	9.4	7.0	1.7	5.0	3.7	28.6	10.5	25.2	38.4	34.6	6.4
	KIZ2005006216	58.0	45.6	7.8	4.8	10.0	8.2	6.7	1.5	5.0	3.5	27.4	9.2	23.8	35.9	32.5	5.5
<i>O. polystigmus</i>	KIZ2001004626	67.8	54.7	10.5	6.5	12.9	7.2	9.6	1.7	5.9	4.5	33.1	11.6	30.9	44.1	39.9	5.6
	KIZ2001004627	62.7	52.4	6.6	3.9	11.9	5.9	7.7	1.5	4.8	4.3	31.4	11.5	28.8	41.7	39.2	6.1
<i>O. polystigmus</i>	KIZ2001004628	45.8	37.4	5.3	2.9	8.9	4.2	5.1	1.2	3.3	2.9	23.9	7.2	20.4	30.6	28.5	4.3
	KIZ2001004629	51.9	42.5	7.5	3.2	9.5	5.1	5.9	1.6	3.8	3.3	25.6	9.2	22.9	32.5	29.1	6.1
	KIZ2001004630	41.8	33.7	6.6	3.1	8.2	4.3	5.2	1.4	3.6	2.8	19.9	8.5	18.8	27.4	25.0	3.5
	KIZ2001004631	44.5	36.0	5.8	3.0	8.6	4.6	5.9	1.4	3.4	3.3	21.8	8.3	20.6	28.9	27.5	4.0
	KIZ2001004632	49.5	39.9	6.9	3.5	9.6	5.1	6.2	1.2	3.8	3.0	25.5	9.3	21.3	32.0	30.1	4.7
	KIZ2001004633	51.0	41.2	6.6	3.7	9.9	4.9	6.3	1.6	3.4	3.4	24.5	8.5	22.7	32.8	29.2	4.2
	KIZ2001004634	55.2	44.4	6.6	4.0	10.5	5.6	7.4	1.5	4.5	3.3	26.8	10.0	24.4	35.3	33.4	5.2

Table A2. Continued.

Species	Voucher number	CPD	DFL	DFBL	PFL	PFBL	VFL	VFBL	AFL	AFBL	MBL	OSBL	ISBL	DAN	DPN	DAPN
<i>O. andongensis</i> sp. nov.	GXNU20220601	6.7	10.8	6.9	11.4	2.3	8.2	2.1	8.7	4.3	6.9	8.3	6.3	4.3	4.7	1.5
	GXNU20220602	6.6	10.7	5.8	9.1	2.3	7.1	2.2	8.7	4.4	7.0	7.9	5.7	4.6	4.8	1.2
	GXNU20220603	5.3	10.5	6.3	9.6	2.1	7.3	2.0	9.4	4.0	6.0	7.8	5.5	4.1	4.7	1.2
	GXNU20220604	5.2	9.3	5.3	8.2	2.2	5.7	2.0	7.4	3.9	4.7	7.3	5.2	3.6	4.2	1.1
	GXNU20220605	5.0	8.5	4.9	7.2	1.9	6.0	1.7	7.3	3.7	4.6	5.3	3.8	3.2	4.0	0.9
	GXNU20220606	3.7	7.1	4.2	6.8	1.4	4.9	1.4	5.8	2.8	3.9	4.9	2.3	2.8	3.4	0.8
	GXNU20220607	4.3	6.6	3.9	6.2	1.6	4.7	1.1	6.1	2.5	4.1	4.6	2.7	2.8	3.2	0.7
	GXNU20220608	4.4	6.8	3.9	6.7	1.7	4.6	1.2	6.4	3.2	4.0	5.5	2.4	3.2	3.5	0.9
	GXNU20220609	3.9	7.1	3.8	6.5	1.6	4.9	1.5	6.8	3.1	4.7	5.8	3.8	2.9	3.0	0.8
	GXNU20220610	4.1	6.8	3.3	6.0	1.2	4.7	1.1	5.6	2.5	4.0	4.2	2.8	2.5	2.9	0.9
<i>O. guananensis</i>	KIZ2010003067	7.2	12.7	6.8	11.6	2.8	8.8	3.0	10.5	5.3	9.1	11.3	7.8	5.1	5.7	1.4
	KIZ2010003068	6.9	11.0	6.0	10.5	2.3	8.0	2.2	9.5	4.5	7.6	9.8	5.9	4.8	5.0	1.8
	KIZ2010003069	6.1	10.0	5.4	8.9	2.1	7.6	1.9	8.5	4.0	7.6	8.8	6.3	4.3	4.7	1.2
	KIZ2010003070	5.7	9.7	5.8	8.6	2.3	6.7	1.7	7.6	3.6	6.9	7.9	5.0	4.1	4.8	1.6
	KIZ2010003071	5.5	9.5	5.6	8.7	1.7	6.3	2.1	8.2	3.8	5.9	7.4	3.4	4.1	4.5	0.9
	KIZ2010003072	8.1	12.7	7.0	10.5	3.2	10.1	2.2	10.5	4.8	9.2	11.8	6.8	5.9	6.2	1.8
<i>O. guilinensis</i>	ASIZB208001	38.3	12.2	6.8	10.7	2.7	9.0	2.2	10.9	4.3	7.1	7.4	4.6	5.7	6.0	1.9
	ASIZB208002	12.6	12.8	5.9	10.5	2.9	8.4	2.3	10.1	5.1	6.9	7.4	5.2	4.1	4.8	1.5
	ASIZB208003	35.4	11.6	6.3	10.9	3.1	8.3	2.2	9.8	4.8	8.2	6.7	4.4	5.1	5.6	1.7
	ASIZB208004	52.3	12.0	4.8	10.3	2.1	7.3	2.3	9.8	4.2	6.0	7.7	5.1	4.8	5.0	1.7
	ASIZB208005	48.6	11.5	5.5	9.6	2.9	7.9	2.2	9.7	4.6	6.4	5.9	4.5	4.9	5.1	1.4
	ASIZB208006	7.6	8.7	5.4	8.0	2.0	6.3	1.8	8.1	3.8	4.7	5.3	4.4	3.8	4.5	1.3
	ASIZB208007	6.4	11.4	5.6	10.5	2.2	7.2	1.7	8.8	4.5	6.1	7.6	4.6	4.1	4.9	1.0

Species	Voucher number	CPD	DFL	DFBL	PFL	PFBL	VFL	VFBL	AFL	AFBL	MBL	OSBL	ISBL	DAN	DPN	DAPN
<i>O. luochengensis</i>	KIZ2010003073	8.6	13.0	7.5	10.9	2.9	8.5	2.2	11.4	5.0	6.1	7.3	4.4	5.0	5.6	1.4
	KIZ2010003074	6.6	12.7	6.7	11.7	2.8	9.0	2.3	10.9	4.4	6.7	7.7	4.5	4.9	5.3	1.3
	KIZ2010003075	7.5	13.2	6.9	12.7	3.1	10.1	2.4	11.6	4.9	8.5	9.3	6.2	5.2	5.8	1.2
	KIZ2010003076	7.5	12.3	6.8	11.9	2.9	9.3	2.3	10.9	5.1	7.2	8.3	4.6	5.0	5.4	1.5
	KIZ2010003077	7.1	11.4	6.3	10.8	3.0	8.2	1.9	9.6	4.6	7.5	9.4	5.6	5.0	5.2	2.0
	KIZ2010003242	6.8	12.7	6.6	11.6	3.0	9.8	2.7	10.5	5.0	6.4	6.7	4.8	4.9	5.4	1.3
	KIZ2010003243	8.7	12.6	7.3	12.0	3.6	9.3	2.4	10.5	4.9	7.2	7.4	4.8	5.2	6.0	2.1
	KIZ2010003244	6.0	11.3	6.0	11.3	3.4	8.6	2.0	9.6	4.2	6.4	6.6	5.1	4.7	5.0	1.4
<i>O. platycephalus</i>	KIZ2003007105	8.9	13.6	6.8	12.9	3.5	11.5	2.7	12.1	4.9	9.2	10.9	6.3	5.7	6.2	1.8
	KIZ2003007106	7.9	12.0	6.4	11.5	2.5	9.7	2.1	10.5	5.2	6.9	8.2	5.3	4.9	5.1	1.6
	KIZ2003007110	7.5	9.5	6.0	9.4	2.5	8.8	2.2	8.8	4.6	6.5	7.0	4.2	4.0	4.9	1.5
	KIZ2005006211	5.8	8.5	4.1	8.5	1.9	7.6	1.6	8.2	3.7	5.4	5.5	4.2	4.0	4.3	1.2
	KIZ2005006212	5.7	8.0	4.3	8.5	2.0	7.2	1.8	7.4	3.5	4.6	5.6	3.4	3.0	3.4	0.9
	KIZ2005006214	5.8	9.5	4.6	9.1	1.8	7.7	1.8	8.4	3.7	4.8	4.9	4.1	3.9	4.1	1.1
	KIZ2005006215	6.1	9.4	4.6	9.1	2.3	8.0	2.0	8.8	3.7	4.7	6.1	3.9	4.0	4.6	1.3
	KIZ2005006216	5.5	8.8	4.5	9.3	2.1	8.0	1.8	8.2	3.8	3.8	5.8	3.7	3.2	4.0	1.0
<i>O. polystigmus</i>	KIZ2001004626	7.3	10.1	6.0	8.3	2.0	7.0	1.7	8.6	4.3	6.5	7.9	4.7	4.8	5.4	1.1
	KIZ2001004627	5.8	8.9	4.8	7.1	2.0	6.3	1.6	8.1	3.9	6.4	5.4	3.5	3.4	4.4	1.0
<i>O. polystigmus</i>	KIZ2001004628	3.2	6.8	3.7	6.2	1.6	5.9	1.4	6.1	4.1	3.0	4.6	3.2	2.7	3.3	1.1
	KIZ2001004629	4.2	7.5	4.2	7.0	1.8	5.2	1.1	6.8	3.6	4.9	5.5	3.1	2.9	3.3	1.2
	KIZ2001004630	3.9	6.7	3.6	5.3	1.5	4.9	1.0	5.0	2.6	2.9	4.6	1.7	2.7	3.2	0.7
	KIZ2001004631	4.3	6.1	3.2	5.2	1.5	4.5	1.4	5.4	2.6	3.5	4.9	2.7	2.3	3.0	1.1
	KIZ2001004632	3.8	7.1	3.6	5.6	1.1	5.9	1.1	6.9	3.9	3.7	3.8	2.4	2.8	3.5	0.9
	KIZ2001004633	5.0	8.1	4.0	8.0	1.7	5.9	1.2	7.5	3.3	5.0	6.1	4.7	3.0	3.5	1.0
	KIZ2001004634	4.3	7.8	5.4	7.0	1.9	6.0	1.6	7.4	4.0	5.9	5.8	4.1	3.0	3.6	1.1



# New records of rove beetles from the Province of Quebec, and additional provincial records in Canada (Coleoptera, Staphylinidae)

Nicolas Bédard<sup>1</sup>, Adam Brunke<sup>2</sup>, Pierrick Bloin<sup>1</sup>, Ludovic Leclerc<sup>1,3</sup>

1 Natural Resources Canada, Canadian Forestry Service, Laurentian Forestry Centre, 1055, rue du P.E.P.S., C. P. 10380, Quebec, QC G1V 4C7, Canada

2 Canadian National Collection of Insects, Arachnids and Nematodes, Agriculture and Agri-Food Canada, 960 Carling Avenue, Ottawa, ON, K1A 0C6, Canada

3 Laval University, 12325, rue de l'Université, Quebec, QC G1V 0A6, Canada

Corresponding author: Nicolas Bédard ([nicolas.bedard@nrcan-rncan.gc.ca](mailto:nicolas.bedard@nrcan-rncan.gc.ca))

## Abstract

We newly report 25 provincial records of rove beetles (Coleoptera: Staphylinidae) from the province of Quebec from the following subfamilies: Steninae (1), Euaesthetinae (1), Omaliinae (2), Oxyporinae (1), Paederinae (1), Proteininae (1), Pselaphinae (2), Scaphidiinae (2), Scydmaeninae (2), Staphylininae (11) and Tachyporinae (1). Among these, two species are also reported for the first time from Ontario, two from Nova Scotia, and five are new Canadian records. We also report the first supporting data for *Sunius melanocephalus* (Fabricius, 1792) and *Scopaeus minutus* Erichson, 1840 for Quebec, and of *Arpedium schwarzi* Fauvel, 1878, *Phyllodrepa punctiventris* (Fauvel, 1878), and *Sepedophilus basalis* (Erichson, 1839) for Ontario. Specimen data and diagnoses are provided for each species, as well as references for identification where available.

**Key words:** Euaesthetinae, Omaliinae, Paederinae, Proteininae, Pselaphinae, Scaphidiinae, Staphylininae, Steninae, Tachyporinae



Academic editor: Zi-Wei Yin

Received: 12 January 2024

Accepted: 24 January 2024

Published: 1 April 2024

ZooBank: <https://zoobank.org/BACE4334-CEC3-48F2-A9A1-A77D1F106FD3>

**Citation:** Bédard N, Brunke A, Bloin P, Leclerc L (2024) New records of rove beetles from the Province of Quebec, and additional provincial records in Canada (Coleoptera, Staphylinidae). ZooKeys 1196: 303–329. <https://doi.org/10.3897/zookeys.1196.118698>

**Copyright:** © Copyright work is made by His Majesty or by an officer or servant of the Crown in the course of his duties.

This is an open access article distributed under terms of the CC0 Public Domain Dedication.

## Introduction

The rove beetles (Staphylinidae) are one of the most speciose insect groups, with more than 66,000 described species (Newton 2022) and many more to discover. However, faunistic knowledge and a precise inventory are still lacking in most parts of the world. Many recent works (e.g., Brunke and Marshall 2011; Brunke et al. 2011, 2012a, 2021; Webster and Demerchant 2012a, 2012b, Webster et al. 2012a, 2012b, 2012c, 2012d, 2012e, 2012f, 2016; Brunke 2016; Klimaszewski et al. 2016, 2017, 2020, 2021) have documented and greatly expanded the knowledge on species diversity in Canada. In the latest checklist of the beetles of Canada and Alaska (Bousquet et al. 2013), there were 769 species of rove beetles known from the province of Quebec. Since then, this number has significantly increased, whether through the descriptions of new species, or by more extensive inventories resulting in the discovery of broader distributions for described species. In recent years, molecular-based approaches

to faunistics have provided several important additions to the Staphylinidae of Canada and underlined the necessity for a deeper and more extensive taxonomic study of Nearctic beetles (Hebert et al. 2016; Pentinsaari et al. 2019; Brunke et al. 2021). Despite the enormous changes to the fauna of Canada and Quebec since Bousquet et al. (2013), many staphylinid groups remain in the same or similar state of knowledge as reported in Brunke et al. (2012b). The small size of most species, their great diversity, and the lack of easily observed, external diagnostic characters in many groups have traditionally made these beetles less attractive for collectors, but their ubiquity and diversity of ecological roles make them extremely useful tools for ecological and conservation studies (Pohl et al. 2008).

Following the examples set by the above cited works, and in order to better document species in northeastern Canada, the authors have increased their efforts in the last few years to collect and identify many specimens of rove beetles from various locations in the province of Quebec. This collecting effort, in conjunction with intensive curatorial work in some major collections, has led to the discovery of several unrecorded species in the province and elsewhere in Canada. We report 25 new records of Staphylinidae in Quebec (excluding the Aleocharinae, which will be treated in a separate paper), with two additions to the Ontario fauna and two from Nova Scotia. We also provide images for poorly known species that have not been clearly illustrated previously in the North American taxonomic literature.

## Materials and methods

Acronyms of collections referred to in this publication are as follows:

- CCC** Claude Chantal Insect collection (private collection), Varenne, Quebec, Canada
- CTC** Claude Tessier Insect collection (private collection), Cap-Rouge, Quebec, Canada
- CMNC** Canadian Museum of Nature, Gatineau, Quebec, Canada
- CNC** Canadian National Collection of Insects, Arachnids, and Nematodes, Agriculture and Agri-Food Canada, Ottawa, Ontario, Canada
- DEBU** University of Guelph Insect Collection, University of Guelph, Guelph, Ontario, Canada
- LFC** Laurentian Forestry Center (Natural Resources Canada), René-Martineau Insectarium, Quebec, Quebec, Canada
- LLC** Ludovic Leclerc Insect Collection (private collection), Quebec, Quebec, Canada
- NBC** Nicolas Bédard Insect Collection (private collection), Quebec, Quebec, Canada
- ORC** Ouellet-Robert Collection, Université de Montréal, Montréal, Quebec, Canada
- PBC** Pierrick Bloin Insect Collection (private collection), Quebec, Quebec, Canada
- PdTC** Pierre de Tonnancour Insect Collection (private collection), Quebec, Quebec, Canada

**RVC** Robert Vigneault Insect Collection (private collection), Oka, Quebec, Canada  
**SDC** Stéphane Dumont Insect Collection (private collection), Montréal, Quebec, Canada

Canadian province and territory abbreviations:

**AB** Alberta  
**BC** British Columbia  
**LB** Labrador  
**MB** Manitoba  
**NB** New Brunswick  
**NF** Newfoundland  
**NS** Nova Scotia  
**NT** Northwest Territories  
**NU** Nunavut  
**ON** Ontario  
**PE** Prince Edward Island  
**QC** Quebec  
**SK** Saskatchewan  
**YT** Yukon Territory

Most specimens from 2020–2023 were collected using various active methods, such as using an entomological aspirator and by sifting various substrates (wood chips, decaying plant matter, etc.). Many individuals were captured in different types of traps, mainly pitfall traps baited with vinegar and ethanol, but also using white tulle fabric interception traps and standard flight-interception traps with collection pans underneath. Some species were also attracted with UV light, either suspended on a white sheet or combined with a white-cross-vane. Many, mostly older records, were found after consulting several collections.

Identifications were made by using available literature (see documentation under each species) or by comparing with voucher specimens housed in the LFC or the CNC. Most specimens were dissected, and their genitalia were mounted in Canada balsam or Euparal, on a microslide with the specimens. Specimens requiring confirmation were validated with external expertise, with detailed pictures or through physical examination. The illustrations were made using a Canon EOS 90D camera with a Canon MP-E 65mm f/2.8 1–5× lens, mounted on Cognisys Stackshot Macro-Rail. The images were processed and stacked using Helicon Focus, and final adjustments were made using Adobe Lightroom/Photoshop.

## **New provincial and Canadian records**

Adventive species are indicated with an asterisk (\*) after the name. Only examined specimens deposited in private or public collections are reported under specimen data. The occurrence records from various websites, such as iNaturalist or BugGuide, are reported as “Internet data”, but only if the pictures were detailed enough for confident identification. The distribution of each species in Canada is based on the most recent available work, with new territory records placed in bold.

Label data are provided in chronological order for every species within each regional county municipality (MRC). Some data were translated from French to English, and various details known but not necessarily appearing on the labels (e.g., current MRC, GPS coordinates, collecting technique, general habitat, etc.) have been added. Each recent record follows the format: **COUNTRY: PROVINCE – County/Regional county municipality**, City [more precise location when necessary](GPS points), date of collecting, collector(s), collection method (number of specimen(s), collection abbreviation in which they are deposited). For older specimens, labels were reported verbatim, since data were frequently incomplete or imprecise.

### **Family Staphylinidae Latreille, 1802**

#### **Subfamily Steninae MacLeay, 1825**

#### ***Stenus (Stenus) colon* Say, 1831**

Fig. 1

**Note.** This species was previously only known to reach Ontario in Canada (Bousquet et al. 2013). It can be separated from the other *Stenus* species by the wide reniform macula on each elytron, pale femora, usually with dark band at mid-length, and the head broader than the elytra. In the northeast, it is unmistakable and does not resemble any other known species. It resembles to the more southerly distributed *Stenus renifer* Lec., from which it can be readily distinguished by its larger size, broader elytra, and denser abdominal punctuation.

**Specimen data. CANADA: QUEBEC – MRC de Memphremagog**, Pottton (45.0162, -72.4344), 20.VII-5.VIII.2022, N. Bédard, pitfall trap on a sandy river shore (1, NBC). – **Ville de Québec, Cap-Rouge** (46.7543, -71.3464), 29.VI.2023, C. Tessier, on a river bank (3, CTC). – **Ville de Lévis**, St-Nicolas (46.6902, -71.3120), 29.IX.2009, C. Tessier, sifting grass pile near a wetland (1, CTC).

**Distribution in Canada.** ON, QC (Bousquet et al. 2013) - **New to Quebec.**

#### **Subfamily Euaesthetinae Thomson, 1859**

#### ***Euaesthetus similis* Casey, 1884**

**Note.** See Puthz (2014) for identification and illustrations. The available collection data (Puthz 2014) indicate that this species is predominantly found near water, inhabiting wetlands and areas along rivers. One specimen was collected in a muskrat nest. Less often, the species has also been collected in drier microhabitats including an alvar and cotton fields, although both of these habitats may experience flooding during heavy rains. Males can be easily recognized among other *Euaesthetus* by their strongly iridescent elytra and bifurcate parameres of the aedeagus (Puthz 2014).

**Specimen data. CANADA: QUEBEC – MRC de-la-Vallée-du-Richelieu**, Carignan (45.475882, -73.274623), 6.V.2022, N. Bédard, sifting river debris (1, NBC). – **MRC de Memphrémagog**, Pottton (45.0259, -72.4279), 5.VIII.2022, L. Leclerc, pitfall trap baited with apple cider vinegar (2, LLC).

**Distribution in Canada.** ON, QC, NB (Puthz, 2014) - **New to Quebec.**

**Subfamily Omaliinae MacLeay, 1825**

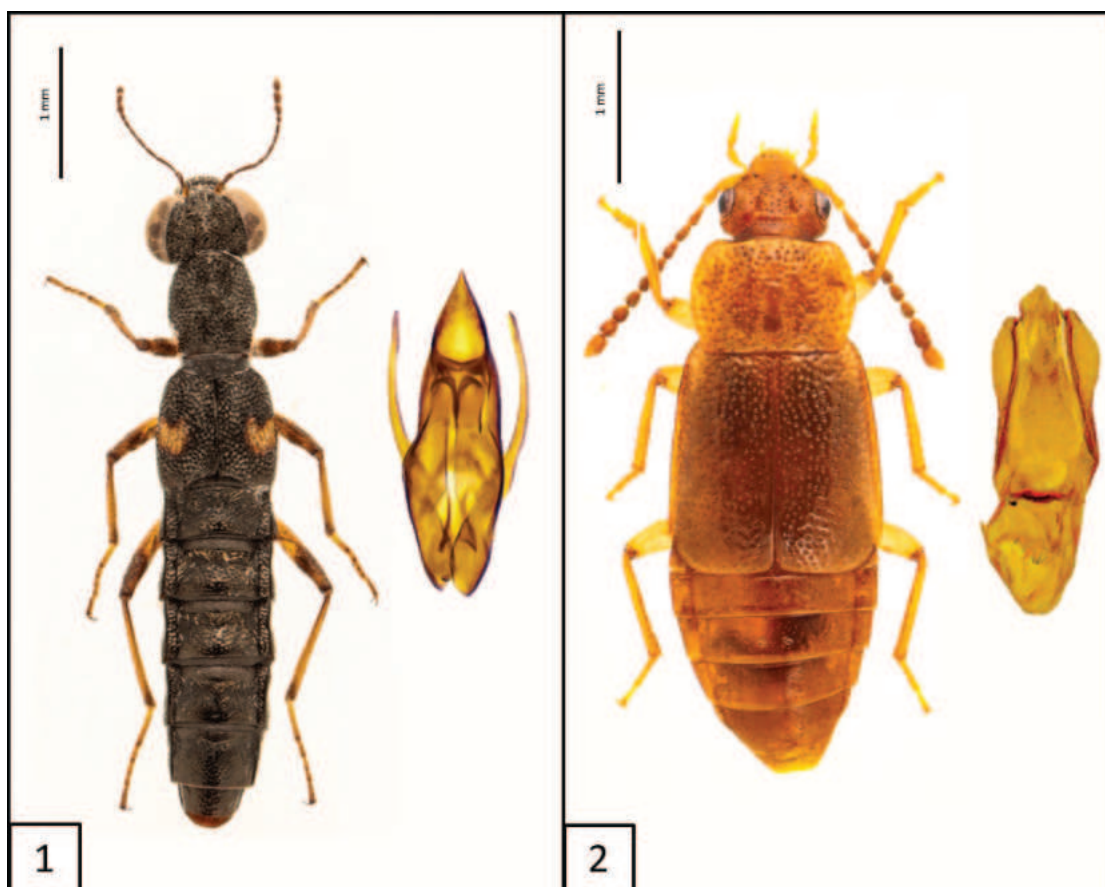
***Arpedium schwarzi* Fauvel, 1878**

Fig. 2

**Note.** See Campbell (1984) for identification. *Arpedium schwarzi* was previously recorded in Ontario, Canada, only from specimens collected at the hedgerow edges of soybean fields (Brunke et al. 2014, see supplementary material). Vouchers were deposited in DEBU, but the specimen data were not published. They are provided below, along with a new record from Quebec.

**Specimen data. CANADA: ONTARIO - Huron Co.,** Auburn (43.729, -81.528), 23.XI.2009, A. Brunke, forested hedgerow beside soybean field, pitfall (1, DEBU); Auburn (43.745, -81.508), 27.X.2010, forested hedgerow beside soybean field, near river, pitfall (1, DEBU); Auburn (43.745, -81.514), 10.XI.2010, forest hedgerow beside soybean field, pitfall (1, DEBU); Brucefield (43.509, -81.528), 23.XI.2009, A. Brunke, hedgerow near ditch, pitfall (3, DEBU). **QUEBEC - MRC de Memphrémagog,** Magog (45.281547, -72.171752), 25.V.2023, P. Bloin, sifted from *Sphagnum* moss in a bog (1, PBC).

**Distribution in Canada.** ON, QC (Bousquet et al. 2013) - **New to Quebec, supporting data for Ontario.**



Figures 1, 2. Habitus and aedeagus of 1 *Stenus colon* Say, 1831, aedeagus dorsal view 2 *Arpedium schwarzi* Fauvel, 1878, aedeagus ventral view.

***Phyllodrepa punctiventris* (Fauvel, 1878)**

Fig. 3

**Note.** *Phyllodrepa punctiventris* is easily distinguished from other species in eastern North America by the entirely pale body. In the case of teneral specimens, it can be recognized by the pronotum with microsculpture of transverse waves across the entire disc, elytra without scratch-like sculpture between the punctures and elytral punctures in clear longitudinal rows. The parameres of the aedeagus are also distinctive (Fig. 3). Little has been published about the species' microhabitat preferences, but it may live in bird nests or tree-holes, as one of the Quebec specimens was collected in a canopy trap and one specimen from Washington DC (CNC) was collected from an oak tree-hole. We are not aware of previously published specimen data for Ontario, so the data are provided below.

**Specimen data. CANADA: ONTARIO – Chatham-Kent Region**, Rondeau Provincial Park, Nature Centre, at blacklight at edge of forest, 31.V.1985, L. LeSage (1, CNC). **QUEBEC – MRC des Deux-Montagnes**, Parc National d'Oka (45.4767, -74.0537), 27.V.2002, R. Vigneault [Collected with permit] (1, RVC); Same general locality and collector but 20.V.2017 (1, RVC); Same general locality and collector but 2.V.2018, white tulle fabric interception trap in a compost site (1, LLC). – **MRC du Haut-St-Laurent**, Havelock (45.026750, -73.800528), 3–18.VI.2023, N. Bédard, Canopy cross-vane trap with fermentation bait (1, NBC).

**Distribution in Canada.** ON, QC (Bousquet et al. 2013) - **New to Quebec, supporting data for Ontario.**

**Subfamily Paederinae Fleming, 1821**

***Scopaeus (Scopaeus) minutus* Erichson, 1840\***

**Note.** See Brunke and Marshall (2011) for illustrations and identification. This adventive species was first reported from Montreal, Quebec, Canada, by Frisch et al. (2002) without presenting precise occurrences or vouchers. Additional data were provided by Brunke and Marshall (2011) for Ontario and by Webster et al. (2016) for New Brunswick, and we here provide the first distribution data for Quebec.

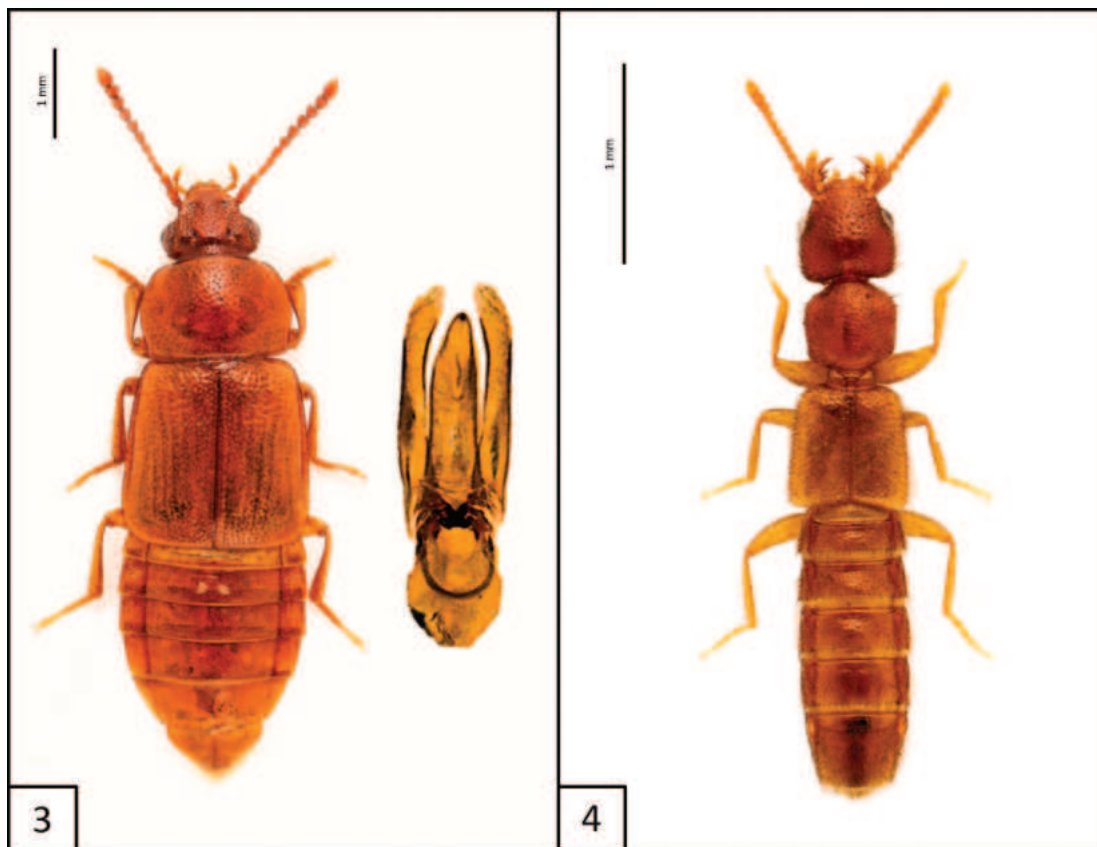
**Specimen data. CANADA: QUEBEC - Ville de Lévis**, Saint-Nicolas (-71.3120, 46.6902), 14.V.2022, L. Leclerc, sifted from wood debris and *Sphagnum* sp. (1, LLC). - **Ville de Québec**, St-Augustin-de-Desmaures (46.7371, -71.4122), 6.V.2023, N. Bédard, sifting moss on a disturbed field (3, NBC). - **MRC de Portneuf**, Pont-Rouge (46.7543, -71.7183), 1.VIII.2022, L. Leclerc, ultraviolet cross-vane panel trap (1, LLC); same locality except 22.IV.2023, L. Leclerc, by sifting *Betula* and *Populus* leaf litter in a sandpit (2, LLC).

**Distribution in Canada.** ON, QC, NB (Webster et al. 2016) - **Supporting data for Quebec.**

***Hypomedon debilicornis* (Wollaston, 1857)\***

Fig. 4

**Note.** As reported by Schülke and Smetana (2015), this cosmopolitan species has been recorded from Nearctic, Neotropical, Palearctic, Oriental, and



Figures 3, 4. Habitus and aedeagus of 3 *Phyllodrepa punctiventris* (Fauvel, 1878), aedeagus ventral view 4 *Hypomedon debilicornis* (Wollaston, 1857), habitus only.

Australian regions. Notably, this species exhibits parthenogenesis wherein females evolved without sexual reproduction, a factor that is believed to have facilitated its spread (Owen and Allen 2000). The species can be distinguished from other *Medonina* in eastern Canada by its pale body, small but protruding eyes, transverse subapical antennomeres, smooth lateral pronotal margins and lack of velvety appressed pubescence on the forebody. We here extend its distribution northward and newly report the species from Quebec and Canada.

**Specimen data. CANADA: QUEBEC - MRC Marguerite-D'Youville**, Saint-Amable (45.6431, -73.3341), 31.VIII.2023, L. Leclerc, by sifting wood chips heap (2, CNC; 5, LLC; 1, PBC; 1, NBC).

**Distribution in Canada. QC - New to Canada and Quebec.**

### ***Sunius melanocephalus* (Fabricius, 1792)\***

**Note.** See Assing (1995, 2008) and Brunke and Marshall (2011) for identification and illustrations. As in *Scopaeus minutus*, no voucher data were provided with the first Quebec record (Campbell and Davies 1991). The species was recorded for the first time in North America by Hoebeke (1991), and Brunke and Marshall (2011) added records for Ontario. We here provide supporting data for Quebec, including those for the original record, and the oldest available Canadian records for the species thus far. The species has occurred in North America since at least 1924 (Hoebeke 1991).

**Specimen data. CANADA: ONTARIO - Ottawa Reg.,** Kinburn, 10.X.1967, J.M. Campbell & A. Smetana, ex. nest of *Microtus pennsylvanicus* (1, CNC); Ottawa [Shirley's Bay], 2.V.1979, A. & Z. Smetana (2, CNC); Fitzroy Provincial Park, 2–3.V.1979, A.&Z. Smetana (1, CNC); Kanata, 25.IV.1969, A. Smetana (1, CNC); Ottawa, 12.IV.1959, J.E.H. Martin (2, CNC). - **Toronto Reg.,** Toronto [Islington], 24.VIII.1990, S. Snäll (1, CNC); Toronto, 12.IX.1990, S. Snäll, lakeshore (1, CNC). **QUEBEC - Parc de la Gatineau,** King Mountain, 20.IV.1968, A. Smetana (1, CNC). - **MRC de-la-Vallée-du-Richelieu,** Carignan (45.475882, -73.274623), 6.V.2022, N. Bédard, Sifting grass pile near an urban forest (3, NBC). - **MRC de l'Île-d'Orléans,** Saint-Pierre-de-l'Île-d'Orléans (46.8813, -71.0551), 10.IX.2022, L. Leclerc, sifted from *Populus* and *Betula* leaf litter (1, LLC). - **MRC des Jardins-de-Napierville,** Sainte-Clothilde [Piège #1 carottes] 17.VI.1985, Guy Boivin (1, CNC). - **Ville de Québec,** Sainte-Foy (46.7923, -71.2803), sifted from *Robinia pseudoacacia* leaf litter (2, LLC); Cité-Universitaire (46.7863, -71.2686), 26.IV.2023, L. Leclerc, sifted from wood chips (2, PBC).

**Distribution in Canada.** ON, QC (Bousquet et al. 2013) - **Supporting data for Quebec.**

### Subfamily Oxyporinae

#### *Oxyporus ashei* Campbell, 1978

Fig. 5

**Note.** See Campbell (1978) for identification. *Oxyporus ashei* was described by Campbell (1978) based on four specimens from North Carolina. We newly record it here from southern Canada (QC, ON), extending its distribution far northward. This species is rarely collected but can be easily recognized by the mostly pale orange-yellow body dorsally, contrasting with the dark ventral head and thorax. Its color pattern is strikingly similar to the distantly related and common eastern species *Pseudoxyporus lateralis* (Gravenhorst, 1802) but can be distinguished by the much shorter antennae and entirely dark mandibles.

**Specimen data. CANADA: QUEBEC – MRC des Deux-Montagnes,** Parc National d'Oka (45.472273, -74.049343), 1.VII.2018, R. Vigneault, white tulle fabric interception trap [Collected with permit] (1, RVC).

**Internet data. CANADA: ONTARIO-** York Co., King City (43.9635, -79.5227), 2.VIII.2021, Shuk Han (Nancy) Mak, Recorded through iNaturalist (Obs.: 89701768).

**Distribution in Canada.** ON, QC - **New to Ontario, Quebec, and Canada.**

### Subfamily Proteininae Erichson, 1839

#### *Proteinus parvulus* LeConte, 1863

**Note.** See Webster et al. (2016) for illustrations and identification. The species was described by LeConte (1863) from "Lake Superior". This was later corroborated by records from Ontario by Hubbard et al. (1878). More recently, Webster et al. (2016) have extended its known range by recording it from six Canadian provinces (see below). Although recognized as a transcontinental species in Canada, the distribution appeared disjunct as there have been no

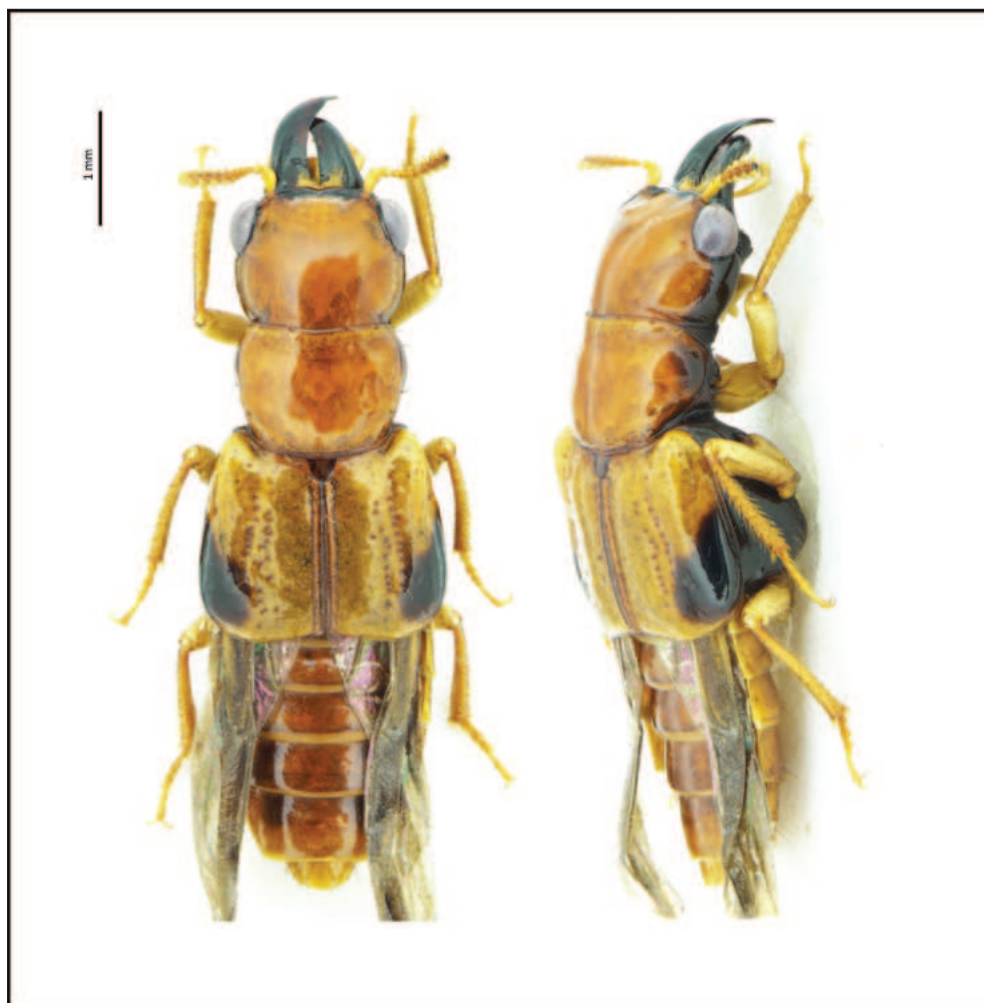


Figure 5. Habitus of *Oxyporus ashei* Campbell, 1978, dorsal and lateral views.

published records of its presence in Quebec until now. We here support this distribution with the first vouchers of the species from Quebec.

**Specimen data. CANADA: QUEBEC - MRC La Jacques-Cartier, Lac-Croche** (47,389896, -71,811252), 8–22.VII.2020, Christian Hébert (Canadian Forest Service), pitfall trap, projet d'aire protégée Ya'nienhonhndeh [2020-3-8822], (1, LFC); same information but (47,419579, -71,801022), 22.VII-6.VIII.2020, [2020-3-9022], (1, LFC); same information but (47,403227, -71,796046) [2020-3-8891], (1, LFC); same information but (47,259286, -71,659231), multi-directional impact trap [2020-3-8943], (1, LFC); same information but (47,371618, -71,782273) multi-directional impact trap [2020-3-8943], (2, LFC).

**Distribution in Canada.** YT, BC, AB, SK, MB ON, QC, NB (Webster et al. 2016) - **New to Quebec.**

#### **Subfamily Pselaphinae Latreille, 1802**

#### ***Eutyphlus schmitti* Raffray, 1904**

**Note.** See Owens and Carlton (2016) for illustrations and identification. The first five specimens were found in Berlese-Tullgren extractions of forest leaf

litter collected on Mont Écho in 2012 (one on 14 June, and four on 20 July). All of these specimens come from stands dominated by *Acer saccharum*, *Betula papyrifera*, and *Fagus grandifolia*. It represents the first record of this genus and species in Quebec and Canada. Another specimen was found in 2016 in southern Quebec, in a pitfall trap in a maple-dominated forest. *Eutyphlus schmitti* is present in mountainous regions from Quebec and New Hampshire, southward to North Carolina and westward to Ohio (Owens and Carlton 2016; present study). It was found to be particularly abundant in old-growth hardwood forests in New Hampshire (Chandler 1987).

**Specimen data. CANADA: QUEBEC - MRC du Brôme-Missisquoi**, Sutton (45.10389, -72.50861) 14.VI.2012, P.M. Brousseau, maple forest (1, ORC); same but 20.VII.2012 (4, ORC). - **MRC du Granit**, Lac Mégantic [148-101], 21.VII.2016, MFFP, pitfall trap 2016-0004 (1, LFC).

**Distribution in Canada. QC** (Owens and Carlton 2016) - **New to Quebec and Canada.**

### ***Thesium cavifrons* (LeConte, 1863)**

**Note.** See Grigarick and Schuster (1980) and Chandler (1989) for identification and illustrations. This species is the only *Thesium* in northeast North America (Chandler 2000). It can be readily distinguished from the other members of Euplectini by the carinate prosternum and the clearly separated mesocoxal cavities. In addition to the literature cited above for its identification, photos of the holotype are accessible via the MCZ website (type #27740).

**Specimen data. CANADA: QUEBEC - Gatineau City**, Buckingham (45°34'N, 75°28'W) 3–10.VII.2000, C. Hébert (Canadian Forest Service), Projet Verglas (1, CNC).

**Distribution in Canada. ON, QC** (Bousquet et al. 2013) - **New to Quebec.**

### **Subfamily Scydmaeninae Leach, 1815**

#### ***Euconnus (Euconnus) remiformis* Stephan & Chandler, 2021**

**Note.** See Stephan et al. (2021 [2020]) for identification and illustrations. This and the following species were recently described in a Nearctic revision of the subgenus *Napochus* (Stephan et al. 2021 [2020]), from specimens collected in several eastern states. Both were initially described in the subgenus *Napochus*, but shortly after their description, Jałoszyński (2021) synonymized the subgenus with *Euconnus* s. str. *Euconnus remiformis* is mostly known from the southeastern United States, but was also reported from the northeast based on a single specimen from Maine (Stephan et al. 2021 [2020]). The present record supports a more widespread distribution in the north.

**Specimen data. CANADA: QUEBEC - MRC du Haut-St-Laurent**, Havelock (45.0258, -73.7993), 3–17.VII.2023, N. Bédard, Interception trap in an oak and maple forest (1, NBC).

**Distribution in Canada. QC** (Stephan et al. 2021 [2020]) - **New to Quebec and Canada.**

### ***Euconnus (Euconnus) separatus* Stephan & Chandler, 2021**

**Note.** See Stephan et al. 2021 [2020] for identification and illustrations. This species was known to occur as far north as the Upper Peninsula of Michigan, south to Florida, where it is rather common (Stephan et al. 2021 [2020]). Therefore, its presence in southern Quebec and Canada was expected and it is likely even more widespread in eastern Canada (Ontario and New Brunswick) given greater sampling effort, and modern taxonomic revision available.

**Specimen data. CANADA: QUEBEC - MRC du Haut-St-Laurent,** Havelock (45.0258, -73.7993), 3–17.VII.2023, N. Bédard, Interception trap in an oak and maple forest (1, NBC).

**Distribution in Canada. QC** (Stephan et al. 2021 [2020]) - **New to Quebec and Canada.**

### **Subfamily Scaphidiinae Latreille, 1806**

#### ***Baeocera inexpectata* Löbl & Stephan, 1993**

**Note.** See Löbl and Stephan (1993) for illustrations and identification. Initially described only from Saskatchewan (Löbl and Stephan 1993), this species was recently found in New Brunswick by Webster et al. (2012e), greatly extending its range eastward. The authors suggested that it was likely to be found in the intervening territories, and this is supported by the new record from Quebec. This small species is a member of the *congener* group of species and can be easily identified by the shape and the structures of the male genitalia, with each paramere bearing a medial membranous lobe.

**Specimen data. CANADA: QUEBEC - MRC de Manicouagan,** Pointe-aux-Outardes (49.0943, -88.3005), 24.VI.2021, N. Bédard [#2559], handpicked in tide debris on a beach (1, NBC).

**Distribution in Canada. SK, QC, NB** (Bousquet et al. 2013) - **New to Quebec.**

#### ***Scaphisoma americanum* (Löbl, 1987)**

**Note.** See Löbl (1987) for illustrations and identification. This species was described in the genus *Caryoscapha* Ganglbauer by Löbl (1987) from various locations in eastern North America, the northernmost records being from Illinois. Despite its relatively large body, it remained overlooked in most of its range. The genus was later synonymized with *Scaphisoma* by Leschen and Löbl (2005). We report for the first time its presence in Canada, based on specimens from Quebec, Ontario, and Nova Scotia.

**Specimen data. CANADA: ONTARIO - Haldimand-Norfolk Reg.,** Cronmiller property [~6 km W St. Williams] (42°40'18"N, 80°29'24"W), 31.V-15.VI.2011, Brunke & Paiero, forest near vernal pools, malaise (1, DEBU); Turkey Point Provincial Park (42°41'48"N, 80°19'48"W) 19.V.2011, A. Brunke, forest site 1, Berlese leaf and log litter (1, DEBU). - **Northumberland Co.,** Peter's Woods Provincial Nature Reserve (44°7'27"N, 78°2'21"W), 12.XI.2011, Brunke & Paiero, forest (1, DEBU); same except 6.X.2011 (2, DEBU); same except 27.VI.2011 (1, DEBU);

Barr property [~ 7km NE Centreton], 1–16.VI.2011, Brunke & Paiero, field site 2, malaise, (1, DEBU). **QUEBEC - MRC de l'Île-d'Orléans**, Saint-Pierre-de-l'Île-d'Orléans (46.8772, -71.0620), 11.VI.2022, L. Leclerc, beaten from fresh *Cerioporus squamosus* (3, LLC); **Ville de Québec**, Pointe-de-Sainte-Foy (46.7506, -71.3183), 11.VI.2023, L. Leclerc, sifted from fresh *Pleurotus ostreatus* (4, LLC) - **Montréal**, 1.IX.1972, E.J. Kiteley (5, CNC); same except 31.VIII.1979 (3, CNC); same except 14.VI.1983 (1, CNC). - **MRC de Bécancour**, Bécancour (Rivière Godfroy) (46.2977, -72.5321), 4.IX.2023, N. Bédard, sifted from *Hericium coraloides* (7, NBC; 1, LLC). **NOVA SCOTIA - Cape Breton Highlands National Park**, Lone Shieling, 1.VII.1983, R. Vockeroth, malaise trap (1, CNC).

**Distribution in Canada.** ON, QC, NS - **New to Quebec, Ontario, Nova Scotia, and Canada.**

### Subfamily Staphylininae Latreille, 1802

#### *Gabrius amilius* Smetana, 1995

Fig. 6

**Note.** This rare species was first recorded in Canada by Brunke and Marshall (2011) from a single specimen captured in Ontario. Consistent with known habitat data, the specimen reported below was caught in a deciduous forest, and represents the first known occurrence of this species in Quebec.

**Specimen data.** **CANADA: QUEBEC - Ville de Gatineau**, Forêt Boucher (45.4208, -75.8167), 17.VI.2023, F. Génier & S. Laplante (1, CMNC).

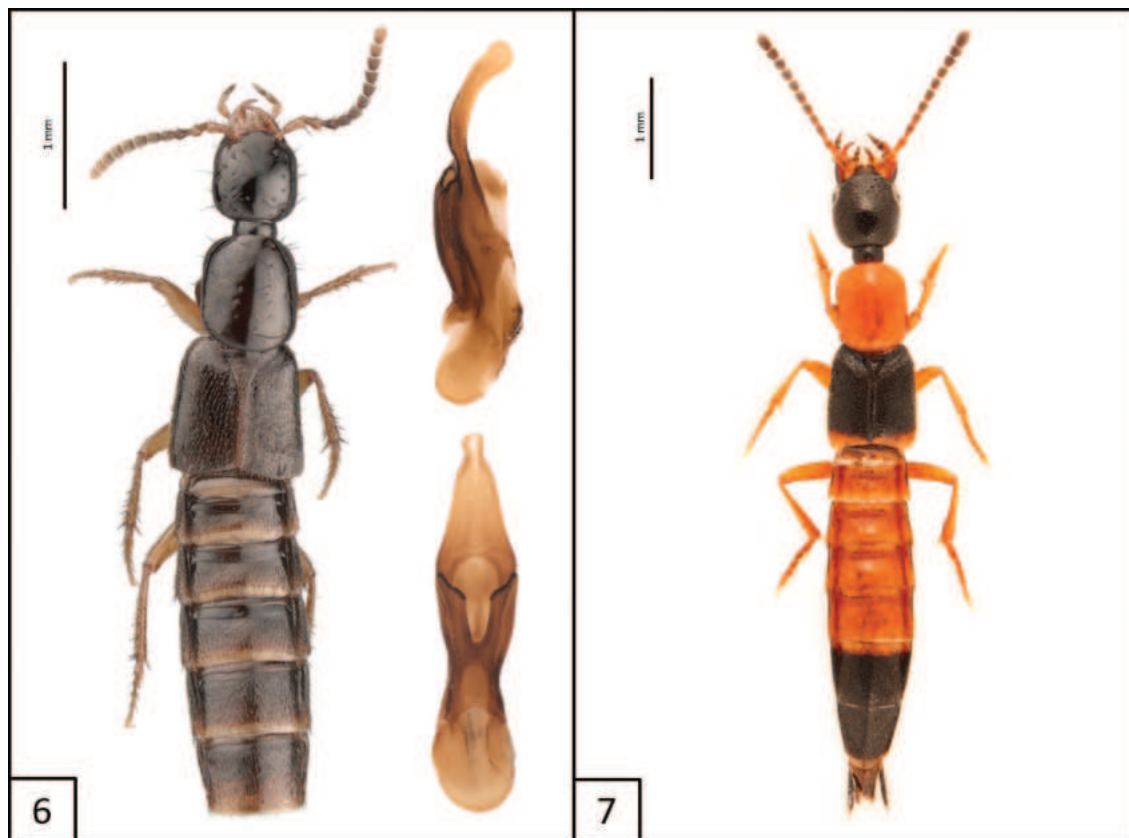
**Distribution in Canada.** ON, QC (Bousquet et al. 2013) - **New to Quebec.**

#### *Neobisnius jucundus* (Horn, 1884)

Fig. 7

**Note.** See Frank (1981) for identification. *Neobisnius jucundus* was originally described by Horn in 1884, based on two female specimens from South Carolina. It has since been found to have a widespread presence in North America, extending into several Canadian provinces (Bousquet et al. 2013). Here we further extend its known Canadian distribution to include southern Quebec. It becomes the fifth species of the genus known from Quebec. Among the bicolored species of the genus, it can be recognized in eastern Canada by the following combination of characters: head longer than wide and with obvious microsculpture dorsally; eyes occupying ~ 1/3 of head length; elytra narrowly pale at apex (< 40%); one or more palpomeres of maxillary palpus darkened. The species can also be recognized by the distinctive shape of the aedeagus (Frank 1981).

**Specimen data.** **CANADA: QUEBEC - MRC des Deux-Montagnes**, Parc national d'Oka (45.476466, -74.054149), 11.V.2023, R. Vigneault, white tulle fabric tissue in a compost site [Collected with permit] (1, RVC). - **MRC de Memphrémagog**, Potton (45.0259, -72.4279), 5.VI.2022, L. Leclerc, N. Bédard & P. Bloin, handpicked under flood debris (1, LLC; 3, NBC; 1, PBC); same locality, except 16.VI.2022 (1, PBC); same locality except 20.VII-5.VIII.2022, pitfall trap baited with apple cider vinegar (1, LLC). - **MRC du Granit**, Saint-Augustin-de-Woburn



Figures 6, 7. Habitus and aedeagus of 6 *Gabrius amulius* Smetana, 1995, aedeagus ventral and lateral views 7 *Neobisnius jucundus* (Horn, 1884), aedeagus ventral view.

(45.416694, -70.879500), 12.V.2022, sandy-gravelly bank of a small river littered with woody debris, N. Bédard & P. Bloin (3, NBC; 1, PBC).

**Distribution in Canada.** BC, AB, SK, MB, ON, QC, NB (Bousquet et al. 2013) - **New to Quebec.**

#### *Ocypus nitens* (Schrank, 1781)\*

**Note.** See Brunke et al. (2011) and Brunke (2016) for illustrations and identification. This large adventive species is native to Europe, the Caucasus, Iran, and Turkey (Herman 2001), and was first detected in eastern North America in Massachusetts in 1944 (Newton 1987). For more than fifty years, it apparently remained confined to a small area in New England (Newton 1987; Brunke 2016), but it has since expanded rapidly its range to Maine by 1989, Rhode Island by 1995 (Brunke et al. 2011), New York by 2010, Vermont and Ontario by 2014 (Brunke 2016) and New Brunswick by 2018 (Knopf and Gilmore 2018). Records from BugGuide were mentioned in Brunke (2016), but those from iNaturalist were not considered, and are here referred-to because they represent most of the observations available for the province of Quebec and Nova Scotia, and greatly extend its known range. The species has been known from Quebec since at least 2013 according to iNaturalist records. There were 38 iNaturalist observations for the province of Quebec, 33 of which were confirmed and verified. These data (grouped here) represent

a widespread area in southern Quebec, reaching its northernmost limit at the level of Montreal and Sherbrooke south to Godmanchester and Potton. We also provide physical specimen data to support the presence of *Ocypus nitens* in Quebec.

**Specimen data. CANADA: QUEBEC - Montréal** (45.5436, -73.6901), 31.V.2018, S. Dumont, pitfall trap (1, SDC); (45.5430 -73.6911), 13.VI.2023, handpicked under a rock (2, SDC); (45.5436, -73.6901), 20.X.2023, pitfall trap (2, SDC); 23.X.2023 (1, SDC); 12.XI.2023 (5, SDC); 16.XI.2023 (2, SDC), 17.XI.2023 (2, SDC). - **MRC de Brome-Missisquoi**, Saint-Armand (45.0221, -73.0582), 29.VII.2017, L. Leclerc, under hardwood log (1, LLC). - **MRC de Deux-Montagnes**, Parc national d'Oka, (Grande Baie, 45.4906, -74.0111), 9.X.2019, 14:00, P. de Tonnancour, climbing tree trunk [Collected with permit] (1, PdTC). - **MRC de Memphremagog**, Potton (45.0162, -72.4344), 15–29.VII.2022, N. Bédard, pitfall trap in a mixed maple forest, det.: NB (1, NBC); Stanstead-Est (45.1578, -72.0291), 28.IV.2018, S. Mailhot, caught in flight (1, LLC). - **MRC du Val-Saint-François**, Racine (45.459475, -72.161956), 15.V.2021, P. Bloin, under log of deciduous tree (1, PBC). - **MRC Les Appalaches**, Adstock (46.0049, -71.1104), 5.XI.2022, P. Bloin, sifted from moss in a balsam fir stand (1, PBC).

**Internet data. CANADA: NOVA SCOTIA - Annapolis Co.**, Clementsvale (44.635474, -65.566914), 19.X.2021, Alexis Orion, Recorded through INaturalist (Obs.: 99352464); Lake La Rose (44.705801, -65.440164), 20.III.2022, Ashlea Viola (@ashlea03), Recorded through INaturalist (Obs.: 109590192); Round Hill (44.769997, -65.409845), 14.VI.2022, (@spaceexplorer), Recorded through INaturalist (Obs.: 121718039). - **Lunenburg Co.**, Chelsea (44.374644, -64.727725), 13.IV.2022, Heather Haughn (@hhaughn), Recorded through INaturalist (Obs.: 111330891); Chelsea (44.374808, -64.727878), 13.IX.2022, Heather Haughn (@hhaughn), Recorded through INaturalist (Obs.: 134902909); Chelsea (44.374642, -64.727708), 16.IX.2022, Heather Haughn (@hhaughn), Recorded through INaturalist (Obs.: 135278623); Conquerall (44.311425, -64.554755), 6.VII.2023, Jamie VanBuskirk (@jamievanbuskirk), Recorded through INaturalist (Obs.: 171483228). - **Kings Co.**, Kentville (45.076912, -64.494473), 22.V.2022, (@kmelville), Recorded through INaturalist (Obs.: 118447209); Bishopville (45.014267, -64.275407), XII.2022, (@cricket\_toadums), Recorded through INaturalist (Obs.: 144268319); Kentville (45.062484, -64.56368), 13.V.2023, Dan Casey (@dan\_casey), Recorded through INaturalist (Obs.: 172019838); Casey Corner (45.01433, -64.566744), VI.2023, (@cricket\_toadums), Recorded through INaturalist (Obs.: 169149071).

**Distribution in Canada. ON, QC, NB, NS** (Brunke 2016) - **New to Quebec and Nova Scotia.**

### ***Platydracus exulans* (Erichson, 1839)**

**Note.** See Brunke et al. (2011) for illustrations and identification. This native species was reported from Quebec by Downie and Arnett (1996) without any further information, but because this record was later presumed to be based on a misidentified specimen (Brunke et al. 2011), it was not reported for Quebec by Bousquet et al. (2013). In Ontario, it has been collected only twice (once with two specimens) and, moreover, 44 years apart at the same locality near the

Ottawa River in the Ottawa area. The Quebec specimen was also found along the Ottawa River further east and it is not clear whether these are vagrant specimens or if there is an apparently disjunct northern population of this species.

**Specimen data. CANADA: QUEBEC - MRC de Vaudreuil-Soulanges**, Rigaud (45.4906, -74.2919), 3.VII.2020, N. Bédard, UV light trap (1, NBC).

**Distribution in Canada.** ON, QC (Bousquet et al. 2013) - **New to Quebec.**

### ***Philonthus hepaticus* Erichson, 1840**

Fig. 8

**Note.** See Smetana (1995) for identification. Majka et al. (2009b) documented a significant range extension for this *Philonthus* species, shedding light on existing distribution gaps within the eastern rove beetle fauna. While this species displays a bipartite distribution pattern in Canada, Smetana (1995) indicated that it is a transcontinental species, with its presence in Quebec highly expected. *Philonthus hepaticus* has an extremely broad range in the New World and occurs south to Chile and Argentina. It has also become adventive in Australia and New Zealand (Newton 2022). This species probably also occurs in at least some parts of southern Ontario.

**Specimen data. CANADA: QUEBEC - Ville de Québec**, Cité-Universitaire (46.7863, -71.2686), 30.V.2023, 18:00–21:00, L. Leclerc, white tulle fabric interception trap (1, LLC); Plaines d'Abraham (46.7950, -71.2285) 2.IX.2023, L. Leclerc, sifted from wood chips heap (4, LLC); Sainte-Foy (46.7874, -71.2914), 28.IX.2023, L. Leclerc, sifted from decaying grass heap (1, LLC); 30.IX.2023 (1, LLC); 5.X.2023 (1, LLC); 9.X.2023 (1, LLC); 11.X.2023 (1, LLC). - **MRC des Deux-Montagnes**, Parc National d'Oka (45.4767, -74.0537), 10.XI.2020, R. Vigneault, white tulle fabric interception trap in a compost site [Collected with permit] (1, RVC); 25.X.2022 (2, RVC).

**Distribution in Canada.** BC, QC, NB (Bousquet et al. 2013) - **New to Quebec.**

### ***Philonthus sanguinolentus* (Gravenhorst, 1802)\***

**Note.** See Smetana (1995) and Klimaszewski et al. (2013) for illustrations and identification. This adventive Palearctic species was initially restricted in North America to the Pacific coast (Smetana 1995), but was discovered in 2013 (collected in 2011) for the first time in Ontario (Klimaszewski et al. 2013). In 2017, a photo record of a specimen from Quebec, Canada was published on BugGuide (see "Internet data" below). We hereby support this new Quebec record with specimen data below.

**Specimen data. CANADA: QUEBEC - Ville de Québec**, Cap-Rouge (46.7519, -71.3069), 17.VII.2022, P. Bloin, by sweeping vegetation along the railway track (1, PBC); Sainte-Foy (46.7874, -71.2914), 23.VII.2023, L. Leclerc, sifted from a decaying grass heap (1, LLC).

**Internet data. CANADA: QUEBEC - MRC de la Haute-Yamaska**, Granby, 17.VIII.2017, J. Brodeur, recorded through BugGuide (<https://BugGuide.net/node/view/1425701>).

**Distribution in Canada.** ON, QC (Bousquet et al. 2013) - **New to Quebec.**

### ***Quedius cinctus* (Paykull, 1790)\***

**Note.** See Majka et al. (2009a) and Smetana (1971) for illustrations and identification. Known to be present in North America since at least 1942 (Smetana 1971). This adventive species was recorded for the first time in Canada by Majka et al. (2009a) from specimens collected on carrion in New Brunswick in 2007. Across its native western Palaearctic range, this species lives mainly in decaying organic substances, very often near or directly in human settlements (Smetana 1971). Brunke and Marshall (2011) reported it from Ontario based on specimens collected from rotting *Cerioporus* (= *Polyporus*) *squamosus* in 2008.

**Specimen data.** **CANADA: QUEBEC - Ville de Québec**, Plaines d'Abraham (46.795042, -71.228484), 6.IX.2022, P. Bloin, sifted from wood chips and plant waste (2, PBC, 1, NBC); Sainte-Foy (46.7874, -71.2914), 24.X.2022, white tulle fabric interception trap (4, LLC), 5.V.2023 (1, LLC), 9.X.2023, sifted from decaying grass heap (1, LLC), 10.X.2023 (1, LLC), 14.X.2023 (1, LLC), 17.X.2023 (1, LLC); Cité-Universitaire (46.7863, -71.2686), 15.X.2022, L. Leclerc, N. Bédard & P. Bloin, sifted from fresh wood chips pile (1, LLC), 23.X.2022 (2, LLC), 25.X.2022 (4, LLC; 4, NBC; 4, PBC), 4.XI.2022, white tulle fabric interception trap (4, LLC). - **MRC de Deux-Montagnes**, Oka (45.4993, -74.0203), 3.IV.2020, R. Vigneault, white tulle fabric interception trap in a compost site (1, RVC); Parc national d'Oka (45.4767, -74.0537), 22.III.2021, R. Vigneault, white tulle fabric interception trap in a compost site [Collected with permit] (1, RVC); 12.X.2022, P. de Tonnancour and R. Vigneault, white tulle fabric interception trap [Collected with permit] (2, PdTC; 1, RVC). - **MRC de l'Île-d'Orléans**, Saint-Pierre-de-l'Île-d'Orléans (46.8809, -71.0636), 5.X.2023, 16:00–18:00, L. Leclerc, white tulle fabric interception trap (1, LLC). - **MRC de Vaudreuil-Soulanges**, Terrasse-Vaudreuil (45.3923, -73.9922), 26-IX-2011, P. de Tonnancour, fermented cantaloup (1, PdTC); 27.IX.2018, P. de Tonnancour, attracted to a compost heap (1, PdTC); 7.X.2021, P. de Tonnancour, composted grass clippings (1, PdTC); 30.IX.2023, 15:00–17:00, P. de Tonnancour, white tulle fabric interception trap (1, PdTC). - **Ville de Gatineau**, Aylmer [Ouest Forêt Boucher], 15.IV.2010, V. Théberge & L. LeSage, Berlese of porcupine dung in a hollow base of a large maple tree, in a mixed forest (1, CNC); same except 6.IV.2010 (4, CNC).

**Distribution in Canada.** ON, QC, NB (Bousquet et al. 2013) - **New to Quebec.**

### ***Hypnogyra gularis* (LeConte, 1880)**

Fig. 9

**Note.** See Smetana (1982) for identification. This species has been previously reported from New Brunswick (Webster et al. 2012h) and Ontario (Bousquet et al. 2013). Not much has been reported about its biology, though Smetana (1982) suspected that it prefers microhabitats similar to those of the Central European species, *H. angularis* (Ganglbauer, 1895), which is associated with tree-holes and similar microhabitats, and often cohabitates with wood-nesting ants. One of us (AJB) has repeatedly collected series of this species in tree-holes (oaks, beech, sugar maple) in Ontario, confirming the hypothesis of Smetana (1982).

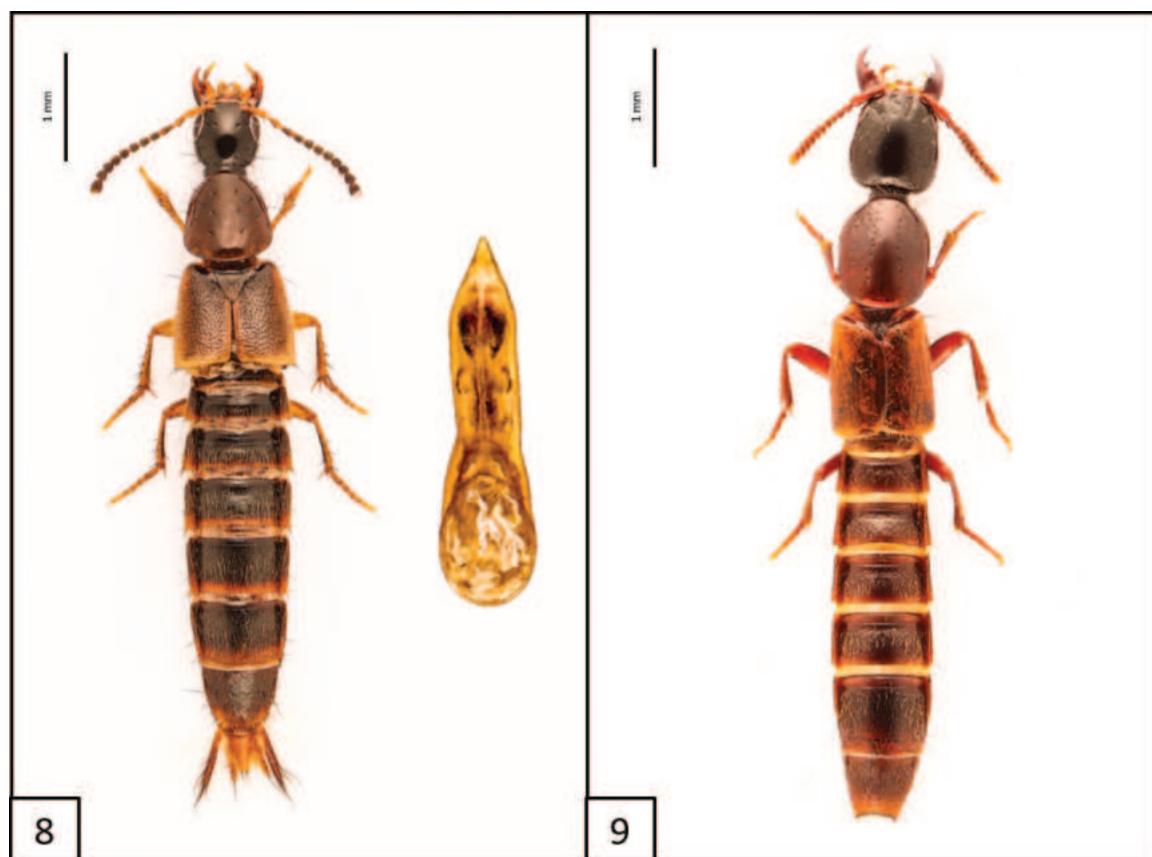
**Specimen data. CANADA: QUEBEC – Ville de Québec**, Sainte-Foy (46.7874, -71.2914), 17.V.2021, L. Leclerc, white tulle fabric interception trap (1, LLC). – **MRC des Deux-Montagnes**, Parc National d’Oka (45.4767, -74.0537), 5.V.2019, R. Vigneault, white tulle fabric interception trap in a compost site [Collected with permit] (1, LLC); 20.V.2019 (11, LLC); La Grande Baie (45.4927, -74.0056), 10.V.2022, 15:00–16:00, P. de Tonnancour, white tulle fabric interception trap in a sugar maple stand [Collected with permit] (1, PdTC). – **MRC du Haut-St-Laurent**, Havelock (45.026750, -73.800528), 3–18.VI.2023, N. Bédard, Canopy cross-vane trap with fermentation bait (1, NBC); Same locality and collector but 18.VI-3.VII.2023, interception trap in a maple and oak forest (1, NBC).

**Distribution in Canada.** ON, QC, NB (Bousquet et al. 2013) - **New to Quebec.**

***Gauropterus fulgidus* (Fabricius, 1787)\***

Fig. 10

**Note.** See Smetana (1982) for identification. This very characteristic and large xantholinine beetle was accidentally introduced to North America from Europe in the 19<sup>th</sup> century and is now found in both the western and eastern parts of North America (Smetana 1982). We report here the first occurrences of this species in the province of Quebec.



**Figures 8, 9.** Habitus and aedeagus of **8** *Philonthus hepaticus* Erichson, 1840, aedeagus ventral view **9** *Hypnogyra gularis* (LeConte, 1880), habitus only.

**Specimen data. CANADA: QUEBEC – MRC des Deux-Montagnes**, Parc National d’Oka (45.476714, -74.053690), 27.V.2023, R. Vigneault, white tulle fabric interception trap in a compost site [Collected with permit] (1, NBC). – **Ville de Québec**, Beauport (46.9421, -71.1987), 21.V.2021, N. Bédard, white tulle fabric interception trap (1, NBC); Sainte-Foy (46.7921, -71.2806), 15.X.2022, L. Leclerc, sifted from dried vegetal debris (2, LLC); Cité-Universitaire (46.7863, -71.2686), 26.X.2022, P. Bloin, sifted from wood chips (2, PBC).

**Distribution in Canada.** ON, QC (Bousquet et al. 2013) - **New to Quebec.**

### ***Phacophallus pallidipennis* (Motschulsky, 1858)\***

Fig. 11

**Note.** See Smetana (1982) for identification. This Oriental species is adventive in Europe, North America, Africa and the Australian region, and was initially identified in North America in 1904 along the western coast. Since then, it has been observed in various locations across the continent. The first detection in the eastern part of North America was in New York in 1931 (Smetana 1982). The records given below represent its first detection in Canada and are the northernmost known. It is generally a species that is more commonly found in warmer and southern regions of North America (Smetana 1982). It was previously reported as *Phacophallus tricolor* in most recent works (including Smetana 1982), but was synonymized with *Phacophallus pallidipennis* by Bordoni (2002).

**Specimen data. CANADA: QUEBEC – MRC de Marguerite-D’Youville**, Varennes, C. Chantal, 8.IX.2020 (1), 11.IX.2020 (2), 17.X.2020 (2), 23.X.2020 (4), 17.VIII.2021 (2), sifting dead grass (13, CCC). – **Ville de Québec**, Cité-Universitaire (46.7861, -71.2687), 23.X.2022, L. Leclerc, white tulle fabric interception trap (2, LLC); same locality except 26.X.2022, N. Bédard, sifting decomposing wood chips (1, NBC); same locality and method except 28.X.2022 (3, PBC).

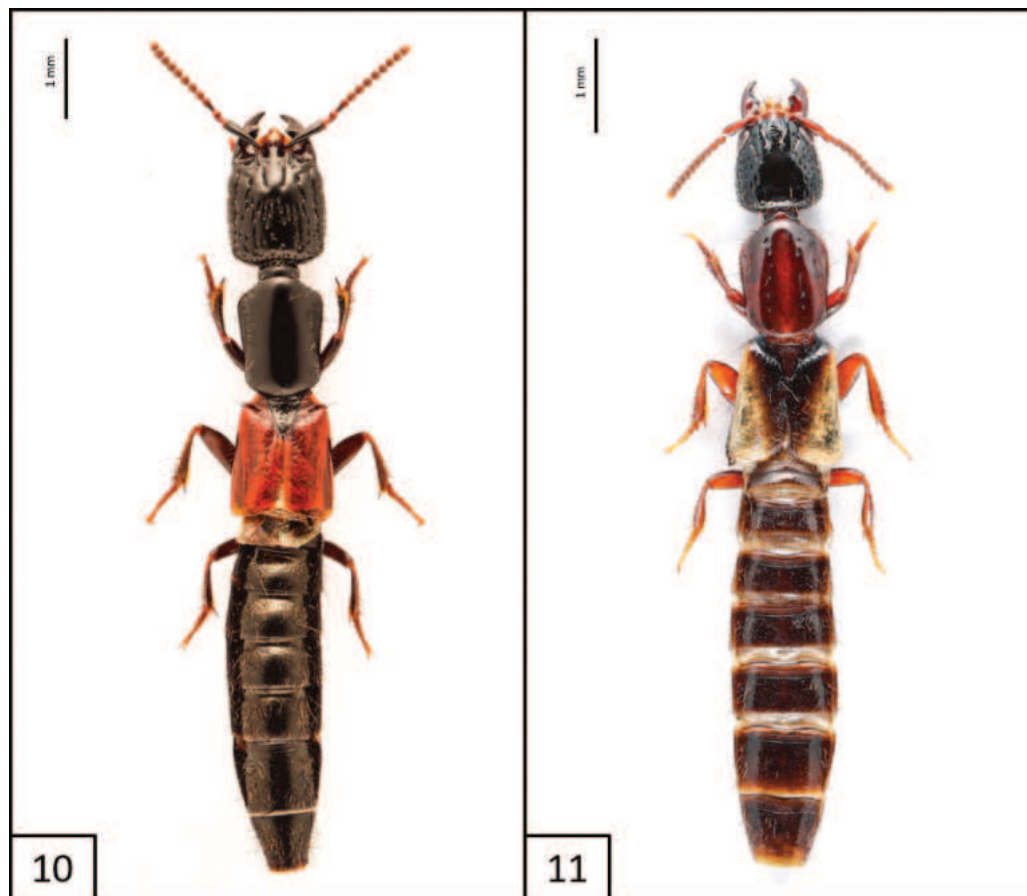
**Distribution in Canada.** QC. - **New to Quebec and Canada.**

### ***Xantholinus linearis* (Olivier, 1795)\***

**Note.** See Brunke and Majka (2010) for illustrations and identification. This introduced species was recently detected in Quebec based on specimens captured by the authors. However, in the future, by inspecting older or uncured material in collections, older specimens may be found. This species has been present in the maritime provinces of Canada and eastern North America since at least 1949 (Brunke and Majka 2010) but was first detected in North America in 1930 (British Columbia) (Smetana 1982).

**Specimen data. CANADA: QUEBEC – MRC du Granit**, Stratford (45.760829, -71.345770), 18.VIII.2023, N. Bédard, Handpicked in a parking lot (1, NBC). – **MRC La-Côte-de-Beaupré**, Saint-Joachim (47.0669, -70.8014), 15.X.2022, P. Bloin, flying on a warm fall day (1, PBC). – **Ville de Lévis**, Saint-Romuald (46.7390, -71.2615), 29.IV.2023, L. Leclerc, sifted from *Quercus* and *Acer* leaf litter (1, LLC).

**Distribution in Canada.** BC, AB, ON, QC, NB, NS, PE, NF (Bousquet et al. 2013) - **New to Quebec.**



Figures 10, 11. Habitus of 10 *Gauropterus fulgidus* (Fabricius, 1787) 11 *Phacophallus pallidipennis* (Motschulsky, 1858).

### Subfamily Tachyporinae MacLeay, 1825

#### *Sepedophilus basalis* (Erichson, 1839)

Fig. 12

**Note.** See Campbell (1976) for identification. *Sepedophilus basalis* is listed as occurring in Ontario by Bousquet et al. (2013) and Ontario and Quebec by Newton (2022). However, we have corresponded with these authors and could not determine a published voucher-based source for the records. It is possible the Quebec record came from the historical account by Provancher (1877: 243), although misidentifications with other species were common before the modern revision by Campbell (1976). The inclusion of this species in the Ontario fauna likely came from unpublished data of specimens deposited in the CNC. We here provide voucher data for *Sepedophilus basalis*, which occurs in Canada, broadly from southern Ontario to southern Quebec.

**Specimen data. CANADA: QUEBEC – MRC de Bécancour**, Bécancour (Rivière Godefroy) (46.2977, -72.5301), 25.V.2022, N. Bédard, sifted from debris near a river (3, NBC). – **MRC des Deux-Montagnes**, Parc National d’Oka (45.472273, -74.049343), 11.V.2023, R. Vigneault, white tulle fabric interception trap in a compost site [Collected with permit] (1, NBC); same but 13.V.2023 (1, NBC). **ONTARIO – Chatham-Kent Reg.**, Rondeau Provincial Park, 11–25.V.1985, L. LeSage & A. Woodliffe, intercept trap 4, white pine stand (1, CNC); same except 2–13.VII.1985, intercept trap in maple beech forest (2, CNC); Rondeau Provincial



Figure 12. Habitus of *Sepedophilus basalis* (Erichson, 1839) dorsal and lateral views, and aedeagus (ventral view).

Park, 25–28.V.1985, L. LeSage & A. Smetana, intercept trap in maple beech forest (1, CNC); same except 14.VI.-2.VII.1985 (1, CNC); Rondeau Provincial Park, 14.VI.-2.VII.1985, L. LeSage & D.M. Wood, intercept trap in maple beech forest (1, CNC); Rondeau Provincial Park, [South Point Trail], 31.V.1985, A. Smetana (5, CNC); Rondeau Provincial Park, [N end South Point Trail], 3.VI.1985, A. Davies & J.M. Campbell, under bark of fallen tree (5, CNC); Rondeau Provincial Park [Spicebush Trail], 4.VI.1985, A. Davies & J.M. Campbell, sifting mushrooms and litter (4, CNC); same except under bark of fallen tree (2, CNC); Rondeau Provincial Park, [Harrison Trail], 30.V.1985, A. Smetana (2, CNC); Rondeau Provincial Park [South Point], 2.VI.1985, A. Davies & J.M. Campbell, moss on log in pond (1, CNC); Rondeau Provincial Park [Tulip Tree Trail], 5.VI.1985, A. Davies & J.M. Campbell, sifting beech and maple litter near water (1, CNC); **Elgin Co.**, J.F. Pearce Park, 5.VI.1981, L. LeSage (1, CNC). – **Halton Reg.**, Milton, 21–30.VIII.1981, M. Sanborne (1, CNC). – **Leeds and Grenville Co.**, 2 km SE Spencerville, 30.IV.1979, A.& Z. Smetana (1, CNC). – **Ottawa Reg.**, 5 km NW South March, 24.IV.1979, A.& Z. Smetana (1, CNC).

**Distribution in Canada.** ON, QC - New to Quebec, supporting data for Ontario.

## Discussion

Distribution data of 27 species of rove beetles (excluding Aleocharinae) are provided for the Province of Quebec, 25 of which are new records, increasing the total number of staphylinid species in Quebec to 863 (Bédard, unpublished database). Approximately one-third of the newly recorded species (10 out of 27) are considered adventive in North America. Notably, these adventive species were predominantly found in human-disturbed habitats, including compost heaps and wood chip piles. These man-made habitats offer favorable conditions for introduced species as they tend to be warmer and to have more stable temperatures than the surrounding environments as a result of the heat generated by decomposition. This phenomenon was observed in several beetle families in Europe, where warm-loving species tended to thrive farther north in compost compared to other microhabitats (Ødegaard and Tømmerås 2000). Some of the species we report here, including *Gauropterus fulgidus*, *Phacophallus pallidipennis*, *Philonthus sanguinolentus* and *Hypomedon debilicornis* appear to follow this principle.

Moreover, sifting these different substrates also revealed new records of species from largely tropical genera, such as *Echiaster* Erichson, 1839 and *Atanygnathus* Jakobson, 1909. These species could not be identified but are not among the described North American species. They could not be treated in this paper because the genera are unrevised across most of their distribution. The occurrence of these species in Canada may be attributed to the transport of “contaminated” plant material (Klimaszewski and Brunke 2018). In the case of many species in the present paper, large accumulations of wood chips could be considered refugia for these species, allowing them to survive harsh winters and expand further into synanthropic and natural environments (Ødegaard and Tømmerås 2000).

The detection of the above rove beetle species in Quebec is likely due to a very recent intensification of sampling effort in the province, combined with the use of alternative collection methods. *Hypnogyra gularis*, *Oxyporus ashei*, and *Quedius cinctus* were mainly collected using the white tulle fabric interception trap, which seems to effectively capture small, cryptic species and those that are highly local and frequently disperse to patchy or ephemeral microhabitats (de Tonnancour et al. 2017). Notably, while Quebec was included in several broad taxonomic works (e.g., Klimaszewski et al. 2018, 2021) and has been the site of several forestry studies (Paquin and Dupérré 2001; Klimaszewski et al. 2007), the province has never been the focus of recent faunistic or revisionary research on rove beetles. The present paper has begun to narrow this knowledge gap and with continued sampling and taxonomic effort, we hope to better understand the true diversity of Staphylinidae in Quebec.

## Acknowledgments

We would like to thank to Pierre de Tonnancour and Robert Vigneault for providing specimen data for *Quedius cinctus*, Stéphane Dumont and Pierre de Tonnancour for *Ocypus nitens*, François Génier for the pictures and data of *Gabrius amulius*, and the data of *Scaphisoma americanum*. We would also like to thank Pierre-Marc Brousseau for the data and details about *Eutyphlus schmitti*, Jean Brodeur who agreed to share his image record of *Philonthus sanguinolentus*, and Robert Vigneault for contributing his specimen of *Oxyporus ashei*. We thank

Claude Tessier for the records of *Stenus colon* and for the detailed pictures of the aedeagus. Many thanks go to Dr. Donald Chandler (University of New Hampshire, United States) for the confirmations of the *Euconnus* spp., and to Anthony Davies (Canadian National Collection of Insects, Arachnids and Nematodes, Canada) for *Thesium cavifrons*. AJB would like to thank S. Paiero (University of Guelph Insect Collection, Canada) for arranging the loan of the specimens from DEBU.

## Additional information

### Conflict of interest

The authors have declared that no competing interests exist.

### Ethical statement

No ethical statement was reported.

### Funding

This study received financial support from A-base funding to AB from the Government of Canada (Agriculture and Agri-food Canada: Systematics of Beneficial Arthropods – J-002276).

### Author contributions

All authors have contributed equally.

### Author ORCIDs

Nicolas Bédard  <https://orcid.org/0009-0004-7649-100X>

Adam Brunke  <https://orcid.org/0000-0003-1158-936X>

Pierrick Bloin  <https://orcid.org/0009-0009-3260-9017>

Ludovic Leclerc  <https://orcid.org/0009-0006-2381-9627>

### Data availability

All of the data that support the findings of this study are available in the main text.

## References

- Assing V (1995) Über *Sunius fallax* (LOKAY, 1919)(Col., Staphylinidae). Entomologische Nachrichten und Berichte 38(1994): 267–269.
- Assing V (2008) A revision of the *Sunius* species of the Western Palaearctic region and Middle Asia (Coleoptera: Staphylinidae: Paederinae). Linzer Biologische Beiträge 40(1): 5–135.
- Bordoni A (2002) Xantholinini della Regione Orientale (Coleoptera: Staphylinidae): Classificazione, Filogenesi e Revisione Tassonomica. Monografie di Museo Regionale di Scienze Naturali, Torino, 998 pp.
- Bousquet Y, Bouchard P, Davies AE, Sikes D (2013) Checklist of beetles (Coleoptera) of Canada and Alaska. Pensoft Series Faunistica No. 109, Sofia-Moscow, 402 pp. <https://doi.org/10.3897/zookeys.360.4742>
- Brunke A (2016) First detection of the adventive large rove beetle *Ocypus nitens* (Schrank) in Canada and an update of its Nearctic distribution using data generated by the public. Biodiversity Data Journal 11(4): e11012. <https://doi.org/10.3897/BDJ.4.e11012>

- Brunke AJ, Majka CG (2010) The adventive genus *Xantholinus* Dejean (Coleoptera, Staphylinidae, Staphylininae) in North America: New records and a synthesis of distributional data. *ZooKeys* 65: 51–61. <https://doi.org/10.3897/zookeys.65.574>
- Brunke A, Marshall S (2011) Contributions to the faunistics and bionomics of Staphylinidae (Coleoptera) in northeastern North America: Discoveries made through study of the University of Guelph Insect Collection, Ontario, Canada. *ZooKeys* 75: 29–68. <https://doi.org/10.3897/zookeys.75.767>
- Brunke A, Newton A, Klimaszewski J, Majka C, Marshall S (2011) Staphylinidae of Eastern Canada and Adjacent United States. Key to Subfamilies; Staphylininae: Tribes and Subtribes, and Species of Staphylinina. *Canadian Journal of Arthropod Identification* 12: 1–110. <https://doi.org/10.3752/cjai.2011.12>
- Brunke AJ, Klimaszewski J, Dorval JA, Bourdon C, Paiero SM, Marshall SA (2012a) New species and distributional records of Aleocharinae (Coleoptera, Staphylinidae) from Ontario, Canada, with a checklist of recorded species. *ZooKeys* 186: 119–206. <https://doi.org/10.3897/zookeys.186.2947>
- Brunke A, Klimaszewski J, Anderson RS (2012b) Present taxonomic work on Staphylinidae (Coleoptera) in Canada: Progress against all odds. *ZooKeys* 186: 1–5. <https://doi.org/10.3897/zookeys.186.3252>
- Brunke A, Bahlai CA, Klimaszewski J, Hallett RH (2014) Rove beetles (Coleoptera: Staphylinidae) in Ontario, Canada soybean agroecosystems: assemblage diversity, composition, seasonality, and habitat use. *Canadian Entomologist* 146(6): 652–670. <https://doi.org/10.4039/tce.2014.19>
- Brunke AJ, Pentinsaari M, Klimaszewski J (2021) Integrative taxonomy of Nearctic and Palaearctic Aleocharinae: New species, synonymies, and records (Coleoptera, Staphylinidae). *ZooKeys* 1041: 27–99. <https://doi.org/10.3897/zookeys.1041.64460>
- Campbell JM (1976) A revision of the genus *Sepedophilus* Gistel (Coleoptera: Staphylinidae) of America north of Mexico. *Memoirs of the Entomological Society of Canada* 108(S99): 1–89. <https://doi.org/10.4039/entm10899fv>
- Campbell JM (1978) New species of *Oxyporus* (Coleoptera: Staphylinidae) from North America. *Canadian Entomologist* 110(8): 805–813. <https://doi.org/10.4039/Ent110805-8>
- Campbell JM (1984) A revision of the North American Omaliinae (Coleoptera: Staphylinidae): The genera *Arpedium* Erichson and *Eucnecosum* Reitter. *Canadian Entomologist* 116(4): 487–527. <https://doi.org/10.4039/Ent116487-4>
- Campbell JM, Davies A (1991) Family Staphylinidae: rove beetles. In: Bousquet Y (Ed.) Checklist of beetles of Canada and Alaska. Publication 1861/E, Research Branch, Agriculture Canada, Ottawa, Ontario, 86–124.
- Chandler DS (1987) Species richness and abundance of Pselaphidae (Coleoptera) in old-growth and 40-year-old forests in New Hampshire. *Canadian Journal of Zoology* 65(3): 608–615. <https://doi.org/10.1139/z87-095>
- Chandler DS (1989) The Pselaphidae (Coleoptera) of Latimer County, Oklahoma, with revisions of four genera from eastern North America. Part 1. Faroninae and Euplectinae. *Transactions of the American Entomological Society* 115: 503–529.
- Chandler DS (2000) [2001] Subfamily Pselaphinae Latreille 1802. In: Newton AF, Thayer MK, Ashe JS, Chandler DS (Eds) Family 22. Staphylinidae Latreille, 1802. In: Arnett Jr RH., Thomas MC (Eds) *American Beetles, Archostemata, Myxophaga, Adephaga, Polyphaga: Staphyliniformia*. Volume 1. CRC Press, Boca Raton, Florida, [xv +] 286–295: 344–354.

- de Tonnancour P, Anderson RS, Bouchard P, Chantal C, Dumont S, Vigneault R (2017) New Curculionoidea (Coleoptera) records for Quebec, Canada. *ZooKeys* 681: 1–95. <https://doi.org/10.3897/zookeys.681.12469>
- Downie NM, Arnett Jr RH (1996) *The beetles of northeastern North America*, Vol. 1 & 2, Sandhill Crane Press, Gainesville Florida, 1721 pp.
- Frank JH (1981) Revision of the New World species of the genus *Neobisnius* Ganglbauer (Coleoptera, Staphylinidae, Staphylininae). *Occasional Papers of the FSCA* 1: 1–60.
- Frisch J, Burckhardt D, Wolters V (2002) Rove beetles of the subtribe Scopaeina Mulsant & Rey (Coleoptera: Staphylinidae) in the West Palaearctic: Phylogeny, biogeography, and species catalogue. *Organisms, Diversity & Evolution* 2(1): 27–53. <https://doi.org/10.1078/1439-6092-00032>
- Grigarick AA, Schuster RO (1980) Discrimination of Genera of Euplectini of North and Central America (Coleoptera, Pselaphidae) (Vol. 87). University of California Press 87: 1–6. [79 pls.]
- Hebert PD, Ratnasingham S, Zakharov EV, Telfer AC, Levesque-Beaudin V, Milton MA, Pederson S, Janetta P, DeWaard JR (2016) Counting animal species with DNA barcodes: Canadian insects. *Philosophical Transactions of the Royal Society B: Biological Sciences* 371(1702): 1–10. <https://doi.org/10.1098/rstb.2015.0333>
- Herman L (2001) Catalog of the Staphylinidae (Insecta, Coleoptera): 1758 to the end of the second millennium. *Bulletin of the American Museum of Natural History* 2001(265): 1–4218. <https://doi.org/10.1206/0003-0090.265.1.1>
- Hoebeke ER (1991) *Sunius melanocephalus* (Coleoptera: Staphylinidae), a Palearctic rove beetle new to North America. *Entomological News* 102(1): 19–24.
- Hubbard HG, Schwarz EA, LeConte JL (1878) *The Coleoptera of Michigan*. *Proceedings of the American Philosophical Society* 17(101): 593–669.
- Jałoszyński P (2021) Taxonomy of *Euconnus* complex. Part XXIII. Status of *Napochus* Thomson, *Pycnophus* Casey, and *Filonapochus* Franz revisited (Coleoptera, Staphylinidae, Scydmaeninae). *Zootaxa* 5026(2): 255–270. <https://doi.org/10.11646/zootaxa.5026.2.6>
- Klimaszewski J, Brunke AJ (2018) Canada's adventive Rove Beetle (Coleoptera, Staphylinidae) fauna: a long-term case study on the detection, origin, introduction pathways, and dynamic distribution of non-native beetles. *Biology of Rove Beetles (Staphylinidae) Life History, Evolution, Ecology and Distribution*: 65–79. [https://doi.org/10.1007/978-3-319-70257-5\\_5](https://doi.org/10.1007/978-3-319-70257-5_5)
- Klimaszewski J, Langor D, Savard K, Pelletier G, Chandler DS, Sweeney J (2007) Rove beetles (Coleoptera: Staphylinidae) in yellow birch-dominated stands of southeastern Quebec, Canada: diversity, abundance, and description of a new species. *The Canadian Entomologist* 139(6): 793–833. <https://doi.org/10.4039/n06-057>
- Klimaszewski J, Brunke A, Assing V, Langor DW, Newton AF, Bourdon C, Pelletier G, Webster RP, Herman L, Perdereau L, Davies A, Smetana A, Chandler DS, Majka C, Scudder GGE (2013) Synopsis of adventive species of Coleoptera (Insecta) recorded from Canada. Part 2: Staphylinidae. *Pensoft, Sofia-Moscow*, 360 pp.
- Klimaszewski J, Larson DJ, Labrecque M, Bourdon C (2016) Twelve new species and fifty-three new provincial distribution records of Aleocharinae rove beetles of Saskatchewan, Canada (Coleoptera, Staphylinidae). *ZooKeys* 610: 1–45. <https://doi.org/10.3897/zookeys.610.9361>
- Klimaszewski J, Webster RP, Langor DW, Brunke A, Davis A, Bourdon C, Labrecque M, Newton AF, Dorval JA, Frank HJ (2018) *Aleocharinae Rove Beetles of Eastern Canada*

- (Coleoptera, Staphylinidae, Aleocharinae): A Glimpse of Megadiversity. Springer Editions, Cham, 906 pp. <https://doi.org/10.1007/978-3-319-77344-5>
- Klimaszewski J, Hoebeke RE, Godin B, Davies A, Perry KL, Bourdon C, Winchester N (2020) Aleocharine Rove beetles of British Columbia: A hotspot of Canadian Biodiversity (Coleoptera: Staphylinidae). Springer Editions, Cham, 631 pp. <https://doi.org/10.1007/978-3-030-36174-7>
- Klimaszewski J, Brunke A, Sikes DS, Pentisaari M, Godin B, Webster RP, Davies A, Bourdon C, Newton AF (2021) A Faunal Review of Aleocharine Beetles in the Rapidly Changing Arctic and Subarctic Regions of North America (Coleoptera: Staphylinidae). Springer Editions, Cham, 712 pp. <https://doi.org/10.1007/978-3-030-68191-3>
- Knopf E, Gilmore W (2018) The first recorded occurrences of *Platydracus immaculatus* (Mannerheim) and *Ocypus nitens* (Schrank), (Coleoptera; Staphylinidae), in New Brunswick, Canada. *Journal of the Acadian Entomological Society* 14: 25–27.
- LeConte JL (1863) New species of North American Coleoptera. Part I. Smithsonian Miscellaneous Collections 6(167): 1–264. <https://doi.org/10.5962/bhl.title.51303>
- Leschen RA, Löbl I (2005) Phylogeny and classification of Scaphisomatini Staphylinidae: Scaphidiinae with notes on mycophagy, termitophily, and functional morphology. *Coleopterists Bulletin* 59(3): 1–63. [https://doi.org/10.1649/0010-065X\(2005\)059\[0001:PACOSS\]2.0.CO;2](https://doi.org/10.1649/0010-065X(2005)059[0001:PACOSS]2.0.CO;2)
- Löbl I (1987) Contribution to the knowledge of the genus *Caryoscapha* Ganglbauer (Coleoptera: Scaphidiidae). *Coleopterists Bulletin* 41(4): 385–391.
- Löbl I, Stephan K (1993) A review of the species of Baeocera Erichson (Coleoptera, Staphylinidae, Scaphidiinae) of America north of Mexico. *Revue Suisse de Zoologie* 100: 675–733. <https://doi.org/10.5962/bhl.part.79880>
- Majka CG, Michaud JP, Moreau G (2009a) Adventive species of *Quedius* (Coleoptera, Staphylinidae) in North America: A survey and new Canadian record. *ZooKeys* 22: 341–345. <https://doi.org/10.3897/zookeys.22.207>
- Majka CG, Michaud JP, Moreau G, Smetana A (2009b) *Philonthus hepaticus* (Coleoptera, Staphylinidae) in eastern Canada: Are distribution gaps distinctive features or collecting artifacts? *ZooKeys* 22: 1–347. <https://doi.org/10.3897/zookeys.22.208>
- Newton AF (1987) Four *Staphylinus* (*sensu lato*) Species New to North America, with Notes on Other Introduced Species (Coleoptera: Staphylinidae). *Coleopterists Bulletin* 41(4): 381–384.
- Newton AF (2022) StaphBase. In: Bánki O, Roskov Y, Döring M, Ower G, Hernández Robles DR, Plata Corredor CA, Stjernegaard Jeppesen T, Örn A, Vandepitte L, Hobern D, Schalk P, DeWalt RE, Ma K, Miller J, Orrell T, Aalbu R, Abbott J, Adlard R, Adriaenssens EM, et al. (Eds) *Catalogue of Life Checklist* (Aug 2022). <https://doi.org/10.48580/dfs-3gk> [Accessed 26/11/2023]
- Ødegaard F, Tømmerås BÅ (2000) Compost heaps—Refuges and stepping-stones for alien arthropod species in northern Europe. *Diversity & Distributions* 6(1): 45–59. <https://doi.org/10.1046/j.1472-4642.2000.00071.x>
- Owen J, Allen AJW (2000) *Hypomedon debilicornis* (Wollaston, 1857)(Col.: Staphylinidae) breeding in Surrey. *Entomologist's Record and Journal of Variation* 112(4): 154–158.
- Owens BE, Carlton CE (2016) Revision of *Eutyphlus* LeConte (Coleoptera: Staphylinidae: Pselaphinae), with description of a new species and phylogenetic placement within the tribe Trichonychini. *Coleopterists Bulletin* 70(1): 1–29. <https://doi.org/10.1649/072.070.0102>

- Paquin P, Dupérré N (2001) Beetles of the boreal forest: a faunistic survey carried out in western Quebec. In Proceedings of the Entomological Society of Ontario 132: 57–98.
- Pentinsaari M, Anderson R, Borowiec L, Bouchard P, Brunke A, Douglas H, Smith A, Hebert P (2019) DNA barcodes reveal 63 overlooked species of Canadian beetles (Insecta, Coleoptera). ZooKeys 894: 53–150. <https://doi.org/10.3897/zookeys.894.37862>
- Pohl G, Langor D, Klimaszewski J, Work T, Paquin P (2008) Rove beetles (Coleoptera: Staphylinidae) in northern Nearctic forests. Canadian Entomologist 140(4): 415–436. <https://doi.org/10.4039/n07-LS03>
- Provancher L (1877) Petite faune entomologique du Canada. Volume I, les Coléoptères. Presses de C. Darveau, Quebec, 785 pp.
- Putz V (2014) Nordamerikanische Arten der Gattung *Euaesthetus* GRAVENHORST (Coleoptera, Staphylinidae) 115. Beitrag zur Kenntnis der Euaesthetinen. Linzer Biologische Beiträge 115: 845–876.
- Schülke M, Smetana A (2015) Staphylinidae. Catalogue of Palaearctic Coleoptera 2(1): 304–900.
- Smetana A (1971) Revision of the tribe Quediini of North America north of Mexico (Coleoptera: Staphylinidae). Memoirs of the Entomological Society of Canada 103(79): 1–303. <https://doi.org/10.4039/entm10379fv>
- Smetana A (1982) Revision of the subfamily Xantholininae of America north of Mexico (Coleoptera: Staphylinidae). Memoirs of the Entomological Society of Canada 114(S120): 1–389. <https://doi.org/10.4039/entm114120fv>
- Smetana A (1995) Rove beetles of the subtribe Philonthina of America North of Mexico (Coleoptera: Staphylinidae) Classification, Phylogeny, and taxonomic revision. Memoirs on Entomology International. Associated Publishers, 946 pp.
- Stephan KH, Chandler DS, O’Keefe ST, Riley EG (2021) [2020] A revision of the North American species of *Euconnus* (*Napochus*) Thomson, north of Mexico (Coleoptera: Staphylinidae: Scydmaeninae). American Entomological Society, 319 pp. <https://doi.org/10.1649/0010-065X-75.4.868>
- Webster RP, Demerchant I (2012a) New Staphylinidae (Coleoptera) records with new collection data from New Brunswick, Canada: Oxyporinae. ZooKeys 186: 263–271. <https://doi.org/10.3897/zookeys.186.2502>
- Webster RP, Demerchant I (2012b) New Staphylinidae (Coleoptera) records with new collection data from New Brunswick, Canada: Paederinae. ZooKeys 186: 273–292. <https://doi.org/10.3897/zookeys.186.2504>
- Webster RP, Sweeney JD, Demerchant I (2012a) New Staphylinidae (Coleoptera) records with new collection data from New Brunswick, Canada: Omaliinae, Micropeplinae, Phloeocharinae, Olisthaerinae, and Habrocerinae. ZooKeys 186: 7–29. <https://doi.org/10.3897/zookeys.186.2495>
- Webster RP, Sweeney JD, Demerchant I (2012b) New Staphylinidae (Coleoptera) records with new collection data from New Brunswick and eastern Canada: Tachyporinae. ZooKeys 186: 55–82. <https://doi.org/10.3897/zookeys.186.2491>
- Webster RP, Sweeney JD, Demerchant I (2012c) New Staphylinidae (Coleoptera) records with new collection data from New Brunswick, Canada: Scaphidiinae, Piestinae, Osorinae, and Oxytelinae. ZooKeys 186: 239–262. <https://doi.org/10.3897/zookeys.186.2506>
- Webster RP, Chandler DS, Sweeney JD, Demerchant I (2012d) New Staphylinidae (Coleoptera) records with new collection data from New Brunswick, Canada: Pselaphinae. ZooKeys 186: 31–53. <https://doi.org/10.3897/zookeys.186.2505>

- Webster RP, Klimaszewski J, Sweeney JD, Demerchant I (2012e) New Staphylinidae (Coleoptera) records with new collection data from New Brunswick, and an addition to the fauna of Quebec, Canada: Aleocharinae. *ZooKeys* 186: 83–118. <https://doi.org/10.3897/zookeys.186.2655>
- Webster RP, Smetana A, Sweeney JD, Demerchant I (2012f) New Staphylinidae (Coleoptera) records with new collection data from New Brunswick and an addition to the fauna of Quebec: Staphylininae. *ZooKeys* 186: 293–348. <https://doi.org/10.3897/zookeys.186.2469>
- Webster RP, Davies A, Klimaszewski J, Bourdon C (2016) Further contributions to the staphylinid fauna of New Brunswick, Canada and the USA, with descriptions of two new *Proteinus* species (Coleoptera, Staphylinidae). *ZooKeys* 573: 31–83. <https://doi.org/10.3897/zookeys.573.7830>



# Two new records and description of a new *Perinereis* (Annelida, Nereididae) species for the Saudi Arabian Red Sea region

Marcos A. L. Teixeira<sup>1</sup>, Chloé Julie Loïs Fourreau<sup>2</sup>, Juan Sempere-Valverde<sup>1,3</sup>, Susana Carvalho<sup>1,4</sup>

1 *Biological and Environmental Science and Engineering Division (BESE), King Abdullah University of Science and Technology (KAUST), Thuwal 23955-6900, Saudi Arabia*

2 *Molecular Invertebrate Systematics and Ecology (MISE) Lab, Graduate School of Engineering and Science, University of the Ryukyus, Nishihara, Okinawa, Japan*

3 *Laboratorio de Biología Marina/Estación de Biología Marina del Estrecho (Ceuta), Departamento de Zoología, Facultad de Biología, Universidad de Sevilla, Avda. Reina Mercedes s/n, 41012, Sevilla, Spain*

4 *Marine Science Program, Biological and Environmental Science and Engineering Division, King Abdullah University of Science and Technology, Thuwal, 23955, Saudi Arabia*

Corresponding author: Susana Carvalho ([susana.carvalho@kaust.edu.sa](mailto:susana.carvalho@kaust.edu.sa))

## Abstract

Annelid biodiversity studies in the Red Sea are limited and integrative taxonomy is needed to accurately improve reference libraries in the region. As part of the bioblitz effort in Saudi Arabia to assess the invertebrate biodiversity in the northern Red Sea and Gulf of Aqaba, *Perinereis* specimens from intertidal marine and lagoon-like rocky environments were selected for an independent assessment, given the known taxonomic ambiguities in this genus. This study used an integrative approach, combining molecular with morphological and geographic data. Our results demonstrate that specimens found mainly in the Gulf of Aqaba are not only morphologically different from other five similar *Perinereis* Group I species reported in the region, but phylogenetic analysis using available COI sequences from GenBank revealed different molecular operational taxonomic units, suggesting an undescribed species, *P. kaustiana* **sp. nov.** The new species is genetically close and shares a similar paragnath pattern to the Indo-Pacific distributed *P. helleri*, in particular in Area III and Areas VII–VIII. Therefore, we suggest it may belong to the same species complex. However, *P. kaustiana* **sp. nov.** differs from the latter mainly in the shorter length of the postero-dorsal tentacular cirri, median parapodia with much longer dorsal cirri, posteriormost parapodia with much wider and greatly expanded dorsal ligules. Additionally, two new records are reported for the Saudi Neom area belonging to *P. damietta* and *P. suzensis*, previously described only for the Egyptian coast (Suez Canal) and are distributed sympatrically with the new species, but apparently not sympatric with each other.

**Key words:** Gulf of Aqaba, mtCOI-5P, NEOM, north-eastern Red Sea, Polychaeta, Saudi Arabia, taxonomy

## Introduction

Based on genetic databases (i.e., BOLD and GenBank), and despite the recent advances in integrative studies focused on polychaetes (i.e., Nygren et al. 2010; Villalobos-Guerrero et al. 2021; Teixeira et al. 2023), there are still many taxonomic ambiguities and unidentified annelid species in some groups of



Academic editor: Andrew Davinack

Received: 5 November 2023

Accepted: 26 January 2024

Published: 1 April 2024

ZooBank: <https://zoobank.org/C1537B91-98F4-41E2-A930-51BA8F4E8118>

Citation: Teixeira MAL, Fourreau CJL, Sempere-Valverde J, Carvalho S (2024) Two new records and description of a new *Perinereis* (Annelida, Nereididae) species for the Saudi Arabian Red Sea region. ZooKeys 1196: 331–354. <https://doi.org/10.3897/zookeys.1196.115260>

Copyright: © Marcos A. L. Teixeira et al. This is an open access article distributed under terms of the Creative Commons Attribution License (Attribution 4.0 International – CC BY 4.0).

Nereididae (i.e., Martin et al. 2021; Elgetany et al. 2022). *Perinereis* Kinberg, 1865 is one of the most diverse genera in this family, currently including between 97 (Wilson et al. 2023) to 106 (WoRMS Editorial Board 2024) valid species distributed worldwide. From these, approximately 16 species are reported for the Arabian Peninsula (Ocean Biodiversity Information System, OBIS; Mohammad 1971; Wehe and Fiege 2002). Due to apparent similar paragnath patterns, overall body features and lack of detailed systematic studies, *Perinereis* species are often problematic to identify to the species level (Bakken and Wilson 2005; Yousefi et al. 2011). This has led to informal denomination of species complexes and recognition of geographic morphs and varieties such as *P. cultrifera* (Grube, 1840) species group (type locality: Naples, Italy; Scaps et al. 2000) and the *P. nuntia* (Lamarck, 1818) species (type locality: Gulf of Suez, Egypt) group (Wilson and Glasby 1993; Glasby and Hsieh 2006; Sampértegui et al. 2013), both reported for the Red Sea (OBIS). Thanks to molecular data, it is now easier to screen for potential new species with apparent similar morphotypes. Recent evidence comparing populations from different regions has shown that when specimens differ genetically, further analysis of the diagnostic morphological features often leads to the recognition of distinct features that were previously overlooked (i.e., Sampértegui et al. 2013; Teixeira et al. 2022b). A recent review on meiofauna (Cerca et al. 2018) and recent polychaete studies (i.e., Abe et al. 2019; Tilic et al. 2019; Martin et al. 2020), including from Nereididae (Glasby et al. 2013; Sampieri et al. 2021; Teixeira et al. 2022a, b) also demonstrate that cryptic and pseudo-cryptic species often have geographically restricted distributions, with the range of cryptic species being smaller than the parent morphospecies.

The Egyptian side of the Red Sea has been the focus of an increasing amount of polychaete studies either reviewing existing species groups (i.e., Villalobos-Guerrero 2019) or describing new species that were previously considered cryptic (i.e., Elgetany et al. 2022). The northern Saudi Arabian Red Sea and Gulf of Aqaba, despite being expected to host a large biodiversity (Roberts et al. 2002; DiBattista et al. 2016), has seen comparatively few biodiversity studies involving molecular techniques, particularly for polychaetes. To address this gap, and document the invertebrate biodiversity of the region, a bioblitz was conducted in the Neom region (northern Saudi Arabian Red Sea and Gulf of Aqaba) to document the local biodiversity, with emphasis on mobile invertebrates and cryptobenthic fish. As part of this effort, this study used a molecular approach, combined with morphological and geographic data, to investigate *Perinereis* samples collected from marine intertidal and lagoon-like rocky environments of the northern Red Sea. In particular, we aimed to assess species distributions and to investigate whether specimens collected belonged to existing *P. cultrifera* group, *P. nuntia* group, to other similar *Perinereis* species reported for the region, or if new species were undescribed.

## Material and methods

### Sampling effort

The NEOM bioblitz sampling campaign surveyed 38 shallow and coral reef sites up to 25 meters depth and some intertidal habitats, along the northern

region of the Saudi Arabian Red Sea and Gulf of Aqaba (Neom area). This initiative aims to initiate a biodiversity inventory of marine benthic invertebrates (mainly mobile) and cryptobenthic fish in the Red Sea using DNA barcoding and metabarcoding. Only intertidal marine and lagoon-like rocky environments were considered for the purpose of this study, in order to perform an independent assessment within *Perinereis*, given the known taxonomic ambiguities in several species within the genus from this particular habitat.

A total of 36 *Perinereis* specimens (atokous) were hand-collected on rocky shores, in coarse-grained sediments under cobbles and rocks. Specimens were found in Magna (centre of Gulf of Aqaba; 28°26'57.3"N, 34°45'35.4"E), Shushah Island (27°56'13.7"N, 34°54'36.1"E) and lagoon-like environments at Almojawah Bay (South of Gulf of Aqaba; 28°10'18.1"N, 34°38'57.6"E) and Duba (Al Muwaileh; 27°37'04.4"N, 35°31'26.7"E), in May 2023. Two specimens collected in the northern region of Portugal (Canto Marinho, 41°44'13.2"N, 8°52'33.6"W) belonging to *Perinereis oliveirae* (Horst, 1889), were previously collected by the first author of this work, and due to misidentifications with the *P. cultrifera* morphotype in genetic databases, were used in this study for comparison purposes.

Table 1 details the number of original specimens collected for each sampling location, which correspond to the same number of COI sequences analysed. The number of COI sequences from *Perinereis* species publicly available in GenBank, respective sampling area and references are also detailed in Table 1 and were used for comparison purposes. The collected Red Sea *Perinereis* specimens were deposited at NTNU University Museum, Trondheim, Norway (**NTNU-VM**, Bakken et al. 2024; vouchers: NTNU-VM-86010–NTNU-VM-86044). *Perinereis oliveirae* specimens are deposited at Biological Research Collection of the Department of Biology of the University of Aveiro (**CoBI** at **DBUA**; curated by Ascensão Ravara: aravara@ua.pt; vouchers: DBUA0002494.02.v01 and DBUA0002494.02.v02), Portugal. Specimens that were exhausted in the DNA analysis were assigned only with the Process ID from the BOLD systems (<http://v4.boldsystems.org/>), corresponding to MTPNO009-23 (Gulf of Aqaba, Magna). Some specimens were preserved in 96% ethanol and others in formalin with a respective sample tissue preserved in ethanol for molecular work (detailed in Suppl. material 1).

### DNA extraction, PCR amplification, and alignments

DNA sequences of the 5' end of the mitochondrial cytochrome oxidase subunit I (mtCOI-5P) were obtained for all the collected *Perinereis* specimens and used for the main analysis. A representative number of specimens per location for the new species were also sequenced using the mitochondrial 16S rRNA and D2 region of nuclear 28S rRNA, for future reference purposes.

DNA extraction was performed using QuickExtract DNA Extraction Solution (Lucigen) with 50 µl of the reagent per Eppendorf. The tubes were then transferred to a heat block at 65 °C for 30 min and then an additional 2 min at 98 °C. Depending on the specimen size, only a small amount of tissue (i.e., a single parapodium) or the posterior end of the worm was used.

PCR reactions were performed using a premade PCR mix from VWR containing 10 µl per tube of Red Taq DNA polymerase Master Kit (2 mM, 1.1×), 0.5 µl of each primer (10 mM) and 1 µl of DNA template in a total 12 µl volume reaction.

**Table 1.** Species, number of sequences (*n*), geographic location, and their respective GenBank COI accession numbers for the original material and sequence data used from other studies.

Species	GenBank COI	Region	Location	<i>n</i>	Reference
<i>Perinereis kaustiana</i> sp. nov.	PP279005, PP279009, PP279010, PP279017– PP279020, PP279029, PP279035	Red Sea	Saudi Arabia, Gulf of Aqaba (Magna)	9	This study
	PP279008, PP279025		Saudi Arabia, Shushah Island	2	
	PP279004		Saudi Arabia, Duba (Al Muwaileh)	1	
<i>Perinereis suezensis</i>	PP279006, PP279007, PP279015, PP279016, PP279021, PP279023, PP279024, PP279026– PP279028, PP279036, PP279038, PP279039		Saudi Arabia, Shushah Island	13	
	OP612968–OP612972		Egypt, Gulf of Suez	5	
<i>Perinereis damietta</i>	PP279034		Saudi Arabia, Gulf of Aqaba (Magna)	1	This study
	PP279014, PP279037		Saudi Arabia, Duba (Al Muwaileh)	2	
	PP279002, PP279011– PP279013, PP279030– PP279033		Saudi Arabia, Gulf of Aqaba (Almojawah Bay)	8	
	OP610122–OP610126		Egypt, Gulf of Suez	5	Elgetany et al. (2022)
<i>Perinereis fayedensis</i>	OP605759–OP605763		Egypt, Gulf of Suez	5	
<i>Perinereis oliveirae</i>	PP279003, PP279022	NE Atlantic	Portugal, Canto Marinho	2	This study
" <i>Perinereis cultrifera</i> "	KR916909–KR916912		Portugal, Areosa Beach	5	Lobo et al. (2016)
<i>Perinereis helleri</i>	JX420256	Malaca Strait	Malaysia, Port Dickson	1	Glasby et al. (2013)
" <i>Perinereis nuntia</i> "	MH337359	Andaman Sea	India, Adaman and Nicobar Islands	1	Sivaraj and Thivikaran, unpublished
	JX420257	Java Sea	Indonesia, Pari Island	1	Glasby et al. (2013)
<i>Perinereis marionii</i>	OP347380	NE Atlantic	Great Britain, Plymouth	1	Teixeira et al. (2022b)
	OP347386		Portugal, Canto Marinho	1	
<i>Perinereis vallata</i>	HQ705192–HQ705196	South Pacific Ocean	Chile, Concepción	5	Sampértegui et al. (2013)
<i>Perinereis euiini</i>	KY249122–KY249124	Yellow Sea	South Korea, Gusan-myeon	3	Park and Kim (2017)
	MN256544–MN256546	South China Sea	China, Xiamen	3	Xing and Zhang, unpublished
<i>Perinereis anderssoni</i>	MH143495, MH143498, MH143502, MH143503, MH143522	NW Atlantic	Brasil, Espirito Santo	5	Paiva et al. (2019)
<i>Alitta virens</i>	OP038747, OP038760, OP038799, OP038806, OP038851	North Sea	Sweden, Tjärnö-Salto canal	5	Teixeira et al. (2022a)

Table 2 displays the PCR conditions, primers and sequence lengths for the different markers. Amplification success was screened in a 1% agarose gel, using 1 µl of PCR product. Successful PCR products were then purified using the Exonuclease I and Shrimp Alkaline Phosphatase (ExoSAP-IT, Applied biosystems) protocol, according to manufacturer instructions. Cleaned up amplicons were sent to KAUST Sanger sequencing service for forward sequencing.

The obtained trace files were edited and aligned in MEGA software v. 11.0.10 (<https://www.megasoftware.net/>; Tamura et al. 2021). COI sequences were blasted in GenBank to access possible existing matches (NCBI; <https://blast>).

**Table 2.** Primers and PCR conditions used in this study.

Marker	Primer	Fragment	Direction (5'–3')	PCR thermal cycling conditions	Reference
COI	PolyLCO	658bp	(F) GAYTATWTTCAACAAATCATAAAGATATTGG	1) 94 °C (1 min); 2) 5 cycles: 94 °C (40 s), 45 °C (40 s), 72 °C (1 min); 3) 35 cycles: 94 °C (40 s), 51 °C (40 s), 72 °C (1 min); 4) 72 °C (5 min).	Carr et al. (2011)
	PolyHCO		(R) TAACTTCWGGGTGACCAAA RAATCA		
16S	16SAR-L	c.365bp	(F) CGCCTGTTTATCAAAAACAT	1) 94 °C (3 min); 2) 40 cycles: 94 °C (30 s), 52 °C (30 s), 72 °C (1 min); 3) 72 °C (7 min).	Kessing et al. (2004)
	16SANN-F		(F) GCGGTATCCTGACCGRCAWAAGGTA		
	16SBR-H		(R) CCGGTCTGAACTCAGATCACGT		
28S	28sC2	c.500bp	(F) ACTCTCTCTTCAAAGTTCTTTTC	1) 96 °C (4 min); 2) 45 cycles: 94 °C (30 s), 55 °C (30 s), 72 °C (1 min); 3) 72 °C (8 min).	Hassouna et al. (1984)
	28s-D2		(R) TCCGTGTTTCAAGACGG		

ncbi.nlm.nih.gov/Blast.cgi). GenBank sequences batch for the original material are COI, PP279002–PP279039; 16S, PP264567–PP264572, PP264574, PP264575; 28SD2, PP264613, PP264614, PP264616. The dataset used for molecular analysis and its metadata can be accessed at the BOLD Systems under the project “*Perinereis* Saudi NEOM (DS-MTPNO)”, publicly available with the DOI: <https://doi.org/10.5883/DS-MTPNO>. The alignments (fasta and nexus format) for each individual marker and Suppl. material 1 are also publicly available online at Figshare: <https://www.doi.org/10.6084/m9.figshare.25097756>.

### Phylogenetic analysis and MOTU clustering

For comparison purposes, GenBank COI sequence data from *P. marionii* (Audouin & Milne Edwards, 1833); *P. vallata* (Grube, 1857); *P. helleri* (Grube, 1878); *P. cultrifera*; *P. euiini* Park & Kim, 2017; *P. anderssoni* Kinberg, 1865; *P. nuntia* (Lamarck, 1818); *P. fayedensis* Elgetany, Struck & Glasby, 2022; *P. suezensis* Elgetany, Struck & Glasby, 2022; *P. damietta* Elgetany, Struck & Glasby, 2022; and the outgroup *Alitta virens* (M. Sars, 1835) completed the final dataset (Table 1, Suppl. material 1). The phylogenetic analysis was performed through maximum likelihood (ML) for the entire dataset. Best-fit models were selected using the Akaike Information Criterion in MEGA. The phylogenetic relationship analysis was executed with 500 bootstrap runs using the General Time-Reversible model with gamma distributed rates and a portion of the sites invariable (GTR+G+I). The final version of the tree was edited with the software Inkscape v. 1.2 (<https://www.inkscape.org>).

Three delimitation methods were applied to obtain Molecular Operational Taxonomic Units (MOTUs): The Barcode Index Number (BIN), which makes use of the Refined Single Linkage (RESL) algorithm available only in BOLD (Ratnasingham and Hebert 2013); the Assemble Species by Automatic Partitioning (ASAP, Puillandre et al. 2021), implemented in a web interface (<https://bioinfo.mnhn.fr/abi/public/asap/asapweb.html>) with default settings using the Kimura-2-Parameter (K2P) distance matrix; lastly, the Poisson Tree Processes (bPTP; Zhang et al. 2013) performed in a dedicated web interface (<https://species.h-its.org/>), using the ML phylogeny obtained above, for 500000 MCMC generations and twenty-five percent of the samples discarded as burn-in.

The mean genetic distances for mtCOI (K2P; Kimura 1980) within and between MOTUs were calculated in MEGA.

## Morphological analysis

Specimens were studied using a Leica stereo microscope (model M205 C). Stereo microscope images were taken with a Flexacam C3 camera. Compound microscope images of parapodia and chaetae were obtained with a Leica DM2000 LED imaging light microscope, equipped with a Flexacam C3 camera, after mounting the parapodia on a slide preparation using Aqueous Permanent Mounting Medium (Supermount). Parapodial and chaetal terminology in the taxonomic section follows Bakken and Wilson (2005) with the modifications made by Villalobos-Guerrero and Bakken (2018). The final figure plates were edited with the software Inkscape v. 1.2.

For measuring length of dorsal ligules, not only the lengths of the tips were considered, but the proximal part of the ligules was also included (e.g., Conde-Vela and Salazar-Vallejo 2015; Villalobos-Guerrero and Carrera-Parra 2015; Teixeira et al. 2022b). Like Hutchings et al. (1991), a specimen is described as having a greatly expanded dorsal notopodial ligule posteriorly only if the dorsal ligule is more than two times as long as the ventral ligule. For analysis of variation, only complete specimens were considered; total length (**TL**), length up to chaetiger 15 (**L15**), width at chaetiger 15 (**W15**) were measured with a millimetre rule under the stereomicroscope. Number of chaetigers (**NC**) were also taken into consideration. TL was measured from anterior margin of prostomium to the end of the pygidium, and W15 were measured excluding parapodia. Measurements of the length of the antennae (**AL**), palps (**PL**), dorsal cirri (**DCL**), dorsal ligule (**DLL**), ventral cirri (**VCL**), ventral ligule (**VLL**), median ligule, the length and width of the head (**HL** and **HW**, respectively), and the length of all four tentacular cirri, including the longest one (postero-dorsal cirri, **DPCL**), were also retrieved. Heterogomph falciger blade size comparison (short, long, and extra-long) based on Wilson et al (2023). Spiniger serration based on the comparison between *P. cultrifera* (lightly serrated) and *P. rullieri* (coarsely serrated) from Pilato (1974).

Paragnath counts were performed to compare patterns with other morphologically similar Group I *Perinereis* species (Hutchings et al. 1991). Pharynx paragnath terminology follows Bakken et al. (2009) and paragnath description of areas VII and VIII follow Conde-Vela (2018).

Terminology for molecular vouchers follows Pleijel et al. (2008) and Astrin et al. (2013). Overall description follows a similar structure to those of Villalobos-Guerrero (2019). Dates of sample collection follow the DD/MM/YY format.

## Results

### Phylogenetic analyses

The phylogenetic reconstruction recovered ten MOTUs of *Perinereis* (Fig. 1A), the delimitation of which are cohesively supported by the three species-delimitation tests applied, except for MOTU 1 and GB1, which are clustered together with the ASAP method. Sequences from *P. fayedensis* and *P. anderssoni* are not present in BOLD and have no associated BIN.

In this phylogenetic tree, *P. suzensis* (MOTU 1) and *P. fayedensis* (MOTU GB1) are sister to each other, and their lineage splits early compared to the

other analysed species of *Perinereis*. The basal node support for the six molecular groups (2, 4, GB2, and GB4–GB6) is very low. The 36 Red Sea specimens sequenced in the present study clustered into three clades that correspond to *P. suezensis* (MOTU 1, Fig. 1D) and *P. damietta* (MOTU 2, Fig. 1C), as well as a molecular cluster exclusively harbouring sequences of specimens belonging to *P. kaustiana* sp. nov. (MOTU 3, Fig. 1E). The new species is sister to a group (MOTU GB3) including sequences attributed to *Perinereis helleri* from Malaysia (JX420256 from Glasby et al. (2013)), as well as two sequences probably misidentified as *Perinereis nuntia* from India and Indonesia (MH337359 from Sivaraj and Thivikaran (unpublished) and JX420257 from Glasby et al. 2013). This relationship was supported with 83% bootstrap replications. The genetic divergence between *P. kaustiana* sp. nov. and GB3 sequences group (19.9%, COI K2P) was higher than between the closely related but recently established as distinct species, *P. suezensis* and *P. fayedensis* (~ 6%, COI K2P). MOTU 4 grouped our sequences of *P. oliveirae* with *P. cultrifera* sequences from Lobo et al. (2016). Table 3 shows all the COI distances between and within the analysed taxa from Fig. 1.

## Taxonomic account

### Family Nereididae Blainville, 1818

### Genus *Perinereis* Kinberg, 1865

#### *Perinereis kaustiana* sp. nov.

<https://zoobank.org/378AABC8-4C46-43FF-9A0F-5F6703B4A801>

Figs 1A, B, E; 2A–J; 3A–I

*Nereis Perinereis helleri* Grube, 1878: 81–82; Horst 1924: 172–173, pl 34, figs 3, 4.

*Perinereis helleri* Monroe, 1931: 14–15, fig. 8a–c.; Russell 1962: 7; Rozbaczylo and Castilla 1973: 220–221; Hartmann Schröder 1979: 116.

*Perinereis cultrifera* var. *helleri* Fauvel 1932: 105–106.

*Perinereis carniguina* Grube, 1878: 87, pl 4, fig. 8.

**Material examined. Holotype and hologenophore:** NTNU-VM-86011, Saudi Arabia (Red Sea), Gulf of Aqaba, Magna, 28°26'57.3"N, 34°45'35.4"E, intertidal, rocky beach among coarse-grained sand under rocks, collected by Marcos A. L. Teixeira and Chloé Julie Loïs Fourreau, 11/05/2023, GenBank (mtCOI): PP279020.

**Paratypes and paragenophores:** 7 specimens, NTNU-VM-86010, NTNU-VM-86012–NTNU-VM-86017, Saudi Arabia (Red Sea), Gulf of Aqaba, Magna, 28°26'57.3"N, 34°45'35.4"E, intertidal, rocky beach under rocks among coarse-grained sand, collected by Marcos A. L. Teixeira and Chloé Julie Loïs Fourreau, 11/05/2023, GenBank (mtCOI): PP279009–PP279010, PP279017–PP279019, PP279029, and PP279035.

**Non-types.** 2 specimens, NTNU-VM-86019, NTNU-VM-86020, Saudi Arabia (Red Sea), Shushah Island, 27°56'13.7"N, 34°54'36.1"E, intertidal, rocky beach under rocks among coarse-grained sand, collected by Marcos A. L. Teixeira, 05/05/2023. 1 specimen, NTNU-VM-86018, Saudi Arabia (Red Sea), Dubai, Al Muwaileh, 27°37'04.4"N, 35°31'26.7"E, lagoon environment, intertidal, under rocks among coarse-grained sand, collected by Marcos A. L. Teixeira and Chloé

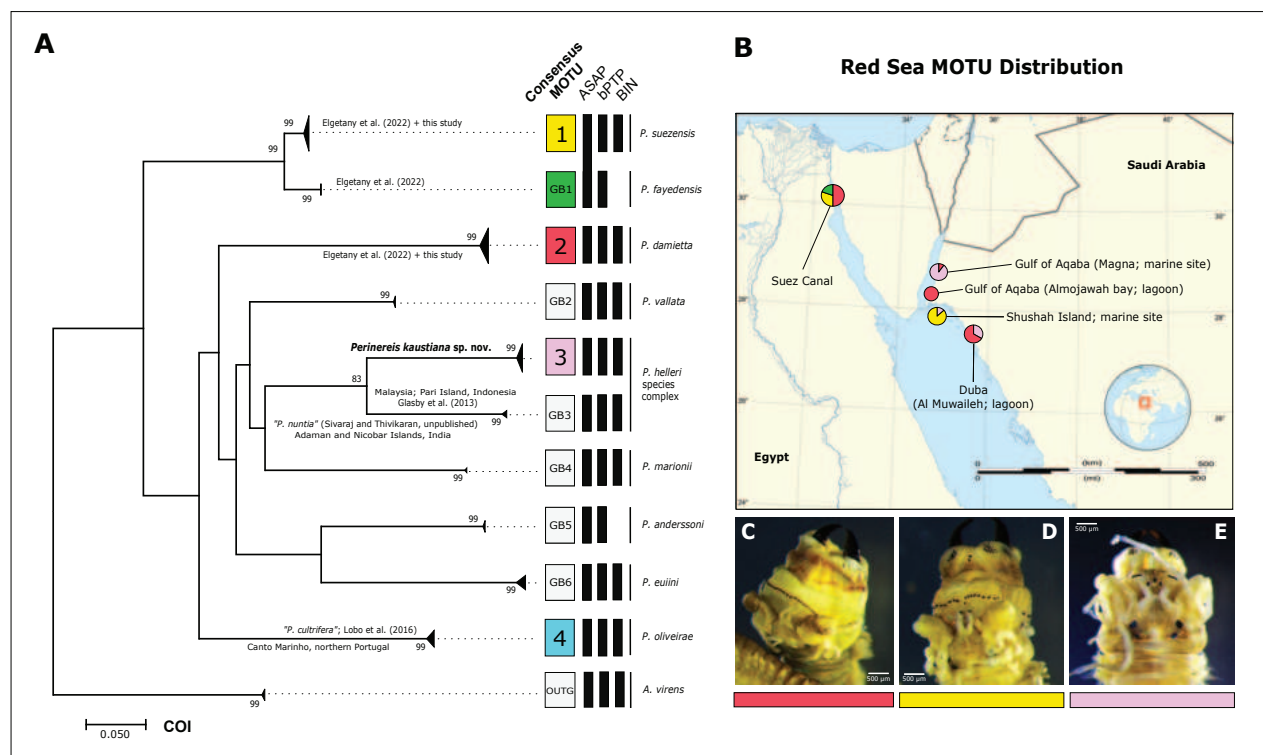


**Figure 1.** Phylogenetic tree and MOTU distribution for the three sampled Red Sea *Perinereis* species **A** maximum likelihood phylogeny based on COI sequences, with information regarding the different MOTU delineation methods. Numbered MOTUs (1–4) contain original sequences from *Perinereis* specimens analysed in this study; MOTUs “GB” are based on *Perinereis* sequences mined from GenBank; MOTU “OUTG” correspond to the rooted outgroup, *Alitta virens*. Bootstrap values lower than 80% not displayed **B** Red Sea MOTU distribution; each coloured pie corresponds to a unique species and respective abundance proportion; larger pie charts indicate higher number of sympatric species. Species from the Suez Canal based on mined GenBank sequences from Elgetany et al. (2022); abundance proportion based on type material **C** *Perinereis damietta*, focus on prostomium and pharynx, dorsal view, specimen NTNU-VM-86031 **D** *Perinereis suezensis*, focus on prostomium and pharynx, dorsal view, specimen NTNU-VM-86032 **E** *Perinereis kaustiana* sp. nov., focus on prostomium and pharynx, dorsal view, specimen NTNU-VM-86011. Scale bars: 500 µm (**C–E**).

Julie Loïs Fourreau, 18/05/2023. 1 specimen, MTPN009-23, Saudi Arabia (Red Sea), Gulf of Aqaba, Magna, 28°26'57.3"N, 34°45'35.4"E, intertidal, rocky beach under rocks among coarse-grained sand, collected by Marcos A. L. Teixeira and Chloé Julie Loïs Fourreau, 11/05/2023.

**Diagnosis.** Four pairs of tentacular cirri, postero-dorsal one reaching chaetiger 7–9; ratio of DPCL / HL = 3.6×. Eversible pharynx with one pair of dark brown curved jaws with seven or eight denticles; two longitudinal canals emerging from the pulp cavity, both in the mid-section of the jaw. Pharynx consisting of maxillary and oral rings with conical shaped paragnaths. Maxillary ring: Area I = 2 small paragnaths arranged in a longitudinal line. Area II = Cluster of 5–7 small paragnaths. Area III = central patch of nine small paragnaths, lateral patches with two small paragnaths each. Area IV = 13 small paragnaths arranged in wedge shape without any bars. Oral ring: Area V = a triangle of three large paragnaths. Area VI (a+b) = two narrow bar-shaped paragnaths, one on each side, displayed as a straight line. Areas VII–VIII = 20–24 small paragnaths in total; Area VII, ridge region with two transverse paragnaths, furrow regions with two longitudinal paragnaths each; Area VIII, ridge regions with one paragnath

**Table 3.** Mean intra (in bold) and inter-MOTU COI genetic distances (K2P; %), for the eleven analysed species/MOTUs in Fig. 1.

	1	2	3	4	5	6	7	8	9	10	11
<i>P. kaustiana</i> sp. nov. (M. 3)	<b>1.0 ± 0.2</b>										
<i>P. helleri</i> (M. GB3)	19.9 ± 2.4	<b>0.5 ± 0.2</b>									
<i>P. suzezensis</i> (M. 1)	25.8 ± 3.2	26.7 ± 3.2	<b>1.1 ± 0.2</b>								
<i>P. damietta</i> (M. 2)	23.8 ± 3.2	25.5 ± 3.2	25.9 ± 3.1	<b>0.8 ± 0.2</b>							
<i>P. fayedensis</i> (M. GB1)	25.3 ± 3.2	25.8 ± 3.2	5.8 ± 1.0	25.0 ± 3.0	<b>0.0 ± 0.0</b>						
<i>P. euiini</i> (M. GB6)	24.6 ± 3.2	25.5 ± 3.2	27.0 ± 3.4	25.3 ± 3.2	27.2 ± 3.4	<b>0.6 ± 0.2</b>					
<i>P. oliveirae</i> (M. 4)	25.8 ± 3.2	25.7 ± 3.2	25.4 ± 3.2	27.3 ± 3.4	24.8 ± 3.1	26.3 ± 3.3	<b>0.6 ± 0.2</b>				
<i>P. anderssoni</i> (M. GB5)	26.7 ± 3.4	24.6 ± 3.3	24.9 ± 3.1	26.4 ± 3.3	23.7 ± 3.0	22.3 ± 2.8	26.6 ± 3.4	<b>0.2 ± 0.1</b>			
<i>P. vallata</i> (M. GB2)	23.1 ± 3.0	22.0 ± 2.8	23.2 ± 3.0	22.0 ± 2.8	22.6 ± 2.9	24.1 ± 3.1	23.6 ± 2.9	24.3 ± 3.2	<b>0.1 ± 0.1</b>		
<i>P. marionii</i> (M. GB4)	25.9 ± 3.3	22.8 ± 3.0	25.2 ± 3.2	27.3 ± 3.4	23.8 ± 3.0	24.0 ± 3.2	23.6 ± 3.0	23.1 ± 3.0	21.1 ± 2.7	<b>0.3 ± 0.2</b>	
<i>A. virens</i> (OUTG)	29.3 ± 3.9	28.1 ± 3.5	27.5 ± 3.4	29.6 ± 3.6	27.5 ± 3.3	28.5 ± 3.5	27.6 ± 3.4	27.6 ± 3.5	26.3 ± 3.1	26.5 ± 3.2	<b>0.2 ± 0.1</b>

each, furrow regions with two longitudinal paragnaths each. Dorsal cirrus longer than ventral cirrus throughout the body; much longer in median chaetigers, ratio DCL / VCL = 2.8–3×. Ventral cirri of median chaetigers shorter than ventral ligule, ratio of VCL / VLL = 0.7×. Dorsal ligule oval, ending tip gradually becomes thinner throughout the body; finger-like tip in median and posterior parapodia. Dorsal ligules of median chaetigers subequal to dorsal cirri, tips shorter than dorsal cirri. Posterio-most dorsal ligules greatly expanded (3× the length of the ventral ligule) and visibly much wider (2.5–3× the width of median ligule) than anterior and median ones (2× the width of median ligule). Pygidial cirri as long as last 12–14 chaetigers.

**Molecular Data.** MtCOI-5P, 16S, and 28S sequences as in specimens NTNU-VM-86010–NTNU-VM-86020 and MTPNO009-23 (Table 1; Suppl. material 1). GenBank accession numbers: PP279004, PP279005, PP279008–PP279010, PP279017–PP279020, PP279025, PP279029, PP279035 (mtCOI- 5P); PP264567–PP264572, PP264574, PP264575 (16S); PP264613, PP264614, PP264616 (28S-D2). *Perinereis kaustiana* sp. nov. clearly differs from the remaining species of the COI phylogeny, grouping in MOTU 3 (Fig. 1A). No GenBank BLAST match to date. Sister species with *P. helleri*. Intraspecific mtCOI-5P mean distances below 1%. Interspecific mtCOI-5P mean distances to the closest and distant neighbour are 19.9% (K2P, *P. helleri*) and 26.7% (K2P, *P. anderssoni*) respectively. DOI for the species' Barcode Index Number (BIN): <https://doi.org/10.5883/BOLD:AFJ4260>.

**Distribution and habitat.** Confined to the northeastern Red Sea (Duba, Shushah Island) and Gulf of Aqaba (Magna) so far. **Type locality:** Saudi Arabia, Gulf of Aqaba: Magna region (marine site), 28°26'57.3"N, 34°45'35.4"E. Specimens collected both in lagoon-like environments and fully marine sites in rocky areas, usually among coarse-grained sand under rocks. Apparently more abundant and easier to find in marine sites from the Gulf of Aqaba. Can be found in sympatry with *P. damietta* (Fig. 1B, C) and *P. suzezensis* (Fig. 1B, D). The latter two species as described by Elgetany et al. (2022).

**Etymology.** The species designation pays tribute to the King Abdullah University of Science and Technology (KAUST) in Saudi Arabia, a globally recognized graduate-level research institution. This naming honours KAUST's substantial

and enduring contributions to marine science, particularly in advancing our understanding of the Red Sea over the course of more than a decade. Through its dedicated research efforts, KAUST has significantly enriched the scientific community's knowledge of this unique marine environment.

**Description.** Specimens used: NTNU-VM-86011 (holotype) and NTNU-VM-86015 (paratype), both preserved in ethanol 96%, stored at NTNU University Museum (Norway, NTNU-VM).

**Body/measurements:** Body with a prominent dorsal blood vessel (Fig. 2I); stout anteriorly, posteriorly gradually tapering toward pygidium. Colour in preserved specimens is yellowish-brown. Holotype, NTNU-VM-86011, large specimen, complete, TL = 55 mm, L15 = 7 mm, W15 = 2.12 mm, with 115 chaetigers. Paratype, NTNU-VM-86015, small specimen, complete, TL = 24 mm, L15 = 5 mm, W15 = 1.06 mm, with 85 chaetigers.

**Head** (Fig. 2A, B, E, J): Prostomium pyriform, 1.2× wider than long; 2.5× longer than antennae. Palps with a round or conical palpostyle (Fig. 2A); palpophore longer than wide, subequal to the entire length of prostomium. Antennae separated, gap half of antennal diameter (Fig. 2E); tapered, less than half the length of the palpophore. Eyes black, anterior and posterior pairs well separated (Fig. 2J). Anterior pair of eyes oval shaped, as wide as antennal diameter; posterior pair of eyes round or oval shaped, subequal width to anterior pair. Distance between the anterior eyes 1.25× longer than posterior ones. Nuchal organs covered by the tentacular belt.

**Tentacular cirri:** Tentacular cirri longer than mid body width. Tentacular cirri pattern: postero-dorsal cirri twice longer than antero-dorsal ones; postero-dorsal reaching chaetiger 7–9 (Fig. 2I). Antero-dorsal cirri reaching chaetigers 3 and 4; 1.7× longer than palpophore. Antero-ventral cirri 1.4× shorter than postero-ventral ones; antero-ventral shorter than palpophore. Dorsal cirrophores wrinkled, cylindrical.

**Pharynx:** Pair of dark brown curved jaws with 7–8 denticles; two longitudinal canals emerging from the pulp cavity, both in the mid-section of the jaw (Fig. 2C). Pharynx consisting of maxillary and oral rings with conical shaped paragnaths (Fig. 2A, B). Maxillary ring: Area I = two small paragnaths arranged in a longitudinal line (Fig. 2F). Area II = Cluster of 5–7 small paragnaths (Fig. 2F). Area III = central patch of nine small paragnaths, lateral patches with two small paragnaths each (Fig. 2D). Area IV = 13 small paragnaths arranged in wedge shape without any bars (Fig. 2D). Oral ring: Area V = a triangle of three large paragnaths (Fig. 2E). Area VI (a+b) = two narrow bar-shaped paragnaths, one on each side, displayed as a straight line (Fig. 2E). Areas VII–VIII = 20–24 small paragnaths in total; Area VII, ridge region with two transverse paragnaths, furrow regions with two longitudinal paragnaths each (Fig. 2G); Area VIII, ridge regions with one paragnath each, furrow regions with two longitudinal paragnaths each (Fig. 2G).

**Notopodia:** Dorsal cirri slender, tapering, subequal to dorsal ligule in anterior (Fig. 3A) and median (Fig. 3B) parapodia, 1.8× shorter in posterior ones (Fig. 3C); cirri longer than proximal part of dorsal ligule in anterior and median parapodia, 1.4× shorter in posterior ones. Dorsal cirri longer than ventral one throughout the body, much longer in median chaetigers; 1.7× longer in anterior and posterior parapodia, 2.4× in median ones. Dorsal ligules oval, ending tip gradually becomes thinner throughout the body; finger-like tip in median and

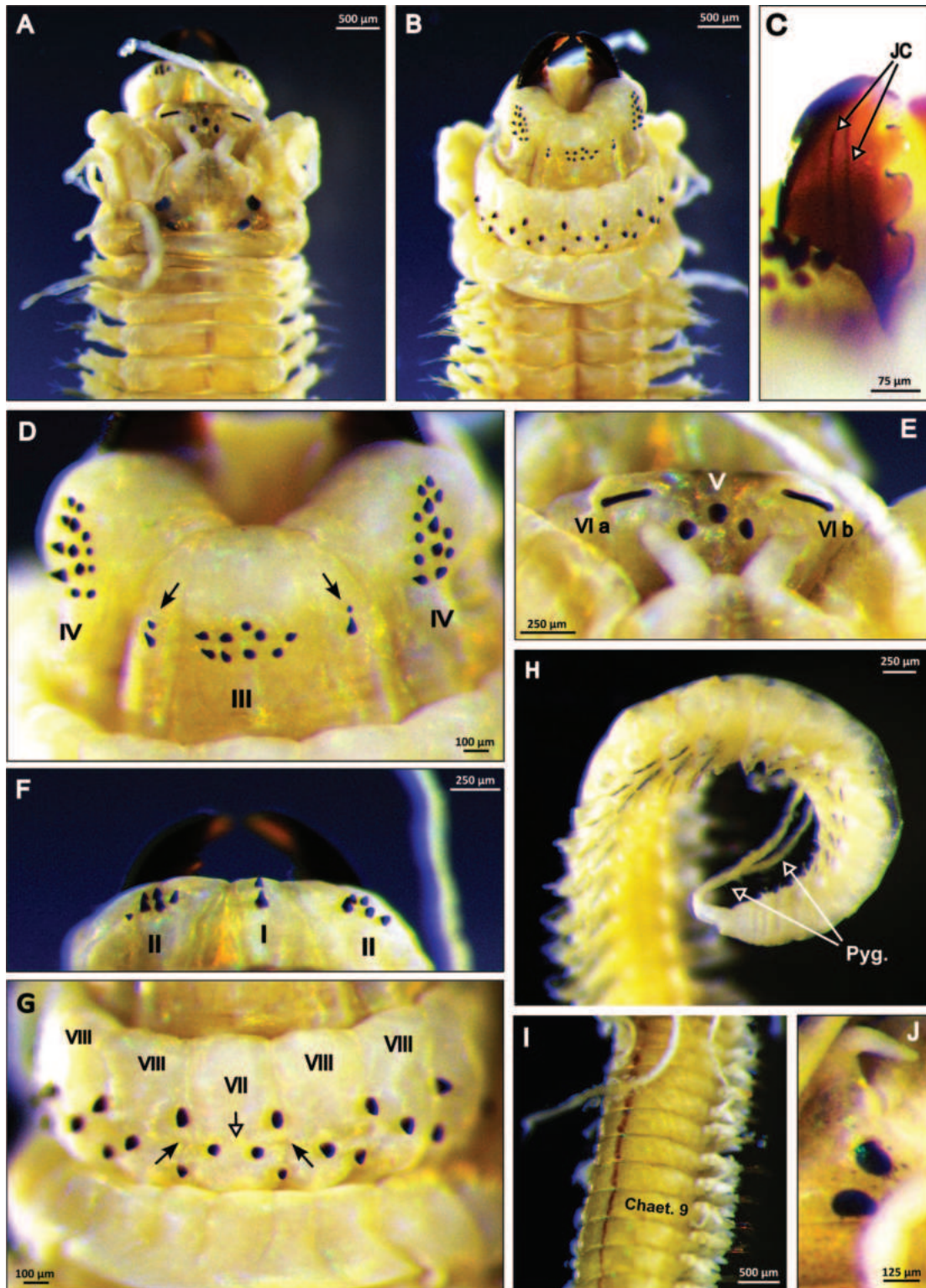


**Figure 2.** *Perinereis kaustiana* sp. nov. All pictures are from the holotype (NTNU-VM-86011) if not stated otherwise **A** anterior end, prostomium, dorsal view **B** anterior end, prostomium, ventral view **C** jaws and respective jaw canals (JC), dorsal view **D** pharynx, maxillary ring (Areas III and IV), ventral view; black arrows, lateral patches with two paragnaths each **E** pharynx, oral ring (Areas VI), dorsal view **F** pharynx, maxillary ring (Areas I and II), dorsal view **G** pharynx, oral ring (Areas VII–VIII), ventral view; black arrows, furrow regions; white arrows, ridge regions **H** posterior end; white arrows, pygidial cirri, paratype (NTNU-VM-86015) **I** anterior body, tentacular cirri reaching chaetiger 9, paratype (NTNU-VM-86015) **J** worm's eyes, right side, paratype (NTNU-VM-86015). Abbreviations: chaet., chaetiger; Pyg., Pygidium. Scale bars: 500  $\mu$ m (**A**, **B**, **I**); 250  $\mu$ m (**E**, **F**, **H**); 100  $\mu$ m (**D**, **G**); 125  $\mu$ m (**J**); 75  $\mu$ m (**C**).

posterior parapodia (Fig. 3A–C). Dorsal ligules 1.4× longer and twice as wider as median ligules in anterior parapodia (Fig. 3A), 1.6× longer and twice wider in median ones (Fig. 3B), twice longer and 2.5–3.0× wider than median ligules in posterior parapodia (Fig. 3C). Posteriormost dorsal ligules greatly expanded; 3× the length of the ventral ligule; visibly much wider (2.5–3×) than median ligule (Fig. 3C, I). Distal part of dorsal ligules slightly longer than proximal one in anterior and median parapodia, 1.5× shorter in posterior ones.

**Neuropodia:** Ventral cirri slender with tapering tip, 1.35× shorter throughout the body (Fig. 3A–C). Neuroacicular ligules subequal to ventral ligule in anterior parapodia, 1.3–1.4× longer in median and posterior ones. Ventral ligules oval in anterior parapodia, gradually becomes thinner throughout the body with a tapering tip; ventral ligules 1.4× shorter than dorsal ligules in anterior parapodia (Fig. 3A), twice shorter in median ones (Fig. 3B), 2.5–3× shorter in posterior parapodia (Fig. 3C).

**Chaetae:** Notochaetae with homogomph spinigers; spinigers with lightly serrated blade, evenly spaced (Fig. 3D), numerous and present throughout the whole body. Neurochaetal supra-acicular fascicle with homogomph spinigers (Fig. 3F) and heterogomph falcigers (Fig. 3H) present throughout the whole body; spinigers with coarsely serrated blade, present in the dorsal most position; falcigers with slender serrated long blade (Fig. 3H). Neurochaetal subacicular fascicle with heterogomph spinigers (Fig. 3G) and heterogomph falcigers (Fig. 3E) both present throughout the whole body; spinigers with lightly serrated blades (Fig. 3G); falcigers similar to supra-acicular ones (Fig. 3H), present in the ventral most position.

**Pygidium:** With a pair of long cylindrical slender anal cirri, as long as last 12–14 chaetigers (Fig. 2H).

**Remarks.** Some nereidid species groups can have similar morphological features, including paragnath patterns, that may cause misidentifications. The new species COI clade revealed no GenBank match based on the BLAST tool. *Perinereis kaustiana* sp. nov. and a sequence belonging to a specimen from Malaysia identified as *P. helleri* (type locality: Bohol, Philippines) not only are sister to each other and phylogenetically close (Fig. 1A;  $19.9 \pm 2.4\%$  K2P COI distance), but they also seem to share the same paragnath sizes, shapes and patterns (Park and Kim 2017: 255, fig. 4e; sampled in South Korea; no molecular data available), including in Area III, with the presence of lateral patches with two paragnaths each (Fig. 2D) and the same paragnath arrangements in the furrow and ridge regions of Areas VII–VIII (Fig. 2G). This makes them morphologically very similar and possibly belonging to the same cryptic complex, which could range from the Red Sea to the Indo-Pacific based on the available COI data. However, *P. kaustiana* sp. nov. seems to differ from *P. helleri* in some key features: shorter postero-dorsal tentacular cirri, reaching up to chaetiger 9, instead of the reported chaetiger 16 for *P. helleri*; median parapodia with much longer dorsal cirri (3×) compared to ventral one; posteriormost parapodia with much wider dorsal ligule (2.5–3.0×) than the median ligule (Fig. 3C, I) and dorsal ligule greatly expanded (3× longer than ventral ligule). Based on parapodia drawings from Hutchings et al. (1991: 255, fig. 9; Syntype ZMB Q3464), the ratio between dorsal and ventral cirri in *P. helleri* is subequal to slightly longer than ventral cirri throughout the body and posteriormost dorsal ligules with double the width of median ones and slightly expanded (up to 2× the length of

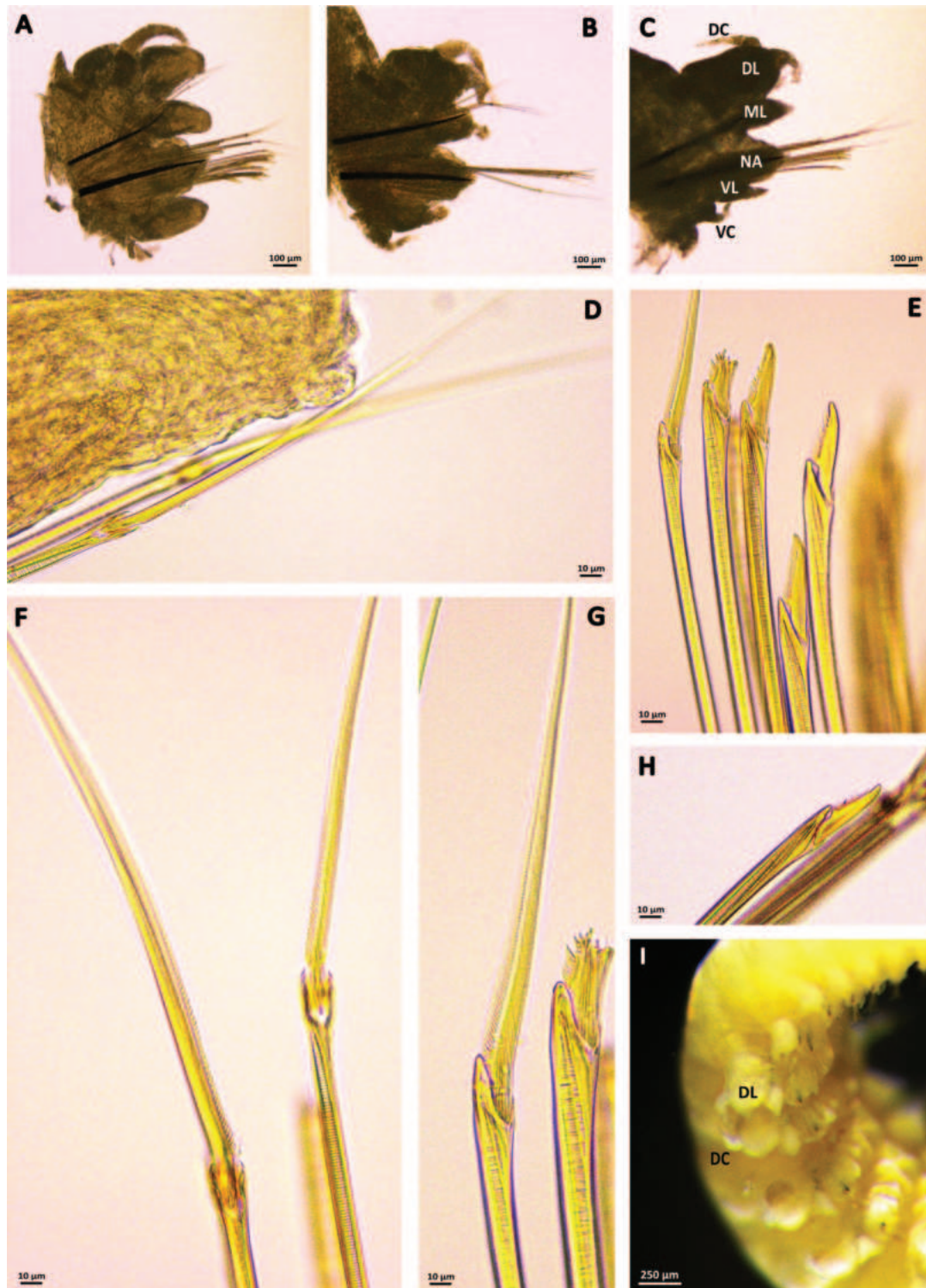


**Figure 3.** *Perinereis kaustiana* sp. nov. Parapodia and types of chaetae. All images are from the holotype (NTNU-VM-86011) **A** right parapodium, posterior view, chaetiger 9 **B** right parapodium, posterior view, chaetiger 46 **C** right parapodium, posterior view, chaetiger 96 **D** notochaetae: homogomph spiniger with lightly serrated blade, chaetiger 9 **E** neurochaetae, subacicular fascicle: heterogomph falcigers (centre) and heterogomph spinigers with lightly serrated blade (left), chaetiger 9 **F** neurochaetae, supra-acicular fascicle: homogomph spiniger with coarsely serrated blade, chaetiger 9 **G** neurochaetae, subacicular fascicle: heterogomph spiniger with lightly serrated blade, chaetiger 9 **H** neurochaetae, supra-acicular fascicle: heterogomph falciger, chaetiger 56 **I** posterior end, focused on chaetiger 97 and chaetiger 98. Abbreviations: DC, Dorsal cirri; DL, Dorsal ligule; ML, Median ligule; NA, Neuroacicular ligule; VL, Ventral ligule; VC, Ventral cirri. Scale bars: 250  $\mu\text{m}$  (**I**); 100  $\mu\text{m}$  (**A–C**); 10  $\mu\text{m}$  (**D–H**).

**Table 4.** Comparison between selected characters in the most morphologically similar species to *P. kaustiana* sp. nov., reported for the Arabian Peninsula and Mediterranean Sea and lacking DNA data. The Indo-Pacific *P. helleri* is also included. Morphological details of paragnath patterns for *P. cultrifera* and *P. rullieri* species complexes also includes partial data from topotypical specimens belonging to the private collection of the first author, to be published in the forthcoming future.

Characters	<i>P. kaustiana</i> sp. nov.	<i>P. helleri</i> (Grube, 1878)	<i>P. cultrifera</i> (Grube, 1840)	<i>P. rullieri</i> Pilato, 1974
Colouration	Yellowish to yellowish brown	Creamy pink or pale brown	Yellowish brown to dark brown; faint narrow transverse pigmented bands on several anterior chaetigers	Yellowish brown to dark brown
Paragnaths Area I	2 small paragnaths arranged in a longitudinal line	Usually 2 small paragnaths arranged in a longitudinal line; occasionally 1	Usually 2 paragnaths arranged in a longitudinal line; occasionally 1	Usually one; may have 2 paragnaths arranged in a longitudinal line
Paragnaths Area II	Cluster of 5–7 small paragnaths	Cluster of 4–17 small paragnaths	Diagonal band of 3–15 large paragnaths	Cluster of 3–15 small paragnaths
Paragnaths Area III	Central patch of 9 small paragnaths + lateral patches with 2 paragnaths each	Central patch of 11–20 small paragnaths + lateral patches with 2 or 3 paragnaths each	Central patch of 5–11 large paragnaths, lateral patch absent	Central patch of 5–16 small paragnaths + lateral patches (may be present only on a single side) with 1 paragnath each
Paragnaths Area IV	13 small paragnaths arranged in wedge shape without any bars.	10–19 small paragnaths arranged in wedge shape, without any bars.	6–20 paragnaths arranged in wedge shape, without any bars.	10–25 paragnaths arranged in wedge shape without any bars.
Paragnaths Area V	Triangle of 3 paragnaths	Triangle of 3 paragnaths	Variable. Usually a triangle of 3 paragnaths; may occasionally display a single paragnath or have 4 paragnaths arranged in rhomboid shape	Usually a triangle of 3 paragnaths; may occasionally display a single paragnath
Paragnaths Areas VI (a+b)	2 narrow, straight bars	2 narrow, straight bars	Variable, usually 2 broader and straight bars; may have narrow and/or arcuate and/or short bars	Variable, usually 2 narrower and straight bars; may be very short
Paragnaths Areas VII, VIII	Area VII, ridge region with 2 transverse paragnaths, furrow regions with 2 longitudinal paragnaths each; 20–24 total.	Area VII, ridge region with 2 transverse paragnaths, furrow regions with 2 longitudinal paragnaths each; 21–40 total	Usually arranged in two regular rows of large paragnaths; 20–50 total	Usually arranged in two irregular rows of small paragnaths; 20–40 total
Postero-dorsal cirri	Medium sized, reaching up to chaetiger 9	Long sized, reaching up to chaetiger 16	Small sized, reaching up to chaetigers 4 and 5	Medium sized, reaching up to chaetigers 6–8
Homogomph spiniger serration (neurochaetal supra-acicular fascicle)	Coarsely serrated	No data	Lightly serrated	Coarsely serrated
Heterogomph falcigers	Present with long blades	Present with long blades	Present with short blades	Present with long blades
Parapodia	Posteriormost dorsal ligules greatly expanded (3× longer than ventral ligule) and much wider (2.5–3× wider than median ligule) than in anterior and median ones. Median dorsal cirri much longer than ventral ones (ratio 2.8–3×)	Posteriormost dorsal ligule expanded (1.9–2× longer than ventral ligule). Dorsal cirri subequal to ventral cirri throughout the body	Posteriormost dorsal ligule expanded (1.5–1.8× longer than ventral ligule); may be greatly expanded (> 2×)	Posteriormost dorsal ligule expanded (1.5–1.8× longer than ventral ligule); may be greatly expanded (> 2×)
Type locality	Gulf of Aqaba, Saudi Arabia (Red Sea)	Philippines, Bohol (Pacific)	Naples, western Italy (Mediterranean)	Sicily, Eastern Italy (Mediterranean)
Reference	This study	Mohammad 1971; Hutchings et al. 1991	Hutchings et al. 1991; Pilato 1974	Pilato 1974

the ventral ligules; Table 4). Furthermore, *P. helleri* from Hutchings et al. (1991) does not seem to possess ligules with finger-like ending tips.

Other species with similar paragnath patterns are *Perinereis anderssoni* (Kinberg 1865: 167–179; Park and Kim 2017: 255, fig. 4d) and *Perinereis rullieri*

(Pilato 1974: 25–36, figs 1–4), which share the same small sized paragnaths as *P. kaustiana* sp. nov., but instead the former two species possess only one paragnath in each lateral patch of Area III and paragnaths in Areas VII and VIII are usually arranged in two regular rows, without any discernible pattern in the furrow or ridge regions. *Perinereis anderssoni* is reported in the Atlantic region of the American continent (type locality: Rio de Janeiro, Brazil), while *P. rullieri* is apparently restricted to the Mediterranean Sea (type locality: between Aci Trezza and Augusta, eastern coast of Sicily, Italy). Moreover, the morphological similar lineages found within the *Perinereis cultrifera* (Grube 1840: 74, fig. 6; Hutchings et al. 1991: 253–254, fig. 8a–c) species complex, including *P. euiini* (Park and Kim 2017: 252–260, figs 1, 2, 4a, b, 5, tables 1, 4, described for South Korea), are different from *P. kaustiana* sp. nov. due to the overall larger paragnath sizes, lack of any lateral patches in Area III, and the presence of shorter heterogomph falcigers (Park and Kim 2017: 254, fig. 2L). Specimens of *Perinereis cultrifera* from Lobo et al. (2016) were misidentified and are in fact *P. oliveirae* (Horst 1889: 38–45, plate 3; Fauvel 1923: 354, fig. 138 e–k), the latter characterised by the presence of three paragnaths in lateral patches in Area III, while this feature is absent in *P. cultrifera*. *Perinereis oliveirae* is described for the northern Iberian Peninsula, having also very long bar-shaped paragnaths in Areas VI and very short tentacular cirri compared to length of the head (reaching chaetigers 1 and 2). These features were confirmed based on the two *P. oliveirae* specimens from this study and samples from the private collection of the first author of this study.

Apart from the above-mentioned species, based on WoRMS (<https://www.marinespecies.org/>; Read and Fauchald 2024), OBIS (<https://mapper.obis.org/>), the *Perinereis* checklist from Mohammad (1971) for the Arabian Gulf and the annotated checklist of polychaete species around the Arabian Peninsula from Wehe and Fiege (2002), there are five additional *Perinereis* species with just a single bar-shaped paragnath on each side of Area VI (*Perinereis* species Group I, Hutchings et al. 1991) reported for the Arabian Peninsula: *P. perspicillata* (Grube, 1878) (Bonyadi-Naeini et al. 2018: 1973, table 4); *P. iranica* Bonyadi-Naeini, N. Rastegar-Pouyani, E. Rastegar-Pouyani, Glasby & Rahimian, 2018: 1965–1976, figs 2, 3, table 4; *P. obfuscata* (Grube, 1878) (Bonyadi-Naeini et al. 2018: 1973, table 4); *P. striolata* (Grube, 1878) (Bonyadi-Naeini et al. 2018: 1973, table 4) and *P. floridana* (Ehlers, 1868: 269–748, pls XII–XXIV), as interpreted by Bonyadi-Naeini et al. (2018: 1972–1973, table 4). None of the above species share the same morphotype as *P. kaustiana* sp. nov., differing in the paragnath numbers and arrangement, as well as the length of the postero-dorsal cirri and types of chaetae, as described in the taxonomic key below. Additionally, four *Perinereis* Group I species reported mainly for the Mediterranean Sea were added to the key due to geographical proximity for comparison purposes: *Perinereis cultrifera*, *Perinereis rullieri*, *Perinereis macropus* (Claparède, 1870: 444–448, pl. VIII, fig. 1), and *Perinereis tenuisetis* (Fauvel, 1915) (Guerne and Richard 1916: 88–92, pl. VII, figs 1–10; Mahcene et al. 2023). A comparison between selected characters in the most morphologically similar species to *P. kaustiana* sp. nov., some lacking DNA data and reported for the Arabian Peninsula and Mediterranean Sea, are summarised in Tables 4, 5 (including *P. helleri*).

**Table 5.** Comparison between selected characters in the most morphologically similar species to *P. kaustiana* sp. nov., reported for the Arabian Peninsula and Mediterranean Sea and lacking DNA data.

Characters	<i>P. iranica</i> Bonyadi-Naeini et al. (2018)	<i>P. perspicillata</i> Grube, 1878	<i>P. macropus</i> (Claparède, 1870)	<i>P. floridana</i> (Ehlers, 1868)
Colouration	Creamy with orange pigmentation in anterior body	No data	Greenish; white pigmented dots in prostomium and anterior region (based on the drawings)	No data
Paragnaths Area I	Cluster of 4–6 paragnaths	Cluster of 6–8 paragnaths	Cluster of 4 paragnaths	1 large paragnath.
Paragnaths Area II	12–15 paragnaths	Cluster of paragnaths	20–25 paragnaths arranged in wedge shape	Group of paragnaths in three oblique rows
Paragnaths Area III	Central patch of 30–45 paragnaths, lateral patch absent	Central patch, lateral patch absent	Central patch of 30–35 paragnaths + lateral patches with 4 paragnaths each	Group of very small paragnaths in three parallel rows
Paragnaths Area IV	40–47 paragnaths arranged in wedge shape without any bars.	Cluster of very dark paragnaths	25–27 paragnaths arranged in an inverse triangle	Group of paragnaths in four parallel rows, the last shorter than the others and ending in a cluster in the central corner
Paragnaths Area V	5 paragnaths in one row, median one larger than others	Triangle of 3 paragnaths	5 paragnaths in one row + single middle paragnath on top of the row	1 large paragnath
Paragnaths Area VI (a+b)	2 long, arcuate bars	2 large transversal bars	2 slightly arcuate transversal bars	1 single, broad, flat, somewhat triangular paragnath
Paragnaths Areas VII and VIII	3 rows, two distal most rows composed of large paragnaths and proximal row comprising small paragnaths; 25–31 total	Central group with three rows, lateral ones with one row	Band of 50–55 paragnaths	Group of large paragnaths in two distinct rows
Postero-dorsal cirri	Very small, reaching up to chaetiger 2	No data	Very small, reaching up to chaetiger 2	Extend back to chaetiger 5
Homogomph spiniger serration (neurochaetal supra-acicular fascicle)	No data	No data	No data	No data
Heterogomph falcigers	Present with short blades	No data	Short blades	Present with short, sickle-shaped blades
Parapodia	Posteriormost dorsal ligule greatly expanded	No data	Posteriormost dorsal ligule not expanded	No data
Type locality	Iran (Persian Gulf)	Philippines (Pacific)	Naples, western Italy (Mediterranean)	Caribbean Sea
Reference	Bonyadi-Naeini et al. 2018	Fauvel 1911; Mohammad 1971	Claparède 1870	Wesenberg-Lund 1949; Bonyadi-Naeini et al. 2018

**Key to the *Perinereis* species Group I reported for the Arabian Peninsula and Mediterranean Sea, including the Indo-Pacific ingroup *P. helleri***

- 1 Area V, usually a triangle of 3 paragnaths or more .....2
- Area V, a single paragnath or absence.....8
- 2 Area I, a small cluster of 4–8 paragnaths.....3
- Area I, 1 to 3 paragnaths; if more than 1, arranged in a longitudinal line...4
- 3 Area III, cluster of paragnaths, lateral patches absent; Area VI, a large transversal bar .....***P. perspicillata***
- Area III, cluster of paragnaths, lateral patches present, 4 paragnaths each; Area VI, a short arcuate bar .....***P. macropus***
- 4 Large paragnath sizes; Area III, lateral patches absent. Short heterogomph falcigers .....5
- Small paragnath sizes; Area III, lateral patches with 1 or 2 paragnaths each. Long heterogomph falcigers .....6

- 5 Area V, one row of 5 paragnaths, median one larger than others; Area VI, a long clear arcuate bar ..... ***P. iranica***
- Area V, a triangle of 3 paragnaths; Area VI, a short straight bar, may be slightly arcuate ..... ***P. cultrifera* (complex)**
- 6 Area III, lateral patches with 1 paragnath each (may be present only on a single side)..... ***P. rullieri* (complex)**
- Area III, lateral patches with 2 paragnaths each ..... **7**
- 7 Length of postero-dorsal cirri extends back to chaetiger 16 (range 8–16). Dorsal cirri subequal to slightly longer than ventral one throughout the body. Posteriormost dorsal ligules expanded. Indo-Pacific variant..... ***P. helleri***
- Length of postero-dorsal cirri extends back to chaetigers 7–9. Dorsal cirri of median segments much longer than ventral cirri (DCL / VCL = 2.8–3×). Posteriormost dorsal ligules greatly expanded. Red Sea variant ..... ***P. kaustiana* sp. nov.**
- 8 Area V, absence of paragnaths. Homogomph falcigers present; heterogomph falcigers absent ..... ***P. tenuisetis***
- Area V, a single paragnath. Homogomph falcigers absent; heterogomph falcigers usually present\* ..... **9**
- 9 Area I, 1 large paragnath..... ***P. floridana***
- Area I, a small cluster of 3–9 paragnaths..... **10**
- 10 Tentacular cirri reaching backwards to chaetiger 1 ..... ***P. obfuscata***
- Tentacular cirri reaching backwards to chaetigers 6 and 7..... ***P. striolata***

## Discussion

Our molecular data provides compelling evidence for the existence of a new, deeply divergent, and completely sorted species within the *Perinereis* species Group I in the Red Sea. At first glance, *P. kaustiana* sp. nov. can be easily misidentified as the well-known and allegedly cosmopolitan *P. cultrifera*, due to the classic two bar shaped paragnaths in Areas VI and proximity with the Mediterranean Sea. This might be the reason the latter is usually reported for the Red Sea (Wehe and Fiege 2002; Bonyadi-Naeini et al. 2018; OBIS), but a greater sampling effort in the central and southern Red Sea regions are needed to confirm this. Morphological features, such as the paragnath arrangement, as well as the length of tentacular cirri and ratios within the parapodia also allowed the distinction of *P. kaustiana* sp. nov. from other similar species (see taxonomic key and Tables 4, 5). Upon careful morphological examination, *P. kaustiana* sp. nov. is morphologically closer to the Indo-Pacific *P. helleri*, than it is to the European *P. cultrifera*, based mainly on paragnath patterns, particularly in Areas III (Fig. 2D) and VII and VIII (Fig. 2G), and similar length of the falciger blades. Paragnath features in Areas VII and VIII lends support to the taxonomic importance of highlighting faint ridges and furrows in the ventral oral ring for certain *Perinereis* species (Conde-Vela 2018), which usually are not accounted in species descriptions due to no apparent pattern being found (i.e., Teixeira et al. 2022a). *Perinereis kaustiana* sp. nov. and *P. helleri* are also phylogenetically closely related (Fig. 1A), despite being divergent lineages, with genetic distances that are in the range used for delimitating polychaete species (i.e., Kvist 2016; Lobo et al. 2016; Nygren et al. 2018). This situ-

\* No available chaetae data for *P. striolata*.

ation, together with the absence or subtle morphological differences previously overlooked, resembles cryptic lineages within a species complex (Teixeira et al. 2022b, 2023), and further sampling efforts between the Red Sea to the Indo-Pacific region are needed to assess this.

The new species is so far unique to the northern Red Sea and apparently easy to find in the rocky beaches of the Gulf of Aqaba. Considering the high rate of endemism in the Red Sea (DiBattista et al. 2016), this species may indeed be endemic to this Sea, although further sampling across this region and the Indo-Pacific area might prove it to be more widespread. In the remaining sampling sites further south, along the northern Saudi coast, *P. kaustiana* sp. nov. is outcompeted by the sympatric distributed *Perinereis nuntia* species group, which seems to be the dominant coastal annelid in the region (Fig. 1B). The latter is also a species complex with several different species recently revised by Villalobos-Guerrero (2019). Our specimens initially identified as belonging to the *P. nuntia* complex revealed at least two different morphotypes, which after further morphological (mainly based on paragnath patterns, Fig. 1C, D) and molecular review corresponded to the new species recently described by Elgetany et al. (2022) for the neighbouring Egyptian coast (Suez Canal), namely *P. damietta* (Fig. 1C) and *P. suezensis* (Fig. 1D). These species are sympatric with *P. kaustiana* sp. nov., but apparently not sympatric with each other in the studied region (Fig. 1B). *Perinereis damietta* (which is morphologically more similar to *P. heterodonta* Gravier, 1899 than to *P. nuntia* according to Elgetany et al. (2022)), was found mainly in lagoon-like environments, whereas *P. suezensis* only in fully marine areas. *Perinereis kaustiana* sp. nov. shared both marine and lagoon-like habitats, with all the three sampled species found in intertidal coarse-grained sand, under rocks or cobbles. As speculated by Elgetany et al. (2022), *P. damietta* seems to have a slightly wider habitat preference, since some of our specimens (from Al Muwaileh lagoon) also occurred sub-tidally, attached to small rocks at approximately 1 meter depth.

## Acknowledgements

Thanks are due to the remaining NEOM bioblitz 2023 expedition Team: Gustav Paulay (Team Leader), Robert Lasley, Diana Noto, Morgan Bennett-Smith, Daisuke Uyeno, Eléfanti Soma, Viktor Peinemann, Matthew David Tietbohl, and the crew of Al Azizi. Thanks are due to the Biodiversity & Ecosystem Management Lab (BEM, at KAUST) Team members: Fern Lyne-Temple, Gloria L. Gil Ramos, Ronald C. Cadiz, Rodrigo Villalobos, Norah Almutairi, João Gabriel Duarte Rosado, and João Cúrdia for helping to organise the sampling campaign. We are also in debt to current and previous members of the NEOM Environmental Authority Department and Education, Research, and Innovation Foundation (ERIF), namely Ameer Eweida, Flor Torres, Ana Manjua, Deborah Colbourne, Abdulkader Khamis, and Vibeke Svensson. Furthermore, we would like to thank the reviewers, including Christopher J. Glasby, the Copy Editor Nathalie Yonow and the Subject Editor Andrew Davinack for the reviewing process of our manuscript.

## Additional information

### Conflict of interest

The authors have declared that no competing interests exist.

## Ethical statement

Sampling of marine invertebrates followed the Institutional Biosafety and Bioethics Committee (IBEC; reference 22IBEC073) and approved by the Saudi National Committee of Bio-Ethics (NCBE; IBEC Registration Number with NCBE, Kingdom of Saudi Arabia: HAP-02-J-042)

## Funding

This study was funded by the NEOM research grant #5209 “Biodiversity baseline assessment and monitoring” (RGC/3/5209-01-01) and King Abdullah University of Science and Technology baseline grant to Susana Carvalho (BAS/1/1109-01-01).

## Author contributions

Conceptualization: MALT, CJLF, JSV, SC. Data curation: MALT. Formal analysis: MALT. Funding acquisition: SC. Investigation: CJLF, MALT. Methodology: MALT, JSV. Project administration: SC. Resources: SC. Supervision: SC. Visualization: CJLF. Writing – original draft: MALT. Writing – review and editing: JSV, SC, CJLF.

## Author ORCIDs

Marcos A. L. Teixeira  <https://orcid.org/0000-0002-2228-2673>

Chloé Julie Loïs Fourreau  <https://orcid.org/0000-0002-0062-2876>

Juan Sempere-Valverde  <https://orcid.org/0000-0001-5856-9214>

Susana Carvalho  <https://orcid.org/0000-0003-1300-1953>

## Data availability

New sequence data and specimen metadata were uploaded in the project “*Perinereis* Saudi NEOM (DS-MTPNO)” within BOLD (<https://v4.boldsystems.org/>) and in the following link: <https://dx.doi.org/10.5883/DS-MTPNO>. The COI alignments (FASTA and NEXUS formats) are publicly available online at Figshare (DOI: <https://www.doi.org/10.6084/m9.figshare.25097756>). GenBank accession numbers: PP279002–PP279039 (mtCOI- 5P); PP264567–PP264572, PP264574, PP264575 (16S); PP264613, PP264614, PP264616 (28SD2). See Suppl. material 1 for more details. The new biological material from the Red Sea is deposited at NTNU University Museum (NTNU-VM), Trondheim, Norway. Specimens from *Perinereis oliveirae* are deposited at the Biological Research Collection (Marine Invertebrates) of the Department of Biology of the University of Aveiro (CoBI at DBUA), Portugal. All specimens are available upon request.

## References

- Abe H, Tanaka M, Taru M, Abe S, Nishigaki A (2019) Molecular evidence for the existence of five cryptic species within the Japanese species of *Marphysa* (Annelida: Eunicidae) known as “Iwa-mushi”. *Plankton & Benthos Research* 14(4): 303–314. <https://doi.org/10.3800/pbr.14.303>
- Astrin J, Zhou X, Misof B (2013) The importance of biobanking in molecular taxonomy, with proposed definitions for vouchers in a molecular context. *ZooKeys* 365: 67–70. <https://doi.org/10.3897/zookeys.365.5875>
- Bakken T, Wilson RS (2005) Phylogeny of nereidids (Polychaeta, Nereididae) with paragnaths. *Zoologica Scripta* 34(5): 507–547. <https://doi.org/10.1111/j.1463-6409.2005.00200.x>
- Bakken T, Glasby CJ, Wilson RS (2009) A review of paragnath morphology in Nereididae (Polychaeta). *Zoosymposia* 2(1): 305–316. <https://doi.org/10.11646/zoosymposia.2.1.21>

- Bakken T, Hårsaker K, Daverdin M (2024) Marine invertebrate collection NTNU University Museum. Version 1.1682. Norwegian University of Science and Technology. [Occurrence dataset] <https://doi.org/10.15468/ddbs14> [accessed via GBIF.org on 2024-02-05]
- Bonyadi-Naeini A, Rastegar-Pouyani N, Rastegar-Pouyani E, Glasby CJ, Rahimian H (2018) Intertidal polychaetes from Abu Musa Island, Persian Gulf, with a new species from the *Perinereis cultrifera* species complex (Annelida: Nereididae). *Journal of the Marine Biological Association of the United Kingdom* 98(8): 1965–1976. <https://doi.org/10.1017/S0025315417001564>
- Carr CM, Hardy SM, Brown TM, Macdonald TA, Hebert PDN (2011) A Tri-Oceanic Perspective: DNA Barcoding Reveals Geographic Structure and Cryptic Diversity in Canadian Polychaetes. *PLOS ONE* 6(7): e22232. <https://doi.org/10.1371/journal.pone.0022232>
- Cerca J, Purschke G, Struck TH (2018) Marine connectivity dynamics: Clarifying cosmopolitan distributions of marine interstitial invertebrates and the meiofauna paradox. *Marine Biology* 165(8): e123. <https://doi.org/10.1007/s00227-018-3383-2>
- Claparède E (1870) Les Annélides Chétopodes du Golfe de Naples. Supplément. *Mémoires de la Société de physique et d'histoire naturelle de Genève*. 20(2): 365–542. <https://doi.org/10.5962/bhl.title.2142>
- Conde-Vela VM (2018) New species of *Pseudonereis* Kinberg, 1865 (Polychaeta: Nereididae) from the Atlantic Ocean, and a review of paragnath morphology and methodology. *Zootaxa* 4471(2): 245–278. <https://doi.org/10.11646/zootaxa.4471.2.2>
- Conde-Vela VM, Salazar-Vallejo SI (2015) Redescriptions of *Nereis oligohalina* (Rioja, 1946) and *N. garwoodi* Gonzalez-Escalante & Salazar-Vallejo, 2003 and description of *N. confusa* sp. n. (Annelida, Nereididae). *ZooKeys* 518: 15–49. <https://doi.org/10.3897/zookeys.518.9564>
- DiBattista JD, Roberts MB, Bouwmeester J, Bowen BW, Coker DJ, Lozano-Cortés DF, Howard Choat J, Gaither MR, Hobbs J-PA, Khalil MT, Kochzius M, Myers RF, Paulay G, Robitzsch VSN, Saenz-Agudelo P, Salas E, Sinclair-Taylor TH, Toonen RJ, Westneat MW, Williams ST, Berumen ML (2016) A review of contemporary patterns of endemism for shallow water reef fauna in the Red Sea. *Journal of Biogeography* 43(3): 423–439. <https://doi.org/10.1111/jbi.12649>
- Ehlers EH (1868) Die Borstenwürmer (Annelida Chaetopoda) nach systematischen und anatomischen Untersuchungen dargestellt. Wilhelm Engelmann, Leipzig 2: 269–748.
- Elgetany AH, Struck TH, Glasby CJ (2022) Three new species of the genus *Perinereis* (Annelida, Nereididae) from Egyptian coasts. *ZooKeys* 1132: 163–188. <https://doi.org/10.3897/zookeys.1132.87629>
- Fauvel P (1915) Polychètes pelagiques nouvelles des Campagnes de la Princesse-Alice (note préliminaire). *Bulletin de l'Institut océanographique* 305: 1–11.
- Fauvel P (1923) Polychètes errantes. *Faune de France* 5: 1–488. [www.fauvedefrance.org/bibliotheque/docs/P.FAUVEL%28FdeFr05%29Polychetes-errantes.pdf](http://www.fauvedefrance.org/bibliotheque/docs/P.FAUVEL%28FdeFr05%29Polychetes-errantes.pdf)
- Fauvel P (1932) Annelida Polychaeta of the Indian Museum, Calcutta. *Memoirs of the Indian Museum, Calcutta* 12: 1–262. [pls 1–9]
- Glasby CJ, Hsieh HL (2006) New species and new records of the *Perinereis nuntia* species group (Nereididae: Polychaeta) from Taiwan and other Indo-West Pacific shores. *Zoological Studies* 45: 553–577. <https://zoolstud.sinica.edu.tw/Journals/45.4/553.html>
- Glasby CJ, Wei NWV, Gibb KS (2013) Cryptic species of Nereididae (Annelida: Polychaeta) on Australian coral reefs. *Invertebrate Systematics* 27(3): 245–264. <https://doi.org/10.1071/IS12031>

- Grube AE (1840) Actinien, Echinodermen und Würmer des Adriatischen- und Mittelmeers nach eigenen Sammlungen beschrieben. Königsberg: J.H. Bon, 92 pp. <https://doi.org/10.5962/bhl.title.23025>
- Grube A-E (1878) Annulata Semperiana. Beiträge zur Kenntniss der Annelidenfauna der Philippinen nach den von Herrn Prof. Semper mitgebrachten Sammlungen. Mémoires l'Académie Impériale des Sciences de St.- Pétersbourg. <https://doi.org/10.5962/bhl.title.85345>
- Guerne J, Richard J (1916) Résultats des campagnes scientifiques accomplies sur son yacht par Albert Ier, prince souverain de Monaco, fasc. 48. Annelides Polychetes. <https://doi.org/10.5962/bhl.title.2169>
- Hartmann-Schröder G (1979) Zur Kenntnis des Eulitorals der australischen Küsten unter besonderer Berücksichtigung der Polychaeten und Ostracoden. Teil 2. Die Polychaeten der tropischen Nordwestküste Australiens (zwischen Derby im Norden und Port Hedland im Süden). Mitteilungen aus dem Zoologischen Institut und Zoologische Museum der Universität Hamburg 76: 75–218. [pl. 1]
- Hassouna N, Mithot B, Bachellerie JP (1984) The complete nucleotide sequence of mouse 28S rRNA gene. Implications for the process of size increase of the large subunit rRNA in higher eukaryotes. Nucleic Acids Research 12(8): 3563–3583. <https://doi.org/10.1093/nar/12.8.3563>
- Horst R (1889) Contributions towards the knowledge of the Annelida Polychaeta. Notes Leyden Museum Jentink 1889: 38–45.
- Hutchings P, Reid A, Wilson RS (1991) *Perinereis* (Polychaeta, Nereididae) from Australia, with redescriptions of six additional species. Records of the Australian Museum 43(3): 241–274. <https://doi.org/10.3853/j.0067-1975.43.1991.47>
- Kessing B, Croom H, Martin A, McIntosh C, Palumbi S, Owen MW (2004) The simple fool's guide to PCR, version 1.0. In: Special Publication. Dept. of Zoology, University of Hawaii, Honolulu. [https://www.academia.edu/18102912/The\\_simple\\_fool\\_s\\_guide\\_to\\_PCR](https://www.academia.edu/18102912/The_simple_fool_s_guide_to_PCR)
- Kimura (1980) A simple method for estimating evolutionary rate of base substitutions through comparative studies of nucleotide sequences. Journal of Molecular Evolution 16: 111–120. <https://doi.org/10.1007/BF01731581>
- Kinberg JGH (1865) Annulata nova. [Continuatio.]. Öfversigt af Königlich Vetenskapsakademiens förhandlingar, Stockholm 22: 167–179.
- Kvist S (2016) Does a global DNA barcoding gap exist in Annelida? Mitochondrial DNA. Part A, DNA Mapping, Sequencing, and Analysis 27: 2241–2252. <https://doi.org/10.3109/19401736.2014.984166>
- Lobo J, Teixeira MAL, Borges LMS, Ferreira MSG, Hollatz C, Gomes PA, Sousa R, Ravara A, Costa MH, Costa FO (2016) Starting a DNA barcode reference library for shallow water polychaetes from the southern European Atlantic coast. Molecular Ecology Resources 16(1): 298–313. <https://doi.org/10.1111/1755-0998.12441>
- Mahcene HR, Villalobos-Guerrero TF, Kurt G, Denis F, Daas T (2023) A new species of *Perinereis* Kinberg, 1865 (Annelida: Nereididae) from the Western Mediterranean Sea revealed by morphological and molecular approaches. Mediterranean Marine Science 24(2): 454–460. <https://doi.org/10.12681/mms.33969>
- Martin D, Gil J, Zanol J, Meca MA, Portela RP (2020) Digging the diversity of Iberian bait worms Marphysa (Annelida, Eunicidae). PLOS ONE 15(1): e0226749. <https://doi.org/10.1371/journal.pone.0226749>
- Martin D, Aguado MT, Fernández Álamo M-A, Britayev TA, Böggemann M, Capa M, Faulwetter S, Fukuda MV, Helm C, Petti MAV, Ravara A, Teixeira MAL (2021) On the Diversity of Phyllodocida (Annelida: Errantia), with a Focus on Glyceridae, Goniadidae,

- Nephtyidae, Polynoidae, Sphaerodoridae, Syllidae, and the Holoplanktonic Families. *Diversity* 13(3): e131. <https://doi.org/10.3390/d13030131>
- Mohammad M-BM (1971) Intertidal polychaetes from Kuwait, Arabian Gulf, with descriptions of three new species. *Journal of Zoology (London, England)* 163(3): 285–303. <https://doi.org/10.1111/j.1469-7998.1971.tb04536.x>
- Monro CCA (1931) Polychaeta, Oligochaeta, Echiuroidea and Sipunculoidea. *Scientific Reports of the Great Barrier Reef (Qld) Expedition 1928–29. Scientific Reports British Museum* 4: 1–37. [Natural History]
- Nygren A, Eklöf J, Pleijel F (2010) Cryptic species of *Notophyllum* (Polychaeta: Phylodocidae) in Scandinavian waters. *Organisms, Diversity & Evolution* 10(3): 193–204. <https://doi.org/10.1007/s13127-010-0014-2>
- Nygren A, Parapar J, Pons J, Meißner K, Bakken T, Kongsrud JA, Oug E, Gaeva D, Sikorski A, Johansen RA, Hutchings PA, Lavesque N, Capa M (2018) A mega-cryptic species complex hidden among one of the most common annelids in the North East Atlantic. *PLOS ONE* 13(6): e0198356. <https://doi.org/10.1371/journal.pone.0198356>
- Paiva PC, Mutaquilha BF, Coutinho MCL, Santos CSG (2019) Comparative phylogeography of two coastal species of *Perinereis* Kinberg, 1865 (Annelida, Polychaeta) in the South Atlantic. *Marine Biodiversity* 49(3): 1537–1551. <https://doi.org/10.1007/s12526-018-0927-0>
- Park T, Kim W (2017) Description of a New Species for Asian Populations of the “Cosmopolitan” *Perinereis cultrifera* (Annelida: Nereididae). *Zoological Science* 34(3): 252–260. <https://doi.org/10.2108/zs160154>
- Pilato G (1974) *Perinereis rullieri*, nuova specie di nereidi (Annelida, Polychaeta) delle coste Siciliane. *Animalia, Catania* 1: 25–37.
- Pleijel F, Jondelius U, Norlinder E, Nygren A, Oxelman B, Schander C, Sundberg P, Thollesson M (2008) Phylogenies without roots? A plea for the use of vouchers in molecular phylogenetic studies. *Molecular Phylogenetics and Evolution* 48(1): 369–371. <https://doi.org/10.1016/j.ympev.2008.03.024>
- Puillandre N, Brouillet S, Achaz G (2021) ASAP: Assemble species by automatic partitioning. *Molecular Ecology Resources* 21(2): 609–620. <https://doi.org/10.1111/1755-0998.13281>
- Ratnasingham S, Hebert PDN (2013) A DNA-Based Registry for All Animal Species: The Barcode Index Number (BIN) System. *PLOS ONE* 8(7): e66213. <https://doi.org/10.1371/journal.pone.0066213>
- Read G, Fauchald K [Eds] (2024) World Polychaeta Database. *Perinereis cultrifera* (Grube, 1840). World Register of Marine Species. <https://www.marinespecies.org/aphia.php?p=taxdetails&id=130408> [Accessed on 15 January 2024]
- Roberts CM, McClean CJ, Veron JEN, Hawkins JP, Allen GR, McAllister DE, Mittermeier CG, Schueler FW, Spalding M, Wells F, Vynne C, Werner TB (2002) Marine biodiversity hotspots and conservation priorities for tropical reefs. *Science* 295: 1280e1284. <https://doi.org/10.1126/science.1067728>
- Rozbaczylo N, Castilla JC (1973) El genero *Perinereis* (Annelida, Polychaeta, Nereidae) en Chile. *Studies on the Neotropical Fauna* 8(2): 215–232. <https://doi.org/10.1080/01650527309360463>
- Russell E (1962) Some nereid polychaetes from Queensland. *University of Queensland Papers. Department of Zoology* 2: 1–12.
- Sampértegui S, Rozbaczylo N, Canales-Aguirre CB, Carrasco F, Hernández CE, Rodríguez-Serrano E (2013) Morphological and molecular characterization of *Perinereis gualpensis* (Polychaeta: Nereididae) and its phylogenetic relationships with other

- species of the genus off the Chilean coast, Southeast Pacific. *Cahiers de Biologie Marine* 54: 27–40.
- Sampieri BR, Vieira PE, Teixeira MAL, Seixas VC, Pagliosa PR, Amaral ACZ, Costa FO (2021) Molecular diversity within the genus *Laeonereis* (Annelida, Nereididae) along the west Atlantic coast: Paving the way for integrative taxonomy. *PeerJ* 9: e11364. <https://doi.org/10.7717/peerj.11364>
- Scaps P, Rouabah A, Leprêtre A (2000) Morphological and biochemical evidence that *Perinereis cultrifera* (Polychaeta: Nereididae) is a complex of species. *Journal of the Marine Biological Association of the United Kingdom* 80(4): 735–736. <https://doi.org/10.1017/S0025315400002587>
- Tamura K, Stecher G, Kumar S (2021) MEGA11: Molecular Evolutionary Genetics Analysis Version 11. *Molecular Biology and Evolution* 38(7): 3022–3027. <https://doi.org/10.1093/molbev/msab120>
- Teixeira MAL, Bakken T, Vieira PE, Langeneck J, Sampieri BR, Kasapidis P, Ravara A, Nygren A, Costa FO (2022a) The curious and intricate case of the European *Hediste diversicolor* (Annelida, Nereididae) species complex, with description of two new species. *Systematics and Biodiversity* 20(1): e2116124. <https://doi.org/10.1080/14772000.2022.2116124>
- Teixeira MAL, Langeneck J, Vieira PE, Hernandez JC, Sampieri BR, Kasapidis P, Mucciolo S, Bakken T, Ravara A, Nygren A, Costa FO (2022b) Reappraisal of the hyperdiverse *Platynereis dumerilii* (Annelida: Nereididae) species complex in the North Atlantic, with the description of two new species. *Invertebrate Systematics* 36(11): 1017–1061. <https://doi.org/10.1071/IS21084>
- Teixeira MAL, Vieira PE, Pleijel F, Langeneck J, Sampieri BR, Hernandez JC, Ravara A, Costa FO, Nygren A (2023) Revealing the diversity of the green *Eulalia* (Annelida, Phyllodoceidae) species complex along the European coast, with description of three new species. *Organisms, Diversity & Evolution* 23(3): 477–503. <https://doi.org/10.1007/s13127-022-00597-1>
- Tilic E, Feerst KG, Rouse GW (2019) Two new species of *Amphiglena* (Sabellidae, Annelida), with an assessment of hidden diversity in the Mediterranean. *Zootaxa* 4648(2): 337–353. <https://doi.org/10.11646/zootaxa.4648.2.8>
- Villalobos-Guerrero TF (2019) Redescription of two overlooked species of the *Perinereis nuntia* complex and morphological delimitation of *P. nuntia* (Savigny in Lamarck, 1818) from the Red Sea (Annelida, Nereididae). *Zoosystema* 41: 465–496. <https://doi.org/10.5252/zoosystema2019v41a24>
- Villalobos-Guerrero TF, Bakken T (2018) Revision of the *Alitta virens* species complex (Annelida: Nereididae) from the North Pacific Ocean. *Zootaxa* 4483(2): 201–257. <https://doi.org/10.11646/zootaxa.4483.2.1>
- Villalobos-Guerrero TF, Carrera-Parra LF (2015) Redescription of *Alitta succinea* (Leuckart, 1847) and reinstatement of *A. acutifolia* (Ehlers, 1901) n. comb. based upon morphological and molecular data (Polychaeta: Nereididae). *Zootaxa* 3919(1): 157–178. <https://doi.org/10.11646/zootaxa.3919.1.7>
- Villalobos-Guerrero TF, Park T, Idris I (2021) Review of some *Perinereis* Kinberg, 1865 (Annelida: Nereididae) species of Group 2 sensu Hutchings, Reid & Wilson, 1991 from the Eastern and South-eastern Asian seas. *Journal of the Marine Biological Association of the United Kingdom* 101(2): 279–307. <https://doi.org/10.1017/S0025315421000126>
- Wehe T, Fiege D (2002) Annotated checklist of the polychaete species of the seas surrounding the Arabian Peninsula: Red Sea, Gulf of Aden, Arabian Sea, Gulf of Oman, Arabian Gulf. *Fauna of Arabia* 19: 7–238.

- Wilson RS, Glasby CJ (1993) A revision of the *Perinereis* species group (Polychaeta: Nereididae). Records of the Australian Museum 45(3): 253–277. <https://doi.org/10.3853/j.0067-1975.45.1993.23>
- Wilson RS, Glasby CJ, Bakken T (2023) The Nereididae (Annelida) – diagnoses, descriptions, and a key to the genera. ZooKeys 1182: 35–134. <https://doi.org/10.3897/zookeys.1182.104258>
- WoRMS Editorial Board (2024) World Register of Marine Species. <https://www.marine-species.org/aphia.php?p=taxdetails&id=129380> [Accessed 17 Jan 2024]
- Yousefi S, Rahimian H, Nabavi M, Glasby CJ (2011) Nereididae (Annelida: Polychaeta) from intertidal habitats in the Gulf of Oman, Iran. Zootaxa 3013(1): 48–64. <https://doi.org/10.11646/zootaxa.3013.1.2>
- Zhang J, Kapli P, Pavlidis P, Stamatakis A (2013) A general species delimitation method with applications to phylogenetic placements. Bioinformatics 29(22): 2869–2876. <https://doi.org/10.1093/bioinformatics/btt499>

## Supplementary material 1

### Supplementary data

Authors: Marcos A. L. Teixeira, Chloé Julie Loïs Fourreau, Juan Sempere-Valverde, Susana Carvalho

Data type: xlsx

Explanation note: Voucher data, origin of the specimens and GenBank accession numbers for each of the analysed genetic markers original to this study and molecular metadata used for comparison purposes or as outgroups.

Copyright notice: This dataset is made available under the Open Database License (<http://opendatacommons.org/licenses/odbl/1.0/>). The Open Database License (ODbL) is a license agreement intended to allow users to freely share, modify, and use this Dataset while maintaining this same freedom for others, provided that the original source and author(s) are credited.

Link: <https://doi.org/10.3897/zookeys.1196.115260.suppl1>